



**Maria Margarida
Feitor Pintão
Moreno Antunes**

**Conversão catalítica de sacarídeos em 2-furaldeído
e 5-hidroximetil-2-furaldeído**

**Catalytic routes to convert saccharides to furanic
aldehydes**



**Maria Margarida
Feitor Pintão
Moreno Antunes**

Conversão catalítica de sacarídeos em 2-furaldeído e 5-hidroximetil-2-furaldeído

Catalytic routes to convert saccharides to furanic aldehydes

Tese apresentada à Universidade de Aveiro para cumprimento dos requisitos necessários à obtenção do grau de Doutor em Química, realizada sob a orientação científica da Doutora Anabela Valente Investigadora Auxiliar do Departamento de Química, CICECO da Universidade de Aveiro, e do Doutor Martyn Pillinger, Investigador Auxiliar do Departamento de Química, CICECO da Universidade de Aveiro.

Financial support from FCT, POCI 2010, OE, FEDER, FCT project POCT1/QUI/56112/2004, Research Unit 62/94, project PEst-C/QUI/UI0062/2011, FSE under the III Community Support Framework



FCT Fundação para a Ciência e a Tecnologia
MINISTÉRIO DA EDUCAÇÃO E CIÊNCIA



UNIÃO EUROPEIA
Fundo Europeu
de Desenvolvimento Regional



QUADRO
DE REFERÊNCIA
ESTRATÉGICO
NACIONAL
PORTUGAL 2007-2013

To my dear parents, sister and beloved Miguel.

the jury

President

Prof. Doutor Mário Guerreiro da Silva Ferreira

Professor Catedrático do Departamento de Engenharia de Materiais e Cerâmica da Universidade de Aveiro

Prof. Doutor Carlos de Pascoal Neto

Professor Catedrático do Departamento de Química da Universidade de Aveiro

Prof. Doutora Maria Filipa Gomes Ribeiro

Professora Associada com Agregação do Departamento de Engenharia Química e Biológica, Instituto Superior Técnico, Lisboa

Prof. Doutor José Eduardo dos Santos Félix Castanheiro

Professor Auxiliar do Departamento de Química da Universidade de Évora

Doutora Anabela Tavares Aguiar Valente

Investigadora Auxiliar do Departamento de Química, CICECO, Universidade de Aveiro (Orientadora)

Doutor Martyn Pillinger

Investigador Auxiliar do Departamento de Química, CICECO, Universidade de Aveiro (Co-Orientador)

acknowledgements

To my supervisors Doctor Anabela Valente and Doctor Martyn Pillinger. To Doctor Anabela Valente I want to express my sincere gratification for all the support given over these last years, right from the start, for the valuable scientific values, inspiration, motivation, patience to clarify my doubts, for understanding the worst moments I passed through, the friendship always demonstrated, and above all for being always present during my thesis project. To Doctor Martyn Pillinger for having accepted me as PhD student, for all the knowledge and friendship transmitted through these last years. It was an honor working with him.

I am very grateful to Professor Isabel Gonçalves for motivating me to carry out research work at CICECO, which was the beginning of a scientific research journey, and for the support and friendship.

A special thanks to Doctor Sérgio Lima who was a fantastic lab-mate and for his patience, precious know-how and continuous collaboration throughout this thesis.

I wish to acknowledge Professor Filipa Ribeiro and Doctor Auguste Fernandes for the fruitful discussions and support in the measurements of the acid properties and catalysts tested in Chapter 3. Doctor Silvia Rocha and MSc Magda Santos are acknowledged for the assistance in the GC×GC-ToFMS analyses.

I acknowledge Doctor Nikolai Ignatyev from PC-RL, Ionic Liquids Research Laboratory, Merck KGaA, Darmstadt, Germany for the collaboration in the work of Chapter 8 and for supplying an ionic liquid.

For the technical support in characterization techniques, I acknowledge Doctor Maria Rosário Soares (powder XRD, CICECO), MSc Maria Celeste Azevedo (thermal analyses and vibrational spectroscopy, CICECO), Lic. Maria João Bastos (nitrogen sorption isotherms, Department of Materials and Ceramic Engineering), Lic. Hilário Tavares (liquid state NMR, Department of Chemistry), Lic. Manuela Marques (elemental analyses) and Isabel Martins (solid state NMR, Department of Chemistry). Doctor Fernando Domingues (Department of Chemistry) is acknowledged for the access to one of the HPLC equipments which was important for the success of this work.

A special thanks to my dear colleagues of the laboratory, besides Doctor Sérgio Lima, Doctors Patrícia Neves, Sofia Bruno and Ana Gomes for their unconditional and friendly support and for always making me feel like I was at home, and to my former lab-colleagues Doctors Sandro Gago and Salete Balula for the good moments when I arrived at Aveiro.

To my very close friends Vânia Fernandes, Graziella Portella and Marisa Resende for always being there for me, for the supporting and listening moments which helped me to manage stress.

To António Cavaleiro for all the help he gave me.

To my parents and sister for supporting me with love throughout all my journeys.

To Miguel Pereira for listening to me from the start, and for the unconditional love.

To the University of Aveiro, in particular to CICECO and to the Department of Chemistry for accepting me as a PhD student and for providing me all the necessary conditions to carry out my research and to Fundação para a Ciência e Tecnologia (FCT) and European Social Fund (FSE) for the PhD grant (SFRH/BD/61648/2009) and all the granted subsidies. This work was partly funded by the FCT project POCI/QUI/56112/2004.

palavras-chave

Biorefinarias, biomassa, carboidratos, 2-furaldeído, 5-hidroxiacetil-2-furaldeído, catálise ácida, materiais porosos, líquidos iônicos.

Resumo

Os carboidratos constituem os polímeros naturais mais abundantes na Terra, e a sua valorização química é de grande interesse no contexto das biorefinarias. O objetivo deste trabalho centrou-se na conversão de carboidratos (monossacarídeos e polissacarídeos) em 2-furaldeído (Fur) e 5-hidroxiacetil-2-furaldeído (Hmf) na presença de catalisadores ácidos, em reatores descontínuos. Fur e Hmf são considerados compostos “plataforma” porque podem ser convertidos numa grande variedade de produtos químicos e materiais (alternativos aos derivados do petróleo). Testaram-se catalisadores ácidos heterogêneos como alternativa aos ácidos minerais que são comumente usados como catalisadores homogêneos para a produção industrial do Fur. Por outro lado utilizou-se água ou um líquido iônico como solvente para a dissolução dos carboidratos no meio reacional. As temperaturas reacionais foram superiores a 150 °C quando o solvente era a água, e inferiores a 150 °C no caso de líquidos iônicos. Com o intuito de identificar os produtos reacionais (solúveis e insolúveis), utilizaram-se diferentes técnicas nomeadamente espectroscopia de infravermelho, espectroscopia de RMN de estado líquido e sólido, TGA, DSC e GCxGC-ToFMS. Obtiveram-se misturas complexas de produtos reacionais e discutiram-se aspetos mecanísticos.

A estabilidade térmica do catalisador é importante uma vez que a formação de matéria carbonácea insolúvel é característica destes sistemas reacionais tornando-se necessário proceder à regeneração do catalisador por calcinação. Os catalisadores testados foram ácidos inorgânicos nanoporosos, cristalinos ou amorfos, com tamanho de partícula nano ou micrométrico, especificamente silicoaluminofosfatos, aluminossilicatos e óxidos mistos de zircónio e tungsténio. Estes tipos de materiais são versáteis uma vez que as suas propriedades físico-químicas podem ser modificadas no sentido de melhorar os seus desempenhos catalíticos na conversão de diferentes tipos de substratos (ex. através da criação de mesoporos nos materiais e/ou modificação das propriedades ácidas). Os materiais testados exibiram melhores desempenhos catalíticos para a conversão de pentoses em Fur do que para a de hexoses em Hmf, quando o solvente era a água. Em suma, os catalisadores apresentaram boa estabilidade hidrotérmica. No caso dos sistemas reacionais à base de líquidos iônicos foram verificados elevados rendimentos em Fur e Hmf, especialmente quando os substratos eram a D-frutose ou polissacarídeos relacionados. Contudo, os catalisadores sofreram desativação tal que as reações catalíticas ocorreram em fase homogénea. Conforme explicado numa revisão bibliográfica sobre o estado da arte da conversão catalítica de carboidratos em Fur e Hmf usando líquidos iônicos, o desenvolvimento de sistemas catalíticos heterogêneos à base de líquidos iônicos representa um grande desafio.

Keywords

Biorefineries, biomass, carbohydrates, 2-furaldehyde, 5-hydroxymethyl-2-furaldehyde, acid catalysis, porous materials, ionic liquids.

Abstract

The conversion of plant biomass-derived carbohydrates (preferably non-edible) into added-value products is envisaged to be at the core of the future biorefineries. Carbohydrates are the most abundant natural organic polymers on Earth. This work deals with the chemical valorisation of plant biomass, focusing on the acid-catalysed conversion of carbohydrates (mono and polysaccharides) to furanic aldehydes, namely 2-furaldehyde (Fur) and 5-hydroxymethyl-2-furaldehyde (Hmf), which are valuable platform chemicals that have the potential to replace a variety of oil derived chemicals and materials. The investigated reaction systems can be divided into two types depending on the solvent used to dissolve the carbohydrates in the reaction medium: water or ionic liquid-based systems. The reaction temperatures were greater than 150 °C when the solvent was water, and lower than 150 °C in the cases of the ionic liquid-based catalytic systems. As alternatives to liquid acids (typically used in the industrial production of Fur), solid acid catalysts were investigated in these reaction systems. Aiming at the identification of (soluble and insoluble) reaction products, complementary characterisation techniques were used namely, FT-IR spectroscopy, liquid and solid state NMR spectroscopy, TGA, DSC and GC×GC-ToFMS analyses. Complex mixtures of soluble reaction products were obtained and different types of side reactions may occur. The requirements to be put on the catalysts for these reaction systems partly depend on the type of carbohydrates to be converted and the reaction conditions used. The thermal stability is important due to the fact that formation of humins and catalyst coking phenomena are characteristically inherent to these types of reactions systems leading to the need to regenerate the catalyst which can be effectively accomplished by calcination. Special attention was given to fully inorganic nanoporous solid acids, amorphous or crystalline, and consisting of nano to micro-size particles. The investigated catalysts were silicoaluminophosphates, aluminosilicates and zirconium-tungsten mixed oxides which are versatile catalysts in that their physicochemical properties can be fine-tuned to improve the catalytic performances in the conversion of different substrates (e.g. introduction of mesoporosity and modification of the acid properties). The catalytic systems consisting of aluminosilicates as solid acids and water as solvent seem to be more effective in converting pentoses and related polysaccharides into Fur, than hexoses and related polysaccharides into Hmf. The investigated solid acids exhibited fairly good hydrothermal stabilities. On the other hand, ionic liquid-based catalytic systems can allow reaching simultaneously high Fur and Hmf yields, particularly when Hmf is obtained from D-fructose and related polysaccharides; however, catalyst deactivation occurs and the catalytic reactions take place in homogeneous phase. As pointed out in a review of the state of the art on this topic, the development of truly heterogeneous ionic liquid-based catalytic systems for producing Fur and Hmf in high yields remains a challenge.

Published SCI papers

7- Antunes, M. M.; Lima, S.; Fernandes, A.; Candeias, J.; Pillinger, M.; Rocha, S. M.; Ribeiro, M. F.; Valente, A. A. : Catalytic Dehydration of D-xylose to 2-Furaldehyde in the Presence of Zr-(W, Al) Mixed Oxides. Tracing By-Products Using Two-Dimensional Gas Chromatography-Time-of-Flight Mass Spectrometry. *Catalysis Today* **2012**, 195, 127-135.

6-Antunes, M. M.; Lima, S.; Pillinger, M.; Valente, A. A.: Coupling of Nanoporous Chromium, Aluminium Containing Silicates with an Ionic Liquid for the Transformation of Glucose Into 5-(Hydroxymethyl)-2-furaldehyde. *Molecules* **2012**, 17, 3690-3707.

5-Antunes, M. M.; Lima, S.; Fernandes, A.; Pillinger, M.; Ribeiro, M. F.; Valente, A. A.: Aqueous-Phase Dehydration of Xylose to Furfural in the Presence of MCM-22 and ITQ-2 Solid Acid Catalysts. *Applied Catalysis A: General* **2012**, 417-418, 243-252.

4-Lima, S.; Antunes, M. M.; Fernandes, A.; Pillinger, M.; Ribeiro, M. F.; Valente, A. A.: Catalytic Cyclodehydration of Xylose to Furfural in the Presence of Zeolite H-Beta and a Micro/Mesoporous Beta/TUD-1 Composite Material. *Applied Catalysis A: General* **2010**, 388, 141-148.

3-Lima, S.; Antunes, M.M.; Fernandes, A.; Pillinger, M.; Ribeiro, M. F.; Valente, A. A.: Acid-Catalysed Conversion of Saccharides into Furanic Aldehydes in the Presence of Three-Dimensional Mesoporous Al-TUD-1. *Molecules* **2010**, 15, 3863-3877.

2-Lima, S.; Fernandes, A.; Antunes, M. M.; Pillinger, M.; Ribeiro, F.; Valente, A. A.: Dehydration of Xylose into Furfural in the Presence of Crystalline Microporous Silicoaluminophosphates. *Catalysis Letters* **2010**, 135, 41-47.

1-Lima, S.; Neves, P.; Antunes, M. M.; Pillinger, M.; Ignatyev, N.; Valente, A. A.: Conversion of Mono/di/polysaccharides into Furan Compounds Using 1-Alkyl-3-methylimidazolium Ionic Liquids. *Applied Catalysis A: General* **2009**, 363, 93-99.

General list of abbreviations

AAL	α -Angelica lactone
^{27}Al MAS NMR	^{27}Al Magic-angle spinning nuclear magnetic resonance
AEL	Aluminophosphate-eleven (AIPO-11)
AFI	Aluminophosphate-five (AIPO-5)
AFR	Aluminophosphate-forty (AIPO-40)
Al_{fr}	Framework aluminium
Al_{ext-fr}	Extraframework aluminium
AS	Acid sites
a.t.	Ambient temperature
ATR	Attenuated total reflectance
B	Brönsted acid sites
BAL	β -Angelica lactone
BAMA	2,5-bis(aminomethyl)furan
BEA	Beta zeolite
BET	Brunauer, Emmett and Teller
BJH	Barrett-Joyner-Halenda
BS	Base sites
BuOH	n-Butanol
C_{Cel}	Conversion of D-cellobiose
C_{Fru}	Conversion of D-fructose
C_{Fur}	Conversion of 2-furaldehyde
C_{Glu}	Conversion of D-glucose
C_{Sub}	Conversion of substrate
C_{Suc}	Conversion of D-sucrose
C_{Xyl}	Conversion of D-xylose
CBC	Carbon based catalysts
^{13}C CP MAS NMR	^{13}C cross polarisation, magic-angle spinning, nuclear magnetic resonance
^{13}C NMR	^{13}C nuclear magnetic resonance

Cel	D-cellobiose
CH	Conventional heating method
CIMV	Compagnie Industrielle de la Matière Végétale
DFF	Diformylfuran
DFP	Difuranpropane
DFT	Density functional theory
DHMF	2,5-Dihydroxymethylfuran
DHMTFH	2,5-Di-(hydroxymethyl)tetrahydrofuran
DMA	Dimethylacetamide
DMF	2,5-Dimethylfuran
DMFA	N,N-Dimethylformamide
DMSO	Dimethylsulfoxide
D_p	Maximum at the pore size distribution
DOP	Degree of polymerisation
DR UV-vis	Diffuse reflectance ultraviolet visivel
DSC	Differential scanning calorimetry
DTHFP	(Di-tetrahydrofuran)propane
FA	Furfuryl alcohol
FAU	Faujasite zeolite
FDCA	2,5-Furandicarboxylic acid
FFAA	5-Formylfuran-2-acetic acid
FFDI	2,5-Furfuryldiisocyanate
FT-IR	Fourier transform infrared
Fru	D-fructose
Fur	2-Furaldehyde
GC-MS	Gas chromatography-mass spectrometry
Glu	D-glucose
HAF	2-(2'-Hydroxyacetyl)furan
HAFF	2-(2'-Hydroxyacetyl)furan formate
HB-HMF	3-(Hydroxybutenyl)-hydroxymethylfuran
HCW	Hot compressed water
HHMMF	4-Hydroxy-2-(hydroxymethyl)-5-methyl-3(2H)-furanone

HHT	4-Hydroxy-2,3,5-hexanetrione
HKPA	5-Hydroxy-4-keto-2-pentenoic acid
Hmf	5-Hydroxymethyl-2-furaldehyde
HMFA	5-Hydroxymethyl-furoic acid
HMFI	5-(Hydroxymethyl)furfurylidene ester
HMFIA	5-(Hydroxymethyl)furfurylidene acetophenone
HMPT	Hexamethylphosphotriamide
HMTHFA	5-Hydroxymethyltetrahydro-2-furaldehyde
¹H NMR	¹ H nuclear magnetic resonance
HPAs	Heteropolyacids
HPLC	High performance liquid chromatography
HRTEM	High resolution transmission electron microscopy
HT	Hydrotalcite
IBMK	Isobutylmethylketone
ICP-AES	Inductively coupled plasma atomic emission spectroscopy
IL(s)	Ionic liquid(s)
InsolOrg	Water-insoluble organic matter
Ipr	1,3-bis(2,6-diisopropylphenyl)imidazolylidene
IUPAC	International union of pure and applied chemistry
L	Lewis acid sites (not associated with numbers)
Mal	D-maltose
Man	D-mannose
MCFAT	Methyl furan-2-carboxylate
MF	2-Methyl-2-furaldehyde
MFI	Mordenite framework inverted
MFF	5-Methyl-2-furaldehyde
MOR	Mordenite
MPY	1-Methyl-2-pyrrolidone
MR	Membered ring
MTC	Multi turbin column
MTHF	Methyltetrahydrofuran
MTHFAT	Methyltetrahydrofuran-2-carboxylate

MW	Microwave
PEC	Pure energy corporation
PSD	Pore size distribution
PTFE	Polytetrafluoroethylene
PVP	Poly-(1-vinyl-2-pyrrolidinone)
S	Selectivity
SAPOS	Silicoaluminophosphates
S_{BET}	BET specific surface area
SEM	Scanning electron microscopy
S_{EXT}	External specific surface area
S_{Fur}	Selectivity of 2-furaldehyde
S_{Hmf}	Selectivity of 2-hydroxymethyl-2-furaldehyde
S_{meso}	Mesoporous specific surface area
SPME/GCxGC-ToFMS	Solid-phase microextraction coupled with comprehensive two-dimensional gas chromatography with a time-of-flight mass spectrometry
Suc	D-sucrose
TEM	Transmission electron microscopy
TGA	Thermogravimetric analysis
THF	Tetrahydrofuran
THFA	Tetrahydrofurfuryl alcohol
THFAC	Tetrahydrofuran-2-carboxylic acid
THFAM	Tetrahydrofuran-2-methanamine
THFF	Tetrahydro-2-furaldehyde
TIC GC x GC-ToFMS	Total ion chromatogram by comprehensive two-dimensional gas chromatography with a time-of-flight mass spectrometry
TMS	Tetramethylsilane
Tol	Toluene
p-TsOH	para-Toluenesulfonic acid
TUD-1	Technische Universital Delft, number one
TY	Theoretical yield
USDOE	US department of energy

V_{micro}	Microporous volume
V_{meso}	Mesoporous volume
V_p	Total pore volume
V_{S.T.P.}	Volume adsorbed at a standard temperature and pressure conditions
Wt	Water
Y	Yield
Y_{Cel}	Yield of D-cellobiose
Y_{Hmf}	Yield of 5-hydroxymethyl-2-furaldehyde
Y_{Fru}	Yield of fructose
Y_{Fur}	Yield of 2-furaldehyde
Y_{Glu}	Yield of D-glucose
Y_{Man}	Yield of D-mannose
Y_{Suc}	Yield of D-sucrose
Y_{Xyl}	Yield of D-xylose
XRD	X-ray diffraction
Xyl	D-xylose

List of abbreviations of ionic liquids

[Amim] ⁺	1-Allyl-3-methylimidazolium cation
[Amim]Cl	1-Allyl-3-methylimidazolium chloride
[Asbi] ⁺	3-Allyl-1-(4-sulfobutyl)imidazolium cation
[Asbi]CF ₃ SO ₃	3-Allyl-1-(4-sulfobutyl)imidazolium trifluoromethane sulfonate
[Ascbi]CF ₃ SO ₃	3-Allyl-1-(4-sulfurylchloridebutyl)imidazolium trifluoromethane sulfonate
[B ₂ im] ⁺	Butyl-3-methyl-imidazolium cation
[B ₄ N] ⁺	1-Tetra-butyl ammonium cation
[B ₄ N]Cl	1-Tetra-butyl ammonium chloride
[B ₄ N]HSO ₄	1-Tetra-butylammonium hydrogen sulfate
[B ₄ P] ⁺	1-Tetra-butyl phosponium cation
[B ₄ P]HSO ₄	1-Tetra-butyl hydrogen sulfate
[Bdmim]Cl	1-Butyl-2,3-dimethylimidazolium chloride
[Bemim]Cl	1-Benzyl-3-methylimidazolium chloride
[Bm ₂ im] ⁺	Butyl-2,3-dimethylimidazolium cation
[Bm ₂ im]Cl	Butyl-2,3-dimethylimidazolium chloride
[Bmim] ⁺	1-Butyl-3-methyl imidazolium cation
[Bmim]BF ₄	1-Butyl 3-methyl imidazolium tetrafluoroborate
[Bmim]Br	1-Butyl-3-methyl imidazolium bromide
[Bmim]Cl	1-Butyl-3-methyl imidazolium chloride
[Bmim]CH ₃ COO	1-Butyl-3-methyl imidazolium acetate
[Bmim]CF ₃ COO	1-Butyl-3-methyl imidazolium trifluoromethane acetate
[Bmim](CF ₃ SO ₂) ₂ N	1-Butyl-3-methylimidazolium bistriflate imide
[Bmim]CF ₃ SO ₃	1-Butyl-3-methylimidazolium trifluoromethane sulfonate
[Bmim]saccharine	1-Butyl-3-methylimidazolium saccharine
[Bmim]SCN	1-Butyl-3-methylimidazolium thiocyanate
[Bmim]HPO ₄	1-Butyl-3-methylimidazolium hydrogen phosphate
[Bmim]HSO ₄	1-Butyl-3-methyl imidazolium hydrogen sulfate
[Bmim]PF ₆	1-Butyl-3-methyl imidazolium hexafluorophosphate
[Bmim]TolSO ₃	1-Butyl-3-methylimidazolium p-toluenesulfonate

[Bmpy] ⁺	1-Butyl-1-methylpyridinium cation
[Bmpy]Cl	1-Butyl-3-methylpyridinium tetrafluoroborate
[Bpy]AlCl ₄	1-Butylpyridinium tetrachloroaluminate
[Bpy]BF ₄	1-Butylpyridinium tetrafluoroborate
[Cho] ⁺	Choline cation
[Cho]Cl	Choline chloride
[Cho]HSO ₄	Choline hydrogen sulfate
[Dmim] ⁺	1-Decyl-3-methylimidazolium cation
[Dmim]Cl	1-Decyl-3-methylimidazolium cation
[EH ₃ N] ⁺	1-Ethylammonium cation
[EH ₃ N]NO ₃	1-Ethylammonium nitrate
[Emim] ⁺	1-Ethyl-3-methylimidazolium cation
[Emim]AlCl ₄	1-Ethyl-3-methylimidazolium tetrachloroaluminate
[Emim]BF ₄	1-Ethyl-3-methylimidazolium tetrafluoroborate
[Emim]Br	1-Ethyl-3-methylimidazolium bromide
[Emim]Cl	1-Ethyl-3-methylimidazolium chloride
[Emim]HSO ₄	1-Ethyl-3-methylimidazolium hydrogen sulfate
[Emim]CF ₃ SO ₃	1-Ethyl-3-methylimidazolium trifluoromethane sulfonate
[E ₄ N]Cl	Tetraethylammonium chloride
[E ₃ Nmeo] _n Cl	Poly(triethyl-ammonium methylene ethylene oxide)
[Epy] ⁺	1-Ethylpyridinium cation
[Epy]Cl	1-Ethylpyridinium chloride
[Hmim] ⁺	1-H-3-Methylimidazolium cation
[Hmim]CH ₃ SO ₃	1-H-Methylimidazolium methyl sulfonate
[Hmim]Cl	1-H-3-Methylimidazolium chloride
[Hmim]HSO ₄	1-H-3-Methyl imidazolium hydrogen sulfonate
[Hpy] ⁺	1-H-Pyridinium cation
[Hpy]Cl	1-H-Pyridinium chloride
[Hpy]ToISO ₃	1-H-Pyridinium p-toluene sulfonate
[Hxmim] ⁺	1-Hexyl-3-methylimidazolium cation
[Hxmim]Cl	1-Hexyl-3-methylimidazolium chloride
[Hxpy] ⁺	1-Hexylpyridium cation

[Mim]Cl	1,3-Dimethylimidazolium chloride
[M ₃ BeN]Cl	Trimethylbenzylammonium chloride hydrated
[M ₃ HN]Cl	Trimethylammonium chloride hydrated
[M ₂ N]Cl	Dimethylammonium chloride hydrated
[M ₄ N]Cl	Tetramethylammonium chloride hydrated
[M ₃ PhN]Cl	Trimethylphenylammonium chloride hydrated
[Morph] ⁺	Morpholinium cation
[Morph]HSO ₄	Morpholinium hydrogen sulfonate
[Mscbi] ⁺	3-Methyl-1-(4-chlorosulfonylbutyl)imidazolium cation
[NMM] ⁺	N-Methylmorpholinium cation
[NMM]CH ₃ SO ₃	N-Methylmorpholinium methyl sulfonate
[NMM]HSO ₄	N-Methylmorpholinium hydrogen sulfonate
[NMP]	N-Methylpyrrolidinium
[NMP]CH ₃ SO ₃	N-Methylpyrrolidinium methyl sulfonate
[NMP]HSO ₄	N-Methylpyrrolidinium hydrogen sulfonate
[Omim] ⁺	1-Octyl-3-methylimidazolium cation
[Omim]Cl	1-Octyl-3-methylimidazolium chloride
[Pcohpy]Cl	3-Chloro-2-hydroxypropyl pyridinium chloride
[Pcmopy]Cl	3-Chloro-2-methoxypropyl pyridinium chloride
[Sbmim] ⁺	1-(4-Sulfonic acid) butyl-3-methylimidazolium cation
[Sbmim]Cl	1-(4-Sulfonic acid) butyl-3-methylimidazolium chloride
[Sbmim]HSO ₄	1-(4-Sulfonic acid) butyl-3-methylimidazolium hydrogen sulfate
[Spmim] ⁺	1-(4-Sulfonic acid) propyl-3-methylimidazolium cation
[Spmim]Cl	1-(4-Sulfonic acid) propyl-3-methylimidazolium chloride
TES[Pmim]Cl	1-Triethoxysilyl-propyl-3-methyl-imidazolium chloride
[TMG] ⁺	Tetramethylguanidinium cation
[TMG]CF ₃ CO ₂	Tetramethylguanidium trifluoromethane acetate
[TMG]Lac	Tetramethylguanidium lactate

General Index

Published SCI papers	i
General list of abbreviations	iii
List of abbreviations of ionic liquids.....	xiii

CHAPTER 1

Conversion of carbohydrate biomass to furanic aldehydes.....	1
1.1. Renewable sources for energy and chemicals	3
1.2. Biomass as a renewable source	5
1.3. Furanic aldehydes as platform chemicals	14
1.3.1. 2-Furaldehyde.....	16
1.3.1.1. Industrial production.....	16
1.3.1.2. Applications	23
1.3.2. 5-Hydroxymethyl-2-furaldehyde and applications.....	26
1.4. Catalytic conversion of saccharides into furanic aldehydes	30
1.4.1. Reaction mechanism of the conversion of saccharides to furanic aldehydes.....	30
1.4.2. Type of acid catalysts.....	37
1.4.3. Conversion of saccharides to furanic aldehydes in the presence of heterogeneous catalysts	46
1.5. Conversion of saccharides into furanic aldehydes using ionic liquid (IL) based catalytic systems.....	71
1.5.1. ILs as solvents (an acid catalyst is added).....	75
1.5.1.1. ILs coupled with homogeneous liquid acid catalysts	78
1.5.1.2. ILs coupled with homogeneous/heterogeneous solid acid catalysts.....	83
1.5.2. ILs as acid solvents/catalysts (dual function).....	99
1.5.3. Recycling of IL-based catalytic systems	103
1.6. References.....	111

CHAPTER 2

Experimental	135
2.1. Preparation of the catalysts	137
2.1.1. Silicoaluminophosphates (SAPOs)	137
2.1.2. Mesoporous aluminosilicate (Al-TUD-1).....	139
2.1.3. Zeolite BEA and BEATUD-1 composite.....	140
2.1.4. Zeolite MCM-22 and the related delaminated material ITQ-2.....	142
2.1.5. ZrW(X)	144
2.1.6. Chromium-incorporated nanoporous materials.....	146
Al-TUD-1, Cr-Al-TUD-1 and Cr-TUD-1.....	146
BEA, BEATUD-1, Cr-BEA and Cr-BEATUD-1	147
2.2. Characterisation of the catalysts.....	148
2.3. Catalytic tests	151
2.3.1. Aqueous–phase reaction systems	152
2.3.2. Ionic liquid-based catalytic systems.....	154
2.3.3. Recovery of the solid acid catalysts	156
2.4. Quantification of reaction products.....	157
2.5. Identification of the reaction products	159
2.6. References.....	160

CHAPTER 3

Reaction of D-xylose in the presence of crystalline microporous silicoaluminophosphates (SAPOs).....	163
3.1. Introduction	165
3.1.1. SAPO-5	167
3.1.2. SAPO-11	168
3.1.3. SAPO-40	169
3.2. Results and discussion.....	170
3.2.1. Catalyst characterisation	170
3.2.2. Catalytic dehydration of D-xylose.....	175
3.2.2.1. Catalytic performance of SAPOs.....	175
3.2.2.2. Catalyst stability	181

3.3. Conclusions	184
3.4. References.....	184

CHAPTER 4

Conversion of saccharides in the presence of Three-Dimensional Mesoporous Al-TUD-1	193
4.1. Introduction	195
4.2. Results and discussion.....	197
4.2.1. Catalyst characterisation	197
4.2.2. Hydrolysis/dehydration of carbohydrates to Fur/Hmf	203
4.2.3. Catalytic reactions of pentose-based carbohydrates to Fur.....	204
4.2.4. Catalytic reactions of the hexose-based carbohydrates to Hmf	205
4.2.5. Catalyst stability.....	212
4.3. Conclusions	213
4.4. References.....	214

CHAPTER 5

Reaction of D-xylose in the presence of zeolite Beta (BEA) and a micro/mesoporous (BEATUD-1) composite material	219
5.1. Introduction	221
5.1.1. Zeolite Beta (BEA)	223
5.1.2. Microporous/mesoporous BEATUD-1	224
5.2. Results and discussion.....	225
5.2.1. Catalysts characterisation.....	225
5.2.2. Catalytic dehydration of D-xylose	237
5.2.2.1. Catalytic performance of zeolite BEA and composite BEATUD-1.....	237
5.2.2.2. Identification of the reaction products	242
5.2.2.3. Catalytic stability	249
5.3. Conclusions	251
5.4. References.....	252

CHAPTER 6

Reaction of D-xylose in the presence of zeolite MCM-22 and delaminated ITQ-2.....	265
6.1. Introduction	267
6.1.1. Zeolite MCM-22	268
6.1.2. Delaminated ITQ-2.....	270
6.2. Results and discussion.....	272
6.2.1. Catalyst characterisation	272
6.2.2. Catalytic dehydration of D-xylose.....	285
6.2.2.1. Catalytic performance of H-MCM-22 and ITQ-2(24) in water-organic biphasic solvent system.....	285
6.2.2.2. Catalytic performance of H-MCM-22 and ITQ-2(24) using solely water as solvent..	290
6.2.2.3. Identification of the reaction products	292
6.2.2.4. Catalyst stability	294
6.3. Conclusions	296
6.4. References.....	297

CHAPTER 7

Reaction of D-xylose in the presence of mixed zirconium tungsten oxides	307
7.1. Introduction	309
7.1.1. Mixed zirconium-tungsten materials, ZrWX (X=Cl, NO ₃) and ZrWAl	310
7.2. Results and discussion.....	312
7.2.1. Catalyst characterisation	312
7.2.2. Catalytic dehydration of D-xylose.....	322
7.2.2.1. Catalytic performance of ZrW(X), ZrW-MP and ZrWAl-MP materials.....	322
7.2.2.2. Identification of the reaction products	324
7.2.2.3. Catalyst stability	331
7.3. Conclusions	334
7.4. References.....	335

CHAPTER 8

Conversion of saccharides into furanic aldehydes using homogeneous ionic liquid-based catalytic systems.....	343
8.1. Introduction	345
8.2. Results and discussion.....	346
8.2.1. [Emim]HSO ₄ characterisation	346
8.2.2. Dehydration of monosaccharides in ionic liquids.....	348
8.2.2.1. Reaction using [Emim]HSO ₄ -based catalytic systems under N ₂ atmosphere.....	348
8.2.2.2. Reaction using [Emim]HSO ₄ -based catalytic systems under reduced pressure.....	351
8.2.2.3. Reaction of hexoses using [Emim]HSO ₄ /co-solvent systems under N ₂ atmosphere	352
8.2.2.4. One-pot hydrolysis/dehydration of di/polysaccharides in ionic liquids.....	354
8.2.2.5. Identification of the reaction products	356
8.2.2.6. IL stability and reuse under N ₂ atmosphere.....	359
8.2.2.7. IL stability and reuse under reduced pressure	361
8.3. Conclusions	361
8.4. References.....	362

CHAPTER 9

Conversion of D-glucose in the presence of micro/mesoporous (chromium, aluminium)-containing silicates using an ionic liquid solvent	365
9.1. Introduction	367
9.1.1. Cr-TUD-1 and Cr-Al-TUD-1	368
9.1.2. Cr-BEA and Cr-BEATUD-1	369
9.2. Results and discussion.....	370
9.2.1. Catalyst characterisation	370
9.2.2. Catalytic dehydration of D-glucose.....	377
9.2.2.1. Catalytic performance of Cr-TUD-1, Cr-Al-TUD-1, Cr-BEA and Cr-BEATUD-1 in the presence of [Bmim]Cl, DMSO or water	378
9.2.2.2. Catalyst stability	380
9.3. Conclusions	387
9.4. References.....	388

CHAPTER 10

Conclusions and outlook	399
10.1. Conclusions	401
10.2. References.....	409

List of Figures

CHAPTER 1

Figure 1.1- Raw materials basis of the chemical industry in an historical perspective.	4
Figure 1.2 – Conversion of biomass into energy and other products.....	5
Figure 1.3 - Biomass conversion into fuels, heat and power by a thermochemical process.....	6
Figure 1.4- Biomass conversion to ethanol by a biochemical process.....	7
Figure 1.5 - Biomass deconstruction into primary biorefinery building blocks.	12
Figure 1.6 - Schematic representation of transformation of sugar cane into 2-furaldehyde (Fur) and 5-hydroxymethyl-2-furaldehyde (Hmf).	13
Figure 1.7- Clean fractionation process.	14
Figure 1.8 – Simplified representation of the conversion of carbohydrates to 5-hydroxymethyl-2-furaldehyde (Hmf) and 2-furaldehyde (Fur)	15
Figure 1.9 –The Batch process of Quaker Oats.	17
Figure 1.10- Flow diagram of the sulfite pulping process.....	20
Figure 1.11- 2-Furaldehyde (Fur) platform for biofuels.	25
Figure 1.12- Production of tridecane from 2-furaldehyde (Fur).	26

Figure 1.13- Some added value chemicals from 5-hydroxymethyl-2-furaldehyde (Hmf).	29
Figure 1.14- Reaction routes of 5-hydroxymethyl-2-furaldehyde (Hmf) to kerosene and diesel range intermediates proposed by James.	30
Figure 1.15- Mechanistic proposal for the hydrolysis of cellulose.....	31
Figure 1.16- Reaction mechanism for the dehydration of D-xylose (Xyl) to 2-furaldehyde (Fur) proposed by Antal.	32
Figure 1.17- By-products formed by decomposition reactions of D-xylose (Xyl) in acidic medium or condensation or resinification or 2-furaldehyde (Fur).....	33
Figure 1.18- Isomerisation of D-glucose to D-fructose followed by the acid-catalysed to dehydration to 5-hydroxymethyl-2-furaldehyde (Hmf).....	34
Figure 1.19- Reaction mechanism of the dehydration of D-fructose to 5-hydroxymethyl-2-furaldehyde (Hmf) proposed by Antal.	34
Figure 1.20- Reaction mechanism for the dehydration of D-fructose to 5-hydroxymethyl-2-furaldehyde (Hmf) based on the acyclic route.....	35
Figure 1.21- Reaction mechanism for the dehydration of D-fructose to 5-hydroxymethyl-2-furaldehyde (Hmf) proposal by Caratzoulas.	36
Figure 1.22- 5-Hydroxymethyl-2-furaldehyde (Hmf) reaction products.....	37
Figure 1.23- Conversion of saccharides to 2-furaldehyde (Fur) and 5-hydroxymethyl-2-furaldehyde (Hmf) using an aqueous-organic biphasic solvent system, under batch operation mode.	47

Figure 1.24- Typical pore widths of micro-, meso- and macroporous materials.	48
Figure 1.25- Mineral acids used as catalysts coupled with ILs as solvents in the dehydration of D-fructose to 5-hydroxymethyl-2-furaldehyde (Hmf).	78
Figure 1.26- Putative nucleophilic mechanism for halide participation in the dehydration of D-fructose into 5-hydroxymethyl-2-furaldehyde (Hmf); X ⁻ represents a halide ion.	79
Figure 1.27- Homogeneous organic Brønsted acids coupled with ILs as solvents in the dehydration of D-fructose to 5-hydroxymethyl-2-furaldehyde (Hmf).	81
Figure 1.28- Brønsted liquid acid catalysts coupled with ILs as solvents in the dehydration of D-glucose to 5-hydroxymethyl-2-furaldehyde (Hmf). Reaction conditions: 9 wt.% sac, 1 mol.% cat, T=120 °C, reaction time= 3h.	82
Figure 1.29- Mineral and organic acid catalysts coupled with ILs as solvents in the dehydration of cellulose to 5-hydroxymethyl-2-furaldehyde (Hmf).	82
Figure 1.30- Soluble organic solid acids coupled with ILs in the dehydration of D-fructose or D-glucose into 5-hydroxymethyl-2-furaldehyde (Hmf).	84
Figure 1.31- Lewis acid catalysts coupled with ILs as solvents in the dehydration of D-fructose to 5-hydroxymethyl-2-furaldehyde (Hmf); Ipr=1,3-bis(2,6-diisopropylphenyl)imidazolylidene.	87
Figure 1.32- Lewis acid catalysts coupled with ILs as solvents in the dehydration of D-glucose to 5-hydroxymethyl-2-furaldehyde (Hmf). Ipr=1,3-bis(2,6-diisopropylphenyl)imidazolylidene; HAP=hydroxyapatite.	90
Figure 1.33- Chromium-catalysed isomerisation of D-glucose to D-fructose.	91

Figure 1.34- Soluble solid catalysts coupled with ILs as solvents in the dehydration of disaccharides (e.g. D-maltose, D-cellobiose and D-sucrose) and polysaccharides (e.g. cellulose and inulin) to 5-hydroxymethyl-2-furaldehyde (Hmf).	93
Figure 1.35- Insoluble organic acids resins coupled with ILs as solvents in the dehydration of D-fructose to 5-hydroxymethyl-2-furaldehyde (Hmf).	96
Figure 1.36- ILs as solvents coupled with inorganic solid acids (e.g microporous H-ZSM-5, H-Beta and H-Mordenite, mesoporous SBA-15-SO ₃ H, zirconium and other oxides)in the dehydration of hexoses to 5-hydroxymethyl-2-furaldehyde (Hmf).....	98
Figure 1.37- Acidic ILs used in the dehydration of hexoses (D-fructose unless otherwise indicated) to 5-hydroxymethyl-2-furaldehyde (Hmf).....	100

CHAPTER 2

Figure 2.1- Schematic representation of the aqueous-phase acid hydrolysis and dehydration of saccharides into 2-furaldehyde (Fur) and 5-hydroxymethyl-2-furaldehyde (Hmf), using a biphasic solvent system (A) or solely water as solvent (B).	153
Figure 2.2- Schematic representation of the acid hydrolysis and dehydration of saccharides into 2-furaldehyde (Fur) and 5-hydroxymethyl-2-furaldehyde (Hmf) using an IL-based catalytic system under biphasic solvent conditions (A) or using an acid-functionalised IL without adding a solid acid catalyst (B) or using an IL as solvent coupled with a solid acid catalyst (C).....	155
Figure 2.3- Experimental setup used for the D-xylose/[Emim]HSO ₄ reaction system under reduced pressure (Chapter 8).	156
Figure 2.4- Centrifuge (A) used to separate the solid from the liquid phases; Oven used to dry the powdered catalysts recovered (B) and muffle furnace used for calcination (C).	157

CHAPTER 3

Figure 3.1- SM1, SM2 and SM3 mechanism in the transformation of AlPOs to SAPOS.....	166
Figure 3.2- AFI framework type viewed along [001].....	168
Figure 3.3- AEL framework type viewed along [001].....	168
Figure 3.4- AFR framework type viewed along [001].....	169
Figure 3.5- Powder XRD patterns of the fresh and used SAPO materials.....	171
Figure 3.6- N ₂ adsorption-desorption isotherms measured at -196 °C and pore size distribution curves for SAPO-5 (orange), SAPO-11a (green), SAPO-11b (red) and SAPO-40 (blue).....	172
Figure 3.7- SEM images of the SAPO materials.....	173
Figure 3.8- Simplified representation of the dehydration of D-xylose (Xyl) to 2-furaldehyde (Fur).....	176
Figure 3.9- Kinetic profile of the D-xylose (Xyl) reaction in the presence of SAPO-5 (–), SAPO-11a (▲), SAPO-11b (●) and SAPO-40 (◆). Reaction conditions: 0.3 Wt:0.7 Tol (v/v) biphasic solvent system, 170 °C, 600 r.p.m, 20 g _{cat} .dm ⁻³ , 0.67 M Xyl.	177
Figure 3.10- Kinetic profile of the dependence of the selectivity of 2-furaldehyde (S _{Fur}) on conversion of D-xylose (C _{Xyl}), in the presence of SAPO-5 (–), SAPO-11a (▲), SAPO-11b (●) and SAPO-40 (◆). Reaction conditions: 0.3 Wt:0.7 Tol (v/v) biphasic solvent system, 170 °C, 600 r.p.m, 20 g _{cat} .dm ⁻³ , 0.67 M Xyl.	178
Figure 3.11- SEM images of SAPO-11a fresh and after catalysis.....	179

Figure 3.12- DSC curves for the two SAPO-11 samples, fresh and after 4 h of reaction: SAPO-11a fresh (pink); SAPO-11a recovered (red); SAPO-11b fresh (green); SAPO-11b recovered (blue). Reaction conditions: 0.3 Wt:0.7 Tol biphasic solvent system, 170 °C, 20 g_{cat}.dm⁻³, 0.67 M Xyl.182

Figure 3.13- Yields of 2-furaldehyde (Y_{Fur}) in recycling runs in the presence of the SAPOs samples (4 h, 170 °C): Run 1-black bar, run 2-orange bar, run 3-green bar. Reaction conditions used: 0.3 Wt:0.7 Tol (v/v) biphasic solvent system, 170 °C, 20 g_{cat}.dm⁻³, 0.67 M Xyl.....183

Figure 3.14- Conversions of D-xylose (C_{Xyl}) in recycling runs in the presence of the SAPOs samples (4 h, 170 °C): Run 1-black bar, run 2-orange bar, run 3- green bar. Reaction conditions: 0.3 Wt:0.7 Tol (v/v) biphasic solvent system, 170 °C, 20 g_{cat}.dm⁻³, 0.67 M Xyl.....183

CHAPTER 4

Figure 4.1- Representative structure of MCM-41.....195

Figure 4.2 - Representative structure of MCM-48.....196

Figure 4.3- Powder XRD pattern for Al-TUD-1.....198

Figure 4.4- Representative SEM image of Al-TUD-1.....198

Figure 4.5- Representative TEM image of A) TUD-1 and B) Al-TUD-1.....199

Figure 4.6- N₂ adsorption-desorption isotherm measured at -196 °C of Al-TUD-1. Red line is the desorption branch; green line is the adsorption branch.....200

Figure 4.7- ²⁷Al MAS NMR spectrum of Al-TUD-1.....201

Figure 4.8- Simplified representation of the acid hydrolysis and dehydration of saccharides to 2-furaldehyde (Fur) and 5-hydroxymethyl-2-furaldehyde (Hmf).....203

Figure 4.9- Dehydration of D-xylose in the presence of Al-TUD-1: (●) conversion of D-xylose (C_{Xyl}); (X) yield of 2-furaldehyde (Y_{Fur}). Reaction conditions: 0.3 Wt:0.7 Tol (v/v) biphasic solvent system, 170 °C, 20 $g_{cat}\cdot dm^{-3}$, 0.67 M Xyl.....204

Figure 4.10- Dehydration of D-xylan in the presence of Al-TUD-1: (●) yield of D-xylose (Y_{Xyl}); (X) yield of 2-furaldehyde (Y_{Fur}). Reaction conditions: 0.3 Wt:0.7 Tol (v/v) biphasic solvent system, 170 °C, 20 $g_{cat}\cdot dm^{-3}$, 33.3 $g\cdot dm^{-3}$ D-xylan.....205

Figure 4.11 -Dehydration of D-fructose in the presence of Al-TUD-1: (●) conversion of D-fructose (C_{Fru}), (▲) yield of glucose (Y_{Glu}), (◇) yield of 5-hydroxymethyl-2-furaldehyde (Y_{Hmf}), (-) yield of D-mannose (Y_{Man}) and (X) yield of 2-furaldehyde (Y_{Fur}) are also shown. Reaction conditions: 0.3 Wt:0.7 Tol (v/v) biphasic solvent system, 170 °C, 20 $g_{cat}\cdot dm^{-3}$, 0.67 M Fru.....206

Figure 4.12 - Dehydration of D-glucose in the presence of Al-TUD-1: (▲) conversion of D-glucose (C_{Glu}), (●) yield of D-fructose (Y_{Fru}), (◇) yield of 5-hydroxymethyl-2-furaldehyde (Y_{Hmf}), (-) yield of D-mannose (Y_{Man}), and (X) yield of 2-furaldehyde (Y_{Fur}) are also shown. Reaction conditions used: 0.3 Wt:0.7 Tol (v/v) biphasic solvent system, 170 °C, 20 $g_{cat}\cdot dm^{-3}$, 0.67 M Glu.....206

Figure 4.13- Hydrolysis and dehydration of D-sucrose in the presence of Al-TUD-1: (*) conversion of sucrose (C_{Suc}): (●) yield of D-fructose (Y_{Fru}), (▲) yield of D-glucose (Y_{Glu}), (◇) yield of 5-hydroxymethyl-2-furaldehyde (Y_{Hmf}), (-) yield of D-mannose (Y_{Man}), (X) yield of 2-furaldehyde (Y_{Fur}). Reaction conditions: 0.3 Wt:0.7 Tol (v/v) biphasic solvent system, 170 °C, 20 $g_{cat}\cdot dm^{-3}$, 0.29 M Suc.....208

Figure 4.14- Hydrolysis and dehydration of D-cellobiose in the presence of Al-TUD-1: (*) conversion of D-cellobiose (C_{Cel}), (●) yield of 2-furaldehyde (Y_{Fur}), (▲) yield of D-glucose (Y_{Glu}), (◇) yield of 5-hydroxymethyl-2-furaldehyde (Y_{Hmf}), (-) yield of D-mannose (Y_{Man}), (X) yield of 2-furaldehyde (Y_{Fur}). Reaction conditions: 0.3 Wt:0.7 Tol (v/v) biphasic solvent system, 170 °C, 20 $g_{cat}\cdot dm^{-3}$, 0.29 M Cel.209

Figure 4.15- Hydrolysis and dehydration of inulin in the presence of Al-TUD-1: (●) yield of D-fructose (Y_{Fru}), (▲) yield of D-glucose (Y_{Glu}), (-) yield of D-mannose (Y_{Man}), and (◇) yield of 5-

hydroxymethyl-2-furaldehyde (Y_{Hmf}). Reaction conditions: 0.3 Wt:0.7 Tol (v/v)biphasic solvent system, 170 °C, 20 $g_{cat}\cdot dm^{-3}$, 33.3 $g\cdot dm^{-3}$ inulin.210

Figure 4.16- Reaction mechanism proposed by Aida et al. for the conversion of D-glucose (Glu) to 2-furaldehyde (Fur); tau= tautomerisation, RA=retro aldol.....212

Figure 4.17- Catalytic performance of Al-TUD-1 in four consecutive 6 h batch runs at 170 °C. Reaction conditions: Wt:Tol (0.3:0.7 v/v)biphasic solvent system, 20 $g_{cat}\cdot dm^{-3}$, and 0.67 M Xyl. ...213

CHAPTER 5

Figure 5.1- Structure of an amorphous and crystalline aluminosilicate.222

Figure 5.2- Structure of zeolite BEA viewed along [100] (A and B) and along [001] (C).222

Figure 5.3- Framework structures of A) polymorph A, B) polymorph B and C) polymorph C of zeolite Beta, showing the different stackings of the 12-MR pores as A) ABAB (shears with alternating translations), B) ABCABC (shears in the same direction) and C) AA.....224

Figure 5.4- Powder XRD patterns of the fresh and recovered catalysts.226

Figure 5.5- TEM images of BEA (a and b) and BEATUD-1 (c and d). The amorphous carbon support film used for BEA (b) appears as the mottled background in the upper and lower right-hand parts of the micrograph; a holey carbon film was used for BEATUD-1 to clearly distinguish the mesoporous silica matrix of the composite from the background of the support.....227

Figure 5.6- N_2 adsorption-desorption isotherms measured at -196 °C and pore size distribution curves for BEA (Δ), BEATUD-1 (O) and TUD-1 (-).....231

Figure 5.7- ^{27}Al MAS NMR spectra of BEA (green) and BEATUD-1 (blue).233

Figure 5.8- FT-IR spectra of BEA and BEATUD-1 after pyridine adsorption and outgassing at 150 °C.....234

Figure 5.9- FT-IR spectra of BEA and BEATUD-1 after pyridine adsorption and outgassing at 150 °C.....235

Figure 5.10- Effect of the outgassing temperature on BEA and BEATUD-1 after pyridine adsorption.....236

Figure 5.11- Schematic representation of the reaction of D-xylose (Xyl) to 2-furaldehyde (Fur) under aqueous-organic biphasic solvent conditions. The dots represent the powdered solid acid catalyst.....238

Figure 5.12- D-xylose conversion (C_{Xyl}) in the presence of BEA1.0 (Δ), BEA0.4 (\blacktriangle), physical mixture BEA0.4/TUD0.6 (\times), or BEATUD-1 (O) for 0.3 Wt:0.7 Tol (v/v) biphasic solvent system ; BEATUD-1 (\bullet) or BEA (-) for solely Wt (0.3 cm³), 170 °C, 0.67 M Xyl . Amount of catalyst in the reaction medium: 20 g_{cat}.dm⁻³ for BEA1.0 and BEATUD-1; 8 g_{BEA}.dm⁻³ for BEA0.4 and 8 g_{BEA}.dm⁻³ + 12 g_{TUD-1}.dm⁻³ for BEA0.4/TUD0.6.....240

Figure 5.13- Dependence of the yield of 2-furaldehyde (Y_{Fur}) on time for the reaction of D-xylose in the presence of BEA1.0 (Δ), BEA0.4 (\blacktriangle), physical mixture BEA0.4/TUD0.6 (\times), or BEATUD-1 (O) for 0.3 Wt:0.7 Tol (v/v) biphasic solvent system; BEATUD-1 (\bullet) or BEA (-) for solely Wt (0.3 cm³), 170 °C, 0.67 M Xyl. Amount of catalyst in the reaction medium: 20 g_{cat}.dm⁻³ for BEA1.0 and BEATUD-1; 8 g_{BEA}.dm⁻³ for BEA0.4 and 8 g_{BEA}.dm⁻³ + 12 g_{TUD-1}.dm⁻³ for BEA0.4/TUD0.6.....240

Figure 5.14- Yield of 2-furaldehyde (Y_{Fur}) versus the conversion of D-xylose (C_{Xyl}) for the reaction of D-xylose in the presence of BEA1.0 (Δ), BEA0.4 (\blacktriangle), physical mixture BEA0.4/TUD0.6 (\times), or BEATUD-1 (O) for 0.3 Wt:0.7 Tol (v/v) biphasic solvent system; BEATUD-1 (\bullet) or BEA (-) for solely Wt (0.3 cm³) 170 °C, 0.67 M Xyl. Amount of catalyst in the reaction medium: 20 g_{cat}.dm⁻³ for BEA1.0 and BEATUD-1; 8 g_{BEA}.dm⁻³ for BEA0.4 and 8 g_{BEA}.dm⁻³ + 12 g_{TUD-1}.dm⁻³ for BEA0.4/TUD0.6.....241

Figure 5.15- ^1H NMR spectra of the solution obtained after separation of the solid phase from the reaction mixture of D-xylose (Xyl) in the presence of BEA using D_2O as solvent (C). The spectra of 2-furaldehyde, Fur (A) and D-xylose, Xyl (B) are given for comparison. Reaction conditions: D_2O (1 cm^3), 8 h, $170\text{ }^\circ\text{C}$, $20\text{ g}_{\text{BEA}}\cdot\text{dm}^{-3}$, 0.67 M Xyl243

Figure 5.16- ^{13}C NMR spectrum of the reaction solution obtained after the reaction of D-xylose (Xyl) in the presence of BEA using D_2O as solvent (C). The spectra of D-xylose, Xyl (A) and 2-furaldehyde, Fur (B) are given for comparison. Reaction conditions: D_2O (1 cm^3), 8 h, $170\text{ }^\circ\text{C}$, $20\text{ g}_{\text{BEA}}\cdot\text{dm}^{-3}$, 0.67 M Xyl244

Figure 5.17- ^{13}C NMR spectrum of 2-furaldehyde (Fur) in DMSO-d_6 (A); ^{13}C NMR spectrum of the solution obtained after washing the used BEA with DMSO-d_6 (B); ^{13}C CP MAS NMR spectrum of BEA after catalysis using D_2O as solvent (C). Reaction conditions: D_2O (1 cm^3), 8 h, $170\text{ }^\circ\text{C}$, $20\text{ g}_{\text{BEA}}\cdot\text{dm}^{-3}$, 0.67 M Xyl246

Figure 5.18- ^1H NMR spectrum of the solution obtained after washing the used BEA with DMSO-d_6 . Reaction conditions: D_2O (1 cm^3), 8 h, $170\text{ }^\circ\text{C}$, $20\text{ g}_{\text{BEA}}\cdot\text{dm}^{-3}$, 0.67 M Xyl247

Figure 5.19- FT-IR spectra of BEA before and after reaction of D-xylose (Xyl) using D_2O as solvent. Reaction conditions: D_2O (1 cm^3), 8 h, $170\text{ }^\circ\text{C}$, $20\text{ g}_{\text{BEA}}\cdot\text{dm}^{-3}$, 0.67 M Xyl . The spectra of D-xylose (Xyl) and 2-furaldehyde (Fur) are given for comparison.248

Figure 5.20- DSC curves for fresh BEA and BEATUD-1 and after 98% of D-xylose conversion (C_{Xyl}). Reaction conditions: 0.3 Wt:0.7 Tol (v/v) biphasic solvent system, $170\text{ }^\circ\text{C}$, $20\text{ g}_{\text{BEA}}\cdot\text{dm}^{-3}$, 0.67 M Xyl249

Figure 5.21- Catalytic performance of BEA and BEATUD-1 in four consecutive 6 h batch runs. Reaction conditions: 0.3 Wt:0.7 Tol (v/v) biphasic solvent system, 8 h, $170\text{ }^\circ\text{C}$, $20\text{ g}_{\text{BEA}}\cdot\text{dm}^{-3}$, 0.67 M Xyl250

CHAPTER 6

Figure 6.1- Structures of a MWW-type framework projected along [001] (A), and projected along [100] (B).....	269
Figure 6.2- Structure of a MWW-type framework viewed normal to [001].	269
Figure 6.3- Schematic representation of MWW-type zeolite and ITQ-2 from Pre-MCM-22; HMI-hexamethylenamine, CTMAOH-cetyltrimethylammonium hydroxyde.	270
Figure 6.4- Schematic structure of ITQ-2.	271
Figure 6.5- Powder XRD patterns of as-prepared and (for H-MCM-22(24) and ITQ-2(24)) used/calcined (after catalysis) catalysts.....	273
Figure 6.6- SEM images of a) Na-MCM-22(24) and b) ITQ-2(24).	274
Figure 6.7- SEM images of a) HMCM-22(24) and b) HMCM-22(38).....	274
Figure 6.8- TEM images of a) Na-MCM-22(24) and an b) ITQ-2(24) layer, viewed along the 10-MR channels, perpendicular to the z-direction.	275
Figure 6.9- N ₂ adsorption-desorption isotherms measured for Na-MCM-22(24) and ITQ-2(24), at -196 °C.	276
Figure 6.10- N ₂ adsorption-desorption isotherms measured for H-MCM-22(24), Na-MCM-22(38) and H-MCM-22(38), at -196 °C.....	276
Figure 6.11- ²⁷ Al MAS NMR spectra of the as-prepared catalysts: (Na,H)-MCM-22 and ITQ-2(24).	280

Figure 6.12- Schematic representation of non-equivalent tetrahedral positions in one layer of MCM-22 . The T1 and T3-T8 sites may be occupied by Al and Si, while T2 sites contain only Si. ...280

Figure 6.13- FT-IR spectra, in the framework region of H-MCM-22(24) and ITQ-2(24).....281

Figure 6.14- FT-IR spectra of ITQ-2(24), H-MCM-22(24) and H-MCM-22(38) after pyridine adsorption and outgassing at 150 °C.282

Figure 6.15- FT-IR spectra of ITQ-2(24), H-MCM-22(24) and H-MCM-22(38) after pyridine adsorption and outgassing at 150 °C.283

Figure 6.16- Kinetic profiles of the reaction of D-xylose (Xyl) in the presence of Na-MCM-22(24) (▲), H-MCM-22(24) (x), H-MCM-22(38) (+) or ITQ-2(24) (●). Reaction conditions: 0.3 Wt:0.7 Tol(v/v) biphasic solvent system, 170 °C, 20 g_{cat}.dm⁻³, 0.67 M Xyl.286

Figure 6.17- Dependence of the yield of 2-furaldehyd (Y_{Fur}) on the conversion of D-xylose (C_{Xyl}) curves for Na-MCM-22(24) (▲), H-MCM-22(24) (x), H-MCM-22(38) (+) or ITQ-2(24) (●). Reaction conditions: 0.3 Wt:0.7 Tol (v/v) biphasic solvent system, 170 °C, 20 g_{cat}.dm⁻³, 0.67 M Xyl.....286

Figure 6.18- Kinetic profiles of the reaction of the conversion of D-xylose (C_{Xyl}) for H-MCM-22(24)(x), ITQ-2(24) (●) and H₂SO₄ (▲), used as catalysts. Reaction conditions: 1 cm³ Wt or 4 mM H₂SO₄, 170 °C, 20 g_{cat}.dm⁻³, 0.67 M Xyl.....291

Figure 6.19- Dependence of the yield of 2-furaldehyde (Y_{Fur}) on the conversion of D-xylose (C_{Xyl}) for H-MCM-22(24) (x), ITQ-2(24) (●) and H₂SO₄ (▲), used as catalysts. Reaction conditions: 1 cm³ Wt or 4 mM H₂SO₄, 170 °C, 20 g_{cat}.dm⁻³, 0.67 M Xyl. The kinetic profile for H₂SO₄ was measured until 72 h of reaction.....291

Figure 6.20-¹H NMR spectrum of the solution obtained after separation the solid phase from the reaction mixture of D-xylose(Xyl) in the presence of ITQ-2(24) using D₂O as solvent. The spectra of

2-furaldehyde and D-xylose (Xyl) are given for comparison. Reaction conditions: D₂O (1 cm³), 24 h, 170 °C, 20 g_{BEA}.dm⁻³, 0.67 M Xyl.293

Figure 6.21-¹³C NMR spectrum of the reaction solution obtained after the reaction of D-xylose (Xyl) in the presence of ITQ-2(24) using D₂O as solvent. The spectra of 2-furaldehyde (Fur) and D-xylose (Xyl) are given for comparison. Reaction conditions: D₂O (1 cm³), 8 h, 170 °C, 20 g_{BEA}.dm⁻³, 0.67 M Xyl.....293

Figure 6.22- Possible pathways for the formation of by-products in the D-xylose (Xyl) to 2-furaldehyde (Fur) reaction systems.294

Figure 6.23- DSC curves for the as-prepared H-MCM-22(24) (green line) and ITQ-2(24) (red line) catalysts, and the respective solids recovered from the reaction of D-xylose (Xyl) after ca. 98% of conversion was reached (used catalysts). Reaction conditions: 0.3 Wt:0.7 Tol (v/v) biphasic solvent system, 170 °C, 20 g_{cat}.dm⁻³, 0.67 M Xyl.....295

Figure 6.24- Yield of 2-furaldehyde (Y_{Fur}) in four consecutive 6 h batch runs of the reaction of D-xylose (Xyl) in the presence of regenerated catalysts H-MCM-22(24) or ITQ-2(24). Reaction conditions: 0.3 Wt:0.7 Tol (v/v) biphasic solvent system, 170 °C, 20 g_{cat}.dm⁻³, 0.67 M Xyl.....296

CHAPTER 7

Figure 7.1- Formation of Brönsted acid site mechanism.311

Figure 7.2- XRD patterns of the unused and recycled catalysts. For ZrW(Cl) and ZrW(NO₃) the main peaks of the ZrO₂ crystalline phases are marked as (■) m-ZrO₂ and (●) t-ZrO₂.....315

Figure 7.3- SEM images (top) and chemical mapping (Zr-red; W-dark blue; Al-light blue) for: a) ZrW(Cl), b) ZrW-MP, c) ZrWAl-MP.316

Figure 7.4- Nitrogen adsorption-desorption isotherms measured at -196 °C for ZrWCl (■), ZrW-MP (unused (▲); recycled (X)) and ZrWAl-MP (●). The inset shows the respective pore size distribution curves using the same symbols.	317
Figure 7.5- Raman spectra of unused and recycled catalysts.	319
Figure 7.6- FT-IR spectra of ZrWAl-MP, ZrW-MP, ZrW(NO ₃) and ZrW(Cl) after pyridine adsorption and outgassing at 150 °C.	320
Figure 7.7- Effect of the outgassing temperature on ZrWAl-MP after pyridine adsorption.	321
Figure 7.8- Yield of 2-furaldehyde (Y _{Fur}) versus reaction time for the catalysts ZrW(Cl) (■), ZrW(NO ₃) (▲), ZrW-MP (●), and ZrWAl-MP ((+)) for 0.3 Wt:0.7 Tol (v/v) biphasic solvent system and (X) for solely Wt (1 cm ³). Reaction conditions: 170 °C, 20 g _{cat} ·dm ⁻³ , 0.67 M Xyl.	322
Figure 7.9- Yield of 2-furaldehyde (Y _{Fur}) versus conversion of D-xylose (C _{Xyl}) for the catalysts ZrW(Cl) (■), ZrW(NO ₃) (▲), ZrW-MP (●), and ZrWAl-MP ((+)) for 0.3 Wt:0.7 Tol (v/v) biphasic solvent system and (X) for solely Wt (1 cm ³). Reaction conditions: 170 °C, 20 g _{cat} ·dm ⁻³ , 0.67 M Xyl.	323
Figure 7.10- Products formed in the reaction of D-xylose (Xyl) in the presence of ZrWAl-MP, using solely water (1 cm ³) as solvent, at 170 °C, identified by GCxGC-ToFMS.	325
Figure 7.11- TIC GCxGC-ToFMS representation (1 D and 3 D) of the reaction mixture with D-xylose (Xyl) as the substrate. Reaction conditions: solely Wt (1 cm ³), 170 °C, 20 g _{cat} ·dm ⁻³ , 0.67 M Xyl, 4 h.	325
Figure 7.12- TIC GCxGC-ToFMS representation (1 D and 3 D) of the reaction mixture for 2-furaldehyde (Fur) as substrate, in the presence of ZrWAl-MP using solely Wt as solvent. Reaction conditions: Solely Wt (1 cm ³), 170 °C, 0.67 M Fur, 6 h.	329

Figure 7.13- TGA (represented as (mass of InsolOrg)/(initial mass of D-Xylose) and DSC curves for the ZrWAl-MP catalyst separated (washed/dried) from the reaction mixture after reaching at least 98% of D-xylose conversion (C_{Xyl}), using the 0.3 Wt:0.7 Tol (v/v) biphasic solvent system (red lines) or solely Wt (1 cm^3)(green lines). Reaction conditions: $170\text{ }^\circ\text{C}$, $20\text{ g}_{\text{cat}}\cdot\text{dm}^{-3}$, 0.67 M Xyl332

Figure 7.14- Yield of 2-furaldehyde (Y_{Fur}) in recycling runs of the reaction of D-xylose (Xyl) in the presence of ZrWAl-MP or ZrW-MP. Reaction conditions: 0.3 Wt:0.7 Tol (v/v) biphasic solvent system, $170\text{ }^\circ\text{C}$, $20\text{ g}_{\text{cat}}\cdot\text{dm}^{-3}$, 0.67 M Xyl , 4 h.333

CHAPTER 8

Figure 8.1- Molecular structures of [Emim]HSO₄ and [Bmim]Cl.....346

Figure 8.2- ¹H NMR spectra of fresh and recovered (from a catalytic test) [Emim]HSO₄.347

Figure 8.3- ¹³C NMR spectra of fresh and recovered (from a catalytic test) [Emim]HSO₄.347

Figure 8.4- Conversion of D-Xylose (C_{Xyl}) (○) and yield of 2-furaldehyde (Y_{Fur}) (+) versus time for the reaction carried out in [Emim]HSO₄/Tol . Reaction conditions: 0.3 Wt:0.7 Tol (v/v)biphasic solvent system, $100\text{ }^\circ\text{C}$, 0.67 M Xyl348

Figure 8.5- FT-IR spectra of [Emim]HSO₄ as acquired (blue line), [Emim]HSO₄ after the control experiment (vacuum drying, pink line) and the distillate obtained in that experiment (red line). 351

Figure 8.6- Yields of 2-furaldehyde, Y_{Fur} (from Xyl/D-xylan) or 5-hydroxymethyl-2-furaldehyde, Y_{Hmf} (from the remaining substrates) obtained in IL co-solvent biphasic system at $100\text{ }^\circ\text{C}$ (initial concentration of feedstock of $100\text{ g}\cdot\text{dm}^{-3}$ or $120\text{ g}\cdot\text{dm}^{-3}$ for pentose or hexose-based carbohydrates, respectively, in the IL). In general, theoretical yields vary between 70 and 80 wt.%.355

Figure 8.7- ¹³ C CP MAS NMR spectrum of the recovered solid after a catalytic batch run using D-xylose (Xyl)/[Emim]HSO ₄ at 100 °C/4 h.	357
Figure 8.8- FT-IR spectra of [Emim]HSO ₄ as acquired (blue line), and dark solid phase obtained from the reaction of D-xylose (Xyl) using [Emim]HSO ₄ at 100 °C/4 h.	358
Figure 8.9- Conversion of D-xylose (C _{xyl}) to 2-furaldehyde (Fur) in [Emim]HSO ₄ /Tol for four consecutive 4 h runs at 100 °C, using the same IL charged initially to the reaction vessel. Reaction conditions: 0.3 Wt:0.7 Tol (v/v) biphasic solvent system, 100 °C, 0.67 M Xyl.	359
Figure 8.10- FT-IR spectra of pure [Emim]HSO ₄ (IL) and IL recovered from the reaction of D-xylose (Xyl) carried out in [Emim]HSO ₄ /Tol under nitrogen, or in [Emim]HSO ₄ under reduced pressure. The spectra of D-xylose (Xyl) and 2-furaldehyde (Fur) are given for comparison.	360

CHAPTER 9

Figure 9.1- Simplified representation of aluminium (A) and chromium (B)- containing silicates in which Al ⁴⁺ and Cr ⁶⁺ are in tetrahedral coordination (charges are not represented for the sake of simplicity).	368
Figure 9.2- Powder XRD patterns of the fresh TUD-1 related materials (Al-TUD-1, Cr-TUD-1, and Cr-Al-TUD-1) and of the respective recW solids. The inset shows the low angle powder XRD patterns.	371
Figure 9.3- Powder XRD patterns of the fresh zeolite BEA-related materials and of the respective recW solids.	372
Figure 9.4- High resolution TEM images of a) Cr-BEA and b) Cr-BEATUD-1.	373
Figure 9.5- N ₂ adsorption-desorption isotherms at -196 °C of Al-TUD-1 (■), Cr-Al-TUD-1 (▲) and Cr-TUD-1 (○). The insets show the respective PSD curves (with matching symbols).	375

Figure 9.6- N₂ adsorption-desorption isotherms at -196 °C of BEA (■), Cr-BEA (▲), BEATUD-1 (O) and Cr-BEATUD-1 (X). The insets show the respective PSD curves (with matching symbols).....376

Figure 9.7- Diffuse reflectance UV-vis spectra of the chromium-containing materials and the respective recC solids.....377

Figure 9.8- Conversion of D-glucose (Glu) into 5-(hydroxymethyl)-2-furaldehyde (Hmf) using a solid acid/[Bmim]Cl catalytic system. Reaction conditions: monophasic solvent system, [Bmim]Cl (0.3 cm³), 120 °C, 15 g_{cat}·dm⁻³, 0.28 M Glu, 3 h.378

Figure 9.9- FT-IR ATR spectra of prepared materials and the respective recW solids.....381

Figure 9.10- FT-IR ATR spectra of prepared materials and the respective recW solids in the range 300-1800 cm⁻¹.382

Figure 9.11- FT-IR ATR spectra of fresh [Bmim]Cl and the recovered ionic liquid (recIL) phases for the different solid acid/IL systems [denoted recIL(name of solid acid)].....383

Figure 9.12- DSC curves for the recW solids related to the chromium containing solid acids and, for comparison, for fresh Cr-TUD-1 and Cr-Al-TUD-1.....385

Figure 9.13- UV-vis spectra of the recIL phases related to the chromium-containing solids, and of chromium salts dissolved in the IL ([Bmim]Cl) before and after heating at 120 °C for 3 h.387

CHAPTER 10

Figure 10.1- Solid acid catalysts tested in the hydrolysis/dehydration of saccharides into 2-furaldehyde (Fur) and to 5-hydroxymethyl-2-furaldehyde (Hmf) in the aqueous phase.402

Figure 10.2- Saccharides investigated in the hydrolysis/dehydration of saccharides into 2-furaldehyde (Fur) and to 5-hydroxymethyl-2-furaldehyde (Hmf) in the aqueous phase.403

Figure 10.3- Saccharides investigated in the hydrolysis/dehydration of saccharides to 2-furaldehyde (Fur) and into 5-hydromethyl-2-furaldehyde (Hmf) in the ionic liquid-based catalytic systems.....406

Figure 10.4- Ionic liquids tested in the hydrolysis/dehydration of saccharides into 2-furaldehyde (Fur) and to 5-hydromethyl-2-furaldehyde (Hmf) in the ionic liquid-based catalytic systems for the conversion of saccharides: [Emim]HSO₄ as solvent and catalyst or added in catalytic amounts, and chromium containing micro/mesoporous materials coupled to [Bmim]Cl (Cr-Al-TUD-1, Cr-TUD-1, Cr-BEA, Cr-BEATUD-1).407

List of tables

CHAPTER 1

Table 1.1- Simplified representation of molecular structures of saccharides and lignin.	9
Table 1.2 -Industrial, patented, and other studied processes for production of 2-furaldehyde (Fur).....	21
Table 1.3- Pilot scale processes to produce 2-furaldehyde (Fur) that operate with sulfite liquor. .	22
Table 1.4- Catalysts tested in the conversion of pentoses and related di/polysaccharides.....	39
Table 1.5- Catalysts tested in the conversion of hexoses and related di/polysaccharides.....	41
Table 1.6. Catalytic results reported for the conversion of saccharides (and levoglucosan) to 2-furaldehyde (Fur) and 5-hydroxymethyl-2-furaldehyde (Hmf) in the presence of insoluble solid acid catalysts.	54
Table 1.7- Names, abbreviations and structures of cations of ionic liquids	74
Table 1.8- Hydrolysis/Dehydration of di/polysaccharides or lignocellulosic biomass into 5-hydroxymethyl-2-furaldehyde/2-furaldehyde (Hmf/Fur) using ILs.	76
Table 1.9- Summary of the recycling procedures and efficiency of IL based catalytic systems. ...	107

CHAPTER 2

Table 2.1- List of chemicals used in the syntheses of SAPOs catalysts.	137
Table 2.2- Chemicals used in the synthesis of Al-TUD-1 catalyst.....	139
Table 2.3- Chemicals used in the syntheses of zeolite BEA and BEATUD-1 as catalysts.....	140

Table 2.4- Chemicals used in the syntheses of zeolite MCM-22 and delaminated ITQ-2 catalysts.....	142
Table 2.5- Chemicals used in the syntheses of the ZrW(X) catalysts.	144
Table 2.6 - Chemicals used in the syntheses of Al-TUD-1, Cr-AITUD-1, Cr-TUD-1, BEA, BEATUD-1, Cr-BEA and Cr-BEATUD-1 catalysts.	146
Table 2.7- Chemicals used in the catalytic tests and HPLC calibrations.....	151

CHAPTER 3

Table 3.1- Structural and textural properties of the SAPOs samples.....	170
Table 3.2- Acid properties of SAPOs measured by FT-IR of adsorbed pyridine.	175
Table 3.3- Catalytic results for the SAPOs samples for the conversion of D-xylose (Xyl) to 2-furaldehyde (Fur) and comparison with literature data for other solid acid catalysts tested under similar conditions.	177
Table 3.4- Reaction of D-xylose (Xyl) in the presence of SAPOs-11, at 160-180 °C.	180

CHAPTER 4

Table 4.1- Si/Al molar ratio and textural properties of the prepared Al-TUD-1, and comparison with literature data for this type of material tested as catalyst in different reaction systems (liquid or gas-phase).....	200
Table 4.2- Acid properties of Al-TUD-1 measured by FT-IR of adsorbed pyridine and comparison with literature data.	202
Table 4.3- Performance of Al-TUD-1 in the reaction of D-fructose (Fru) or D-glucose (Glu) using the biphasic solvent system (Wt:Tol) and comparison with literature data for zeolites as catalysts.....	207

Table 4.4- Catalytic performance of Al-TUD-1 in the conversion of D-sucrose (Suc) or D-cellobiose (Cel) into D-fructose (Fru), D-glucose (Glu) and 5-hydroxymethyl-2-furaldehyde (Hmf), and comparison with the literature data for zeolite H-Y. 210

CHAPTER 5

Table 5.1-Elemental composition and textural properties of BEA, BEATUD-1 and TUD-1 and comparison with literature data. 229

Table 5.2- Acid properties measured by FT-IR of adsorbed pyridine of BEA and BEATUD-1 and comparison with literature data. 236

Table 5.3- Catalytic performance of BEA, BEATUD-1 or TUD-1 in the reaction of D-xylose (Xyl) using the biphasic solvent system (Wt:Tol) and comparison with literature data for other catalysts. 238

CHAPTER 6

Table 6.1- Elemental composition and textural properties of (Na,H)-MCM-22 and ITQ-2(24)catalysts and comparison with literature data for other delaminated zeolites. 277

Table 6.2- Acid properties measured by FT-IR of adsorbed pyridine of (Na,H)-MCM-22 and ITQ-2(24) catalysts and comparison with literature data. 284

Table 6.3- Catalytic performance of aluminosilicates tested as catalysts in the reaction of D-xylose (Xyl), using a biphasic solvent system (Wt:Tol) at 170 °C, and comparison with literature data with other catalysts. 288

CHAPTER 7

Table 7.1- Elemental composition and specific surface area of the prepared materials ZrW(Cl), ZrW(NO₃), ZrW-MP, ZrWAl-MP and bulk ZrO₂. 313

Table 7.2- Acid properties measured by FT-IR of adsorbed pyridine of the prepared materials: (ZrW(Cl), ZrW(NO₃), ZrW-MP, ZrWAl-MP and bulk ZrO₂) after outgassing at 150 °C..... 321

Table 7.3- By-products detected by GCxGC-ToFMS for the reaction of D-xylose (Xyl) in the presence of ZrWAl-MP, at 170 °C..... 326

CHAPTER 8

Table 8.1- Conversion of mono/disaccharides into 2-furaldehyde (Fur) and/or 5-hydroxymethyl-2-furaldehyde (Hmf) in the ionic liquids [Emim]HSO₄ or [Bmim]Cl. 349

CHAPTER 9

Table 9.1- Physicochemical properties of the prepared materials and comparison data with the literature. a) 374

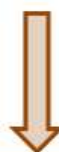
Table 9.2- Catalytic results for the reaction of D-glucose (Glu) in the presence of the prepared materials, using [Bmim]Cl as solvent, at 120 °C (Catalytic BR), and related catalytic tests for investigating catalyst stability (experiments (i), (ii), and (iii)) 379

CHAPTER 1

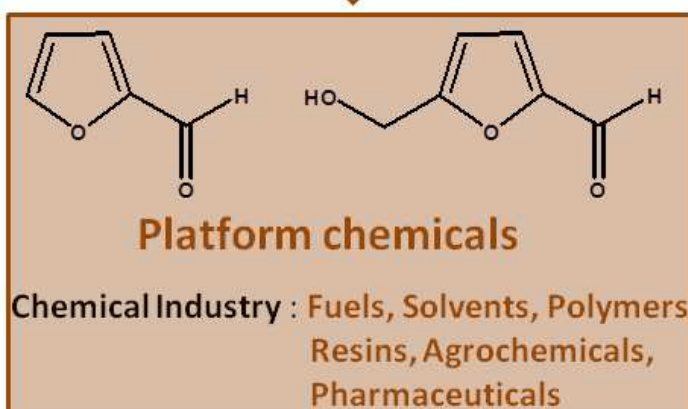
Conversion of carbohydrate biomass to furanic aldehydes



Hydrolysis/
Dehydration



Catalytic system



Index

CHAPTER 1	1
Conversion of carbohydrate biomass to furanic aldehydes.....	1
1.1. Renewable sources for energy and chemicals	3
1.2. Biomass as a renewable source	5
1.3. Furanic aldehydes as platform chemicals	14
1.3.1. 2-Furaldehyde	16
1.3.1.1. Industrial production.....	16
1.3.1.2. Applications.....	23
1.3.2. 5-Hydroxymethyl-2-furaldehyde and applications	26
1.4. Catalytic conversion of saccharides to furanic aldehydes	30
1.4.1. Reaction mechanism of the conversion of saccharides to furanic aldehydes.....	30
1.4.2. Type of acid catalysts	37
1.4.3. Conversion of saccharides to furanic aldehydes in the presence of heterogeneous catalysts.....	46
1.5. Conversion of saccharides to furanic aldehydes using ionic liquid (IL) based catalytic systems.....	71
1.5.1. ILs as solvents (an acid catalyst is added)	75
1.5.1.1. ILs coupled with homogeneous liquid acid catalysts	78
1.5.1.2. ILs coupled with homogeneous/heterogeneous solid acid catalysts	83
1.5.2. ILs as acid solvents/catalysts (dual function)	99
1.5.3. Recycling of IL-based catalytic systems.....	103
1.6. References.....	111

1.1. Renewable sources for energy and chemicals

Energy is the base of life of a modern industrial society. It is related to almost everything that man does or wishes to do. In its many useful forms, it is a basic element that influences and limits human standard of living and technological progress. Clearly, it is an essential support system for all of us.¹ The intense population growth is expected to contribute to the growing worldwide demand for energy.² Key strategies for efficient energy consist essentially of a safe supply, low implementation costs, and environmental sustainability. Coal became the primary energy resource and was the majority of coal produced is burned to produce heat and electric power. Other uses include the production of synthetic fuels and feedstock for the petrochemical industry.^{1,3} During processing and/or combustion of coal, several compounds can be released into the environment as harmful pollutants: sulfur dioxide, sulfur trioxide, nitrogen oxides, hydrogen chloride, mercury vapor and a wide variety of trace metals are some examples.¹⁻³ Furthermore the use of coal may result in the production of CO₂ which is the most important greenhouse gas in the atmosphere, or volatile organic solvent emissions. The combustion of coal releases more CO₂ per unit of heat released than combustion of oil or gas, since it has the lowest H/C ratio of the fossil fuels. Besides the greenhouse gas emissions, other issues, such as global warming or natural resource depletion, are becoming worldwide environmental concerns.² A growing interest in obtaining cleaner fuels from coal (e.g. increasing demand for low sulfur coal) was noticed.²⁻¹¹ A coal-based economy remained prevalent until the discovery of petroleum (in the middle of XX century). Oil and natural gas began to substitute coal, in a fossil fuel based economy (i.e. as raw materials for the production of energy such as, heat, steam, electric power, and of solid, liquid or gaseous fuels).^{12,13} Natural gas started to be widely adopted for cooking, space heating, water heating and industrial uses in most urban areas, once it was possible to transport natural gas through a pipeline grid system. Pipelines were developed with the purpose of transporting oil from the producing regions to the refineries. An oil well is drilled to bring liquid petroleum to the surface and the first pipeline was built in 1859 in Titusville, Pennsylvania.¹

Indeed the fossil fuel era had a large impact on civilisation and industrial development. However, the threat to oil supplies in 1973 (the first oil shock), due to the depletion of the reserves of fossil fuels, and environmental issues led to major increases in oil prices.¹ Intensive research programs started to be developed. The future energy production needs to be as clean as possible and economically viable. Renewable energy sources have become desirable because they

can alleviate our dependence on the inevitable depletion of non-renewable fossil fuels, replacing part of the crude oil and natural gas which are the current major raw materials.^{10,11,14-25} Based on the predicted end of cheap oil by 2040,^{1,26} Lichtenthaler et al.¹⁵ reported that the curve for the utilisation of biofeedstocks should rise and intersect the one for fossil raw materials between 2030-2040 (Figure 1.1). According to these data, the transition in the evolution to a more bio-based system continues somewhat inhibited by the cheaper fossil raw materials. Until the mid-1800s, renewable biomass sources, in the form of wood and farm residues/wastes, supplied the vast majority of the world's energy and fuel needs, and were the first principal sources of fuel and construction materials because of the little capital technological investment needed.^{1,2} Afterwards, coal and fossil fuels slowly displaced biomass consumption and became the preferred energy sources. Presently, considerable achievements and rapid progress are being made in areas such as hydropower, geothermal energy, solar thermal technology, wind energy conversion, photovoltaics and biomass conversion.^{2,11,17,27-29} Due to the first oil shock in the mid 1970s mentioned above, there is a reborn interest in using biomass to reduce oil consumption and imports.¹⁴

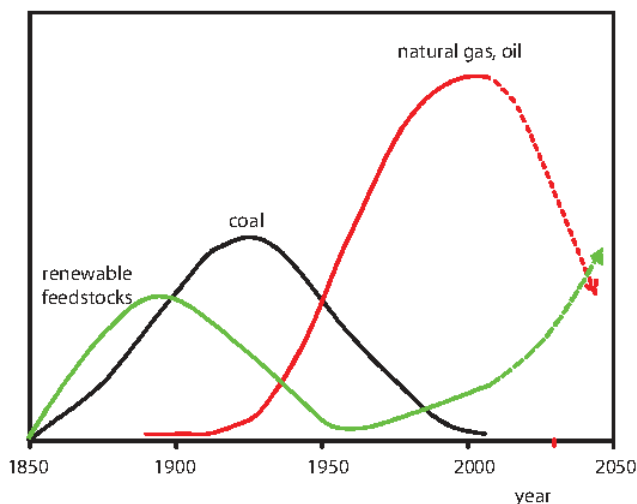


Figure 1.1- Raw materials basis of the chemical industry in an historical perspective [adapted from ¹⁵].

1.2. Biomass as a renewable source

Biomass is non-fossil organic matter with chemical energy content, essentially of plant origin (phytomass), and a renewable, relatively inexpensive and widely dispersed carbon source.^{1,11,13,15,17-19,21-23,28-35} An increasing usage of biomass is expected for the production of biofuels and other chemicals.^{5,36,37} Plant biomass can convert CO₂ from the atmosphere to sugars (plus molecular oxygen) by photosynthesis, which is an initial key step in the growth of biomass plants (Figure 1.2).^{1,38} It is the photosynthetic capability of plants to utilise CO₂ from the atmosphere that leads to the designation of a “carbon neutral” fuel from biomass (assuming that no extra carbon is introduced into the atmosphere).³⁹ Considering that over the entire globe, plant photosynthesis captures only 0.1% of the solar energy, and according to data obtained from the USA department of energy for the global primary energy production in the form of oil, coal, natural gas, nuclear power, hydroelectric power and other forms (including renewable energy), the energy stored in biomass each year worldwide is seven times greater than the annual production of energy.⁴⁰ Biomass is therefore seen as one of the most important keys towards sustainability (renewable source of organics and stored energy).^{15,17-19,21-23,41}

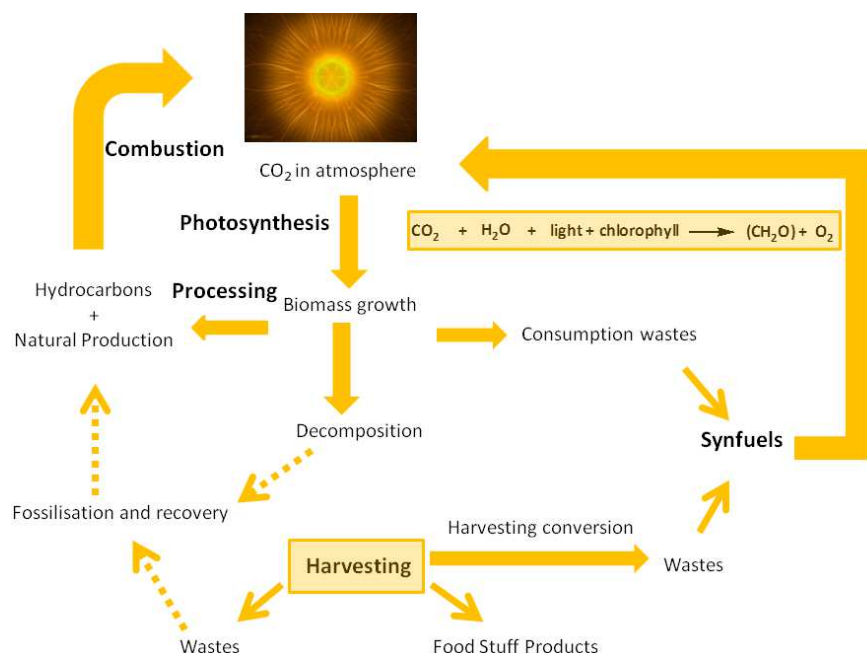


Figure 1.2- Conversion of biomass into energy and other products [adapted from ¹].

Biomass can be harvested for food, fiber, construction materials or left to natural decomposition. After a long period of time, the decomposition products from biomass and the wastes from the harvesting can be partially recovered as fossil fuels. Alternatively, the wastes can be converted to energy (heat, power) and synthetic fuels by suitable conversion processes which are essentially thermochemical and biochemical.^{1,39} An example of a thermochemical conversion process is known as the gasification process where the biomass is heated under air, O₂ and steam giving origin to a gas mixture, referred as syngas (Figure 1.3).³⁹ An example of biological conversion of biomass is that used for bioethanol production (Figure 1.4).

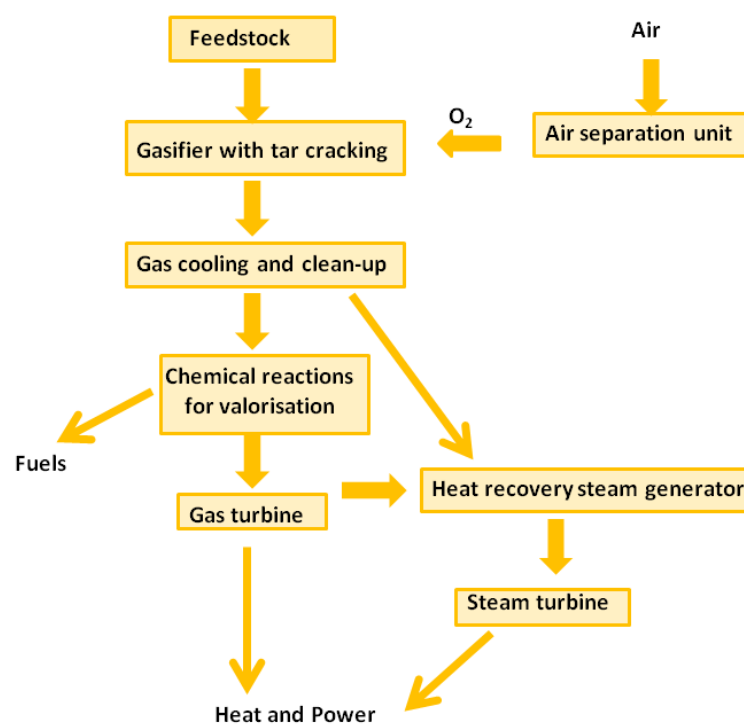


Figure 1.3- Biomass conversion into fuels, heat and power by a thermochemical process [adapted from ³⁹].

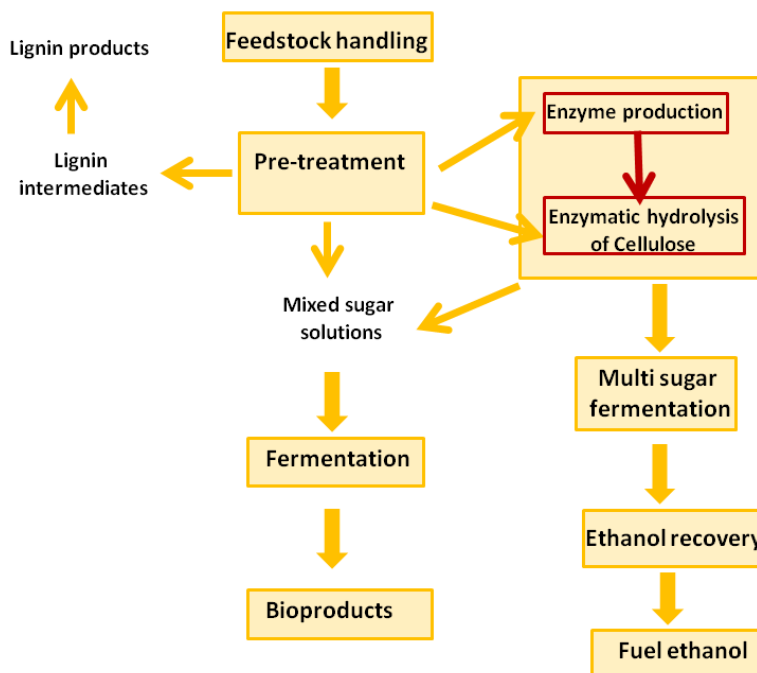


Figure 1.4- Biomass conversion to ethanol by a biochemical process [adapted from ³⁹].

Although promising, the use of biomass energy can be affected by the potentially damaging environmental effect of continued fossil fuel usage. Another limitation on the use of biomass compared to other fossil fuel energy is related to the more difficult conversion into convenient forms of energy, chemicals and products,³⁹ partly due to the complex structure of lignocellulosic biomass that provides protection and structural integrity to the plant. On the other hand, the diversity of biomass composition offers great opportunities to produce a wide range of new and existing chemicals. Challenges include developing viable approaches for the chemical valorisation of lignocellulosic matter which can be found in municipal solid wastes, forestry and agricultural residues and some industrial wastes.^{39,42}

The main components of lignocellulosic biomass are the carbohydrates cellulose (ca. 40% dry weight of wood)^{23,25,41,43} and hemicelluloses (ca. 20-35%), and lignin (ca. 15-30%), (Table 1.1).^{23,25,36,44-46} One can imagine that cellulose forms a skeleton which is surrounded by other substances functioning as matrix (hemicelluloses) and encrusting (lignin) materials.^{44,45} The three components are located on the cell walls of the plants. Lignin is a cross-linked biopolymer with a high-energy content and built of substituted phenolic units.^{34,39} Cellulose consists of D-anhydroglucopyranose units linked by β -(1,4)-glycosidic bonds, forming a linear structure whose chains are strongly interconnected through hydrogen bonding and van der Waals forces

(forming essentially crystalline structures), with a degree of polymerisation (DOP) going from 10000 in native wood to 1000 in bleached kraft pulp.^{4,39} Each D-anhydroglucopyranose unit possesses hydroxyl groups at C-2, C-3 and C-6 positions.^{43,47} In D-glucose, C-1 refers to the aldehyde anomeric carbon centre of the hemiacetal functional group: in cellulose, the C-1 of one glucose unit is linked to C-4 of the next glucose unit via β -(1,4)-glycosidic bonds (Table 1.1).⁴⁸ Hemicelluloses are heterogeneous biopolymers (amorphous structures) which bind strongly to cellulose by hydrogen bonds. Hemicelluloses are composed mainly of five-carbon monosaccharides (pentoses such as xylose and arabinose) and some six-carbon monosaccharides (e.g. D-mannose, D-glucose and D-galactose).^{4,39} The most prevalent hemicellulose is D-xylan, composed of D-xylopyranosyl units linked by β -1,4-glycosidic bonds. In hardwood, the D-xylan backbone is modified with various side chains, including 4-O-methyl-D-glucuronic acid linked to D-xylose units via α -(1,2)-glycosidic bonds and acetic acid that esterifies the D-xylose units at the O-2 or O-3 positions (Table 1.1). In non-acetylated softwood xylans, there are L-arabinofuranose residues attached to the main chain by α -(1,2) and/or α -(1,3)-glycosidic linkages (Table 1.1).⁴⁹ Hemicellulose polymers are almost always branched possessing a wide variety of substituents as specified for D-xylan (e.g. 4-O methyl glucuronic and galacturonic acid residues).⁵⁰ Sugars are linked together by α -(1,4) or β -(1,4)- glycosidic bonds, occasionally by α -(1,3) and/or α -(1,2)-glycosidic bonds (e.g. xylan polysaccharides composed of (pentose) xylose units) or yet by α -(1,2)- β -glycosidic bonds (e.g. sucrose, Table 1.1).⁵¹⁻⁵⁴

Hemicelluloses possess a lower DOP (50-300) than cellulose and are more vulnerable to chemical attack (e.g. hydrolysis).²⁵ Although abundant, cellulose and hemicelluloses are difficult to dissolve in water, particularly in the former case.³⁹ The hemicelluloses and lignin provide a protective cover in the surroundings of cellulose and should be removed to enable the efficient hydrolysis of cellulose.³⁹ The removal of this protective cover is possible by a chemical treatment using an appropriate acid catalyst.²⁵ The high level of hydrogen bonding among the polysaccharide chains makes it difficult to depolymerise cellulose. Starch and inulin are less abundant carbohydrates than cellulose and hemicelluloses.^{4,36} Inulin is a polymer composed of fructose units linked by β -(2,1) glycosidic bonds (Table 1.1). Starch consists of glucose units joined by α -glycosidic bonds and is composed of amilopectin (ca. 75-80 wt.%) and amylose (ca. 20-25 wt.%, Table 1.1).^{55,56} In amilopectin the glucose units are linked in a linear fashion via α -(1,4)-glycosidic bonds and branching occurs via α -(1,6)-glycosidic bonds. Amylose is essentially a linear polymer made up of α -(1,4)-glycosidic bonds; it is less soluble in water than amilopectin and is hydrolysed more slowly.⁵⁷ Other carbohydrates include disaccharides like D-cellobiose (two

glucose units linked by a β -(1,4)-glycosidic bond), D-maltose (two glucose units linked by a α -(1,4)-glycosidic bond) and D-sucrose (one glucose and one fructose units linked via an ether bond between C-1 on the glucosyl unit and C-2 on the fructosyl unit; α -D-glucopyranosyl-(1-2)- β -D-fructofuranoside). D-glucose and D-xylose are the most common hexoses and pentoses, respectively.³⁴

Table 1.1- Simplified representation of molecular structures of saccharides and lignin.

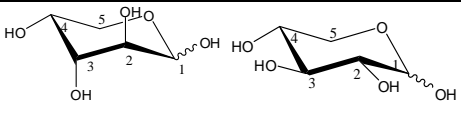
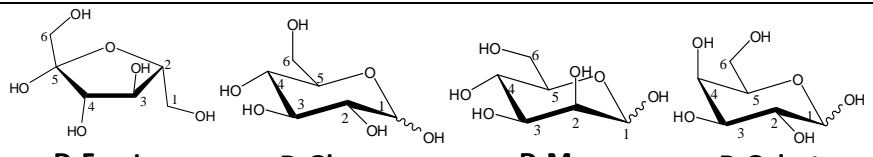
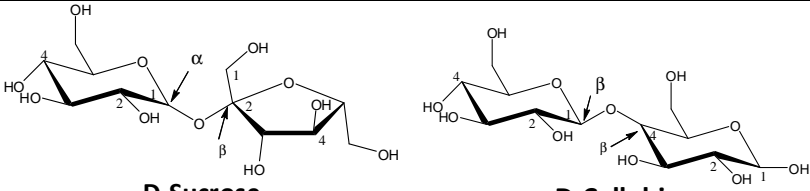
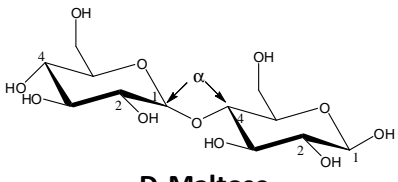
Monosaccharides- Pentoses	
	<p>D-Arabinose D-Xylose</p>
Monosaccharides- Hexoses	
	<p>D-Fructose D-Glucose D-Mannose D-Galactose</p>
Disaccharides	
	<p>D-Sucrose D-Cellobiose</p>
	<p>D-Maltose</p>

Table 1.1- Continued.

Polysaccharides

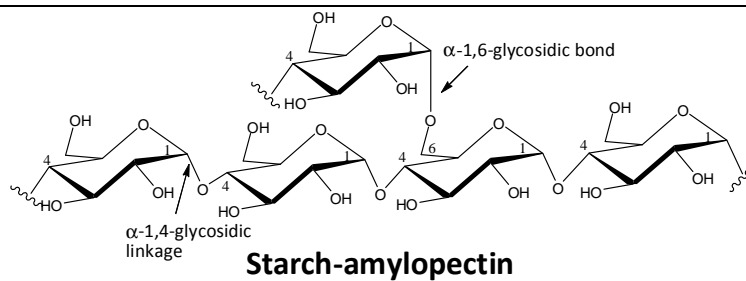
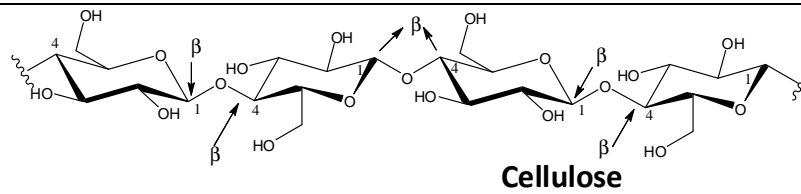
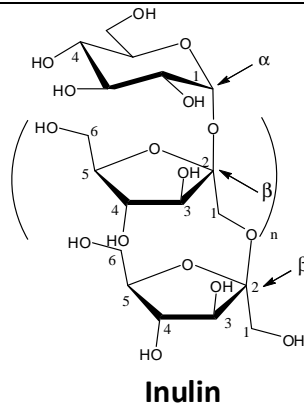
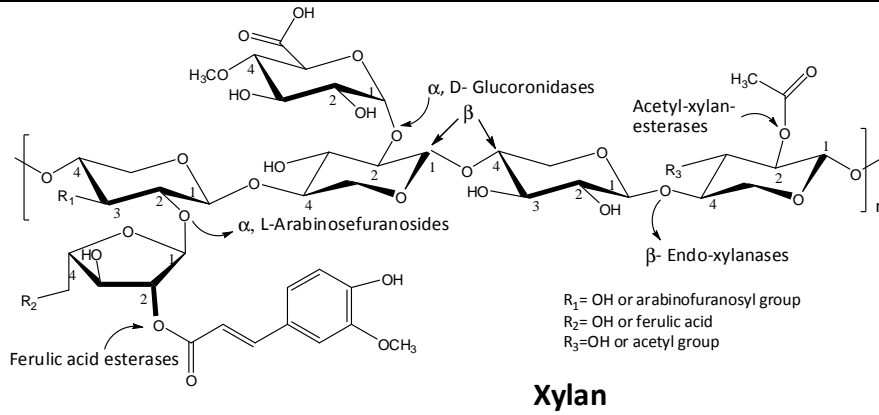
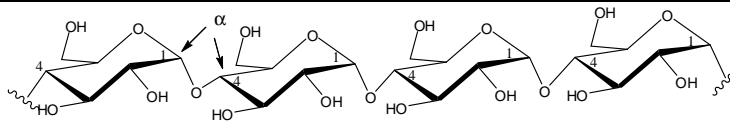
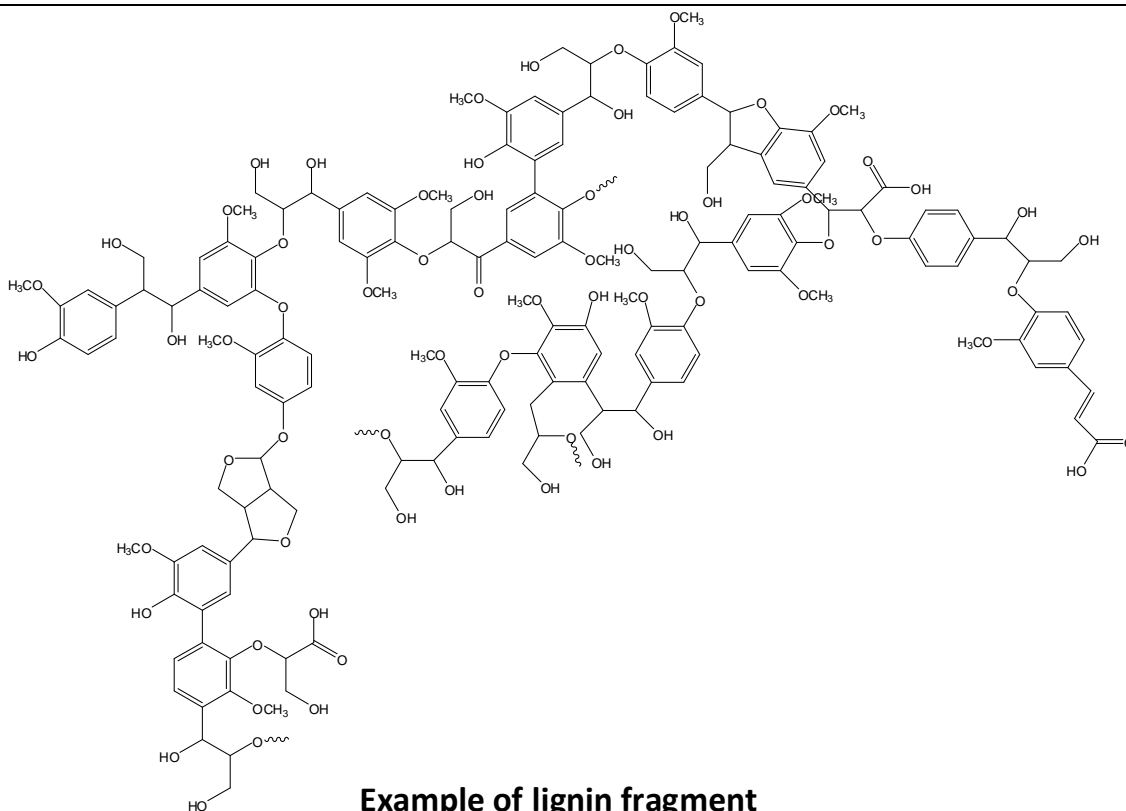


Table 1.1- Continued.

**Starch-amilose****Example of lignin fragment**

Biomass conversion processes can allow large molecules to be broken down into smaller ones, and the reduction in the degree of oxygen-functionalities.⁵⁸⁻⁶⁰ The selective deconstruction of biomass may allow a complex mixture of monomeric and polymeric materials to be converted into streams of primary biorefinery building blocks (high molecular weight biopolymers, low molecular weight chemicals or intermediates), which can be subsequently transformed into added value chemicals (Figure 1.5).^{61,62}

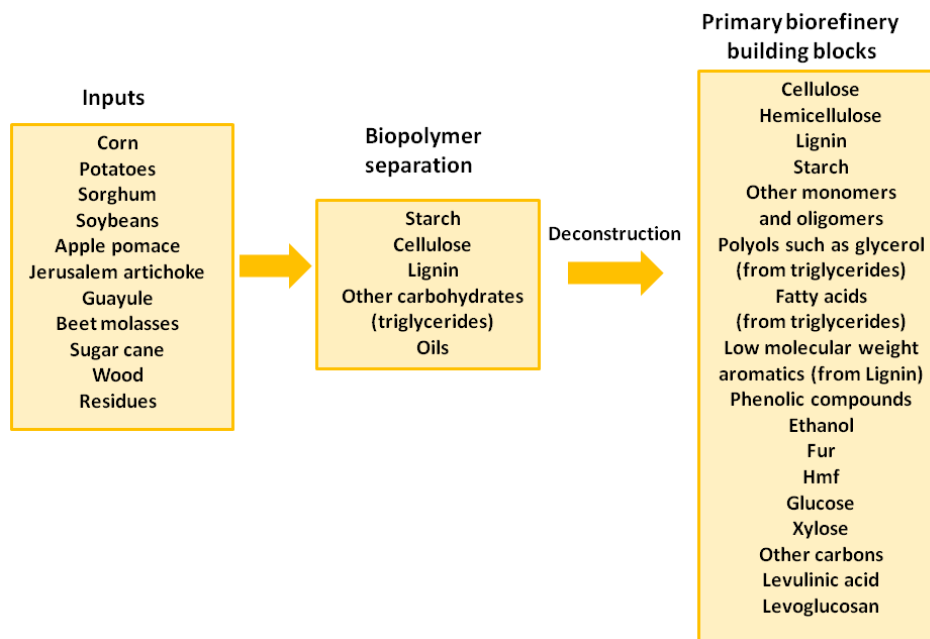


Figure 1.5- Biomass deconstruction into primary biorefinery building blocks [adapted from ³⁹].

Sugar cane processing gives bagasse consisting of cellulose (43.6%), hemicelluloses (33.5%), lignin (18.1%), ash (2.3%), wax (0.8%) and others (0.7%).⁶³ It is produced in large quantities by sugar and alcohol industries (the world annual production of bagasse is ca. 54 million dry tones. In Brazil, sugars from sugarcane are used to produce the fuel bioethanol.⁶⁴ In the U.S.A. bioethanol is derived from starch in corn grain; starch was the first major carbohydrate biopolymer to be used for energy production.³⁹ Sugar cane may be used as a biomass source for displacing fossil fuels in which 2-furaldehyde (Fur) and 5-hydroxymethyl-2-furaldehyde (Hmf) are intermediates (Figure 1.6).

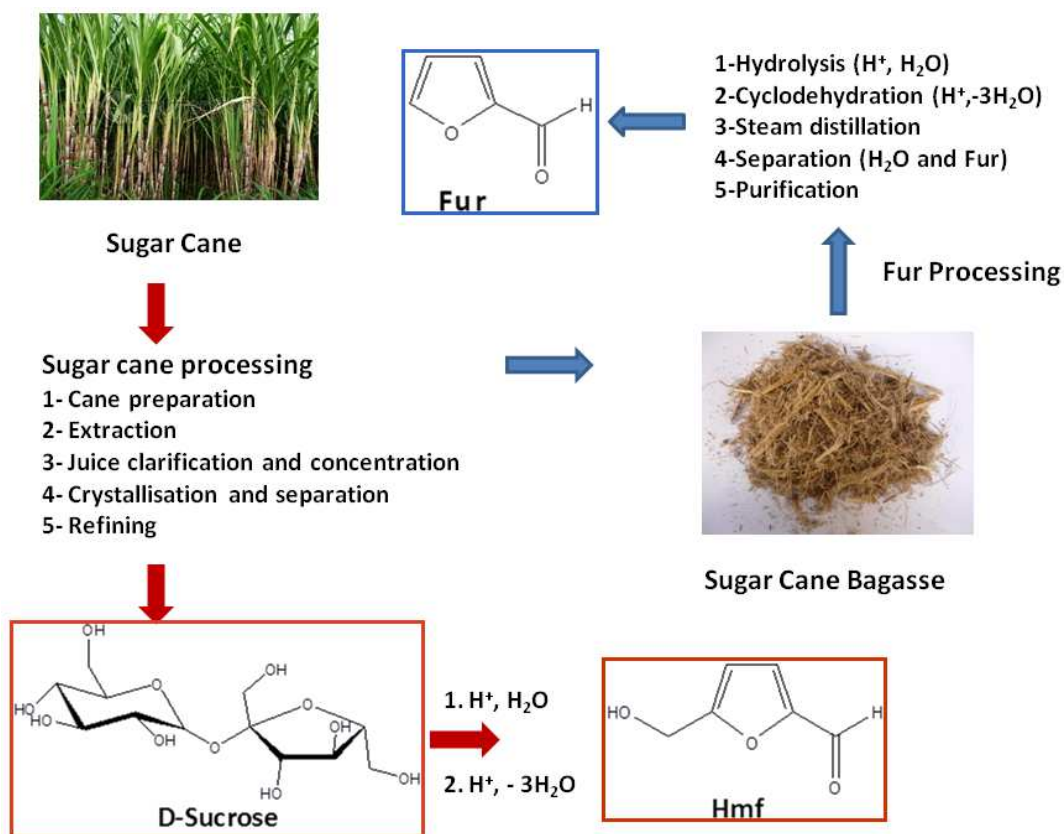


Figure 1.6- Schematic representation of transformation of sugar cane into 2-furaldehyde (Fur) and 5-hydroxymethyl-2-furaldehyde (Hmf) [adapted from ⁶⁵].

The three main biopolymers of lignocellulosic feedstocks (cellulose, hemicelluloses and lignin) can be separated by a wide variety of methods to give separated polymer streams for further processing to final products.^{23,39,66} The pulp and paper industry describes these processes as pulping: e.g. Kraft pulping,⁶⁷ sulfite pulping,⁵⁸ organosolv.^{68,69} Different approaches have been described in the literature for the fractionation of lignocellulosic feedstocks such as that shown in Figure 1.7 in which the pretreatment consists in using a mixture of water and organic solvents and a liquid acid.

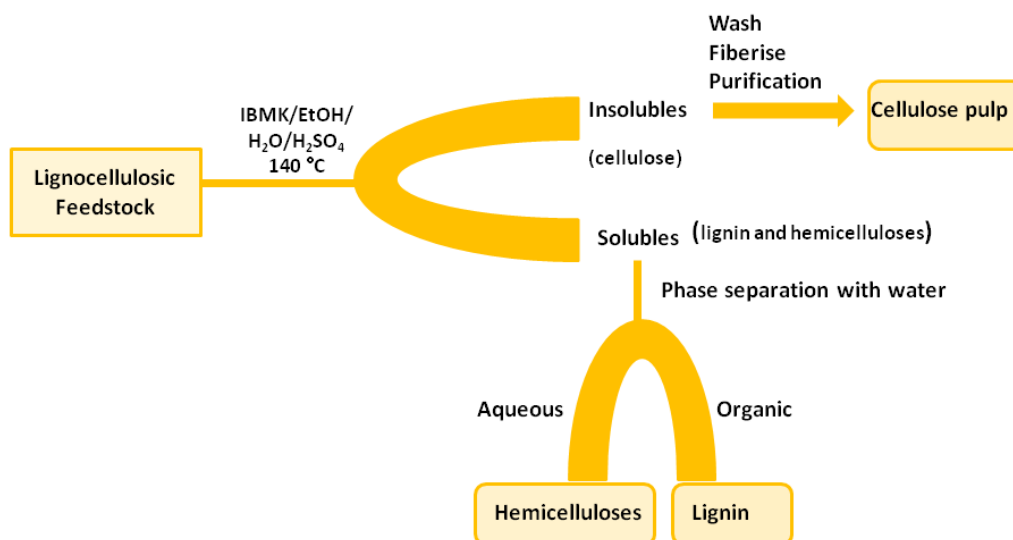


Figure 1.7- Clean fractionation process [adapted from ³⁹].

1.3. Furanic aldehydes as platform chemicals

One of the most important chemical transformations of carbohydrates is the hydrolysis of cellulose and hemicelluloses into the constituent monosaccharides, essentially hexoses and pentoses, and the dehydration of the latter into the furanic aldehydes, Hmf and Fur, respectively (Figure 1.8). These reactions are promoted by an acid which can be a liquid acid, an insoluble solid (e.g. zeolites) in water or an organic solvent, or alternatively an ionic liquid medium can be used.^{18,32,58-60,70-73} These different types of reaction media will be discussed in Sections 1.4 and 1.5.

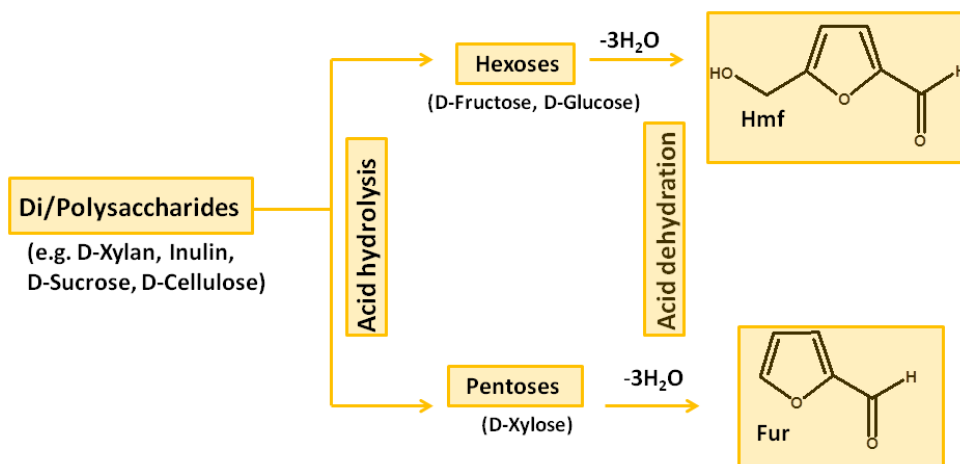
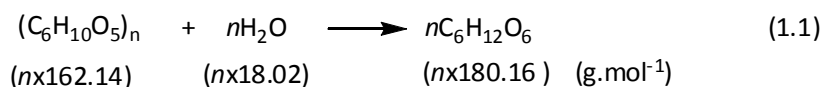
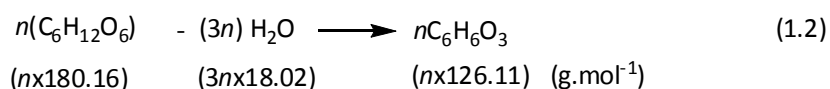


Figure 1.8- Simplified representation of the conversion of carbohydrates to 5-hydroxymethyl-2-furaldehyde (Hmf) and 2-furaldehyde (Fur) [adapted from ⁴].

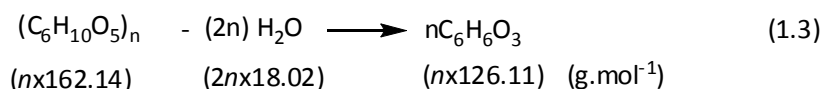
The conversion of biomass to the furanic aldehydes Fur and Hmf as platform chemicals, is considered an important route for achieving sustainable supply of energy and chemicals.^{25,71,74,75} The conversion of polysaccharides to Hmf and Fur requires acidic reaction conditions and when it is 100% selective, H₂O is the only co-product. Coupling the hydrolysis and dehydration reactions gives a positive net production of water. The stoichiometry of these reactions is given for Hmf production in Equations (1.1)-(1.3), being similar for Fur production. The hydrolysis reaction of polysaccharides consumes one molecule of water per monosaccharide formed (equation 1.1), whereas the dehydration of each molecule of monosaccharide gives one molecule of furanic aldehyde plus three molecules of water (equation 1.2).



Equation 1.1- Stoichiometry of the complete hydrolysis of a polysaccharide containing n hexose units.



Equation 1.2- Stoichiometry of the dehydration of the hexose molecules to 5-hydroxymethyl-2-furaldehyde (Hmf).



Equation 1.3- Stoichiometry of the overall hydrolysis-dehydration reaction scheme.

The theoretical yield of Hmf ($\text{C}_6\text{H}_6\text{O}_3$) obtained from a polysaccharide $((\text{C}_6\text{H}_{10}\text{O}_5)_n)$ is about 78 wt.%. In the case of Fur ($\text{C}_5\text{H}_4\text{O}_2$, $96.08 \text{ g} \cdot \text{mol}^{-1}$), obtained from a polysaccharide with n pentose unit $((\text{C}_5\text{H}_{10}\text{O}_4)_n)$, $132.11 \text{ g} \cdot \text{mol}^{-1}$ the theoretical yield is about 73 wt.%. Detailed reaction mechanisms will be presented later.

1.3.1. 2-Furaldehyde

2-Furaldehyde (Fur) was discovered by Döbereiner in 1821.³⁷ It was obtained as a by-product during the synthesis of formic acid. Afterwards, Emmett observed that Fur can be obtained from vegetable substances. Later, in 1840, Stenhouse found that Fur could be produced by distilling a wide variety of crop materials (e. g. corn cobs, oat husks, bran, sawdust, sugar cane bagasse, rice and peanut) from agricultural waste rich in pentosans using an aqueous solution of H_2SO_4 , and he attributed the empirical formula $\text{C}_5\text{H}_4\text{O}_2$ to Fur.^{76,77} The chemical structure of Fur was determined by the chemist Carl Harries in 1901 as cited by Dalin Yebo.⁷⁸ It consists of a furanic ring (aromatic character) with an aldehyde substituent group (Figures 1.6 and 1.8), has a boiling point of $161.7 \text{ }^\circ\text{C}$,^{79,80} and is a colourless liquid that in the presence of oxygen suffers auto-oxidation becoming dark red/brown in colour.⁷² Generally, Fur is produced from pentosans such as xylans which are acid-hydrolysed to D-xylose (an aldopentose) and the latter is dehydrated into Fur (Figure 1.8).²⁵

1.3.1.1. Industrial production

The industrial production of Fur was stimulated by the necessity of the USA to become self-sufficient in war periods. Therefore between 1914 and 1918 they started to explore processes to transform agricultural residues into valuable products. However, the large-scale production of

Fur only started in 1921 with the Quaker Oats company.⁵⁸ Ever since Fur has been produced on an industrial scale, commonly using aqueous sulfuric acid medium.^{25,58-60,73} The commercial processes for the production of Fur are based on the use of either batch or continuous reactors where hemicellulose feedstocks are treated with an acid to hydrolyse the hemicelluloses fraction into essentially D-xylose which is further dehydrated into Fur.²⁵

The batch process of Quaker Oats in 1921 was the first industrial process of Fur production.^{58,81,82} A simplified representation of this process is given in Figure 1.9. The raw materials (oat hulls harvested from their cereal mill in Cedar Rapids, Iowa) were mixed with a diluted solution of H_2SO_4 in a reactor heated at $153\text{ }^\circ\text{C}$ for 5 to 8 h. The reaction temperature was limited because the reactors could not support too high pressures. Therefore compensation factors such as increasing the residence time and the amount of H_2SO_4 had to be taken into consideration. These strategies led to the formation of strongly acidic residues and acid corrosion hazards, favouring secondary reactions, which lowered the Fur yield of the process. At the end of the reaction, a mixture of Fur (35%) and water (65%) was obtained. This mixture was steam-stripped to an azeotropic distillation column. According to Brownlee's optimum conditions (at 25.4% of initial water content),⁸³ the initial H_2SO_4 concentration was 6.05 wt.%, the Fur in the distillate and in the residue was 52.3% and 9.9% of the theoretical yield (73 wt.%) respectively, giving an overall yield of 62.2%.⁵⁸

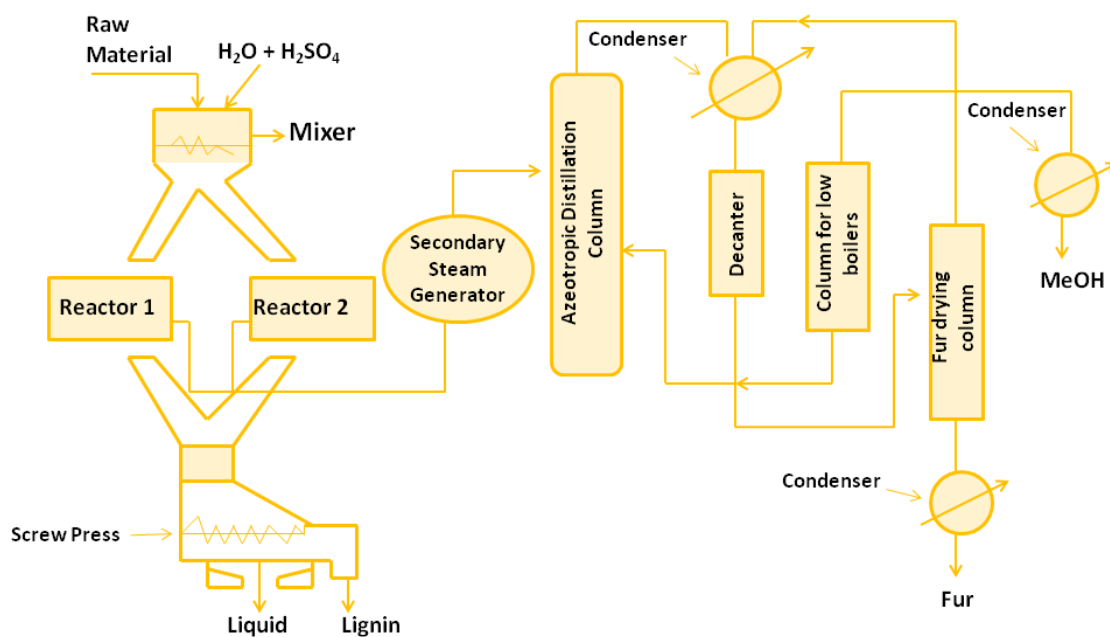


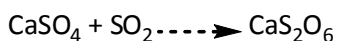
Figure 1.9-The batch process of Quaker Oats [adapted from ⁵⁸].

In the older industrial commercial processes (Quaker-Oats, Agrifurane, Rosenlew, Escher Wyss or Chinese) that ran at temperatures below 200 °C (Table 1.2), yields of Fur of up to 50% of the theoretical value were obtained while in the “analytic Fur process”, 100% Y_{Fur} was observed.⁵⁸ According to Zeitsch the reason for these huge differences is related to the reactions that Fur suffers within the liquid and vapor media. In the “analytical Fur process” for the quantitative determination of the pentose, the substance to be analysed is added to H_3PO_4 saturated with NaCl to increase the achievement of the boiling point, which is ca. 110 °C, temperature at which the water vapor undergoes superheating. In the case of the conventional processes mentioned above, the remaining Fur in the liquid phase reacts with itself or with intermediates of the conversion of pentosans to Fur in the presence of an acid catalyst. On the other hand, in the case of the analytical process, the mixture is brought to boiling and is maintained as such throughout the digestion period. In this process Fur is shifted from the liquid into the vapor phase where it does not undergo loss reactions, since the vapor phase does not contain the active acid species. This cannot be achieved in conventional industrial processes, because at any pressure, condensing steam is thermodynamically incapable of inducing an aqueous pentose solution to boil (due to the elevated boiling point). Thus Fur generated is left temporarily in the liquid phase.⁵⁸

Several advances have been made to avoid Fur loss reactions in the liquid phase. Improved Fur yields were obtained by processes operating at higher temperatures (> 200 °C) such as Supratherm, Stakes, Suprayield and Montane (Table 1.2). The current production of Fur uses high pressure steam to heat the reaction.⁸⁴ Due to the entropy effect at higher temperatures, the formation of larger molecules by condensation of Fur is avoided.^{84,85} The Suprayield process is a good example that demonstrates this effect. It was invented by Zeitsch in 1999,⁸⁶ and developed by International Furan Technology Ltd. in South Africa, which is a member of DalinYebo group (further founded in 2001).⁸⁷ In this process, the liquid phase is heated to the primary temperature (240 °C) with steam for a short time (the secondary temperature should not be below 180 °C to avoid slow reactions).^{58,85} The higher the primary temperature the lower is the need for an acid, which should not be H_2SO_4 (to avoid losses by sulfonation) nor HCl (causes corrosion) or HNO_3 (due to nitration). H_3PO_4 was the preferred acid because it does not cause any side reaction.^{58,78} During the heating, the steam (Fur-water vapor mixture) condenses and the moisture content of the reactor is increased.⁸⁵ When the pressure in the reactor is gradually decreased below the vapor pressure of the liquid, the liquid phase boils and the Fur is removed from the reaction solution through a stripping column. The Fur rich vapor mixture formed is then condensed.^{58,84,85} As long as the vapor is separated from the liquid phase, the solution cools and

the vapor pressure decreases, making it necessary to continue lowering the reactor pressure.⁸⁵ The limited solubility of Fur in water (8.3% at 20 °C),⁸⁴ facilitates the separation of the Fur rich lower phase from the upper phase in a decanter. After the separation, the commercial product is obtained by purification processes (e.g. by distillation) while the water-rich upper phase is recycled from the decanter back to the stripper column as reflux.⁸⁴ Apart from Suprayield, there are other patented processes, such as Verdernikovs,⁸⁸⁻⁹⁰ CIMV (Compagnie Industrielle de la Matière Végétale),⁹¹ Lignol,^{92,93} MTC (Multi-Turbin-Column),⁹⁴ or Chempolis.^{95,96} The CIMV is the only technology in the world today that can cleanly recycle the three main components of the vegetable matter (cellulose, hemicelluloses and lignin) of lignocellulosic feedstock, and separate them into intermediary products, such as sugar syrup, for both chemical and biotechnology industries. The refining of these syrups (mainly composed of C-5 sugars and principally D-xylose) results in the production of Fur and its many derivatives.⁹⁷ In the case of the MTC process, extractions with toluene and distillation under reduced pressure were carried out to prevent reactions of Fur with organic acids.⁸⁵ Not all the processes need an acid since the organic acids formed as by-products of the decomposition of the raw materials may act as catalysts in autocatalytic reaction mechanisms. Some of these processes are represented in Table 1.2 (Rosenlew, Supratherm, Stakes, CIMV or Chempolis).

Fur can be obtained via sulfite pulping (discovery by Tilghman in 1866) which allow white cellulose fibers to be obtained by treating wood in aqueous solution of calcium bisulfite $\text{Ca}(\text{HSO}_3)_2$ under reduced pressure (Figure 1.10). Lignin present in the wood reacts with sulfite to form water-soluble sulfonic acids, liberating the fibers of the wood. The reaction requires a temperature of 140 °C and the presence of an acid to permit the conversion of pentosans to Fur. The Fur yield can be increased by recovering the Fur that exists in the liquor.⁵⁸ However, the pentose in calcium sulfite waste liquors is not used to produce Fur because during the digestion at higher pressures a super saturation with CaSO_4 occurs, due to the reduction of sulfur dioxide to dithionate (Equation 1.4). Some processes that operate with sulfite liquor to produce Fur are listed in Table 1.3.⁵⁸



Equation 1.4- Reduction of SO_2 to S_2O_6 .⁵⁸

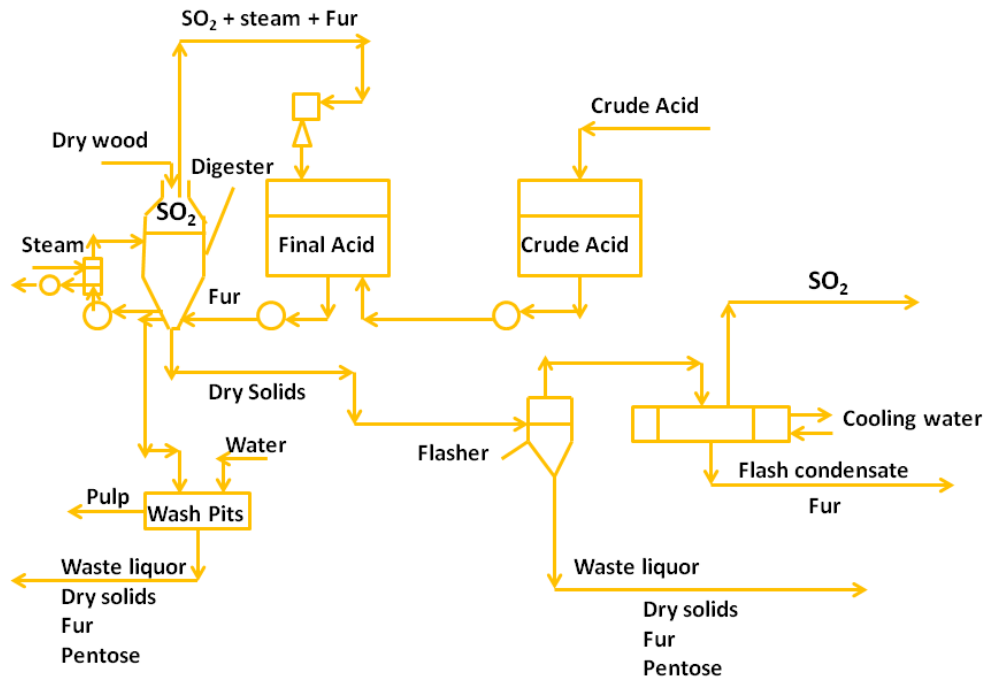


Figure 1.10- Flow diagram of the sulfite pulping process [adapted from ⁵⁸].

Table 1.2 -Industrial,^a patented,^b and other studied^c processes for production of 2-furaldehyde (Fur).

Industrial Process	Country	Catalyst	Reactor (operation mode)	Temperature (°C)	Reaction Time (h)	Y _{Fur} (wt. %)	Process duration	Ref
Quaker Oats ^a	U.S.A.	H ₂ SO ₄	Batch	153	5	50	1921-1961	⁵⁸
Quaker Oats ^a	U.S.A.	H ₂ SO ₄	Continuous	184	1	55	1961-1997	^{58,72,98}
Natta ^a	nf ^d	HCl	Batch	nf ^d	nf ^d	nf ^d	nf ^d	^{41,99}
Natta ^b	nf ^d	HCl	Continuous	20-25, ¹⁰⁰ 190- 200, ¹⁰¹ 300 ¹⁰²	3-8, ¹⁰⁰ 24 ¹⁰²	70-80	1954-1957	¹⁰⁰⁻¹⁰²
Roni and Sebara ^a	nf ^d	H ₂ SO ₄	nf ^d	177-161	nf ^d	nf ^d	nf ^d	⁴¹
Duipopetrovski ^a	nf ^d	HCl	nf ^d	nf ^d	nf ^d	nf ^d	nf ^d	⁴¹
Chinese ^a	China	H ₂ SO ₄	Batch	160	4-5	35-50	nf-2004	^{58,72,98,103,104}
West Pro modified Chinese Huaxia Technology ^a	China	H ₂ SO ₄	Continuous	< 200	nf ^d	98.9-99.5	2004-to present	^{25,72,85}
Agrifurane (Petrole chimie) ^a	France	H ₂ SO ₄	Batch	177-161	nf ^d	40- 50 ⁸⁵	1981- Abandoned	^{58,72,85,98,105}
Escher Wyss ^a	Germany	H ₂ SO ₄	Continuous	170	0.75	40-50 ⁸⁵	Abandoned	^{58,72,85,98,106}
Rosenlew ^a	Sweden and Finland	Autocatalytic (acid by-products)	Continuous	180 ⁹⁸	2	40-50 ⁸⁵	nf ^d	^{58,72,85,98,106}
Supratherm ^b	Germany	H ₂ SO ₄ or autocatalytic	Continuous	200-230 ^{58,107}	Few s ^{58,107}	High	1988	⁵⁸
Stake ^b	Canada	Autocatalytic	Continuous ¹⁰⁸⁻¹¹⁰	230	0.105	66	1978	⁵⁸
Suprayield ^{a,b,e}	South Africa	H ₃ PO ₄ or autocatalytic	Continuous	240-180 ^{25,58,85}	0.0014- 0.017 ^{25, 103}	70 ^{25,85} to 80 ¹⁰³	1999	^{58,85,86,103,104}
Biofine ^a	U.S.A.	H ₂ SO ₄	Continuous	190-200	0.33	70-84	1988-1996	^{8,85,111-113}
Vedernikov ^b	Latvia	H ₂ SO ₄	Continuous	170	1	70-80	1996-1999	^{85,88-90,114,115}
MTC ^{a,f}	The Netherlands	H ₂ SO ₄	Continuous	nf ^d	0.41	>86	2010-to present	^{8,85}
CIMV ^{a,g}	France	Autocatalytic	Continuous	100-120 ¹¹⁶	1-3 ¹¹⁶	nf ^d	1999-to present	^{8,91,116-118}
Lignol ^a	Canada	Acetic acid	Continuous ¹¹⁹	180-200 ^{93,120}	0.5-1.5 ¹²⁰	nf ^d	2001-2009 ^{119,121}	⁸

Chempolis ^a	Finland	Autocatalytic	Continuous	110-125 ^{95,96}	0.33-1.33 ^{95,96}	nf ^d	1997-to present	¹¹⁸
Montane et al. ^c	Spain	H ₂ SO ₄	Continuous	220-240	Few min	50-65	2002	¹²²
Rong Xing et al. ^c	U.S.A	HCl or H ₂ SO ₄	Continuous	110-220	3 h	92.2 [HCl]	2011	¹²³
a) Industrial process. b) patented process. c) other processes. d) nf = information not found. e) Suprayield process was recently owned by the Proserpine Corporative Sugar Milling Association Ltd., Australia, ^{85,124} and by the India Arcoy Biorefinery Private Ltd. ^{8,85,125} f) MTC process (Multi-Turbin-Column) was developed by Technical University of Delft. ^{8,85} g) CIMV-Compagnie Industrielle de la Matière Végétale.								

Table 1.3- Pilot scale processes to produce 2-furaldehyde (Fur) that operate with sulfite liquor.⁵⁸

Industrial Process	Country	Reactor	Temperature (°C)	Reaction Time (h)	Observations
Voest-Alpine	Austria	Continuous	150-180 ^{126,127}	0.17-0.42 ^{126,127}	Without any applications since the use of calcium liquor was prohibitive due to fouling and with magnesium sulfite pulping there is no incentive to make Fur since there is no effluent.
Reactive Desorption	Czechoslovakia	Continuous	140-220	nf ^b	Steam injection was thermodynamically incapable of boiling sulfite liquor, and consequently any Fur formed in this column remained dissolved in the liquid phase, where it reacts with itself, with intermediates of the conversion of the pentose to Fur and with other ingredients of liquor, thus incurring many losses.
Enforced Ebullition ^a	Germany	Continuous	240-234	nf ^b	In addition to steam as primary heating agent, a hot gas is used to bring the liquor from the steam condensation temperature to boiling, to avoid the loss reactions of Fur with itself and with intermediates of the conversion of the pentose to Fur. Nevertheless the decomposition of the pentose with lignosulfonated and other ingredients is not avoided.
a) No reference to pilot scale testing. b) nf = Information not found.					

During the 1990s, the world production of Fur changed from developed countries to developing countries (China).⁷² The inexpensive Fur imports from China and the Dominican Republic led to the closure of USA plants (between 1995 and 2003);⁷² and since 2005, U.S.A. is no longer a Fur producer.¹²⁰ In 1998 the world market for Fur was ca. 142 000 ton.year⁻¹.^{41,128} In 2005 it was estimated to be between 250 000-300 000 ton.year⁻¹,^{11,25,72} which was continued until 2011;^{4,99} very recently this value was reported to be 400 000 ton.year⁻¹.⁸⁰ China is the biggest Fur producer (ca. 200 000 ton.year⁻¹), and exporter, accounting for over 70% of the global Fur production (with tendency to increase).^{25,72,79,99,129} The other main producers are the Dominican Republic (32 000 ton.year⁻¹, 2005) and South Africa (20 000 ton.year⁻¹, 2005).^{25,72} In 2009, 5 000 ton.year⁻¹ of Fur were planned to be produced by the Suprayield process in Proserpine, Australia (by the Propersine Corporation Sugar Milling Association Ltd).^{85,124} Afterwards in 2010, the India Arcoy Biorefinery Private Ltd at Panoli, Ankleshwar (Gujarat Province) plans to produce Fur at 11 000 ton.year⁻¹ based on this Suprayield one process.^{85,125} The MTC, a similar process to the Suprayield had a capacity to produce ca. 10 000 ton.year⁻¹.^{8,85} Gravitis in 2000 and 2001 reported that a plant in Russia based on the Verdernikov process,⁸⁸⁻⁹⁰ produces 4 300 ton of Fur and 8 800 ton of ethanol per year.^{130,131}

The International Furan Chemicals B. V. founded in 1994 in the Netherlands is the leading market provider in the field of Fur and furfuryl alcohol worldwide: Fur is produced in one of the world's largest Fur facilities, Central Romana Corporation, located in the Dominican Republic, and converted to furfuryl alcohol at the related party, TransFuran Chemicals in Belgium.⁶⁵ The DalinYebo group founded in 2001 also markets and sells Fur.¹³²

1.3.1.2. Applications

Fur is a key chemical used in the synthesis of a wide range of added-value compounds and non-petroleum derived chemicals that have several present and potential applications in plastics, pharmaceutical,^{58,106,130} and agrochemical industries.⁵⁸ Presently Fur is used as a solvent to remove aromatic compounds from lubricating oils and diesel fuels,^{58,106,130} and to obtain unsaturated compounds from vegetable oils to make drying oils; as a fungicide for growing plants and wood; and as a nematocide.⁵⁸ The major use of Fur (ca. 65%) is as an intermediate for the synthesis of furfuryl alcohol (FA) which in turn is essentially used for producing furan resins, which

are used as binding agents in foundry technologies (e.g. urea furan resin, a binding material used in metallurgy for heavy metals and precision casts and dies).^{71,80,106,130,133-136} Fur is used as an intermediate to produce surface coatings,⁷² polymers,^{71,72} mortar, adhesives for foundry cores and moulds, boiler, and floor grouting (by FA),⁷² nylons and lubricants.^{106,130}

Figure 1.11 illustrates some of the added-value products obtainable from Fur.^{80,137} Fur can be hydrogenated to tetrahydro-2-furaldehyde (THFF) (which in turn by self-aldol condensation can be converted to a diesel fuel),¹³⁸ furfuryl alcohol (FA) (for furanic resins or plastics),^{80,137,139,140} 2-methylfuran (MF), tetrahydrofurfuryl alcohol (THFA) and methyltetrahydrofuran (MTHF).^{11,32,75,80,113} FA is one of the most common products of Fur produced worldwide representing 65% of Fur conversion.⁵⁸ MTHF (20 wt.% oxygen content) was approved by the USDOE (US Department of Energy) for use as gasoline additive in P series type fuels and is a component of P-series fuel.^{11,141} P series fuels are defined as renewable and non-petroleum clear liquid fuels that can substitute gasoline and are used in flex-fuel vehicles (FFVs) and spark-ignition engines.¹⁴² Besides MTHF, P series fuels contain a mixture of ethanol (55%) and pentane-plus (27.5%) and normal butane (in a vestigious quantity).¹⁴³ It was patented in 1997,¹⁴⁴ and an exclusive license for commercialisation is owned by the Pure Energy Corporation (PEC) since 1998, when P-Series were recognised as alternative fuels in accordance with the Energy Police Act of 1992.¹⁴³ Over aqueous phase processing, Fur is an intermediate that can produce liquid straight-chain alkanes in the range C₈₋₁₃ useful to make jet and diesel fuels.^{11,123,138,145-147} Jet fuels are complex hydrocarbon mixtures that consist of different classes such as paraffin, naphthene and aromatics, which were especially designed as an aviation fuel for use in aircraft by gas-turbine engines.^{145,148,149} Fur can be transformed into furan, a widely used solvent in industry, by pyrolysis (which promotes the break of the aldehyde group) or by hot alkali (since fused alkali allows the oxidation of the aldehyde group into furoic acid and subsequent decarboxylation).¹⁵⁰ Furthermore furan gives THF (by hydrogenation),^{106,140} acetylfuran and difuranpropane (DFP) that by hydrogenation gives (Di-tetrahydrofuran)propane (DTHFP).¹⁰⁶ Furoic acid is converted to tetrahydrofuran-2-carboxylic acid (THFAC) by hydrogenation, or to methylfuran-2-carboxylate (MCFAT) by esterification.¹⁰⁶ Methyltetrahydrofuran-2-carboxylate (MTHFAT) and tetrahydrofuran-2-methanamine (THFAM) are other Fur derivatives.¹⁰⁶

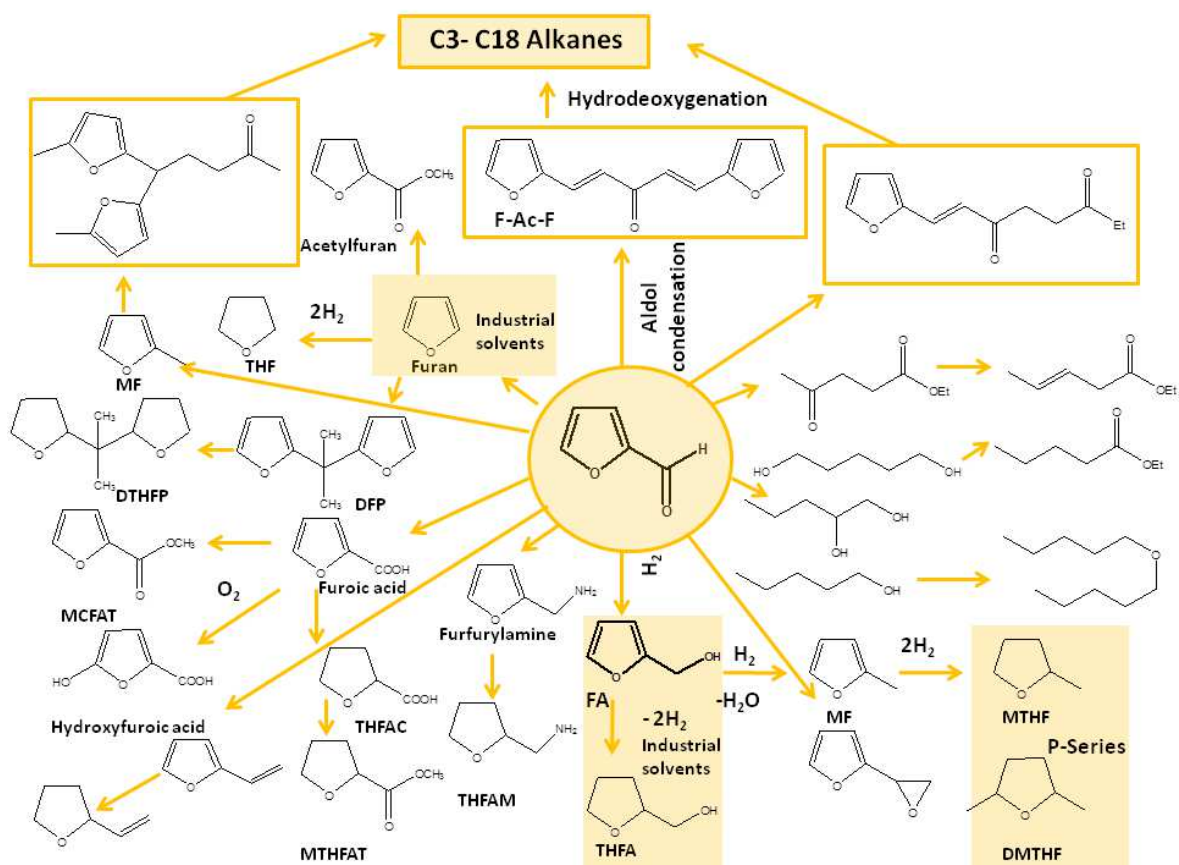


Figure 1.11- 2-Furaldehyde (Fur) platform for biofuels [adapted from ^{80,106,137,140,151}].

Desirable jet and diesel fuel range alkanes (C8-C13) can be obtained by base-catalysed aldol condensation of Fur into higher molecular weight products which can subsequently undergo dehydration and hydrogenation to give linear alkanes such as tridecane (Figure 1.12). Xing et al.¹⁴⁵ achieved high yields of alkanes by this procedure. The aldol condensation occurs between the carbonyl group of Fur and the carbonyl group of acetone, forming a β -hydroxycarbonyl derivative, which by dehydration gives origin to α,β -unsaturated carbonyl compounds: Fur-acetone monomer (F-Ac, C8 product) and Fur-acetone dimer (F-Ac, C13 product).^{152,153} Further hydrogenation gives alcohol H-dimer or spiro H-dimer. Tridecane is finally produced by hydrodeoxygenation. Xing et al.¹⁴⁵ used a bi-functional Pt/SiO₂-Al₂O₃ catalyst.

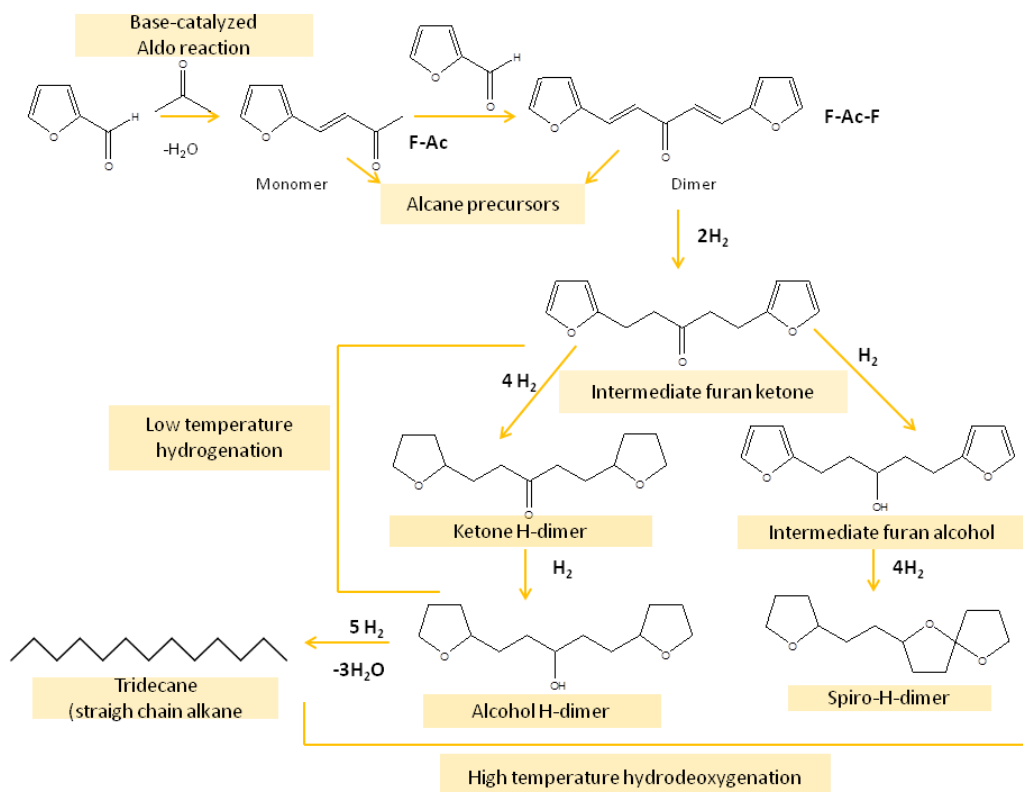


Figure 1.12- Production of tridecane from 2-furaldehyde (Fur) [adapted from ^{145,154}].

1.3.2. 5-Hydroxymethyl-2-furaldehyde and applications

Hmf is a yellow solid which melts at relatively low temperatures (28-34 °C) and has a boiling point of 114-116 °C (for a pressure of 1 mmHg).¹⁵⁵ Hmf was discovered in 1895 by Düll¹⁵⁶ and Kiermeyer¹⁵⁷ while developing methods to prepare oxymethyl-2-furaldehyde. While Düll heated inulin with oxalic acid, Kiermeyer used sugar cane. Later, in 1919, Middendorp¹⁵⁸ presented a full and detailed study concerning the synthesis, physical characterisation and chemical behaviour of Hmf. Hmf is a more functionalised molecule than Fur; it consists simultaneously of a primary aromatic alcohol, an aromatic aldehyde (apart from the furan ring system) (Figures 1.6 and 1.8). Hmf has a weak cytotoxicity and mutagenicity in humans, except for Hmf concentrations above to 12 mM.¹⁵⁹ Above these values it is cytotoxic, causing irritation to eyes, the respiratory tract, the skin and the mucous membrane.¹⁶⁰ Hmf is present in many foods in low quantities.¹³⁷ Some examples comprise honey,¹⁶¹⁻¹⁶³ fruit juices,^{161,162,164,165} milk,^{161,166,167} vinegars,^{161,168} jams and

alcoholic products,¹⁶¹ biscuits^{161,162,169} and meat products.¹⁷⁰ Higher amounts were found in bread,^{169,171} coffee,^{170,172} dried fruits, juices, caramel products,¹⁷⁰ prunes, dark beer, canned peaches and raisins,¹⁷² breakfast cereals,^{162,173} jam,¹⁶² and soy sauce.¹⁵⁹ In fresh food it is absent.¹⁶⁰ Hmf is obtainable from hexose-based polysaccharides such as cellulose or inulin via acid-hydrolysis to D-glucose or D-fructose, respectively, being further dehydrated to Hmf (Figure 1.8).⁴ In 1944, Haworth et al.¹⁷⁴ made an important contribution to the knowledge of the mechanism of formation of Hmf. Newth¹⁷⁵ was the first to publish a review about Hmf in 1951, and many others were followed which keep on growing every year very fast, proving its great importance.^{15,38,71,74,151,176-185}

The production of Hmf has not gone beyond the pilot plant scale.^{186,187} In 1993 an evaluation of the costs to produce Hmf indicated a Hmf marketing price of at least 2500 €.ton⁻¹.¹⁵ More recently, Dumesic reported a techno-economic analysis of Hmf production from D-fructose and referred that the market for Hmf could be comparable with that of terephthalic acid (which in the USA exceeds 4 million metric ton.year⁻¹).²⁰ For the production of Hmf from D-fructose the estimated costs were about \$ 102.4 million for the equipment and \$ 36.4 million for catalyst first charge and \$ 258.500 million for replacement every two years.²⁰ The estimated costs are quite high for a bulk-scale industrial product and the present politico-economical situation still favours the petroleum route.⁷¹

Efforts need to be taken into consideration because worldwide production can be larger for Hmf than for Fur as a result of the more abundant terrestrial resources containing hexoses than those containing pentoses. A successful commercial implementation to produce Hmf depends partly on the feedstocks availability and prices, lower capital costs and higher price for the by-product levulinic acid (which currently is \$ 300.ton⁻¹)²⁰; there are some important challenges to lower the price of Hmf as a biobased platform chemical.

Hmf can be used for the synthesis of dialdehydes, ethers, amino alcohols and other organic intermediates, that lead to solvents (e.g. furan, THFA and FA),¹⁸⁸ surface-active agents, phytosanitary products and phenolic resins.^{34,74,189} FA is obtained by the addition of H₂O to Hmf (Figure 1.13).^{38,190} Phenolic resins are formed by acid catalysed reaction of Hmf with phenol.^{15,71,191} Hmf can be converted into diesel fuel additives^{138,192,193} and biofuels,¹⁹⁴ similar to Fur. To obtain kerosene and other diesel fuel intermediates there is the need to increase the carbon chain length of Hmf,⁷⁰ which is done by aldol condensation and further aqueous phase dehydration-hydrogenation. The aldol condensation of Hmf might consist of a non C-C coupling or a cross

coupling (C-C) reaction.⁷⁰ In the non C-C coupling, furan derivatives (alkoxymethyl-2-furaldehyde ethers or esters) are formed by condensation with lower alcohols or carboxylic acids through the –OH group of Hmf.¹⁹⁵ In the cross coupling reaction, Hmf suffers cross condensation with acetone (or other aldehydes or ketones with at least one acidic α -proton). When using acetone the product obtained is 5-(hydroxymethyl)furfurylidene acetophenone (HMFIA) which by further hydrogenation of the keto group gives origin to 3-(hydroxybutenyl)-hydroxymethylfuran (HB-HMF).^{33,190} 5-(Hydroxymethyl)furfurylidene ester (HMFIE) is obtained by aldol-crossed condensation, (Figure 1.13).^{33,71} Since Hmf does not have an α -H it cannot undergo self-aldol condensation. The resulting condensation compounds are hydrophilic and rich in oxygen. This hydrophilicity can be reduced by subsequent hydrogenolysis giving origin to fuels of kerosene and other diesel range products.⁷⁰

Disubstituted furan derivatives of Hmf include several compounds, such as 2,5-furandicarboxylic acid (FDCA), diformylfuran (DFF) and 2,5-dimethylfuran (DMF) (Figure 1.13).^{15,32-34,38,71,74,140,177,185,196-199} They have potential to replace some important petrochemicals to produce polyesters or to be used as liquid transportation fuels. FDCA is a promising substitute of terephthalic acid,^{177,200} and is obtained by oxidation of DFF, which in turn is obtained by oxidation of Hmf.^{15,33} DMF and 2-methylfuran (MF) are obtained by hydrogenation of Hmf,^{11,32,33,35,38,138,188,201,202} and have the advantage of being less volatile and of 40% higher energy density than ethanol.⁷⁴ 5-(hydroxymethyl)furfurylidene acetophenone (HMFA) is another product of Hmf oxidation.^{71,151} The direct hydrogenation of Hmf leads to the formation of 5-hydroxymethyltetrahydro-2-furaldehyde (HMTHFA),³³ 2,5-dihydroxymethylfuran (DHMF),^{33,140,190,203-208} and 2,5-di-(hydroxymethyl)tetrahydrofuran (DHMTHF).^{33,190,209-211} 2,5-furfuryldiisocyanate (FFDI),⁷¹ and 2,5-bis(aminomethyl)furan (BAMA)^{15,71,151} are other Hmf derivatives. Other applications may include pharmaceuticals with a wide spectrum of biological activities;^{15,212} (e.g. Hmf was found to bind specifically with intracellular sickle hemoglobin (HbS), inhibiting the formation of sickled cells in blood²¹³); thermoresistant polymers synthesized via reactions involving the carboxylic acid groups in FDCA;^{18,38,70,74,140,214} and macrocyclic compounds (e.g. oxo-porphyrines, oxo-annulenes, and alkenyl or alkynyl furans synthesised via reactions involving the dialdehyde group in DFF and FDCA, and possessing biological activity).^{74,177,185} Derivatives of Hmf have been utilized as fungicides, corrosion inhibitors and flavoring agents.¹⁷⁷ Decomposition of Hmf can give levulinic acid and formic acid;^{33,34,38,71,74,190,215} levulinic acid is a versatile chemical for the synthesis of various bulk chemicals with applications as fuel additives,

resin precursors, etc.²¹⁵ Hmf can be converted to Fur by decarboxylation,¹³⁷ or carbonylated into 5-formylfuran-2-acetic acid (FFAA).²¹⁶

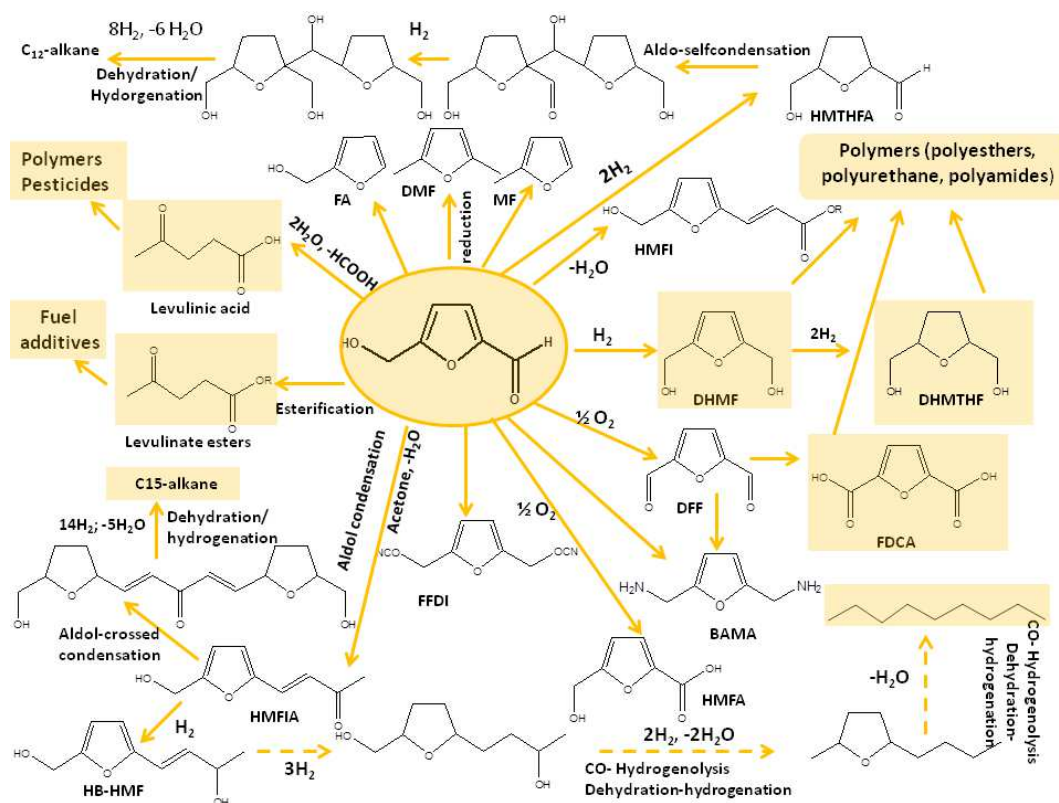


Figure 1.13- Some added value chemicals derived from reactions of 5-hydroxymethyl-2-furaldehyde (Hmf).^{15,33,34,38,71,74,140,151,185,190,202,215}

Until 2000, a way to produce kerosene and other diesel range fuel intermediates from Hmf without the need for complementary feedstocks (e.g. ethanol or acetone) was unknown. James et al.⁷⁰ presented reaction routes where these products could be obtained with Hmf alone as the feedstock, by reacting two or more Hmf molecules through the -OH or -CO groups. These reactions include: the benzoin reaction, the hetero Diels-Alder reaction, acid condensation and ketosination (Figure 1.14).⁷⁰ To obtain the respective fuels hydrogenolysis must then be employed.

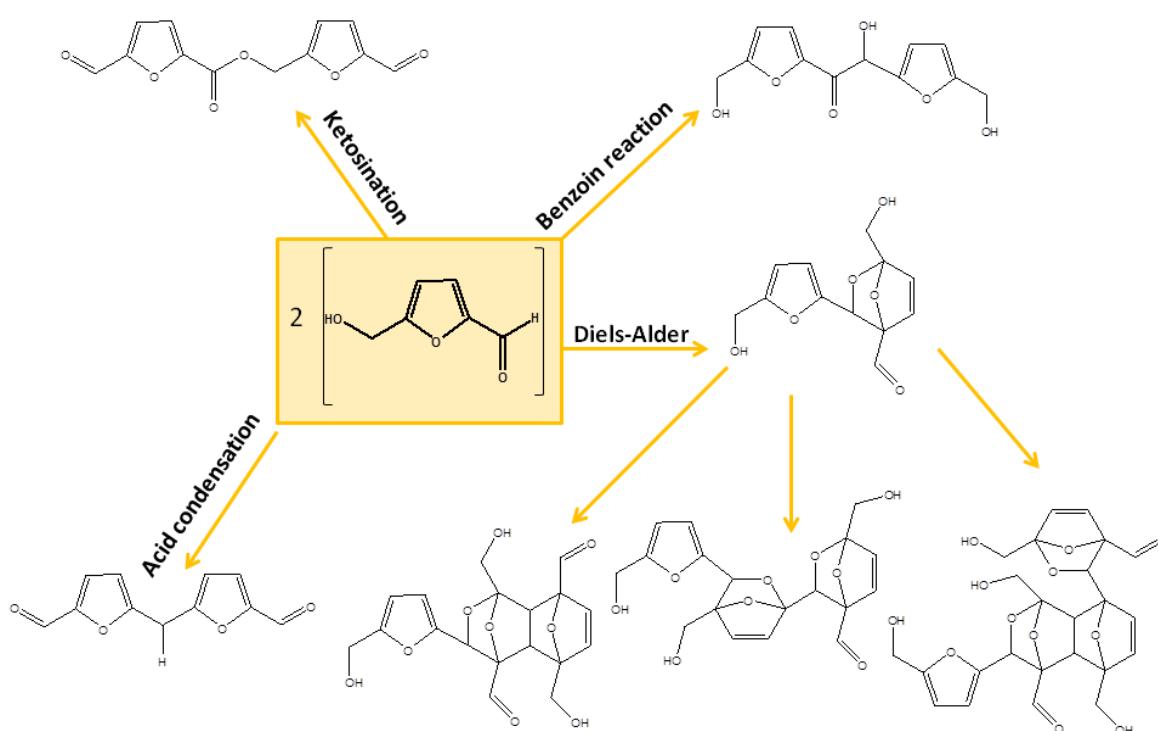


Figure 1.14- Reaction routes of 5-hydroxymethyl-2-furaldehyde (Hmf) to kerosene and diesel range intermediates [adapted from ⁷⁰].

1.4. Catalytic conversion of saccharides to furanic aldehydes

1.4.1. Reaction mechanism of the conversion of saccharides to furanic aldehydes

The mechanisms for the hydrolysis of polysaccharides into the respective pentoses and hexoses and subsequent dehydration into the furanic aldehydes have been extensively investigated using liquid acids, particularly mineral acids such as H_2SO_4 . Some mechanistic aspects are discussed in this Section.

The mechanism of the acid-catalysed hydrolysis of a polysaccharide, proposed by Abatzoglou et al.²¹⁷ is exemplified for the case of cellulose in Figure 1.15. It involves the protonation of the glucosidic oxygen (which is linked to two sugar units) by the proton of the acid, followed by the cleavage of the C-O bond and the simultaneous formation of a lower molecular

weight cellulosic chain and of a relatively unstable carbocation. The formation of this intermediate is faster at the end than in the middle of the chain.²¹⁸ Finally, the carbocation reacts with water giving origin to another smaller cellulosic chain (with a hemiacetal end group) and the acidic H^+ is regenerated.²¹⁷ This sequence of processes is repeated until the monomer (D-glucose) is formed.⁵⁸ This mechanism can also apply for the case of furanosides, characteristic of hemicellulosic structures. The furanosides have a higher reaction rate than the pyranosides.²¹⁷

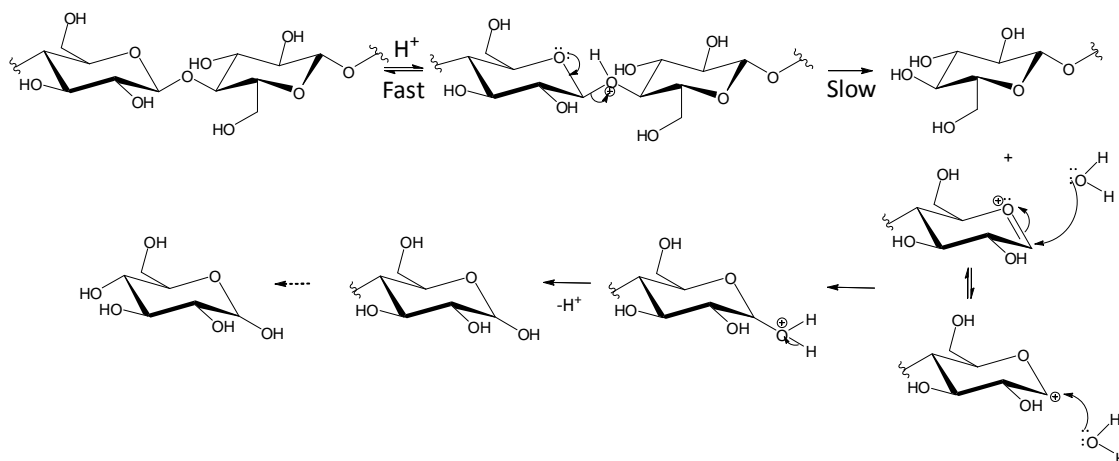


Figure 1.15- Mechanistic proposal for the hydrolysis of cellulose.²¹⁷

In the dehydration of a pentose into Fur, three water molecules are released per Fur molecule that is produced.⁵⁸ Hydroxyl groups are transformed into H_2O^+ by the presence of a Brönsted acid which leads to the release of a water molecule and to the formation of carbocation intermediates. According to Antal et al.²¹⁹ there are two possible mechanisms for the dehydration of D-xylose to Fur. These two mechanisms basically differ in the hydroxyl group that is first protonated. The xylofuranose intermediate can be formed by elimination of the OH group at C-1 (giving xylosyl cation) and subsequent substitution of O-2 at C-5 with simultaneous scission of the C-5-O-5 linkage. Afterwards the loss of two more water molecules leads to the formation of Fur (Figure 1.16).

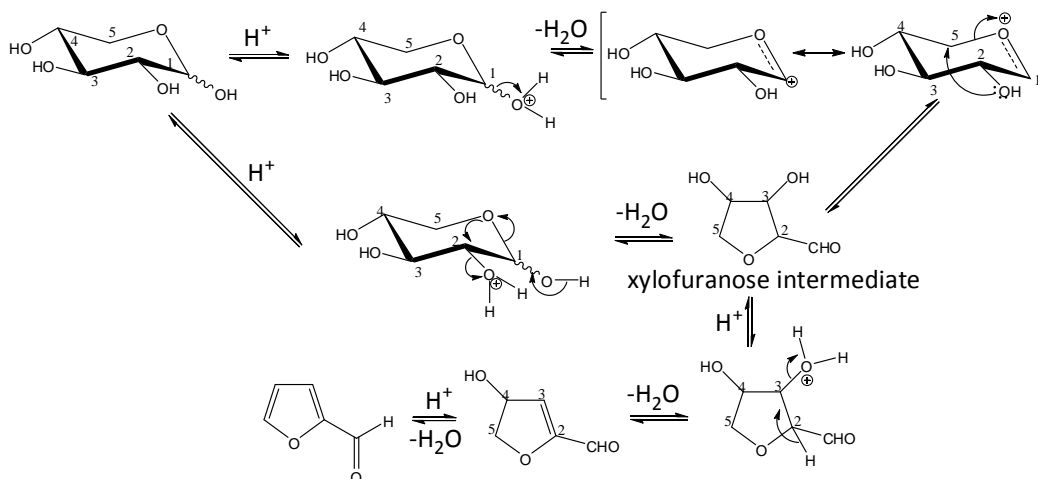


Figure 1.16- Reaction mechanism for the dehydration of D-xylose (Xyl) to 2-furaldehyde (Fur) proposed by Antal et al.²¹⁹

During the dehydration reaction of a pentose into Fur, several side reactions take place. Figure 1.17 shows some of the possible by-products during the dehydration of D-xylose into Fur. D-xylose in an open-chain form can suffer isomerisation into lyxose and xylulose, and decomposition into fragmentation products. Lyxose can undergo dehydration to give Fur.^{219,220} If Fur formed remains in the liquid phase containing the catalytically active species, two types of secondary reactions can take place.⁵⁸ Fur reacts with itself, which is the so-called resinification reaction; Fur reacts with intermediates of the conversion of the pentose, commonly referred as condensation reactions of Fur. According to Antal, Fur does not react directly with D-xylose.^{219,221}

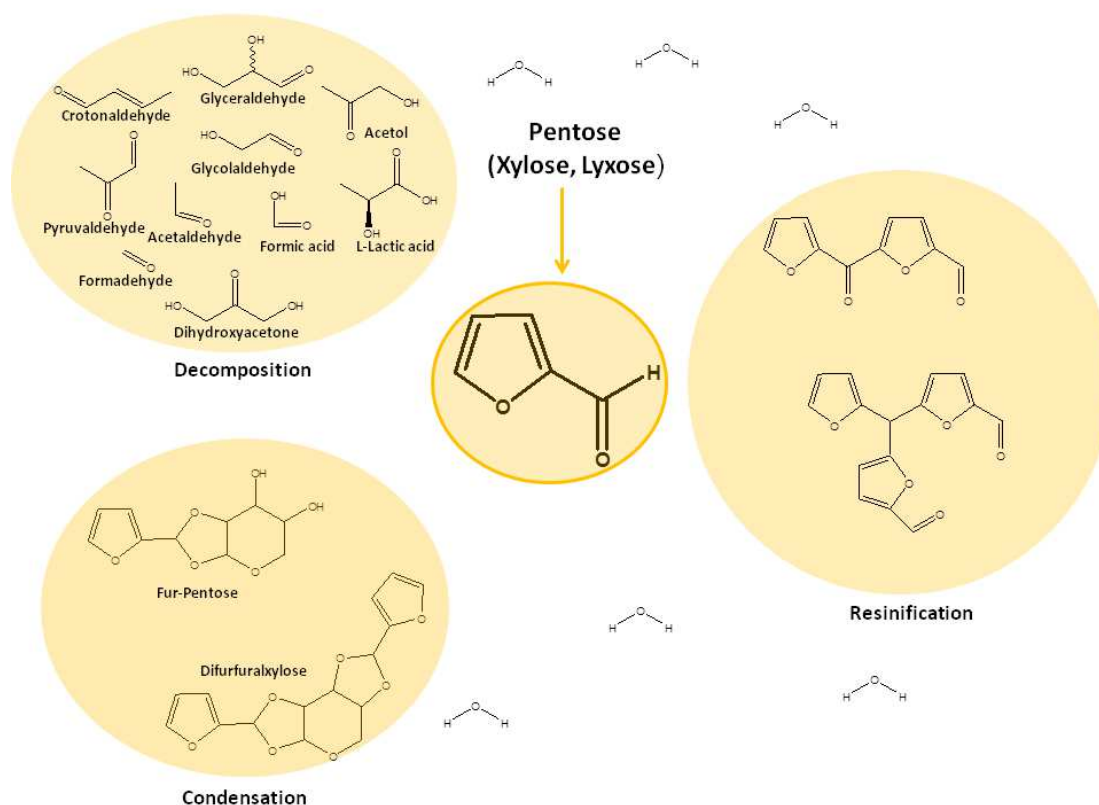


Figure 1.17- By-products formed by decomposition reactions of D-xylose (Xyl) in acidic medium or condensation or resinification of 2-furaldehyde (Fur) [adapted from ^{58,99,219}].

Side reactions may be avoided by reducing the reaction time and increasing the temperature.^{58,133,221} This procedure may decrease the resinification of Fur because higher temperatures inhibit the formation of larger molecules (entropy effect).⁵⁸ On the other hand, Fur loss reactions can be avoided by using as organic co-solvent that extracts Fur from the aqueous phase as it is formed.²²² Fur reaction losses are higher for condensation reactions than for resinification.⁵⁸

The acid catalysed dehydration of hexoses (mainly D-fructose and D-glucose) gives Hmf. D-Fructose as substrate tends to give higher Hmf yields than D-glucose.^{34,74,99,223,224} In the case of aqueous phase reactions considerable amounts of by-products (e.g. levulinic acid and oligomers) are produced.³⁴ In order to enhance selectivity to Hmf in the reaction of D-glucose it is necessary to promote the selective isomerisation of D-glucose to D-fructose prior to the dehydration to Hmf which can be done by the addition of a base catalyst (Figure 1.18).^{34,74,99,201,224}

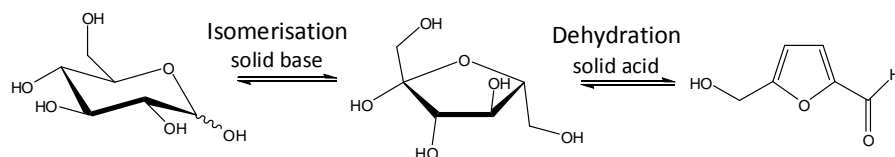


Figure 1.18- Isomerisation of D-glucose to D-fructose followed by the acid-catalysed dehydration to 5-hydroxymethyl-2-furaldehyde (Hmf) [adapted from ^{34,74,99,201,224}].

The type of reaction mechanism is difficult to establish due to the small lifetimes of the intermediate species. Haworth et al.^{174,225} proposed the first mechanism for the dehydration of D-fructose to Hmf, based on the formation of the fructofuranosyl cation as intermediate. The formation of Hmf can proceed by two possible pathways: the acyclic and cyclic route.⁷⁴ In the following works, Antal et al.²²⁶ and Newth¹⁷⁵ proposed the cyclic route due to the evidence of the intermediate enol (Figure 1.19).

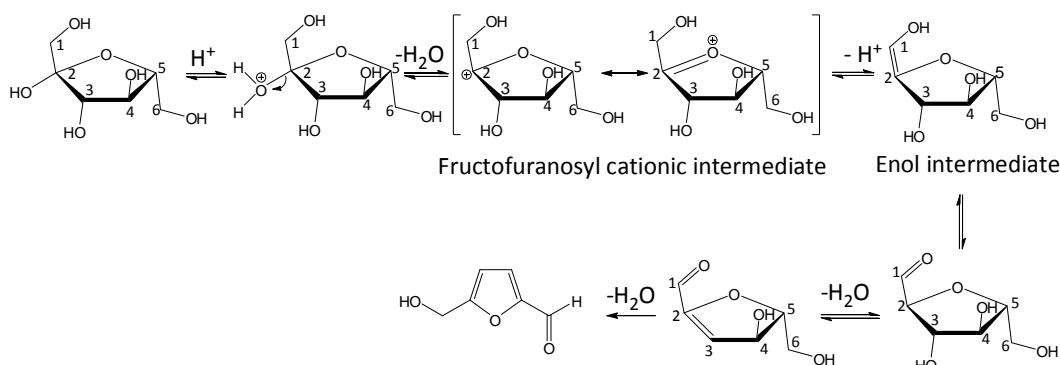


Figure 1.19- Reaction mechanism of the dehydration of D-fructose to 5-hydroxymethyl-2-furaldehyde (Hmf) proposed by Antal et al. [adapted from ²²⁶].

Other authors have suggested the more complex acyclic route through an open-chain 1,2-enediol mechanism.^{74,178,223} In the acyclic route the 1,2-enediol undergoes β-elimination to form deoxy-hexosulose intermediates which suffer dehydration to give Hmf (Figure 1.20). Retro aldol cleavage gives Fur and dehydration of 2,3-enediol gives hydroxyacetylfructose.²²³ For D-glucose or other hexoses the Hmf yields are lower due to their small extension into enol intermediates.²²³

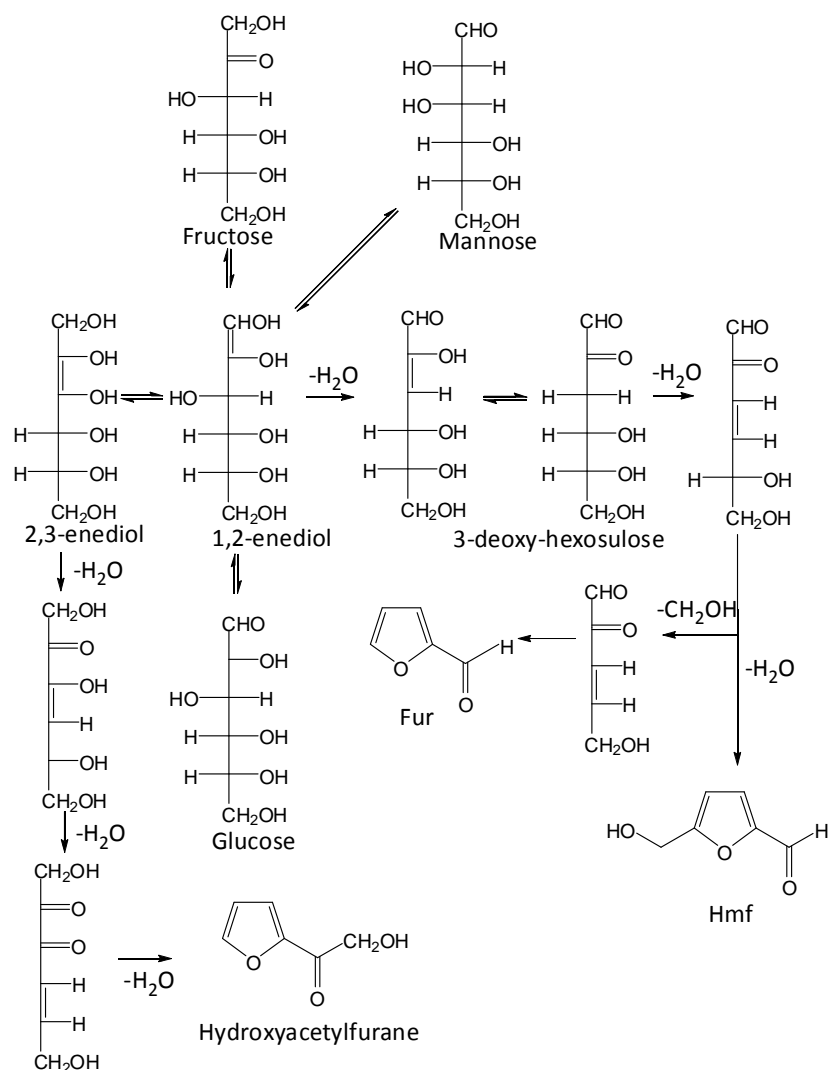


Figure 1.20- Reaction mechanism for the dehydration of D-fructose to 5-hydroxymethyl-2-furaldehyde (Hmf) based on the acyclic route [adapted from ²²³].

More recently, Assary et al.²²⁷ confirmed the mechanistic proposal of Antal et al.²²⁶ by investigating the formation of fructofuranosyl intermediate species, the enol and the aldehyde intermediates in neutral and acidic environments by theoretical studies, including calculations of enthalpies, free energies and effective solvation interaction. In work carried out by Caratzoulas et al.²²⁸ free-energy calculations using hybrid quantum mechanics/molecular simulations indicated that the reaction of D-fructose to Hmf proceeds via intramolecular proton and hydride transfers (Figure 1.21). The first dehydration was similar to the mechanistic proposal by Haworth et al.^{174,225} and developed by Antal et al.,²²⁶ but the second dehydration step was found to involve

three sequential, elementary steps: a) hydride transfer from C-1 to C-2 (Intermediate-1 (I-1) to I-2), b) proton transfer from O-1 to O-3 (I-2 to I-3) and c) dehydration (I-3 to I-4). The third and final dehydration step involves a hydride transfer to C-4 (I-5 to I-6), followed by a proton transfer from C-3 to O-4 (I-6 to I-7) with further water loss.²²⁸

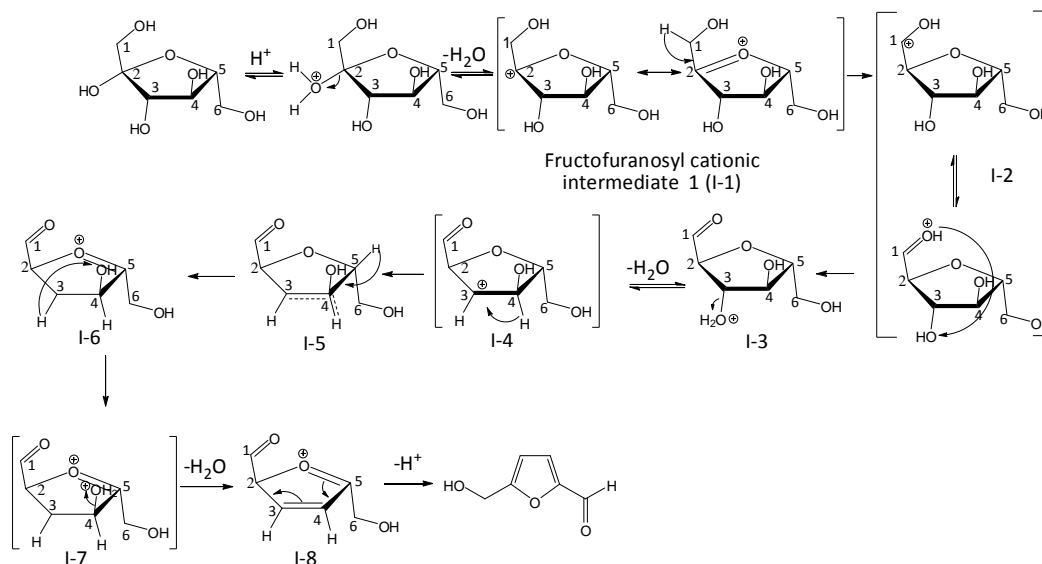


Figure 1.21- Reaction mechanism for the dehydration of D-fructose to 5-hydroxymethyl-2-furaldehyde (Hmf) proposed by Caratzoulas et al. [adapted from²²⁸].

The conversion of hexoses to Hmf may be accompanied by different types of reactions including isomerisation (e.g. D-glucose and D-mannose to D-fructose),^{74,185,224,226,229-232} dehydration (besides Hmf, other by-products may be formed such as 5-methyl-2-furaldehyde (MFF), α -angelica lactone (AAL), β -angelica lactone (BAL), 2-(2-hydroxyacetyl)furan (HAF), 2-(2-hydroxyacetyl)furan formate (HAFF), 4-hydroxy-2,3,5-hexanetrione (HHT), 4-hydroxy-2-(hydroxymethyl)-5-methyl-3(2H)-furanone (HHMMF) and isomaltol),²²⁶ fragmentation reactions of the monosaccharides and condensation reactions.^{74,185,224,226,233,234} Decomposition of Hmf to levulinic and formic acids (I) (favoured at a low pH),^{74,185,224,226,231-233,235,236} self-polymerisation between Hmf molecules (II),^{29,235} or cross polymerisation between Hmf and the hexose (III)^{35,224,235} are possible side-reactions which can lead to the formation of insoluble by-products, humins (favoured at high pHs) (Figure 1.22).^{185,224,226,233,235-237} Self polymerisation between hexose molecules can also take place leading to difructose dianhydrides and levulosans (soluble polymers), in the case of D-fructose.²²⁴ Other by-products during the conversion of D-fructose to

Hmf include dihydroxyacetone and glyceraldehyde from a retro-aldol reaction of D-fructose; pyruvaldehyde by dehydration of glyceraldehyde,^{188,226} and 5-hydroxy-4-keto-2-pentenoic acid (HKPA).^{185,238}

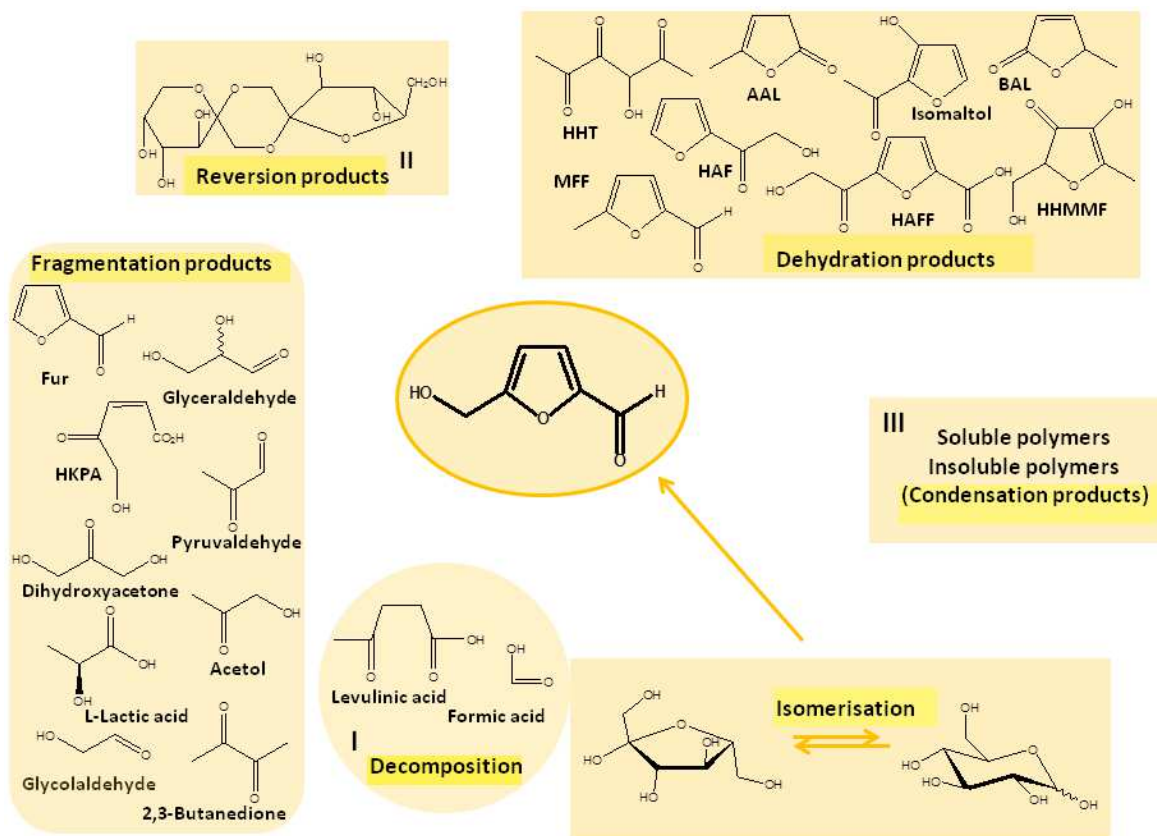


Figure 1.22- 5-Hydroxymethyl-2-furaldehyde (Hmf) reaction products [adapted from ^{185,226,231,235}].

1.4.2. Type of acid catalysts

The syntheses of furan derivatives from saccharides in the presence of catalysts have attracted much attention.⁷⁴ Several types of acid catalysts have been tested for the dehydration of pentoses and hexoses to Hmf and Fur, and may be divided into liquid or solid (soluble or insoluble). These reactions have been studied employing a single solvent (water or organic solvents)^{196,219,229,233,239-254} or a biphasic solvent system (water and an organic co-solvent or two immiscible organic solvents).^{29,145,223,240,247,249,250,255-262} In some cases Hmf or Fur is obtained in a

one-pot hydrolysis/dehydration step from di or polysaccharides in either a mono^{196,239,253,254,263} or biphasic solvent system.^{29,145,256,262} Tables 1.4 and 1.5 show examples of the investigated catalysts, which can be grouped according to their physical state in the pure form (e.g. liquid or solid acids). The investigated (molecular) liquid acids are essentially (inorganic) mineral acids and some organic acids; in general these are Brønsted acids, some are soluble in the reaction medium such as Lewis acid salts and Brønsted heteropolyacids of the Keggin type, and others are insoluble (heterogeneous). In the case of insoluble solid acids some are organic materials such as, acid ion-exchange resins (Brønsted acids), others are inorganic such as zeolites and zeotype materials (possess Brønsted and Lewis acid sites), or hybrid organic-inorganic materials such as mesoporous silicas functionalised with sulfonic acid groups (Brønsted acid sites).

Mineral acids such as H₂SO₄ or HCl have been extensively used as catalysts for the conversion of carbohydrates to furanic aldehydes. In particular H₂SO₄ continues to be the common industrial catalyst. However it poses risks to human health (high toxicity), the environment (due to the difficult catalyst recovery/recycling and sulfur-containing by-products resulting from catalyst residues leading to expensive purification procedures), and equipment corrosion hazards.^{58,240,264} For these reasons the production of Fur and Hmf is one process where the demand for green chemistry is stimulating the use of recyclable and less-toxic acid catalysts.^{265,266}

Heterogeneous acid catalysts are promising alternatives to homogeneous ones because their use may allow overcoming typical disadvantages associated with the use of homogeneous catalysts: e.g. the separation of the catalyst from the reaction products is easier (e.g. via filtration) which can lower the costs of the process, as separation processes typically represent more than half of the total investment in the equipment.^{267,268} Neutralisation steps at the end of the reaction in the presence of mineral acids (with the formation of waste products) are avoided through the use of heterogeneous catalysts. Heterogeneous catalysts can be quite resistant to high temperatures, which is favourable in terms of the catalyst lifetime. Solid acids can lead to higher selectivities towards Hmf than homogeneous ones.^{239,267} The acid properties of solid acid catalysts can be fine-tuned in order to improve the Fur/Hmf yield.⁷⁴ The design of selective catalysts with isolated active sites for one-pot transformation processes is a challenge.²⁶⁹ The literature data related to the use of saccharides to Fur and Hmf using water or organic solvents is summarised in the Section 1.4.2.

Table 1.4- Catalysts tested in the conversion of pentoses and related di/polysaccharides.

Liquid Acids		Solid Acids				
Organic	Inorganic	Soluble	Insoluble			
			Organic	Hybrid	Inorganic	
					Zeolites and Zeotypes	Others
CH ₃ COOH ²⁷⁰ HCOOH ²⁷⁰	HCl ^{29,270-277} HCl(NaCl), HCl(KCl), HCl(CaCl ₂), HCl(KBr), HCl(FeCl ₃) ²⁷² HCl (CrCl ₂) ²⁷⁷ H ₃ PO ₄ ^{29,270,278,279} H ₂ SO ₄ ^{29,231,241,255-257,270,272,275,280,281} HNO ₃ ²⁷⁰	<i>para</i> toluene sulfonic acid (TsOH) ²⁸⁰ Yb(OTf) ₃ ²⁷¹ YCl ₃ ²⁸² CrCl ₂ , CrCl ₃ , CrBr ₃ ²⁷⁷ CrCl ₂ (LiBr), CrCl ₂ (NaBr), CrCl ₃ (LiBr), CrBr ₃ (LiBr) ²⁷⁷ AlCl ₃ ²⁷⁵ AlCl ₃ ·6H ₂ O ²⁸³ SnCl ₂ ²⁷⁵ SnCl ₄ ·5H ₂ O ²⁷⁴ Cs _x H _{3-x} PW ₁₂ O ₄₀ , x < 2.5 ²⁸⁴ H ₃ PW ₁₂ O ₄₀ ^{275,280,284,285} H ₄ SiW ₁₂ O ₄₀ ²⁸⁰ H ₃ PMo ₁₂ O ₄₀ ²⁸⁰ VOPO ₄ ·2H ₂ O, VOHPO ₄ ·0.5H ₂ O, VO(H ₂ PO ₄) ₂ , γ-VOPO ₄ , VO(PO ₃) ₂ ²⁸⁶ (VO) ₂ P ₂ O ₇ ²⁸⁶	Amberlyst-15 240,248,274 Amberlyst-70 271,287 Nafion-SAC-13 271,288 Nafion-117 ²⁸⁸	SBA-15-SH, SBA-15-SO ₃ H(C), ^a SBA-15-SO ₃ H(G), ^b 257 MCM-41-SO ₃ H 240,289 MSHS-SO ₃ H, ^c HMS-SO ₃ H ²⁸⁹ Hybrid SO ₃ H ²⁴⁰ MP-NH-PW ₁₂ O ₄₀ , ^d LP-NH-PW ₁₂ O ₄₀ , ^{e,285} SCBC ^{f,256}	H-Beta ^{249,290} SnBeta ²⁷⁴ H-ZSM-5 ^{220,249} H-Y Faujasite 222,249,271,291,292 H-Mordernite 222,249,292 H-Ferrierite ²⁴⁹ Nu-6, H-Nu-6 del-Nu-6 ²⁶⁵	Cs _{2.5} H _{0.5} PW ₁₂ O ₄₀ , MP _γ -Cs _x PW ₁₂ O ₄₀ , ^g x= 2.5 or 3; y=15 or 34 wt.% LP _γ -Cs _x PW ₁₂ O ₄₀ , ^g y=15 wt.% ²⁸⁴ MP _γ -PW ₁₂ O ₄₀ , ^g LP _γ -PW ₁₂ O ₄₀ , ^h y=15-34 wt.% ²⁸⁵ Niobium silicates: Na-AM-11, H-AM-11, Nb-MCM-41 ^{291,292} γ-Al ₂ O ₃ , SiO ₂ -Al ₂ O ₃ ^{249,271,281} Si, H-SBA-15 ^{257,293} Al-SBA-15 ²⁹⁰ Si, H-MCM-41 ²⁴⁰ Al-MCM-41 ^{290,292,294,295} Al-MCM-48 ²⁹⁰ Pt-MCM-48 ²⁹⁰ MSHS-Al ^{k,289} Al-phosphate complex ²⁸¹ Zr-P ^{i,271} ZrO ₂ ^{296,297} TiO ₂ ^{281,296,297}

Table 1.4- *Continued.*

						$\text{TiO}_2\text{-ZrO}_2$ ^{278,297} $\text{WO}_3\text{-ZrO}_2$ ^{271,278} $\text{SO}_4^{2-}/\text{Al}_2\text{O}_3, \text{SO}_4^{2-}/\text{SiO}_2,$ $\text{SO}_4^{2-}/\text{TiO}_2, \text{SO}_4^{2-}/\text{Fe}_2\text{O}_3$ ²⁵⁵ $\text{SO}_4^{2-}/\text{ZrO}_2$ ^{255,296,298} $\text{S}_2\text{O}_8^{2-}/\text{ZrO}_2$ $\text{S}_2\text{O}_8^{2-}/\text{Al}_2\text{O}_3\text{-ZrO}_2$ ²⁹⁸ $\text{S}_2\text{O}_8^{2-}/\text{ZrO}_2\text{-MCM-41},$ $\text{S}_2\text{O}_8^{2-}/\text{Al}_2\text{O}_3\text{-ZrO}_2\text{-MCM-41}$ ²⁹⁸ MSZ, MSAZ ^{j, 298} $\text{SO}_4^{2-}/\text{Nb}_2\text{O}_5, \text{SO}_4^{2-}/\text{SnO}_2,$ $\text{SO}_4^{2-}/\text{HfO}_2$ ²⁵⁵ $\text{SO}_4^{2-}/\text{ZrO}_2\text{-Al}_2\text{O}_3,$ $\text{SO}_4^{2-}/\text{ZrO}_2\text{-MCM-41},$ $\text{SO}_4^{2-}/\text{ZrO}_2\text{-Al}_2\text{O}_3\text{-MCM-41}$ ²⁹⁸ $\text{SO}_4^{2-}/\text{ZrO}_2\text{-Al}_2\text{O}_3/\text{SBA-15},$ $\text{SO}_4^{2-}/\text{ZrO}_2/\text{SBA-15}$ ²⁹³ $\text{HTiNbO}_5, \text{HTi}_2\text{NbO}_7,$ $\text{HNb}_3\text{O}_8, \text{H}_4\text{Nb}_6\text{O}_{17},$ $\text{H}_2\text{Ti}_3\text{O}_7, \text{exfoliated}$ nanosheets ²⁹⁹ $[\text{RE}(\text{H}_2\text{cmp})\text{H}_2\text{O}]$ ^{l,282}
<p>In brackets are indicated other salts which were sometimes added.</p> <p>a) SBA-15-SO₃H(C)-prepared by co-condensation. b) SBA-15-SO₃H(G)-prepared by grafting.²⁵⁷ c) MSHS-SO₃H- sulfonic acid modified mesoporous shell silica bead.²⁸⁹ d) MP-NH- medium-pore micelle template aminopropyl functionalised silica. e) LP-NH- Large-pore micelle templated aminopropyl functionalised silica.²⁸⁵ f) SCBC- Sulfonated carbon based catalyst.²⁵⁶ g) Mpy- medium-pore micelle templated MCM-41 (3.7 nm) (γ is the loading of heteropolyacid). h) Lpy - Large-pore micelle templated silica (9.6 nm) (γ is the loading of heteropolyacid).^{284,285} i) Zr-P-Zirconium phosphate.²⁷¹ j) MSZ and MSAZ- Mesoporous sulfated zirconia and alumina modified mesoporous sulfated zirconia respectively.²⁹⁸ k) MSHS-SO₃H and MSHS-Al- aluminium modified mesoporous shell silica bead.²⁸⁹ l) [RE(H₂cmp)H₂O]-Rare earth hybrid layered networks formed by rare earth (RE) chloride salts and N-carboxymethyl)iminodi(methylphosphoric acid (H₂cmp)).²⁸²</p>						

Table 1.5- Catalysts tested in the conversion of hexoses and related di/polysaccharides.

Liquid Acids		Solid Acids				
Organic	Inorganic	Soluble	Insoluble			
			Organic	Hybrids	Inorganic	
					Zeolites and Zeotypes	Others
Oxalic acid 70,177,233 Maleic acid 70,177,233,300 CH ₃ SO ₃ H ^{198,235,301} CF ₃ SO ₃ H ^{198,301-303} HCOOH ^{243,304,305} CH ₃ COOH ^{301,304-307} CF ₃ COOH ¹⁹⁸ Citric acid ^{233,308} Nicotinic acid ³⁰⁸ para-toluene sulfonic acid (TsOH) ^{70,177,229,233,235,309-311}	HCl ^{29,35,196,198,229,230,233,235,237,242,243,258,259,300-302,304-307,312-322} HCl(NaCl) ^{235,258} HCl(LiCl), HCl(KCl), HCl(CsCl), HCl(CaCl ₂), HCl(MgCl ₂), HCl(KBr), HCl(NaBr) ²⁵⁸ HCl(AlCl ₃), HCl(CrCl ₃), HCl(LaCl ₃) ^{235,258} HCl(Na ₂ SO ₄) ²³³ N(CH ₃) ₃ /HCl, NH(CH ₃) ₂ /HCl ³²³ H ₃ PO ₄ ^{29,35,198,233,243,278,279,300,301,305,306,308,319,324,325} Pyridine /H ₃ PO ₄ ^{70,177,308} α- Picoline /H ₃ PO ₄ , Collidine/H ₃ PO ₄ ^{70,177,308} NaH ₂ PO ₄ ³⁰⁸ (NH ₄) ₂ HPO ₄ ³⁰⁸	AlCl ₃ ^{201,242,304,307,312,323,326-329} AlCl ₃ (Et ₄ NCl) ³²³ AlCl ₃ .6H ₂ O ^{305,314,318,326} AlCl ₃ (NaCl) ³²⁶ AlBr ₃ ³²⁶ Al ₂ (SO ₄) ₃ ^{242,312} Al ₂ (SO ₄) ₃ ²⁴² Al(NO ₃) ₃ ³¹² CrCl ₂ ^{73,196,201,230,242,253,305,309,310,313,322,327-332} CrCl ₂ (LiCl), CrCl ₂ (LiBr) ²⁵³ CrCl ₃ ^{196,201,253,263,310,312,324,327-337} CrCl ₃ (LiCl) ^{253,263,335} CrCl ₃ (LiBr) ^{253,263} CrCl ₃ (NaCl), CrCl ₃ (KCl), CrCl ₃ (NaBr), CrCl ₃ (KBr), CrCl ₃ (NH ₄ Cl), CrCl ₃ (NH ₄ Br), CrCl ₃ (NH ₄ I) ²⁶³ CrCl ₃ .6H ₂ O ^{252,305,313,318,323,331,336,338-340} CrBr ₃ ^{196,201,253} Cr ₂ (SO ₄) ₃ ³¹² CrSO ₄ ²⁴² Cr(NO ₃) ₃ ^{253,324} ZnCl ₂ ^{230,242,304,305,310,313,341}	Amberlyst-15 ^{35,229,243,245-247,260,302,306,309-311,342-344} Amberlyst-36 ³⁰⁹ Amberlyst-70 ^{302,345,346} Amberlite-IR118, Amberlite-IR120 ³⁴⁷ Dowex50-WX-8 ^{259,306,348} Dowex50-WX-4 ²⁵³ Diaion-PK216 ^{18,347,348} Diaion-PK208, Diaion-PK228, Lewatit-SC-108 ³⁴⁷ Levait-SPC-108 ^{349,350} Lewatit-S2328, Lewatit-K1131, Lewatit-K1469, Lewatit-K2641 ³⁵¹ Nafion ²⁴⁵ Nafion-NR50 ²²⁹ NKC-9 ^{304,335} OC-1052 ³²⁰	SCBC ^{a, 256} AC-SO ₃ H, ^b Glu-TsOH ^{c,246} TP-A380, ^d TAA-A380, ^e TP-SBA-15, ^f TAA-SBA-15 ^{g 346,352} SBA-15-SO ₃ H ^{352,353} SSA-SBA-15, ^h GCC, FCC, CCC, LCC, BCC, JCC ^{i,354} Carb-SO ₃ H ^{j,302} MIL-101-H ₃ PW ₁₂ O ₄₀ ^{k,355} BHC ^{l,356} (it was considered a homegeneous hybrid catalyst)	H-MCM-22 ²⁹⁵ γ ²⁴⁴ H-Y Faujasite ^{244,245,261,309,357,358} Na-Beta ³⁵⁹ SiO ₂ -H-Beta ²⁵⁰ H-Beta ^{229,245,246,250,261,290,309,358,359} Ti-Beta Sn-Beta (HCl) ³⁶⁰ H-Mordernite ^{223,250,261,309,358} SiO ₂ -H-Mordernite ²⁵⁰ Na-ZSM-5 ^{304,359} H-ZSM-5 ^{229,250,261,309,313,359} SiO ₂ -H-ZSM-5 ²⁵⁰ H-MFI ³⁵⁸ LZy ³⁶¹	Cs _{2.5} H _{0.5} PW ₁₂ O ₄₀ ^{245,335} Cs ₃ PW ₁₂ O ₄₀ ^{315,362} Zn _{1.5} PW ₁₂ O ₄₀ ³⁶² Ag ₃ PW ₁₂ O ₄₀ ³¹⁵ Si-H-SBA-15 ^{346,353} Al-MCM-20 ³⁵⁷ Al-MCM-41 ^{290,357} Al-MCM-48 ²⁹⁰ TS-1, Sn-MCM-41, Ti-MCM-41 ³⁶⁰ Pt-MCM-48 ²⁹⁰ SO ₄ ²⁻ /ZrO ₂ /SBA-15 ³³⁵ ZrO ₂ ^{296,297,363-369} SO ₄ ²⁻ -ZrO ₂ ^{229,245,296,364,367,370} SO ₄ ²⁻ -ZrO ₂ /Al ₂ O ₃ ³⁷⁰ WO ₃ -ZrO ₂ ^{245,278} Zr ₃ (PO ₄) ₂ ^{239,264,335,371} ZrPP, TPP ^{m,239} TiO ₂ ^{296,297,363,365,366,368,372} TiO ₂ -HCl ³⁶⁵ TiO ₂ -H ₃ PO ₄ ^{239,365}

Table 1.5. *Continued.*

H_2SO_4 ^{29,35,70,177,196,198,201,231,233,242-244,253,256,258,259,300-302,304-307,312,313,316,318,319,324,327,334,335,338,353,363,366} Pyridine (H_2SO_4) ^{70,177,308} H_2SO_4 (Na_2SO_4) ²⁵⁸ H_2SO_4 (LiCl), H_2SO_4 (LiBr) ²⁵³ H_2SO_4 (NaCl), $\text{H}_2\text{SO}_4(\text{CrCl}_3 \cdot 6\text{H}_2\text{O})$ ³⁴⁰ $\text{HCl} + \text{H}_2\text{SO}_4$ ²³³ $\text{NaHSO}_4 \cdot \text{H}_2\text{O}(\text{Et}_4\text{NCl})$ ³²³ HI ^{70,177} HBr ^{235,312} VCl_4 ²⁰¹ H_2IrCl_6 ³¹² GeCl_4 ³⁷³ SnCl_4 ^{252,263,327,329,336,374} $\text{SnCl}_4 \cdot 4\text{H}_2\text{O}$ ³⁷³ $\text{SnCl}_4 \cdot 5\text{H}_2\text{O}$ ^{252,305,360} $\text{SnCl}_4(\text{NH}_4\text{Br})$ ²⁶³ TiCl_4 ³²⁸ HClO_4 ²³⁵ HNO_3 ^{198,243,300,304,305,319}	ZnSO_4 ^{242,312} CuCl ^{196,201,329} CuSO_4 ³¹² CuCl_2 ^{201,304,306,327-329} $\text{CuCl}_2 \cdot 2\text{H}_2\text{O}$ ^{252,305,323} $\text{CuCl}_2 \cdot 2\text{H}_2\text{O}(\text{Et}_4\text{NCl})$ ³²³ CuClBr_2 ²⁰¹ FeCl_2 ^{201,242,328,329,375,376} FeCl_3 ^{201,242,252,263,304,305,310,312,323,328,329,333,375} $\text{FeCl}_2 \cdot 4\text{H}_2\text{O}$ ²⁵² $\text{FeCl}_3 \cdot 6\text{H}_2\text{O}$ ³⁰⁵ $\text{FeCl}_3(\text{NH}_4\text{Br})$ ^{263,375} $\text{FeCl}_3(\text{Et}_4\text{NBr})$ ^{323,375} $\text{FeCl}_3(\text{Et}_4\text{NCl}), \text{FeCl}_3(\text{LiCl}),$ $\text{FeCl}_3(\text{NaCl}), \text{FeCl}_3(\text{KCl}),$ $\text{FeCl}_3(\text{LiBr}), \text{FeCl}_3(\text{NaBr}),$ $\text{FeCl}_3(\text{KBr})$ ³⁷⁵ $\text{Fe}_2(\text{SO}_4)_3$ ^{242,312} FeSO_4 ²⁴² $\text{Fe}(\text{NO}_3)_3$ ³¹² $\text{Fe}(\text{NO}_3)_2/\text{Et}_4\text{NBr},$ $\text{Fe}(\text{NO}_3)_3/\text{Et}_4\text{NBr}$ ³⁷⁵ VCl_3 ²⁰¹ CoCl_2 ^{242,377} CoSO_4 ^{242,377} $\text{Co}_2(\text{SO}_4)_3, \text{Co}(\text{NO}_3)_2$ ³⁷⁷ MnCl_2 ^{201,242,329} $\text{MnCl}_2 \cdot 4\text{H}_2\text{O}$ ³⁰⁵ MnSO_4 ²⁴² NiCl_2 ^{242,329} $\text{NiCl}_2 \cdot 6\text{H}_2\text{O}$ ²⁵² NiSO_4 ²⁴²	$\text{TiO}_2(\text{IrCl}_3)$ ³²⁴ $\text{TiO}_2(\text{SO}_4)$ ²⁻³³⁵ $\text{TiO}_2\text{-ZrO}_2$ ^{278,297} Al_2O_3 ^{245,372} $\text{Pt}/\text{Al}_2\text{O}_3$ ³⁷⁸ $\text{Al}_2\text{O}_3\text{-SiO}_2$ ²⁵⁰ AlF-Zr-P ^{n,371} $_2\text{O}_5 \cdot x\text{H}_2\text{O}$ ^{229,335,379-382} NbOPO_4 ^{379-381,383,384} SiO_2 ³⁷² $\text{SiO}_2\text{-gel}$ ³⁸⁵ $\text{B}_2\text{O}_3, \text{P}_2\text{O}_5$ ³²⁵ CeO_2 ³⁷² SnO_2 ³⁶⁰ $\text{Ta}_2\text{O}_5 \cdot n\text{H}_2\text{O}$ ³⁷⁹ $\text{VOPO}_4 \cdot 2\text{H}_2\text{O}/\text{SiO}_2;$ $\text{VOPO}_4 \cdot 2\text{H}_2\text{O}/\text{TiO}_2$ ³⁸⁶ $\text{VOPO}_4 \cdot 2\text{H}_2\text{O}/\gamma\text{-Al}_2\text{O}_3,$ ³⁸⁶ Pillared montmorillonite (PM) clays: H-, Cr-, Fe-PM ^{o,387} Al-PM ^{310,357,387}
--	--	--

Table 1.5. *Continued.*

		TiCl_3 ³¹² ScCl_3 ³⁸⁸ $\text{ScCl}_3 \cdot 6\text{H}_2\text{O}$ ³⁷³ $\text{Sc}(\text{OTf})_3$ ^{245,310,389} GeBr_2 ³⁷³ $\text{Ge}(\text{OEt})_4$ ³⁷³ PdCl_2 ^{201,306,312,328,329,390} RuCl_3 ^{201,251,328,390} $\text{RuCl}_3(\text{MgCl}_2)$, $\text{RuCl}_3(\text{MgSO}_4)$ ²⁵¹ RuSO_4 ^{251,312} RhCl_3 ²⁰¹ MoCl_3 ^{201,323,333} $\text{MoCl}_3(\text{Et}_4\text{NCl})$ ³²³ SnCl_2 ^{307,327,329} $\text{SnCl}_2 \cdot 2\text{H}_2\text{O}$ ^{263,305} $\text{SnCl}_2(\text{NH}_4\text{Br})$ ²⁶³ ZrCl_4 ^{328,373} $\text{Zr}(\text{NO}_3)_4$ ³²⁴ AgNO_3 ³¹⁵ $\text{Ag}_2(\text{SO}_4)$ ^{251,312} $\text{YCl}_3, \text{YCl}_3 \cdot 6\text{H}_2\text{O}$ ³⁸⁸ $\text{PtCl}_2, \text{PtCl}_4$ ^{201,329} IrCl_3 ³²⁴ $\text{IrCl}_3 \cdot \text{H}_2\text{O}$ ³³⁹ $\text{AuCl}_3(\text{HCl})$ ³²⁴ BiCl_3 ³⁷³ WCl_3 ³³³ $\text{WCl}_4, \text{WCl}_6$ ³²⁸ HfCl_4 ³⁷³ LaCl_3 ^{201,242,329,388,390} $\text{La}_2(\text{SO}_4)_3$ ²⁴²				
--	--	--	--	--	--	--

Table 1.5. *Continued.*

		$\text{Yb}(\text{OTf})_3$ ^{389,391} YbCl_3 ^{390,391} NdCl_3 ^{390,391} $\text{Nd}(\text{OTf})_3$ ³⁸⁹ DyCl_3 ^{390,391} EuCl_3 ³⁹⁰ PrCl_3 ^{390,391} HoCl_3 ³⁹⁰ $\text{Ho}(\text{OTf})_3$ ³⁸⁹ SmCl_3 ³⁹⁰ $\text{Sm}(\text{OTf})_3$ ³⁸⁹ $\text{GdCl}_3, \text{TbCl}_3, \text{ErCl}_3, \text{LuCl}_3$ ³⁹⁰ CeCl_3 ^{373,390,391} $\text{Ce}(\text{NH}_4)_3(\text{NO}_3)_6$ ³²⁴ H_3BO_3 ^{262,313,325,392} $\text{H}_3\text{BO}_3(\text{K}_2\text{SO}_4), \text{H}_3\text{BO}_3(\text{LiCl}),$ $\text{H}_3\text{BO}_3(\text{LiBr}), \text{H}_3\text{BO}_3(\text{LiNO}_3),$ $\text{H}_3\text{BO}_3(\text{NaCl}), \text{H}_3\text{BO}_3(\text{NaBr}),$ $\text{H}_3\text{BO}_3(\text{NaNO}_3),$ $\text{H}_3\text{BO}_3(\text{Na}_2\text{SO}_4),$ $\text{H}_3\text{BO}_3(\text{KCl}), \text{H}_3\text{BO}_3(\text{KBr}),$ $\text{H}_3\text{BO}_3(\text{KI}), \text{H}_3\text{BO}_3(\text{KNO}_3)$ ²⁶² $\text{H}_3\text{BO}_3(\text{MgCl}_2),$ $\text{H}_3\text{BO}_3(\text{K}_2\text{SO}_4),$ $\text{H}_3\text{BO}_3(\text{AlCl}_3), \text{H}_3\text{BO}_3(\text{FeCl}_3)$ ²⁶² $(\text{NH}_4)_2\text{SO}_4$ ^{70,177,252,308} $(\text{NH}_4)_2\text{SO}_3$ ³⁰⁸ NH_4NO_3 ²⁵² NH_4Br ^{252,263} NH_4I ²⁶³ NH_4Cl ^{252,308} $\text{NaCl}/\text{NH}_4\text{Cl}$ ²⁵²				
--	--	--	--	--	--	--

Table 1.5. *Continued.*

		E_4NBr^{375} $(NH_4)/OAc^{308}$ $FePW_{12}O_{40}^{315}$ $H_3PW_{12}O_{40}^{198,245,307,315,335,355,362}$ $H_3PMo_{12}O_{40}, H_3SiW_{12}O_{40}$ $H_3SiMo_{12}O_{40}^{198}$ $VOPO_4 \cdot 2H_2O^{386}$ $VO(SO_4)_2^{70,177}$ $[Fe(H_2O)].VOPO_4 \cdot 2H_2O^{386}$ $[Al(H_2O)].VOPO_4 \cdot 2H_2O,$ $[Ga(H_2O)].VOPO_4 \cdot 2H_2O,$ $[Cr(H_2O)].VOPO_4 \cdot 2H_2O,$ $[Mn(H_2O)].VOPO_4 \cdot 2H_2O^{386}$				
<p>In brackets are indicated other salts which were sometimes added.</p> <p>a) SCBC-Sulfonated carbon based catalyst.²⁵⁶ b) AC-SO₃H- Sulfonated activated carbon. c) Glu-TsOH- sulfonated carbonaceous material bearing SO₃H, OH, and COOH groups via one-step hydrothermal carbonisation of D-glucose and para-toluene sulfonic acid (TsOH) under mild conditions.²⁴⁶ d) TP-A380- Thiopropyl groups onto non-porous silica.³⁴⁶ e) TAA-A380- Propylsulfonic acid groups on Tp-A380 (3-(thiopropyl)-propane-1-sulfonic acid functionalised onto non-porous silica.³⁴⁶ f) TP-SBA-15- Thiopropyl functionalised silica SBA-15.³⁴⁶ g) TAA-SBA-15- Propylsulfonic acid groups on Tp-SBA-15 (3-(thiopropyl)-propane-1-sulfonic acid functionalised silica SBA-15).^{346,352} h) SSA-SBA-15- 3-(Propylsulfonyl)-propane-1-sulfonic acid functionalised silica SBA-15.³⁵² i) TESAS-SBA-15- 3-(Propylthio)propane-1-sulfonic acid functionalised silica SBA-15.³⁵² j) Carbonaceous based catalysts: GCC, FCC, CCC, LCC, BCC and JCC- Glucose, fructose, cellulose, lignin and bamboo derived carbonaceous catalyst.³⁵⁴ k) Carb-SO₃H- Vulcan carbonaceous support on sulfonic acid.³⁰² l) MIL-101- chromium based metal-organic framework.³⁵⁵ m) BHC-Betaïne hydrochloride, a co-product of carbohydrate industry. n) ZrPP and TPP- Layered zirconium pyrophosphate, titanium phosphate and cubic titania pyrophosphate.²³⁹ o) AlF-Zr-P-Zirconium phosphate coating on aluminium foams.³⁷¹</p>						

1.4.3. Conversion of saccharides to furanic aldehydes in the presence of heterogeneous catalysts

Since the pentoses and hexoses and the respective di/oligo/polysaccharides are polar and non-volatile compounds, their conversion to Hmf and Fur is restricted to liquid-phase processing. The solubilisation of polysaccharides into the reaction medium is one of the requirements to avoid detrimental mass transfer limitations and to maximise feedstock loadings, which is desirable for process intensification. This is particularly important in the cases of insoluble solid acid catalysts (to avoid detrimental mass transfer limitation associated with the catalyst and reagent being in the solid state). Employing an aqueous-phase reaction medium has important advantages: water is cheap, non-toxic, non-flammable and a clean solvent, increasing the economic feasibility of the process.²⁶⁴ The use of an immiscible organic co-solvent is known to allow enhanced Fur or Hmf yields; in this way the target products are extracted as they are formed from the aqueous phase, avoiding undesired side reactions. Román-Leshkov et al.³⁵ proposed a two-phase reactor system for the dehydration of D-fructose to Hmf (Figure 1.23). The aqueous phase consisted of a mixture of dimethylsulfoxide (DMSO) and poly(1-vinyl-2-pyrrolidinone) allowing the suppression of undesired side reactions; the organic phase consisted of isobutylmethylketone (IBMK) which continuously extracts Hmf. The countercurrent extractor was employed to remove the Hmf remaining in the aqueous phase.³⁵ Afterwards, the same group investigated the solvent effect on the dehydration of D-fructose in biphasic system with saturated inorganic salt, with THF as extract solvent, reaching an outstanding Hmf selectivity of 83%.²⁵⁸ Furthermore, one pot procedures involving multiple catalytic steps such as reaction and separation of products can minimise investment in equipment and energy consumption.²⁶⁹

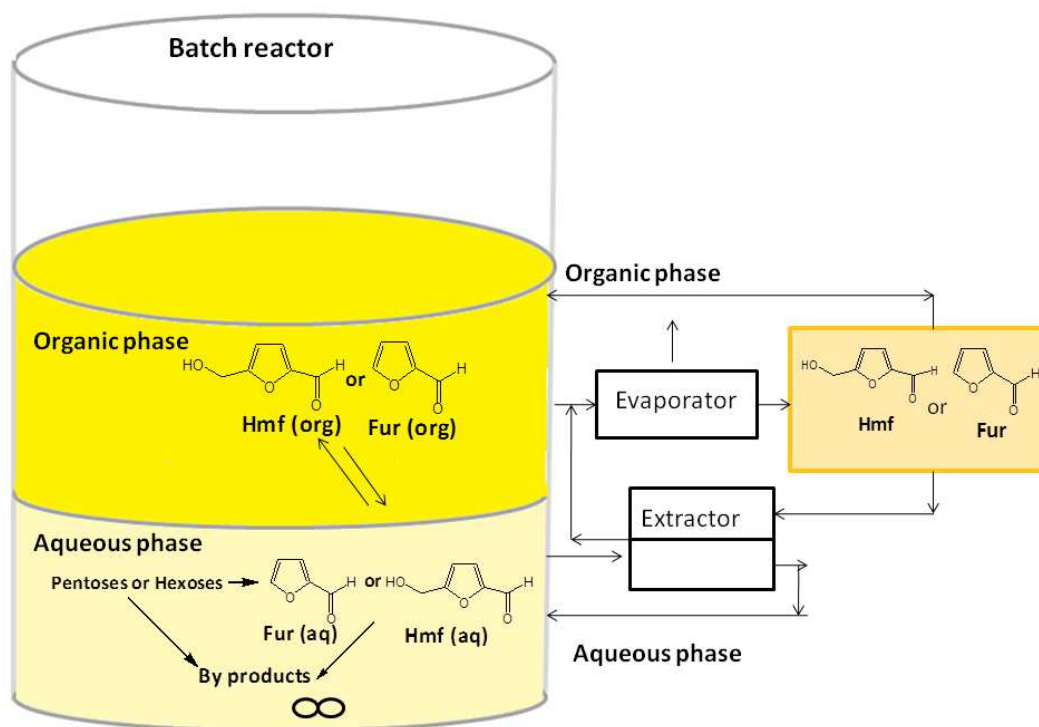


Figure 1.23- Conversion of saccharides to 2-furaldehyde (Fur) and 5-hydroxymethyl-2-furaldehyde (Hmf) using an aqueous-organic biphasic solvent system, under batch operation mode [adapted from ^{35,74}].

Although cellulose is one of the most abundant natural polymers and attractive renewable feedstocks, it is insoluble in water and most organic solvents and not easy to hydrolyse because of its compact crystalline structure (formed mainly by inter- and intra-molecular hydrogen bonds).^{25,393,394} Pre-dissolution treatments applied to cellulose using phosphoric acid can allow the crystallinity of cellulose to be decreased, facilitating its hydrolysis.³⁹⁵⁻³⁹⁹ Phosphoric acid has been successfully used to dissolve cellulose and compares favourably to other inorganic mineral acids due to the fact of being less corrosive and due to its non-toxic properties and low cost.⁴⁰⁰ The addition of H_3PO_4 to cellulose involves an esterification reaction with the $-\text{OH}$ groups of cellulose leading to cellulose- $\text{O}-\text{PO}_3\text{H}_2$ and a competition of H-bond formation between $-\text{OH}$ groups of cellulose chains and H-bond formation between one hydroxyl group of cellulose with H_2O or a hydrogen ion.³⁹⁸ DMSO dissolves fairly well saccharides and leads to quite good Fur/Hmf yields. However DMSO can decompose giving toxic S-containing by-products,³⁴ and its separation from Hmf can be quite energy intensive.^{29,401,402} The alternative use of ionic liquids

based catalytic systems for converting saccharides to furanic aldehydes has been explored in recent years with one of the main advantages being the favourable properties of some ionic liquids in dissolving cellulose and other polysaccharides in comparison with common organic solvents and water.⁴⁰³ The state of the art of this field is presented in Section 1.5. This Section focuses on heterogeneous catalytic systems using only water and/or organic solvents.

Porous solids can be classified according to their pore sizes: micropores possess less than 2 nm in width, mesopores have widths in the range 2 to 50 nm, and macropores have widths above 50 nm, according to IUPAC.^{404,405} Examples of porous materials with different ranges of pores sizes are shown in Figure 1.24.⁴⁰⁶ The porous solids can possess catalytic active sites and function as bulk catalysts, or can be used as (inert) supports for active species (supported catalysts). A wide range of reaction systems based on heterogeneous catalysts using different solvent systems have been investigated in the conversion of saccharides to Hmf and Fur. Table 1.6 collects the catalytic results reported for the conversion of mono/polysaccharides and lignocellulosic feedstocks, using water and/or organic solvents in the presence of heterogeneous acid catalysts.

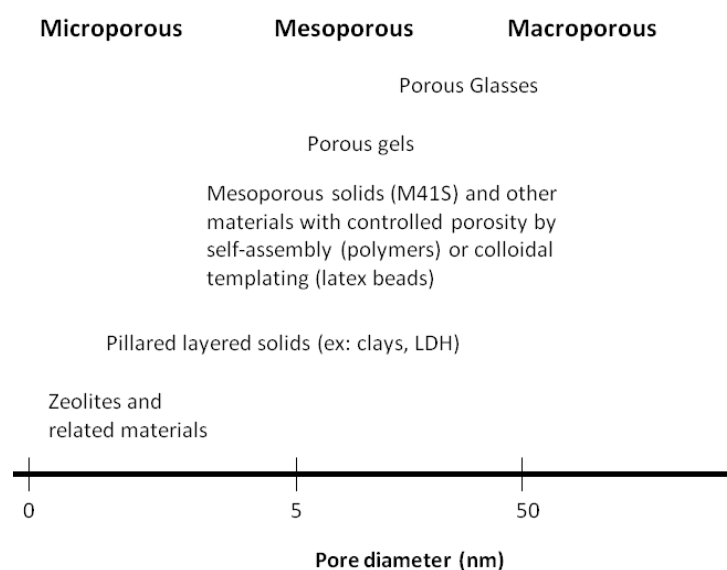


Figure 1.24- Typical pore widths of micro-, meso- and macroporous materials [adapted from ⁴⁰⁶].

The use of porous solid acid catalysts in the hydrolysis/dehydration of polysaccharides into furan derivatives seems attractive although important requirements need to be considered such as, type and density of acid sites, accessibility of the acid sites (avoiding detrimental internal

mass transfer limitations), stability under the applied reaction conditions (e.g. leaching of the active species into solution), leveling-off of the acidity by the type of solvent (e.g. water-tolerance), resistance to thermal and/or chemical treatments for removing insoluble by-products and regenerating the catalyst (allowing extended catalyst lifetimes).³⁶

Crystalline inorganic oxides (such as zeolite H-Beta,^{229,245,246,249,250,261,290,359} H-Ferrierite,²⁴⁹ H-ZSM-5,^{220,229,249,250,261,313,359} H-Mordenite,^{222,223,249,250,261,291,292,407} and H-Y Faujasite^{222,244,245,249,261,271,291,292,357,358,387}), amorphous niobium oxides (such as e.g. Nb₂O₅.nH₂O,^{229,379,380,382,407} Nb₂O₅/PO₄²⁻,^{379-381,383,384} and Nb₂O₅/SO₄²⁻²⁵⁵), exfoliated niobates (e.g. eH₄Nb₆O₁₇ and eHNb₃O₈),²⁹⁹ exfoliated titanates (e.g. eH₂Ti₃O₇²⁹⁹), titanoniobate nanosheets (e.g. HTiNbO₅²⁹⁹), exfoliated titanoniobates (e.g. eHTi₂NbO₇²⁹⁹) and delaminated microporous aluminosilicate (del-Nu-6(1)²⁶⁵) are considered fairly stable and water tolerant porous solid acid catalysts (Table 1.6). Microporous pillared-clay catalysts are layered montmorillonite sheets with intercalated metal oxide pillars and larger pores widths (> 10 Å, enough to accommodate D-glucose, 8.6 Å) than zeolites, promote high conversions with high selectivities to organic acids but low selectivities to Hmf. Lourvanij et al.³⁸⁷ stated that larger pore sizes allowed D-glucose to diffuse into the microporous matrix but also trapped the Hmf molecule, directing the reaction to final organic acids. Some examples are aluminium pillared montmorillonite (Al-PM),^{357,387} Cr-PM, Fe-PM and H-PM³⁸⁷ (Table 1.6). Aluminosilicate catalysts (e.g. zeolite) seem more attractive in terms of costs and/or availability of the sources of the constituent elements (Al, Si) than transition-metal containing ones such as, H-AM-11 (microporous niobium silicate), Nb-MCM-41 (mesoporous niobium silicate),^{291,292} Pt-MCM-48,²⁹⁰ Pt/Al₂O₃,³⁷⁸ WO₃/ZrO₂,^{245,271,278} ZrO₂,^{296,297,363,365-368} TiO₂,^{281,296,297,363,365,366,368,372} TiO₂-ZrO₂,²⁹⁷ Ta₂O₅.nH₂O,³⁷⁹ and CeO₂³⁷² (Table 1.6). Several other advantages in the use of zeolites are reported particularly when compared to acidic ion exchange resins, such as presenting higher selectivities in water; resistance to higher temperatures favouring the formation of Hmf; capacity to adsorb organic acids partly responsible for further degradation of Hmf; easier to regenerate by thermal processes.²²³ However various authors reported that in the case of crystalline microporous solid acids as zeolites and zeotypes, the formation of coke can lead to catalyst surface passivation and pore blockage, resulting in decreasing catalytic activity and/or product selectivity.^{71,220,222,223,249} O'Neill et al.²²⁰ with H-ZSM-5 in the dehydration of D-xylose observed the formation of bulky by-products entrapped in the micropores; Moreau et al.^{222,223} concluded that H-Mordenites or H-Faujasites with higher Si/Al ratio lead to lower selectivities because upon increasing the Si/Al ratio, the acid properties of the catalysts are decreased, and increases secondary reactions with formation of by-products; Kim et

al.²⁴⁹ observed the same behaviour for other zeolites. On the other hand, heavier substrate molecules (e.g. di/polysaccharides) can be too bulky to enter the channels of the microporous structures. The investigation of the microporous acid catalysts in the conversion of saccharides to Fur/Hmf were followed by innovative applications of mesoporous materials possessing Brønsted acid sites such as sulfonic acid groups (firstly tested by Dias et al.²⁴⁰ with MCM-41-SO₃H, and followed by other authors with SBA-15-SO₃H,^{257,352} sulfonic acid modified mesoporous shell silica bead, MSHS-SO₃H,²⁸⁹ and propylthiol mesoporous silica SBA-15-SH,²⁵⁷ Table 1.6). Mesoporous materials possessing both Lewis acid sites and Brønsted acid sites associated with the presence of aluminium were also tested (amorphous SiO₂-Al₂O₃,^{249,250,271,281,407} aluminium modified mesoporous shell silica bead, Al-MSHS,²⁸⁹ aluminium-containing MCM-41 type,^{290,292,294,295,357} MCM-48 type,²⁹⁰ or crystalline mesoporous MCM-20 type,³⁵⁷ Table 1.6). Some zeolites are formed from lamellar precursors (e.g. by thermal treatment) and these may be delaminated to form mesopores from aggregates, enhancing the specific surface area and acid sites accessibility (e.g. ITQ-2,^{408,409} ITQ-6,⁴¹⁰ ITQ-18,^{411,412} Nu-6⁴¹³). These type of materials are quite promising for the conversion of pentoses to Fur.²⁶⁵

Solid acids possessing sulfur-containing surface groups such as (per)sulfate^{229,245,255,293,296,298,367,370} and sulfonic acid^{240,257,289,346,352} have been successfully applied as acid catalysts in the reaction of saccharides to Hmf/Fur (Table 1.6). These types of materials shown in Table 1.6 are organic such as, ion-exchange resins (e.g. Nafion,²⁴⁵ Nafion SAC-13,^{271,288} Nafion-117,²⁸⁸ Nafion NR-50,²²⁹ (perfluorinate sulfonic acid resins) Amberlyst-15,^{35,229,240,243,245-247,260,274,407} Amberlyst-70,^{271,287,345,346,352} Amberlite IR-118,³⁴⁷ (macroreticular resin based on a styrene-divinylbenzene co-polymer) Diaion PK-216,^{18,347,348} Dowex 50wx4,²⁵³ Dowex 50wx8,^{259,348} (microreticular resin based on a styrene-divinylbenzene co-polymers) Lewatit S2328,³⁵¹ Lewatit SCP 108,³⁵⁰ OH1052³²⁰), or others such as phosphonics arylsulfonic acid-functionalised non-ordered silica (SiSphSA),³⁵² thiopropyl groups onto non-porous silica (Tp-A380)³⁴⁶ and propylsulfonic acid groups on Tp-A380 (Taa-A380)³⁴⁶; inorganic such as, versions of (per)sulfate bulk (zirconia, titania, alumina or other metals) (e.g. S₂O₈²⁻/ZrO₂,²⁹⁸ SO₄²⁻/ZrO₂,^{229,245,255,296,298,367,370} SO₄²⁻/TiO₂,²⁵⁵ SO₄²⁻/Al₂O₃,²⁵⁵ SO₄²⁻/Fe₂O₃,²⁵⁵ SO₄²⁻/SnO₂,²⁵⁵ and SO₄²⁻/HfO₂²⁵⁵); alumina or silica-supported (per)sulfate zirconia (e.g. S₂O₈²⁻/Al₂O₃-ZrO₂,²⁹⁸ S₂O₈²⁻/ZrO₂-MCM-41,²⁹⁸ S₂O₈²⁻/Al₂O₃-ZrO₂/MCM-41,²⁹⁸ SO₄²⁻/Al₂O₃-ZrO₂,^{293,298,370} SO₄²⁻/ZrO₂-Al₂O₃/SBA-15,²⁹³ SO₄²⁻/ZrO₂/SBA-15,²⁹³ SO₄²⁻/ZrO₂-MCM-41,²⁹⁸ and SO₄²⁻/Al₂O₃-ZrO₂/MCM-41²⁹⁸); hybrid organic-inorganic such as silicas modified with sulfonic acid surface groups (e.g. MCM-41-SO₃H,^{240,289} SBA-15-SO₃H,^{257,352} HMS-SO₃H,²⁸⁹ and sulfonic acid modified mesoporous shell silica bead, MSHS-SO₃H²⁸⁹), thiopropyl

groups (e.g. Tp-SBA-15³⁴⁶ and SBA-15-SH²⁵⁷) or with thiopropylsulfonic acid groups (e.g. Taa-SBA-15,³⁴⁶ 3-((3-methoxysilyl)-propyl)thio)propane-1-sulfonic acid, TESAS-SBA-15,³⁵² 3-propylsulfonyl)propane-1-sulfonic acid, SSA-SBA-15³⁵²). SBA-15 in particular is a good support for the dispersion of sulfated zirconia or sulfated groups because of its unique surface, pore structure, and hydrothermal stabilities.⁴¹⁴ These types of catalysts present some limitations in terms of thermal stability associated with the sulfur containing groups (SO_4^{2-} groups are unstable at high temperatures (ca. 250 °C^{240,255}) and catalyst regeneration requires a thermal treatment above this temperature for the removal of the accumulated organic matter.^{240,293,370} Alternatives might include regeneration with H_2O_2 ,^{240,257,293} or acetone.²⁵⁷ Another limitation is associated with leaching of sulfur-containing groups during the catalytic reaction.^{255,293,296,298} For example, for materials of the type (per)sulfated zirconia supported on mesoporous silica MCM-41 (some doped with aluminium) used as catalysts in the dehydration of D-xylose, while no leaching of zirconium and aluminium was observed, the sulfur loading dropped by ca. 50%, compromising its reusability.²⁹⁸ Shi et al.²⁵⁷ observed coke formation in 34 wt.% for SBA-15-SO₃H(C) (prepared by co-condensation) which lead to a deactivation of the catalyst. After regeneration with acetone the content of coke was still high (28.2 wt.%), which indicates that part of the accumulated organic matter is not dissolved in acetone and the catalytic activity dropped by ca. 10%. However when regenerated with H_2O_2 the content of coke dropped almost completely (0.4 wt.%) and the catalytic activity was recovered completely. These results indicate that H_2O_2 treatment is an effective method for regenerating sulfonic acid functionalised mesoporous SBA-15 materials. Furthermore no sulfur leaching was observed for SBA-15-SO₃H(C) (S content was similar for the fresh and recovered catalysts) indicating that the material has a high thermal stability.²⁵⁷ MCM-41-SO₃H resulted in a significant decrease in the Fur selectivity (65% to 23%) and C_{Xyl} (37% to 28%) due to the formation of organic by-products (confirmed by colour change of the catalyst) which were not efficiently eliminated by filtration and washing processes.²⁸⁹ The same behaviour was previously noted by Dias et al.²⁴⁰ when the catalyst MCM-41-SO₃H was washed with methanol and treated with H_2O_2 (C_{Xyl} dropped from 62 to 52% and the Fur selectivity from 80% to 34%). On the other hand, despite the lower activity of HMS-SO₃H, and MSHS-SO₃H, the colour of the catalysts remained white after catalysis and no decrease in the selectivity was observed.²⁸⁹

The substitution of sulfur groups by phosphorous has also been investigated in the reaction under study. Solid acids with phosphorous-containing surface groups such as versions of titanium phosphates (e.g. $\alpha\text{-PO}_4^{2-}/\text{TiO}_2$,²³⁹ $\gamma\text{-PO}_4^{2-}/\text{TiO}_2$ ²³⁹), zirconium phosphates (e.g. $\text{PO}_4^{2-}/\text{ZrO}_2$,^{264,271,371} $\gamma\text{-PO}_4^{2-}/\text{ZrO}_2$,^{239,407} and $\text{Al}_2\text{O}_3/\text{PO}_4^{2-}/\text{ZrO}_2$ ³⁷¹), niobium phosphates (e.g. PO_4^{2-}

/Nb₂O₅³⁸¹), pyrophosphates (e.g. cubic zirconium pyrophosphate, C-ZrO₂/P₂O₇,²³⁹ cubic titanium pyrophosphate C-TiP₂O₇²³⁹), metal-oxides with phosphoric acid (e.g. Ta₂O₅.nH₂O/H₃PO₄²⁻,³⁷⁹ TiO₂/H₃PO₄,³⁶⁵ Nb₂O₅/H₃PO₄³⁸¹) or yet layered vanadyl phosphates (VOP) involving both Brønsted and Lewis acid sites were also tested, supported on silica, alumina, or titania (e.g. VOP/SiO₂,³⁸⁶ VOP/Al₂O₃,³⁸⁶ and VOP/TiO₂³⁸⁶) and have been employed with good performances in both activity and selectivity (Table 1.6). The reuse of the phosphorous containing materials was possible after removal of the adsorbed reaction by-products with acetone treatment, which allowed significant improvement of the catalytic performances,^{239,381} or by treatment with a solution of H₃PO₄ without loss in the catalytic activity or selectivity for seven runs.²⁶⁴ No leaching was observed for phosphorous containing materials in aqueous media.²⁷¹ Hybrid organic-inorganic materials with phosphorous tested in the dehydration of D-xylose are exemplified by rare earth hybrid layered networks formed by rare earth chloride salts and N-(carboxymethyl)iminodi(methylphosphoric acid).²⁸²

Mesoporous silica-supported heteropolyacids (HPAs) of the Keggin-type, such as supported H_xPW₁₂O₄₀^{3-x}²⁸⁵ and Cs_xH_{3-x}PW₁₂O₄₀,²⁸⁴ are quite active catalysts in the dehydration of D-xylose, although leaching of the active species was observed (using water and toluene (Wt/Tol) as a biphasic solvent system), resulting in a decrease of the catalytic activity and Fur yields in the subsequent batch runs (Table 1.6). Using DMSO as solvent there was practically no loss of activity.^{284,285} The leaching phenomena is most likely related to relatively weak interactions of the active species (ionic) with the support and solvation effects (when using the biphasic Wt/Tol system), leaving only Keggin anions strongly bound to the surface of the support.²⁸⁵ The compound Ag₃PW₁₂O₄₀ (as a Lewis acid) was tested in the conversion of D-fructose to Hmf, using water/IBMK biphasic system as solvent, and was recycled for 6 batch runs without drop in catalytic activity. The leaching of Ag₃PW₁₂O₄₀ was relatively low, ca. 5% (Table 1.6).³¹⁵ A sulfonated organic heteropolyacid, [MimPS]₃PW₁₂O₄₀, a heteropolyacid salt of an ionic liquid cation functionalised with a propanesulfonate group, 1-(3-sulfonicacid)propyl-3-methylimidazolium phosphotungstate, was very efficient to convert D-fructose to Hmf presenting high stability without loss of activity during 6 recycling runs.³⁶²

Carbon-based catalysts (CBC) are hybrid organic-inorganic catalysts synthesised by incomplete carbonisation of high carbon content materials (e.g. sugars and naphthalene), that have recently been used in biomass conversion and have the advantage of having a high thermal stability, high acidity, low preparation costs and high capacity of recyclability without significant losses.^{246,256,354} Some examples of such catalysts include sulfonated naphthalene-based catalyst

(SCBC),²⁵⁶ lignin-derived carbonaceous catalyst (LCC),³⁵⁴ and Glu-TsOH, a carbon-based catalyst prepared by a facile and eco-friendly approach from D-glucose and *p*-toluenesulfonic acid (*p*-TsOH).²⁴⁶ These types of catalysts compare favourably to strong acidic sulfonated co-polymer resins which have low thermal stability (with temperatures below 130 °C) due to their organic frameworks.⁴¹⁵ CBC have high thermal stability because of their carbon frameworks (Table 1.6).²⁴⁶

In a recent work, Ordonsky et al.⁴⁰⁷ studied the acidity of some of the types of the mentioned materials (alumina, aluminosilicate, zirconium phosphate, niobic acid, ion-exchange resin Amberlyst-15 and zeolite Mordenite) using temperature-programmed desorption of NH₃ and IR spectroscopy of adsorbed pyridine. In that work it was reported that the nature and strength of acid sites plays a crucial role in the selectivity towards Hmf. While the Brønsted acid sites in the case of zeolites and ion-exchange resin led to high selectivities in the dehydration of D-fructose with an increase in the selectivity with the addition of IBMK, the Lewis acidity in the case of phosphate and oxides results in the intensive production of humins from D-fructose at the initial stages of the process, where organic phase addition did not affect selectivity.⁴⁰⁷

Table 1.6- Catalytic results reported for the conversion of saccharides (and levoglucosan) to 2-furaldehyde (Fur) and 5-hydroxymethyl-2-furaldehyde (Hmf) in the presence of insoluble solid acid catalysts.

C_{sub} – Substrate conversion in mol.%; Y_{Fur} - 2-furaldehyde yield in mol.%, Y_{Hmf} - 5-hydroxymethyl-2-furaldehyde yield in mol.%;

AS= Acid sites, $\mu\text{mol.g}^{-1}$; [B]= Concentration of Brönsted acid sites, $\mu\text{mol.g}^{-1}$; BS= Base sites, $\mu\text{mol.g}^{-1}$; [L]= Concentration of Lewis acid sites, $\mu\text{mol.g}^{-1}$,

CO_2 -TPD- Acid properties measured by temperature programmed desorption of the adsorbed CO_2 ,

D_p =Pore width (nm),

IR- NH_3 - Acid properties measured by infrared spectroscopy with ammonium as probe molecule,

IR-py- Acid properties measured by infrared spectroscopy of adsorbed pyridine as probe molecule,

ITA- Intrinsic total acidity, $\mu\text{.eq.g}^{-1}$,

NH_3 -TPD- temperature programmed desorption of the adsorbed ammonia. It usually has coupled TCD (thermal conductivity detector) and it uses helium as a carrier gas,

T-NaOH- Titrating the solid with NaOH, T-Bu NH_2 - Non-aqueous titration with butylamine,

S_{BET} = Specific surface area, $\text{m}^2.\text{g}^{-1}$; V_{micro} = Microporous volume, $\text{cm}^3.\text{g}^{-1}$; V_{meso} = Mesoporous volume, $\text{cm}^3.\text{g}^{-1}$, V_p = Total volume pore, $\text{cm}^3.\text{g}^{-1}$.

Tol-Toluene; DMSO- dimethylsulfoxide; IBMK- Isobutylmethylketone; DMFA-N,N-dimethylformamide; BuOH-Butanol; HCW- Hot compressed water; MPY-1-Methyl-2-pyrrolidone;

PVP- Poly-(1-vinyl-2-pyrrolidinone); THF-Tetrahydrofuran; HMPT- Hexamethylphosphotriamide;

HT- Hydrotalcite; VOP- Vanadyl phosphate, NbOPO_4 - Niobium phosphate;

MW-microwave.

Substrate	Catalyst (composition, acid properties)	Reaction Conditions (Solvent/added catalyst/temperature/time)	C_{sub} (%)	Y_{Hmf} or Y_{Fur} (%)	Ref
Zeolites and Zeotypes					
D-Fructose	Na-Beta (Si/Al=25)	DMSO, 130 °C, 30 min	99	49 Hmf	359
D-Xylose	H-Beta (Si/Al=12.5; 508 S_{BET})	(H_2O , 140 °C, 4 h)/(DMSO, 140 °C, 4 h)/ ($\text{H}_2\text{O}+\text{Tol}$, 140 °C, 4 h)	52/90/90	19/24/40 Fur	249
D-Fructose	H-Beta (Si/Al=15)	H_2O , IBMK, 165 °C, 60 min	85	34 Hmf	261
D-Fructose	H-Beta (Si/Al=12.5±2.5)	DMSO, 120 °C, 120 min, 9.7×10^4 Pa	100	97 Hmf	245
D-Fructose	H-Beta (Si/Al=25)	DMSO, 130 °C, 30 min	99	65 Hmf	359
D-Fructose	H-Beta (590 S_{BET} ; 100 AS by TPD- NH_3)	DMSO, 130 °C, 1.5 h	99	60 Hmf	246
D-Fructose	H-Beta (Si/Al=15.6; 610 S_{BET} ; 0.22 V_{micro} ; 860 AS by TPD- NH_3)	H_2O , 165 °C, 82 min, in an autoclave	35	9.8 Hmf	250

D-Fructose or D-Glucose	H-Beta (Si/Al=12.5)	DMFA, 100 °C, 3 h	Trace	0 Hmf	229
Levoglucosan	H-Beta (Si/Al=25; 0.477 V _p ; 589 S _{BET} ; 143 [B]; 7 [L] by IR-py)	H ₂ O, 450 °C, 2 h	nf ^a	1 Hmf+7 Fur	290
D-Xylose	Sn-Beta (Sn/Si=0.01)	Amberlyst co-catalyst, H ₂ O, 110 °C, 180 min	92	9.5 Fur	274
D-Xylose	Sn-Beta (Sn/Si=0.01)	HCl co-catalyst, H ₂ O, 110 °C, 60 min	77	21 Fur	274
D-Glucose	Sn-Beta (Si/Sn=96)	HCl co-catalyst, H ₂ O, 140 °C, 120 min	nf ^a	11 Fur	360
D-Xylose	H-Ferrierite (Si/Al=10; 390 S _{BET})	(H ₂ O, 140 °C, 4h)/(DMSO, 140 °C, 4 h)/ (H ₂ O+Tol, 140 °C, 4 h)	45/74/80	13/23/35 Fur	249
D-Fructose	Na-ZSM-5 (Si/Al=24)	DMSO, 130 °C, 60 min	1	1 Hmf	359
D-Xylose	H-ZSM-5 (Si/Al=11.5; 572 S _{BET})	(H ₂ O, 140 °C, 4 h)/(DMSO, 140 °C, 4 h)/ (H ₂ O+Tol, 140 °C, 4 h)	57/69/90	17/21/43 Fur	249
D-Xylose	H-ZSM-5 (Si/Al=28; 1.2 D _p)	H ₂ O, 220 °C, 10 min	97	46 Fur	220
D-Fructose or D-Glucose	H-ZSM-5 (Si/Al=45)	DMFA, 100 °C, 3h	Trace	0 Hmf	229
D-Fructose	H-ZSM-5 (Si/Al=25)	H ₂ O, IBMK, 165 °C, 60 min	90	53 Hmf	261
D-Fructose	H-ZSM-5 (Si/Al=24)	DMSO, 130 °C, 30 min	94	48 Hmf	359
D-Fructose	H-ZSM-5 (Si/Al=13; 442 S _{BET} ; 0.18 V _{micro} ; 966 AS by TPD-NH ₃)	(Non solvent, 165 °C, 88 min)/(H ₂ O, 165 °C, 67 min)/(H ₂ O+IBMK, 165 °C, 208 min in an autoclave)	38/38/76	12/11/30 Hmf	250
D-Fructose	H-ZSM-5	DMSO, 110 °C, nf ^a	nf ^a	65 Hmf	313
D-Fructose	SiO ₂ /H-ZSM-5 (Si/Al=14.1; 414 S _{BET} ; 0.17 V _{micro} ; 894 AS by TPD-NH ₃)	H ₂ O, 165 °C, 67 min in an autoclave	22	10 Hmf	250
D-Xylose	H-Mordenite (Si/Al=10; 433 S _{BET})	(H ₂ O, 140 °C, 4 h)/(DMSO, 140 °C, 4 h)/ (H ₂ O+Tol, 140 °C, 4 h)	40/62/81	12/24/35 Fur	249
D-Xylose	H-Mordenite (Si/Al=11)	H ₂ O+Tol, 170 °C, 50 min	37	33 Fur	222
D-Xylose	H-Mordenite (Si/Al=12)	H ₂ O+IBMK, 170 °C, 50 min	36	20 Fur	222
D-Xylose	H-Modernite (Si/Al=6)	H ₂ O+Tol, 160 °C, 6 h	79	28 Fur	291,292
D-Fructose	H-Mordenite (Si/Al=11; 0.192 V _{micro} ; 0.056 V _{meso})	H ₂ O+IBMK, 165 °C, 60 min	76	69 Hmf	223,261
D-Fructose	H-Mordenite (Si/Al=12; 420 S _{BET} ; 1100 AS by TPD-NH ₃ ; 229 [B]; 42 [L] by IR-py; 0.5-0.75 D _p)	H ₂ O, 135 °C, 433 min	7	3 Hmf	407

D-Fructose	H-Mordenite (Si/Al=11.7; 461 S _{BET} ; 0.21 V _{micro} ; 1100 AS by TPD-NH ₃)	(Non solvent, 165 °C, 124 min)/H ₂ O, 165 °C, 117 min)/(H ₂ O+IBMK, 165 °C, 83 min), in an autoclave	55/56/12	27/27/12 Hmf	250
D-Fructose	SiO ₂ /H-Mordenite (Si/Al=13.7; 423 S _{BET} ; 0.2 V _{micro} ; 915 AS by TPD-NH ₃)	(H ₂ O, 165 °C, 182 min)/(H ₂ O+IBMK, 165 °C, 400 min) in an autoclave	56/78	36/53 Hmf	250
D-Xylose	H-Y Faujasite (Si/Al=2.6; 631 S _{BET})	(H ₂ O, 140 °C, 4 h)/(DMSO, 140 °C, 4 h)/(H ₂ O+Tol, 140 °C, 4 h)	71/61/97	22/1/41 Fur	249
D-Xylose	H-Y Faujasite (Si/Al=5)	H ₂ O+Tol, 160 °C, 6 h	94	39 Fur	291,292
D-Xylose	H-Y Faujasite (Si/Al=30; 303 S _{BET} ; 0.028 V _{micro} ; 312 [B]; 208 [L] by TPD-NH ₃)	H ₂ O, 160 °C, 90 min	75	24 Fur	271
D-Xylose	H-Y Faujasite (Si/Al=15)	(H ₂ O+Tol, 170 °C, 50 min)/(H ₂ O+IBMK, 170 °C, 50 min)	51/54	42/30 Fur	222
D-Fructose	H-Y Faujasite (Si/Al=2.4)	DMSO, 120 °C, 120 min, 9.7x10 ⁴ Pa	100	76 Hmf	245
D-Fructose	H-Y Faujasite (Si/Al=15)	H ₂ O, IBMK, 165 °C, 60 min	76	40 Hmf	261
D-Glucose	H-Y Faujasite (515.2 S _{BET} ; 0.74 D _p)	H ₂ O, 150 °C, 2.5 h	56	6 Hmf	357
D-Glucose	H-Y Faujasite (Si/Al=3.3)	H ₂ O, 160 °C, 3 h	68	7 Hmf	244
D-Glucose	H-Y Faujasite (Si/Al=3.3; Na ₂ O= 0.18 wt.%; 645±3 S _{BET} ; AS= 520±10; 0.74 D _p)	H ₂ O, 150 °C, 5 h	87	8 Hmf	387
D-Sucrose	H-Y Faujasite (Si/Al=15)	H ₂ O, 95 °C, 120 min	100	Traces	358
Levogluconan	H-MCM-22 (Si/Al=30; 547 S _{BET} ; 173 [B]; 15 [L] by IR-py)	H ₂ O, 300 °C, 0.3 s	nf ^a	0 Hmf+1 Fur	295
D-Xylose	Nu-6 (2) (Si/Al=36; Na/Al=3.3; 25 S _{BET} ; 0.01 V _p)	H ₂ O, Tol, 170 °C, 6 h	90	22 Hmf	265
D-Xylose	H-Nu-6 (2) (Si/Al=32; Na/Al=1.6; 20 S _{BET} ; 0.01 V _p)	H ₂ O, Tol, 170 °C, 6 h	60/90	28/45 Hmf	265
Amorphous silica					
D-Fructose	SiO ₂ -gel (0.500 g)	H ₂ O, 20 bar of synthetic air, 160 °C, 65 min	52	52 Hmf	385
D-Fructose	SiO ₂	H ₂ O, 120 °C, 5 min	nf ^a	1.2 Hmf	372
D-Xylose	Si-H-SBA-15 (765 S _{BET} , ²⁵⁷ 584 S _{BET} , ²⁹³ 1.09 V _p , ^{257,293} 1.1 D _p , ²⁵⁷ 8.09 D _p ²⁹³)	H ₂ O, Tol, 160 °C, 4 h	39	5 Fur	257,293
D-Fructose	Si-H-SBA-15 (850 S _{BET} ; 8.9 D _p ⁴¹⁶)	H ₂ O, IBMK/2-BuOH, 180 °C, 120 min	59	31 Hmf	346
D-Xylose	Si-H-MCM-41 (833 S _{BET} ; 0.59 V _p)	DMSO, 140 °C, 24 h	86	45 Fur	240
Alumina					
D-Xylose	γ-Al ₂ O ₃ (262 S _{BET} ; 171 [B]; 257 [L] by TPD-NH ₃)	H ₂ O, 160 °C, 90 min	100	10 Fur	271

Table 1.6- Continued.					
D-Xylose	$\gamma\text{-Al}_2\text{O}_3$ (250 S_{BET})	H ₂ O, 160 °C, 60 min	84	18 Fur	281
D-Xylose	$\gamma\text{-Al}_2\text{O}_3$ (213 S_{BET})	(H ₂ O, 140 °C, 4 h)/(DMSO, 140 °C, 4 h)/ (H ₂ O+Tol, 140 °C, 4 h)	84/85/99	21/13/31 Fur	249
D-Fructose	A ₂ O ₃ (262 S_{BET} ; 72 AS by TPD-NH ₃ ; 135 [L] by IR-py; 9.8 D _p)	H ₂ O, 135 °C, 458 min	24	4 Hmf	407
D-Fructose	Al ₂ O ₃	DMSO, 120 °C, 2 h, 9.7x10 ⁴ Pa	40	0 Hmf	245
D-Fructose	Al ₂ O ₃	H ₂ O, 120 °C, 5 min	nf ^a	2 Hmf	372
Modified aluminium					
D-Xylose	Al-Phosphate (155 S_{BET})	(H ₂ O, 160 °C, 60 min)/(H ₂ O, 180 °C, 30 min)/(H ₂ O, 200 °C, 30 min)	18/27/89	11/18/47 Fur	281
D-Glucose	Pt/Al ₂ O ₃	HCW, 1x10 ⁷ Pa, continuous flow, 238-250 °C	22	0	378
Porous metallosilicates					
D-Xylose	Na-AM-11 (Si/Nb=19.5; 489 S_{BET} ; 0.22 V _p)	H ₂ O, Tol, 160 °C, 6 h	77	31 Fur	291,292
D-Xylose	H-AM-11 (Si/Nb=29.2; 328 S_{BET} ; 0.17 V _p)	H ₂ O, Tol, 160 °C, 6 h	85	46 Fur	291,292
D-Xylose	ex-H-AM-11 (Si/Nb=3.7; Nb loading= 19.5 wt.%, 395 S_{BET} ; 0.22 V _p ; prepared by ion-exchange with NH ₄ NO ₃ solution)	H ₂ O, Tol, 160 °C, 6 h	85	39 Fur	291
D-Xylose	Nb-MCM-41 (Si/Nb=2.4, 1040 S_{BET} ; 0.99 V _p ; 4.0 D _p)	H ₂ O, Tol, 160 °C, 6 h	99	39 Fur	291,292
D-Xylose	ex-Nb-MCM-41 (Si/Nb=23; Nb loading= 4.5 wt.%, 827 S_{BET} ; 0.66 V _p ; 3.5 D _p ; prepared by ion-exchange with NH ₄ Cl)	H ₂ O, Tol, 160 °C, 6 h	94	35 Fur	291
Levogluconan	Pt-MCM-48 (410 S_{BET} ; 0.573 V _p ; 5 [B]; 3 [L] by IR-py)	H ₂ O, 450 °C, 2 h	nf ^a	12 Hmf+1 Fur	290
Modified mesoporous silicates with organic groups (hybrids)					
D-Xylose	SBA-15-SO ₃ H (S loading=1.49 mmol.g ⁻¹ ; 747 S_{BET} ; 1.26 V _p ; 6.6 D _p (for fresh)); (S loading=1.48 mmol.g ⁻¹ ; 338 S_{BET} ; 0.42 V _p ; 3.9-5.7 D _p (for used))	H ₂ O, Tol, 160 °C, 4 h	92	68 Fur	257
D-Fructose	SBA-15-pSO ₃ H (S/Si=1.35, 640 S_{BET} ; 4.5 D _p ; 0.90 V _p ; 64 AS)	H ₂ O, IBMK:2-BuOH, 130 °C, 140 min	79	52 Hmf	352
D-Xylose	MSHS-SO ₃ H (Sulfonic acid modified mesoporous shell silica bead; S loading=0.35 mmol.g ⁻¹ ; 432 S_{BET} ; 0.38 V _p ; 3.4 D _p)	H ₂ O, 190 °C, 1 h	64	44 Fur	289
D-Xylose	HMS-SO ₃ H	H ₂ O, 190 °C, 1 h	64	14 Fur	289
D-Xylose	MCM-41-SO ₃ Hc (S loading= 3.9 wt.%; 438 S_{BET} ; 0.24 V _p ; 0.7 H ⁺ m _{eq} .g ⁻¹ by T-NaOH)	DMSO, 140 °C, 24 h	91	75 Fur	240
D-Xylose	MCM-41-SO ₃ H (S loading=1.09 mmol.g ⁻¹ ; 686 S_{BET} ; 0.68 V _p ; 1.9 D _p)	H ₂ O, 170 °C, 1 h	37	24 Fur	289

D-Xylose	SBA-15-SH (Propylthiol mesoporous silica)	H ₂ O, Tol, 160 °C, 4 h	23	0 Fur	²⁵⁷
D-Fructose	Tp-A380 (Thiopropyl groups grafted onto non-porous silica; S loading=0.36 mmol.g ⁻¹ ; 360 S _{BET})	H ₂ O, IBMK/2-BuOH, 180 °C, 120 min, autonomous pressure	62	38 Hmf	³⁴⁶
D-Fructose	Tp-SBA-15 (Thiopropyl functionalised mesoporous silica; S loading=1.1 mmol.g ⁻¹ ; 444 S _{BET} ; 4.1 D _p)	H ₂ O, IBMK/2-BuOH, 180 °C, 120 min, autonomous pressure	61	32 Hmf	³⁴⁶
D-Fructose	Taa-A380 (Propylsulfonic acid groups on Tp-A380; S loading=0.38 mmol.g ⁻¹)	H ₂ O, IBMK/2-BuOH, 180 °C, 120 min, autonomous pressure	67	43 Hmf	³⁴⁶
D-Fructose	Taa-SBA-15 (Propyl sulfonic acid groups on Tp-SBA-15; S loading=2.3 mmol.g ⁻¹ ; 218 S _{BET} ; 7.5 D _p)	H ₂ O, IBMK/2-BuOH, 180 °C, 30 min, autonomous pressure	66	49 Hmf	³⁴⁶
D-Fructose	SSA-SBA-15 (3-(propylsulfonyl)propane-1-sulfonic acid functionalised in SBA-15; S/Si=0.82; 585 S _{BET} ; 4.7 D _p ; 0.86 V _p , 64 AS)	H ₂ O, IBMK/2-BuOH, 130 °C, 140 min	81	53 Hmf	³⁵²
D-Fructose	TESAS-SBA-15 (3-(propylthio)propane-1-sulfonic acid functionalised in SBA-15; S/Si=1.25; 449 S _{BET} ; 4.7 D _p ; 0.72 V _p ; 64 AS)	H ₂ O, IBMK/2-BuOH, 130 °C, 141 min	84	60 Hmf	³⁵²
D-Fructose	Si-SphSA (phosphonic arylsulfonic acid-functionalised non-ordered silica)	H ₂ O, IBMK/2-BuOH, 130 °C, 115 min	79	53 Hmf	³⁵²
Modified ordered mesoporous silicates (with sulfate groups)					
D-Xylose	SO₄²⁻/ZrO₂-Al₂O₃/SBA-15 (ZrO ₂ -Al ₂ O ₃ =12 wt.%, S loading=1.55 wt.%; 276 S _{BET} ; 0.43 V _p , 6.60 D _p ; AS=910 by TPD-NH ₃)	H ₂ O, Tol, 160 °C, 4 h	99	53 Fur	²⁹³
D-Xylose	SO₄²⁻/ZrO₂/SBA-15 (ZrO ₂ = 12 w%, S loading= 1.96 wt.%, 245 S _{BET} ; 0.32 V _p ; 4.94 D _p ; 880 AS by TPD-NH ₃)	H ₂ O, Tol, 160 °C, 4 h	98	44 Fur	²⁹³
Ordered mesoporous aluminosilicates					
Levoglucosan	Al-SBA-15 (632 S _{BET} ; 0.509 V _p ; 4 [B]; 4 [L] by IR-py)	H ₂ O, 450 °C, 2 h	nf ^a	1Hmf+11 Fur	²⁹⁰
D-Xylose	SiO₂-Al₂O₃ (Si/Al=5; 585 S _{BET} ; 342 [B]; 90 [L] by TPD-NH ₃)	H ₂ O, 160 °C, 90 min	90	23 Fur	²⁷¹
D-Xylose	SiO₂-Al₂O₃ (Si/Al=3.3; 572 S _{BET})	(H ₂ O, 140 °C, 4h)/(DMSO, 140 °C, 4 h)/(H ₂ O+Tol, 140 °C, 4 h)	43/91/99	15/11/41 Fur	²⁴⁹
D-Xylose	SiO₂-Al₂O₃ (Si/Al=5, 370 S _{BET} ; Si/Al=30, 470 S _{BET} ; Si/Al=40, 500 S _{BET})	H ₂ O, 160 °C, 60 min	85/78/55	17/19/16 Fur	²⁸¹
D-Fructose	SiO₂-Al₂O₃ (Si/Al=11; 327 S _{BET} ; 12 AS by TPD-NH ₃ ; 28 [B]; 46 [L] by IR-py; 9.5 D _p)	H ₂ O, 135 °C, 500 min	24	6 Hmf	⁴⁰⁷

D-Fructose	SiO ₂ -Al ₂ O ₃ (Si/Al=10.8; 327 S _{BET} ; 225 AS by TPD-NH ₃)	(Non solvent, 165 °C, 135 min)/(H ₂ O, 165 °C, 95 min)/(H ₂ O+IBKM, 165 °C, 105 min) in an autoclave	62/48/50	20/14/16 Hmf	250
D-Xylose	Al-MSHS (Aluminium modified mesoporous shell silica bead; 473.5 S _{BET} ; 0.6 V _p ; 2 D _p)	H ₂ O, 170 °C, 1 h	45	16 Fur	289
D-Glucose	Al-MCM-20 (541.8 S _{BET} ; 2.74 D _p)	H ₂ O, 150 °C, 24 h	60	18 Hmf	357
D-Xylose	Al-MCM-41 (Al ₂ O ₃ loading: 3-4 wt.%; S _{BET} ≥ 800; V _p ≥ 0.70; 3 D _p)	H ₂ O, NaCl, 1-BuOH, 170 °C, 2 h	82	48 Fur	294
D-Xylose	Al-MCM-41 (649 S _{BET} ; 0.35 V _p ; 2. 6 D _p)	H ₂ O, Tol, 160 °C, 6 h	96	47 Fur	292
D-Glucose	Al-MCM-41 (799.8 S _{BET} ; 3.28 D _p)	H ₂ O, 150 °C, 16 h	80	16 Hmf	357
Levoglucosan	Al-MCM-41 (0.636 V _p ; 944 S _{BET} ; 3 [B]; 12 [L] by IR-py)	H ₂ O, 450 °C, 2 h	nf ^a	1 Hmf+14 Fur	290
Levoglucosan	Al-MCM-41 (Si/Al=20; 944 S _{BET} ; 3 [B]; 12 [L] by IR-py)	H ₂ O, 300 °C, 0.3 s	nf ^a	0 Hmf+6 Fur	295
Levoglucosan	Al-MCM-48 (0.573 V _p ; 718 S _{BET} ; 2 [B]; 7 [L] by IR-py)	H ₂ O, 450 °C, 2 h	nf ^a	2 Hmf+10 Fur	290
Layered materials					
D-Fructose	AIVOP (0.8 S _{BET})/CrVOP (10 S _{BET}) ^b	H ₂ O, 80 °C, 2h	76/58	58/58 Hmf	386
D-Fructose	FeVOP (5.3 S _{BET})/MnVOP (3.7 S _{BET})/GaVOP (0.8 S _{BET}) ^b	H ₂ O, 80 °C, 1 h	71/55/52	60/46/39 Hmf	386
D-Fructose	VOP/SiO ₂ (14 wt.% VOP; 200 S _{BET}); VOP/ γ-Al ₂ O ₃ (7.9 wt.%; 100 S _{BET}); VOP/TiO ₂ (9.6 wt.% VOP; 125 S _{BET})	H ₂ O, 80 °C, 1 h	39/38/40	29/32/35 Hmf	386
D-Fructose	Nb ₂ O ₅	H ₂ O, 100 °C, 54-70 h	71-78	18-20 Hmf	382
D-Fructose	Nb ₂ O ₅ (180 S _{BET} ; 242 AS by TPD-NH ₃ ; 11 [B]; 27 [L] by IR-py; 8.0 D _p)	H ₂ O, 135 °C, 250 min	44	13 Hmf	407
D-Fructose	Nb ₂ O ₅ .nH ₂ O (80 wt.% Nb ₂ O ₅ ; 20 wt.% H ₂ O; 108 S _{BET} ; 222 ITA by IR-NH ₃)	H ₂ O, 100 °C, 40 min	42	9 Hmf	380
D-Fructose	Nb ₂ O ₅ .nH ₂ O (70 S _{BET} ; 3500 AS by TPD-NH ₃)	2-BuOH, H ₂ O, 160 °C, nf ^a	79	46 Hmf	379
D-Fructose	Nb ₂ O ₅ .nH ₂ O	DMFA, 100 °C, 3 h	8	0 Hmf	229
D-Glucose	Nb ₂ O ₅ .nH ₂ O	DMFA, 100 °C, 3 h	12	0 Hmf	229
D-Fructose	Nb ₂ O ₅ .nH ₂ O/H ₃ PO ₄ (215 S _{BET} ; 4400 AS ³⁷⁹ by NH ₃ -TPD, 4.3 D _p ³⁸⁴)	BuOH, H ₂ O, 160 °C, 50 min ³⁸⁴	90	89 Hmf	379,384
D-Fructose	NbOPO ₄ (P/Nb= 0.45; 150 S _{BET})	H ₂ O, 100 °C, 30 min	29	29 Hmf	381,383
D-Fructose	NbOPO ₄ (66.7 wt.% Nb ₂ O ₅ ; 15.9 wt.% P ₂ O ₅ ; 2.1 wt.% K ₂ O; 142 S _{BET} ; 283 ITA by IR-NH ₃)	H ₂ O, 110 °C, 30 min	65	23 Hmf	380

D-Glucose	$\text{Nb}_2\text{O}_5 \cdot n\text{H}_2\text{O}/\text{H}_3\text{PO}_4$ (215 S_{BET} ; 4400 AS by NH_3 -TPD; ³⁷⁹ 4.3 D_p ³⁸⁴)	BuOH, H ₂ O, 160 °C, 110 min	68	49 Hmf	384
D-Sucrose	NbOPO_4 (P/Nb=0.53; Nb loading= 3.4 wt.%)	H ₂ O, 100 °C, 4 h	30	27 Hmf	381
Inulin	$\text{Nb}_2\text{O}_5 \cdot n\text{H}_2\text{O}/\text{H}_3\text{PO}_4$ (215 S_{BET} ; 4400 AS by NH_3 -TPD; ³⁷⁹ 4.3 D_p ³⁸⁴)	BuOH, H ₂ O, 160 °C, 140 min	86	54 Hmf	384
Inulin	NbOPO_4 (P/Nb= 0.45; 150 S_{BET})	H ₂ O, 100 °C, 30 min	30	26 Hmf	381
Jerusalem artichoke juice ^c	$\text{Nb}_2\text{O}_5 \cdot n\text{H}_2\text{O}/\text{H}_3\text{PO}_4$ (215 S_{BET} ; 4400 AS by NH_3 -TPD; ³⁷⁹ 4.3 D_p ³⁸⁴)	BuOH, H ₂ O, 160 °C, 150 min	93	51 Hmf	384
D-Xylose	$\text{SO}_4^{2-}/\text{Nb}_2\text{O}_5$ (SO_4^{2-} loading= 0.58 mmol.g ⁻¹ ; 39 S_{BET})	H ₂ O, Tol, 100 °C, 48 h	20	8 Fur	255
D-Fructose	$\text{Ta}_2\text{O}_5 \cdot n\text{H}_2\text{O}$ (41.6 S_{BET} ; 900 AS by NH_3 -TPD)	BuOH, H ₂ O, 160 °C, nf ^a	81	62 Hmf	379
D-Fructose	$\text{Ta}_2\text{O}_5 \cdot n\text{H}_2\text{O}/\text{H}_3\text{PO}_4$ (141.5 S_{BET} ; 1500 AS by NH_3 -TPD)	BuOH, H ₂ O, 160 °C, 100 min	94	90 Hmf	379
D-Glucose	$\text{Ta}_2\text{O}_5 \cdot n\text{H}_2\text{O}/\text{H}_3\text{PO}_4$ (141.5 S_{BET} ; 1500 AS by NH_3 -TPD)	BuOH, H ₂ O, 160 °C, 120 min	68	57 Hmf	379
Inulin	$\text{Ta}_2\text{O}_5 \cdot n\text{H}_2\text{O}/\text{H}_3\text{PO}_4$ (141.5 S_{BET} ; 1500 AS)	BuOH, H ₂ O, 160 °C, 150 min	95	87 Hmf	379
Jerusalem artichoke juice ^c	$\text{Ta}_2\text{O}_5 \cdot n\text{H}_2\text{O}/\text{H}_3\text{PO}_4$ (141.5 S_{BET} ; 1500 AS)	BuOH, H ₂ O, 160 °C, 120 min	91	79 Hmf	379
D-Xylose	RE [H_2cmp] H ₂ O (RE ³⁺ = Y ³⁺ , La ³⁺ , Pr ³⁺ , Nd ³⁺ , Sm ³⁺ , Eu ³⁺ , Gd ³⁺ , Tb ³⁺ , Dy ³⁺ , Ho ³⁺ , Er ³⁺ ; multi-functional rare-earth (RE) hybrid layered networks formed by rare-earth chloride salts and N-(carboxymethyl)iminodi(methylphosphoric acid) (H_5cmp))	H ₂ O, Tol, 170 °C, 4 h	40-77	25-40 Fur	282
D-Glucose	H-pillared montmorillonite (40.9± 8.1 S_{BET} ; 900±70 AS; 1.72±0.01 D_p)	H ₂ O, 150 °C, 12 h	60	13 Hmf	387
D-Glucose	Al-pillared montmorillonite (132 S_{BET} ; 1.08 D_p)	H ₂ O, 150 °C, 5 h	86	13 Hmf	357
D-Glucose	Al-pillared montmorillonite (138±0.8 S_{BET} ; 520±10 AS; 1.08±0.06 D_p)	H ₂ O, 150 °C, 5 h	80	10 Hmf	387
D-Glucose	Cr-pillared montmorillonite (250±21.7 S_{BET} ; 980±170 AS; 1.2±0.03 D_p)	H ₂ O, 150 °C, 5 h	82	13 Hmf	387
D-Glucose	Fe-pillared montmorillonite (231±7.0 S_{BET} ; 930±150 AS; 1.5±0.07 D_p)	H ₂ O, 150 °C, 3.6 h	87	3 Hmf	387
Exfoliated nanosheets					
D-Xylose	$\text{eH}_4\text{Nb}_6\text{O}_{17}$ (136 S_{BET} ; 0.18 V_p ; 204 [B]; 245 [L] by IR-py)	H ₂ O, Tol, 160 °C, 2 h	97	53 Fur	299
D-Xylose	$\text{eH}_2\text{Ti}_3\text{O}_7$ (57 S_{BET} ; 0.03 V_p ; 7 [B]; 135 [L] by IR-py)	H ₂ O, Tol, 160 °C, 2 h	97	44 Fur	299

Table 1.6- <i>Continued.</i>					
D-Xylose	eHTi ₂ NbO ₇ (88 S _{BET} ; 0.08 V _p ; 85 [B]; 226 [L] by IR-py)	H ₂ O, Tol, 160 °C, 2 h	96	51 Fur	299
D-Xylose	eHTiNbO ₅ -MgO (103 S _{BET} ; 0.08 V _p ; 162 [B]; 220 [L] by IR-py)	H ₂ O, Tol, 160 °C, 3 h	90	54 Fur	299
Delaminated microporous aluminosilicate					
D-Xylose	del-Nu-6(1) (Si/Al=29, Na/Al=0.9; 151 S _{BET} ; 0.07 V _p)	H ₂ O, Tol, 170 °C, 1 h	90	48 Fur	265
Titanium oxides					
D-Xylose	HTiNbO ₅ (330 S _{BET} ⁴¹⁷)	H ₂ O, Tol, 160 °C, 6 h	45	26 Fur	299
D-Xylose	TiO ₂ (48 S _{BET} ; 0.120 V _p ; 4.6 D _p ; 161 AS by TPD-NH ₃ ; 83.9 BS by TPD-CO ₂)	HCW, 250 °C, 5 min	72	31 Fur	296,297
D-Xylose	TiO ₂ (8.7 S _{BET})	H ₂ O, 160 °C, 60 min	80	33 Fur	281
D-Fructose	Anatase TiO ₂	(HCW, 200 °C, 5 min, MW)/(HCW, 200 °C, 5 min, sand bath)	84/65	38/27 Hmf +5/5 Fur	366
D-Fructose	Anatase-TiO ₂ (4.7 S _{BET} ; 79 AS by TPD-NH ₃ ; 42 BS by TPD-CO ₂)	H ₂ O, 200 °C, 5 min	98	22 Hmf	368
D-Fructose	Anatase TiO ₂	H ₂ O, 200 °C, 300 s	nf ^a	21 Hmf+2 Fur	363
D-Fructose	TiO ₂	H ₂ O, n-BuOH, 200 °C, 1.38x10 ⁷ Pa, 3 min	nf ^a	18 Hmf	365
D-Fructose	TiO ₂ (326 S _{BET} ; 0.3 V _p)	(H ₂ O, 120 °C, 5 min, MW)/(H ₂ O, 120 °C, 15 min, MW) / (acetonitrile, 120 °C, 5 min, MW)	nf ^a	34/36/29 Hmf	372
D-Fructose	TiO ₂ (326 S _{BET} ; 0.3 V _p)	(DMSO, 140 °C, 5 min, MW)/(MPY, 140 °C, 5 min, MW)/(H ₂ O+IBMK, 130 °C, 5 min, MW)	nf ^a	54/37/40 Hmf	372
D-Glucose	Anatase TiO ₂	(H ₂ O, 200 °C, 300 s)/(HCW, 200 °C, 200 s)	nf ^a	20/16 Hmf +2/2 Fur	363
D-Glucose	Anatase TiO ₂	HCW, 200 °C, 3 min, MW	42	7 Hmf+1 Fur	366
D-Glucose	Anatase-TiO ₂ (4.7 S _{BET} ; 79 AS by TPD-NH ₃ ; 42 BS by TPD-CO ₂)	H ₂ O, 200 °C, 5 min	83	19 Hmf	368
D-Glucose	TiO ₂ (48 S _{BET} ; 0.120 V _p ; 4.6 D _p ; 161 AS by TPD-NH ₃ ; 84 BS by TPD-CO ₂)	HCW, 250 °C, 5 min	78	27 Hmf+4 Fur	296,297
D-Glucose	TiO ₂ (326 S _{BET} ; 0.3 V _p)	(H ₂ O, 120 °C, 5 min)/(DMSO, 140 °C, 5 min)/(MPY, 150 °C, 5 min)/(H ₂ O+IBMK, 130 °C, 5 min)	nf ^a	25/37/30/26 Hmf	372

D-Glucose	TiO₂	(0.15 M HCl, H ₂ O, IBMK, 180 °C, 6.9x10 ⁶ Pa, 2 min)/(0.10 M H ₃ PO ₄ , H ₂ O, IBMK, 180 °C, 6.9x10 ⁶ Pa, 2 min)	nf ^a	37/33 Hmf	³⁶⁵
D-Glucose	TiO₂	(H ₂ O+IBMK, 180 °C, 3.4E6 Pa, 2 min)/(H ₂ O+n-BuOH, 200 °C, 1.38Ex10 ⁷ Pa, 3 min)/(H ₂ O+n-BuOH+IBMK, 180 °C, 1.38x10 ⁷ Pa, 2 min)/(H ₂ O+IBMK+4 methy-2-pentanol, 180 °C, 1.38x10 ⁷ Pa, 2 min)	nf ^a	29/13/12/14 Hmf	³⁶⁵
D-Maltose	TiO₂ (326 S _{BET} ; 0.3 V _p)	(H ₂ O, 120 °C, 5 min)/(DMSO, 140 °C, 5 min)	nf ^a	11/14 Hmf	³⁷²
D-Sucrose	TiO₂ (326 S _{BET} ; 0.3 V _p)	(H ₂ O, 120 °C, 10 min)/(DMSO, 140 °C, 5 min)/(MPY, 140 °C, 5 min)/(H ₂ O+IBMK, 130 °C, 5 min)	nf ^a	15/21/12/15 Hmf	³⁷²
D-Sucrose	TiO₂	H ₂ O, n-BuOH, 180 °C, 1.38x10 ⁷ Pa, 3 min	nf ^a	16 Hmf	³⁶⁵
D-Cellobiose	TiO₂ (326 S _{BET} ; 0.3 V _p)	(H ₂ O, 120 °C, 5 min)/(DMSO, 140 °C, 5 min)	nf ^a	15/19 Hmf	³⁷²
D-Xylan	TiO₂ (48 S _{BET} ; 0.120 V _p ; 4.6 D _p ; 161 AS by TPD-NH ₃ ; 83.9 BS by TPD-CO ₂)	HCW, 250 °C, 5 min	67 ²⁹⁷ /62 ²⁹⁶	26 Fur	^{296,297}
Cellulose	TiO₂ (48 S _{BET} ; 0.120 V _p ; 4.6 D _p ; 161 AS by TPD-NH ₃ ; 83.9 BS by TPD-CO ₂)	HCW, 250 °C, 5 min	62 ²⁹⁷ /60 ²⁹⁶	12 Hmf+3 Fur	^{296,297}
Cellulose	TiO₂	H ₂ O, IBMK, 270 °C, 6.9x10 ⁶ Pa, 60 min, continuous process	80	35 Hmf	³⁶⁵
Starch	TiO₂	H ₂ O, IBMK, 180 °C, 6.9x10 ⁶ Pa, 2 min	nf ^a	15 Hmf	³⁶⁵
Lite corn syrup	TiO₂	H ₂ O, IBMK, 180 °C, 6.9x10 ⁶ Pa, 2 min	nf ^a	27 Hmf	³⁶⁵
Honey	TiO₂	H ₂ O, IBMK, 170 °C, 6.9x10 ⁶ Pa, 2 min	nf ^a	26 Hmf	³⁶⁵
Sugarcane bagasse	TiO₂ (48 S _{BET} ; 0.120 V _p ; 4.6 D _p ; 161 AS by TPD-NH ₃ ; 83.9 BS by TPD-CO ₂)	HCW, 250 °C, 5 min	nf ^a	7 Hmf+9 Fur	^{296,297}
Rice husk	TiO₂ (48 S _{BET} ; 0.120 V _p ; 4.6 D _p ; 161 AS by TPD-NH ₃ ; 83.9 BS by TPD-CO ₂)	HCW, 250 °C, 5 min	nf ^a	3 Hmf+8 Fur	²⁹⁷
Cornocobs	TiO₂ (48 S _{BET} ; 0.120 V _p ; 4.6 D _p ; 161 AS by TPD-NH ₃ ; 83.9 BS by TPD-CO ₂)	HCW, 250 °C, 5 min	nf ^a	8 Hmf+10 Fur	²⁹⁷

Zirconium oxides					
D-Xylose	ZrO ₂ (124 S _{BET} ; 0.234 V _p ; 4.3 D _p ; 232 AS by TPD-NH ₃ ; 129 BS by TPD-CO ₂)	HCW, 250 °C, 5 min	65 ²⁹⁶ /66 ²⁹⁷	26 Fur	^{296,297}
D-Fructose	ZrO ₂ (27.1 S _{BET})	H ₂ O, 200 °C, 5 min	80	36 Hmf	³⁶⁷
D-Fructose	ZrO ₂ (27.1 S _{BET})	Acetone, DMSO, 180 °C, 5 min	75	46 Hmf	³⁶⁷
D-Fructose	ZrO ₂	HCW, 200 °C, 5 min, MW	65	31 Hmf+3 Fur	³⁶⁶
D-Fructose	ZrO ₂ (110 S _{BET} ; 670 AS by TPD-NH ₃ ; 550 BS by TPD-CO ₂)	H ₂ O, 200 °C, 5 min	92	15 Hmf	³⁶⁸
D-Fructose	ZrO ₂	H ₂ O, 200 °C, 300 s	nf ^a	15 Hmf+1 Fur	³⁶³
D-Glucose	ZrO ₂	H ₂ O, 200 °C, 300 s	nf ^a	5 Hmf+1 Fur	³⁶³
D-Glucose	ZrO ₂	H ₂ O, IBMK, flow system, 180 °C, 3.4x10 ⁶ Pa, 2 min	nf ^a	21 Hmf	³⁶⁵
D-Glucose	ZrO ₂ (124 S _{BET} ; 0.234 V _p ; 4.3 D _p ; 232 AS by TPD-NH ₃ ; 129 BS by TPD-CO ₂)	HCW, 250 °C, 5 min	76	17 Hmf+3 Fur	^{296,297}
D-Glucose	ZrO ₂	HCW, 200 °C, 5 min, MW	57	10 Hmf+1 Fur	³⁶⁶
D-Glucose	ZrO ₂ (110 S _{BET} ; 670 AS; 550 BS)	H ₂ O, 200 °C, 5 MW	51	5 Hmf	³⁶⁸
D-Xylan	ZrO ₂ (124 S _{BET} ; 0.234 V _p ; 4.3 D _p ; 232 AS by TPD-NH ₃ ; 129 BS by TPD-CO ₂)	HCW, 250 °C, 5 min	49 ²⁹⁶ /51 ²⁹⁷	23 Fur	^{296,297}
Cellulose	ZrO ₂ (124 S _{BET} ; 0.234 V _p ; 4.3 D _p ; 232 AS by TPD-NH ₃ ; 129 BS by TPD-CO ₂)	HCW, 250 °C, 5 min	38 ²⁹⁶ /45 ²⁹⁷	8 Hmf+2 Fur	^{296,297}
Sugar Cane Bagasse	ZrO ₂ (124 S _{BET} ; 0.234 V _p ; 4.3 D _p ; 232 AS by TPD-NH ₃ ; 129 BS by TPD-CO ₂)	HCW, 250 °C, 5 min	nf ^a	4 Hmf+7 Fur	^{296,297}
Rice Husk	ZrO ₂ (124 S _{BET} ; 0.234 V _p ; 4.3 D _p ; 232 AS by TPD-NH ₃ ; 129 BS by TPD-CO ₂)	HCW, 250 °C, 5 min	nf ^a	2 Hmf+5 Fur	²⁹⁷
Corcob	ZrO ₂ (124 S _{BET} ; 0.234 V _p ; 4.3 D _p ; 232 AS by TPD-NH ₃ ; 129 BS by TPD-CO ₂)	HCW, 250 °C, 5 min	nf ^a	6 Hmf+7 Fur	²⁹⁷
D-Xylose	TiO ₂ -ZrO ₂ (187 S _{BET} ; 0.391 V _p ; 2.5 D _p ; 645 AS by TPD-NH ₃ ; 712 BS by TPD-CO ₂)	HCW, 250 °C, 5 min	79	34 Fur	²⁹⁷
D-Glucose	TiO ₂ -ZrO ₂ (187 S _{BET} ; 0.391 V _p ; 2.5 D _p ; 645 AS by TPD-NH ₃ ; 712 BS by TPD-CO ₂)	HCW, 250 °C, 5 min	84	29 Hmf+5 Fur	²⁹⁷
D-Xylan	TiO ₂ -ZrO ₂ (173 S _{BET} ; 0.335 V _p ; 3.1 D _p)	Acetone, DMSO, 250 °C, 5 min	22	17 Fur	²⁹⁷

D-Xylan	TiO ₂ -ZrO ₂ (187 S _{BET} ; 0.391 V _p ; 2.5 D _p ; 645 AS by TPD-NH ₃ , 712 BS by TPD-CO ₂)	HCW, 250 °C, 5 min	75	27 Fur	²⁹⁷
Cellulose	TiO ₂ -ZrO ₂ (187 S _{BET} ; 0.391 V _p ; 2.5 D _p ; 645 AS by TPD-NH ₃ ; 712 BS by TPD-CO ₂)	HCW, 250 °C, 5 min	71	14 Hmf+2 Fur	²⁹⁷
Cellulose	TiO ₂ -ZrO ₂ (173 S _{BET} ; 0.335 V _p ; 3.1 D _p)	Acetone, DMSO, 250 °C, 5 min	37	11 Hmf+2 Fur	²⁹⁷
Sugarcane bagasse	TiO ₂ -ZrO ₂ (187 S _{BET} ; 0.391 V _p ; 2.5 D _p ; 645 AS by TPD-NH ₃ ; 712 BS by TPD-CO ₂)	HCW, 250 °C, 5 min	nf ^a	7 Hmf+9 Fur	²⁹⁷
Rice husk	TiO ₂ -ZrO ₂ (187 S _{BET} ; 0.391 V _p ; 2.5 D _p ; 645 AS by TPD-NH ₃ ; 712 BS by TPD-CO ₂)	HCW, 250 °C, 5 min	nf ^a	3 Hmf+9 Fur	²⁹⁷
Corncob	TiO ₂ -ZrO ₂ (187 S _{BET} ; 0.391 V _p ; 2.5 D _p ; 645 AS by TPD-NH ₃ ; 712 BS by TPD-CO ₂)	HCW, 250 °C, 5 min	nf ^a	8 Hmf+10 Fur	²⁹⁷
D-Xylose	WO _x -ZrO ₂ (149 S _{BET} ; 138 [B]; 186 [L] by TPD-NH ₃)	H ₂ O, 160 °C, 90 min	96	16 Fur	²⁷¹
D-Fructose	WO ₃ -ZrO ₂	DMSO, 120 °C, 2 h, 9.7x10 ⁴ Pa	100	94 Hmf	²⁴⁵
D-Xylan	WO ₃ -ZrO ₂ (92 S _{BET} ; 0.189 V _p ; 3.4 D _p)	Acetone, DMSO, 250 °C, 5 min	25	17 Fur	²⁷⁸
Cellulose	WO ₃ -ZrO ₂ (92 S _{BET} ; 0.189 V _p ; 3.4 D _p)	Acetone, DMSO, 250 °C, 5 min	60	14 Hmf+3 Fur	²⁷⁸
Tabioca flour	WO ₃ -ZrO ₂ (92 S _{BET} ; 0.189 V _p ; 3.4 D _p)	Acetone, 230 °C, 5 min	60	22 Hmf+2 Fur	²⁷⁸
Corncob	WO ₃ -ZrO ₂ (92 S _{BET} ; 0.189 V _p ; 3.4 D _p)	Acetone, 250 °C, 5 min	53	11 Hmf+4 Fur	²⁷⁸
Other oxides					
D-Fructose	CeO ₂	H ₂ O, 120 °C, 5 min	nf ^a	1 Hmf	³⁷²
Ion-exchange resins					
D-Fructose	Nafion	DMSO, 120 °C, 2 h, 9.7x10 ⁴ Pa	100	94 Hmf	²⁴⁵
D-Xylose	Nafion SAC-13 (231 S _{BET} ; 140 [B] by TPD-NH ₃) ^d	H ₂ O, 160 °C, 240 min	22	11 Fur	²⁷¹
D-Xylose	Nafion SAC-13 (111000 AS)	DMSO, 125 °C, 8 h	87	55 Fur	²⁸⁸
D-Xylose	Nafion 117 (53000 AS)	DMSO, 150 °C, 2 h	91	60 Fur	²⁸⁸
D-Fructose	Nafion NR-50	DMFA, 100 °C, 3 h	~100	45 Hmf	²²⁹
D-Glucose	Nafion NR-50	(DMFA, 100 °C, 3 h)/(HT+DMFA, 100 °C, 3 h)	34/60	0/27 Hmf	²²⁹
D-Xylose	Amberlyst-15 (4.6 H ⁺ m _{eq} ·g ⁻¹ by T-NaOH)	DMSO, 140 °C, 24 h	90	63 Hmf	²⁴⁰
D-Xylose	Amberlyst-15	H ₂ O, 110 °C, 60 min	66	24 Hmf	²⁷⁴
D-Fructose	Amberlyst-15	DMFA, 100 °C, 180 min	~100	73 Hmf	²²⁹
D-Fructose	Amberlyst-15	HT, DMFA, 100 °C, 3h	~100	76 Hmf	²²⁹
D-Fructose	Amberlyst-15	H ₂ O, DMSO, PVP, IBMK/2-BuOH, 90 °C, ^e	76	59 Hmf	³⁵

D-Fructose	Amberlyst-15 (0.15-0.053 D _p)	DMSO, 120 °C, 2 h, N ₂ under 1.01x10 ⁵ Pa or 9.7x10 ⁴ Pa	100	100 Hmf	245
D-Fructose	Amberlyst-15	(DMFA, 80 °C, 2h)/(DMFA, 100 °C, 2 h)	88/100	77/90 Hmf	247
D-Fructose	Amberlyst-15	(Metanol+THF, 120 °C, 3 h)/(THF, 120 °C, 20 min)/(methanol, 120 °C, 3h)	97/98/96	29/48/17 Hmf	260
D-Fructose	Amberlyst-15 (SO ₃ H loading=4.7 mmol.g ⁻¹ ; 53 S _{BET} ; 4700 AS by TPD-NH ₃)	DMSO, 130 °C, 1.5 h	~100	84 Hmf	246
D-Fructose	Amberlyst-15	Isopropyl alcohol, 120 °C, 4 h	nf ^a	60 Hmf	243
D-Fructose	Amberlyst-15 (53 S _{BET} ; 4700 [B] by IR-py; 30 D _p)	H ₂ O, 135 °C, 408 min	32	18 Hmf	407
D-Glucose	Amberlyst-15	DMFA, 100 °C, 3 h	69	0 Hmf	229
D-Glucose	Amberlyst-15	(HT, DMFA, 80 °C, 4.5 h)/(HT, DMFA, 80 °C, 9 h)	60/73	76/42 Hmf	229
D-Glucose	Amberlyst-15	HT, DMFA, 100 °C, 3 h	64	38 Hmf	229
D-Glucose	Amberlyst-15	HT, DMFA, 80 °C, 9 h	73	42 Hmf	247
D-Sucrose	Amberlyst-15	HT, DMFA, 120 °C, 3h	58	54 Hmf	229
D-Cellobiose	Amberlyst-15	HT, DMFA, 120 °C, 3h	52	35 Hmf	229
D-Xylose	Amberlyst-70	H ₂ O, Tol, 175 °C, 4 h	81	54 Fur	287
D-Xylose	Amberlyst-70 (0.32 S _{BET} ; 2860 [B] by TPD-NH ₃) ^d	H ₂ O, 160 °C, 240 min	38	20 Fur	271
D-Fructose	Amberlyst-70 (36 S _{BET} ; 22 D _p) ⁴¹⁸	H ₂ O, IBMK/2-BuOH, 180 °C, 10 min, autonomous pressure	86	67 Hmf	346
D-Fructose	Amberlyst-70 (2550 AS)	H ₂ O, IBMK/2-BuOH, 130 °C, 225 min	85	60 Hmf	352
D-Glucose	Amberlyst-70 (≥ 2.55 eq. H ⁺ . kg ⁻¹)	H ₂ O, methanol, 170 °C, 80 min	~100	7 Hmf	345
D-Fructose	Amberlite IR-118	DMSO, 80 °C, 200 h	nf ^a	94 Hmf	347
D-Fructose	Diaion PK 216	DMSO, 80 °C, 500 min	nf ^a	90 Hmf	347
D-Fructose	Diaion PK 216	(H ₂ O, MPY, 90 °C, 18 h)/(DMSO, IBMK, 90 °C, 12 h)	98/90	83/73 Hmf	18
D-Fructose	Diaion PK 216	H ₂ O, acetone, 150 °C, 15 min	95	73 Hmf	348
D-Sucrose	Diaion PK 216	(H ₂ O, MPY, 90 °C, 21 h)/(DMSO, IBMK, 90 °C, 21 h)	58/55	43/38 Hmf	18
Inulin	Diaion PK 216	(H ₂ O, MPY, 90 °C, 21 h)/(DMSO, IBMK, 90 °C, 21 h)	100/100	69/62 Hmf	18

D-Tagatose	Dowex 50wx4	DMSO, 120 °C, 2 h	nf ^a	55 Hmf	253
D-Fructose	Dowex 50wx8-100	H ₂ O, acetone, 150 °C, 15 min	95	73 Hmf	348
D-Fructose	Dowex 50wx8-100	Acetone, DMSO, 150 °C, 20 min	99	87 Hmf	259
D-Fructose	Lewatit S2328 (5.39 meq. H ⁺ .g ⁻¹)	H ₂ O, 90 °C, 180 h	nf ^a	3 Hmf	351
D-Fructose	Lewatit SCP 108 (0.95 eq. H ⁺ .g ⁻¹)	H ₂ O, DMSO, IBMK, 76 °C for 100 h in a continuous mode plus 2 h of IBMK	nf ^a	97 Hmf	350
D-Fructose	Lewatit SCP 108 (0.95 eq. H ⁺ .g ⁻¹)	(HMPT, 76 °C, 100 h)/(MPY, 76 °C, 100 h)/(DMFA, 76 °C, 100 h)/(Acetonitrile, 76 °C, 100 h)/(Pyridine, 76 °C, 100 h)	nf ^a	33/88/ 84/10/5 Hmf	350
D-Fructose	OH1052 (1.38 meq. H ⁺ .g ⁻¹)	H ₂ O, ROX activated carbon to Hmf adsorption, 90 °C, 48 h	77	51 Hmf	320
Phosphate/(Per)Sulfate Zirconium based solid acids					
D-Xylose	PO ₄ ²⁻ /ZrO ₂ (168 S _{BET} ; 1362 [B]; 5.1 [L] by TPD-NH ₃)	H ₂ O, 160 °C, 90 min	42	58 Fur	271
D-Fructose	PO ₄ ²⁻ /ZrO ₂ (P/Zr=1.8; 38.1 S _{BET})	H ₂ O, 240 °C, 3.35x10 ⁴ Pa, 120 s	81	50 Hmf	264
D-Fructose	PO ₄ ²⁻ /ZrO ₂ (P/Zr=1.8; 63.6 S _{BET})	Sub-critical water, 240 °C, 3.35x10 ⁴ Pa, 180 s	97	54 Hmf	264
D-Fructose	γ-PO ₄ ²⁻ /ZrO ₂ (6 S _{BET})	H ₂ O, 100 °C, 30 min	39	29 Hmf	239
D-Fructose	PO ₄ ²⁻ /ZrO ₂ (89 S _{BET})	H ₂ O, 135 °C, in autoclave, under N ₂ , 238 min	13	6 Hmf	371
D-Fructose	PO ₄ ²⁻ /ZrO ₂ (93 S _{BET} ; 111 AS by TPD-NH ₃ ; 45 [B]; 92 [L]; 8.5 D _p)	H ₂ O, 125 °C, 308 min	42	12 Hmf	407
D-Glucose	PO ₄ ²⁻ /ZrO ₂ (P/Zr=1.8; 63.6 S _{BET})	Sub-critical water, 240 °C, 3.35x10 ⁴ Pa, 180 s	53	21 Hmf	264
D-Fructose	C-ZrO ₂ /P ₂ O ₇ (12 S _{BET} ; cubic zirconium pyrophosphate)	H ₂ O, 100 °C, 30 min	44	44 Hmf	239
Inulin	C-ZrO ₂ /P ₂ O ₇ (12 S _{BET} ; cubic zirconium pyrophosphate)	H ₂ O, 100 °C, 30 min	26	26 Hmf	239
D-Fructose	Al foam /PO ₄ ²⁻ /ZrO ₂ (ZrP loading = 16 wt.%; 198 S _{BET} ; ZrP=zirconium phosphate)	H ₂ O, 135 °C, autoclave, under N ₂ , 250 min	18	7 Hmf	371
D-Xylose	SO ₄ ²⁻ /ZrO ₂ (S loading=0.37 mmol.g ⁻¹ ; 90 S _{BET})	H ₂ O, Tol, 160 °C, 4 h	86	37 Fur	298
D-Xylose	SO ₄ ²⁻ /ZrO ₂ (SO ₄ ²⁻ loading=0.39 mmol.g ⁻¹ ; 152 S _{BET})	H ₂ O, Tol, 100 °C, 48 h	21	9 Fur	255
D-Xylose	SO ₄ ²⁻ /ZrO ₂ (243 S _{BET} ; 0.390 V _p ; 3.6 D _p ; 734 AS by TPD-NH ₃ ; 70.5 BS by TPD-CO ₂)	HCW, 250 °C, 5 min	69	29 Fur	296
D-Fructose	SO ₄ ²⁻ /ZrO ₂ (154 S _{BET})	H ₂ O, 200 °C, 5 min	89	33 Hmf	367
D-Fructose	SO ₄ ²⁻ /ZrO ₂ (154 S _{BET})	Acetone, DMSO, 180 °C, 5 min	91	66 Hmf	367
D-Fructose	SO ₄ ²⁻ /ZrO ₂	DMFA, 100 °C, 3 h	57	21 Hmf	229

D-Fructose	$\text{SO}_4^{2-}/\text{ZrO}_2$ (6.9 S_{BET} ; 0.008 V_p ; 1830 AS by TPD-NH ₃ ; 320 BS by TPD-CO ₂)	DMSO, 130 °C, 4 h, under N ₂	100	72 Hmf	370
D-Fructose	$\text{SO}_4^{2-}/\text{ZrO}_2$	DMSO, 120 °C, 2 h, 9.7x10 ⁴ Pa	100	92 Hmf	245
D-Glucose	$\text{SO}_4^{2-}/\text{ZrO}_2$ (6.9 S_{BET} ; 0.008 V_p ; 1830 AS by TPD-NH ₃ ; 320 BS by TPD-CO ₂)	DMSO, 130 °C, 4 h, under N ₂	95	19 Hmf	370
D-Glucose	$\text{SO}_4^{2-}/\text{ZrO}_2$	DMFA, 100 °C, 3 h	7	0 Hmf	229
D-Glucose	$\text{SO}_4^{2-}/\text{ZrO}_2$ (243 S_{BET} ; 0.390 V_p ; 3.6 D_p ; 734 AS by TPD-NH ₃ ; 70.5 BS by TPD-CO ₂)	HCW, 250 °C, 5 min	78	22 Hmf+2 Fur	296
D-Xylan	$\text{SO}_4^{2-}/\text{ZrO}_2$ (243 S_{BET} ; 0.390 V_p ; 3.6 D_p ; 734 AS by TPD-NH ₃ ; 70.5 BS by TPD-CO ₂)	HCW, 250 °C, 5 min	58	24 Fur	296
Cellulose	$\text{SO}_4^{2-}/\text{ZrO}_2$ (243 S_{BET} ; 0.390 V_p ; 3.6 D_p ; 734 AS by TPD-NH ₃ ; 70.5 BS by TPD-CO ₂)	HCW, 250 °C, 5 min	55	11 Hmf+2 Fur	296
Sugarcane bagasse	$\text{SO}_4^{2-}/\text{ZrO}_2$ (243 S_{BET} ; 0.390 V_p ; 3.6 D_p ; 734 AS by TPD-NH ₃ ; 70.5 BS by TPD-CO ₂)	HCW, 250 °C, 5 min	-	6 Hmf+7 Fur	296
D-Xylose	$\text{S}_2\text{O}_8^{2-}/\text{ZrO}_2$ (S loading=0.33 mmol.g ⁻¹ ; 85 S_{BET})	H ₂ O, Tol, 160 °C, 4 h	80	38 Fur	298
D-Xylose	$\text{SO}_4^{2-}/\text{Al}_2\text{O}_3\text{-ZrO}_2$ (S loading=0.38 mmol.g ⁻¹ ; Al loading= 0.28 mmol.g ⁻¹ ; 94 S_{BET})	H ₂ O, Tol, 160 °C, 4 h	86	42 Fur	298
D-Xylose	$\text{SO}_4^{2-}/\text{Al}_2\text{O}_3\text{-ZrO}_2$ (580 AS by TPD-NH ₃)	H ₂ O, Tol, 160 °C, 4 h	99	41 Fur	293
D-Fructose	$\text{SO}_4^{2-}/\text{Al}_2\text{O}_3\text{-ZrO}_2$ (Zr/Al=9; 11 S_{BET} ; 0.015 V_p ; 1790 AS by TPD-NH ₃ ; 350 BS by TPD-CO ₂)	DMSO, 130 °C, 4 h, under N ₂	100	64 Hmf	370
D-Glucose	$\text{SO}_4^{2-}/\text{Al}_2\text{O}_3\text{-ZrO}_2$ (Zr/Al=1; 27 S_{BET} ; 0.038 V_p ; 1550 AS by TPD-NH ₃ ; 520 BS by TPD-CO ₂)	DMSO, 130 °C, 4 h, under N ₂	99	48 Hmf	370
D-Xylose	$\text{S}_2\text{O}_8^{2-}/\text{Al}_2\text{O}_3\text{-ZrO}_2$ (S loading=0.45 mmol.g ⁻¹ ; Al loading= 0.31 mmol.g ⁻¹ ; 91 S_{BET})	H ₂ O, Tol, 160 °C, 4 h	87	40 Fur	298
D-Xylose	$\text{SO}_4^{2-}/\text{ZrO}_2\text{-MCM-41}$ (S loading=0.90 mmol.g ⁻¹ ; Zr loading=0.96 mmol.g ⁻¹ ; 426 S_{BET})	H ₂ O, Tol, 160 °C, 4 h	94	40 Fur	298
D-Xylose	$\text{S}_2\text{O}_8^{2-}/\text{ZrO}_2\text{-MCM-41}$ (S loading=1.20 mmol.g ⁻¹ ; Zr loading=0.93 mmol.g ⁻¹ ; 382 S_{BET})	H ₂ O, Tol, 160 °C, 4 h	95	43 Fur	298
D-Xylose	$\text{SO}_4^{2-}/\text{Al}_2\text{O}_3\text{-ZrO}_2\text{/MCM-41}$ (S loading=0.40 mmol.g ⁻¹ ; Al loading=0.12 mmol.g ⁻¹ ; Zr loading=1.01 mmol.g ⁻¹ ; 394 S_{BET})	H ₂ O, Tol, 160 °C, 4 h	50	23 Fur	298

Table 1.6- <i>Continued.</i>					
D-Xylose	$S_2O_8^{2-}/Al_2O_3-ZrO_2/MCM-41$ (S loading=0.70 mmol.g ⁻¹ ; Al loading=0.10 mmol.g ⁻¹ ; Zr loading=0.90 mmol.g ⁻¹ ; 359 S _{BET})	H ₂ O, Tol, 160 °C, 4 h	84	41 Fur	298
Phosphate/ (Per)Sulfate Titanium, aluminium and other based solid acids					
D-Fructose	$\alpha-PO_4^{2-}/TiO_2$ (8.7 S _{BET})	H ₂ O, 100 °C, 30 min	29	29 Hmf	239
D-Glucose	TiO_2/H_3PO_4	H ₂ O, IBMK, 180 °C, 6.9x10 ⁶ Pa, 2 min	nf ^a	33 Hmf	365
Inulin	$\gamma-PO_4^{2-}/TiO_2$ (4.5 S _{BET})	H ₂ O, 100 °C, 30 min	32	31 Hmf	239
D-Fructose	C- TiP_2O_7 (10.5 S _{BET} ; cubic titanium pyrophosphate)	H ₂ O, 100 °C, 30 min	25	25 Hmf	239
D-Xylose	SO_4^{2-}/TiO_2 (SO ₄ ²⁻ loading:0.64 mmol.g ⁻¹ ; 126 S _{BET})	H ₂ O, Tol, 100 °C, 48 h	39	17 Fur	255
D-Xylose	SO_4^{2-}/Al_2O_3 (SO ₄ ²⁻ loading:0.92 mmol.g ⁻¹ ; 209 S _{BET})	H ₂ O, Tol, 100 °C, 48 h	7	2 Fur	255
D-Xylose	SO_4^{2-}/SiO_2 (SO ₄ ²⁻ loading: 0.04 mmol.g ⁻¹ ; 147 S _{BET})	H ₂ O, Tol, 100 °C, 48 h	2	1 Fur	255
D-Xylose	SO_4^{2-}/Fe_2O_3 (SO ₄ ²⁻ loading:0.37 mmol.g ⁻¹ ; 67 S _{BET})	H ₂ O, Tol, 100 °C, 48 h	16	1 Fur	255
D-Xylose	SO_4^{2-}/SnO_2 (SO ₄ ²⁻ loading:0.64 mmol.g ⁻¹ ; 139 S _{BET} and calcined at 500 °C)	H ₂ O, Tol, 100 °C, 48 h	61	29 Fur	255
D-Xylose	SO_4^{2-}/SnO_2 (SO ₄ ²⁻ loading:0.68 mmol.g ⁻¹ ; 125 S _{BET} and calcined at 450 °C)	H ₂ O, Tol, 100 °C, 48 h	75	29 Fur	255
D-Xylose	SO_4^{2-}/HfO_2 (SO ₄ ²⁻ loading:0.22 mmol.g ⁻¹ ;158 S _{BET})	H ₂ O, Tol, 100 °C, 48 h	42	10 Fur	255
Supported HPAs					
D-Xylose	$Cs_{2.5}H_{0.5}PW_{12}O_{40}$ (128 S _{BET})	H ₂ O, Tol, 160 °C, 8h	45	21 Fur	284
D-Fructose	$Cs_{2.5}H_{0.5}PW_{12}O_{40}$ (116 S _{BET})	DMSO, 120 °C, 2 h, 9.7x10 ⁵ Pa	100	91 Hmf	245
D-Fructose	$Cs_3PW_{12}O_{40}$	DMSO, 120 °C, 2 h	96	73 Hmf	362
D-Fructose	$Cs_3PW_{12}O_{40}$	H ₂ O, IBMK, 120 °C, 60 min	47	40 Hmf	315
D-Glucose	$Cs_3PW_{12}O_{40}$	H ₂ O, IBMK, 130 °C, 4 h	33	13 Hmf	315
D-Fructose	$Zr_{1.5}PW_{12}O_{40}$	DMSO, 120 °C, 2 h	97	51 Hmf	362
D-Fructose	$Ag_3PW_{12}O_{40}$ (W loading=69.2 wt.%; P loading=1.0 wt.%; Ag loading=10.1 wt. %; W:P:Ag=12:1:3; 5.1 S _{BET} ; 0.87 D _p ; 3010 AS by IR-py)	(H ₂ O, IBMK, 120 °C, 60 min)/(H ₂ O, IBMK, 120 °C, 90 min)/(H ₂ O, IBMK, 130 °C, 60 min)	83/93/nf ^a	79/78/88 Hmf	315
D-Glucose	$Ag_3PW_{12}O_{40}$ (W loading=69.2 wt.%; P loading=1 wt.%; Ag loading=10.1 wt. %; W:P:Ag=12:1:3; 5.1 S _{BET} ; 0.87 D _p ; 3010 AS by IR-py)	H ₂ O, IBMK, 130 °C, 4 h	90	76 Hmf	315
D-Xylose	$MP34PWb_{12}O_{40}$ (233 S _{BET} ; 0.198 V _p ; 12-tungstophosphoric acid immobilised in medium mesoporous silica in butanol)	(H ₂ O, Tol, 160 °C, 4 h)/(DMSO, 140 °C, 4 h)	80/49	42/52 Fur	285

D-Xylose	MP34CsPW₁₂O₄₀ (705 S _{BET} ; 0.552 V _p ; cesium salt of 12-tungstophosphoric acid supported on medium pore MCM-41)	(H ₂ O, Tol, 160 °C, 8 h)/(DMSO, 140 °C, 4 h)	77/91	45 Fur	²⁸⁴
D-Xylose	LP15CsPW₁₂O₄₀ (608 S _{BET} ; 1.421 V _p ; cesium salt of 12-tungstophosphoric acid supported on large pore micelle template silica)	(H ₂ O, Tol, 160 °C, 4 h)/(DMSO, 140 °C, 4 h)	65/70	26/24 Fur	²⁸⁴
D-Xylose	LP34PWb₁₂O₄₀ (520 S _{BET} ; 1.392 V _p ; 12-tungstophosphoric acid immobilised in large mesoporous silica)	(H ₂ O, Tol, 160 °C, 4 h)/(DMSO, 140 °C, 4 h)	82/53	48/50 Fur	²⁸⁵
D-Xylose	MPNHPW₁₂O₄₀ (481 S _{BET} ; 0.3 V _p ; 12-tungstophosphoric acid immobilised in medium pore amino-functionalised silica)	H ₂ O, Tol, 160 °C, 4 h	68	18 Fur	²⁸⁵
D-Xylose	LPNHPW₁₂O₄₀ (663.6 S _{BET} ; 2 V _p ; 12-tungstophosphoric acid immobilised in large pore amino-functionalised silica)	H ₂ O, Tol, 160 °C, 4 h	64	18 Fur	²⁸⁵
D-Fructose	[MIMPS]₃PW₁₂O₄₀ (Heteropolyacid salt of an ionic liquid cation functionalised with a propanesulfonated group, 1-(3-sulfonicacid)propyl-3-methyl imidazolium phosphotungstate)	(IBMK, 120 °C, 2 h)/(DMSO, 120 °C, 2 h)/(n-BuOH, 120 °C, 2h)/(sec-BuOH, 120 °C, 2 h)/(iso-BuOH, 120 °C, 2 h)	99/99/99/ 100/99	44/76/75 /99/57 Hmf	³⁶²
Carbon based catalysts					
D-Xylose	SCBC (S loading=1.46 mmol.g ⁻¹ ; 1.1 S _{BET} ; 0.7 V _p ; sulfonated carbon-based catalysts)	Acetone, DMSO, H ₂ O, 200 °C, 10 min	45	9 Fur	²⁵⁶
D-Fructose	SCBC (S loading=1.46 mmol.g ⁻¹ ; 1.1 S _{BET} ; 0.7 V _p ; sulfonated carbon-based catalysts)	Acetone, DMSO, H ₂ O, 200 °C, 10 min	95	28 Hmf+1 Fur	²⁵⁶
D-Glucose	SCBC (S loading=1.46 mmol.g ⁻¹ ; 1.1 S _{BET} ; 0.7 V _p ; sulfonated carbon-based catalysts)	Acetone, DMSO, H ₂ O, 200 °C, 10 min	29	6 Hmf+1 Fur	²⁵⁶
D-Xylan	CBC (S loading=1.46 mmol.g ⁻¹ ; 1.1 S _{BET} ; 0.7 V _p ; sulfonated carbon-based catalysts)	Acetone, DMSO, H ₂ O, 230 °C, 5 min	-	10 Fur	²⁵⁶
Cellulose	CBC (S loading=1.46 mmol.g ⁻¹ ; 1.1 S _{BET} ; 0.7 V _p ; sulfonated carbon-based catalysts)	Acetone, DMSO, H ₂ O, 230 °C, 7 min	-	7 Hmf+1 Fur	²⁵⁶
Cassava Waste	CBC (S loading=1.46 mmol.g ⁻¹ ; 1.1 S _{BET} ; 0.7 V _p ; sulfonated carbon-based catalysts)	Acetone, DMSO, H ₂ O, 250 °C, 1 min	-	12 Hmf+3 Fur	²⁵⁶
D-Fructose	LCC (CH _{0.94} O _{0.37} S _{0.027} ; lignin-derived carbonaceous catalyst)	(H ₂ O, DMSO, MW 100W, 110 °C, 10 min)	98	84 Hmf	³⁵⁴
D-Fructose	Ac-SO₃H (SO ₃ H loading= 0.6 mmol.g ⁻¹ ; 506 S _{BET} ; 2700 AS by TPD-NH ₃ ; sulfonated activated carbon)	DMSO, 130 °C, 1.5 h	~100	81 Hmf	²⁴⁶

D-Fructose	Glu-TsOH ($< 1 S_{\text{BET}}$; 2000 AS by TPD-NH ₃ ; carbonaceous catalyst formed in an eco-friendly approach between D-glucose and p-toluene sulfonic acid)	DMSO, 130 °C, 1.5 h	~100	91 Hmf	²⁴⁶
a) nf- information not found. b) Although the authors considered these compounds as heterogeneous catalysts, recent studies demonstrated that at least for VOPs the catalytic reaction is homogeneous in nature. ²⁸⁶ c) The aqueous extract of the Jerusalem artichoke was processed by cation and anion exchange to remove the various ions, and ultrafiltration dialysis to remove protein. d) Weak LAS were detected from the silica matrix by IR-NH ₃ . e) Chosen from a set of values in which the reaction time was from 8 to 16 h.					

1.5. Conversion of saccharides to furanic aldehydes using ionic liquid (IL) based catalytic systems

The poor solubility of polysaccharides (especially that of cellulose, the most abundant source of hexoses for Hmf) in almost any solvent may be a problem when considering the use of solid acid catalysts due to the possible severe diffusion limitations. Some approaches prior to the reaction in the presence of a solid acid may be pre-treating the carbohydrate feedstock by pre-dissolution, which allows transforming the crystalline and recalcitrant cellulose structure (natural form) into an amorphous form that is faster hydrolysed than the crystalline form. This is important because the crystalline form is resistant to chemical and biological transformations (the glycosidic bonds are protected by the tight packing of cellulose chains in microfibrils). Many authors have been making efforts to selectively convert saccharides into Hmf and Fur in ionic liquids (ILs) in order to enhance the solubility of the substrate in the reaction medium, improve yields of target products and facilitate catalyst recycling.⁴⁰³

ILs were first introduced in 1914 by Paul Walden who reported the physical properties of ethyl ammonium nitrate $[\text{EtNH}_3]\text{NO}_3$ formed by neutralisation of ethylamine with concentrated nitric acid.⁴¹⁹ Nevertheless the earliest report on ILs applied to polysaccharides is only dated after two decades in a patent from 1934 focusing on the molten salt N-ethylpyridinium chloride that dissolved cellulose.⁴²⁰ In 1948 they emerged as mixtures of aluminium(III) chloride and 1-ethylpyridinium bromide.⁴²¹ Chemical and physical properties of derivatives of 1-butylpyridinium tetrachloroaluminate ($[\text{Bpy}]\text{AlCl}_4$) were found to have some limitations since it was liquid at ambient temperature only within a very narrow composition range.⁴²² Some years later, 1-ethyl-3-methylimidazolium tetrachloroaluminate ($[\text{Emim}]\text{AlCl}_4$) appeared with a much wider liquid range becoming the first IL system liquid at ambient temperature. Since then a wide number of potential applications of ILs as solvents in organic synthesis have been developed incorporating many different ions (Table 1.7).⁴²³

ILs are defined as a class of non-molecular ionic solvents consisting of ion pairs; an organic heterocyclic cation (e.g. dialkylimidazolium) and an inorganic (e.g. chloride or nitrate) or organic anion (e.g. trifluoromethane sulfonate or acetate) that usually melt at or below 100 °C. Their versatility allows them to be referred to as “designer solvents”, because they may be tailored through the modification of the constituent ions to meet desired properties, such as

polarity, hydrophilicity, and miscibility with solutes or other solvents, and acid-base properties.^{424,425} The cations in ILs are responsible for their physical properties (such as melting point, viscosity and density) whereas the anions control chemical properties and reactivity.⁴²⁶

The requirements of a certain solvent to dissolve cellulose are highly demanding such as: i) dissolution of cellulose (preferably more than 10 wt.%) at low temperature ; ii) melting point lower than 20 °C; iii) high thermal stability (> 200 °C); iv) non-volatile; v) non-toxic, vi) chemically stable; vii) no undesired cellulose decomposition; viii) easy recyclable process; ix) cost effective.¹⁶ Compared to common organic solvents used in carbohydrate chemistry, ILs have interesting properties and different reviews describe their numerous advantages,⁴⁰³ besides they fulfill some of the “Green Chemistry” requirements. They have almost no vapour pressure, avoiding atmospheric pollution problems (emission and explosion risks) typically associated with volatile organic solvents and products contamination with the solvent in distillation processes. ILs remain liquid through a wide range of temperatures and are quite stable at high temperatures. They are fairly air- and water-stable (water is intrinsically associated with the hydrolysis/dehydration processes), and in some cases they can be recycled efficiently. ILs also have relatively moderate surface tensions compared to organic solvents and even when compared to water.⁴²⁷ ILs display singular solubilisation properties for cellulose (and other polysaccharides), as the dissolution of the latter in ILs, breaks down crystalline domains leaving the polysaccharide chains more exposed and the glycosidic bonds more accessible to active species.⁴²⁸⁻⁴³⁰ In the specific case of [Bmim]Cl, an NMR study demonstrated that the solubility of cellulose is due to the disruption of the hydrogen bonds in cellulose by the chloride anions of the IL.⁴³¹ Hence, through the use of ILs it is possible to affect the thermodynamic and kinetic barriers commonly associated with the transformation of the polysaccharides in water or common organic solvents.^{428-430,432} Therefore ILs open up a window of opportunities for the dissolution of carbohydrates and their ability to dissolve cellulose is dependent on the degree of polymerisation (DOP), its crystallinity, and on the operating conditions.²³⁴

The most effective ILs for dissolving cellulose or cellulosic biomass have included those composed of imidazolium or pyridinium cations with short aliphatic chain substituent groups and anions, which are strong hydrogen bond acceptors, such as chloride and acetate, for disrupting the extensive hydrogen bond network of cellulose (Table 1.7).^{184,420,426,428-430,433-448} The efficiency of the IL-based reaction system may be further improved through the use of MW heating (in bulk heating), instead of conventional heating (CH, using an external heating source involving conduction/convection),^{343,449,450} since the dielectric properties of ILs allow the MW absorption in

bulk heating to be extremely efficient.^{334,451,452} However, apart from the advantages mentioned, one of the disadvantages they present is related to their viscosity being relatively high compared to conventional solvents (66 to 1110 cP at 20-25 °C), and hence the design of less viscous ILs is still a challenge for many applications.⁴⁵³

Two main approaches have been successfully used as tools in different perspectives regarding the application of ILs in the acid-catalysed hydrolysis/dehydration of saccharides to Fur and Hmf, under mild reaction conditions: i) ILs as solvents (an acid catalyst is added) or ii) acid solvents/catalysts (dual function). Ideally, the IL dissolves the substrate (and the catalyst when the IL is not acidic) but not the target products, simplifying the product separation process and avoiding product and/or catalyst loss/decomposition in more laborious/demanding work-up procedures. Accordingly, in the case of Fur production, the product separation is possible by decantation, and in the case of Hmf (solid) by filtration. However, Fur and Hmf are soluble in the IL systems which have been investigated (Tables 1.7 and 1.8). When the target products are soluble in the IL, it may be beneficial to use a co-solvent for in situ extraction of those products as they are formed (a biphasic liquid-liquid system). Nevertheless, the addition of a co-solvent may cause cross-contamination requiring additional purification steps (Table 1.8). In the case of Fur production, a cleaner approach may be to evaporate the product as it is formed.

High expectations on ILs for these reaction systems are evident and have already deserved patent applications.^{194,454-457} A review about the use of imidazolium salts in the conversion of biomass was published in 2010.¹⁸⁴ More recently Zakrzewska et al.⁴⁵⁸ focused specifically on Hmf production by means of the IL-mediated conversion of hexoses or related di/polysaccharides and summarised studies published until July 2010. A minireview by Ståhlberg et al.⁴⁵⁹ has focused on issues of process technology of the synthesis of Hmf using ILs, and a review by A. Rosatella et al.¹⁸⁵ addresses the toxicological and environmental impact issues regarding the preparation of Hmf, which includes ILs as solvents. A recent review about ILs used in the hydrolysis/dehydration reaction of saccharides (pentoses or hexoses) into furanic aldehydes was published.⁴ The research and development of IL-based catalytic systems for the chemical valorisation of (highly complex) biomass can be made by looking at how each type of IL-based catalytic system performed for different types of carbohydrates (containing pentoses and hexoses). The latter approach has good prospects to convert different saccharides into Fur+Hmf (including stability and recycling efficiency) which are desirable for process intensification.

Several published works have focused on a specific substrate, which leaves gaps in the knowledge of the potential of the investigated IL-based catalytic systems for converting different carbohydrate feedstocks.

In the following Sections IL-mediated production of Fur and Hmf from biomass is summarised, in the perspective of the type of IL-based catalytic system (IL as solvents coupled with a Brönsted or Lewis acid catalyst or acidic ILs working as solvents and catalysts), crossing information of different scientific contributions having in common the application of a specific type of IL-based catalytic system, and promising achievements in the reactions of different mono/di/polysaccharides are reported. Comparisons of product selectivity should only be made for similar saccharide (or saccharide conversions). Since this was often not possible between different works, the results are focused in terms of Hmf and Fur molar yields (denoted Y , equation 1.5) and in terms of molar conversions of saccharides (denoted $C_{\text{saccharide}}$, equation 1.6): n_0 (saccharide), n_t (saccharide) and n_t (Fur or Hmf) are the initial moles of saccharide, the moles of saccharide, Fur or Hmf at a reaction time t , respectively. Furthermore the investigated ILs are given in Table 1.7.

$$Y_{\text{Fur or Hmf}} (\% \text{ at a reaction time } t) = \frac{n_t (\text{Fur or Hmf})}{n_0 (\text{if monosaccharide}) \text{ or } 2 n_0 (\text{if disaccharide})} \times 100 \quad (1.5)$$

$$C_{\text{saccharide}} (\% \text{ at a reaction time } t) = \frac{n_0 (\text{saccharide}) - n_t (\text{saccharide})}{n_0 (\text{saccharide})} \times 100 \quad (1.6)$$

Table 1.7- Names, abbreviations and structures of cations of ionic liquids.

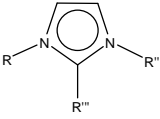
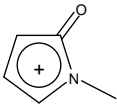
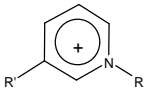
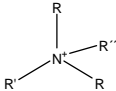
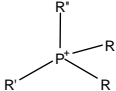
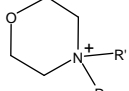
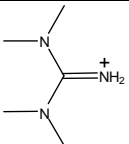
Structure	R	R'	R''	Abbreviation
	H	H	CH ₃	[Hmim]
	CH ₃ CH ₂	H	CH ₃	[Emim]
	CH ₃ (CH ₂) ₃	H	CH ₃	[Bmim]
	CH ₃ (CH ₂) ₅	H	CH ₃	[Hxmim]
	CH ₃ (CH ₂) ₇	H	CH ₃	[Omim]
	CH ₃ (CH ₂) ₉	H	CH ₃	[Dmim]
	CH ₃ (CH ₂) ₃	H	CH ₃ (CH ₂) ₃	[B ₂ im]
	CH ₂ CH=CH ₂	H	CH ₃	[Amim]
	(CH ₂) ₄ SO ₃ H	H	CH ₂ CH=CH ₂	[Asbi]
	(CH ₂) ₄ SO ₂ Cl	H	CH ₂ CH=CH ₂	[Ascbi]
	(CH ₂) ₄ SO ₂ Cl	H	CH ₃	[Mscbi]
	(CH ₂) ₄ SO ₃ H	H	CH ₃	[Sbmim]
	(CH ₂) ₃ SO ₃ H	H	CH ₃	[Spmim]
	CH ₃ (CH ₂) ₃	CH ₃	CH ₃	[Bm ₂ im]

Table 1.7- Continued.

	—	—	—	[NMP]
	H	H	—	[Hpy]
	CH ₃ CH ₂	H	—	[Epy]
	CH ₃ (CH ₂) ₅	H	—	[Hxpy]
	CH ₃ (CH ₂) ₃	CH ₃	—	[Bmpy]
	CH ₂ CHOHCH ₂ Cl	H	—	[Pcohy]
	H ₂ CH(OCH ₃)CH ₂ Cl	H	—	[Pcmopy]
	CH ₃ (CH ₂) ₃	CH ₃ (CH ₂) ₃	CH ₃ (CH ₂) ₃	[B ₄ N]
	CH ₃ CH ₂	CH ₃ CH ₂	CH ₃ CH ₂	[E ₄ N]
	CH ₃ CH ₂	CH ₂ (CHO)CH ₂	CH ₃ CH ₂	[E ₃ Nmeo]
	CH ₃	CH ₃	CH ₃	[M ₄ N]
	CH ₃	C ₆ H ₅ CH ₂	CH ₃	[M ₃ BeN]
	CH ₃	H	H	[M ₂ H ₂ N]
	CH ₃	H	CH ₃	[M ₃ HN]
	CH ₃	C ₆ H ₅	CH ₃	[M ₃ PhN]
	CH ₃ (CH ₂) ₃	(CH ₂) ₂ OH	—	[Cho]
	CH ₃ (CH ₂) ₃	CH ₃ (CH ₂) ₃	CH ₃ (CH ₂) ₃	[B ₄ P]
	H	H	—	[Morph]
	H	CH ₃	—	[NMM]
	—	—	—	[TMG]
	—	—	—	[TMG]

1.5.1. ILs as solvents (an acid catalyst is added)

When ILs are used as solvents in the conversion of polysaccharides into furanic compounds, the catalysts used are Lewis acids (e.g. transition metal salts) or Brönsted acids (mineral acids, heteropolyacids and organic acids). The investigated ILs were essentially those containing an alkyl or allyl-substituted imidazolium cation and a halide anion, which have interesting solubilisation properties for saccharides and are readily available (Table 1.8). Fur and Hmf are fairly stable in these types of ILs.²³¹ Density functional theory (DFT) calculations revealed that the imidazolium IL solvent “switches” the dehydration of D-fructose from a

thermodynamically unfavourable reaction to a thermodynamically favourable one, activating the reactants, stabilising the products, and enhancing Hmf yield.⁴³² The water concentration in the ILs is an important issue since it has been reported that ILs enhance the water auto-ionisation process (influencing the pKw values of water), increasing the concentration of both [H⁺] and [OH⁻] in the IL-water mixtures, enabling acid- and/or base-catalysed reactions to occur.⁴⁶⁰ According to Zhang et al.,⁴⁶⁰ the values of Kw of water in IL-water mixtures under mild conditions (typically employed in biomass conversion using ILs) are similar to that of water under high temperature and pressure conditions.⁴⁶⁰ The loadings of substrate may enhance formation of humins (dark-brown compounds) as reported by Qi et al.³³⁶

Table 1.8 shows the results for the hydrolysis/dehydration of di/polysaccharides. The values of the yields (denoted Y) are given in wt.% unless specified otherwise. In general, the best results were chosen when the reaction conditions were optimised.

Table 1.8- Hydrolysis/Dehydration of di/polysaccharides or lignocellulosic biomass into 5-hydroxymethyl-2-furaldehyde/2-furaldehyde (Hmf/Fur) using ionic liquids.

Substrate	Acid added/IL /co-solvent	Reaction conditions (°C/ h)	Y _{Fur/Hmf} ^a (wt.%)	Ref
DISACCHARIDES (TY Hmf= 74 wt.%)^b				
D-Cellobiose	CrCl ₃ /[Bmim]Cl/n.u. ^c	140/0.08	20	336
	(CuCl ₂ +CrCl ₂)/[Emim]Cl/n.u. ^c	100/3	<10	329
	CrCl ₃ .6H ₂ O/[E ₄ N]Cl/n.u. ^c	130/0.17	22	305
	SnCl ₄ /[Emim]BF ₄ /n.u. ^c	100/3	20	374
	GeCl ₄ /[Bmim]Cl/n.u. ^c	120/0.5	15	373
D-Maltose	CuCl ₂ /CrCl ₂ /[Emim]Cl/n.u. ^c	100/3	<6	329
	GeCl ₄ /[Bmim]Cl/n.u. ^c	120/0.5	9	373
D-Sucrose	HCl/[Omim]Cl/n.u. ^c	120/1.5	58	230
	CrCl ₃ /[Bmim]Cl/n.u. ^c	100/0.08	28	336
	CrCl ₂ /HCl/[Omim]Cl/n.u. ^c	120/1	82	230
	CrCl ₃ .6H ₂ O/[E ₄ N]Cl/n.u. ^c	130/0.17	28	305
	SnCl ₄ /[Emim]BF ₄ /n.u. ^c	100/6	23	374
	GeCl ₄ /[Bmim]Cl/n.u. ^c	120/0.5	21	373
	IrCl ₃ /[Bmim]Cl/n.u. ^c	100/3	14	324
	p-TsOH ^e /[Cho]Cl/n.u. ^c	100/1	9	310
	n.u./[Hmim]Cl/n.u. ^c	90/1	37	342
n.u./[NMM]CH ₃ SO ₃ /DMFA-LiBr ^d	90/1.5	18	461	
Lactose	CrCl ₂ /H ₂ SO ₄ /[Emim]Cl/n.u. ^c	120/2	8	253
POLYSACCHARIDES				
Cellulose (TY Hmf ≅ 74 wt.%)	HCl/[Emim]Cl/n.u. ^c	105/4	30 ^f	317
	HCl/[Emim]Cl/acetoneitrile	110/3	29 ^f	301
	HCl/[Emim]Cl/H ₂ O	110/3	25 ^f	301
	HCl/[Bmim]Cl/(H ₂ O+H ₂ SO ₄)	90/1.08	20 ^f	301
	CuCl ₂ /CrCl ₂ /[Emim]Cl/n.u. ^c	120/ 8	58	329

Table 1.8- Continued.

Cellulose (TY Hmf \cong 74 wt.%)	CrCl ₂ /HCl/[Emim]Cl/(DMA-LiCl)	140/2	54 ^f	196	
	n.u./[Emim]Cl/(DMA-LiCl)	140/2	4 ^f	196	
	CrCl ₃ /[Bmim]Cl/n.u. ^c	150/0.17	54 ^f	336	
	CrCl ₃ /[Bmim]Cl/n.u. ^c	^h /0.033	62 ^f	334	
	CrCl ₃ .6H ₂ O/[Bmim]Cl	^h /0.042	62 ^f	337	
	CrCl ₃ /[Bmim]Cl/n.u. ^c	160/0.1	55 ^f	340	
	CrCl ₃ /[Bmim]Cl/H ₂ O	140/0.67	53 ^f	335	
	CrCl ₃ /LiCl/[Bmim]Cl/H ₂ O	140/0.67	62 ^f	335	
	CrCl ₂ /[Bmim]Cl/n.u. ^c	120/6	34	309	
	lpr-CrCl ₂ ⁱ /[Bmim]Cl/n.u. ^c	120/12	48	309	
	GeCl ₄ /[Bmim]Cl/n.u. ^c	120/0.5	37 ^f	373	
	FeCl ₂ /[Sbmim]SO ₄ /(IBMK)	150/5	34+19 ^g	376	
	CoSO ₄ /[Sbmim]HSO ₄ /IBMK	150/5	24+17 ^g	377	
	n.u./[Sbmim]HSO ₄ /(IBMK+H ₂ O)	150/5	15+8 ^g	376	
	n.u./[Sbmim]HSO ₄ /(IBMK+H ₂ O)	150/5	15+8 ^g	377	
	Amberlyst-36/[Bmim]Cl/n.u. ^c	120/6	20	309	
	H-Y/[Bmim]Cl/n.u. ^c	120/6	36	309	
	p-TsOH ^e /[Bmim]Cl/n.u. ^c	120/6	21	309	
	Inulin (TY Hmf \cong 74 wt.%)	[Cho]Cl/citric acid	80/2	40	316
		[Cho]Cl/oxalic acid	80/2	44	316
[Cho]Cl/oxalic acid/ethyl acetate		80/2	50	316	
p-TsOH ^e /[Cho]Cl/n.u. ^c		90/1	57 ^f	310	
Amberlyst-70/[Bmim]Cl/glycerol carbonate		110/ ⁱ	60 ^f	302	
Amberlyst-15/[Emim]HSO ₄		100/0.083	65 ^f	344	
Amberlyst-15/([Bmim]HSO ₄ + [Bmim]Cl)/n.u. ^c		80/1.1	82 ^f	344	
SnCl ₄ /[Emim]BF ₄		100/3	40 ^f	374	
BHC ^j /[Cho]Cl/(H ₂ O+IBMK)		100/1	19	356	
Starch (TY Hmf \cong 74 wt.%)	HCl/[Omim]Cl/ethyl acetate	120/1	30	322	
	CrCl ₂ /HCl/[Omim]Cl/ethyl acetate	120/1	60	322	
	SnCl ₄ /[Emim]BF ₄ /n.u. ^c	100/24	47 ^f	374	
Xylan oat (TY Fur \cong 73 wt.%)	CrCl ₂ /HCl/[Emim]Cl/n.u. ^c	140/2	25 ^f	277	
Pine Wood	CrCl ₃ /[Bmim]Cl/n.u. ^c	^h /0.05	52+31 ^{f,g}	337	
	TFA ^k /[Bmim]Cl/H ₂ O	120/2h	4	462	
Wheat straw	CrCl ₃ /LiCl/[Bmim]Cl/n.u. ^c	160/0.25	61 ^f	335	
Rice straw	CrCl ₃ /[Bmim]Cl/n.u. ^c	^h /0.05	47+25 ^{f,g}	337	
Corn stalk	CrCl ₃ /[Bmim]Cl/n.u. ^c	^h /0.05	45+23 ^{f,g}	337	
Corn stover	CrCl ₃ /HCl/[Emim]Cl/DMA	140/2	48+34 ^{f,g}	196	

a) Yield of 2-furaldehyde from pentose-based saccharides; yield of 5-hydroxymethyl-2-furaldehyde from hexose-based saccharides. b) Theoretical yield (TY) of 2-furaldehyde or 5-hydroxymethyl-2-furaldehyde. c) n.u. =not used. d) DMFA-dimethylformamide. e) *para*-toluene sulfonic acid. f) Yield given in (mol%). g) 5-hydroxymethyl-2-furaldehyde +2-furaldehyde yield. h) Temperature not mentioned (MW, 400 W). i) lpr-(1,3-bis(2,6-diisopropylphenyl)imidazolidene) chloride. j) Time not mentioned. j) BHC- Betaine hydrochloride, a co-product of carbohydrate industry. k-TFA-trifluoroacetic acid.

1.5.1.1. ILs coupled with homogeneous liquid acid catalysts

A range of liquid Brønsted acid catalysts have been tested using ILs as solvents in the reaction of monosaccharides, mainly D-fructose (Figures 1.25 and 1.27) and D-glucose (Figure 1.28) or polysaccharides (e.g. cellulose, Figure 1.29). The liquid Brønsted acid catalysts mostly used include inorganic HCl, H₂SO₄, HNO₃, H₃PO₄ mineral acids (Figure 1.25)^{196,198,230,306,317,334,463} or organic acetic, citric, oxalic, malonic, and maleic acids (Figures 1.27 and 1.28).^{198,202,306,316,463,464} Various ILs used as solvents with mineral acids as catalysts in the dehydration of monosaccharides (D-xylose, D-fructose or D-glucose), can be employed with or without a co-solvent at reaction temperatures in the range of 80-120 °C, reaction times from 1 min to 12 h and using MW or conventional heating (CH) methods.^{196,198,231,306} In the case of Hmf production from D-fructose (4-10 wt.%), high (80-95%) Y_{Hmf} were obtained, using H₂SO₄ as catalyst coupled with different ILs ([Emim]Cl, [Hpy]Cl or [Bmim]Cl at 80-120 °C (Figure 1.25).^{196,231,306,338,353,463} These results showed the positive effect of sulfuric acid (no Hmf was formed in the absence of the catalyst).³³⁸

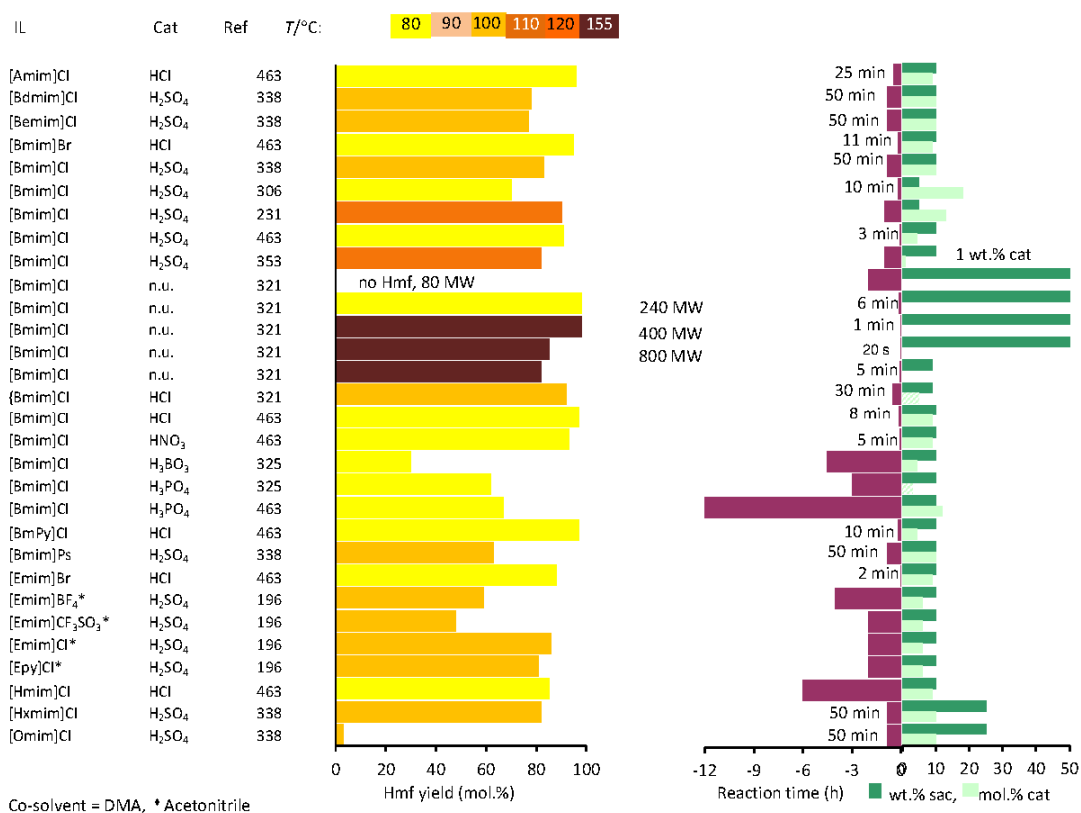


Figure 1.25- Mineral acids used as catalysts coupled with ILs as solvents in the dehydration of D-fructose to 5-hydroxymethyl-2-furaldehyde (Hmf).

In [Hxmim]Cl and [Omim]Cl, the H_2SO_4 (10 mol.%) had no catalytic effect ($Y_{\text{Hmf}} < 10\%$) due to the bulky groups that prevent the H^+ of the acid to react with D-fructose. However, increasing the content of H_2SO_4 to 25 mol.% facilitated the contact of the H^+ ions with D-fructose, reaching 82% Y_{Hmf} in the case of [Hxmim]Cl (Figure 1.25).³³⁸

It was postulated that the anion Cl^- played an important role in the enolisation step, acting as nucleophile and attacking a fructofuranosyl oxocarbenium ion (primary intermediate) to form a 2-deoxy-2-halo intermediate that is less prone to side reactions, as well as reversion to D-fructose; the latter intermediate then loses HCl to form the enol intermediate (Figure 1.26).¹⁹⁶

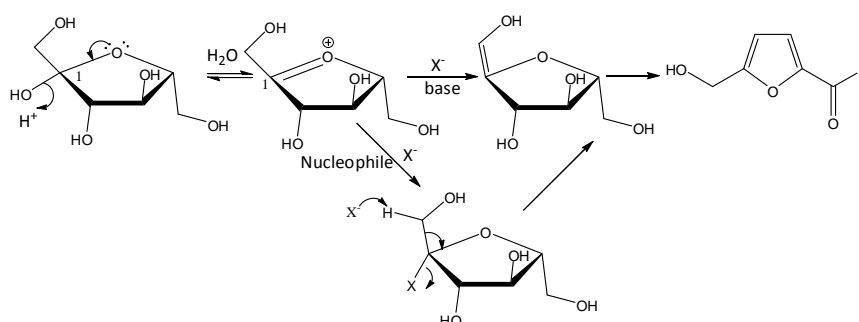


Figure 1.26- Putative nucleophilic mechanism for halide participation in the dehydration of D-fructose into 5-hydroxymethyl-2-furaldehyde (Hmf); X^- represents a halide ion [adapted from ¹⁹⁶].

Using HNO_3 resulted in a higher Hmf yield than that with H_3PO_4 possibly due to the stronger acidity of the former (based on pK_a values for aqueous solutions) although this trend may not necessarily be in line with that for ILs as solvents.¹⁹⁸ The use of HCl as catalyst in ILs is also very effective for Hmf production from D-fructose (Figure 1.25). For a series of self-made ILs containing imidazolium or pyridinium cations and using HCl as catalyst (9 mol.%), Li et al.⁴⁶³ reported far better results for the halide (Cl^- or Br^-)-containing ILs than for BF_4^- and PF_6^- . In line with this trend, better results were also found for [Emim]Cl in comparison to [Emim] BF_4 for the $[\text{H}_2\text{SO}_4/\text{IL}/\text{DMA}]$ system.¹⁹⁶ The superior results for the Cl^- containing IL compared to the “nonbasic” (poor coordination ability) BF_4^- and PF_6^- containing ILs, may be partly related to the lower affinity of the latter ILs towards D-fructose or cationic intermediates, in comparison to the Cl^- -containing IL.^{196,311,430,465-467} On the other hand, the stability of HCl may be influenced by the type of the IL (possibly more stable in Cl^- -containing ILs). The $\text{HCl}/[\text{Bmim}]\text{Cl}$ system was effective even for D-fructose loadings as high as 50 wt.% (67% Y_{Hmf} (78% C_{Fru}) at 80 °C/55 min).⁴⁶³ These

results are promising in comparison to those for the aqueous phase reaction of D-fructose at 80–95 °C, in the presence of HCl (>0.25 M) or acid resins (e.g. 20% Y_{Hmf} after several h).²²⁶ The use of high concentrations of HCl may allow high Y_{Hmf} to be reached at lower reaction temperatures and longer reaction times. Lai et al.⁴³² for the reaction of D-fructose (20 wt.%) in HCl/[Bmim]Cl, with a HCl loading of 50 mol.%, achieved a 80% Y_{Hmf} at a.t./70 h. The addition of tetrahydrofuran (THF) as immiscible co-solvent to the system HCl/[Bmim]Cl enhanced the reaction rate and gave comparable Hmf yields in only 24 h). Furthermore the IL was recycled in an efficient way (Section 1.5.3).⁴³² The use of IL-based systems instead of conventional acidic aqueous solutions (typically involving high temperatures) avoid Hmf loss reactions via its decomposition into formic and levulinic acids.²⁰¹ The influence of water in the IL system on the reaction of D-fructose was investigated in detail for the HCl/[Bmim]Cl system at 80 °C, and it was found that the reaction rate decreased with increasing water concentration (up to ca. 30 wt.%). Nevertheless, increasing reaction times allowed similarly high Hmf yield to be reached.⁴⁶³ Although mineral acids have been used with success, Li et al.³²¹ obtained a high Hmf yield without using a catalyst under MW. At 240 W the dehydration of D-fructose (50 wt.%) gave 98% Y_{Hmf} at 80 °C/6 min; at 400 W the same Y_{Hmf} was reached at 155 °C in only 1 min. At a potency higher than 400 W, a fast D-fructose consumption (> 90% in 30 s) was observed, but a lower Y_{Hmf} (80% in 20 s).³²¹ In an oil bath and solely [Bmim]Cl (9 wt.% D-fructose) an inferior 82% Y_{Hmf} (84% C_{Fru}) was obtained at 155 °C/5 min. The addition of 5 mol.% of HCl to [Bmim]Cl gave 92% Y_{Hmf} (96% C_{Fru}) at 100 °C/30 min. Using H₂O (instead of [Bmim]Cl) with 1 mol.% HCl gave a much lower Y_{Hmf} of only 11% (39% C_{Fru}) at 100 °C/420 min.³²¹ This proved that [Bmim]Cl played an important role in promoting the reaction, and the combination with MW produced great benefits for the selective dehydration of D-fructose.³²¹

Organic acids have as well been successfully coupled with ILs as solvents for the conversion of saccharides into furanic aldehydes under moderate reaction conditions (Figure 1.27); they are more attractive in comparison to inorganic acids in that they may be obtained from renewable biomass and may be biodegradable. For example, the reaction of D-fructose (10 wt.%) in the presence of maleic acid (7.6 mol.%) in [Bmim]Cl gave 88% Y_{Hmf} at 80 °C/50 min, which is similar to the best results reported for inorganic liquid acids (Figures 1.25 and 1.27).⁴⁶³ CF₃SO₃H in [Bmim]Cl provided better Y_{Hmf} (88% at 96% C_{Fru}) than H₂SO₄ (ca. 85% Y_{Hmf}) or CuCl₂ (ca. 80% Y_{Hmf}) due to the stronger proton donor ability it presents.³⁰³ In the absence of a catalyst, the Y_{Hmf} was only 48% indicating the excellent synergistic effect of the catalyst. The authors reported equally high Y_{Hmf} (ca. 90%) for imidazolium cations with alkyl chain substituent groups of less than four carbon

atoms ([Mim]Cl, [Emim]Cl, [Bmim]Cl). Longer alkyl chains prevent the H of C-2 of the imidazolium cation to contact with the -OH group of D-fructose to dehydrate into Hmf ($Y_{\text{Hmf}} < 15\%$ with [Hxmim]Cl, [Omim]Cl and [Dmim]Cl).³⁰³ Varying the anion to [Bmim]BF₄, [Bmim]PF₆, [Bmim]CF₃SO₃H or [Bmim]SCN also gave very poor $Y_{\text{Hmf}} (< 20\%)$. Molecular simulation studies indicated that the Cl⁻ anion has a stronger interaction with D-fructose. The Cl⁻ ions in ILs may tend to form strong hydrogen bonds between two adjacent -OH groups in D-fructose (OH-Cl-OH).³⁰³

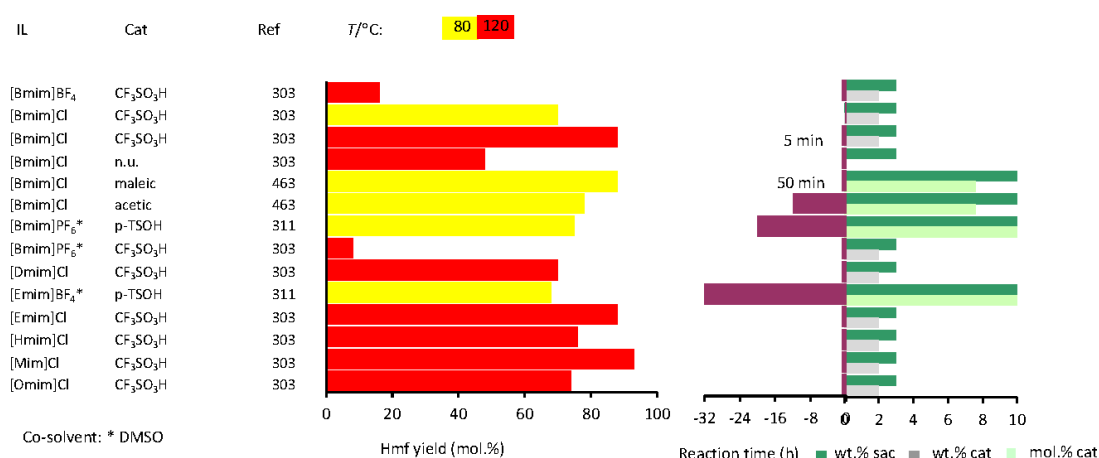


Figure 1.27- Homogeneous organic Brønsted acids coupled with ILs as solvents in the dehydration of D-fructose to 5-hydroxymethyl-2-furaldehyde (Hmf).

The results reported to date using liquid Brønsted acid catalysts in ILs as solvents in the reaction of D-fructose to Hmf (Figures 1.25 and 1.27) are, in general, more attractive than those for D-glucose (Figure 1.28). The reaction of D-fructose (10 wt.%) in [Emim]Cl, without adding an acid, gave ca. 40% Y_{Hmf} (58% C_{Fru}) and 70% Y_{Hmf} (100% C_{Fru}) at 100 °C and 120 °C, respectively, after 3 h reaction. The same IL was ineffective in converting D-glucose into Hmf ($Y_{\text{Hmf}} < 5\%$, even at the higher temperature of 180 °C).²⁰¹ Hence, D-glucose is a more demanding substrate than D-fructose for Hmf production. Nevertheless, for the reaction of D-glucose, considerably higher Y_{Hmf} have been reported using Brønsted acid catalyst/IL systems (Figure 1.28) in comparison to acidic ILs (discussed in Section 1.5.2), possibly due to the stronger bulk acidity in the latter case. Different inorganic (H₂SO₄, HNO₃, HCl, H₃PO₄) and organic (CH₃SO₃H, CF₃SO₃H) liquid acids have been tested in the conversion of D-glucose, using [Bmim]Cl as solvent (Figure 1.28).^{198,230,231,317,334}

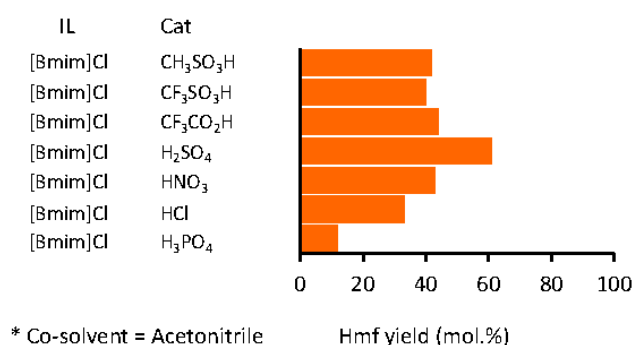


Figure 1.28- Brønsted liquid acid catalysts coupled with ILs as solvents in the dehydration of D-glucose (Glu) to 5-hydroxymethyl-2-furaldehyde (Hmf).¹⁹⁸ Reaction conditions: 9 wt.% sac, 1 mol.% cat, T=120 °C, reaction time= 3 h.

D-Sucrose,²³⁰ starch,³²² cellulose³¹⁷ and other biomass derived feedstocks have been converted into 30-60% Y_{Hmf} , using HCl in imidazolium chloride ILs (Table 1.8). Similar 25 mol.% and 29 mol.% Y_{Hmf} were obtained by adding H₂O or acetonitrile to the [Emim]Cl/HCl/cellulose system; (5 wt.% cellulose, 15 wt.% H₂O or 10 wt.% acetonitrile, and 1 wt.% HCl) at 110 °C/3 h.³⁰¹ Dee et al.³⁰¹ coupled [Bmim]Cl to several mineral and organic acids (e.g. HCl, H₂SO₄, CH₃SO₃H, CF₃COOH, CH₃COOH and H₃PO₄) in H₂O from 4.6 wt.% cellulose giving a similar ca. 20 mol.% Y_{Hmf} for the first four acids ($pK_a \leq -1.9$) at 90 °C in 0.9 h-2 h (Table 1.8, Figure 1.29). H₃PO₄ and CH₃COOH (acids with a $pK_a \geq 2$ had not given Hmf).³⁰¹ Using [Bmim]CH₃COO instead of [Bmim]Cl with H₂SO₄, the catalyst becomes inactive due to the strong affinity of CH₃COO⁻ for the H⁺ of H₂SO₄.³⁰¹

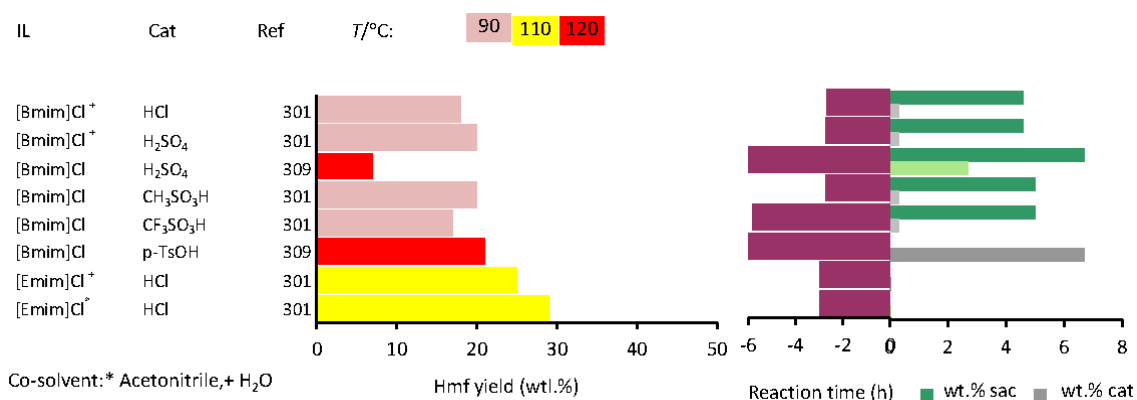


Figure 1.29- Mineral and organic acid catalysts coupled with ILs as solvents in the dehydration of cellulose to 5-hydroxymethyl-2-furaldehyde (Hmf).

To obtain Fur, pentose based carbohydrates are used as feedstocks but poorer results were obtained. The reaction of D-xylose in $\text{H}_2\text{SO}_4/[\text{Bmim}]\text{Cl}$ gave only 13% Y_{Fur} (100% C_{Xyl}) at 120 °C/1.5 h (6 mol.% H_2SO_4 ; 5 wt.% D-xylose),²³¹ while Binder et al.²⁷⁷ reported 10 mol.% Y_{Fur} from xylan (5 wt.%) using HCl (25 mol.%) and $[\text{Emim}]\text{Cl}/\text{DMA}$ (5 wt.% IL) at 140 °C/2 h.²⁷⁷

1.5.1.2. ILs coupled with homogeneous/heterogeneous solid acid catalysts

Different types of solid acid catalysts have been investigated in the conversion of saccharides into Hmf/Fur, using ILs as solvents. Some are soluble (such as betaine hydrochloride,³⁵⁶ Keggin type heteropolyacids,¹⁹⁸ or metal chloride salts),^{196,201,305,306,309,313,322-324,328-332,334-339,373,374,468-472} while others are insoluble (such as organic ion-exchange acid resins,^{302,304,306,309,311,343} carbon-based catalysts,³⁵⁴ microporous zeolites,^{309,313} zirconium oxides,^{364,369} sulfated zirconia,³⁶⁴ other inorganic oxides (P_2O_5 and B_2O_5),³²⁵ or hybrid organic-inorganic, like SBA-15- SO_3H ³⁵³).

Betaine hydrochloride-based catalyst (denoted BHC), a co-product of the sugar beet industry coupled to $[\text{Cho}]\text{Cl}$ (Choline chloride), gave interesting results as a homogeneous acid catalyst in the dehydration of D-fructose to Hmf (Figure 1.30).³⁵⁶ The homogeneous system ($[\text{Cho}]\text{Cl}/\text{BHC}/\text{H}_2\text{O}$), with a mass ratio of [10/0.5/2] (5 wt.% BHC, 10 wt.% D-fructose), reached 81% Y_{Hmf} at 110 °C/1 h. With the addition of IBMK, a slightly improved 84% Y_{Hmf} was obtained under the same conditions (Figure 1.30).³⁵⁶ $[\text{Cho}]\text{Cl}$ was beneficial for the production of Hmf as in its absence lower Y_{Hmf} were obtained. For the system $[\text{glycerol}/\text{BHC}]$ with a mass ratio of [50:50] and $[\text{H}_2\text{O}/\text{IBMK}/\text{BHC}]$, in 2 h the Y_{Hmf} was 57% at 110 °C. Hmf is less reactive with $[\text{Cho}]\text{Cl}$ than with glycerol or H_2O .³⁵⁶ The efficiency of the ($[\text{Cho}]\text{Cl}/\text{BHC}/\text{H}_2\text{O}$) system also depended on the D-fructose and BHC contents. Higher amounts of D-fructose and BHC resulted in a lower 50% Y_{Hmf} (40 wt.% fructose, 10 wt.% BHC). Higher concentrations of D-fructose led to degradation of Hmf to soluble and insoluble humins; BHC amounts > 5 wt.% limit the reaction due to diffusion problems caused by the high viscosity of the system.³⁵⁶ This system was especially successful for D-fructose. For D-glucose the presence of AlCl_3 (10 mol.%) is required to promote the isomerisation into D-fructose, reaching 40% Y_{Hmf} (temperature and time not mentioned). Recycling tests in order to recover the IL were applied with success (Section 1.5.3).³⁵⁶ A BHC

homogeneous catalyst (5 wt.%) coupled to ([Cho]Cl/H₂O/IBMK) was also applied in the conversion of inulin (15 wt.%), giving a Y_{Hmf} of 19 wt.% (52 mol.%) at 100 °C/1h (Table 1.8, Figure 1.33).³⁵⁶

Heteropolyacids (HPAs) are easier and safer to handle than liquid acids; HPAs of the keggin-type gave comparable or superior results to those observed for liquid acid catalysts in the reaction of D-glucose using imidazolium-chloride ILs as solvents (Figure 1.30).¹⁹⁸ The trend in catalytic activity in the reaction of D-glucose (9 wt.%) in HPA/[Bmim]Cl at 120 °C/3 h correlated with the trend in the acidity of the HPA: 12-TPA>12-MPA>12-TSA>12-MSA; 12-TPA=12-tungstophosphoric acid (H₃PW₁₂O₄₀); 12-MPA=12-molybdophosphoric acid (H₃PMo₁₂O₄₀); 12-TSA=12-tungstosilicic acid (H₃SiW₁₂O₄₀); 12-MSA=molybdosilicic acid (H₃SiMo₁₂O₄₀) (Figure 1.30).¹⁹⁸

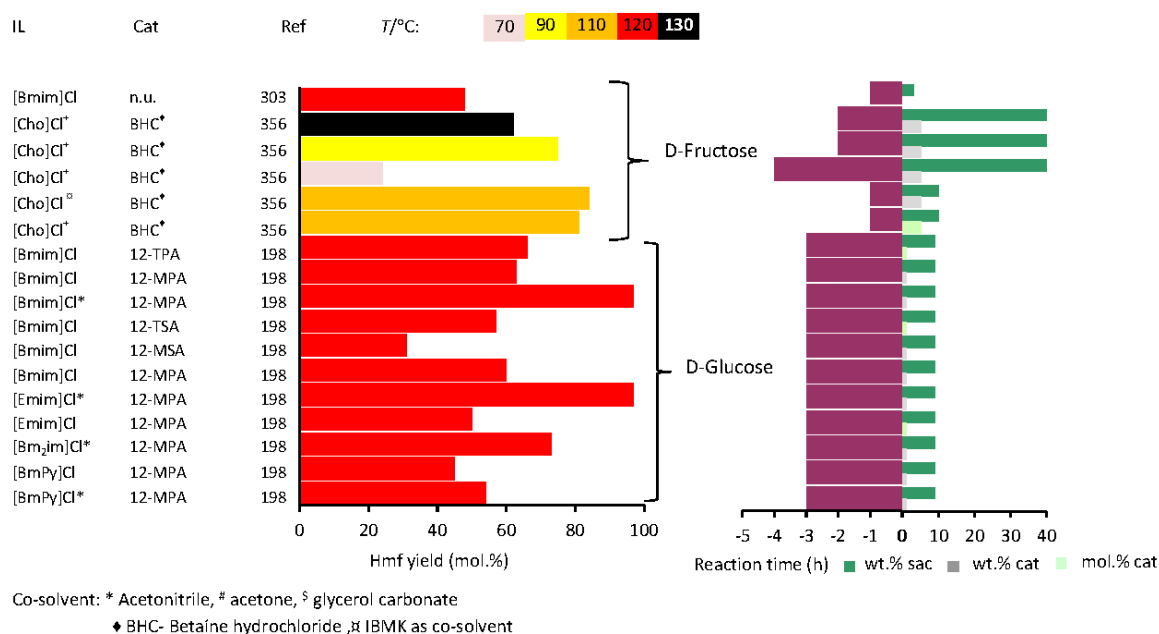


Figure 1.30- Soluble organic solid acids coupled with ILs in the dehydration of D-fructose or D-glucose (Glu) into 5-hydroxymethyl-2-furaldehyde (Hmf).

With 12-MPA as catalyst, the ILs [Bm₂im]Cl and [BmPy]Cl were less effective solvents than [Bmim]Cl and it was postulated that these differences could be due to differences in the acid-base properties of the IL medium.¹⁹⁸ The formation of humins in the reaction of D-glucose (9 wt.%) could be suppressed by coupling the HPA/IL system with acetonitrile as co-solvent (ca. 40 wt.% in the IL), giving an outstanding result of 98% Y_{Hmf} (99% C_{Glu}) in the case of 12-MPA/([Bmim]Cl or

[Emim]Cl) at 120 °C/3 h.¹⁹⁸ Besides decreasing the viscosity of the IL, which may improve mass transfer rates, acetonitrile may have an effect of leveling-off the acid strength of the reaction medium.^{198,343,449,450} On the other hand, non-protic solvents, such as acetonitrile and DMSO, may influence the equilibrium of mutarotation of hexoses (water concentration in the system may also influence the extent of this process) which may affect the selectivity of the catalytic system.^{226,473,474}

Several transition metal and lanthanide chloride salts as catalysts dissolved in ILs, mainly 1-alkyl-3-methylimidazolium chloride, were investigated in the conversion of saccharides into Hmf, especially for D-fructose (Figure 1.31).^{196,201,202,230,306,322,328,330,331,334,336,374,455,457,468,470,471,475} In the case of D-glucose dehydration almost no catalyst besides chromium chloride (CrCl₂) was effective (Figure 1.32).^{196,201,230,322,330,334,336,374,455,457,468,470,471,475} Zhao et al.²⁰¹ patented the application of such processes, and some of these represented major breakthroughs in the selective conversion of D-glucose (Figure 1.32) and related di/polysaccharides into Hmf (Figure 1.34).^{194,201,329} Y_{Hmf} values in the range 59-83% have been reported for the reaction of D-fructose (10 wt.%) using metal Lewis catalysts in [Emim]Cl at (80-120 °C)/(1.5-3h) (Figure 1.31).^{196,201,470,471} Chromium salts were the most used. By MW heating Qi et al.³³⁶ obtained 78% Y_{Hmf} from D-fructose (5 wt.%) at 100 °C within only 1 min by using CrCl₃/[Bmim]Cl (10 mol.% salt; IL with less than 1% H₂O, Figure 1.31); good results were obtained in recycling runs (Section 1.5.3). Yong et al.³³⁰ tested the CrCl₂/[Bmim]Cl system in the presence of a bulky N-heterocyclic carbene (NHC), namely 1,3-bis(2,6-diisopropylphenyl)imidazolyliidene (Ipr), and obtained 96% Y_{Hmf} at 100 °C/6 h (9 mol.% catalyst, 10 wt.% D-fructose and CH method, Figure 1.31). NHC ligands are interesting because they offer a great deal of flexibility as the catalytic activity can be modified by varying their stereo and electronic properties.³³⁰ In this study, the authors concluded that bulky NHC ligands such as Ipr inhibit the Cr centre from reacting with [Bmim]Cl to form a sterically crowded metal centre, thereby providing a higher catalytic efficiency since the initiation of the reaction by binding of the substrate to the metal centre will be inhibited if the centre is sterically crowded.³³⁰ The stability of the IL was confirmed by recycling procedures (Section 1.5.3). Using DMSO instead of IL drastically decreased the Y_{Hmf} to 41%.^{330,455,457,468}

Good results were obtained with ([Bmim]Cl/CrCl₃·6H₂O) and ([Bmim]Cl/CrCl₂; 6 mol.% catalyst and 10 wt.% D-fructose): 80 and 60% Y_{Hmf} respectively (100% C_{Fru}) at 80 °C/3 h.³³¹ The higher catalytic activity of Cr³⁺ is due to the increased Lewis acidity compared to Cr²⁺, which limits the concentration of intermediates that are prone to bimolecular condensation reactions that

lead to humins.³³¹ Other ILs were tested instead of [Bmim]Cl: [Bemim]Cl and [Bmim]TolSO₃ reached 71% and 66% Y_{Hmf} , respectively, at 100 °C/2 h; [Hxmim]Cl and [Bdmim]Cl (44-49% Y_{Hmf} at 90-92% C_{Fru}); [Omim]Cl gave a very poor Y_{Hmf} (< 1%).³³⁸ These results are in agreement with the discussion in “the ILs coupled to Brönsted catalysts Section”, in that the catalytic activity decreases with the length of the alkyl group.^{303,338} The anions of ILs used also play a role in the D-fructose dehydration: the interaction of the acidic H⁺ in [Bmim]TolSO₃ with D-fructose is more difficult than in [Bmim]Cl, and Cl⁻ acts as nucleophile promoting the reaction in a more favourable way than the p-toluenesulfonate anion.³³⁸

Gruber et al.¹⁹⁴ reported lower yields when the CrCl₂/IL system contained acetic or propanoic acids as co-solvents (10 wt.% D-fructose; 6 mol.% catalyst; IL=([Emim]Cl+[Hmim]Cl); 29 or 40% Y_{Hmf} were obtained respectively. However, the main products formed were 5-(acetoxymethyl)-2-furaldehyde or 5-(propionyloxy)methyl-2-furaldehyde, respectively, which are promising fuels/fuel additives.

Despite their contribution to important mechanistic insights, in the chromium-based catalytic processes, Cr⁶⁺ can be formed, posing serious risks to human health and the environment, which would mean that their implementation on an industrial scale would be subject to very stringent regulations. Therefore several other different inorganic chloride salts have been tested. Zhao et al.²⁰¹ reported 63-83% Y_{Hmf} for FeCl₂, FeCl₃, CuCl, CuCl₂, VCl₃, MoCl₃, PdCl₂, PtCl₂, PtCl₄, RuCl₃, RhCl₃, AlCl₃ as catalysts (6 mol.%), using [Emim]Cl as solvent at 80 °C/3 h (10 wt.% D-fructose, Figure 1.31). The best result was obtained for PtCl₂.²⁰¹ Using H₂SO₄ as catalyst (1.8-18 mol.%) instead of a metal Lewis acid, under similar reaction conditions, gave similar 75-80% Y_{Hmf} .²⁰¹ Other inorganic chloride salts (SnCl₄, BiCl₃, ScCl₃ and CeCl₃ in 10 mol.%) resulted in Y_{Hmf} less than 8% with [Bmim]Cl at 100 °C/5 min (5 wt.% D-fructose).³⁷³ However, using SnCl₄ (10 mol.%) coupled to [Emim]BF₄, Hu et al.³⁷⁴ reported 62% Y_{Hmf} (100% C_{Fru}) for the reaction of D-fructose (20 wt.%) at 100 °C/3 h; compared to chromium chloride catalysts, SnCl₄ has lower toxicity and in what concerns recycling tests it was successful too.³⁷⁴

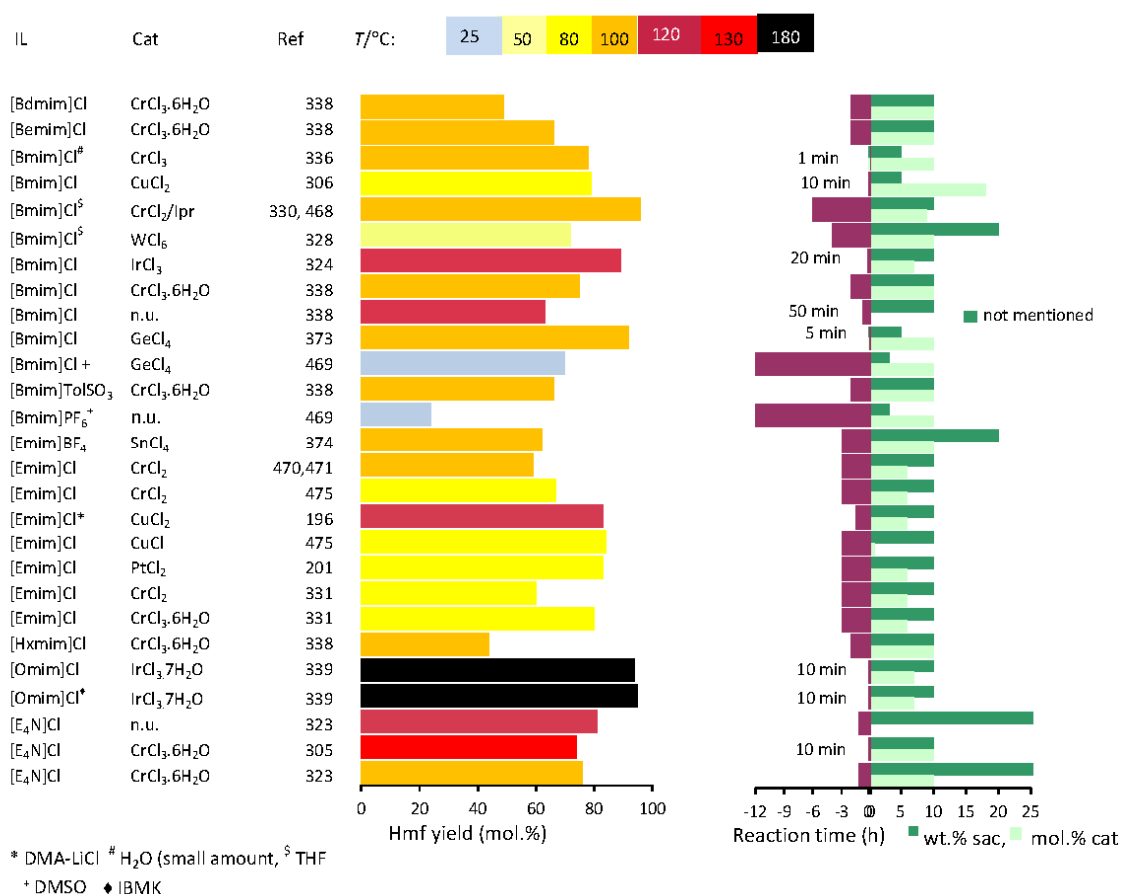


Figure 1.31- Lewis acid catalysts coupled with ILs as solvents in the dehydration of D-fructose to 5-hydroxymethyl-2-furaldehyde (Hmf); lpr=1,3-bis(2,6-diisopropylphenyl)imidazolylidene.

Using GeCl₄ (10 mol.% based on 3.3. wt.% D-fructose), [Bmim]Cl under very mild reaction conditions and DMSO (50 wt.% to the IL) as co-solvent, Zhang et al.⁴⁶⁹ obtained 70% Y_{Hmf} at 25 °C/12 h (Figure 1.31). In the absence of the IL the Y_{Hmf} was only 39% within 12 h, which proved that the IL promotes the dehydration reaction; and are relatively easy to recover for further reuse (recycling tests in Section 1.5.3).⁴⁶⁹ However, not all ILs, under the same conditions, are promising for this type of reaction: with [Bmim]CH₃COO, the Y_{Hmf} was < 5%, possibly due to side reactions between D-fructose and the imidazolium ring induced by the strongly basic acetate group. In the case of [Bmim]BF₆, the low nucleophilicity of BF₆⁻ compared to Cl⁻ might hamper the D-fructose dehydration, leading to a lower 25% Y_{Hmf}.⁴⁶⁹ In the case of the salts RuCl₃, WCl₄ and WCl₆, 45-63% Y_{Hmf} were reached under very mild reaction conditions (at 50 °C/4 h). The best results were observed for the tungsten-containing systems.³²⁸ This was a very good result when compared to chromium chloride (CrCl₂ or CrCl₃) which gave Y_{Hmf} < 5%.³²⁸ In the case of WCl₆, the 63% Y_{Hmf} at

80 °C was slightly lower than that at 50 °C (ca. 62% Y_{Hmf}), which encouraged the authors to test lower temperatures (42% Y_{Hmf} at 22 °C/4 h and 53% Y_{Hmf} at 30 °C/4 h).³²⁸ Coupling the $\text{WCl}_6/[\text{Bmim}]\text{Cl}$ system (10 mol.% salt) with THF as immiscible co-solvent for the in situ extraction of Hmf gave 72% Y_{Hmf} compared to 63% Y_{Hmf} for the monophasic solvent system at 50 °C/4 h (20 wt.% D-fructose), meaning that THF was able to remove the water produced during the dehydration step. THF gave better results than IBMK, Tol, or ethyl acetate as co-solvents.^{328,455} The $\text{WCl}_6/[\text{Bmim}]\text{Cl}/\text{THF}$ biphasic solvent system could be operated in a batch, semi-batch, or continuous mode. The latter produced superior Hmf yield due to a continuous extraction of the Hmf phase, allowing the IL purification (by water removal). Further details on the recycling procedures are described in Section 1.5.3.^{328,455}

Other type of ILs, without imidazolium cations, were reported by Cao et al.,³²³ and Hmf yields in the range 64 to 81% Y_{Hmf} (100% C_{Fru}) were obtained with the ILs $[\text{M}_4\text{N}]\text{Cl}$, $[\text{E}_4\text{N}]\text{Cl}$, $[\text{B}_4\text{N}]\text{Cl}$, $[\text{M}_3\text{BeN}]\text{Cl}$, $[\text{M}_3\text{PhN}]\text{Cl}$, $[\text{M}_3\text{HN}]\text{Cl}$, $[\text{M}_2\text{H}_2\text{N}]\text{Cl}$ and $[\text{Cho}]\text{Cl}$ from D-fructose (50 wt.%) at 120 °C/70 min,³²³ in which the best result was obtained with $[\text{E}_4\text{N}]\text{Cl}$ (recycling tests in Section 1.5.3).³²³ However at 100 °C, only 33% Y_{Hmf} was achieved by $[\text{E}_4\text{N}]\text{Cl}$. To improve this result, a Lewis acid co-catalyst (10 mol.% $\text{CrCl}_3 \cdot 6\text{H}_2\text{O}$, FeCl_3 , $\text{CuCl}_2 \cdot 2\text{H}_2\text{O}$, MoCl_3 , AlCl_3) or $\text{NaHSO}_4 \cdot \text{H}_2\text{O}$ was added, which led to an improvement in the Y_{Hmf} to 68-83% (100% C_{Fru}) at 100 °C/70 min.³²³ These results are comparable with the results obtained by Zhao et al.²⁰¹ with $[\text{Emim}]\text{Cl}$, although Cao et al.³²³ used a higher concentration of D-fructose (50 wt.% compared to 10 wt.%) which seems to be preferred in Hmf production processes.

For the more demanding substrate D-glucose, catalytic systems of the type $\text{MCl}_x/(\text{imidazolium})$, with $\text{M}=\text{chromium}$ or tin, gave more than 60% Y_{Hmf} (Figure 1.32).^{196,201,230,322,330,334,336,374,455,457,468,470,471,475}

Outstanding results were reported in a pioneering work by Zhao et al.²⁰¹ using various metal chlorides as catalysts (9 mol.% based on D-glucose) for the catalytic conversion of D-glucose (10 wt.%) in $[\text{Emim}]\text{Cl}$, in which CrCl_2 was found to be the best catalyst giving nearly 70% Y_{Hmf} (90% C_{Glu}) at 100 °C/3 h. This proves that CrCl_2 improves the Y_{Hmf} , as when using $[\text{Emim}]\text{Cl}$ in the absence of catalyst, no Hmf was formed and the C_{Glu} was only 40%, and when using H_2SO_4 instead of CrCl_2 very poor results were achieved (ca. 12% Y_{Hmf} at 95% C_{Glu} , Figure 1.32).²⁰¹ Binder et al.¹⁹⁶ added LiCl to this system and reported that it did not affect the yield of Hmf, while the absence of CrCl_2 , led to a Y_{Hmf} less than 1%,¹⁹⁶ similar to that reported by Zhao for $\text{LiCl}/[\text{Emim}]\text{Cl}$.²⁰¹ Zhang et al.³³¹ reported 55% Y_{Hmf} (ca. 90% C_{Glu}) and 58% Y_{Hmf} (ca. 90% C_{Glu}) with CrCl_2 and CrCl_3 , respectively, instead of $\text{CrCl}_3 \cdot 6\text{H}_2\text{O}$. These results indicate that $\text{CrCl}_3 \cdot 6\text{H}_2\text{O}$ is more active in the

isomerisation of D-glucose to D-fructose and in the dehydration of D-fructose. The difference in the Hmf yield between CrCl_3 and $\text{CrCl}_3 \cdot 6\text{H}_2\text{O}$ might also be related to their different solubilities in $[\text{Emim}]\text{Cl}$ which is related to their solid state structure. The dissolution in $[\text{Emim}]\text{Cl}$ implies the introduction of the Cl^- of the IL in the coordination sphere of chromium.³³¹ This process is difficult for CrCl_3 because it involves a substantial perturbation of the octahedrally coordinated chromium ions (of its Cl-bridged octahedral CrCl_6 network), and there is not an energy benefit from the substitution of a bridging Cl ligand by a terminal one, which makes CrCl_3 insoluble in $[\text{Emim}]\text{Cl}$ in the absence of D-glucose. However, solubility tests suggested that a carbonyl moiety is necessary to favour CrCl_3 dissolution; therefore the presence of D-glucose provides a slow dissolution.³³¹ On the other hand, in $\text{CrCl}_3 \cdot 6\text{H}_2\text{O}$, the Cr^{3+} centers are present as isolated hexa aquo-chromium cations ($\text{Cr}(\text{OH}_2)_6$) interconnected through a hydrogen-bonding network between Cl^- anions and H_2O ligands which rapidly decomposes in highly polar $[\text{Emim}]\text{Cl}$.³³¹ Using other ILs, such as $[\text{Bmim}]\text{Cl}$, $[\text{Hxmim}]\text{Cl}$, $[\text{Bdmim}]\text{Cl}$, $[\text{Bemim}]\text{Cl}$ and $[\text{Bmim}]\text{ToISO}_3$, with $\text{CrCl}_3 \cdot 6\text{H}_2\text{O}$ (25 mol.% based on 10 wt.% D-fructose), Y_{Hmf} (55-65%) were obtained at 120 °C/1 h.³³⁸ Several other chloride salts consisted of Na, Li, La, Al, Mn, Fe, Cu, V, Mo, Pd, Pt, Ru or Rh were tested in $[\text{Emim}]\text{Cl}$, but failed to succeed (Y_{Hmf} was always less than 10%), because in general, they catalysed undesired reaction pathways or D-glucose conversion was negligible (which was the case with La^{3+} , Na^+ , Li^+ , Mn^{3+} , Cu^{2+}).²⁰¹ $Y_{\text{Hmf}} < 8\%$ (50-70% C_{Glu}) were also reported with the system $\text{IrCl}_3/[\text{Bmim}]\text{Cl}$ (7 mol.% catalyst; 10 wt.% D-glucose).³²⁴ Ståhlberg et al.³⁹¹ explored lanthanide salts (CeCl_3 , PrCl_3 , NdCl_3 , DyCl_3 , YbCl_3 , $\text{Yb}(\text{CF}_3\text{SO}_3)_3$ (10 mol.%) with IL= $[\text{Bmim}]\text{Cl}$ or $[\text{Emim}]\text{Cl}$ but the Y_{Hmf} were less than 24% at 140 °C/6 h (10 wt.% D-glucose).³⁹¹ In the presence of catalytic amounts of SnCl_4 (10 mol.%) and using different ILs ($[\text{Bmim}]\text{X}$, with $\text{X}=\text{Cl}^-$, BF_4^- , PF_6^- , $(\text{CF}_3\text{SO}_2)_2\text{N}^-$, CF_3CO_2^- , CF_3SO_3^- , saccharine; $[\text{Emim}]\text{BF}_4$) at 100 °C/3 h, Hu et al.³⁷⁴ reported some interesting results for the reaction of D-glucose (10 wt.%), and the best result (for $[\text{Emim}]\text{BF}_4$) gave 57% Y_{Hmf} (97% C_{Glu}), which was considerable better than the result obtained for $[\text{Bmim}]\text{BF}_4$ (37% Y_{Hmf} at 88% C_{Glu} , Figure 1.32). Differences in acidity of the IL medium may affect the catalytic results. It has been reported that $[\text{Emim}]\text{BF}_4$ tends to be more acidic than $[\text{Bmim}]\text{BF}_4$ and that minor amounts of water in the IL may significantly influence the acidity of the IL medium.⁴⁶⁵ On the other hand, poorer results observed for the ILs containing the anions Cl^- , $(\text{CF}_3\text{SO}_2)_2\text{N}^-$, CF_3CO_2^- , CF_3SO_3^- , and saccharin were attributed to the superior coordinating ability of these species towards the Sn^{4+} cation, inhibiting the interactions of the metal with D-glucose required for the isomerisation to D-fructose to selectively form Hmf.³⁷⁴ When ethylene glycol was added to the $\text{SnCl}_4/[\text{Emim}]\text{BF}_4$ system, a five-membered ring chelate complex with Sn was formed inhibiting the reaction of D-glucose ($C_{\text{Glu}} < 5\%$). Other

alcohols (ethanol and 1,3-propanediol) which formed an acyclic and a six-membered ring chelate complex with Sn did not affect the reaction.³⁷⁴ Accordingly, five-membered ring chelate structures are more stable than the acyclic and six-membered ring chelate structures.³⁷⁴ More recently, Zhang et al.³⁷³ tested several different types of ILs ([Bmim]Cl, [Bmim]A, with $A=CH_3COO^-$, BF_4^- , and $(CF_3SO_2)_2N^-$, and [cation]Cl, with cation=[Hmim]⁺, [Omim]⁺ and [Dmim]⁺) with $GeCl_4$, in which the best result was obtained for [Bmim]Cl (38% Y_{Hmf} , Figure 1.32). The addition of 5 Å molecular sieves increased the Y_{Hmf} to 48%.³⁷³

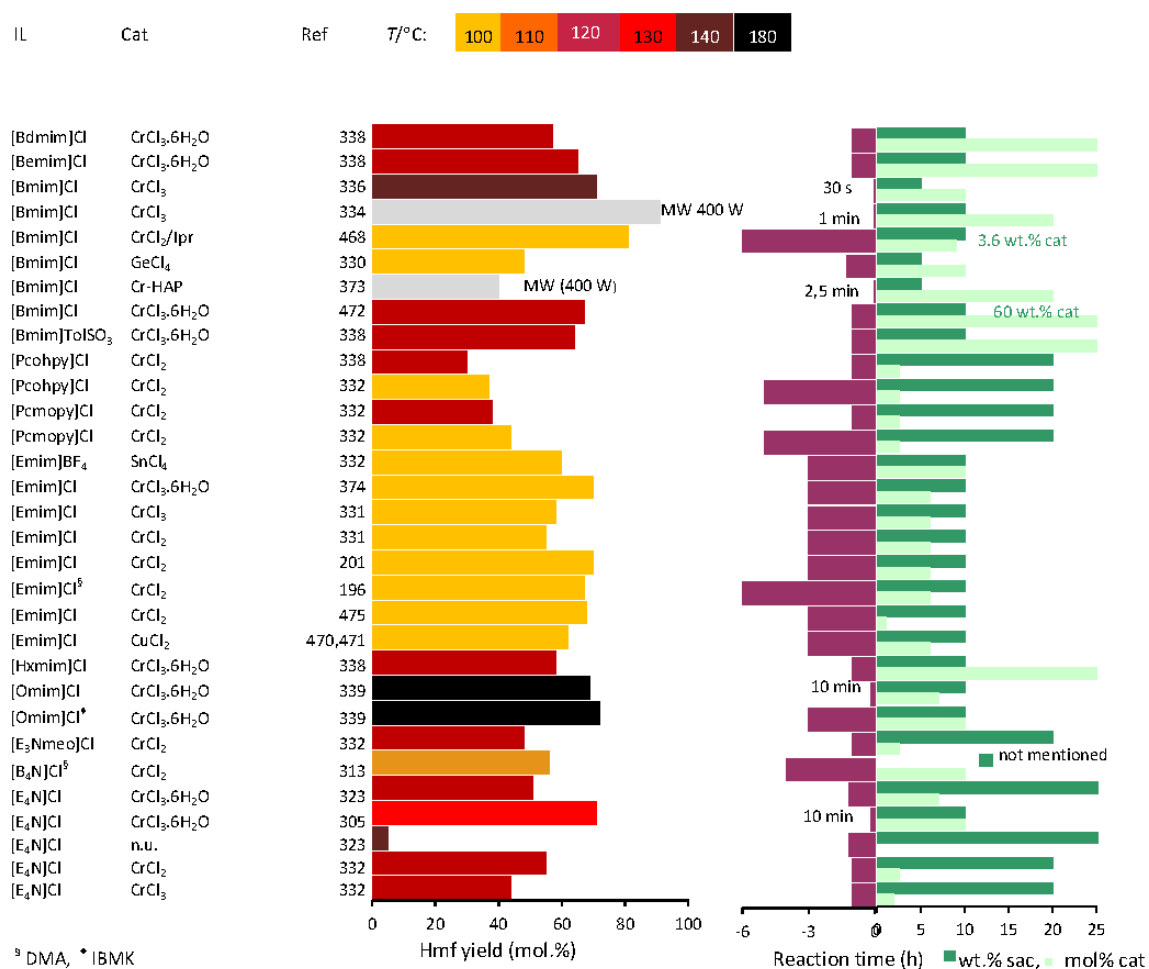


Figure 1.32- Lewis acid catalysts coupled with ILs as solvents in the dehydration of D-glucose to 5-hydroxymethyl-2-furaldehyde (Hmf). lpr=1,3-bis(2,6-diisopropylphenyl)imidazolylidene; HAP=hydroxyapatite.

The results mentioned above indicate a determinant role of the $CrCl_2$ catalyst in the selectivity of this reaction. The high selectivity of D-glucose to Hmf in the presence of the

CrCl_2 /[Emim]Cl system seems to be related to the metal coordination ability. Several authors suggested the formation of [Emim]CrCl₃ by CrCl_2 , and that the CrCl_3^- anion may act as a Lewis acid in proton transfer to facilitate the isomerisation of D-glucose to D-fructose, followed by dehydration to Hmf (Figure 1.33).^{196,201,334,391} Spectroscopic, kinetic, and density functional theory calculations have given mechanistic insights into the D-glucose isomerisation using the CrCl_2 /imidazolium chloride ILs system. The transient self-organisation of the Lewis acidic Cr^{2+} centers into binuclear complexes containing the open form of the hexose is involved in the hydride shift (between C2 and C1 of the open form hexose) step, involving an enediolate intermediate (Figure 1.33), which is favoured by the dynamic nature of the chromium complexes and the presence of moderately basic sites in the IL (high concentration of the free basic Cl^- ions of the IL facilitates proton transfer and forms a hydrogen-bonding network with the -OH groups of D-glucose).^{470,471}

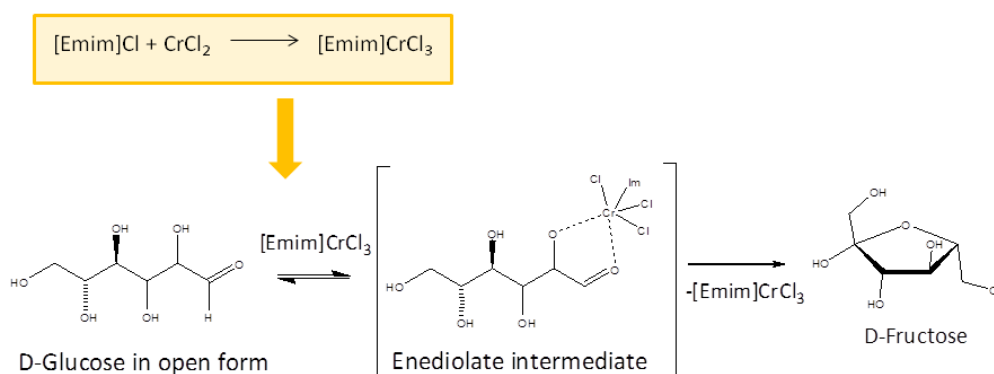


Figure 1.33- Chromium-catalysed isomerisation of D-glucose to D-fructose [adapted from 196,201,334,391].

The poorer results for other metal chlorides in comparison to the CrCl_x /IL systems may be rationalised on the basis of differences in reaction mechanisms (e.g. ytterbium less prone to form complexes with imidazolium chlorides).³⁹¹

The multi component system Ipr/CrCl_2 /[Bmim]Cl gave 81% Y_{Hmf} in the reaction of D-glucose (10 wt.%) at 100 °C/6 h, and only 32% Y_{Hmf} with DMSO instead of the IL.^{330,468} It was also observed that the MW method appeared to be more favourable than the CH method for Hmf production. Li et al.³³⁴ reported 91% Y_{Hmf} from D-glucose (10 wt.%) in CrCl_3 /[Bmim]Cl (6 mol.%); (400 W, temperature not mentioned), compared to 17% Y_{Hmf} when using CH at 100 °C/1 h (Figure

1.32). The presence of the IL was essential because when water was used instead of the IL, less than 1% Y_{Hmf} was obtained.³³⁴

The expensive prices of [Emim]Cl used by Zhao et al.²⁰¹ in the dehydration of D-glucose led to the search of cheaper ionic liquids. Since [B₄N]Cl is non-toxic and cheap it can be seen as an alternative to imidazolium-based ILs.³¹³ [B₄N]Cl coupled to CrCl₂/DMA gave 56% Y_{Hmf} (10 mol.% catalyst) at 110 °C/4 h (Figure 1.32).³¹³ [E₄N]Cl coupled to CrCl₂ (0.03 M)/DMSO/Benzene gave 55% Y_{Hmf} at 120 °C/1 h,³³² which was improved when [E₄N]Cl was coupled to CrCl₃·6H₂O (10 mol.%) with an outstanding result of 71% Y_{Hmf} at 130 °C/10 min.³⁰⁵ Aprotic acids (DMSO or DMFA) instead of [E₄N]Cl gave lower Y_{Hmf} of 22 and 42%, respectively, under the same reaction conditions, showing the good effect of the IL.³⁰⁵ Other ILs ([Pcohpy]Cl, [Pcmopy]Cl and [E₃Nmeo]Cl) were also tested with CrCl₂ as catalyst (0.03 M) but lower Hmf yields were obtained (30, 38 and 48% respectively) at 120 °C/1 h (Figure 1.32).³³² These unsatisfactory results might be related with the possible instability of the hydroxyl group in the IL (especially for [Pcohpy]Cl), which easily undergoes dehydration to form a double bond, and subsequently polymerisation.³³² Cheaper ILs such as [Bpy]BF₄ were also tested using SnCl₄ (10 mol.% instead of chromium catalysts at 100 °C/3 h, but the Y_{Hmf} was only 20% (80% C_{Glu}),³⁷⁴ despite better than the series of inorganic chloride salts tested by Zhao et al.²⁰¹

The results mentioned above for chromium catalysts fostered much research in CrCl_x/IL catalytic systems for producing Hmf from D-glucose and related di/polysaccharides (Figures 1.32 and 1.34).

The hydrolysis/dehydration reactions of the disaccharides D-cellobiose, D-maltose, and D-sucrose into Hmf have been explored, using MCl_x/(imidazolium-IL) systems, in which M=Cr, Sn, Ge, Ir or Au (Table 1.8).^{196,230,305,322,324,329,334,374} In the case of D-sucrose, the best result is reported from Chun et al.²³⁰ that used a Brønsted and Lewis acid catalyst system: (CrCl₂ or ZnCl₂)/HCl coupled to [Omim]Cl obtaining a maximum 82 wt.% Y_{Hmf} from D-sucrose (20 (wt/v)%) at 120 °C/0.5 h (Figure 1.34).²³⁰ Aqueous solutions of HCl (0.0-0.5M) were used firstly to promote the hydrolysis of D-sucrose, and (CrCl₂ or ZnCl₂)/IL was added to promote the selective dehydration of the monosaccharides to give Hmf.²³⁰ For D-cellobiose, Hu et al.^{305,374} reported 22-23 wt.% Y_{Hmf} using the system SnCl₄/[Emim]BF₄ at 100 °C/3 h, or [E₄N]Cl /CrCl₃·6H₂O at 130 °C/10 min (Table 1.8, Figure 1.34). Binder et al.²⁵³ reported that CrCl₂/[Emim]Cl (6 mol.% catalyst) can also be used to produce Hmf from other hexoses: D-mannose, D-lactose, D-galactose and D-tagatose (10 wt.%). 57% Y_{Hmf} was obtained for D-mannose and 14-17% for the other substrates at 120 °C/2 h.

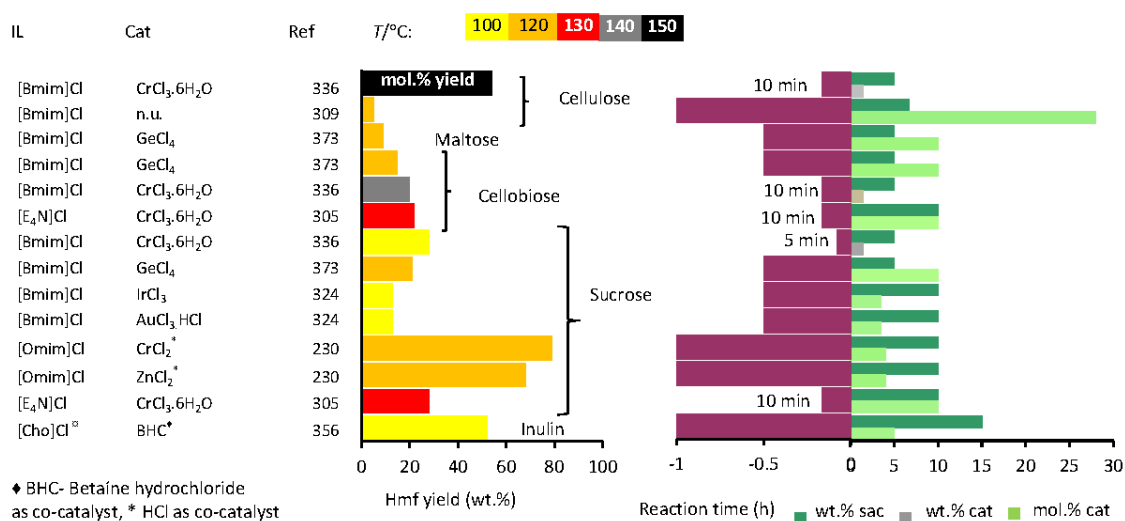


Figure 1.34- Soluble solid catalysts coupled with ILs as solvents in the dehydration of disaccharides (e.g. D-maltose, D-cellobiose and D-sucrose) and polysaccharides (e.g. cellulose and inulin) to 5-hydroxymethyl-2-furaldehyde (Hmf).

The conversion of polysaccharides, such as cellulose and starch, and lignocellulosic biomass, such as corn stover, into Hmf (in which Fur may also be formed) has been successfully carried out in the presence of transition metal Lewis acid catalyst/IL systems (Table 1.8.).^{196,322,329,334-337,373,374} One of the main objectives would be to improve Hmf yields directly from cellulose because it has a rather inexpensive availability from non-food resources. Su et. al.³²⁹ reported a one-pot catalytic of crystalline cellulose to Hmf; the cellulose was pre-dissolved in the (catalyst/IL) system at 100 °C/1 h before initiating the reaction (1 cm³ of H₂O per gram of cellulose), depolymerising cellulose much faster than aqueous H₂SO₄. The resulting D-glucose was converted to Hmf under mild reaction conditions. Catalytic amounts of a pair of metal chloride salts (CuCl₂/CrCl₂) dissolved in [Emim]Cl as solvent were used; (6 total mol.% (Cu+Cr) with respect to D-glucose units in the loaded cellulose (10 wt.%), mole fraction of CuCl₂=0.17) and ca. 55% Y_{Hmf} was obtained at 120 °C/8 h for twelve replicate experiments (further details on the recycling procedures are given in Section 1.5.3).³²⁹

The DMA/LiCl system is good to dissolve cellulose (≥ 15 wt.% DMA/LiCl versus ≤ 0.7 wt.% DMA),¹⁹⁶ as the association of the lithium cations with DMA to form DMA.Li⁺ macrocations results in high concentrations of weakly ion paired chloride ions that can form hydrogen bonds with the hydroxyl groups of cellulose, disrupting its intra and inter chain hydrogen bonds.⁴⁷⁶ Therefore, the

multicomponent catalyst consisting of CrCl_x (25 mol.%) and HCl (6 mol.%) was incorporated in the solvent system (DMA-LiCl)/[Emim]Cl (60 wt.% IL; DMA with 10 mol.% LiCl) for the production of Hmf from cellulose (4 wt.%) and corn stover (10 wt.%), giving 54 mol.% and 48 mol.% Y_{Hmf} at 140 °C/2 h, and 34 mol.% Y_{Fur} for corn stover.¹⁹⁶ This system proposed by Binder et al.¹⁹⁶ is effective in dissolving cellulose but since (DMA/LiCl) is miscible with most other solvents, it may be less effective than the system ($\text{CuCl}_2/\text{CrCl}_2$)/[Emim]Cl, proposed by Yu et al.³²⁹ for the extraction of Hmf and reuse of the IL in further runs (detailed in Section 1.5.3). Nevertheless, the work of Binder et al.¹⁹⁶ is relevant as it was the first reporting on Hmf production from raw lignocellulosic biomass (dry corn stover) in an IL. The authors provided a new concept for the use of biomass as a raw material for renewable energy, and the biomass components which were not converted into Hmf (such as lignin) were reformed to produce H_2 for subsequent Hmf hydrogenolysis to give DMF. Other authors already assessed the effectiveness of the CrCl_3 /[Bmim]Cl catalytic system from cellulose giving good Hmf yield within a few minutes, using the MW method (Table 1.8).^{334,336,340} Li et al.³³⁴ reported 62 mol.% Y_{Hmf} within only 2 min (400 W, temperature not mentioned; 10 wt.% catalyst relative to saccharide and 5 wt.% cellulose), demonstrating the outstanding effect of the MW heating in comparison with CH (17 mol.% Y_{Hmf} at 100 °C/4 h).³³⁴ By adding LiCl (50 mol.% Cr+50 mol.% Li) to the CrCl_3 /[Bmim]Cl system, Wang et al.³³⁵ obtained ca. 62 mol.% Y_{Hmf} from 2.5 wt.% cellulose at 140 °C/40 min, or 61 mol.% Y_{Hmf} from 2.5 wt.% wheat straw at 160 °C/15 min (Table 1.8). The (CrCl_3 +LiCl)/[Bmim]Cl catalytic system was recycled with success (Section 1.5.3) and gave better results for the conversion of cellulose to Hmf than the catalysts H_2SO_4 (20 mol.% Y_{Hmf}), NKC-9 (macroporous styrene-based sulfonic acid resin; 18 mol.% Y_{Hmf}), $\text{H}_3\text{PW}_{12}\text{O}_{40}$ (12 mol.% Y_{Hmf}), $\text{CS}_{2.5}\text{H}_{0.5}\text{PMO}_{12}\text{O}_{40}$ (10 mol.% Y_{Hmf}), sulfated titania, SBA-15 supported sulfated zirconia, Nb_2O_5 and $\text{Zr}_3(\text{PO}_4)_2$ (< 5 mol.% Y_{Hmf}) under similar reaction conditions (140 °C/40 min), using MW.³³⁵

Tan et al.³⁰⁹ obtained 48 wt.% and 34 wt.% Y_{Hmf} respectively when using [Bmim]Cl coupled to lpr-CrCl_2 (12 h) and CrCl_2 (6 h), respectively from cellulose (6.7 wt.%) at 120 °C in which the reaction with lpr-CrCl_2 was extracted two times with diethyl ether to prevent Hmf decomposition.

The lignocellulosic feedstock, rice straw, pine wood, and corn stalk gave 45-52 mol.% Y_{Hmf} and 23-31 mol.% Y_{Fur} within 3 min.³³⁷ Wu et al.³⁴⁰ obtained 55 mol.% Y_{Hmf} at 160 °C/6 min from cellulose (Table 1.8). Using the catalytic system ($\text{HCl}+\text{CrCl}_2$)/[Omim]Cl and ethyl acetate as co-solvent, Chun et al.³²² investigated the production of Hmf from different starch sources (20 wt.%) using in a first stage aqueous HCl (0.5 M) to promote the hydrolysis reaction, followed by the addition of this mixture to CrCl_2 /[Omim]Cl/ethyl acetate to perform the selective dehydration into

Hmf. A 60 wt.% Y_{Hmf} (no Fur was detected) was reached in the case of tapioca starch at 120 °C/1 h (Table 1.8). Hu et al.³⁷⁴ obtained, in a one-pot process, 40 mol% Y_{Hmf} (100% of conversion) from inulin (20 wt.%), using the catalytic system $\text{SnCl}_4/[\text{Emim}]\text{BF}_4$ (10 mol.% SnCl_4) at 100 °C/3 h.³⁷⁴

For the production of Fur, Binder et al.²⁷⁷ investigated the reaction of D-xylose (10 wt.%) using the systems $[\text{Bmim}]\text{Br}$ (20 wt.%) coupled to DMA (55% Y_{Fur} at 100 °C/4 h) or $[\text{Emim}]\text{Cl}$ (5 wt.%) coupled to DMA (45% Y_{Fur} at 2 h), and CrCl_2 or CrCl_3 as catalysts (6 mol.%). A mechanism was proposed, in which chromium, acting as a Lewis acid, promotes the isomerisation of D-xylose to xylulose through a 1,2-hydride shift, and xylulose is dehydrated to Fur. The use of $(\text{CrCl}_x+\text{HCl})/[\text{Emim}]\text{Cl}$ (10 mol.% each catalyst) in the reaction of xylan (5 wt.% of birchwood, beechwood, oat hull, or corn stover) gave 18-25 mol.% Y_{Fur} at 140 °C/ 2 h.²⁷⁷

The replacement of homogeneous acid catalysts by heterogeneous ones may increase the cost-competitiveness and decrease the environmental impact of IL-based systems for biomass conversion processes.

Sulfonic ion-exchange acid resins based on a styrene-divinylbenzene copolymer, such as Amberlyst-15, NKC-9 (macroreticular resin) and DowexR-50WX8 (microreticular resin) have performed well in the dehydration of D-fructose, using ILs as solvents, giving high Hmf yields (Figure 1.35).^{201,306,311,343} Lansalot-Matras et al.³¹¹ reported on the dehydration of D-fructose in the presence of Amberlyst-15 as catalyst (2:1 mass ratio of catalyst/D-fructose) and $([\text{Bmim}]\text{PF}_6$ or $[\text{Bmim}]\text{BF}_4)$ in DMSO as solvent system (5:3 v/v), reaching 70-87% Y_{Hmf} , respectively, at 80 °C/32 h; 10 wt.% D-fructose in IL+DMSO (Figure 1.35). Under similar reaction conditions, in pure DMSO, only traces of Hmf yields were achieved in 44 h.³¹¹ The presence of $[\text{Bmim}]\text{BF}_4$ in DMSO improved the Y_{Hmf} to 36% after 32 h which illustrates the positive effect of ILs as solvents. In solely $[\text{Bmim}]\text{BF}_4$, D-fructose is not completely soluble and a maximum 52% Y_{Hmf} was achieved. DMSO was required to enhance the solubility of D-fructose in these ILs as well as to prevent the formation of Hmf by-products, such as humins.³¹¹

Despite enhancing the solubility of the substrates in the IL medium, the addition of miscible co-solvents may also decrease the viscosity and density of the IL medium (particularly when the co-solvents possess higher dielectric constants).^{449,450} Addition of acetone, DMSO, methanol, ethanol or ethyl acetate (3-7 wt.% in the IL) to the system Amberlyst-15/ $[\text{Bmim}]\text{Cl}$ gave 78-82% Y_{Hmf} (91-95% C_{Fru}) at 25 °C/6 h (5 wt.% D-fructose was pre-dissolved in the IL at 80 °C/ 20 min, prior to the addition of the solid acid at a.t.; resin/D-fructose mass ratio of 1).³⁴³

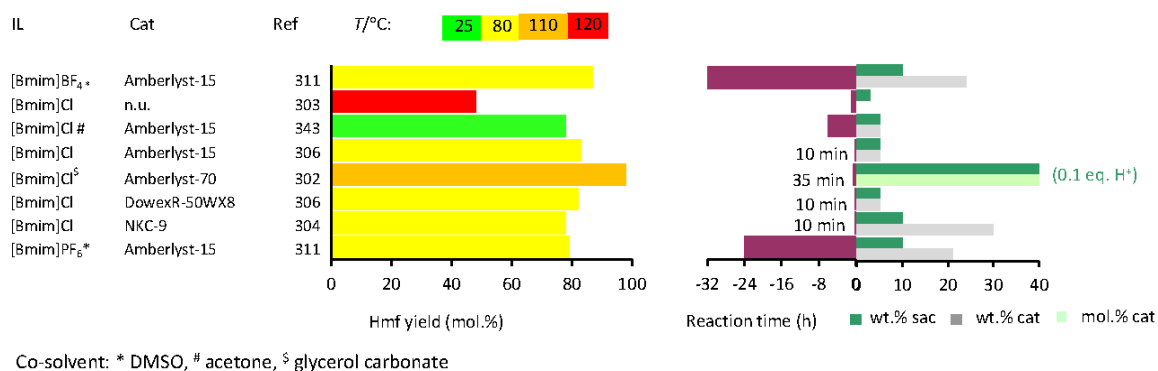


Figure 1.35- Insoluble organic acid resins coupled with ILs as solvents in the dehydration of D-fructose to 5-hydroxymethyl-2-furaldehyde (Hmf).

For rapidly reaching higher reaction temperatures MW irradiation was employed using Amberlyst-15/[Bmim]Cl to convert D-fructose into Hmf and 82% Y_{Hmf} was achieved (ca. 100 % C_{Fru}) at 100 °C/3 min or 120 °C/1 min (details about recycling in Section 1.5.3).³⁰⁶ This work compares favourably with that of Swatloski et al.,⁴³⁶ who tested a similar IL ([Emim]Cl) with mixtures of chromium(II) chloride associated with N-heterocyclic carbenes (9 mol.% based on D-fructose), at the same temperature of 100 °C but using CH with an external heat source (65-96% Y_{Hmf} within 6 h).

Mixtures of ILs and glycerol or glycerol carbonate (cheap, safe, and prepared from renewable resources) have been identified by Benoit et al.³⁰² as interesting solvent systems for the acid-catalysed conversion of D-fructose and inulin. Amberlyst-70 coupled with an IL/(glycerol carbonate) (65:35) solvent system gave 98% Y_{Hmf} at 110 °C/35 min from D-fructose (40 wt.%) (Figure 1.35), while the reaction of 20 wt.% inulin in [Bmim]Cl/(glycerol carbonate) (10:90) gave 60% Y_{Hmf} at 110 °C (time not mentioned). A phosphotungstic acid ($\text{H}_3\text{PW}_{12}\text{O}_{40}$) supported in a chromium based metal organic framework (MIL-101) coupled to [Emim]Cl gave 84% Y_{Hmf} from D-fructose at 80 °C and 1 h, and only 21% Y_{Hmf} from D-glucose even at 100 °C and 3 h, showing again the better efficiency of D-fructose.³⁵⁵

Solid acids coupled with ILs have been poorly explored in the biomass conversion processes using other sources besides D-fructose or D-glucose. Nevertheless, protonic forms of ion-exchange acid resins (Amberlyst 15DRY, Dowex 50WX8, macroporous styrene-based sulfonic acid resin NK-9, perfluorinate sulfonic acid resin Nafion NR50) coupled with [Bmim]Cl as solvent promote the depolymerisation/hydrolysis of cellulose,⁴⁷⁷⁻⁴⁸¹ and performed comparably to

concentrated H_2SO_4 .⁴⁸⁰ [Bmim]Cl coupled to sulfonated resins (Amberlyst-15 and Amberlyst-36), organic p-TsOH or mineral acid (H_2SO_4) from cellulose gave low Y_{Hmf} (7-21 wt.%) at 120 °C/6 h.³⁰⁹ These weak results in strongly acidic conditions speeded up cellulose hydrolysis, but also promoted the decomposition of Hmf into levulinic acid which explains the low Hmf yield obtained.³⁰⁹

As an alternative to the use of ILs as solvents in the presence of an ion-exchange resin, acidic ILs (which will be further discussed in Section 1.5.2) have been successfully used in the one-pot hydrolysis/dehydration of inulin. While a mixture of [Emim]HSO₄ and a solid acid resin (5 wt.% of Amberlyst-15 in the IL) gave 65 mol.% Y_{Hmf} at 100 °C/5 min,³⁴⁴ 82 mol.% Y_{Hmf} was reported when using [Bmim]HSO₄ and [Bmim]Cl in two different stages: primary hydrolysis of inulin (5 wt.%) in [Bmim]HSO₄ gave 82% Y_{Fru} at 80 °C/5 min, followed by the addition of a mixture of Amberlyst-15 and [Bmim]Cl for the subsequent dehydration of the D-fructose to Hmf at 80 °C/60 min (details about the recycling process in Section 1.5.3).³⁴⁴

Guo et al.³⁵⁴ reported the dehydration of D-fructose (10 wt.%) into Hmf in the presence of carbonaceous catalysts using [Bmim]Cl. The best result was obtained with 10 wt.% LCC (lignin derived carbonaceous catalyst) with 84% Y_{Hmf} (98% C_{Fru}) at 110 °C/10 min, using DMSO as co-solvent (DMSO/IL ratio=4/6) and MW (100 W) (Figure 1.36). The addition of DMSO promoted the reaction, because in its absence the yield of Hmf was lower (71% at 100% C_{Fru}).³⁵⁴ Without IL the Hmf yield decreased drastically to 38% (100% C_{Fru}) at 150 °C/1 h.³⁵⁴ For comparison, with D-glucose and the LCC catalyst (5 wt.%), for the same mixture of [Bmim]Cl and DMSO under MW (100 W) gave a lower 68% Y_{Hmf} (99% C_{Glu}) even at a higher temperature of 160 °C/50 min.³⁵⁴

Mesoporous SBA-15 functionalised with a propylsulfonic acid group, SBA-15-SO₃H in catalytic amounts (1 wt.%) coupled to [Bmim]Cl was very efficient in the dehydration of D-fructose (10 wt.%) to Hmf with 81% Y_{Hmf} (100% C_{Fru}) at 120 °C/1 h (Figure 1.36), which was successfully recycled as detailed in Section 1.5.3.³⁵³

Several solid oxides (e.g. ZrO₂, B₂O₃ and P₂O₅) were tested in the dehydration of D-fructose.^{325,364} Qi et al.³⁶⁴ reported for bulk ZrO₂ (2 wt.% catalyst) in [Bmim]Cl, 55% Y_{Hmf} (60% C_{Fru}) at 100 °C/0.5 h. Similar yields were also obtained from the more demanding D-glucose (2.5 wt.%) in the presence of ZrO₂ (1 wt.%) using a mixture of [Hxmim]Cl and water (MW, 700 W), 53% Y_{Hmf} at 200 °C/10 min (Figure 1.36),³⁶⁹ however without water the Y_{Hmf} at 200 °C/1 min was only 10% (70% C_{Glu}). The addition of protic solvents (e.g. methanol or ethanol) to the IL had a synergistic effect (similar to water), promoting the isomerisation to D-fructose (4-23% Y_{Fru}) and

18-53% Y_{Hmf} ; in contrast for aprotic solvents (e.g. DMSO, DMFA or acetone) the Y_{Hmf} was less than 10%.³⁶⁹ Nevertheless, in the absence of IL, either protic (butanol) or aprotic (DMSO or DMA), gave no Hmf, possibly due to the fact that [Bmim]Cl dissolves better the ions and disrupt H-bonds due to its polarity.³¹³

Higher Hmf yields were reported for P_2O_5 (5 mol.%)/[Bmim]Cl under mild conditions with 82% Y_{Hmf} at 50 °C/1 h (Figure 1.36).³²⁵ Other ILs ([Emim]Cl, [Emim]Br, [Bmim]Br) were also quite effective for P_2O_5 leading to 62-68% Y_{Hmf} at 80 °C/0.5 h.³²⁵ The success of this system was mainly attributed to the acidic properties of P_2O_5 , as in its absence no Hmf was formed in 1 h.³²⁵ Sulfated zirconium ($\text{ZrO}_2/\text{SO}_4^{2-}$, 2 wt.%) coupled to several ILs ([Bmim]Cl, [Emim]Cl or [Hxmim]Cl), in the dehydration of D-fructose (5 wt.%) under MW, reached 88% Y_{Hmf} (96% C_{Fru}), 82% (88% C_{Fru}), and 89% (100% C_{Fru}), respectively, at 100 °C/0.5 h.³⁶⁴ Acidic ILs ([Emim]HSO₄ and [Bmim]HSO₄) coupled to $\text{ZrO}_2/\text{SO}_4^{2-}$ were very active (ca. 100% C_{Fru}) but less efficient (36-43% Y_{Hmf}) due to the formation of insoluble humins promoted by the strong acidity of ILs.³⁶⁴ The basic [Bmim]CH₃COO gave no Hmf (75% C_{Fru}), possibly due to the leveling-off of the acidity of $\text{ZrO}_2/\text{SO}_4^{2-}$.³⁶⁴ Nevertheless, the higher activity of $\text{ZrO}_2/\text{SO}_4^{2-}$ in [Bmim]Cl from D-fructose (compared to ZrO_2) is related to the higher number of acid sites (recycling details in Section 1.5.3).³⁶⁴

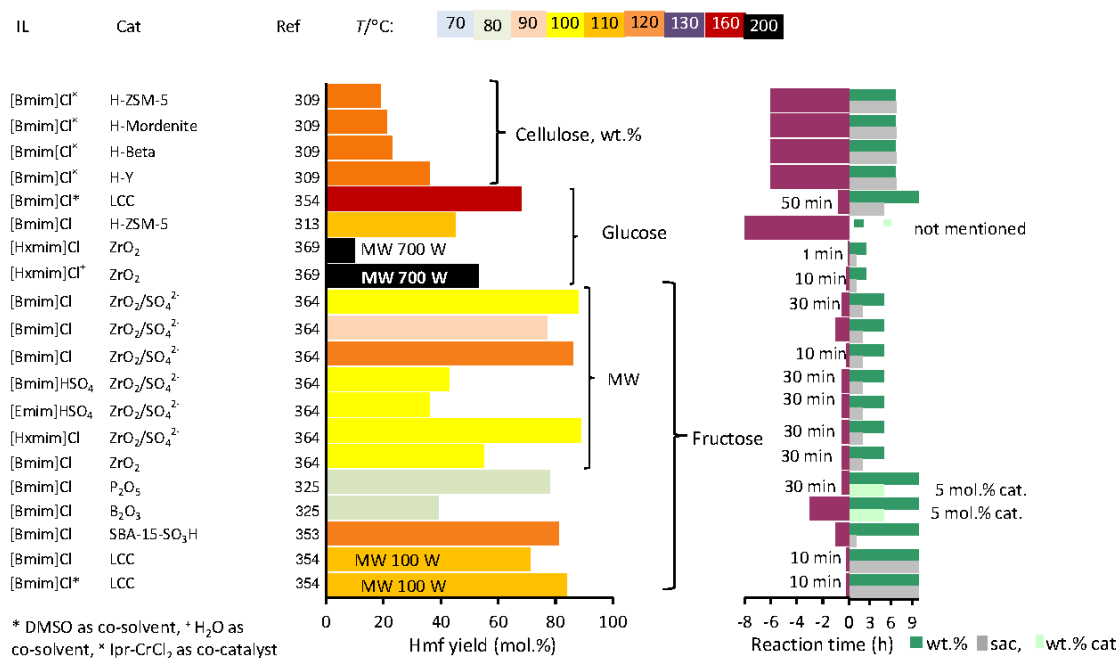


Figure 1.36- ILs as solvents coupled with inorganic solid acids (e.g microporous H-ZSM-5, H-Beta and H-Mordenite, mesoporous SBA-15-SO₃H, zirconium and other oxides) in the dehydration of hexoses to 5-hydroxymethyl-2-furaldehyde (Hmf).

Degimenci et al.⁴⁸² immobilised a thin IL layer (1-triethoxysilyl)-propyl-3-methylimidazolium chloride, TES-[Pmim]Cl, on a mesoporous silica (SBA-15) to create a local reaction microenvironment on the solid support, through the silanol groups of the IL on the surface of SBA-15.⁴⁸² Afterwards the subsequent introduction of CrCl₂ led to the formation of weakly bound active species (Cr²⁺) with a high mobility (CrCl₂-Im-SBA-15), which was beneficial for the selective conversion of D-glucose (10 wt.%) to Hmf: the system (H₂O/CrCl₂/[Pmim]Cl) gave no Hmf whereas in the system (H₂O/CrCl₂-Im-SBA-15), 23% Y_{Hmf} (50% C_{Glu}) was obtained at 150 °C/3 h.⁴⁸² The immobilised IL stabilises the active mobile [CrCl₄]²⁻ complexes and avoids excessive interactions with water which may favour non-selective routes of sugar conversion and catalyst deactivation pathways.⁴⁸² The addition of DMSO/2-BuOH/IBMK to CrCl₂-Im-SBA-15, suppressed the production of insoluble humins and led to 35% Y_{Hmf} (50% C_{Glu}).⁴⁸²

Protonic forms of crystalline microporous zeolites of the type Faujasite Y, Beta, and ZSM-5, have been investigated in the hydrolysis of cellulose, using [Bmim]Cl as solvent (10 wt.% zeolite; 5 wt.% cellulose; MW, 240 W), giving more than 30% yield of D-glucose in less than 10 min.⁴⁷⁴ Tan et al.³⁰⁹ tested the system [Bmim]Cl/H-Y/CrCl₂ for the reaction of cellulose (6.7 wt.%, 6.7 wt.% zeolite, < 1 wt.% CrCl₂) and obtained 36 wt.% Y_{Hmf} at 120 °C/6 h.³⁰⁹ Other zeolites (H-Beta, H-Mordenite and H-ZSM-5) gave lower 19-23 wt.% Y_{Hmf} (Figure 1.36).³⁰⁹ The assessment of the homo/heterogeneous catalytic nature of the insoluble solid acid/IL system is a critical issue, which will be discussed in Section 1.5.3. (“Recycling of IL-based catalytic systems”).

1.5.2. ILs as acid solvents/catalysts (dual function)

ILs may possess intrinsic acid properties associated with the constituent anions (amphoteric HSO₄⁻) and/or the cations (e.g. [Asbi]⁺, [Ascbi]⁺, [Hmim]⁺, [Sbmim]⁺, [Spmim]⁺),⁴⁸³ and may play a role as acid catalysts and solvents, where a synergy could be expected from the coupling of the acid and saccharide solubilisation properties of the ILs. Acidic ILs have also been used as catalysts with different solvents. The results shown in Figure 1.37 have been reported for acidic ILs used in the dehydration of D-fructose. 70-92% Y_{Hmf} were obtained under quite moderate reaction conditions, for the dehydration of D-fructose (10-35 wt.%) at 80-90 °C, in about 30 min to 1 h, using the ILs, [Hmim]Cl or [Sbmim]HSO₄, without adding any other solvent (Figure 1.37).^{202,342,463} Hu et al.²⁰² under similar reaction conditions, reported [Hpy]Cl was similarly

effective in the reaction of D-fructose (31 wt.%) giving 70% Y_{Hmf} (97% C_{Fru}) at 80 °C/1 h. In contrast, $[\text{EH}_3\text{N}]\text{NO}_3$, $[\text{TMG}]\text{CF}_3\text{CO}_2$, $[\text{TMG}]\text{Lac}$ (Lac=lactate) and $[\text{Hpy}]\text{ToISO}_3$ (ToISO₃=p-toluenesulfonate) gave $Y_{\text{Hmf}} < 8\%$ (14-34 wt.% D-fructose).⁴⁴⁶ Moreau et al.³⁴² were pioneering in assessing the recyclability of the dual function $[\text{Hmim}]\text{Cl}$ (detailed in Section 1.5.3).³⁴² The use of $[\text{Bmim}]\text{HSO}_4$ as catalyst instead of H_2SO_4 , and $[\text{Bmim}]\text{Cl}$ as solvent, gave 80% Y_{Hmf} at 80 °C/30 min; (7.7 mol.% acid, 10 wt.% D-fructose; Figure 1.37).⁴⁶³ Adding an immiscible co-solvent to the acidic IL reaction medium allows the in situ extraction of Hmf as it is formed, which promotes the reaction of D-fructose to Hmf and avoids decomposition of the latter through its reactions with intermediate products in the acidic IL phase. On the other hand, as mentioned before, the addition of an appropriate organic solvent may allow the viscosity of the reaction solution to be decreased (minimising mass transfer limitations).^{343,449,450}

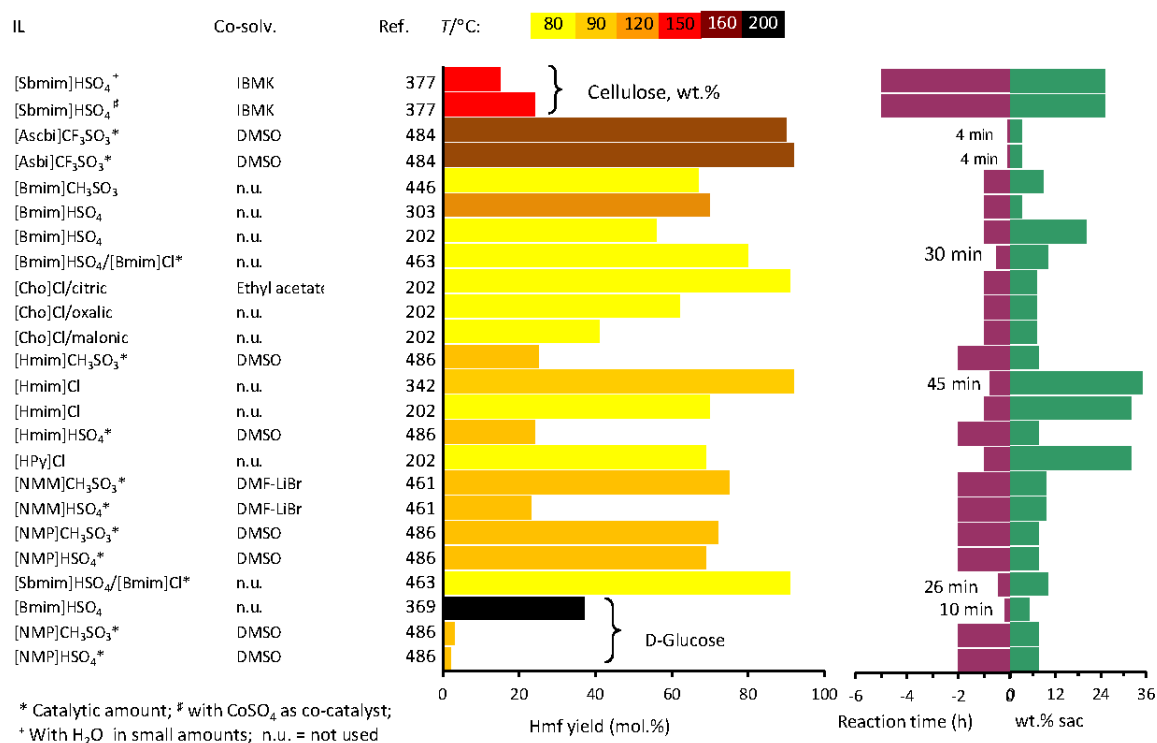


Figure 1.37- Acidic ILs used in the dehydration of hexoses (D-fructose unless otherwise indicated) to 5-hydroxymethyl-2-furaldehyde (Hmf).

It was reported that the Lewis acidic $[\text{Ascbi}]\text{CF}_3\text{SO}_3$ acts more effectively (in terms of Hmf yield) than its Brønsted acidic counterpart $[\text{Asbi}]\text{CF}_3\text{SO}_3$ for the dehydration of D-fructose (78% and 62% Y_{Hmf} , respectively, under MW, 200 W, with DMSO as co-solvent and at 80 °C/4 min).

However, in the presence of water (formed in the dehydration reaction) the hydrolysis of [Ascbi]CF₃SO₃ into [Asbi]CF₃SO₃ takes place.⁴⁸⁴ Nevertheless, the Brønsted IL was quite effective when the temperature was raised from 80 to 160 °C (Y_{Hmf} increased from 60 to 92%). Similar results (83% Y_{Hmf} at 100 °C/2 min) were reported for the Brønsted-Lewis catalyst [Hmim]SO₃Cl under similar conditions (MW, 200 W, DMSO), giving better results than Brønsted [Hmim]HSO₄ IL (71% Y_{Hmf}).⁴⁸⁵

The nature of the cation may influence the Hmf yield. For protic ILs considerably higher Hmf yields were reported for [NMP]HSO₄ (69% Y_{Hmf} at 99% C_{Fru}) and [NMP]CH₃SO₃ (72% Y_{Hmf} at 83% C_{Fru}) at 90 °C/2 h, than for [Hmim]HSO₄ (24% Y_{Hmf} at 46% C_{Fru}) or [Hmim]CH₃SO₃ (25% Y_{Hmf} at 40% C_{Fru}) used in catalytic amounts (7.5 mol.%) and with DMSO as solvent (ca. 7.5 wt.% D-fructose).⁴⁸⁶ These results correlated with the higher acidity of the [NMP]⁺-containing ILs. For these ILs, the effects of the anions HSO₄⁻ or CH₃SO₃⁻ (for each cation [NMP]⁺ or [Hmim]⁺) seemed less pronounced than those of the cations (for each anion).⁴⁸⁶

An interesting “green” approach consisted of using eutectic mixtures containing [Cho]Cl and an organic acid (citric, malonic, and oxalic acids).^{202,306,311} [Cho]Cl/citric acid (30-35 mol.% citric acid in [Cho]Cl) gave ca. 91% Y_{Hmf} (98% C_{Fru}) at 80 °C/1 h from D-fructose (7 wt.%) using ethyl acetate as co-solvent for in situ extraction of Hmf.²⁰² Ethyl acetate favours the reaction because it dissolves Hmf but not D-fructose and is only slightly soluble in [Cho]Cl/citric acid.²⁰² The recycling of [Cho]Cl/citric acid is discussed in detail in Section 1.5.3 and Table 1.9.²⁰² [Cho]Cl/citric acid and [Cho]Cl/oxalic acid were both effective in the one-pot conversion of inulin (6-10 wt.%), giving 40 and 44 wt.% Y_{Hmf} (91% and 100 mol.% of conversion), respectively, at 80 °C/2 h (Table 1.8).³¹⁶ When adding ethyl acetate as co-solvent to [Cho]Cl/oxalic acid, 50 wt.% Y_{Hmf} (100 mol.% of conversion) is obtained at 80 °C/ 2h.³¹⁶ Furthermore the system [Cho]Cl/oxalic acid was recycled with success as explained in Section 1.5.3.^{202,316} In a different approach, [Cho]Cl has been used as additive for preparing low melting carbohydrate mixtures with p-TsOH as catalyst (10 mol.%). 67% Y_{Hmf} at 100 °C/30 min from D-fructose, 25 mol.% Y_{Hmf} from D-sucrose at 100 °C/1 h and 57 mol.% Y_{Hmf} from inulin at 90 °C/1 h were obtained.³¹⁰

Acidic IL-based systems are generally less effective for Hmf production from D-glucose and related di/polysaccharides than from D-fructose and related ones (Figure 1.37). Tong et al.⁴⁸⁶ tested the protic ILs [NMP]HSO₄ and [NMM]CH₃SO₃ and DMSO as solvent under the same experimental conditions as those used for D-fructose, which gave very poor results (2-3 Y_{Hmf} at 90 °C/2 h).⁴⁸⁶ The Brønsted acidic ILs [Hmim]HSO₄ or [Bmim]HSO₄ coupled with CrCl₃ and using

MW (20 mol.% catalyst, 5 wt.% D-glucose) gave poor results: $Y_{\text{Hmf}} < 10\%$ at 120 °C/min. These results were worse than those obtained with the system [Emim]Cl/CrCl₃.³³⁶

For the reaction of D-sucrose (25 wt.%) in [Hmim]Cl, Hmf was selectively formed from the fructofuranosyl units (ca. 100%); glucopyranosyl units gave essentially D-glucose at 90 °C/30 min (Table 1.8);³⁴² recycling was not achieved with success (Section 1.5.3).³⁴²

The acidic IL [Sbmim]HSO₄ was poorly efficient in converting cellulose into Hmf.³⁷⁶ The poor results reported for the acidic ILs in the conversion of cellulose into Hmf may be related to the poor selectivity of the conversion of monosaccharides into Hmf, since the hydrolysis step has been effectively carried out using different acidic ILs (such as e.g. [Sbmim]HSO₄, [Bmim]HSO₄/[Bmim]Cl, [Sbmim]Cl, [Spimim]Cl).^{300,376,487,488} The addition of an aqueous solution of Lewis acid FeCl₂ (5 wt.%) to the acidic IL system [Sbmim]HSO₄/IBMK, in the hydrolysis of microcrystalline cellulose (ca. 6 wt.%), was found to enhance the Y_{Hmf} and Y_{Fur} at 150 °C/5 h from 15 wt.% and 7 wt.% (70 wt.% of conversion), respectively (without FeCl₂) to 34 wt.% and 19 wt.% (84 wt.% of conversion) with FeCl₂.³⁷⁶ Recycling details are described in Section 1.5.3. A similar activity was observed when catalytic amounts of CoSO₄ were coupled to the IL [Sbmim]HSO₄ with IBMK as co-solvent in the conversion of cellulose (24 wt.% Y_{Hmf} and 17 wt.% Y_{Fur} for 84 wt.% of conversion) at 150 °C/300 min.³⁷⁷ In the absence of CoSO₄, the Y_{Hmf} and Y_{Fur} decreased to 15 wt.% and 8 wt.% (70% of conversion), respectively.³⁷⁷ Kim et al.⁴⁸⁹ tested various bisulfate ILs [Bmim]HSO₄, [Hmim]HSO₄, [Morph]HSO₄, [B₄N]HSO₄, [B₄P]HSO₄, [Cho]HSO₄ in the conversion of agar using a catalytic amount of ILs in aqueous solutions at 121 °C/15 min, in which the highest Hmf yield was reported for [B₄N]HSO₄ (2 wt.% Y_{Hmf}).⁴⁸⁹

In order to obtain Fur, acidic ILs were employed using [Sbmim]HSO₄ as catalyst (50 wt.%) and D-xylose in a mixture of H₂O/IBMK.²⁷⁵ An outstanding result of 91 wt% Y_{Fur} (95% C_{Xyl}) was obtained at 150 °C/25 min, comparing favourably to Lewis acids (AlCl₃, SnCl₂, 72-78 wt.% Y_{Fur}), mineral acids (HCl or H₂SO₄, 70-72 wt.% Y_{Fur}) or HPA H₃PW₁₂O₄₀ (48 wt.% Y_{Fur}). The acidic IL [Bmim]HPO₄ was also tested but was less effective under the same conditions (68 wt.% Y_{Fur} at 80% C_{Xyl}). Recycling tests are detailed in the next Section (1.5.3).²⁷⁵

1.5.3. Recycling of IL-based catalytic systems

Several types of homogeneous IL-based catalytic systems have been reused in consecutive runs without observing a decrease in Fur/Hmf yields (Table 1.9), such as solid acid catalysts soluble in the IL (BHC/[Cho]Cl/H₂O, seven runs),³⁵⁶ mineral acids coupled to ILs (HCl/[Bmim]Cl, six runs),⁴³² metal chlorides (CrCl₃/[Bmim]Cl, six runs),³³⁶ (Ipr-CrCl₂/[Bmim]Cl, four runs),^{330,468} (GeCl₄/[Bmim]Cl, five runs),³⁷³ (SnCl₄/[Emim]BF₄, four runs),³⁷⁴ (IrCl₃/[Omim]Cl, five runs),³³⁹ (CrCl₃.6H₂O/[E₄N]Cl, five runs),³⁰⁵ [(CrCl₃+LiCl)/[Bmim]Cl, three runs],³³⁵ (CuCl₂/CrCl₂/[Emim]Cl; twelve runs).³²⁹ Insoluble (solid acid)/IL catalytic systems have been less explored and can be recycled without the need for separating the solid acid from the IL,³⁰⁶ similar to that performed for soluble acid/IL systems. Insoluble solid acids coupled to ILs commonly include ion-exchange resins, such as Amberlyst-15/[Bmim]Cl (seven runs).³⁰⁶ Although insoluble resins/IL catalytic systems are recycled as mixtures, an interesting recycling process for the regeneration of ILs was reported using an ion-exchange resin for converting [Bmim]HSO₄ into [Bmim]Cl. The regeneration of the used ion-exchange resin (into the Cl⁻ form) with NaCl gave NaHSO₄ as product, which, in turn, could be used in the conversion of [Bmim]Cl to [Bmim]HSO₄, giving NaCl as co-product (used for regenerating the used ion-exchange resin).³⁴⁴ Other inorganic oxides include ZrO₂/SO₄²⁻/[Bmim]Cl (six runs),³⁶⁴ and hydroxyapatite supported chromium chloride coupled to [Bmim]Cl (five runs).⁴⁷² Hybrid materials (organic-inorganic) coupled to IL have been recently tested achieving interesting results (SBA-15-SO₃H/[Bmim]Cl, three times).³⁵³ Attempting to facilitate the separation of Hmf from the IL and recycling, silica gel-supported ionic liquids (ILIs), (ILIS-SO₃H and ILIS-SO₂Cl, seven runs) gave good results.⁴⁸⁴ In contrast, the analogous sulfuric acid (SiO₂-SO₃H) and sulfonylchloride (SiO₂-SO₂Cl) modified silica gels exhibited a drastic decrease of Hmf yield in only three runs (the authors did not explain the catalyst deactivation phenomena, Table 1.9).⁴⁸⁴ Bifunctional ILs (acidic ILs that work as solvents and catalysts) are yet another class of IL-based catalytic systems that can be reused without significant drops in the Fur/Hmf yields (e.g. [Hmim]Cl, five runs),³⁴² ([NMP]CH₃SO₃/DMSO, five runs),⁴⁸⁶ and acidic ionic liquid coupled to soluble inorganic solids (FeCl₂/[Sbmim]HSO₄/IBMK, five runs),³⁷⁶ or with a co-solvent ([Sbmim]HSO₄/IBMK, five runs).²⁷⁵ Other types of ILs include ([Cho]Cl/citric acid/ethyl acetate), eight runs),²⁰² and ([Cho]Cl/oxalic acid/ethyl acetate, six runs).³¹⁶

The first step of the recycling procedures commonly involves the solvent extraction of the target products Fur/Hmf, using organic solvents, which are poorly miscible with the IL medium (Table 1.9). Extracting solvents include ethyl acetate,^{202,275,305,306,316,335,336,364,373,374,486} IBMK,^{329,356} THF,^{353,432} diethyl ether,^{330,342,376,468} and toluene (Table 1.9). The addition of ethyl acetate is favourable for enhancing the Hmf yield, avoiding both thermal decomposition and polymerisation reactions between Hmf.³⁰⁶ Besides presenting a low boiling point, ethyl acetate can reduce the energy costs and allow the IL to be easily reused because the IL and substrate are not soluble in ethyl acetate (Table 1.9). These solvents can as well extract small amounts of water from the IL/catalyst phase when used as co-solvents, working as in situ Fur/Hmf extraction.⁴³² For example, for the system [NMP]CH₃SO₃/DMSO, DMSO was separated from the IL phase by distillation under reduced pressure and pure Hmf was further obtained after drying with anhydrous sodium sulfate.⁴⁸⁶ However the use of high-boiling point miscible co-solvents, such as DMSO (miscible with a wide range of polar and non-polar solvents), may require energy intensive and laborious separation processes to recover Hmf (b.p. 114-116 °C at 1x10² Pa) from the reaction medium. In this sense, low boiling co-solvents, such as acetonitrile (which gave interesting results, as discussed above in Section 1.5.2¹⁹⁸), or mixing different ILs,^{344,463} might be preferable.

In the system BHC/[Cho]Cl/H₂O, the Hmf (and other products) were extracted from the BHC/IL (D-fructose) phase, by decantation with IBMK.³⁵⁶ A pair of metal chlorides in the IL (CuCl₂/CrCl₂/[Emim]Cl (cellulose)) was separated from the target product by IBMK.³²⁹ In other systems, Fur or Hmf (and other products) were extracted and separated from SBA-15-SO₃H/[Bmim]Cl (D-fructose) using THF followed by an evaporation step,³⁵³ or simple extraction from HCl/[Bmim]Cl (fructose),⁴³² by THF from CrCl₃/[Bmim]Cl (D-glucose),³³⁶ GeCl₄/[Bmim]Cl (D-fructose),³⁷³ SnCl₄/[Emim]BF₄ (D-glucose),³⁷⁴ [Cho]Cl/citric acid (D-fructose),²⁰² [Cho]Cl/oxalic acid (inulin),³¹⁶ [Sbmim]HSO₄/IBMK (D-xylose),²⁷⁵ by ethyl acetate, or from Ipr-CrCl₂/[Bmim]Cl (D-fructose and D-glucose),^{330,468} and acidic [Hmim]Cl (D-fructose and D-sucrose) by diethyl ether.³⁴² Some authors added water to the IL-based catalytic system after the reaction to decrease the IL viscosity (accompanied by accumulation of by-products), before the extraction: CrCl₃.6H₂O/[E₄N]Cl (D-glucose) by ethyl acetate,³⁰⁵ (CrCl₃+LiCl)/[Bmim]Cl (cellulose and wheat straw),³³⁵ Amberlyst-15/[Bmim]Cl (D-fructose),³⁰⁶ ZrO₂/SO₄²⁻/[Bmim]Cl (D-fructose),³⁶⁴ and FeCl₂/[Sbmim]HSO₄/IBMK (cellulose) by diethyl ether, in which water and IBMK were added afterwards.³⁷⁶ The latter system was used with success in five consecutive runs but decreases in the values of the yields of Hmf and Fur were observed from the first to the second run, which were attributed to the incomplete extraction of by-products from the IL prior to recycling (Table

1.9).³⁷⁶ In the system [NMP]CH₃SO₃/DMSO (D-fructose), the biggest part of Hmf was extracted from the DMSO phase and the remaining IL phase was further extracted with ethyl acetate after water addition.⁴⁸⁶ Recently Wei et al.³³⁹ developed an interesting vacuum distillation process for continuous extraction of Hmf from the IrCl₃/[Omim]Cl phase (D-fructose, D-glucose). The Hmf yield in the recycled system was sometimes higher than the one with the fresh catalyst, which was attributed to small amounts of D-fructose from the previous cycle.^{305,306,330,364,468} Prior to the next run, the catalyst/IL was pre-heated to water and residual solvent removal at 50 °C;⁴³² at 50 °C for 24 h,²⁰² 60 °C for 24 h,^{275,306,336} 65 °C for 24 h³⁰⁵ or 75 °C for 12 h⁴⁸⁶ in a vacuum oven; at 65 °C in a vacuum drier,³³⁵ and at 100 °C for 2 h.^{329,330,468} It is essential to dry the IL, or otherwise the Hmf yields decrease in consecutive batch runs.³²⁹

Many authors reported that no fresh catalyst is required in a new run.^{202,305,306,316,329,330,335,336,339,353,356,364,373,374,376,432,468} A comparison with a recycling test with/without addition of fresh catalyst was similar, meaning the homogeneous catalyst was well retained in the IL.³²⁹ By pH measurements Lai et al.⁴³² also proved that the catalyst was fully retained in the IL. Heterogeneous SBA-15-SO₃H catalyst was reported to be stable, low cost, low toxic, being quite promising for this reaction.^{305,353}

The gradual accumulation of water and other by-products in the recycled IL medium may eventually lead to a decay in the overall efficiency of these catalytic processes and therefore require the purification of the IL medium at a certain stage (Table 1.9).^{202,342,432} The accumulation of water has a negative effect on the catalytic reaction in consecutive batch runs because the IL may form a hydrogen bonded complex with water, possible leveling off the acidity of the IL.^{450,460} Unavoidable accumulation of humins was noticed with an increasing number of recycling runs.^{336,339,356} Non-volatile by-products, including humins, may be precipitated from the IL medium by adding a miscible solvent to the IL with appropriate polarity (e.g. ethanol), being further removed by filtration^{316,339} (Table 1.9). The removal of dark solid known as humins by filtration might increase the lifetime of the catalytic system.³²⁹

The effectiveness of IL-based catalytic systems is also dependent on the substrate used. Yong et al.^{330,468} recycled system was efficient for D-fructose but not for D-glucose in which the Hmf yield decreased gradually with further runs.^{330,468} The different catalytic results in recycling runs for the two hexoses may be due to the high concentration of by-products retained in the IL-based catalytic system in the case of D-glucose (less selective reaction) than that of D-fructose, causing inhibitory effects.^{330,468} Moreau et al.³⁴² also reported a less efficient separation of Hmf from the IL when using D-sucrose as the substrate; according to the authors D-glucose does not

significantly react with the IL and accumulates in the IL medium (being more difficult to extract from less polar solvents such as diethyl ether).³⁴² In the case of insoluble solid acid/IL catalytic systems, the removal of insoluble humins from the IL medium may require the separation of the solid acid from the IL medium. With $\text{ZrO}_2/\text{SO}_4^{2-}$ as catalyst, the decrease in the catalytic activity after the 10th run was attributed to a decrease of acid sites in the catalyst (catalyst surface passivation) by accumulated by-products and a decrease in the contents of SO_4^{2-} in the catalyst (leaching).³⁶⁴ Subsequently, the removal of organic matter from the used solid acid may be performed by thermal degradation or by chemical attack using oxidising agents. The solid acid may need to be regenerated to recover its initial acid properties (e.g. through ion-exchange).⁴⁹⁰

In general, the number of recycling runs reported in the literature is less than ten. Performing more runs and elemental analysis of the recovered IL medium can help to better assess the recycling efficiency of the different approaches of the IL-based catalytic systems. Certain homogeneous acid/IL catalytic systems suffer loss of catalysts during the work-up procedures, possibly due to catalyst deactivation in the IL and/or the inhibitor effect of water (when no drying processes are mentioned). Such cases were observed in the system $\text{Ipr-WCl}_6/[\text{Bmim}]\text{Cl}$ in which the separation of accumulated by-products from the IL phase (by filtration) and the addition of fresh catalyst was required to maintain the high Hmf yield, being poorly attractive with respect to the catalyst recycling.³²⁸ In $\text{IrCl}_3/[\text{Bmim}]\text{Cl}$, the loss of IrCl_3 from the IL medium during the solvent extraction process led to a decrease in product yield in recycling runs (Table 1.9).³²⁴ Degirmenci et al.⁴⁸² developed a promising catalytic system by coordinating CrCl_2 to $[\text{Pmim}]\text{Cl}$, avoiding catalytic species from excessive interaction with the solvent. However, chromium leaching in recycling runs for the system $\text{CrCl}_2/[\text{Pmim}]\text{Cl}/\text{SBA-15}$ led to a drop in catalytic activity.

Table 1.9- Summary of the recycling procedures and efficiency of IL based catalytic systems. ^a

Substrate/IL/Catalyst added/Co-solvent	Separation of the target reaction product	Separation of by-products from the IL system	No. Runs ^b	Variation of Y_{Hmf} or Y_{Fur} ^c	Ref
Homogeneous Brönsted catalyst + IL					
D-Fructose/[Bmim]Cl/HCl	Solvent extraction using THF	Heating under vacuum (50 °C) for water removal after run 3	6	≈ (Hmf)	432
Homogeneous Lewis catalyst + IL					
D-Fructose/[Bmim]Cl/WCl ₆ /THF	Solvent extraction using THF (Continuous or batch operation modes)	Heating under vacuum	5	≈ (Hmf)	455
D-Fructose/[Bmim]Cl/ WCl ₆ /THF	Solvent extraction using THF (Semi-batch operation mode)	IL mixture was filtered after run 5 to remove insoluble by-products	8	↓ (Hmf) after run 5 unless by-products were removed and fresh catalyst WCl ₆ added to the IL mixture	328
D-Fructose/[Bmim]Cl/IrCl ₃	Solvent extraction using ethyl acetate after addition of water	Heating under vacuum (80 °C, 30-60 min) for water and ethyl acetate removal	5	≈ Hmf (run1-run2), ↓ run 2 to run 5 (loss of IrCl ₃ in work-up procedures)	324
D-Fructose/[Bmim]Cl/GeCl ₄	Solvent extraction using ethyl acetate		5	≈ (Hmf)	373
D-Fructose/[Cho]Cl/BHC/H ₂ O/IBMK	Open vessel mode for continuous water removal	Water and IBMK separation by decantation	7	≈ (Hmf). After run7 ↓(Hmf) due to accumulation of humins	356
D-Fructose/[E ₄ N]Cl/NaHSO ₄ ·H ₂ O	Solvent extraction using THF	Hmf is separated from THF by evaporation	14	↑ (run1-run4) system remained active, ↓ (run 4-run8) loss of catalyst in the extraction or accumulation of by-products, ↑ (run8-run9) addition of NHSO ₄ ·2H ₂ O, ↓ (run9-run10) without adding NHSO ₄ ·2H ₂ O, loss of catalytic activity, ↑ (run 11-run 14) addition of catalyst in each run	323
D-Fructose, D-Glucose/[Bmim]Cl/ Ipr/ CrCl ₂	Solvent extraction using diethyl ether	Pre-heating (100 °C/2 h) for water and diethyl ether removal	4	For D-fructose: ≈ (Hmf) For D-glucose: ↓ (Hmf)	330,468
D-Fructose, D-Glucose/[Omim]Cl/IrCl ₃			5	≈ (Hmf) for D-fructose and D-glucose	339

Table 1.9- <i>Continued.</i>					
D-Glucose/[Emim]BF₄/SnCl₄	Solvent extraction using ethyl acetate		4	≈ (Hmf)	374
D-Glucose/[Bmim]Cl/CrCl₃	Solvent extraction using ethyl acetate	Heating under vacuum (60 °C, 24 h) for water and AcOEt removal	6	≈ (Hmf) until run 5, ↓ run 5 to run 6	336
D-Glucose/[E₄N]Cl/CrCl₃.6H₂O	Solvent extraction using ethyl acetate after addition of water (to decrease the viscosity)	Heating under vacuum oven (65 °C, 24 h) for water and residual AcOEt removal	5	≈ (Hmf)	305
Cellulose/[Sbmim]HSO₄/FeCl₂/IBMK	Solvent extraction using diethyl ether and water	Removal of the solvent, diethyl ether and water (Incomplete extraction of by-products from the IL)	5	↓ (Hmf, Fur)	376
Cellulose/[Emim]Cl/CrCl₂/CuCl₂	Solvent extraction using IBMK	Water removal	3	≈ (Hmf)	329
Cellulose, Wheat Straw/[Bmim]Cl/CrCl₃/LiCl	Water was added to decrease the viscosity of IL; Solvent extraction using ethyl acetate	Heating under vacuum (65 °C) for water removal	3	≈(Hmf)	335
Insoluble solid acid + IL					
D-Fructose/[Bmim]Cl/LCC/DMSO	Solvent extraction using ethyl acetate	LCC was filtered, ashed and dried in air for Hmf removal	5	≈ (Hmf)	354
D-Fructose/[Bmim]Cl/ZrO₂/SO₄²⁻	Solvent extraction with ethyl acetate after addition of water		10	≈ (Hmf) until run 6, ↓ run 6 to run10	364
D-Fructose/[Bmim]Cl/SBA-15-SO₃H	Solvent extraction using THF		3	≈ (Hmf)	353
D-Fructose/[Bmim]Cl/Amberlyst-15	Solvent extraction using ethyl acetate after addition of water	Heating under vacuum (60 °C, 24 h) for water and ethyl acetate removal. Recycling of (Amberlyst+IL) mixture	7	≈ (Hmf)	306
D-Fructose/[Bmim]Cl/Amberlyst-15			10	≈ (Hmf)	304
D-Glucose/Cr-HAP/[Bmim]Cl			5	≈ (Hmf)	472
Acidic IL					
D-Xylose/[Sbmim]HSO₄/H₂O/IBMK	Solvent extraction using ethyl acetate	Heating under vacuum (60 °C, 24 h) for water and ethyl acetate removal	5	≈ (Fur)	275

D-Fructose/[Hmim]Cl	Solvent extraction using diethyl ether	Water removal	5	≈ (Hmf)	342
D-Fructose/[Cho]Cl/citric acid/AcOEt	Intermittent solvent extraction using ethyl acetate	Heating under vacuum (50 °C, 24 h) for water removal after run 6	8	Y _{Hmf} reached the level of that in the first run after water removal	202
D-Fructose/[Cho]Cl/citric acid/AcOEt	Continuous extraction with ethyl acetate	Heating under vacuum (50 °C, 24 h) for water removal after run 4	8	Y _{Hmf} reached the level of that in the first run after water removal	202
D-Fructose/[Asbi]CF₃SO₃/DMSO			7	≈ (Hmf)	484
D-Fructose/[Acsbi]CF₃SO₃/DMSO			7	≈ (Hmf)	484
D-Fructose/[NMP]CH₃SO₃/DMSO	Distillation under reduced pressure (to separate DMSO); Solvent extraction using ethyl acetate	Heating under vacuum (75 °C, 12 h) for water and ethyl acetate removal	5	≈ (Hmf)	486
D-Glucose/[Hxmim]Cl/H₂O/ZrO₂	Solvent extraction using ethyl acetate		5	≈ (Hmf)	369
Inulin/[Cho]Cl/oxalic acid/AcOEt	Solvent extraction using ethyl acetate	Distillation of volatiles. Extraction of non-volatile sugar derivatives using ethanol as solvent	6	≈ (Hmf)	316
Cellulose/[Sbmim]HSO₄/IBMK	Solvent extraction using ethyl acetate and water	Water and IBMK removal	5	↓ Hmf run 1 to run 2 (non complete extraction of small by-products) ≈ Hmf (run 2 to run 5)	377

a) If a procedure was not adopted or nothing was mentioned, the cell is empty. Batch operation mode, unless specified otherwise. b) Number of catalytic runs. c) Product yield (Fur or Hmf as indicated in parenthesis) in recycling runs increases (↑), decreases (↓) or is reasonably steady (≈).

For insoluble solid acid/IL catalytic systems, an important issue is whether the catalytic reaction is heterogeneous or homogeneous in nature. This point is seldom addressed in the published literature related to solid acid/IL catalytic systems used in the conversion of carbohydrates into Hmf/Fur. The stability of the inorganic solid acid catalysts, in ILs is rather unexplored.⁴⁹¹ Interesting results were reported for the system Cr-HAP/[Bmim]Cl, which was used in five consecutive batch runs of the reaction of D-glucose without drop of Hmf yield (Table 1.9).⁴⁷² In that study, the assessment of the homo/heterogeneous nature of the catalytic reaction was not addressed. Ion-exchange reactions between acid-form zeolites and ILs can take place giving homogeneous (soluble) active acid species.⁴⁹²⁻⁴⁹⁴ The same can apply for ion-exchange resins.^{477-479,490,495-497} Nevertheless, using Brønsted solid acids (possessing an insoluble anionic polymeric framework) instead of homogeneous acids may be advantageous in that the formation of by-products in reactions involving the free anions is avoided (e.g. sulfur containing by-products, in the case of H₂SO₄ as catalyst, causing downstream contaminations and affecting the yields of Fur/Hmf and, on the other hand, the regeneration of the acid properties of the catalytic system can be more efficient than that for soluble acid catalysts.⁴⁹⁰

This work focuses on the conversion of saccharides into Fur and/or Hmf using heterogeneous catalysts in an aqueous medium (Chapters 3-7) or using an ionic liquid medium (Chapters 8, 9). The production of Hmf has not reached the industrial scale; the same does not apply for Fur. As mentioned previously, sulfuric acid is used in most of these industrial processes and presents several drawbacks, which can be avoided with the use of heterogeneous catalysts. The objectives of this work included: (i) use of heterogeneous catalysts with promising catalytic performances in terms of activity, selectivity and stability, leading to high Fur/Hmf yields; (ii) identification of the reaction (by)products in order to get mechanistic insights into the overall reaction mechanism; (iii) understanding of catalyst deactivation phenomena; (iv) efficient regeneration and reuse of the catalysts. The catalytic performance of crystalline microporous silicoaluminophosphates (SAPOs) with different pore sizes (Chapter 3), zeolite Beta and a composite material consisting of zeolite Beta nanocrystals (Si/Al=12) embedded in a purely siliceous TUD-1 mesoporous matrix (BEATUD-1, Chapter 5) were investigated in the dehydration of D-xylose to Fur. The zeolite MCM-22, delaminated ITQ-2 (Chapter 6) and mixed zirconium oxides (Chapter 7) were also tested. Aluminium-containing mesoporous TUD-1 (denoted Al-TUD-1, Si/Al=21) was tested as a heterogeneous catalyst in the conversion of different types of saccharides to Fur/Hmf (Chapter 4).

The use of ionic liquid (IL) based catalytic systems aimed at obtaining high Fur/Hmf yields using relatively high initial concentrations of carbohydrates and mild reaction conditions. The acid ionic liquid [Emim]HSO₄ (with solvent-catalyst dual function) was tested in the conversion of mono/di/polysaccharides into Fur/Hmf (Chapter 8). The dehydration of (demanding) D-glucose into Hmf was investigated using [Bmim]Cl as solvent and (chromium, aluminium)-containing silicates (Chapter 9). Special attention was given to the recovery and reuse of the IL-based catalytic systems.

1.6. References

- (1) Klass, D. L.: Energy Consumption, Reserves, Depletion, and Environmental Issues. In *Biomass for Renewable Energy, Fuel and Chemicals*; Academic Press: London, U.K., 1998; pp 1-28.
- (2) Knill, C. J.; Kennedy, J. F.: Cellulosic Biomass Derived Products. In *Polysaccharides: Structural diversity and functional versatility*; Dumitriu, S., Ed.; Marcel Dekker: New York, USA, 2005; pp 937-956.
- (3) Srivastava, R. D.; McIlvried, H. G.; Winslow, J. C.; Maronde, C. P.; Noceti, R. P.: Coal Technology for Power, Liquid Fuels and Chemicals. In *Kent and Riegel's Handbook of Industrial Chemistry and Biotechnology*; 11 th ed.; Kent, J. A., Ed.; Springer: New York, USA, 2007; Vol. 2; pp 843-906.
- (4) Lima, S.; Antunes, M. M.; Pillinger, M.; Valente, A. A.: Ionic Liquids as Tools for the Acid-Catalyzed Hydrolysis/Dehydration of Saccharides to Furanic Aldehydes. *ChemCatChem* **2011**, *3*, 1686-1706.
- (5) Persin, Z.; Kleinschek, K. S.; Foster, T. J.; Dam, J. E. G. V.; Boeriu, C. G.; Navard, P.: Challenges and Opportunities in Polysaccharides Research and Technology: The EPNOE Views for the Next Decade in the Areas of Materials, Food and Health Care. *Carbohydr. Polym.* **2011**, *84*, 22-32.
- (6) Shen, L.; Patel, M. K.: LCA Single Score Analysis of Man Made Cellulose Fibres. *Lenzinger Berichte* **2010**, *88*, 60-66.
- (7) Vlachos, D. G.; Caratzoulas, S.: The Roles of Catalysis and Reaction Engineering in Overcoming the Energy and the Environment Crisis. *Chemical Engineering Science* **2010**, *65*, 18-29.
- (8) Jong, W. D.; Marcotullio, G.: Overview of Biorefineries Based on Co-Production of Furfural, Existing Concepts and Novel Developments. *International Journal of Chemical Reactor Engineering* **2010**, *8*, 1-24.
- (9) Farrell, A. E.; Gopal, A. R.: Bioenergy Research Needs for Heat, Electricity, and Liquid Fuels. *Mrs Bulletin* **2008**, *33*, 373-380.
- (10) Lynd, L. R.; Wang, M. Q.: A Product Non-Specific Framework for Evaluating the Potential of Biomass Based Products to Displace Fossil Fuels. *Journal of Industrial Ecology* **2003**, *7*, 17-32.
- (11) Huber, G. W.; Iborra, S.; Corma, A.: Synthesis of Transportation Fuels from Biomass: Chemistry, Catalysts, and Engineering. *Chemical Reviews* **2006**, *106*, 4044-4098.
- (12) Mamman, A. S.; Lee, J. M.; Kim, Y. C.; Hwang, I. T.; Park, N. J.; Hwang, Y. K.; Chang, J. S.; Hwang, J. S.: Furfural: Hemicellulose/xylo-derived biochemical. *Biofuels Bioproducts & Biorefining-Biofpr* **2008**, *2*, 438-454.
- (13) Marshall, A. L.; Alaimo, P. J.: Useful Products From Complex Starting Materials: Common Chemicals From Biomass Feedstocks. *Chemistry- A European Journal* **2010**, *16*, 4970-4980.
- (14) Stephanopoulos, G.: Challenges in Engineering Microbes for Biofuels Production. *Science* **2007**, *315*, 801-804.

- (15) Lichtenthaler, F. W.; Peters, S.: Carbohydrates as Green Raw Materials for the Chemical Industry. *Comptes Rendus Chimie* **2004**, *7*, 65-90.
- (16) Zhang, Y. H. P.: Reviving the Carbohydrate Economy via Multi-Product Lignocellulose Biorefineries. *Journal of Industrial Microbiology & Biotechnology* **2008**, *35*, 367-375.
- (17) Huber, G. W.; Corma, A.: Synergies Between Bio- and Oil-Refineries for the Production of Fuels From Biomass. *Angewandte Chemie-International Edition* **2007**, *46*, 7184-7201.
- (18) Chheda, J. N.; Dumesic, J. A.: An Overview of Dehydration, Aldol-Condensation and Hydrogenation Processes for Production of Liquid Alkanes from Biomass Derived Carbohydrates. *Catalysis Today* **2007**, *123*, 59-70.
- (19) Gallezot, P.: Catalytic Conversion of Biomass: Challenges and Issues. *ChemSusChem* **2008**, *1*, 734-737.
- (20) Kazi, F. K.; Patel, A. D.; Ruiz, J. C. S.; Dumesic, J. A.; Anex, R. P.: Techno-Economic Analysis of Dimethylfuran (Dmf) and Hydroxymethylfurfural (Hmf) Production From Pure Fructose in Catalytic Processes. *Chemical Engineering Journal* **2011**, *169*, 329-338.
- (21) Alonso, D. M.; Bond, J. Q.; Dumesic, J. A.: Catalytic Conversion of Biomass to Biofuels. *Green Chemistry* **2010**, *12*, 1493-1513.
- (22) Petrus, L.; Noordermeer, M. A.: Biomass to Biofuels, a Chemical Perspective. *Green Chemistry* **2006**, *8*, 861-867.
- (23) Ragauskas, A. J.; Williams, C. K.; Davison, B. H.; Britovsek, G.; Cairney, J.; Eckert, C. A.; Frederick, W. J.; Hallett, J. P.; Leak, D. J.; Liotta, C. L.; Mielenz, J. R.; Murphy, R.; Templer, R.; Tschaplinski, T.: The Path Forward for Biofuels and Biomaterials. *Science* **2006**, *311*, 484-489.
- (24) Peterson, A. A.; Vogel, F.; Lachance, R. P.; Froling, M.; Antal, M. J.; Tester, J. W.: Thermochemical Biofuel Production in Hydrothermal Media: A review of Sub- and Supercritical Water Technologies. *Energy & Environmental Science* **2008**, *1*, 32-65.
- (25) Mamman, A. S.; Lee, J. M.; Kim, Y. C.; Hwang, I. T.; Park, N. J.; Hwang, Y. K.; Chang, J. S.; Hwang, J. S.: Furfural: Hemicellulose/Xylose Derived Biochemical. *Biofuels Bioproducts & Biorefining* **2008**, *2*, 438-454.
- (26) Campbell, C. J.; Laherrère, J. H.: The End of Cheap Oil. *Scientific American* **1998**, 78-83.
- (27) Lichtenthaler, F. W.: Carbohydrate-Based Oproduct Lines: The Key Sugars of Biomass: Availability, Present Non Food Uses and Potential Future Development Lines. In *Biorefineries Industrial Processes and Products-Status Quo and Future Directions*; Kamm, B., Gruber, P. R., Kamm, M., Eds.; Wiley-VCH: New York, USA, 2006; Vol. 2; pp 2-59.
- (28) Briens, C.; Piskorz, J.; Berruti, F.: Biomass Valorization for Fuel and Chemicals Production - A Review. *International Journal of Chemical Reactor Engineering* **2008**, *6*, 1-49.
- (29) Chheda, J. N.; Roman-Leshkov, Y.; Dumesic, J. A.: Production of 5-Hydroxymethylfurfural and Furfural by Dehydration of Biomass Derived Mono- and Polysaccharides. *Green Chemistry* **2007**, *9*, 342-350.
- (30) Turley, D. B.: The Chemical Value of Biomass In *Introduction to Chemicals From Biomass*; Clark, J., Deswarte, F., Eds.; Wiley: New York, USA, 2008; pp 21-46.
- (31) Huber, G. W.: Synergien Zwischen Bio- und Ölraffinerien bei der Herstellung von Biomassetreibstoffen. *Angewandte Chemie* **2007**, *119*, 7320-7338.
- (32) Román-Leshkov, Y.; Barrett, C. J.; Liu, Z. Y.; Dumesic, J. A.: Production of Dimethylfuran for Liquid Fuels From Biomass-Derived Carbohydrates. *Nature* **2007**, *447*, 982-985.
- (33) Chheda, J. N.; Huber, G. W.; Dumesic, J. A.: Liquid-Phase Catalytic Processing of Biomass Derived Oxygenated Hydrocarbons to Fuels and Chemicals. *Angewandte Chemie-International Edition* **2007**, *46*, 7164-7183.
- (34) Corma, A.; Iborra, S.; Velty, A.: Chemical Routes for the Transformation of Biomass into Chemicals. *Chemical Reviews* **2007**, *107*, 2411-2502.
- (35) Román-Leshkov, Y.; Chheda, J. N.; Dumesic, J. A.: Phase Modifiers Promote Efficient Production of Hydroxymethylfurfural From Fructose. *Science* **2006**, *312*, 1933-1937.
- (36) Rinaldi, R.; Schuth, F.: Design of Solid Catalysts for the Conversion of Biomass. *Energy & Environmental Science* **2009**, *2*, 610-626.
- (37) Döbereiner, J. W.: Ueber Die Medicinische und Chemische Anwendung und die Vortheilhafte Darstellung der Ameisensäure. *Annalen der Pharmacie* **1832**, *3*, 141-146.

- (38) Boisen, A.; Christensen, T. B.; Fu, W.; Gorbanev, Y. Y.; Hansen, T. S.; Jensen, J. S.; Klitgaard, S. K.; Pedersen, S.; Riisager, A.; Ståhlberg, T.; Woodley, J. M.: Process Integration for the Conversion of Glucose to 2,5-Furandicarboxylic Acid. *Chemical Engineering Research & Design* **2009**, *87*, 1318-1327.
- (39) Decker, S. R.; Sheehan, J.; Dayton, D. C.; Bozell, J. J.; Adney, W. S.; Harnes, B.; Thomas, S. R.; Bain, R. L.; Caernik, S.; Zhang, M.; Himmel, M. E.: Biomass Conversion. In *Kent and Riegel's Handbook of Industrial Chemistry and Biotechnology*; 11 th ed.; Kent, J. A., Ed.; Springer: New York, USA, 2007; Vol. 2; pp 1499-1548.
- (40) USA-Energy-Information-Administration: Natural Gas Consumption Reflects Shifting Sectoral Patterns. In *Today in Energy*; Energy, U. S. D. o., Ed.: Washing D.C., 2012.
- (41) Kamm, B.; Kamm, M.; Gruber, P. R.; Kromus, S.: Biorefinery System- An Overview. In *Biorefineries Industrial Processes and Products-Status Quo and Future Directions*; Kamm, B., Gruber, P. R., Kamm, M., Eds.; Wiley-VCH: New York, USA, 2006; Vol. 1; pp 1-40.
- (42) Gravitis, J.; Vedernikov, N.; Zandersons, J.; Kokorevics, A.; Mochidzuki, K.; Sakoda, A.; Suzuki, M.: Chemicals and Biofuels from Hardwoods, Fuel Crops and Agricultural Wastes. In *2nd Annual Partnerships for Environmental Improvement and Economic Development Conference: Wood and Cellulose: Building Blocks for Chemicals, Fuels and Advanced Materials*: University of New York, College of Environmental Science and Forestry, USA, 2000.
- (43) Sjöström, E.: The Structure of Wood. In *Wood Chemistry: Fundamentals and Applications*; Academic Press: San Diego, USA, 1993; pp 13-17.
- (44) Gruyter, W. D.: Cellulose. In *Wood: Chemistry, Ultrastructure, Reactions*; Fengel, D., Vegener, G., Eds.; Gruyter, W. De.: Berlin; New York, 1989; pp 66-105.
- (45) Gruyter, W. D.: Polyoses (Hemicelluloses). In *Wood: Chemistry, Ultrastructure, Reactions*; Fengel, D., Veneger, G., Eds.; Gruyter, W. De.: Berlin; New York, 1989; pp 106-131.
- (46) Wyman, C. E.: Potential Synergies and Challenges in Refining Cellulosic Biomass to Fuels, Chemicals, and Power. *Biotechnology Progress* **2003**, *19*, 254-262.
- (47) Klemm, D.; Heublein, B.; Fink, H. P.; Bohn, A.: Cellulose: Fascinating Biopolymer and Sustainable Raw Material. *Angewandte Chemie-International Edition* **2005**, *44*, 3358-3393.
- (48) Nelson, D. L.; Cox, M. M.: The Foundations of Biochemistry. In *Lehninger Principles of Biochemistry*; 5 th ed.; Freeman, W. H. and Company: New York, USA, 2008; pp 1-40.
- (49) Shallom, D.; Shoham, Y.: Microbial Hemicellulases. *Current Opinion in Microbiology* **2003**, *6*, 219-228.
- (50) Perez, J.; Dorado, J. M.; Rubia, T. d. I.; Martinez, J.: Biodegradation and Biological Treatments of Cellulose, Hemicellulose and Lignin: An Overview. *International Microbiology : The Official Journal of the Spanish Society for Microbiology* **2002**, *5*, 53-63.
- (51) Chen, J.; Seviour, R.: Medicinal Importance of Fungal Beta-(1 -> 3), (1 -> 6)-Glucans. *Mycological Research* **2007**, *111*, 635-652.
- (52) Nestor, G.; Kenne, L.; Sandstrom, C.: Experimental Evidence of Chemical Exchange Over the Beta(1 -> 3) Glycosidic Linkage and Hydrogen Bonding Involving Hydroxy Protons in Hyaluronan Oligosaccharides by NMR Spectroscopy. *Organic & Biomolecular Chemistry* **2010**, *8*, 2795-2802.
- (53) Lapcik, L.; Smedt, S. D.; Demeester, J.; Chabreck, P.: Hyaluronan: Preparation, Structure, Properties, and Applications. *Chemical Reviews* **1998**, *98*, 2663-2684.
- (54) Zinbo, M.; Timell, T. E.: Studies on a Native Xylan from Norway Spruce (*Picea Abies*). I. Isolation and Constitution. *Sven. Papperstidn.-Nord. Cellul.* **1967**, *70*, 695-701.
- (55) Erickson, M. S.; Brown, W. H.; Poon, T.: *Student Solutions Manual: Introduction to Organic Chemistry*; 3 rd ed.; Wiley-VCH: Hoboken, New Jersey, USA, 2005.
- (56) Petit, B. C.; Escher, F.; Nuessli, J.: Structural Features of Starch-Flavor Complexation in Food Model Systems. *Trends in Food Science & Technology* **2006**, *17*, 227-235.
- (57) Khouw, B. H.; Pritchard, H. O.: The Latent Heat of Vaporization of an Organic Solid: An Undergraduate Experiment. *Journal of Chemical Education* **1975**, *52*, 729.
- (58) Zeitsch, K. J.: *The Chemistry and Technology of Furfural and its Many By-Products*; 1st ed.; Elsevier Science B. V.: Amsterdam, The Netherlands, 2000; Vol. 13.
- (59) Lichtenthaler, F. W.: Carbohydrates as Organic Raw Materials. In *Workshop Conference at the Technische Hochschule Darmstadt*; Lichtenthaler, F. W., Ed.; VCH, Weinheim, Germany: Darmstadt, Germany, 1991; Vol. 1; pp 367.

- (60) Bozell, J. J.: Feedstocks for the Future Using Technology Development as a Guide to Product Identification. In *Feedstocks for the Future: Renewables for the Production of Chemicals and Materials*; Bozell, J. J. P. M. K., Ed., 2006; Vol. 921; pp 1-12.
- (61) Murphy, D. J.: *Designer Oil Crops: Breeding, Processing and Biotechnology*; VCH: Weinheim, Germany, 1994.
- (62) Röbbelen, G.; Downey, R. K.; Ashi, A.: *Oil Crops of the World: their Breeding and Utilization*; McGraw-Hill: University of Michigan, USA, 1989.
- (63) Sun, J. X.; Xu, F.; Sun, X. F.; Sun, R. C.; Wu, S. B.: Comparative Study of Lignins from Ultrasonic Irradiated Sugarcane Bagasse. *Polymer International* **2004**, *53*, 1711-1721.
- (64) Goldenberg, J.; Monaco, L. C.; Macedo, I. C.: The Brazilian Fuel-Alcohol Program. In *Renewable Energy: Sources for Fuels and Electricity*; Johansson, T. B., Kelly, H., Reddy, A. K. N., Williams, R. H., Burnham, L., Eds.; Island Press: Washington, DC, 1993; pp 841-864.
- (65) International-Furan-Chemicals-B.-V.: Production of Furfural. International Furan Chemicals B. V.: The Netherlands, 1994; Vol. 2012.
- (66) Sannigrahi, P.; Pu, Y.; Ragauskas, A.: Cellulosic Biorefineries-Unleashing Lignin Opportunities. *Current Opinion in Environmental Sustainability* **2010**, *2*, 383-393.
- (67) Chakar, F. S.; Ragauskas, A. J.: Review of Current and Future Softwood Kraft Lignin Process Chemistry. *Industrial Crops and Products* **2004**, *20*, 131-141.
- (68) Rodriguez, A.; Jimenez, L.: Pulping with Organic Solvents other than Alcohols. *Afinidad* **2008**, *65*, 188-196.
- (69) Lopez, F.; Alfaro, A.; Jimenez, L.; Rodriguez, A.: Alcohols as Organic Solvents for the Obtainment of Cellulose Pulp. *Afinidad* **2006**, *63*, 174-182.
- (70) James, O. O.; Maity, S.; Usman, L. A.; Ajanaku, K. O.; Ajani, O. O.; Siyanbola, T. O.; Sahu, S.; Chaubey, R.: Towards the Conversion of Carbohydrate Biomass Feedstocks to Biofuels via Hydroxymethylfurfural. *Energy & Environmental Science* **2010**, *3*, 1833-1850.
- (71) Moreau, C.; Belgacem, M. N.; Gandini, A.: Recent Catalytic Advances in the Chemistry of Substituted Furans from Carbohydrates and in the Ensuing Polymers. *Topics in Catalysis* **2004**, *27*, 11-30.
- (72) Win, D. T.: Furfural- Gold From Garbage. *Australian Journal of Technology* **2005**, *8*, 185-190.
- (73) Yan, L.; Zuojun, W.; Chuanjie, C.; Yingxin, L.: Preparation of 5-Hydroxymethylfurfural by Dehydration of Carbohydrates. *Progress in Chemistry* **2010**, *22*, 1603-1609.
- (74) Tong, X.; Ma, Y.; Li, Y.: Biomass Into Chemicals: Conversion of Sugars to Furan Derivatives by Catalytic Processes. *Applied Catalysis A-General* **2010**, *385*, 1-13.
- (75) Dutta, S.; De, S.; Saha, B.; Alam, M. I.: Advances in Conversion of Hemicellulosic Biomass to Furfural and Upgrading to Biofuels. *Catalysis Science & Technology* **2012**, *2*, 2025-2036.
- (76) Brady, J. E.; Russel, J. W.; Holum, J. R.: Organic Compounds and Biochemicals. In *Chemistry: Matter and its Changes*; 3rd ed.; Brennan, D., Ford, E., Smith, R., Swain, E., Eds.; John Wiley & Sons Canada, Ltd.: Hoboken, New Jersey, USA, 2000; pp 1086-1130.
- (77) Shimanskaya, M.; Lukevits, É.: Catalytic Reactions of Furan Compounds (Review). *Chemistry of Heterocyclic compounds* **1993**, *29*, 1000-1011.
- (78) Dehn, W. M.; Jackson, K. E.: Phosphoric Acid in Organic Reactions. *Journal of the American Chemical Society* **1933**, *55*, 4284-4287.
- (79) Levy, J.; Sakuma, Y. "Furfural," SRI International, Stanford Research Institute, 2001.
- (80) Lange, J.-P.; Heide, E. v. d.; Buijtenen, J. v.; Price, R.: Furfural: A Promising Platform for Lignocellulosic Biofuels. *ChemSusChem* **2012**, *5*, 150-166.
- (81) Sain, B.; Chaudhuri, A.; Borgohain, J. N.; Baruah, B. P.; Ghose, J. L.: Furfural and Furfural Based Industrial Chemicals. *Journal of Scientific & Industrial Research* **1982**, *41*, 431-438.
- (82) Brownlee, H. J.; Miner, C. S.: Industrial Development of Furfural. *Industrial and Engineering Chemistry* **1948**, *40*, 201-204.
- (83) Brownlee, H. J.: Furfural Manufacture from Oat Hulls I - A Study of the Liquid-Solid Ratio. *Industrial and Engineering Chemistry* **1927**, *19*, 422-424.
- (84) Seidel, A.; Kroschwitz, J. I.: *Kirk-Othmer Encyclopedia of Chemical Technology*; 5th ed.; John Wiley & Sons Inc.: Hoboken, New York, USA, 2000; Vol. 12.
- (85) Dautzenberg, G.; Gerhardt, M.; Kamm, B.: Bio-Based Fuels and Fuel Additives from Lignocellulose Feedstock via the Production of Levulinic Acid and Furfural. *Holzforschung* **2011**, *65*, 439-451.

- (86) Zeitsch, K. J.: Process for the Manufacture of Furfural. In *United States Patent: 6,743,928 B1*; International Furan Technology (PTY) limited, Kwa Zulu Natal (ZA): USA, 2004; pp 5.
- (87) Yebo, D.: Innovative Minds. Dalin Yebo: Durban, Republic of South Africa, 2011; Vol. 2012.
- (88) Verdernikov, N.: Process for Production of Furfural. In *Latvijas Republikas Patentu Valde: Latvian Patent LV11032*: Latvia, 1996.
- (89) Vedernikov, N.: Process for Producing of Furfural and Acetic Acid. In *Latvijas Republikas Patentu Valde: Latvian Patent LV11950*: Latvia, 1998.
- (90) Vedernikov, N.: Process for Producing of Furfural and Acetic Acid. In *Latvijas Republikas Patentu Valde: Latvian Patent LV12131*: Latvia, 1998.
- (91) Mlayah, B. B.; Delmas, M.; Avignon, G.: Installation for Implementing a Method for Producing Paper Pulp, Lignins and Sugars and Production Method Using Such an Installation. In *United States Patent: US 8,157,964 B2*; Compagnie Industrielle de la Matiere Vegetable, Levallois-Perret, France: USA, 2012; pp 9.
- (92) MacLachlan, R.; Turner, D.; Rushton, M.; Pye, E. K.: Cellulosic Ethanol-The Renewable Fuel for the Future. Lignol, Innovations: Vancouver, British Columbia, Canada, 2012; Vol. 2012.
- (93) Zhang, Y. H. P.: Method and Apparatus for Lignocellulosic Pretreatment Using a Super Cellulose-Solvent and Highly Volatile Solvents. In *United States Patent Applications: US 2009/0229599 A1*: USA, 2009; pp 18.
- (94) Jong, W. D.; Cardoso, M. A. T.; Spronsen, J. V.; Witkamp, G.-J.: Process for the Treatment of Lignocellulosic Biomass. In *International Application Published under the Patent Cooperation Treaty (PCT): WO 2011/149341 A1*; Technische Universiteit Delft: The Netherlands, 2011; pp 15.
- (95) Rousu, P.; Rousu, P.; Rousu, E.: Process for Producing Pulp With a Mixture of Formic Acid and Acetic Acid as Cooking Chemical. In *United States Patent: US 6,562,191 B1*; Chempolis Oy, Oulu, Finland: USA, 2003; pp 5.
- (96) Rousu, P.; Rousu, P.; Rousu, E.: Method of Producing Pulp Using Single Stage Cooking With Formic Acid and Washing With Performic Acid. In *United States Patent: 6,156,156*; Chempolis Oy, Oulun, Finland: Patent, 2000; pp 7.
- (97) Scholastique, T.; Delmas, M.: The End of Fossil-Based Commodities. CIMV, Compagnie Industrielle de la Matière Végétale: Levallois-Perret, France, 2012; Vol. 2012.
- (98) Dias, A. S.; Lima, S.; Pillinger, M.; Valente, A. A.: Furfural and Furfural-Based Industrial Chemicals. In *Ideas in Chemistry and Molecular Sciences: Advances in Synthetic Chemistry*; Pignataro, B., Ed.; Wiley-VCH: Weinheim, Germany, 2010; pp 165-186.
- (99) Karinen, R.; Vilonen, K.; Niemela, M.: Biorefining: Heterogeneously Catalyzed Reactions of Carbohydrates for the Production of Furfural and Hydroxymethylfurfural. *ChemSusChem* **2011**, *4*, 1002-1016.
- (100) Natta, G.: Production of Furfural and Acetic Acid from Pentosan Containing Material. In *United States Patent Office: 2,689,256*; Oronzio De Nora Impianti Electrochimici, Milan, Italy: USA, 1954; pp 4.
- (101) Wenzl, H. F. J.: *The Chemical Technology of Wood (translated from the German by Brauns, F. E. and Braus, D. A.)*; Academic press: New York, USA, 1970.
- (102) Natta, G.: Continuous Process for the Production of Fufural and Acetic Acid from Vegetative Material. In *United States Patent Office: 2,818,413*; Oronazio de Nora Impianti Electrochimici, Milan, Italy: USA, 1957; pp 8.
- (103) Markert, F.: Sustainability, Environmental, and Safety Aspects in the Production of Biocomposites. In *ICCM-17, 17th International Conference on Composite Materials*; RSC, Advancing the Chemical Sciences: Edinburgh International Convention Centre, UK, 2009.
- (104) Arnold, D. R.; Buzzard, J. L.: A Novel and Patented Process for Furfural Production. In *South African Chemical Engineering Congress*; Proceedings of the South African Chemical Engineering Congress: Sun City, South Africa, 2003.
- (105) Gaset, A.; Delmas, M.: Procédé de Preparation de Composes Cetoniques en Particulier de Composed Furanniques ou Composes Cetoniques a Longues Chaines, Composes Furanniques et Composes Cetoniques a Longues Chaines Prebares par Mise en Oeuvre Dudit Pocede. In *French Patent:FR 19810024468*; Agrifurane, S. A., France: France, 1983.

- (106) Wondu-Business-and-Technology-Services; Environmental-and-Farm-Management-Research-and-Development-Program, R.-I.-R.-a.-D.-C.: *Furfural Chemicals and Biofuels From Agriculture: A Report for the Rural Industries Research and Development Corporation*: Australia, 2006.
- (107) Zeitsch, K. J.: Process for Producing Furfural. In *United States Patent: 4,912,237*; Fried Krupp Gesellschaft mit Beschränkter Haftung, Essen, Federal Republic Of Germany: USA, 1990; pp 10.
- (108) Lipinsky, E. S.; Bywater, I.; Scott, K.: Chemicals from Biomass Via the Converttech System. In *Chemistry of Renewable Fuels and Chemicals : Symposium at the 217 th ACS National Meeting*; American Chemical Society, Division of Fuel Chemistry: Anaheim, California, USA, 1999; pp 210-214.
- (109) Brown, D. B.: Apparatus for Conveying Particulate Material. In *United States Patent: 4,186,658*; Stake Technology Ltd. Ottawa, Canada: USA, 1980; pp 12.
- (110) Brown, D. B.; Bender, R.: Apparatus for Discharge of Pressure Cooked Particulate or Fibrous Material. In *United States Patent: 4,211,163*: USA, 1980; pp 7.
- (111) Fitzpatrick, S. W.: Lignocellulose Degradation to Furfural and Levulinic Acid. In *United States Patent: 4,897,497*; Biofine Incorporated, Wilmington, Delaware, USA: USA, 1990; pp 6.
- (112) Fitzpatrick, S. W.: Lignocellulosic Degradation. In *European Patent Specification: EP 0 365 666 B1*; Biofine Incorporated, Wilmington, Delaware, USA: USA, 1995; pp 11.
- (113) Hayes, D. J.; Fitzpatrick, S.; Hayes, M. H. B.; Ross, J. R. H.: The Biofine Process: Production of Levulinic Acid, Furfural, and Formic Acid from Lignocellulosic Feedstocks. In *Biorefineries Industrial Processes and Products-Status Quo and Future Directions*; Kamm, B., Gruber, P. R., Kamm, B., Eds.; Wiley-VCH: New York, USA, 2006; Vol. 2; pp 139-164.
- (114) Gravitis, J.; Zandersons, J.; Vedernikov, N.; Kruma, I.; Ozols-Kalnins, V.: Clustering of Bio-Products Technologies for Zero Emissions and Eco-Efficiency. *Industrial Crops and Products* **2004**, *20*, 169-180.
- (115) Verdernikov, N.: New Technology for Furfural and Bioethanol Production From Low Quality Foliage Wood. In *10th International Symposium on Wood and Pulping Chemistry*: Yokohama, Japan, 1999; Vol. 1; pp 468-470.
- (116) Lam, H. Q.; Bigot, Y. L.; Delmas, M.; Avignon, G.: Matières Premières: La pâte de Sorgho Sucrier. *Technologies* **1999**, 74-75.
- (117) Delmas, M.; Mlayah, B. B.: Organic Pulping of Cereal Straw: from the Pilot Plant to the First Factory. In *"Proceedings of the 16 th European Biomass Conference & Exhibition from Research to Industry and Markets", Management of Environmental Quality: An International Journal*; Emerald, Research You Can Use: Convention and Exhibition Centre, Feria Valencia, Valencia, Spain, 2008; Vol. 20; pp 1660-1665.
- (118) Leponiemi, A.: Fibres and Energy From Wheat Straw by Simple Practise. Aalto University School of Chemical Technology, 2011.
- (119) Peng, C. A.: Biorefining: Back to the Future. *Innovation* **2002**, 12-15.
- (120) Kim, T. H.; Lee, Y. Y.: Pretreatment of Corn Stover by Soaking in Aqueous Ammonia. *Applied Biochemistry and Biotechnology* **2005**, *121-124*, 1119-1131.
- (121) Arato, C.; Pye, E. K.; Gjennestad, G.: The Lignol Approach to Biorefining of Woody Biomass to Produce Ethanol and Chemicals. *Applied Biochemistry and Biotechnology* **2005**, *121*, 871-882.
- (122) Montane, D.; Salvado, J.; Torras, C.; Farriol, X.: High-Temperature Dilute-Acid Hydrolysis of Olive Stones for Furfural Production. *Biomass & Bioenergy* **2002**, *22*, 295-304.
- (123) Xing, R.; Qi, W.; Huber, G. W.: Production of Furfural and Carboxylic Acids From Waste Aqueous Hemicellulose Solutions From the Pulp and Paper and Cellulosic Ethanol Industries. *Energy & Environmental Science* **2011**, *4*, 2193-2205.
- (124) Propersine-Sugar-Milling-Association: Processing in the Proserpine Area. North Queensland, Australia, 2012; Vol. 2012.
- (125) Arcoy-Industries-India-PVT-LTD: Your Partner in Corrosion Prevention. Gujarat, India, 2012; Vol. 2012.
- (126) Avignon, G.; Jaeggie, W.; Steinmüller, H.; Steiner, T.: Combined Process for Thermally and Chemically Treating Lignocellulose-Containing Biomass and for Producing Furfural and Cellulose-Containing Fiber Masses. In *United States Patent: 4,971,657*; Gesellschaft m.b. H. Voest-Alpine Industrieanlagenbau, Austria: USA, 1990; pp 5.

- (127) Avignon, G.; Jaeggie, W.; Steinmüller, H.; Lackner, K.: Combined Process for Thermally and Chemically Treating Lignocellulose Containing Biomass and for Producing Furfural. In *United States Patent: 4,916,242*; Voest-Alpine Industrieanlagenbau Gesellschaft m.b.H., Linz, Austria: USA, 1990; pp 5.
- (128) McKillip, W. J.; Collin, G.; Höke, H.; Zeitsch, K. J.: Furan and Derivatives. In *Ullmann's Encyclopedia of Industrial Chemistry*; Wiley-VCH: Weinheim, Germany, 2001.
- (129) Gubler, R.; Yokose, K. "Furfural," SRI International, Stanford Research Institute, 2008.
- (130) Gravitis, J.; Verdernikov, N.; Zandersons, J.; Kokorevics, A.; Mochidzuki, K.; Sadoka, A.; Suzuki, M. "Chemicals and Biofuels from Hardwoods, Fuel Crops and Agricultural Wastes," United Nation University Headquarters, 2000.
- (131) Gravitis, J.; Vedernikov, N.; Zandersons, J.; Kokorevics, A.: Furfural and Levoglucosan Production from Deciduous Wood and Agricultural Wastes. In *Chemicals and Materials from Renewable Resources*; Bozell, J. J., Ed.; American Chemical Society: Washington, D.C., USA, 2001; Vol. 784; pp 110-122.
- (132) Yebo, D.: Furfural-What is it? What is it Used for?What is Ecoral™? . Dalin Yebo: Durban, Republic of South Africa, 2011; Vol. 2012.
- (133) Zeitsch, K. J.: Furfural Production Needs Chemical Innovation. *Chemical Innovation* **2000**, 30, 29-32.
- (134) Belgacem, M. N.; Gandini, A.: Furan Base Adhesives. In *Handbook of Adhesive Technology*; Pizzi, A., Mittal, N., Eds.; Marcel Dekker: New York; Basel, 2003; Vol. 3; pp 615-635.
- (135) Corma, A.; Torres, O. d. L.; Renz, M.; Villandier, N.: Production of High Quality Diesel From Biomass Waste Products. *Angewandte Chemie* **2011**, 123, 2423-2426.
- (136) Corma, A.; Torre, O. d. L.; Renz, M.; Villandier, N.: Production of High-Quality Diesel from Biomass Waste Products. *Angewandte Chemie-International Edition* **2011**, 50, 2375-2378.
- (137) Lorenzo, G. A.; Morales, F. J.: Estimation of Dietary intake of 5-Hydroxymethylfurfural and Related Substances From Coffee to Spanish Population. *Food and Chemical Toxicology* **2010**, 48, 644-649.
- (138) Huber, G. W.; Chheda, J. N.; Barrett, C. J.; Dumesic, J. A.: Production of Liquid Alkanes by Aqueous-Phase Processing of Biomass Derived Carbohydrates. *Science* **2005**, 308, 1446-1450.
- (139) Luo, H. S.; Li, H. I.; Zhuang, L.: Furfural Hydrogenation to Furfuryl Alcohol Over a Novel Ni-Co-B Amorphous Alloy Catalyst. *Chemistry Letters* **2001**, 404-405.
- (140) Ruiz, J. C. S.; Luque, R.; Escribano, A. S.: Transformations of Biomass-Derived Platform Molecules: from High Added-Value Chemicals to Fuels Via Aqueous-Phase Processing. *Chemical Society Reviews* **2011**, 40, 5266-5281.
- (141) Paul, S. F.: Alternative Fuel. In *United States Patent: US 6,309,430 B1*; The Trustees of Princeton University, Princeton, New Jersey, USA: USA, 2001; pp 9.
- (142) Paul, S. F.: An Optimized Alternative Motor Fuel Formulation: Natural Gas Liquids, Ethanol, and a Biomass-Derived Ether. In *216 th American Chemical Society Annual Meeting*: Boston, Massachusetts, USA, 1998; pp 373.377.
- (143) Katz, K., R.: Alternative Fuel Transportation Program; P Series Fuels. USA-Department-of-Energy-(DOE), Ed.; Office of Energy Efficient and Renewable Energy: Washington, D. C., USA, 1999; Vol. 64; pp 26821-26829.
- (144) Paul, S. F.: Alternative Fuel. In *United States Patent: 5,697,987*; The Trustees of Princeton University: USA, 1997; pp 10.
- (145) Xing, R.; Subrahmanyam, A. V.; Olcay, H.; Qi, W.; Walsum, G. P. V.; Pendse, H.; Huber, G. W.: Production of Jet and Diesel Fuel Range Alkanes From Waste Hemicellulose Derived Aqueous Solutions. *Green Chemistry* **2010**, 12, 1933-1946.
- (146) Huber, G. W.; O'Connor, P.; Corma, A.: Processing Biomass in Conventional Oil Refineries: Production of High Quality Diesel by Hydrotreating Vegetable Oils in Heavy Vacuum Oil Mixtures. *Applied Catalysis A-General* **2007**, 329, 120-129.
- (147) Bayan, S.; Beati, E.: *La Chimica e L'Industria* **1941**, 23, 432-434.
- (148) Gruter, G. J. M.; Dautzenberg, F.: Method for the Synthesis of 5-Alkoxyethylfurfural Ethers and Their Use. In *United States Patent Application Publication: US 2009/0131690 A1*; Furanix Technologies B. V., Amsterdam, The Netherlands: USA, 2009; pp 8.
- (149) Gruter, G. J. M.; Dautzenberg, F.: Method for the Synthesis of Organic Acid Esters of 5-Hydroxymethylfurfural and their Use. In *European Patent Application: EP 1 834 951 A1*; Avantium International B.V., Amsterdam, The Netherlands: The Netherlands, 2007; pp 11.

- (150) Hurd, C. D.; Goldsby, A. R.; Osborne, E. N.: Furan Reactions II. Furan From Furfural. *Journal of the American Chemical Society* **1932**, *54*, 2532-2536.
- (151) Gandini, A.: Furans as Offspring of Sugars and Polysaccharides and Progenitors of a Family of Remarkable Polymers: A Review of Recent Progress. *Polymer Chemistry* **2010**, *1*, 245-251.
- (152) Fakhfakh, N.; Cognet, P.; Cabassud, M.; Lucchese, Y.; Rios, M. D. D. L.: Stoichio-Kinetic Modeling and Optimization of Chemical Synthesis: Application to the Aldolic Condensation of Furfural on Acetone. *Chemical Engineering and Processing* **2008**, *47*, 349-362.
- (153) West, R. M.; Liu, Z. Y.; Peter, M.; Gaertner, C. A.; Dumesic, J. A.: Carbon-Carbon Bond Formation for Biomass Derived Furfurals and Ketones by Aldol Condensation in a Biphasic System. *Journal of Molecular Catalysis A-Chemical* **2008**, *296*, 18-27.
- (154) Matýakubov, R.; Mammatov, Y. M.: Effect of the Nature of the Solvent on the Rate and Mechanism of the Catalytic Hydrogenation of Difurfurylidene acetone. *Chemistry of Heterocyclic compounds* **1981**, *17*, 651-655.
- (155) Sigma-Aldrich: Ficha de Dados de Segurança: 5-(Hidroximetil)furfural. Sigma-Aldrich, Ed.; Kosher Certificated: Madrid, Spain, 2012.
- (156) Düll, G.: *Chemiker-Zeitung* **1895**, *19*, 216-220.
- (157) Kiermayer, J.: *Chemiker-Zeitung* **1895**, *19*, 1003-1006.
- (158) Middendorp, J. A.: Regarding Oxymethylfurfurol. *Recueil Des Travaux Chimiques Des Pays-Bas Et De La Belgique* **1919**, *38*, 1-71.
- (159) Janzowski, C.; Glaab, V.; Samimi, E.; Schlatter, J.; Eisenbrand, G.: 5-Hydroxymethylfurfural: Assessment of Mutagenicity, DNA-Damaging Potential and Reactivity Towards Cellular Glutathione. *Food and Chemical Toxicology* **2000**, *38*, 801-809.
- (160) Henares, J. A. R.; Cueva, S. P. d. L.: Assessment of Hydroxymethylfurfural Intake in the Spanish Diet. *Food Additives and Contaminants Part a-Chemistry Analysis Control Exposure & Risk Assessment* **2008**, *25*, 1306-1312.
- (161) Matute, A. I. R.; Weiss, M.; Sammataro, D.; Finely, J.; Sanz, M. L.: Carbohydrate Composition of High-Fructose Corn Syrups (HFCS) Used for Bee Feeding: Effect on Honey Composition. *Journal of Agricultural and Food Chemistry* **2010**, *58*, 7317-7322.
- (162) Teixido, E.; Santos, F. J.; Puignou, L.; Galceran, M. T.: Analysis of 5-Hydroxymethylfurfural in Foods by Gas Chromatography-Mass Spectrometry. *Journal of Chromatography A* **2006**, *1135*, 85-90.
- (163) Serrano, S.; Espejo, R.; Villarejo, M.; Jodral, M. L.: Diastase and invertase activities in Andalusian honeys. *International Journal of Food Science and Technology* **2007**, *42*, 76-79.
- (164) Gomis, D. B.; Alvarez, M. D. G.; Naredo, L. S.; Alonso, J. J. M.: High Performance Liquid Chromatographic Determination of Furfural and Hydroxymethylfurfural in Apples Juices and Concentrates. *Chromatographia* **1991**, *32*, 45-48.
- (165) Esteve, M. J.; Frigola, A.; Rodrigo, C.; Rodrigo, D.: Effect of Storage Period Under Variable Conditions on the Chemical and Physical Composition and Colour of Spanish Refrigerated Orange Juices. *Food and Chemical Toxicology* **2005**, *43*, 1413-1422.
- (166) Morales, F. J.; Romero, C.; Perez, S. J.: Evaluation of Heat-Induced Changes in Spanish Commercial Milk: Hydroxymethylfurfural and Available Lysine Content. *International Journal of Food Science and Technology* **1996**, *31*, 411-418.
- (167) Ferrer, E.; Alegria, A.; Courtois, G.; Farre, R.: High-Performance Liquid Chromatographic Determination of Maillard Compounds in Store-Brand and Name-Brand Ultra High Temperature Treated Cows' Milk. *Journal of Chromatography A* **2000**, *881*, 599-606.
- (168) Theobald, A.; Muller, A.; Anklam, E.: Determination of 5-Hydroxymethylfurfural in Vinegar Samples by HPLC. *Journal of Agricultural and Food Chemistry* **1998**, *46*, 1850-1854.
- (169) Jimenez, A. R.; Villanova, B. G.; Hernandez, E. G.: Hydroxymethylfurfural and Methylfurfural Content of Selected Bakery Products. *Food Research International* **2000**, *33*, 833-838.
- (170) Murkovic, M.; Pichler, N.: Analysis of 5-Hydroxymethylfurfural in Coffee, Dried Fruits and Urine. *Molecular Nutrition & Food Research* **2006**, *50*, 842-846.
- (171) Jimenez, A. R.; Hernandez, E. G.; Villanova, B. G.: Browning Indicators in Bread. *Journal of Agricultural and Food Chemistry* **2000**, *48*, 4176-4181.
- (172) Husoy, T.; Haugen, M.; Murkovic, M.; Joebstl, D.; Stolen, L. H.; Bjellaas, T.; Ronningborg, C.; Glatt, H.; Alexander, J.: Dietary Exposure to 5-Hydroxymethylfurfural From Norwegian Food and

Correlations with Urine Metabolites of Short-Term Exposure. *Food and Chemical Toxicology* **2008**, *46*, 3697-3702.

(173) Henares, J. A. R.; Andrade, C. D.; Morales, F. J.: Analysis of Heat-Damage Indices in Breakfast Cereals: Influence of Composition. *Journal of Cereal Science* **2006**, *43*, 63-69.

(174) Haworth, W. N.; Jones, W. G. M.: The Conversion of Sucrose Into Furan Compounds. Part I. 5-Hydroxymethylfurfuraldehyde and Some Derivatives. *Journal of the Chemical Society* **1944**, 667-670.

(175) Newth, F. H.: The Formation of Furan Compound From Hexoses *Advances in Carbohydrate Chemistry* **1951**, *6*, 83-106.

(176) Moye, C. J.; Krzeminski, Z. S.: Formation of 5-Hydroxymethylfurfural from Hexoses. *Australian Journal of Chemistry* **1963**, *16*, 258-269.

(177) Lewkowski, J.: Synthesis, Chemistry (and Applications) of 5-Hydroxymethylfurfural and its Derivatives. *Arkivoc* **2001**, *i*, 17-54.

(178) Feather, M. S.; Harris, J. F.: Dehydration Reactions of Carbohydrates. In *Advances in Carbohydrates Chemistry and Biochemistry*; Tipsom, R. S., Horton, D., Eds.; Academic Press Inc., Elsevier Inc.: New York, USA, 1973; Vol. 28; pp 161-224.

(179) Gaset, A.; Gorrichon, J. P.; Truchot, E.: Procédé D'Obtention de Développements Récents. *Info Chimie* **1981**, *212*, 179-184.

(180) Faury, A.; Gaset, A.; Gorrichon, J. P.: Réactivité et Valorisation Chimique de L'Hydroxyméthyl-5-Furannecarboxaldéhyde-2. *Info Chimie* **1981**, *214*.

(181) Kuster, B. F. M.: 5-Hydroxynethylfurfural (Hmf)- A Review Focusing on its Manufacture. *Stärch-Starke* **1990**, *42*, 314-321.

(182) Cottier, L.; Descotes, G.: 5-(Hydroxymethyl)furfural syntheses and chemical transformations. *Trends in Heterocyclic Chemistry* **1991**, *2*, 233-248.

(183) Ulbricht, R. J.; Northup, S. J.; Thomas, J. A.: A Review of 5-Hydroxymethylfurfural (Hmf) in Paraneural Solutions. *Fundamental and Applied Toxicology* **1984**, *4*, 843-853.

(184) Zhang, Y. H. P.; Chan, J. Y. G.: Sustainable Chemistry: Imidazolium Salts in Biomass Conversion and CO₂ fixation. *Energy & Environmental Science* **2010**, *3*, 408-417.

(185) Rosatella, A. A.; Simeonov, S. P.; Frade, R. F. M.; Afonso, C. A. M.: 5-Hydroxymethylfurfural (HMF) as a Building Block Platform: Biological Properties, Synthesis and Synthetic Applications. *Green Chemistry* **2011**, *13*, 754-793.

(186) Rapp, K. M.: Process for the Preparation of 5-Hydroxymethylfurfural, Including a Crystalline Product, Using Exclusively Water as Solvent. In *European Patent Application: O 230 250 B1*; Süddeutsche Zucker- Aktiengesellschaft Mannheim/Ochsenfurt, Germany: Germany, 1991; pp 12.

(187) Rapp, K. M.: Process for the Preparation of 5-Hydroxymethylfurfural, Including a Crystalline Product, Using Exclusively Water as Solvent. In *European Patent Application: O 230 250 A2*; Süddeutsche Zucker- Aktiengesellschaft Mannheim/Ochsenfurt, Germany: Germany, 1987; pp 10.

(188) Bicker, M.; Hirth, J.; Vogel, H.: Dehydration of Fructose to 5-Hydroxymethylfurfural in Sub- and Supercritical Acetone. *Green Chemistry* **2003**, *5*, 280-284.

(189) Koch, H.; Krause, F.; Steffan, R.; Woelk, H. U.: Usage of Starchy Products for Preparation of Phenolic Resins. *Stärke- Starch* **1983**, *35*, 304-313.

(190) Assary, R. S.; Redfern, P. C.; Hammond, J. R.; Greeley, J.; Curtiss, L. A.: Predicted Thermochemistry for Chemical Conversions of 5-Hydroxymethylfurfural. *Chemical Physics Letters* **2010**, *497*, 123-128.

(191) Lichtenhaler, F. W.: Towards Improving the Utility of Ketoses as Organic Raw Materials. *Carbohydrate Research* **1998**, *313*, 69-89.

(192) Skowronski, R.; Grabowski, G.; Lewkowski, J.; Descotes, G.; Cottier, L.; Neyret, C.: New Chemical Conversions of 5-Hydroxymethylfurfural and the Electrochemical Oxidation of its Derivatives. *Organic Preparations and Procedures International* **1993**, *25*, 353-355.

(193) Florentino, H. Q.; Aguilar, R.; Santoyo, B. M.; Diaz, F.; Tamariz, J.: Total Syntheses of Natural Furan Derivatives Rehmanones A, B, and C. *Synthesis-Stuttgart* **2008**, 1023-1028.

(194) Gruter, G. J. M.; Manzer, L. E.; Dias, A. S. V. D. S.; Dautzenberg, F.; Purmova, J.: Hydroxymethylfurfural Ethers and Esters Prepared in Ionic Liquids. In *United States Patent: US 2010/0081833 A1*; Furanix Technologies B. V., Amsterdam, The Netherlands: USA, 2010; pp 5.

- (195) Gruter, G. J. M.; Dautzenberg, F.: Method for the Synthesis of 5-Alkoxyethylfurfural Ethers and Their Use. In *European Patent Application: EP 1 834 950 A1*; Avantium International B. V., Amsterdam, The Netherlands: The Netherlands, 2007; pp 12.
- (196) Binder, J. B.; Raines, R. T.: Simple Chemical Transformation of Lignocellulosic Biomass into Furans for Fuels and Chemicals. *Journal of the American Chemical Society* **2009**, *131*, 1979-1985.
- (197) Luijckx, G. C. A.; Huck, N. P. M.; Rantwijk, F. v.; Maat, L.; Bekkum, H. v.: Ether Formation in the Hydrogenolysis of Hydroxymethylfurfural Over Palladium Catalysts in Alcoholic Solution. *Heterocycles* **2009**, *77*, 1037-1044.
- (198) Chidambaram, M.; Bell, A. T.: A Two-Step Approach for the Catalytic Conversion of Glucose to 2,5-Dimethylfuran in Ionic Liquids. *Green Chemistry* **2010**, *12*, 1253-1262.
- (199) Gandini, A.; Belgacem, M. N.: Furans in Polymer Chemistry. *Progress in Polymer Science* **1997**, *22*, 1203-1379.
- (200) Bozell, J. J.; Petersen, G. R.: Technology Development for the Production of Biobased Products from Biorefinery Carbohydrates-the US Department of Energy's "Top 10" Revisited. *Green Chemistry* **2010**, *12*, 539-554.
- (201) Zhao, H.; Holladay, J. E.; Brown, H.; Zhang, Z. C.: Metal Chlorides in Ionic Liquid Solvents Convert Sugars to 5-Hydroxymethylfurfural. *Science* **2007**, *316*, 1597-1600.
- (202) Hu, S.; Zhang, Z.; Zhou, Y.; Han, B.; Fan, H.; Li, W.; Song, J.; Xie, Y.: Conversion of Fructose to 5-Hydroxymethylfurfural Using Ionic Liquids Prepared From Renewable Materials. *Green Chemistry* **2008**, *10*, 1280-1283.
- (203) Cottier, L.; Descotes, G. R.; Soro, Y.: Heteromacrocycles from Ring-Closing Metathesis of Unsaturated Furanic Ethers. *Synthetic Communications* **2003**, *33*, 4285-4295.
- (204) Moye, C. J.: 5-Hydroxymethylfurfural. *Reviews of Pure and Applied Chemistry* **1964**, *14*, 161-170.
- (205) Timko, J. M.; Cram, D. J.: Furanyl Unit in Host Compounds. *Journal of the American Chemical Society* **1974**, *96*, 7159-7160.
- (206) Goswami, S.; Dey, S.; Jana, S.: Design and Synthesis of a Unique Ditopic Macrocyclic Fluorescent Receptor Containing Furan Ring as a Spacer for the Recognition of Dicarboxylic Acids. *Tetrahedron* **2008**, *64*, 6358-6363.
- (207) Lichtenthaler, F. W.; Brust, A.; Cuny, E.: Sugar Derived Building Blocks. Part 26. Hydrophilic Pyrroles, Pyridazines and Diazepinones From D-Fructose and Isomaltulose. *Green Chemistry* **2001**, *3*, 201-209.
- (208) Turner, J. H.; Rebers, P. A.; Barrick, P. L.; Cotton, R. H.: Determination of 5-Hydroxymethyl-2-Furaldehyde and Related Compounds. *Analytical Chemistry* **1954**, *26*, 898-901.
- (209) Schiavo, V.; Descotes, G.; Mentech, J.: Catalytic Hydrogenation of 5-Hydroxymethylfurfural in Aqueous Medium. *Bulletin De La Societe Chimique De France* **1991**, 704-711.
- (210) Haworth, W. N.; Jones, W. G. M.; Wiggins, L. F.: The Conversion of Sucrose into Furan Compounds 2. Some 2,5- Disubstituted Tetrahydrofurans and Their Products of Ring Scission. *Journal of the Chemical Society* **1945**, 1-4.
- (211) Cope, A. C.; Baxter, W. N.: Aminoalcohols Containing the 8-Oxa-3-Azabicyclo 3.2.1 Octane Ring System and their Benzoates. *Journal of the American Chemical Society* **1955**, *77*, 393-396.
- (212) Gupta, P.; Singh, S. K.; Pathak, A.; Kundu, B.: Template Directed Approach to Solid-Phase Combinatorial Synthesis of Furan Based Libraries. *Tetrahedron* **2002**, *58*, 10469-10474.
- (213) Abdulmalik, O.; Safo, M. K.; Chen, Q. K.; Yang, J. S.; Brugnara, C.; Ohene-Frempong, K.; Abraham, D. J.; Asakura, T.: 5-Hydroxymethyl-2-Furfural Modifies Intracellular Sick Cell Hemoglobin and Inhibits Sickling of Red Blood Cells. *British Journal of Haematology* **2005**, *128*, 552-561.
- (214) Kröger, M.; Prüsse, U.; Vorlop, K. D.: A New Approach for the Production of 2,5-Furandicarboxylic Acid by *in situ* Oxidation of 5-Hydroxymethylfurfural Starting From Fructose. *Topics in Catalysis* **2000**, *13*, 237-242.
- (215) Girisuta, B.; Janssen, L. P. B. M.; Heeres, H. J.: A Kinetic Study on the Decomposition of 5-Hydroxymethylfurfural Into Levulinic Acid. *Green Chemistry* **2006**, *8*, 701-709.
- (216) Papadogianakis, G.; Maat, L.; Sheldon, R. A.: Catalytic Conversions in Water- A Novel Carbonylation Reaction Catalyzed by Palladium Trisulfonated Triphenylphosphine Complexes. *Journal of the Chemical Society-Chemical Communications* **1994**, 2659-2660.

- (217) Abatzoglou, N.; Chornet, E.: Acid Hydrolysis of Hemicelluloses and Cellulose: Theory and Applications. In *Polysaccharides: Structural, Diversity and Functional Versatility*; Dumitriu, S., Ed.; Marcel Dekker: New York, USA, 1998; pp 1007-1045.
- (218) Xiang, Q.; Lee, Y. Y.; Pettersson, P. O.; Torget, R.: Heterogeneous Aspects of Acid Hydrolysis of Alpha-Cellulose. *Applied Biochemistry and Biotechnology* **2003**, *105*, 505-514.
- (219) Antal, M. J.; Leesomboon, T.; Mok, W. S.; Richards, G. N.: Kinetic Studies of the Reactions of Ketoses and Aldoses in Water at High Temperature 3-Mechanism of Formation of 2-Furaldehyde from D-Xylose. *Carbohydrate Research* **1991**, *217*, 71-85.
- (220) O'Neill, R.; Ahmad, M. N. M.; Vanoye, L.; Aiouache, F.: Kinetics of Aqueous Phase Dehydration of Xylose Into Furfural Catalyzed by ZSM-5 Zeolite. *Industrial & Engineering Chemistry Research* **2009**, *48*, 4300-4306.
- (221) Root, D. F.; Saeman, J. F.; Harris, J. F.; Neill, W. K.: Chemical Conversion of Wood Residues. Part II: Kinetics of the Acid Catalyzed Conversion of Xylose to Furfural. *Forest Products Journal* **1959**, *9*, 158-165.
- (222) Moreau, C.; Durand, R.; Peyron, D.; Duhamet, J.; Rivalier, P.: Selective Preparation of Furfural From Xylose Over Microporous Solid Acid Catalysts. *Industrial Crops and Products* **1998**, *7*, 95-99.
- (223) Moreau, C.; Durand, R.; Razigade, S.; Duhamet, J.; Faugeras, P.; Rivalier, P.; Ros, P.; Avignon, G.: Dehydration of Fructose to 5-Hydroxymethylfurfural Over H-Mordenites. *Applied Catalysis A-General* **1996**, *145*, 211-224.
- (224) Torres, A. I.; Daoutidis, P.; Tsapatsis, M.: Continuous Production of 5-Hydroxymethylfurfural From Fructose: A Design Case Study. *Energy & Environmental Science* **2010**, *3*, 1560-1572.
- (225) Haworth, W. N.; Hirst, E. L.; Nicholson, V. S.: The Constitution of the Disaccharides. Part XIII. The Gamma- Fructose Residue in Sucrose. *Journal of the Chemical Society* **1927**, 1513-1526.
- (226) Antal, M. J.; Mok, W. S. L.; Richards, G. N.: Kinetic-Studies of the Reactions of Ketoses and Aldoses in Water at High Temperature .1. Mechanism of Formation of 5-(Hydroxymethyl)-2-Furaldehyde from D-Fructose and Sucrose. *Carbohydrate Research* **1990**, *199*, 91-109.
- (227) Assary, R. S.; Redfern, P. C.; Greeley, J.; Curtiss, L. A.: Mechanistic Insights into the Decomposition of Fructose to Hydroxy Methyl Furfural in Neutral and Acidic Environments Using High-Level Quantum Chemical Methods. *Journal of Physical Chemistry B* **2011**, *115*, 4341-4349.
- (228) Caratzoulas, S.; Vlachos, D. G.: Converting Fructose to 5-Hydroxymethylfurfural: A Quantum Mechanics/Molecular Mechanics Study of The Mechanism and Energetics. *Carbohydrate Research* **2011**, *346*, 664-672.
- (229) Takagaki, A.; Ohara, M.; Nishimura, S.; Ebitani, K.: A One-Pot Reaction for Biorefinery: Combination of Solid Acid and Base Catalysts for Direct Production of 5-Hydroxymethylfurfural from Saccharides. *Chemical Communications* **2009**, 6276-6278.
- (230) Chun, J.-A.; Lee, J.-W.; Li, Y.-B.; Hong, S.-S.; Chung, C.-H.: Catalytic Production of Hydroxymethylfurfural from Sucrose Using 1-Methyl-3-Octylimidazolium Chloride Ionic Liquid. *Korean Journal of Chemical Engineering* **2010**, *27*, 930-935.
- (231) Sievers, C.; Musin, I.; Marzalletti, T.; Olarte, M. B. V.; Agrawal, P. K.; Jones, C. W.: Acid-Catalyzed Conversion of Sugars and Furfurals in an Ionic-Liquid Phase. *ChemSusChem* **2009**, *2*, 665-671.
- (232) Aida, T. M.; Sato, Y.; Watanabe, M.; Tajima, K.; Nonaka, T.; Hattori, H.; Arai, K.: Dehydration of D-Glucose in High Temperature Water at Pressures up to 80 MPa. *Journal of Supercritical Fluids* **2007**, *40*, 381-388.
- (233) Asghari, F. S.; Yoshida, H.: Acid-Catalyzed Production of 5-Hydroxymethylfurfural From D-fructose in Subcritical Water. *Industrial & Engineering Chemistry Research* **2006**, *45*, 2163-2173.
- (234) Vitz, J.; Erdmenger, T.; Haensch, C.; Schubert, U. S.: Extended Dissolution Studies of Cellulose in Imidazolium Based Ionic Liquids. *Green Chemistry* **2009**, *11*, 417-424.
- (235) Dam, H. E. V.; Kieboom, A. P. G.; Bekkum, H. V.: The Conversion of Fructose and Glucose in Acidic Media- Formation of Hydroxymethylfurfural. *Stärch-Starke* **1986**, *38*, 95-101.
- (236) Hansen, T. S.; Woodley, J. M.; Riisager, A.: Efficient Microwave-Assisted Synthesis of 5-Hydroxymethylfurfural from Concentrated Aqueous Fructose. *Carbohydrate Research* **2009**, *344*, 2568-2572.

- (237) Asghari, F. S.; Yoshida, H.: Kinetics of the Decomposition of Fructose Catalyzed by Hydrochloric Acid in Subcritical Water: Formation of 5-Hydroxymethylfurfural, Levulinic, and Formic Acids. *Industrial & Engineering Chemistry Research* **2007**, *46*, 7703-7710.
- (238) Canterino, M.; Somma, I. D.; Marotta, R.; Andreozzi, R.; Caprio, V.: Production of 5-Hydroxy-4-Keto-2-Pentenoic Acid by Photo-Oxidation of 5-Hydroxymethylfurfural With Singlet Oxygen: A Kinetic Investigation. *Journal of Photochemistry and Photobiology A-Chemistry* **2010**, *210*, 69-76.
- (239) Benvenuti, F.; Carlini, C.; Patrono, P.; Galletti, A. M. R.; Sbrana, G.; Massucci, M. A.; Galli, P.: Heterogeneous Zirconium and Titanium Catalysts for the Selective Synthesis of 5-Hydroxymethyl-2-Furaldehyde from Carbohydrates. *Applied Catalysis A-General* **2000**, *193*, 147-153.
- (240) Dias, A. S.; Pillinger, M.; Valente, A. A.: Dehydration of Xylose Into Furfural Over Micro-Mesoporous Sulfonic Acid Catalysts. *Journal of Catalysis* **2005**, *229*, 414-423.
- (241) Rong, C.; Ding, X.; Zhu, Y.; Li, Y.; Wang, L.; Qu, Y.; Ma, X.; Wang, Z.: Production of Furfural From Xylose at Atmospheric Pressure by Dilute Sulfuric Acid and Inorganic Salts. *Carbohydrate Research* **2012**, *350*, 77-80.
- (242) Rasrendra, C. B.; Makertihartha, I. G. B. N.; Adisasmito, S.; Heeres, H. J.: Green Chemicals From D-glucose: Systematic Studies on Catalytic Effects of Inorganic Salts on the Chemo-Selectivity and Yield in Aqueous Solutions. *Topics in Catalysis* **2010**, *53*, 1241-1247.
- (243) Lai, L.; Zhang, Y.: The Production of 5-Hydroxymethylfurfural from Fructose in Isopropyl Alcohol: A Green and Efficient System. *ChemSusChem* **2011**, *4*, 1745-1748.
- (244) Lourvanij, K.; Rorrer, G. L.: Reactions of Aqueous Glucose Solutions Over Solid Acid Y-Zeolite Catalyst at 110-160 °C. *Industrial & Engineering Chemistry Research* **1993**, *32*, 11-19.
- (245) Shimizu, K.-I.; Uozumi, R.; Satsuma, A.: Enhanced Production of 5-Hydroxymethylfurfural From Fructose With Solid Acid Catalysts by Simple Water Removal Methods. *Catalysis Communications* **2009**, *10*, 1849-1853.
- (246) Wang, J.; Xu, W.; Ren, J.; Liu, X.; Lu, G.; Wang, Y.: Efficient Catalytic Conversion of Fructose into Hydroxymethylfurfural by a Novel Carbon-Based Solid Acid. *Green Chemistry* **2011**, *13*, 2678-2681.
- (247) Ohara, M.; Takagaki, A.; Nishimura, S.; Ebitani, K.: Syntheses of 5-Hydroxymethylfurfural and Levoglucosan by Selective Dehydration of Glucose Using Solid Acid and Base Catalysts. *Applied Catalysis A-General* **2010**, *383*, 149-155.
- (248) Takagaki, A.; Ohara, M.; Nishimura, S.; Ebitani, K.: One-Pot Formation of Furfural from Xylose via Isomerization and Successive Dehydration Reactions over Heterogeneous Acid and Base Catalysts. *Chemistry Letters* **2010**, *39*, 838-840.
- (249) Kim, S. B.; You, S. J.; Kim, Y. T.; Lee, S. M.; Lee, H.; Park, K.; Park, E. D.: Dehydration of D-xylose Into Furfural Over H-Zeolites. *Korean Journal of Chemical Engineering* **2011**, *28*, 710-716.
- (250) Ordonsky, V. V.; van der Schaaf, J.; Schouten, J. C.; Nijhuis, T. A.: The Effect of Solvent Addition on Fructose Dehydration to 5-Hydroxymethylfurfural in Biphasic System Over Zeolites. *Journal of Catalysis* **2012**, *287*, 68-75.
- (251) Tyrlik, S. K.; Szerszen, D.; Olejnik, M.; Danikiewicz, W.: Concentrated Water Solutions of Salts as Solvents for Reaction of Carbohydrates .2. Influence of Some Magnesium Salts and Some Ruthenium Species on Catalysis of Dehydration of Glucose. *Journal of Molecular Catalysis A-Chemical* **1996**, *106*, 223-233.
- (252) Liu, J.; Tang, Y.; Wu, K.; Bi, C.; Cui, Q.: Conversion of Fructose into 5-Hydroxymethylfurfural (Hmf) and its Derivatives Promoted by Inorganic Salt in Alcohol. *Carbohydrate Research* **2012**, *350*, 20-24.
- (253) Binder, J. B.; Cefali, A. V.; Blank, J. J.; Raines, R. T.: Mechanistic Insights on the Conversion of Sugars into 5-Hydroxymethylfurfural. *Energy & Environmental Science* **2010**, *3*, 765-771.
- (254) Caruso, T.; Vasca, E.: Electrogenerated Acid as an Efficient Catalyst for the Preparation of 5-Hydroxymethylfurfural. *Electrochemistry Communications* **2010**, *12*, 1149-1153.
- (255) Suzuki, T.; Yokoi, T.; Otomo, R.; Kondo, J. N.; Tatsumi, T.: Dehydration of Xylose over Sulfated Tin Oxide Catalyst: Influences of the Preparation Conditions on the Structural Properties and Catalytic Performance. *Applied Catalysis A-General* **2011**, *408*, 117-124.
- (256) Daengprasert, W.; Boonnoun, P.; Laosiripojana, N.; Goto, M.; Shotipruk, A.: Application of Sulfonated Carbon-Based Catalyst for Solvothermal Conversion of Cassava Waste to Hydroxymethylfurfural and Furfural. *Industrial & Engineering Chemistry Research* **2011**, *50*, 7903-7910.

- (257) Shi, X.; Wu, Y.; Yi, H.; Rui, G.; Li, P.; Yang, M.; Wang, G.: Selective Preparation of Furfural from Xylose Over Sulfonic Acid Functionalized Mesoporous SBA-15 Materials. *Energies* **2011**, *4*, 669-684.
- (258) Román-Leshkov, Y.; Dumesic, J. A.: Solvent Effects on Fructose Dehydration to 5-Hydroxymethylfurfural in Biphasic Systems Saturated with Inorganic Salts. *Topics in Catalysis* **2009**, *52*, 297-303.
- (259) Qi, X.; Watanabe, M.; Aida, T. M.; Smith, R. L., Jr.: Selective Conversion of D-Fructose to 5-Hydroxymethylfurfural by Ion-Exchange Resin in Acetone/Dimethyl sulfoxide Solvent Mixtures. *Industrial & Engineering Chemistry Research* **2008**, *47*, 9234-9239.
- (260) Zhu, H.; Cao, Q.; Li, C.; Mu, X.: Acidic Resin-Catalysed Conversion of Fructose into Furan Derivatives in Low Boiling Point Solvents. *Carbohydrate Research* **2011**, *346*, 2016-2018.
- (261) Rivalier, P.; Duhamet, J.; Moreau, C.; Durand, R.: Development of a Continuous Catalytic Heterogeneous Column Reactor With Simultaneous Extraction of an Intermediate Product by an Organic-Solvent Circulating in Counter-Current Manner With the Aqueous Phase. *Catalysis Today* **1995**, *24*, 165-171.
- (262) Hansen, T. S.; Mielby, J.; Riisager, A.: Synergy of Boric Acid and Added Salts in the Catalytic Dehydration of Hexoses to 5-Hydroxymethylfurfural in Water. *Green Chemistry* **2011**, *13*, 109-114.
- (263) Wang, C.; Fu, L.; Tong, X.; Yang, Q.; Zhang, W.: Efficient and Selective Conversion of Sucrose to 5-Hydroxymethylfurfural Promoted by Ammonium Halides Under Mild Conditions. *Carbohydrate Research* **2012**, *347*, 182-185.
- (264) Asghari, F. S.; Yoshida, H.: Dehydration of Fructose to 5-Hydroxymethylfurfural in Sub-Critical Water Over Heterogeneous Zirconium Phosphate Catalysts. *Carbohydrate Research* **2006**, *341*, 2379-2387.
- (265) Lima, S.; Pillinger, M.; Valente, A. A.: Dehydration of D-xylose Into Furfural Catalysed by Solid Acids Derived From the Layered Zeolite Nu-6(1). *Catalysis Communications* **2008**, *9*, 2144-2148.
- (266) Clark, J. H.: Solid Acids for Green Chemistry. *Accounts of Chemical Research* **2002**, *35*, 791-797.
- (267) Okuhara, T.: Water-Tolerant Solid Acid Catalysts. *Chemical Reviews* **2002**, *102*, 3641-3665.
- (268) King, C. J.: Separation Process, Introduction. In *Ullmann's Encyclopedia of Industrial Chemistry*; Wiley-VCH Verlag GmbH & Co KGaA, Weinheim, Germany, 2000.
- (269) Climent, M. J.; Corma, A.; Iborra, S.: Heterogeneous Catalysts for the One-Pot Synthesis of Chemicals and Fine Chemicals. *Chemical Reviews* **2011**, *111*, 1072-1133.
- (270) Yemis, O.; Mazza, G.: Acid-Catalyzed Conversion of Xylose, Xylan and Straw Into Furfural by Microwave-Assisted Reaction. *Bioresource Technology* **2011**, *102*, 7371-7378.
- (271) Weingarten, R.; Tompsett, G. A.; Conner, W. C. J.; Huber, G. W.: Design of Solid Acid Catalysts for Aqueous-Phase Dehydration of Carbohydrates: The Role of Lewis and Brønsted Acid Sites. *Journal of Catalysis* **2011**, *279*, 174-182.
- (272) Marcotullio, G.; Jong, W. D.: Chloride Ions Enhance Furfural Formation From D-Xylose in Dilute Aqueous Acidic Solutions. *Green Chemistry* **2010**, *12*, 1739-1746.
- (273) Weingarten, R.; Cho, J.; Conner, W. C., Jr.; Huber, G. W.: Kinetics of Furfural Production by Dehydration of Xylose in a Biphasic Reactor With Microwave Heating. *Green Chemistry* **2010**, *12*, 1423-1429.
- (274) Choudhary, V.; Pinar, A. B.; Sandler, S. I.; Vlachos, D. G.; Lobo, R. F.: Xylose Isomerization to Xylulose and its Dehydration to Furfural in Aqueous Media. *Advanced Synthesis & Catalysis* **2011**, *1*, 1724-1728.
- (275) Tao, F.; Song, H.; Chou, L.: Efficient Process for the Conversion of Xylose to Furfural With Acidic Ionic Liquid. *Canadian Journal of Chemistry-Revue Canadienne De Chimie* **2011**, *89*, 83-87.
- (276) Marcotullio, G.; Heidweiller, H. J.; Jong, W. D.: Reaction Kinetic Assessment for Selective Production of Furfural from C₅ Sugars Contained in Biomass. In *"Proceedings of the 16th European Biomass Conference & Exhibition from Research to Industry and Markets"*, Management of Environmental Quality: An International Journal; 16th ed.; Emerald, Research You Can Use: Convention and Exhibition Centre, Feria Valencia, Valencia Spain, 2008; Vol. 20; pp 1660-1665.
- (277) Binder, J. B.; Blank, J. J.; Cefali, A. V.; Raines, R. T.: Synthesis of Furfural from Xylose and Xylan. *ChemSusChem* **2010**, *3*, 1268-1272.
- (278) Dedsuksophon, W.; Faungnawakij, K.; Champreda, V.; Laosiripojana, N.: Hydrolysis/Dehydration/Aldol-Condensation/Hydrogenation of Lignocellulosic Biomass and Biomass

Derived Carbohydrates in the Presence of Pd/WO₃-ZrO₂ in a Single Reactor. *Bioresource Technology* **2011**, *102*, 2040-2046.

(279) Orozco, A. M.; Al-Muhtaseb, A. a. H.; Albadarin, A. B.; Rooney, D.; Walker, G. M.; Ahmad, M. N. M.: Dilute Phosphoric Acid Catalysed Hydrolysis of Municipal Bio-Waste Wood Shavings Using Autoclave Parr Reactor System. *Bioresource Technology* **2011**, *102*, 9076-9082.

(280) Dias, A. S.; Pillinger, M.; Valente, A. A.: Liquid Phase Dehydration of D-xylose in the Presence of Keggin-Type Heteropolyacids. *Applied Catalysis A-General* **2005**, *285*, 126-131.

(281) Forstner, J.; Unkelbach, G.; Pindel, E.; Schweppe, R.: Heterogen Katalysierte Herstellung von Furfural aus Xylose. *Chemie Ingenieur Technik* **2012**, *84*, 503-508.

(282) Silva, L. C.; Lima, S.; Ananias, D.; Silva, P.; Mafra, L.; Carlos, L. D.; Pillinger, M.; Valente, A. A.; Paz, F. A. A.; Rocha, J.: Multi-Functional Rare-Earth Hybrid Layered Networks: Photoluminescence and Catalysis Studies. *Journal of Materials Chemistry* **2009**, *19*, 2618-2632.

(283) Yang, Y.; Hu, C.-W.; Omar, M. M. A.: Synthesis of Furfural from Xylose, Xylan, and Biomass Using AlCl₃ Center Dot 6H₂O in Biphasic Media via Xylose Isomerization to Xylulose. *ChemSusChem* **2012**, *5*, 405-410.

(284) Dias, A. S.; Lima, S.; Pillinger, M.; Valente, A. A.: Acidic Cesium Salts of 12-Tungstophosphoric Acid as Catalysts for the Dehydration of Xylose into Furfural. *Carbohydrate Research* **2006**, *341*, 2946-2953.

(285) Dias, A. S.; Pillinger, M.; Valente, A. A.: Mesoporous Silica-Supported 12-Tungstophosphoric Acid Catalysts for the Liquid Phase Dehydration of D-Xylose. *Microporous and Mesoporous Materials* **2006**, *94*, 214-225.

(286) Sadaba, I.; Lima, S.; Valente, A. A.; Granados, M. L.: Catalytic Dehydration of Xylose to Furfural: Vanadyl Pyrophosphate as Source of Active Soluble Species. *Carbohydrate Research* **2011**, *346*, 2785-2791.

(287) Telleria, I. A.; Larreategui, A.; Requies, J.; Gueemez, M. B.; Arias, P. L.: Furfural Production From Xylose Using Sulfonic Ion-Exchange Resins (Amberlyst) and Simultaneous Stripping With Nitrogen. *Bioresource Technology* **2011**, *102*, 7478-7485.

(288) Lam, E.; Majid, E.; Leung, A. C. W.; Chong, J. H.; Mahmoud, K. A.; Luong, J. H. T.: Synthesis of Furfural from Xylose by Heterogeneous and Reusable Nafion Catalysts. *ChemSusChem* **2011**, *4*, 535-541.

(289) Jeong, G. H.; Kim, E. G.; Kim, S. B.; Park, E. D.; Kim, S. W.: Fabrication of Sulfonic Acid Modified Mesoporous Silica Shells and Their Catalytic Performance With Dehydration Reaction of D-Xylose Into Furfural. *Microporous and Mesoporous Materials* **2011**, *144*, 134-139.

(290) Kaldstrom, M.; Kumar, N.; Heikkila, T.; Tiitta, M.; Salmi, T.; Murzin, D. Y.: Formation of Furfural in Catalytic Transformation of Levoglucosan Over Mesoporous Materials. *ChemCatChem* **2010**, *2*, 539-546.

(291) Dias, A. S.; Lima, S.; Brandao, P.; Pillinger, M.; Rocha, J.; Valente, A. A.: Liquid-Phase Dehydration of D-xylose Over Microporous and Mesoporous Niobium Silicates. *Catalysis Letters* **2006**, *108*, 179-186.

(292) Valente, A. A.; Dias, A. S.; Lima, S.; Brandão, P.; Pillinger, M.; Plácido, H.; Rocha, J.: Catalytic Performance of Microporous Nb and Mesoporous Nb or Al Silicates in the Dehydration of D-Xylose to Furfural. In *Perspectiva de la investigación sobre materiales en España en el siglo XXI: IX Congreso Nacional de Materiales*; Colección: Congressos n° 53 ed.; Materiales, S. E. d., Ed.; Servizo de Pulicaci3ns da Universidade de Vigo: University of Vigo, Vigo, Spain, 2006; Vol. II; pp 1203-1206.

(293) Shi, X.; Wu, Y.; Li, P.; Yi, H.; Yang, M.; Wang, G.: Catalytic Conversion of Xylose to Furfural Over the Solid Acid SO₄²⁻/ZrO₂-Al₂O₃/SBA-15 catalysts. *Carbohydrate Research* **2011**, *346*, 480-487.

(294) Zhang, J.; Zhuang, J.; Lin, L.; Liu, S.; Zhang, Z.: Conversion of D-xylose into Furfural With Mesoporous Molecular Sieve MCM-41 as Catalyst and Butanol as the Extraction Phase. *Biomass & Bioenergy* **2012**, *39*, 73-77.

(295) Kaldstrom, M.; Kumar, N.; Heikkila, T.; Tiitta, M.; Salmi, T.; Murzin, D. Y.: Transformation of Levoglucosan Over H-MCM-22 Zeolite and H-MCM-41 Mesoporous Molecular Sieve Catalysts. *Biomass & Bioenergy* **2011**, *35*, 1967-1976.

(296) Chareonlimkun, A.; Champreda, V.; Shotipruk, A.; Laosiripojana, N.: Reactions of C-5 and C-6-Sugars, Cellulose, and Lignocellulose Under Hot Compressed Water (HCW) in the Presence of Heterogeneous Acid Catalysts. *Fuel* **2010**, *89*, 2873-2880.

- (297) Chareonlimkun, A.; Champreda, V.; Shotipruk, A.; Laosiripojana, N.: Catalytic Conversion of Sugarcane Bagasse, Rice Husk and Corncob in the Presence of TiO₂, ZrO₂ and Mixed-Oxide TiO₂-ZrO₂ Under Hot Compressed Water (HCW) Conditions. *Bioresource Technology* **2010**, *101*, 4179-4186.
- (298) Dias, A. S.; Lima, S.; Pillinger, M.; Valente, A. A.: Modified Versions of Sulfated Zirconia as Catalysts for the Conversion of Xylose to Furfural. *Catalysis Letters* **2007**, *114*, 151-160.
- (299) Dias, A. S.; Lima, S.; Carriazo, D.; Rives, V.; Pillinger, M.; Valente, A. A.: Exfoliated Titanate, Niobate and Titanoniobate Nanosheets as Solid Acid Catalysts for the Liquid-Phase Dehydration of D-Xylose Into Furfural. *Journal of Catalysis* **2006**, *244*, 230-237.
- (300) Li, C.; Wang, Q.; Zhao, Z. K.: Acid in Ionic Liquid: An Efficient System for Hydrolysis of Lignocellulose. *Green Chemistry* **2008**, *10*, 177-182.
- (301) Dee, S. J.; Bell, A. T.: A Study of the Acid-Catalyzed Hydrolysis of Cellulose Dissolved in Ionic Liquids and the Factors Influencing the Dehydration of Glucose and the Formation of Humins. *ChemSusChem* **2011**, *4*, 1166-1173.
- (302) Benoit, M.; Brissonnet, Y.; Guelou, E.; Vigier, K. D. O.; Barrault, J.; Jerome, F.: Acid-Catalyzed Dehydration of Fructose and Inulin with Glycerol or Glycerol Carbonate as Renewably Sourced Co-Solvent. *ChemSusChem* **2010**, *3*, 1304-1309.
- (303) Shi, C.; Zhao, Y.; Xin, J.; Wang, J.; Lu, X.; Zhang, X.; Zhang, S.: Effects of Cations and Anions of Ionic Liquids on the Production of 5-Hydroxymethylfurfural From Fructose. *Chemical Communications* **2012**, *48*, 4103-4105.
- (304) Du, F.; Qi, X.-H.; Xu, Y.-Z.; Zhuang, Y.-Y.: Catalytic Conversion of Fructose to 5-Hydroxymethylfurfural by Ion-exchange Resin in Ionic Liquid. *Chemical Journal of Chinese Universities-Chinese* **2010**, *31*, 548-552.
- (305) Hu, L.; Sun, Y.; Lin, L.: Efficient Conversion of Glucose into 5-Hydroxymethylfurfural by Chromium(III) Chloride in Inexpensive Ionic Liquid. *Industrial & Engineering Chemistry Research* **2012**, *51*, 1099-1104.
- (306) Qi, X.; Watanabe, M.; Aida, T. M.; Smith, R. L., Jr.: Efficient Process for Conversion of Fructose to 5-Hydroxymethylfurfural With Ionic Liquids. *Green Chemistry* **2009**, *11*, 1327-1331.
- (307) Tao, F.; Song, H.; Chou, L.: Dehydration of Fructose Into 5-Hydroxymethylfurfural in Acidic Ionic Liquids. *Royal Chemical Society Advances* **2011**, *1*, 672-676.
- (308) Mednick, M. L.: The Acid-Base-Catalyzed Conversion of Aldohexose into 5-(Hydroxymethyl)-2-furfural. *Journal of Organic Chemistry* **1962**, *27*, 398-403.
- (309) Tan, M.; Zhao, L.; Zhang, Y.: Production of 5-Hydroxymethylfurfural From Cellulose in CrCl₂/Zeolite/BmimCl System. *Biomass & Bioenergy* **2011**, *35*, 1367-1370.
- (310) Ilgen, F.; Ott, D.; Kralisch, D.; Reil, C.; Palmberger, A.; Koenig, B.: Conversion of Carbohydrates Into 5-Hydroxymethylfurfural in Highly Concentrated Low Melting Mixtures. *Green Chemistry* **2009**, *11*, 1948-1954.
- (311) Lansalot-Matras, C.; Moreau, C.: Dehydration of Fructose into 5-Hydroxymethylfurfural in the Presence of Ionic Liquids. *Catalysis Communications* **2003**, *4*, 517-520.
- (312) Tyrlik, S. K.; Szerszen, D.; Olejnik, M.; Danikiewicz, W.: Selective Dehydration of Glucose to Hydroxymethylfurfural and a One-Pot Synthesis of a 4-Acetylbutyrolactone from Glucose and Trioxane in Solutions of Aluminium Salts. *Carbohydrate Research* **1999**, *315*, 268-272.
- (313) Jadhav, H.; Taarning, E.; Pedersen, C. M.; Bols, M.: Conversion of D-glucose Into 5-Hydroxymethylfurfural (Hmf) Using Zeolite in BmimCl or Tetrabutylammonium Chloride (TBAC)/CrCl₂. *Tetrahedron Letters* **2012**, *53*, 983-985.
- (314) Yang, Y.; Hu, C.-W.; Omar, M. M. A.: Conversion of Carbohydrates and Lignocellulosic Biomass Into 5-Hydroxymethylfurfural Using AlCl₃ Center Dot 6H₂O Catalyst in a Biphasic Solvent System. *Green Chemistry* **2012**, *14*, 509-513.
- (315) Fan, C.; Guan, H.; Zhang, H.; Wang, J.; Wang, S.; Wang, X.: Conversion of Fructose and Glucose into 5-Hydroxymethylfurfural Catalyzed by a Solid Heteropolyacid Salt. *Biomass & Bioenergy* **2011**, *35*, 2659-2665.
- (316) Hu, S.; Zhang, Z.; Zhou, Y.; Song, J.; Fan, H.; Han, B.: Direct Conversion of Inulin to 5-Hydroxymethylfurfural in Biorenewable Ionic Liquids. *Green Chemistry* **2009**, *11*, 873-877.
- (317) Binder, J. B.; Raines, R. T.: Fermentable Sugars by Chemical Hydrolysis of Biomass. *Proceedings of the National Academy of Sciences of the United States of America* **2010**, *107*, 4516-4521.

- (318) Hales, R. A.; Maistre, J. W. L.; Orth-Junior, G. O.: Preparation of Hydroxymethylfurfural. In *United States Patent Office: 3,071,599*; Atlas Chemical Industries, Inc., Wilmington, Delaware, USA: USA, 1963; pp 4.
- (319) Li, C.; Zhao, Z. K.: Efficient Acid-Catalyzed Hydrolysis of Cellulose in Ionic Liquid. *Advanced Synthesis & Catalysis* **2007**, *349*, 1847-1850.
- (320) Vinke, P.; Vanbekkum, H.: The Dehydration of Fructose Towards 5-Hydroxymethylfurfural Using Activated Carbon as Adsorbent. *Stärch-Starke* **1992**, *44*, 90-96.
- (321) Li, C.; Zhao, Z. K.; Cai, H.; Wang, A.; Zhang, T.: Microwave-Promoted Conversion of Concentrated Fructose Into 5-Hydroxymethylfurfural in Ionic Liquids in the Absence of Catalysts. *Biomass & Bioenergy* **2011**, *35*, 2013-2017.
- (322) Chun, J.-A.; Lee, J.-W.; Yi, Y.-B.; Hong, S.-S.; Chung, C.-H.: Direct Conversion of Starch to 5-Hydroxymethylfurfural in the Presence of an Ionic Liquid With Metal Chloride. *Stärch-Starke* **2010**, *62*, 326-330.
- (323) Cao, Q.; Guo, X.; Guan, J.; Mu, X.; Zhang, D.: A Process for Efficient Conversion of fructose into 5-Hydroxymethylfurfural in Ammonium Salts. *Applied Catalysis A-General* **2011**, *403*, 98-103.
- (324) Wei, Z.; Li, Y.; Thushara, D.; Liu, Y.; Ren, Q.: Novel Dehydration of Carbohydrates to 5-Hydroxymethylfurfural Catalyzed by Ir and Au Chlorides in Ionic Liquids. *Journal of the Taiwan Institute of Chemical Engineers* **2011**, *42*, 363-370.
- (325) Ray, D.; Mittal, N.; Chung, W.-J.: Phosphorous Pentoxide Mediated Synthesis of 5-Hmf in Ionic Liquid at Low Temperature. *Carbohydrate Research* **2011**, *346*, 2145-2148.
- (326) Sudipta, D.; Dutta, S.; Saha, B.: Microwave Assisted Conversion of Carbohydrates and Biopolymers to 5-Hydroxymethylfurfural With Aluminium Chloride Catalyst in Water. *Green Chemistry* **2011**, *13*, 2859-2868.
- (327) Chen, T.; Lin, L.: Conversion of Glucose in CPL-LiCl to 5-Hydroxymethylfurfural. *Chinese Journal of Chemistry* **2010**, *28*, 1773-1776.
- (328) Chan, J. Y. G.; Zhang, Y.: Selective Conversion of Fructose to 5-Hydroxymethylfurfural Catalyzed by Tungsten Salts at Low Temperatures. *ChemSusChem* **2009**, *2*, 731-734.
- (329) Yu, S.; Brown, H. M.; Huang, X.; Zhou, X.-D.; Amonette, J. E.; Zhang, Z. C.: Single-Step Conversion of Cellulose to 5-Hydroxymethylfurfural (Hmf), a Versatile Platform Chemical. *Applied Catalysis A-General* **2009**, *361*, 117-122.
- (330) Yong, G.; Zhang, Y.; Ying, J. Y.: Efficient Catalytic System for the Selective Production of 5-Hydroxymethylfurfural from Glucose and Fructose. *Angewandte Chemie-International Edition* **2008**, *47*, 9345-9348.
- (331) Zhang, Y.; Pidko, E. A.; Hensen, E. J. M.: Molecular Aspects of Glucose Dehydration by Chromium Chlorides in Ionic Liquids. *Chemistry-A European Journal* **2011**, *17*, 5281-5288.
- (332) Yuan, Z.; Xu, C.; Cheng, S.; Leitch, M.: Catalytic Conversion of Glucose to 5-Hydroxymethylfurfural Using Inexpensive Co-Catalysts and Solvents. *Carbohydrate Research* **2011**, *346*, 2019-2023.
- (333) Guan, J.; Cao, Q.; Guo, X.; Mu, X.: The Mechanism of Glucose Conversion to 5-Hydroxymethylfurfural Catalyzed by Metal Chlorides in Ionic Liquid: A Theoretical Study. *Computational and Theoretical Chemistry* **2011**, *963*, 453-462.
- (334) Li, C.; Zhang, Z.; Zhao, Z. K.: Direct Conversion of Glucose and Cellulose to 5-Hydroxymethylfurfural in Ionic Liquid Under Microwave Irradiation. *Tetrahedron Letters* **2009**, *50*, 5403-5405.
- (335) Wang, P.; Yu, H.; Zhan, S.; Wang, S.: Catalytic Hydrolysis of Lignocellulosic Biomass Into 5-Hydroxymethylfurfural in Ionic Liquid. *Bioresource Technology* **2011**, *102*, 4179-4183.
- (336) Qi, X.; Watanabe, M.; Aida, T. M.; Smith, R. L., Jr.: Fast Transformation of Glucose and Di-/Polysaccharides into 5-Hydroxymethylfurfural by Microwave Heating in an Ionic Liquid/Catalyst System. *ChemSusChem* **2010**, *3*, 1071-1077.
- (337) Zhang, Z.; Zhao, Z. K.: Microwave-Assisted Conversion of Lignocellulosic Biomass into Furans in Ionic Liquid. *Bioresource Technology* **2010**, *101*, 1111-1114.
- (338) Cao, Q.; Guo, X.; Yao, S.; Guan, J.; Wang, X.; Mu, X.; Zhang, D.: Conversion of Hexose into 5-Hydroxymethylfurfural in Imidazolium Ionic Liquids With and Without a Catalyst. *Carbohydrate Research* **2011**, *346*, 956-959.

- (339) Wei, Z.; Liu, Y.; Thushara, D.; Ren, Q.: Entrainer-Intensified Vacuum Reactive Distillation Process for the Separation of 5-Hydroxymethylfurfural From the Dehydration of Carbohydrates Catalyzed by a Metal Salt-Ionic Liquid. *Green Chemistry* **2012**, *14*, 1220-1226.
- (340) Wu, S.; Wang, C.; Gao, Y.; Zhang, S.; Ma, D.; Zhao, Z.: Production of 5-Hydroxymethylfurfural From Cellulose Catalyzed by Lewis Acid Under Microwave Irradiation in Ionic Liquid. *Chinese Journal of Catalysis* **2010**, *31*, 1157-1161.
- (341) Zheng, B.; Fang, Z.; Cheng, J.; Jiang, Y.: Microwave-assisted Conversion of Carbohydrates into 5-Hydroxymethylfurfural Catalyzed by ZnCl₂. *Zeitschrift Fur Naturforschung Section B-a Journal of Chemical Sciences* **2010**, *65*, 168-172.
- (342) Moreau, C.; Finiels, A.; Vanoye, L.: Dehydration of Fructose and Sucrose into 5-Hydroxymethylfurfural in the Presence of 1-H-3-Methyl Imidazolium Chloride Acting Both as Solvent and Catalyst. *Journal of Molecular Catalysis A-Chemical* **2006**, *253*, 165-169.
- (343) Qi, X.; Watanabe, M.; Aida, T. M.; Smith, R. L., Jr.: Efficient Catalytic Conversion of Fructose into 5-Hydroxymethylfurfural in Ionic Liquids at Room Temperature. *ChemSusChem* **2009**, *2*, 944-946.
- (344) Qi, X.; Watanabe, M.; Aida, T. M.; Smith, R. L., Jr.: Efficient One-Pot Production of 5-Hydroxymethylfurfural From Inulin in Ionic Liquids. *Green Chemistry* **2010**, *12*, 1855-1860.
- (345) Hu, X.; Lievens, C.; Larcher, A.; Li, C.-Z.: Reaction Pathways of Glucose During Esterification: Effects of Reaction Parameters on the Formation of HuminType Polymers. *Bioresource Technology* **2011**, *102*, 10104-10113.
- (346) Crisci, A. J.; Tucker, M. H.; Dumesic, J. A.; Scott, S. L.: Bifunctional Solid Catalysts for the Selective Conversion of Fructose to 5-Hydroxymethylfurfural. *Topics in Catalysis* **2010**, *53*, 1185-1192.
- (347) Nakamura, Y.; Morikawa, S.: The Dehydration of D-Fructose to 5-Hydroxymethyl-2-Furaldehyde. *Bulletin of the Chemical Society of Japan* **1980**, *53*, 3705-3706.
- (348) Qi, X.; Watanabe, M.; Aida, T. M.; Smith, R. L., Jr.: Catalytic Dehydration of Fructose into 5-Hydroxymethylfurfural by Ion-Exchange Resin in Mixed-Aqueous System by Microwave Heating. *Green Chemistry* **2008**, *10*, 799-805.
- (349) Rigal, L.; Gorrichon, J. P.; Gaset, A.; Heughebaert, J. C.: Optimization of the Conversion of D-Fructose to 5-Hydroxymethyl-2-Furancarboxaldehyde in a Water-Solvent-Ion-Exchanger Triphasic System 1. Investigation of the Main Effects of the Major Parameters and of their Interactions on the Reaction. *Biomass* **1985**, *7*, 27-45.
- (350) Gaset, A.; Rigal, L.; Paillassa, G.; Salomé, J.-P.; Flèche, G.: Process for Manufacturing 5-Hydroxymethylfurfural. In *United States Patent: 4,590,283*; Roquette Freres: USA, 1986; pp 6.
- (351) Suarez-Pereira, E.; Rubio, E. M.; Pilard, S.; Mellet, C. O.; Fernandez, J. M. G.: Di-D-fructose Dianhydride-Enriched Products by Acid Ion-Exchange Resin-Promoted Caramelization of D-Fructose: Chemical Analyses. *Journal of Agricultural and Food Chemistry* **2010**, *58*, 1777-1787.
- (352) Crisci, A. J.; Tucker, M. H.; Lee, M.-Y.; Jang, S. G.; Dumesic, J. A.; Scott, S. L.: Add-Functionalized SBA-15-Type Silica Catalysts for Carbohydrate Dehydration. *Advanced Synthesis & Catalysis* **2011**, *1*, 719-728.
- (353) Guo, X.; Cao, Q.; Jiang, Y.; Guan, J.; Wang, X.; Mu, X.: Selective Dehydration of Fructose to 5-Hydroxymethylfurfural Catalyzed by Mesoporous SBA-15-SO₃H in Ionic Liquid [Bmim]Cl. *Carbohydrate Research* **2012**, *351*, 35-41.
- (354) Guo, F.; Fang, Z.; Zhou, T.-J.: Conversion of Fructose and Glucose into 5-Hydroxymethylfurfural With Lignin-Derived Carbonaceous Catalyst under Microwave Irradiation in Dimethyl Sulfoxide Ionic Liquid Mixtures. *Bioresource Technology* **2012**, *112*, 313-318.
- (355) Zhang, Y.; Degirmenci, V.; Li, C.; Hensen, E. J. M.: Phosphotungstic Acid Encapsulated in Metal-Organic Framework as Catalysts for Carbohydrate Dehydration to 5-Hydroxymethylfurfural. *ChemSusChem* **2011**, *4*, 59-64.
- (356) Vigier, K. D. O.; Benguerba, A.; Barrault, J.; Jerome, F.: Conversion of Fructose and Inulin to 5-Hydroxymethylfurfural in Sustainable Betaine Hydrochloride-Based Media. *Green Chemistry* **2012**, *14*, 285-289.
- (357) Lourvanij, K.; Rorrer, G. L.: Reaction Rates for the Partial Dehydration of Glucose to Organic Acids in Solid-Acid, Molecular-Sieving Catalyst Powders. *Journal of Chemical Technology and Biotechnology* **1997**, *69*, 35-44.

- (358) Moreau, C.; Durand, R.; Alies, F. R.; Cotillon, M.; Frutz, T.; Theoleyre, M. A.: Hydrolysis of Sucrose in the Presence of H-Form Zeolites. *Industrial Crops and Products* **2000**, *11*, 237-242.
- (359) Sidhpuria, K. B.; Daniel, A. L. D. S.; Trindade, T.; Coutinho, J. A. P.: Supported Ionic Liquid Silica Nanoparticles (SILnPs) as an Efficient and Recyclable Heterogeneous Catalyst for the Dehydration of Fructose to 5-Hydroxymethylfurfural. *Green Chemistry* **2011**, *13*, 340-349.
- (360) Moliner, M.; Roman-Leshkov, Y.; Davis, M. E.: Tin-Containing Zeolites are Highly Active Catalysts for the Isomerization of Glucose in Water. *Proceedings of the National Academy of Sciences of the United States of America* **2010**, *107*, 6164-6168.
- (361) Jow, J.; Rorrer, G. L.; Hawley, M. C.; Lampert, D. T. A.: Dehydration of D-Fructose to Levulinic Acid over LZV Zeolite Catalyst. *Biomass* **1987**, *14*, 185-194.
- (362) Qu, Y.; Huang, C.; Zhang, J.; Chen, B.: Efficient Dehydration of Fructose to 5-Hydroxymethylfurfural Catalyzed by a Recyclable Sulfonated Organic Heteropolyacid Salt. *Bioresource Technology* **2012**, *106*, 170-172.
- (363) Watanabe, M.; Aizawa, Y.; Iida, T.; Aida, T. M.; Levy, C.; Sue, K.; Inomata, H.: Glucose Reactions With Acid and Base Catalysts in Hot Compressed Water at 473 K. *Carbohydrate Research* **2005**, *340*, 1925-1930.
- (364) Qi, X.; Guo, H.; Li, L.: Efficient Conversion of Fructose to 5-Hydroxymethylfurfural Catalyzed by Sulfated Zirconia in Ionic Liquids. *Industrial & Engineering Chemistry Research* **2011**, *50*, 7985-7989.
- (365) McNeff, C. V.; Nowlan, D. T.; McNeff, L. C.; Yan, B.; Fedie, R. L.: Continuous Production of 5-Hydroxymethylfurfural From Simple and Complex Carbohydrates. *Applied Catalysis A-General* **2010**, *384*, 65-69.
- (366) Qi, X.; Watanabe, M.; Aida, T. M.; Smith, R. L., Jr.: Catalytic Conversion of Fructose and Glucose into 5-Hydroxymethylfurfural in Hot Compressed Water by Microwave Heating. *Catalysis Communications* **2008**, *9*, 2244-2249.
- (367) Qi, X.; Watanabe, M.; Aida, T. M.; Smith, R. L., Jr.: Sulfated Zirconia as a Solid Acid Catalyst for the Dehydration of Fructose to 5-Hydroxymethylfurfural. *Catalysis Communications* **2009**, *10*, 1771-1775.
- (368) Watanabe, M.; Aizawa, Y.; Iida, T.; Nishimura, R.; Inomata, H.: Catalytic Glucose and Fructose Conversions With TiO₂ and ZrO₂ in Water at 473 K: Relationship Between Reactivity and Acid-Base Property Determined by TPD Measurement. *Applied Catalysis A-General* **2005**, *295*, 150-156.
- (369) Qi, X.; Watanabe, M.; Aida, T. M.; Smith, R. L.: Synergistic Conversion of Glucose into 5-Hydroxymethylfurfural in Ionic Liquid-Water Mixtures. *Bioresource Technology* **2012**, *109*, 224-228.
- (370) Yan, H.; Yang, Y.; Tong, D.; Xiang, X.; Hu, C.-W.: Catalytic Conversion of Glucose to 5-Hydroxymethylfurfural Over SO₄²⁻/ZrO₂ and SO₄²⁻/ZrO₂-Al₂O₃ Solid Acid Catalysts. *Catalysis Communications* **2009**, *10*, 1558-1563.
- (371) Ordonsky, V. V.; Schouten, J. C.; Schaaf, J. V. D.; Nijhuis, T. A.: Zirconium Phosphate Coating on Aluminum Foams by Electrophoretic Deposition for Acidic Catalysis. *ChemCatChem* **2012**, *4*, 129-133.
- (372) Dutta, S.; De, S.; Patra, A. K.; Sasidharan, M.; Bhaumik, A.; Saha, B.: Microwave Assisted Rapid Conversion of Carbohydrates Into 5-Hydroxymethylfurfural Catalyzed by Mesoporous TiO₂ Nanoparticles. *Applied Catalysis A-General* **2011**, *409*, 133-139.
- (373) Zhang, Z.; Wang, Q.; Xie, H.; Liu, W.; Zhao, Z.: Catalytic Conversion of Carbohydrates into 5-Hydroxymethylfurfural by Germanium(IV) Chloride in Ionic Liquids. *ChemSusChem* **2011**, *4*, 131-138.
- (374) Hu, S.; Zhang, Z.; Song, J.; Zhou, Y.; Han, B.: Efficient Conversion of Glucose into 5-Hydroxymethylfurfural Catalyzed by a Common Lewis Acid SnCl₄ in an Ionic Liquid. *Green Chemistry* **2009**, *11*, 1746-1749.
- (375) Tong, X.; Li, M.; Yan, N.; Ma, Y.; Dyson, P. J.; Li, Y.: Defunctionalization of Fructose and Sucrose: Iron-Catalyzed Production of 5-Hydroxymethylfurfural From Fructose and Sucrose. *Catalysis Today* **2011**, *175*, 524-527.
- (376) Tao, F.; Song, H.; Chou, L.: Hydrolysis of Cellulose by Using Catalytic Amounts of FeCl₂ in Ionic Liquids. *ChemSusChem* **2010**, *3*, 1298-1303.
- (377) Tao, F.; Song, H.; Chou, L.: Catalytic Conversion of Cellulose to Chemicals in Ionic Liquid. *Carbohydrate Research* **2011**, *346*, 58-63.

- (378) Hashaikheh, R.; Butler, I. S.; Kozinski, J. A.: Selective Promotion of Catalytic Reactions During Biomass Gasification to Hydrogen. *Energy & Fuels* **2006**, *20*, 2743-2747.
- (379) Yang, F.; Liu, Q.; Yue, M.; Bai, X.; Du, Y.: Tantalum Compounds as Heterogeneous Catalysts for Saccharide Dehydration to 5-Hydroxymethylfurfural. *Chemical Communications* **2011**, *47*, 4469-4471.
- (380) Carniti, P.; Gervasini, A.; Biella, S.; Auroux, A.: Niobic Acid and Niobium Phosphate as Highly Acidic Viable Catalysts in Aqueous Medium: Fructose Dehydration Reaction. *Catalysis Today* **2006**, *118*, 373-378.
- (381) Carlini, C.; Giuttari, M.; Galletti, A. M. R.; Sbrana, G.; Armaroli, T.; Busca, G.: Selective Saccharides Dehydration to 5-Hydroxymethyl-2-Furaldehyde by Heterogeneous Niobium Catalysts. *Applied Catalysis A-General* **1999**, *183*, 295-302.
- (382) Carniti, P.; Gervasini, A.; Marzo, M.: Absence of Expected Side Reactions in the Dehydration Reaction of Fructose to Hmf in Water Over Niobic Acid Catalyst. *Catalysis Communications* **2011**, *12*, 1122-1126.
- (383) Armaroli, T.; Busca, G.; Carlini, C.; Giuttari, M.; Galletti, A. M. R.; Sbrana, G.: Acid Sites Characterization of Niobium Phosphate Catalysts and their Activity in Fructose Dehydration to 5-Hydroxymethyl-2-Furaldehyde. *Journal of Molecular Catalysis A-Chemical* **2000**, *151*, 233-243.
- (384) Yang, F.; Liu, Q.; Bai, X.; Du, Y.: Conversion of Biomass into 5-Hydroxymethylfurfural Using Solid Acid Catalyst. *Bioresource Technology* **2011**, *102*, 3424-3429.
- (385) Ribeiro, M. L.; Schuchardt, U.: Cooperative Effect of Cobalt Acetylacetonate and Silica in the Catalytic Cyclization and Oxidation of Fructose to 2,5-Furandicarboxylic Acid. *Catalysis Communications* **2003**, *4*, 83-86.
- (386) Carlini, C.; Patrono, P.; Galletti, A. M. R.; Sbrana, G.: Heterogeneous Catalysts Based on Vanadyl Phosphate for Fructose Dehydration to 5-Hydroxymethyl-2-Furaldehyde. *Applied Catalysis A-General* **2004**, *275*, 111-118.
- (387) Lourvanij, K.; Rorrer, G. L.: Dehydration of Glucose to Organic Acids in Microporous Pillared Clay Catalysts. *Applied Catalysis A-General* **1994**, *109*, 147-165.
- (388) Beckerle, K.; Okuda, J.: Conversion of Glucose and Cellobiose into 5-Hydroxymethylfurfural (Hmf) by Rare Earth Metal Salts in N,N'-Dimethylacetamide (DMA). *Journal of Molecular Catalysis A-Chemical* **2012**, *356*, 158-164.
- (389) Wang, F.; Shi, A.-W.; Qin, X.-X.; Liu, C.-L.; Dong, W.-S.: Dehydration of Fructose to 5-Hydroxymethylfurfural By Rare Earth Metal Trifluoromethanesulfonates in Organic Solvents. *Carbohydrate Research* **2011**, *346*, 982-985.
- (390) Ishida, H.; Seri, K.: Catalytic Activity of Lanthanoide(III) Ions for Dehydration of D-glucose to 5-Hydroxymethylfurfural. *Journal of Molecular Catalysis A-Chemical* **1996**, *112*, L163-L165.
- (391) Ståhlberg, T.; Sörensen, M. G.; Riisager, A.: Direct Conversion of Glucose to 5-(Hydroxymethyl)furfural in Ionic Liquids With Lanthanide Catalysts. *Green Chemistry* **2010**, *12*, 321-325.
- (392) Ståhlberg, T.; Rodriguez, S. R.; Fristrup, P.; Riisager, A.: Metal-Free Dehydration of Glucose to 5-(Hydroxymethyl)furfural in Ionic Liquids with Boric Acid as a Promoter. *Chemistry-A European Journal* **2011**, *17*, 1456-1464.
- (393) Jarvis, M.: Chemistry - Cellulose Stacks Up. *Nature* **2003**, *426*, 611-612.
- (394) Climent, M. J.; Corma, A.; Iborra, S.: Converting Carbohydrates to Bulk Chemicals and Fine Chemicals over Heterogeneous Catalysts. *Green Chemistry* **2011**, *13*, 520-540.
- (395) Wei, S.; Kumar, V.; Banker, G. S.: Phosphoric Acid Mediated Depolymerization and Decrystallization of Cellulose: Preparation of Low Crystallinity Cellulose - A New Pharmaceutical Excipient. *International Journal of Pharmaceutics* **1996**, *142*, 175-181.
- (396) Zhang, Y.-H. P.; Ding, S.-Y.; Mielenz, J. R.; Cui, J.-B.; Elander, R. T.; Laser, M.; Himmel, M. E.; McMillan, J. R.; Lynd, L. R.: Fractionating Recalcitrant Lignocellulose at Modest Reaction Conditions. *Biotechnology and Bioengineering* **2007**, *97*, 214-223.
- (397) Zhang, Y. H. P.; Cui, J. B.; Lynd, L. R.; Kuang, L. R.: A Transition From Cellulose Swelling to Cellulose Dissolution by o-Phosphoric Acid: Evidence From Enzymatic Hydrolysis and Supramolecular Structure. *Biomacromolecules* **2006**, *7*, 644-648.
- (398) Zhang, J.; Zhang, J.; Lin, L.; Chen, T.; Zhang, J.; Liu, S.; Li, Z.; Ouyang, P.: Dissolution of Microcrystalline Cellulose in Phosphoric Acid-Molecular Changes and Kinetics. *Molecules* **2009**, *14*, 5027-5041.

- (399) Whitmore, R. E.; Atalla, R. H.: Factors Influencing the Regeneration of Cellulose-I- From Phosphoric Acid. *International Journal of Biological Macromolecules* **1985**, *7*, 182-186.
- (400) Mosier, N.; Wyman, C.; Dale, B.; Elander, R.; Lee, Y. Y.; Holtzapfle, M.; Ladisch, M.: Features of Promising Technologies for Pre-Treatment of Lignocellulosic Biomass. *Bioresource Technology* **2005**, *96*, 673-686.
- (401) Jones, R. E.; Lange, H. B.: Purification of Hydroxymethylfurfural. In *United States Patent Office: 2,994,645*; Merck & Co., Inc. Rahway, New Jersey, USA: USA, 1961; pp 3.
- (402) Hunter, R. H.: Purification of Hydroxymethylfurfural. In *United States Patent Office: 3,201,331*; Atlas Chemical Industries, Inc., Wilmington, Delaware, USA: USA, 1965; pp 5.
- (403) Bourbigou, H. O.; Magna, L.; Morvan, D.: Ionic liquids and Catalysis: Recent Progress from Knowledge to Applications. *Applied Catalysis A-General* **2010**, *373*, 1-56.
- (404) Sing, K. S. W.; Everett, D. H.; Haul, R. A. W.; Moscou, L.; Pierotti, R. A.; Rouquerol, J.; Siemieniowska, T.: Reporting Physisorption Data for Gas Solid Systems With Special Reference to the Determination of Surface Area and Porosity (Recommendations 1984). *Pure and Applied Chemistry* **1985**, *57*, 603-619.
- (405) Rouquerol, J.; Avnir, D.; Fairbridge, C. W.; Everett, D. H.; Haynes, J. H.; Pernicone, N.; Ramsay, J. D. F.; Sing, K. S. W.; Unger, K. K.: Recommendations for the Characterization of Porous Solids. *Pure and Applied Chemistry* **1994**, *66*, 1739-1758.
- (406) Illia, G. J. D. S.; Sanchez, C.; Lebeau, B.; Patarin, J.: Chemical Strategies to Design Textured Materials: From Microporous and Mesoporous Oxides to Nanonetworks and Hierarchical Structures. *Chemical Reviews* **2002**, *102*, 4093-4138.
- (407) Ordonsky, V. V.; van der Schaaf, J.; Schouten, J. C.; Nijhuis, T. A.: Fructose Dehydration to 5-Hydroxymethylfurfural over Solid Acid Catalysts in a Biphasic System. *ChemSusChem* **2012**, *5*, 1812-1819.
- (408) Corma, A.; Fornes, V.; Pergher, S. B.; Maesen, T. L. M.; Buglass, J. G.: Delaminated Zeolite Precursors as Selective Acidic Catalysts. *Nature* **1998**, *396*, 353-356.
- (409) Corma, A.; Fornes, V.; Triguero, J. M.; Pergher, S. B.: Delaminated Zeolites: Combining the Benefits of Zeolites and Mesoporous Materials for Catalytic Uses. *Journal of Catalysis* **1999**, *186*, 57-63.
- (410) Corma, A.; Díaz, U.; Domine, M. E.; Fornés, V.: New Aluminosilicate and Titanosilicate Delaminated Materials Active for Acid Catalysis, and Oxidation Reactions Using H₂O₂. *Journal of the American Chemical Society* **2000**, *122*, 2804-2809.
- (411) Corma, A.; Fornés, V.; Díaz, U.: ITQ-18 a New Delaminated Stable Zeolite. *Chemical Communications* **2001**, 2642-2643.
- (412) Canós, A. C.; Seguí, V. F.; Morales, F. J.: Microporous Acidic Oxide With Catalytic Properties ITQ-18. In *United States Patent: US 6,696,033 B2*; Consejo Superior de Investigaciones Científicas, Madrid, Spain; Universidad Politecnica de Valencia, Valencia, Spain: Spain 2004.
- (413) Zubowa, H.-L.; Schneider, M.; Schreier, E.; Eckelt, R.; Richter, M.; Fricke, R.: The Influence of the Expanding and Exfoliating Conditions on the Structural Transformation of the Layered zeolite Nu-6(1). *Microporous and Mesoporous Materials* **2008**, *109*, 317-326.
- (414) Zhao, D. Y.; Feng, J. L.; Huo, Q. S.; Melosh, N.; Fredrickson, G. H.; Chmelka, B. F.; Stucky, G. D.: Triblock Copolymer Syntheses of Mesoporous Silica With Periodic 50 to 300 Angstrom Pores. *Science* **1998**, *279*, 548-552.
- (415) Toda, M.; Takagaki, A.; Okamura, M.; Kondo, J. N.; Hayashi, S.; Domen, K.; Hara, M.: Green Chemistry - Biodiesel Made With sugar Catalyst. *Nature* **2005**, *438*, 178-178.
- (416) Zhao, D. Y.; Huo, Q. S.; Feng, J. L.; Chmelka, B. F.; Stucky, G. D.: Nonionic Triblock and Star Diblock Copolymer and Oligomeric Surfactant Syntheses of Highly Ordered, Hydrothermally Stable, Mesoporous Silica Structures. *Journal of the American Chemical Society* **1998**, *120*, 6024-6036.
- (417) Takagaki, A.; Sugisawa, M.; Lu, D. L.; Kondo, J. N.; Hara, M.; Domen, K.; Hayashi, S.: Exfoliated Nanosheets as a New Strong Solid Acid Catalyst. *Journal of the American Chemical Society* **2003**, *125*, 5479-5485.
- (418) Siril, P. R.; Cross, H. E.; Brown, D. R.: New Polystyrene Sulfonic Acid Resin Catalysts With Enhanced Acidic and Catalytic Properties. *Journal of Molecular Catalysis A-Chemical* **2008**, *279*, 63-68.
- (419) Plechkova, N. V.; Seddon, K. R.: Applications of Ionic Liquids in the Chemical Industry. *Chemical Society Reviews* **2008**, *37*, 123-150.

- (420) Graenacher, C.: Cellulose Dissolution. In *United States Patent Office: 1,943,176*; Society of Chemical Industrial, Basle, Basel, Switzerland: USA, 1934; pp 4.
- (421) Hurley, F. H.: Electrodeposition of Aluminum. In *United States Patent Office: 2,446,331*; The William Marsh Rice Institute for the Advancement of Literature, Science and Art, a corporation of Texas: USA, 1948; pp 2.
- (422) Chum, H. L.; Koch, V. R.; Miller, L. L.; Osteryoung, R. A.: Electrochemical Scrutiny of Organometallic Iron Complexes and Hexamethylbenzene in a Room Temperature Molten Salt. *Journal of the American Chemical Society* **1975**, *97*, 3264-3265.
- (423) Fields, M.; Thied, R. C.; Seddon, K. R.; Pitner, W. R.; Rooney, D. W.: Treatment of Molten Salt Reprocessing Wastes. In *World Intellectual Property Organization: WO 99/14160*; British Nuclear Fuels Plc, Great Britain; Fields, M., Great Britain, Thield, R.C., Great Britain, Seddon, K.R. Great Britain, Pitner, W.R. Great Britain, Rooney, D.W. Great Britain: Great Britain, 1999; pp 26.
- (424) Huddleston, J. G.; Visser, A. E.; Reichert, W. M.; Willauer, H. D.; Broker, G. A.; Rogers, R. D.: Characterization and Comparison of Hydrophilic and Hydrophobic Room Temperature Ionic Liquids Incorporating the Imidazolium Cation. *Green Chemistry* **2001**, *3*, 156-164.
- (425) Smiglak, M.; Metlen, A.; Rogers, R. D.: The Second Evolution of Ionic Liquids: From Solvents and Separations to Advanced Materials-Energetic Examples From the Ionic Liquid Cook book. *Accounts of Chemical Research* **2007**, *40*, 1182-1192.
- (426) Murugesan, S.; Linhardt, R. J.: Ionic liquids in Carbohydrate Chemistry - Current Trends and Future Directions. *Current Organic Synthesis* **2005**, *2*, 437-451.
- (427) Martino, W.; Mora, J. F. D. L.; Yoshida, Y.; Saito, G.; Wilkes, J.: Surface Tension Measurements of Highly Conducting Ionic Liquids. *Green Chemistry* **2006**, *8*, 390-397.
- (428) Feng, L.; Chen, Z.-I.: Research Progress on Dissolution and Functional Modification of Cellulose in Ionic Liquids. *Journal of Molecular Liquids* **2008**, *142*, 1-5.
- (429) Zakrzewska, M. E.; Lukasik, E. B.; Lukasik, R. B.: Solubility of Carbohydrates in Ionic Liquids. *Energy & Fuels* **2010**, *24*, 737-745.
- (430) Pinkert, A.; Marsh, K. N.; Pang, S.; Staiger, M. P.: Ionic Liquids and Their Interaction with Cellulose. *Chemical Reviews* **2009**, *109*, 6712-6728.
- (431) Remsing, R. C.; Swatloski, R. P.; Rogers, R. D.; Moyna, G.: Mechanism of Cellulose Dissolution in the Ionic Liquid 1-n-Butyl-3-Methylimidazolium Chloride: a ¹³C- and ^{35/37}Cl- NMR Relaxation Study on Model Systems. *Chemical Communications* **2006**, 1271-1273.
- (432) Lai, L.; Zhang, Y.: The Effect of Imidazolium Ionic Liquid on the Dehydration of Fructose to 5-Hydroxymethylfurfural, and a Room Temperature Catalytic System. *ChemSusChem* **2010**, *3*, 1257-1259.
- (433) Zavrel, M.; Bross, D.; Funke, M.; Buechs, J.; Spiess, A. C.: High-Throughput Screening for Ionic Liquids Dissolving (Ligno-)Cellulose. *Bioresource Technology* **2009**, *100*, 2580-2587.
- (434) Lee, S. H.; Doherty, T. V.; Linhardt, R. J.; Dordick, J. S.: Ionic Liquid-Mediated Selective Extraction of Lignin From Wood Leading to Enhanced Enzymatic Cellulose Hydrolysis. *Biotechnology and Bioengineering* **2009**, *102*, 1368-1376.
- (435) Stinson, S. C.: Fine Chemicals' Healthy Ferment. *Chemical & Engineering News* **1998**, *76*, 57-73.
- (436) Swatloski, R. P.; Spear, S. K.; Holbrey, J. D.; Rogers, R. D.: Dissolution of Cellose With Ionic Liquids. *Journal of the American Chemical Society* **2002**, *124*, 4974-4975.
- (437) Liebert, T.; Heinze, T.: Interaction of Ionic Liquids With Polysaccharides 5. Solvents and Reaction Media for the Modification of Cellulose. *Bioresources* **2008**, *3*, 576-601.
- (438) Fukaya, Y.; Sugimoto, A.; Ohno, H.: Superior Solubility of Polysaccharides in Low Viscosity, Polar, and Halogen-Free 1,3-Dialkylimidazolium Formates. *Biomacromolecules* **2006**, *7*, 3295-3297.
- (439) Zhang, H.; Wu, J.; Zhang, J.; He, J. S.: 1-Allyl-3-Methylimidazolium Chloride Room Temperature Ionic Liquid: A New and Powerful Non-Derivatizing Solvent for Cellulose. *Macromolecules* **2005**, *38*, 8272-8277.
- (440) Wu, J.; Zhang, J.; Zhang, H.; He, J. S.; Ren, Q.; Guo, M.: Homogeneous Acetylation of Cellulose in a New Ionic Liquid. *Biomacromolecules* **2004**, *5*, 266-268.
- (441) Fukaya, Y.; Hayashi, K.; Wada, M.; Ohno, H.: Cellulose Dissolution With Polar Ionic Liquids Under Mild Conditions: Required Factors for Anions. *Green Chemistry* **2008**, *10*, 44-46.

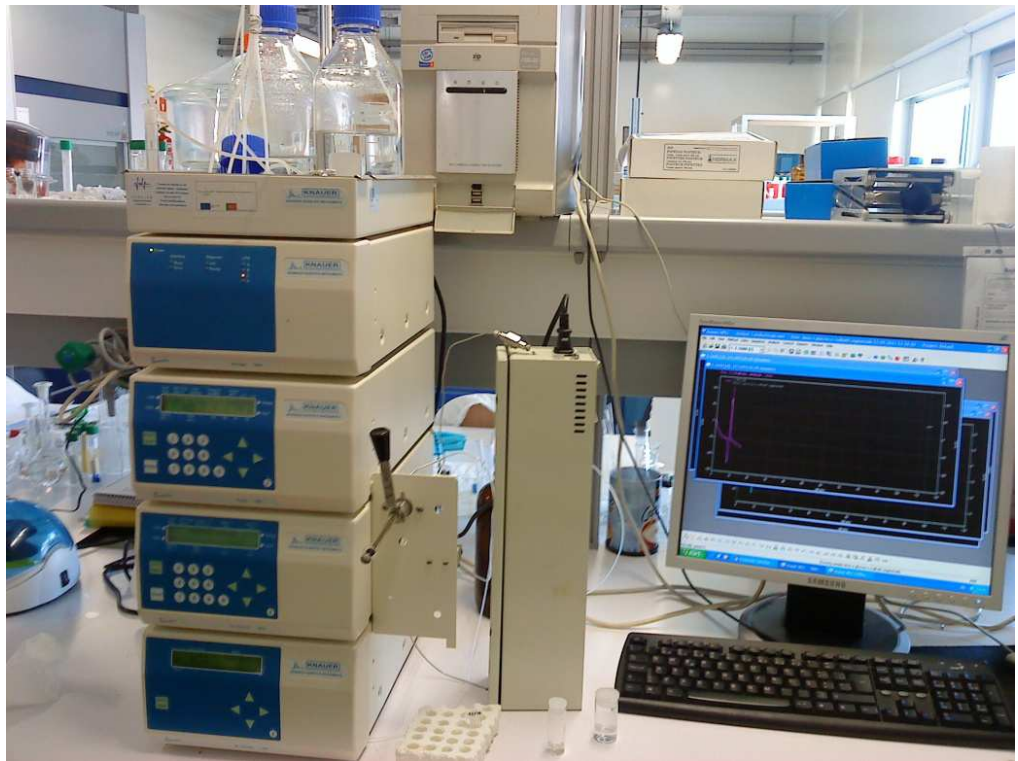
- (442) Egorov, V. M.; Smirnova, S. V.; Formanovsky, A. A.; Pletnev, I. V.; Zolotov, Y. A.: Dissolution of Cellulose in Ionic Liquids as a Way to Obtain Test Materials for Metal-Ion Detection. *Analytical and Bioanalytical Chemistry* **2007**, *387*, 2263-2269.
- (443) Heinze, T.; Schwikal, K.; Barthel, S.: Ionic Liquids as Reaction Medium in Cellulose Functionalization. *Macromolecular Bioscience* **2005**, *5*, 520-525.
- (444) Barthel, S.; Heinze, T.: Acylation and Carbanilation of Cellulose in Ionic Liquids. *Green Chemistry* **2006**, *8*, 301-306.
- (445) Schlufte, K.; Schmauder, H.-P.; Dorn, S.; Heinze, T.: Efficient Homogeneous Chemical Modification of Bacterial Cellulose in the Ionic Liquid 1-N-Butyl-3-Methylimidazolium Chloride. *Macromolecular Rapid Communications* **2006**, *27*, 1670-1676.
- (446) Zimmermann, J.; Ondruschka, B.; Stark, A.: Efficient Synthesis of 1,3-Dialkylimidazolium-Based Ionic Liquids: The Modified Continuous Radziszewski Reaction in a Microreactor Setup. *Organic Process Research & Development* **2010**, *14*, 1102-1109.
- (447) Hermanutz, F.; Gäehr, F.; Uerdingen, E.; Meister, F.; Kosan, B.: New Developments in Dissolving and Processing of Cellulose in Ionic Liquids. *Macromolecular Symposia* **2008**, *262*, 23-27.
- (448) Zhao, H.; Baker, G. A.; Song, Z.; Olubajo, O.; Crittle, T.; Peters, D.: Designing Enzyme-Compatible Ionic Liquids That Can Dissolve Carbohydrates. *Green Chemistry* **2008**, *10*, 696-705.
- (449) Chen, T.; Chidambaram, M.; Liu, Z.; Smit, B.; Bell, A. T.: Viscosities of the Mixtures of 1-Ethyl-3-Methylimidazolium Chloride with Water, Acetonitrile and Glucose: A Molecular Dynamics Simulation and Experimental Study. *Journal of Physical Chemistry B* **2010**, *114*, 5790-5794.
- (450) Seddon, K. R.; Stark, A.; Torres, M. J.: Influence of Chloride, Water, and Organic Solvents on the Physical Properties of Ionic Liquids. *Pure and Applied Chemistry* **2000**, *72*, 2275-2287.
- (451) Hoffmann, J.; Nuchter, M.; Ondruschka, B.; Wasserscheid, P.: Ionic Liquids and Their Heating Behaviour During Microwave Irradiation - A State of the Art Report and Challenge to Assessment. *Green Chemistry* **2003**, *5*, 296-299.
- (452) Palou, R. M.: Ionic liquid and Microwave-Assisted Organic Synthesis: A "Green" and synergic couple. *Journal of the Mexican Chemical Society* **2007**, *51*, 252-264.
- (453) Froeba, A. P.; Kremer, H.; Leipertz, A.: Density, Refractive Index, Interfacial Tension, and Viscosity of Ionic Liquids [Emim]EtSO₄, [Emim]NTf₂, [Emim]NCN₂, and [OMA]NTf₂ in Dependence on Temperature at Atmospheric Pressure. *Journal of Physical Chemistry B* **2008**, *112*, 12420-12430.
- (454) Zhao, H.; Holladay, J. E.; Zhang, Z. C.: Methods for Conversion of Carbohydrates in Ionic Liquids to Value-Added Chemicals. In *United States Patent Application Publication: US 2010/0317879 A1*; Battelle Memorial Institute ATTN: IP Services, Richland, Washington, USA: USA, 2010; pp 16.
- (455) Zhang, Y.; Chan, J. Y. G.: Production of Hydroxymethylfurfural. In *United States Patent Application Publication: US 2009/0313889 A1*; Agency for Science, Technology and Research, Singapore: USA, 2009; pp 20.
- (456) Zhao, H.; Holladay, J. E.; Zhang, Z. C.: Method for Conversion of Carbohydrates in Ionic Liquids to Hydroxymethylfurfural. In *International Application Published under the Patent Cooperation Treaty (PCT): WO/2008/019219 A1*; Battelle Memorial Institute, Pacific Northwest Division, Intellectual Property Legal Services, Richland, USA: USA, 2008; pp 53.
- (457) Zhang, Y.; Ying, J. Y.; Yong, G.: Production of Hydroxymethylfurfural. In *International Application Published Under Patent Cooperation Treaty (PCT): WO 2009/154566 A1*; Agency for Science, Technology and Research, Centros, Singapore: Singapore, 2009; pp 22.
- (458) Zakrzewska, M. E.; Lukasik, E. B.; Lukasik, R. B.: Ionic Liquid-Mediated Formation of 5-Hydroxymethylfurfural-A Promising Biomass-Derived Building Block. *Chemical Reviews* **2011**, *111*, 397-417.
- (459) Ståhlberg, T.; Fu, W.; Woodley, J. M.; Riisager, A.: Synthesis of 5-(Hydroxymethyl)furfural in Ionic Liquids: Paving the Way to Renewable Chemicals. *ChemSusChem* **2011**, *4*, 451-458.
- (460) Zhang, Y.; Du, H.; Qian, X.; Chen, E. Y. X.: Ionic Liquid-Water Mixtures: Enhanced K-w for Efficient Cellulosic Biomass Conversion. *Energy & Fuels* **2010**, *24*, 2410-2417.
- (461) Tong, X.; Ma, Y.; Li, Y.: An Efficient Catalytic Dehydration of Fructose and Sucrose to 5-Hydroxymethylfurfural With Protic Ionic Liquids. *Carbohydrate Research* **2010**, *345*, 1698-1701.
- (462) Ranganathan, M.; Balaram, P.: Trifluoroacetic-Anhydride- A Convenient NMR Solvent for Carbohydrates - 270 MHz ¹H NMR Studies of 2-Acetamido-2-Deoxyhexoses. *Organic Magnetic Resonance* **1980**, *13*, 220-223.

- (463) Li, C.; Zhao, Z. K.; Wang, A.; Zheng, M.; Zhang, T.: Production of 5-Hydroxymethylfurfural in Ionic Liquids Under High Fructose Concentration Conditions. *Carbohydrate Research* **2010**, *345*, 1846-1850.
- (464) Sievers, C.; Olarte, M. B. V.; Marzalletti, T.; Musin, D.; Agrawal, P. K.; Jones, C. W.: Ionic-Liquid-Phase Hydrolysis of Pine Wood. *Industrial & Engineering Chemistry Research* **2009**, *48*, 1277-1286.
- (465) Cui, X.; Zhang, S.; Shi, F.; Zhang, Q.; Ma, X.; Lu, L.; Deng, Y.: The Influence of the Acidity of Ionic Liquids on Catalysis. *ChemSusChem* **2010**, *3*, 1043-1047.
- (466) MacFarlane, D. R.; Pringle, J. M.; Johansson, K. M.; Forsyth, S. A.; Forsyth, M.: Lewis Base Ionic Liquids. *Chemical Communications* **2006**, 1905-1917.
- (467) Katritzky, A. R.; Kuanar, M.; Slavova, I. B. S.; Slavov, S. H.; Dobchev, D. A.; Karelson, M.; Acree, W. E., Jr.: Quantitative Structure-Property Relationship Studies on Ostwald Solubility and Partition Coefficients of Organic Solutes in Ionic Liquids. *Journal of Chemical and Engineering Data* **2008**, *53*, 1085-1092.
- (468) Yong, G.; Zhang, Y.; Ying, J. Y.: Efficient Catalytic System for the Selective Production of 5-Hydroxymethylfurfural From Glucose and Fructose. *Angewandte Chemie* **2008**, *120*, 9485-9488.
- (469) Zhang, Z.; Liu, B.; Zhao, Z.: Conversion of Fructose Into 5-Hmf Catalyzed by GeCl₄ in DMSO and BmimCl System at Room Temperature. *Carbohydr. Polym.* **2012**, *88*, 891-895.
- (470) Pidko, E. A.; Degirmenci, V.; Santen, R. A. V.; Hensen, E. J. M.: Glucose Activation by Transient Cr²⁺ Dimers. *Angewandte Chemie-International Edition* **2010**, *49*, 2530-2534.
- (471) Pidko, E. A.; Degirmenci, V.; Santen, R. A. V.; Hensen, E. J. M.: Glucose Activation by Transient Cr²⁺ dimers. *Angewandte Chemie* **2010**, *122*, 2584-2588.
- (472) Zhang, Z.; Zhao, Z.: Production of 5-Hydroxymethylfurfural From Glucose Catalyzed by Hydroxyapatite Supported Chromium Chloride. *Bioresource Technology* **2011**, *102*, 3970-3972.
- (473) Kjaer, A. M.; Sorensen, P. E.; Ulstrup, J.: Water-Catalyzed Mutarotation of Glucose and Tetra Methyl Glucose in Dioxan, Acetonitrile, and Dimethylsulfoxide. *Journal of the Chemical Society-Perkin Transactions 2* **1978**, 51-59.
- (474) Lichtenthaler, F. W.; Martin, E. C. D.; Rönninger, M. S.; Weber, T.: Practical Routes from Mono- and Disaccharides to Building Blocks with Industrial Application Profiles. In *Carbohydrates as Organic Raw Materials*; VCH: Weinheim, Germany, 1991; pp 207-246.
- (475) Pidko, E. A.; Degirmenci, V.; Hensen, E. J. M.: On the Mechanism of Lewis Acid Catalyzed Glucose Transformations in Ionic Liquids. *ChemCatChem* **2012**, *4*, 1263-1271.
- (476) McCormick, C. L.; Callais, P. A.; Hutchinson, B. H.: Solution Studies of Cellulose in Lithium Chloride and *N, N*-Dimethylacetamide. *Macromolecules* **1985**, *18*, 2394-2401.
- (477) Rinaldi, R.; Palkovits, R.; Schueth, F.: Depolymerization of Cellulose Using Solid Catalysts in Ionic Liquids. *Angewandte Chemie-International Edition* **2008**, *47*, 8047-8050.
- (478) Rinaldi, R.; Palkovits, R.; Schueth, F.: Depolymerization of Cellulose Using Solid Catalysts in Ionic Liquids. *Angewandte Chemie* **2008**, *120*, 8167-8170.
- (479) Kim, S.-J.; Dwiatmoko, A. A.; Choi, J. W.; Suh, Y.-W.; Suh, D. J.; Oh, M.: Cellulose Pretreatment With 1-*n*-Butyl-3-Methylimidazolium Chloride for Solid Acid-Catalyzed Hydrolysis. *Bioresource Technology* **2010**, *101*, 8273-8279.
- (480) Watanabe, H.: The Study of Factors Influencing the Depolymerisation of Cellulose Using a Solid Catalyst in Ionic Liquids. *Carbohydr. Polym.* **2010**, *80*, 1168-1171.
- (481) Schüth, F.; Rinaldi, R.; Engel, P.; Spiess, A.; Büchs, J.: Method for the Hydrolysis of Cellulose Raw Materials. In *World Intellectual Property Organization: WO/2010/111995*; Studiengesellschaft Kohle MBH, Mülheim au der Ruhr, Germany; Rheinisch-Westfälische Technische Hochschule Aachen, Germany: Germany, 2010; pp 14.
- (482) Degirmenci, V.; Pidko, E. A.; Magusin, P. C. M. M.; Hensen, E. J. M.: Towards a Selective Heterogeneous Catalyst for Glucose Dehydration to 5-Hydroxymethylfurfural in Water: CrCl₂ Catalysis in a Thin Immobilized Ionic Liquid Layer. *ChemCatChem* **2011**, *3*, 969-972.
- (483) Hajipour, A. R.; Rafiee, F.: Acidic Brønsted Ionic Liquids. *Organic Preparations and Procedures International* **2010**, *42*, 285-362.
- (484) Bao, Q.; Qiao, K.; Tomida, D.; Yokoyama, C.: Preparation of 5-Hydroxymethylfurfural by Dehydration of Fructose in the Presence of Acidic Ionic Liquid. *Catalysis Communications* **2008**, *9*, 1383-1388.

- (485) Bao, Q.; Qiao, K.; Tomida, D.; Yokoyama, C.: 1-Methylimidazolium Chlorosulfate ([Hmim]SO₃Cl): A Novel Ionic Liquid with Dual Bronsted-Lewis Acidity. *Chemistry Letters* **2010**, *39*, 728-729.
- (486) Tong, X.; Li, Y.: Efficient and Selective Dehydration of Fructose to 5-Hydroxymethylfurfural Catalyzed by Brønsted-Acidic Ionic Liquids. *ChemSusChem* **2010**, *3*, 350-355.
- (487) Amarasekara, A. S.; Owereh, O. S.: Synthesis of a Sulfonic Acid Functionalized Acidic Ionic Liquid Modified Silica Catalyst and Applications in the Hydrolysis of Cellulose. *Catalysis Communications* **2010**, *11*, 1072-1075.
- (488) Amarasekara, A. S.; Owereh, O. S.: Hydrolysis and Decomposition of Cellulose in Bronsted Acidic Ionic Liquids Under Mild Conditions. *Industrial & Engineering Chemistry Research* **2009**, *48*, 10152-10155.
- (489) Kim, C.; Ryu, H. J.; Kim, S. H.; Yoon, J.-J.; Kim, H. S.; Kim, Y. J.: Acidity Tunable Ionic Liquids as Catalysts for Conversion of Agar into Mixed Sugars. *Bulletin of the Korean Chemical Society* **2010**, *31*, 511-514.
- (490) Rinaldi, R.; Meine, N.; Stein, J. V.; Palkovits, R.; Schueth, F.: Which Controls the Depolymerization of Cellulose in Ionic Liquids: The Solid Acid Catalyst or Cellulose? *ChemSusChem* **2010**, *3*, 266-276.
- (491) Glaeser, R.: Novel Process Options for the Application of Zeolites in Supercritical Fluids and Ionic Liquids. *Chemical Engineering & Technology* **2007**, *30*, 557-568.
- (492) Hardacre, C.; Katdare, S. P.; Milroy, D.; Nancarrow, P.; Rooney, D. W.; Thompson, J. M.: A Catalytic and Mechanistic Study of the Friedel-Crafts Benzoylation of Anisole Using Zeolites in Ionic Liquids. *Journal of Catalysis* **2004**, *227*, 44-52.
- (493) Ntais, S.; Moschovi, A. M.; Paloukis, F.; Neophytides, S.; Burganos, V. N.; Dracopoulos, V.; Nikolakis, V.: Preparation and Ion Transport Properties of NaY Zeolite-Ionic Liquid Composites. *Journal of Power Sources* **2011**, *196*, 2202-2210.
- (494) Liu, Z. C.; Meng, X. H.; Zhang, R.; Xu, C. M.: Friedel-Crafts Acylation of Aromatic Compounds in Ionic Liquids. *Petroleum Science and Technology* **2009**, *27*, 226-237.
- (495) Dwiatmoko, A. A.; Choi, J. W.; Suh, D. J.; Suh, Y.-W.; Kung, H. H.: Understanding the Role of Halogen-Containing Ionic Liquids in the Hydrolysis of Cellobiose Catalyzed by Acid Resins. *Applied Catalysis A-General* **2010**, *387*, 209-214.
- (496) Alcalde, E.; Dinares, I.; Ibanez, A.; Mesquida, N.: A general Halide-to-Anion Switch for Imidazolium-Based Ionic Liquids and Oligocationic Systems Using Anion Exchange Resins (A(-) Form). *Chemical Communications* **2011**, *47*, 3266-3268.
- (497) Thuy, B. T. L.; Korth, W.; Aschauer, S.; Jess, A.: Alkylation of Isobutane With 2-Butene Using Ionic Liquids as Catalyst. *Green Chemistry* **2009**, *11*, 1961-1967.

CHAPTER 2

Experimental



Index

CHAPTER 2	135
Experimental	135
2.1. Preparation of the catalysts	137
2.1.1. Silicoaluminophosphates (SAPOs)	137
2.1.2. Mesoporous aluminosilicate (Al-TUD-1).....	139
2.1.3. Zeolite BEA and BEATUD-1 composite.....	140
2.1.4. Zeolite MCM-22 and the related delaminated material ITQ-2	142
2.1.5. ZrW(X)	144
2.1.6. Chromium-incorporated nanoporous materials.....	146
Al-TUD-1, Cr-Al-TUD-1 and Cr-TUD-1.....	146
BEA, BEATUD-1, Cr-BEA and Cr-BEATUD-1	147
2.2. Characterisation of the catalysts.....	148
2.3. Catalytic tests	151
2.3.1. Aqueous–phase reaction systems	152
2.3.2. Ionic liquid-based catalytic systems.....	154
2.3.3. Recovery of the solid acid catalysts	156
2.4. Quantification of reaction products.....	157
2.5. Identification of the reaction products	159
2.6. References.....	160

2.1. Preparation of the catalysts

2.1.1. Silicoaluminophosphates (SAPOs)

The materials described herein were tested as catalysts in Chapter 3. Table 2.1 collects all the materials and reagents used for the synthesis of these catalysts. All materials were used as received.

Table 2.1- List of chemicals used in the syntheses of SAPOs catalysts.

Chemicals	Abbreviation	Supplier	Purity
Silicon, Aerosil A380	Si-A380-M	Merck	
Silicon, Aerosil A380	Si-A380-D	Degussa	
Silicon, AS40	Si-A	Degussa	
Fumed Silica (Aerosil 200 Serva)	Si-A200	Alfa	
Aluminium, Pural SB Al ₂ O ₃ (70 wt.%)	Al-SB	Fluka	
Pseudoboehmite aluminium, Catapal B, Vista, Al ₂ O ₃ (70.7 wt.%)	Al-CB	Alfa	
Pseudoboehmite aluminium, Plural SB Al ₂ O ₃ (75 wt.%)	Al-PSB	Condea	
Orthophosphoric acid, H ₃ PO ₄ , 85 wt.% aqueous solution		Merck	85-88%
Organic template, tripropylamine	TPA	Aldrich	98%
Organic co-template, methylamine (41 wt.% aqueous solution)	MA	Fluka	
Organic template, dipropylamine (99 wt.% aqueous solution)	DPA	Aldrich	
Tetrapropylammonium hydroxide (40 wt.% aqueous solution)	TPAOH	Alfa Aesar	

Special care must be taken in the preparation of silicoaluminophosphate gels, because it has great influence on the nucleation process, induction period and rate of crystallisation and the products obtained.^{1,2} For example, the heating rate of the gel dramatically influences the crystallisation and consequently the SAPO-type phases formed: in this sense, fast heating tends to favour early nucleation of SAPO-5, and after starting to crystallise it is not possible to obtain pure SAPO-40.² Therefore the preparation of the gels requires a strictly reproducible procedure (autoclaves adapted for each heating system) to avoid contamination of SAPO-40.^{1,2} The preparation of the silicoaluminophosphates (SAPOs) was performed by the group of Professor Filipa Ribeiro (IST, Lisbon).

SAPO-5 was prepared according to that described by Weyda et al.¹ A mixture of an aluminophosphate gel and another gel containing the silica source (Aerosil A380) and the organic template, tripropylamine, TPA was used. The aluminophosphate gel was prepared with 85 wt.% of orthophosphoric acid and distilled water. To this mixture was added Plural SB Al₂O₃ (70 wt.%) as an aluminium source. The mixture was stirred for 2 h to obtain a homogeneous gel. The Aerosil A380 was then added and the gel was further stirred for another 1 h, prior to template addition. After another 2 h of stirring, the final homogeneous gel were loaded into 40 cm³ PTFE-coated stainless steel autoclaves and heated under autogeneous pressure, at 170 °C during 11 h. The compositional molar ratio of the final reaction mixture was Al₂O₃:P₂O₅:0.45 SiO₂:TPA:50 H₂O. The solid phase was recovered by centrifugation, washed several times with distilled water, dried overnight at 100 °C and finally calcined at 600 °C for 8 h under air.

Two SAPO-11 samples (SAPO-11a and SAPO-11b) with different morphologies and crystal sizes were prepared by hydrothermal crystallisation according to the procedures described earlier.^{3,5} SAPO-11a was synthesised using only one template (DPA), while SAPO-11b was obtained by using a combination of two templates (DPA as conventional template and MA as co-template). For the preparation of the two samples, pseudoboehmite aluminium (Al-PSB), orthophosphoric acid and silica (Si-A380-D) for the MA and DPA based sample (SAPO-11b) and silica (Si-A) for DPA based sample (SAPO 11a) were used as sources of aluminium, phosphorous and silicon, respectively.⁵ The compositions of the initial gels were: Al₂O₃:P₂O₅:1.5 DPA:0.66 SiO₂:40 H₂O for SAPO-11a (molar ratio) and Al₂O₃:P₂O₅:DPA:0.3 MA:0.66 SiO₂:50 H₂O for SAPO-11b (molar ratio). The homogeneous gels obtained were loaded into PTFE coated stainless steel autoclaves and subjected to crystallisation under autogeneous pressure at 200 °C during 24 h.^{3,5} The final solid phases were recovered by centrifugation, washed several times with distilled water and dried overnight at 100 °C. The template-free materials were obtained using a two step calcination: from a.t. to 500 °C at a heating rate of 5 °C.min⁻¹ under N₂ flow (5 dm³.h⁻¹.g⁻¹), followed by a 2 h isotherm at 500 °C,^{3,5} then up to 650 °C at the same heating rate under air flow, followed by an isotherm at 650 °C for 8 h. White powders were obtained.⁵

SAPO-40 was synthesised accordingly to that described in the literature.^{2,4,6,7} The sources of aluminium, phosphorus and silicon used were pseudoboehmite alumina (Al-CB), orthophosphoric acid (85 wt.%) and fumed silica (Si-A200), respectively. Under continuous stirring, 5.22 g of Al-CB was added slowly to 9.22 g of H₃PO₄ and 5.78 g of distilled water, forming an extremely viscous mixture, slurry A. The solution was then homogenised for 4 h at 20 °C in a closed beaker. A solution B was prepared by mixing 1.04 g of Si-A200 to 40.82 g of the organic

template tetrapropylammonium hydroxide (TPAOH 40 wt.% aqueous solution). After 2 h of stirring at ambient temperature (a.t.), the solution B was poured into a dispersion of solution A and the two phases were vigorously stirred for 90 min. The composition of the final reaction mixture in molar oxide ratios was: $\text{Al}_2\text{O}_3:\text{P}_2\text{O}_5:0.4\text{SiO}_2:(\text{TPA})_2\text{O}:50\text{H}_2\text{O}$. The gel obtained was then poured in a PTFE-lined stainless-steel autoclave, placed in an oven pre-heated at 200 °C and the crystallisation was conducted under static conditions for 160 h. The autoclaves were cooled to a.t. and the crystalline solid was recovered by centrifugation and washed three times with 60 cm³ of distilled water and dried overnight at 100 °C. Finally it was calcined at a rate of 5 °C.min⁻¹ under N₂ flow, from 20 to 550 °C and maintained at that temperature for 8 h under dry air flow.⁸

2.1.2. Mesoporous aluminosilicate (Al-TUD-1)

The material described herein was tested as a catalyst in Chapter 4. Table 2.2 collects all the chemicals used for the synthesis of this catalyst. All reagents were used as received.

Table 2.2- Chemicals used in the synthesis of Al-TUD-1 catalyst.

Chemicals	Abbreviation	Supplier	Purity
Tetraethylorthosilicate	TEOS	Sigma	99.9%
Aluminium(III) isopropoxide	AIP	Fluka	≥99%
Organic template, Triethanolamine	TENA	Aldrich	99.9%
Tetraethylammonium hydroxide, 35 wt.% aqueous solution	TEAOH	Aldrich	99.9%
Isopropanol		Aldrich	99%
Ethanol		Aldrich	99%

Aluminosilicate Al-TUD-1 is synthesised according to its Si/Al ratio, as depending on it, different non-surfactant templates are used.⁹ These organic non-surfactant templates are environmentally friendly, inexpensive, stable,^{10,11} with high boiling point (ca. 340 °C) and good miscibility towards water, alkoxysilanes (Si-source) and with the silica species generated by their hydrolysis.¹¹ Usually triethanolamine, TENA is used for the synthesis of Al-TUD-1 with a high Si/Al ratio,^{9,12} while for the synthesis of Al-TUD-1 possessing low Si/Al ratio tetraethyleneglycol is preferred.^{10,13} When heated, organic meso-sized aggregates can be formed as templates and silica

species condense forming a silica framework.^{10,11} The pore architecture is determined by co-operative organisation of inorganic species and organic templates.¹⁰ The key to a successful formation of mesopores is the control of intermolecular interactions between organic templates and inorganic species, which means to match the type of template molecule with the temperature regime used.¹¹

Al-TUD-1 (with a Si/Al atomic ratio of 25 in the synthesis gel) was prepared as described by Simons et al.¹³ using aluminium(III) isopropoxide (AIP) and tetraethylorthosilicate (TEOS) as aluminium and silicon sources, respectively, and using TENA as organic templating agent. The procedure was as follows: TEOS (17.3 g, 83 mmol) was added to AIP (0.68 g, 3.33 mmol), which was previously dissolved in a mixture of isopropanol (6.5 cm³) and ethanol (6.5 cm³). After stirring at a.t. for a few min, a mixture of TENA (12.51 g, 83.9 mmol) and water (Milli-Q, 9.4 g) was added, followed by the addition of tetraethylammonium hydroxide, TEOH (35 wt.% in Milli-Q water, 11.12 cm³, 27.0 mmol) under vigorous stirring.

The wet gel obtained was stirred at a.t. for 24 h and dried at 98 °C for another 24 h. Then it was hydrothermally treated in a PTFE-lined stainless steel autoclave at 180 °C for 8 h. Finally the solid was calcined at 600 °C in static air for 10 h (heating rate of 1 °C.min⁻¹).

2.1.3. Zeolite BEA and BEATUD-1 composite

The materials described herein were tested as catalysts in Chapter 5. Table 2.3 collects all the chemicals used for the syntheses of the catalysts. All reagents were used as received.

Table 2.3- Chemicals used in the syntheses of zeolite BEA and BEATUD-1 catalysts.

Chemicals	Abbreviation	Supplier	Purity
Tetraethylorthosilicate	TEOS	Sigma	99.9%
Organic template, Triethanolamine	TENA	Aldrich	99.9%
Tetraethylammonium hydroxide, 35 wt.% aqueous solution	TEAOH	Aldrich	99.9%
Ethanol		Panreac	PA

To obtain the zeolite Beta in the proton form (denoted BEA) the commercial ammonium-form of the Beta powder (NH_4BEA , Zeolyst CP814E) was calcined at 550 °C for 10 h with a heating rate of 1 °C.min⁻¹ in static air. Afterwards an interconnected meso- and microporous composite material denoted BEATUD-1 was prepared by embedding H-Beta nanocrystallites in a 3 D mesoporous silica matrix (TUD-1) with a zeolite loading of 40 wt.%, following the procedure described by Maschmeyer et al.^{14,15} The high porosity of the mesoporous matrix allows a higher accessibility to the internal zeolite crystals by external reagents. The silica precursor, tetraethylorthosilicate, TEOS (5.34 g, 25.6 mmol) was added drop by drop to a stirred suspension of BEA (1.0 g) in a mixture of triethanolamine TENA (3.85 g, 25.8 mmol) and water (Milli-Q, 3.0 g). The organic templating agent, a mesopore-forming organic compound, is usually a glycol (with two or more hydroxyl groups) or amine compounds such as TENA (used in the present procedure) and triethylene pentamine with boiling points of at least 150 °C.¹⁵ Then, TEAOH (35 wt.% in Milli-Q water; 3.42 g, 8.2 mmol) was added rapidly under stirring for ca. 2 h. Due to the vigorous stirring, the zeolite particles were homogeneously dispersed in the synthesis mixture before gelation,¹⁴ and due to the rapid increase of the viscosity in the transition of liquid to thick gel the vigorous stirring was maintained during and after gelation.¹⁴ Afterwards the thick gel containing the homogeneous dispersion of zeolite crystals was aged at a.t. in order to complete the hydrolysis and poly-condensation of the inorganic oxide source for 24 h.^{14,15} Afterwards, the gel was dried at 100 °C for another 24 h. Preferably, the organic template should remain in the gel during the drying stage. The dried material that still contains the organic template is heated to a temperature at which there is a substantial formation of mesopores which is typically between the boiling point of Milli-Q water and the boiling point of the organic template.¹⁵ Since the pore-forming step can be performed hydrothermally in a sealed vessel at autogenous pressure,¹⁵ the solid material was transferred to a PTFE-lined autoclave and heated under static conditions at 180 °C for 8 h. The size and volume of the mesopores in the final product depend partly on the temperature and duration of the hydrothermal step. If the temperature and the treatment time are increased, the mesopore diameter and the mesopore volume will be enhanced.¹⁵

The product was recovered, washed with distilled water and dried overnight at 60 °C. Finally, the solid was calcined at 600 °C for 10 h with a heating ramp rate of 1 °C.min⁻¹ in static air to remove organic template agent and the catalyst was finally formed.

The purely siliceous TUD-1 material was prepared using the same procedure as the one described for the composite material but without zeolite.

The catalysts were manually ground using an agate pestle and mortar and subsequently sieved to give a powder with particle sizes of less than 150 μm width.

2.1.4. Zeolite MCM-22 and the related delaminated material ITQ-2

The materials described herein were tested as catalysts in Chapter 6. Table 2.4 collects all the chemicals used for the syntheses of the catalysts. All reagents were used as received.

Table 2.4- Chemicals used in the syntheses of zeolite MCM-22 and delaminated ITQ-2 catalysts.

Chemicals	Abbreviation	Supplier	Purity
Silica, Aerosil 200	Si-A200-D	Degussa	
Sodium aluminate		Riedel-de Hen	
Tetrapropylammonium bromide	TPABr	Fluka	$\geq 99\%$
Tetrapropylammonium hydroxide, 40 wt.% aqueous solution	TPAOH	Alfa Aesar	
Hexamethyleneimine	HMEI	Aldrich	99%
Cetyltrimethylammonium bromide, 20 wt.% aqueous solution	CTMABr	Fluka	$\geq 96\%$
Amberlite IRA-400 (OH)	AIRA-400	Supelco	
NH_4NO_3 , 1 M		Sigma-Aldrich	>98%
NaOH		Prolab	98%
HCl, 37 % aqueous solution		Panreac	Puriss PA (pro-analysis)
Ethanol		Panreac	Puriss PA

The layered zeolite precursors, denoted Pre-MCM-22(X), where X is the Si/Al molar ratio of 30 or 50 used in the synthesis gel, were prepared as described in the literature.^{16,17} The Si/Al ratios were chosen to achieve a compromise between an enhanced acid site density and a successful delamination. Decreasing the aluminium content of the zeolite precursor leads to a lower charge density, and therefore the interactions between the zeolitic layers are weaker, which facilitates the delamination process.¹⁸⁻²¹ In the case of Pre-MCM-22(30), sodium aluminate (53% Al_2O_3 , 47% Na_2O , 0.587 g, 6.10 mmol) and sodium hydroxide (1.03 g, 25.7 mmol) were dissolved in water (Milli-Q, 156 g, 8.67 mol). Hexamethyleneimine (8.36 g, 84.3 mmol) was then added and the mixture was stirred for 45 min, followed by the addition, under agitation, of silica

(Si-A200-D, 11.0 g, 183.1 mmol). The mixture was stirred for a further 2 h to give a gel which was transferred to a 250 cm³ PTFE-lined stainless-steel autoclave, rotated at 50 r.p.m, and heated at 135 °C for 11 days. After this period of time, the autoclave was quenched in cold water. The solid phase was separated by centrifugation and washed thoroughly with deionised water until pH < 9.0, and subsequently dried at 25 °C overnight. Finally, part of the solid was calcined under static air at 540 °C for 6 h, giving Na-MCM-22(24) (in parenthesis, the bulk Si/Al atomic ratio measured by ICP-AES). A similar procedure was followed to prepare Pre-MCM-22(50), which upon calcination gave Na-MCM-22(38).

The delaminated aluminosilicate, ITQ-2, was prepared from Pre-MCM-22(30) as follows: The Pre-MCM-22(30) (10 g) was dispersed in Milli-Q water (20 g), followed by the addition of aqueous cetyltrimethylammonium hydroxide/bromide (100 g, 20 wt.%; 40% exchanged Br/OH; prepared by ion-exchange of CTMABr using Amberlite IRA-400 (OH)) and aqueous tetrapropylammonium hydroxide/bromide (30 g, 40 wt.%; 50% exchanged Br/OH).

CTMAOH/Br was prepared as follows: CTMABr (50 g) was dissolved in 375 cm³ of Milli-Q water (decarbonated at 100 °C for 25 min under N₂). The resin AIRA-400 was pre-washed with 300 cm³ of Milli-Q water under stirring for 1 h. This procedure was repeated twice. Afterwards, 300 cm³ of the washed resin (measured with a graduated cylinder) was added to the aqueous solution of CTMABr (CTMABr (50 g)/Milli-Q water (375 cm³)) under vigorous stirring for 24 h at a.t. Finally, the solution was separated from the resin with a cannula and the resin was further washed following the same procedure described above. The solution was left to evaporate in air to concentrate. The -OH concentration was determined through titration with 0.1 M HCl (standard concentration: 0.10615 M). Thus, CTMABr/OH (20 cm³) was diluted to 100 cm³, and 25 cm³ were titrated with phenolphthalein as indicator.

TPAOH/Br was prepared from a mixture of TPABr (1.2 g) and TPAOH (3 g) in 4 cm³ of Milli-Q water under vigorous stirring at a.t. for 2 h). The resultant mixture possessed pH ≈ 13.5 and was heated at 80 °C with vigorous stirring for 16 h in order to facilitate the swelling of the layers of the precursor material and the final pH was 11.9. The suspension was sonicated using an ultrasound bath (50 W, 50 Hz) during 1 h and after decantation, the supernatant colloid was separated. The pH of the colloid was lowered to ca. 2.0 by adding 6 M HCl in order to facilitate the flocculation of the delaminated solid.

The solid was separated by centrifugation and washed with distilled water. After drying at 60 °C for 12 h, the solid was calcined at 540 °C for 3 h under a flow of N₂ (300 cm³.min⁻¹), and then during 6 h under air (300 cm³.min⁻¹).^{22,23} The catalysts were manually ground using an agate pestle

and mortar and subsequently sieved to give a powder with particle sizes of less than 106 μm width.

An ion-exchange/calcination procedure was applied to Na-MCM-22(24) and Na-MCM-22(38) to give H-MCM-22(24) and H-MCM-22(38), respectively. The ion-exchange procedure consisted of suspending 1 g of the solid material in 15 cm^3 of 1 M NH_4NO_3 and stirring the resultant suspension for 24 h at 80 $^\circ\text{C}$. The ion exchanged materials were washed thoroughly with deionised water, dried at 50 $^\circ\text{C}$ overnight, and finally calcined in air at 540 $^\circ\text{C}$ (heating rate of 1 $^\circ\text{C}\cdot\text{min}^{-1}$) for 6 h.

2.1.5. ZrW(X)

The materials described herein were tested as catalysts in Chapter 7. Table 2.5 collects all the chemicals used for the syntheses of the catalysts. All reagents were used as received.

Table 2.5- Chemicals used in the syntheses of the ZrW(X) catalysts.

Chemicals	Abbreviation	Supplier	Purity
Aluminium nitrate nonahydrate		Riedel-de Hen	$\geq 98.5\%$
Hexadecyltrimethylammonium bromide	HDTMABr	Fluka	$\geq 96\%$
NH_4OH , ca. 13.3 M, 25% of H_2O		Fluka	
$(\text{NH}_4)_2\text{SO}_4$		Panreac	Puriss PA
Ammonium metatungstate hydrate, $(\text{NH}_4)_6\text{W}_{12}\text{O}_{40}\cdot 13\text{H}_2\text{O}$	AMTH	Sigma-Aldrich	99%
AgNO_3		JVP	
$\text{ZrO}(\text{NO}_3)_2\cdot 6\text{H}_2\text{O}$		Sigma-Aldrich	99%
$\text{ZrOCl}_2\cdot 8\text{H}_2\text{O}$		Sigma-Aldrich	99%
Zirconium(IV) propoxide, $\text{Zr}(\text{O-nPr})_4$, 70 wt.% in 1-propanol		Aldrich	
HCl, 37 % aqueous solution		Panreac	Puriss PA
Ethanol		Panreac	Puriss PA

Two samples of zirconium tungsten mixed oxides, ZrW(X) (X=Cl, NO_3) with W/Zr atomic ratio of ca. 0.1 were prepared by the co-precipitation method, in a similar fashion to that reported in the literature by Jacome et al.²⁴ Ammonium metatungstate hydrate ($(\text{NH}_4)_6\text{W}_{12}\text{O}_{40}\cdot 13\text{H}_2\text{O}$) was used as the source of tungsten and $\text{ZrOCl}_2\cdot 8\text{H}_2\text{O}$ (X=Cl) or $\text{ZrO}(\text{NO}_3)_2\cdot 6\text{H}_2\text{O}$ (X= NO_3) were used as

the source of zirconium. For each ZrW(X) material, three solutions were prepared: 50 cm³ of 0.5 M ZrOCl₂·8H₂O or ZrO(NO₃)₂·6H₂O in deionised water (solution A), 1 dm³ of distilled water with pH adjusted to 10 using an aqueous NH₄OH solution (solution B), and 0.2 mmol of ammonium metatungstate dissolved in 20 cm³ of solution B (solution C). Solution A was added drop-wise to solution C, and the pH was adjusted to ca. 10 using a concentrated solution of NH₄OH (25 wt.% H₂O, ca. 13.3 M). The resultant slurries were hydrothermally treated in PTFE-lined stainless steel autoclaves heated at 195 °C for 24 h. Subsequently, the solids were filtered. In the case of ZrW(Cl) the solid was washed with deionised water and the AgNO₃ test was used to confirm the efficient removal of Cl⁻ ions. The prepared materials were dried overnight at 110 °C and then calcined under air at 800 °C for 3 h (heating rate of 1 °C·min⁻¹), and finally ground using an agate pestle and mortar, and sieved to give particles of less than 150 µm width.

A zirconium material (denoted ZrO₂) was prepared in a similar fashion but without adding the tungsten precursor.

Two mesoporous ZrW-MP and ZrWAl-MP materials were prepared via the incipient wetness impregnation method for introducing tungsten (and aluminium) on a pre-prepared templated zirconium hydroxide support (denoted Zr(template)). The Zr(template) solid was prepared by following the procedure described by Ciesla et al.²⁵ (surfactant-based synthesis). A solution of 70 wt.% of zirconium(IV) propoxide (Zr(O-nPr)₄) in 1-propanol (11.34 cm³, 25.64 mmol) was added slowly with stirring to a solution of HDTAMBr (5.0 g, 13.72 mmol) in a mixture of Milli-Q water (230 g) and 37 wt.% of HCl (37.6 cm³, 457.9 mmol). After stirring for 30 min, a solid was obtained, to which was added a solution of (NH₄)₂SO₄ (3.40 g, 25.73 mmol) in Milli-Q water (46 g). The resultant mixture was stirred for 1 h, and then transferred to a polypropylene bottle and heated at 100 °C for 72 h. Finally, the suspension was filtered, and the solid washed consecutively with deionised water (200 cm³), ethanol (200 cm³) and deionised water (200 cm³), followed by drying at 100 °C overnight to give Zr (template).

The alumina-doped tungstated mesoporous zirconia (denoted ZrWAl-MP) was prepared as follows: a solution of ammonium metatungstate hydrate (0.213 g, 0.0668 mmol) and aluminium nitrate nonahydrate (0.210 g, 0.560 mmol) in a mixture of Milli-Q water and ethanol (10 cm³, 1:1 v/v) was added drop-wise with stirring at 100 °C to Zr(template)(3.215 g).²⁶ The drop-wise addition of small aliquots of the solution was alternated with partial drying of the solid at 120 °C for 1 h. After all the solution had been added, the mixture was dried in an oven at 100 °C for 24 h, and the solid was then calcined at 630 °C for 5 h (heating rate of 1 °C·min⁻¹).

The tungsten containing mesoporous zirconia (denoted ZrW-MP) was prepared using the procedure described above for ZrWAl-MP: a solution of ammonium metatungstate hydrate (0.150 g, 0.047 mmol) in a mixture of Milli-Q water and ethanol (10 cm³, 1:1 v/v) was added dropwise with stirring at 100 °C to Zr(template) (1.332 g).

2.1.6. Chromium-incorporated nanoporous materials

The materials described herein were tested as catalysts in Chapter 9. Table 2.6 collects all the chemicals used for the syntheses of the catalysts. All reagents were used as received.

Table 2.6 - Chemicals used in the syntheses of Al-TUD-1, Cr-Al-TUD-1, Cr-TUD-1, BEA, BEATUD-1, Cr-BEA and Cr-BEATUD-1 catalysts.

Chemicals	Abbreviation	Supplier	Purity
Tetraethylorthosilicate	TEOS	Acros	98%
Aluminium(III) isopropoxide	AIP	Aldrich	98%
Organic template, Triethanolamine	TENA	Acros	97%
Tetraethylammonium hydroxide, 35 wt.% aqueous solution	TEAOH	Aldrich	99.9%
Chromium nitrate nonahydrate, Cr(NO ₃) ₃ ·9H ₂ O		Acros	99%
Isopropanol		Riedel-de Häen	99%
Ethanol		Riedel-de Häen	99.8%

Al-TUD-1, Cr-Al-TUD-1 and Cr-TUD-1

The aluminium and/or chromium-containing mesoporous silicas of the type TUD-1 were prepared by hydrothermal synthesis. In particular, Al-TUD-1 was prepared as described previously in Section 2.1.2.^{10,12,13}

Cr-Al-TUD-1 was prepared using the following procedure: TEOS (17.3 g, 83.0 mmol) was added to AIP (0.509 g, 2.5 mmol) and chromium nitrate (0.333 g, 0.8 mmol) dissolved in a mixture of isopropanol (6.5 cm³) and ethanol (6.5 cm³); atomic ratio Si/(Al+Cr)≈25, Si/Cr≈100, Si/Al≈33. After stirring for 30 min, a mixture of TENA (12.5 g, 83 mmol) and Milli-Q water (5.09 g) was

added, followed by addition of TEOH (35 wt.% in Milli-Q water, 17.07 cm³, 41.5 mmol) under vigorous stirring. The clear gel obtained was stirred at a.t. for 24 h and dried at 98 °C for another 24 h, followed by hydrothermal treatment in a PTFE-lined stainless steel autoclave at 180 °C for 8 h. Finally, the solid was calcined at 600 °C in static air for 10 h (heating rate of 1 °C.min⁻¹) to give a yellow powder.

To prepare Cr-TUD-1, a solution of Cr(NO₃)₃.9H₂O (0.38 g, 0.9 mmol) in Milli-Q water (2 cm³) was added dropwise to TEOS (19.91 g, 95.6 mmol); atomic ratio Si/Cr≈100. While stirring, a solution of TENA (14.4 g, 96.5 mmol) in Milli-Q water (3.6 cm³) was added dropwise, followed by the dropwise addition of TEOH (35 wt.% in Milli-Q water, 19.7 cm³, 47.8 mmol). After stirring for 2 h, a clear and pale green gel was obtained. The mixture was aged at a.t. for 24 h, dried at 100 °C for another 24 h, and subsequently subjected to hydrothermal treatment in a stainless steel PTFE-lined autoclave at 180 °C for 8 h. Finally, the solid was calcined at 600 °C for 10 h in air (heating rate of 1 °C.min⁻¹), to give a yellow powder. The prepared materials were manually ground using an agate pestle and mortar and subsequently sieved to give a powder with particle sizes of less than 106 μm width.

BEA, BEATUD-1, Cr-BEA and Cr-BEATUD-1

Commercial zeolite ammonia BEA powder (NH₄-BEA, Zeolyst, CP814) was calcined at 550 °C (1 °C.min⁻¹) in static air for 10 h, to give BEA. To prepare Cr-BEA, an aqueous suspension of NH₄-BEA (2 g) in 200 cm³ of 0.01 M Cr(NO₃)₃.9H₂O was stirred at 25 °C for 2 h. The solid was then filtered and the ion-exchange procedure repeated twice. Finally, the exchanged solid was filtered, thoroughly washed with deionised water at 60 °C, and calcined at 500 °C for 6 h in air (with a heating rate of 1 °C.min⁻¹). The final solid was a yellow powder.

The composite BEATUD-1 was prepared as described previously in Section 2.1.3. using the BEA zeolite,^{14,15} and a similar procedure was used to prepare the composite Cr-BEATUD-1. Firstly, BEA was ion-exchanged with chromium using the same procedure as that described above for Cr-BEA, excluding the final calcination step, giving a green powder. Subsequently, TEOS (5.34 g, 0.025 mmol) was added dropwise to a stirred suspension of this powder (1.00 g) in a mixture of TENA (83.85 g, 25 mmol) and Milli-Q water (2.99 g). Then, TEOH (35 wt.% in Milli-Q water, 3.45 g, 7.5 mmol) was added to the suspension and stirring was continued for 2 h. The gel was aged at

a.t. for 24 h, followed by drying at 100 °C for 24 h. The solid material was transferred to a PTFE-lined autoclave and heated at 180 °C for 8 h under static conditions. Finally, the solid was calcined at 600 °C for 10 h in air (heating rate of 1 °C.min⁻¹). The final solid was a yellow powder. The prepared materials were manually ground using an agate pestle and mortar and subsequently sieved to give a powder with particle sizes of less than 106 µm width.

2.2. Characterisation of the catalysts

ICP-AES measurements for Si (with an error of ca. 7.2%), Al (error of ca. 6%), P (with an error of ca. 10%), Zr and W (error < 10%) and Cr (with an error of ca. 5-10%) were carried out using a Horiba Jobin Yvon modelo Activa M spectrometer (detection limit of ca. 20 µg.dm⁻³) at the Central Laboratory for Analyses, University of Aveiro. Prior to the ICP-AES analyses, the samples (10 mg) were treated with 1 cm³ of HF and HNO₃ and subjected to a microwave treatment. To the resultant solution was added distilled water until 100 cm³ of total volume.

C, N and S chemical analyses (for the IL [Emim]HSO₄, Chapter 8) were performed using a LECO CHNS-932 equipment based on infrared absorption detection method for C and S, and a thermal conductivity detection method for N. The gases used were helium (carrier), oxygen (for combustion at furnace temperature of 1075 °C) and nitrogen (pneumatic) and the analysis time per sample was 4 min.

Powder XRD were collected for all samples at a.t. on a Philips X' Pert MPD diffractometer, equipped with an X'Celerator detector, a graphite monochromator (Cu-Kα X-radiation, λ=1.54060 Å) and a flat plate sample holder, in a Bragg-Brentano para-focusing optics configuration (40 kV, 50 mA). Samples were step-scanned in 0.04° 2θ steps with a counting time of 6 s per step.

Electron microscopies include high resolution transmission electron microscopy (HRTEM) and scanning electron microscopy (SEM). HRTEM was carried out on Hitachi H9000 and JEOL 2200FS instruments. Samples were prepared by spotting continuous (BEA, Chapter 5), holey (BEATUD-1, Chapter 5) or holey amorphous (Na-MCM-22(24) and ITQ-2(24), Chapter 6; Cr-BEA and Cr-BEATUD-1, Chapter 9) carbon film-coated 400 mesh copper grids (Agar Scientific, Stansted, UK) with a suspension of the solid sample in ethanol. SEM images were carried out on a Hitachi SU-70 UHR Schottky instrument for Al-TUD-1 (Chapter 4) and (Na,H)-MCM-22 and ITQ-2(24)

(Chapter 6). In the case of ZrW(Cl), ZrW-MP and ZrWAl-MP, besides SEM images, EDX analyses and elemental mapping were carried out using a Bruker Quantax 400 (Chapter 7).

Thermal analyses (thermogravimetric (TGA) and differential scanning calorimetry (DSC) were also used in the characterisation of the tested catalysts. TGA and DSC were carried out under air with a heating rate of 5 °C.min⁻¹ for SAPOs (Chapter 3), Al-TUD-1 (Chapter 4) and BEA and BEATUD-1 (Chapter 5), and a heating rate of 10 °C.min⁻¹ for (Na,H)-MCM-22 and ITQ-2(24) (Chapter 6), ZrW(Cl), ZrW(NO₃), ZrW-MP and ZrWAl-MP (Chapter 7) and Cr-containing materials (Cr-Al-TUD-1, Cr-TUD-1, Cr-BEA and Cr-BEATUD-1, Chapter 9), using Shimadzu TGA-50 and DSC-50 systems.

The textural parameters were determined from the N₂ adsorption isotherms measured at -196 °C, using a Micromeritics ASAP 2010 instrument for Al-TUD-1 (Chapter 4) and BEA, BEATUD-1 and TUD-1 (Chapter 5), and a Micromeritics instrument Corp Gemini model 2380 for (Na,H)-MCM-22 and ITQ-2(24) (Chapter 6), ZrW(Cl), ZrW(NO₃), ZrW-MP, ZrWAl-MP and ZrO₂ (Chapter 7), and Cr-containing materials (Cr-Al-TUD-1, Cr-TUD-1, Cr-BEA and Cr-BEATUD-1, Chapter 9). Before the measurements the samples were outgassed at 350 °C, under vacuum for Al-TUD-1 (Chapter 4) and BEA, BEATUD-1 and TUD-1 (Chapter 5) or at 250 °C for (Na,H)-MCM-22 and ITQ-2(24) (Chapter 6), ZrW(Cl), ZrW(NO₃), ZrW-MP, ZrWAl-MP and ZrO₂ (Chapter 7) and Cr-containing materials (Cr-Al-TUD-1, Cr-TUD-1, Cr-BEA and Cr-BEATUD-1, Chapter 9). The textural properties include microporous volume (V_{micro} , t -plot method) for SAPOs (Chapter 3), BEA (Chapter 5) and (Na,H)-MCM-22 and ITQ-2(24) (Chapter 6); total pore volume (V_p), using the Gurvitch equation for relative pressure (p/p_0) \approx 0.98 for Al-TUD-1 (Chapter 4), BEA, BEATUD-1 and TUD-1 (Chapter 5), ZrW(Cl), ZrW(NO₃), ZrW-MP and ZrWAl-MP (Chapter 7) and Cr-containing materials (Cr-Al-TUD-1, Cr-TUD-1, Cr-BEA and Cr-BEATUD-1, Chapter 9); microporous external specific surface area (S_{EXT} , t -plot method) for SAPOs (Chapter 3), BEA (Chapter 5), (Na,H)-MCM-22 and ITQ-2(24) (Chapter 6) and Cr-BEA (Chapter 9); BET specific surface area (S_{BET} , calculated for relative pressures (p/p_0) in the range 0.01-0.10 for Al-TUD-1 (Chapter 4), BEA, BEATUD-1 and TUD-1 (Chapter 5), (Na,H)-MCM-22 and ITQ-2(24) (Chapter 6), ZrW(Cl), ZrW(NO₃), ZrW-MP, ZrWAl-MP and ZrO₂ (Chapter 7) and in the range 0.02-0.10 for Cr-containing materials (Cr-Al-TUD-1, Cr-TUD-1, Cr-BEA and Cr-BEATUD-1, Chapter 9); and pore width (D_p) corresponding to the maximum of the BJH pore size distribution curve (PSD) calculated from the adsorption branch of the isotherm for Al-TUD-1 (Chapter 4), BEATUD-1 and TUD-1 (Chapter 5), ITQ-2(24) (Chapter 6), ZrW(Cl), ZrW-MP and ZrWAl-MP (Chapter 7) and Cr-containing materials (Cr-Al-TUD-1, Cr-TUD-1 and Cr-BEATUD-1, Chapter 9).

Solid state NMR (e.g. ^{27}Al magic-angle spinning MAS NMR and ^{13}C CP MAS NMR) was employed. ^{27}Al MAS NMR spectra were measured at 104.26 MHz with a Bruker Avance 400 (9.4 T) spectrometer, using a contact time of 0.6 μs , a recycle delay of 0.8 s, and a spinning rate of 15 kHz for Al-TUD-1 (Chapter 4), BEA and BEATUD-1 (Chapter 5), (Na,H)-MCM-22 and ITQ-2(24) (Chapter 6). Chemical shifts are quoted in ppm from $\text{Al}(\text{H}_2\text{O})_6^{3+}$. The ^{13}C CP MAS NMR spectrum of the used BEA catalyst (washed with methanol and dried overnight at 65 °C) was collected at 100.613 MHz on a 9.4 T Bruker Avance 400 spectrometer with 3.5 μs ^1H 90° pulses, a contact time of 1.5 ms, a spinning rate of 9.0 kHz, and recycle delays of 4 s (Chapter 5).

Other spectroscopies used include Fourier transform infrared (FT-IR), attenuated total reflectance (ATR), Raman and diffuse reflectance UV-vis (DR UV-vis). IR spectra were collected on a FT-IR Unicam Mattson-7000 infrared spectrophotometer using KBr pellets for BEA and BEATUD-1 (Chapter 5), H-MCM-22(24) and ITQ-2(24) (Chapter 6). ATR FT-IR spectra were measured on a Mattson 7000 FT-IR spectrometer equipped with a Specac Golden Gate Mk II ATR accessory having a diamond top-plate and KRS-5 focusing lenses for Cr-containing materials (Cr-AlTUD-1, Cr-TUD-1, Cr-BEA and Cr-BEATUD-1). The Raman spectra were recorded on a Bruker RFS FT-Raman spectrophotometer (100 s^{-1} , $\lambda=1064$ nm, 200-5000 scans with a resolution of 4 cm^{-1}) for ZrW(Cl), ZrW(NO_3), ZrW-MP and ZrWAl-MP (Chapter 7). DR UV-vis spectra were recorded using a Jasco V-560 spectrophotometer and BaSO_4 as reference for Cr-containing materials (Cr-AlTUD-1, Cr-TUD-1, Cr-BEA and Cr-BEATUD-1, Chapter 9).

Acid properties are an important issue in the characterisation of the catalysts. It has been reported in the literature for dehydration reactions in aqueous solutions with solid acid catalysts that gas-phase characterisation of acid sites (AS) can be used for investigating the influence of the acid properties of solid acid catalysts and to predict catalytic activity in the aqueous phase.^{27,28} The acid properties of SAPOs (Chapter 3), Al-TUD-1 (Chapter 4), BEA and BEATUD-1 (Chapter 5), H-MCM-22 and ITQ-2(24) (Chapter 6), ZrW(Cl), ZrW(NO_3), ZrW-MP, ZrWAl-MP (Chapter 7) were measured at IST, Lisbon by the group of Professor Filipa Ribeiro, using a Nexus-Thermo Nicolet FT-IR instrument (64 scans and resolution of 4 cm^{-1}) equipped with a specially designed cell, using self-supported discs (5-10 $\text{mg}\cdot\text{cm}^{-2}$) and pyridine as the basic probe molecule. Pyridine was chosen because its critical dimension of ca. 6.43 Å²⁹ is comparable with the molecular dimensions of D-xylose (6.8 Å along the longest axis).³⁰ After in situ outgassing at 450 °C for 3 h at 10⁻⁶ mbar (for SAPOs (Chapter 3), Al-TUD-1 (Chapter 4), BEA and BEATUD-1 (Chapter 5), H-MCM-22 and ITQ-2(24) (Chapter 6) and at 400 °C for 2 h at 10⁻⁵ mbar for ZrW(Cl), ZrW(NO_3), ZrW-MP and ZrWAl-MP (Chapter 7)), pyridine (99.99%) was contacted with the sample at 150 °C for 10 min and then

evacuated at 150 °C and 350 °C for SAPOs (Chapter 3), Al-TUD-1 (Chapter 4), BEA and BEATUD-1 (Chapter 5) and ZrW(Cl), ZrW(NO₃), ZrW-MP and ZrWAl-MP (Chapter 7) for 30 min or 150 °C for H-MCM-22 and ITQ-2(24) (Chapter 6) for 30 min under vacuum at 10⁻⁶ mbar (in the case of ZrW(X) materials the vacuum applied was 10⁻⁵ mbar). The IR bands at ca. 1540 and 1455 cm⁻¹ are related to pyridine adsorbed on Brønsted acid sites (B) and Lewis acid sites (L), respectively³¹⁻³³ and were used for quantification.³³ In the case of H-MCM-22 and ITQ-2(24) (Chapter 6), the acid properties were investigated by FT-IR studies using collidine (2,4,6-trimethylpyridine) as probe molecule: the FT-IR spectra were recorded with a resolution of 2 cm⁻¹ on a Nicolet Nexus spectrophotometer equipped with an MCT (mercury cadmium telluride) detector. Similar to the procedure applied for the analysis with pyridine, the powdered solids were pressed into self-supported disks (10 mg.cm⁻²) and placed in a quartz IR cell with KBr windows. After in situ outgassing at 450 °C for 4 h, collidine was contacted with the sample at 200 °C for 30 min and then evacuated at 200 °C for further 30 min under vacuum. The IR band at ca. 1635 cm⁻¹ is related to collidine adsorbed on B.

2.3. Catalytic tests

The catalyst experiments can be grouped into the aqueous-phase reaction systems using a solid acid catalyst and the IL-based catalytic systems with or without adding a solid acid catalyst. Table 2.7 collects the chemicals used for the catalytic tests and calibrations. All reagents were used as received.

Table 2.7- Chemicals used in the catalytic tests and HPLC calibrations.

Chemicals	Abbreviation	Supplier	Purity
Sulfuric acid, H ₂ SO ₄		J.T. Baker	95-97%
D-(+)-Xylose		Sigma-Aldrich	99%
D-(-)-Fructose		Aldrich	>99%
D-(+)-Glucose		Sigma-Aldrich	>99%
D-(+)-Cellobiose		Fluka	≥99%
D-(+)-Sucrose		Fluka	≥99%
D-(+)-Maltose monohydrate	Maltose	Riedel-de Häen	
Inulin		Fluka	
4-O-methyl-D-glucurono-D-xylan	Xylan	Sigma	
Cellulose, powder D-natural	Cellulose	Riedel-de Häen	
Starch from potato soluble	Starch	Panreac	PA
1-Ethyl-3-methyl hydrogen sulfate	[Emim]HSO ₄	Merck	

1-Butyl-3-methyl imidazolium chloride	[Bmim]Cl	Fluka	≥ 98%
1-Butyl-3-methyl imidazolium chloride	[Bmim]Cl	Aldrich	≥ 98%
D-(-)-Ribose		Aldrich	98%
D-(-)-Mannitol		Riedel-de Häen	>99%
Sorbitol		Aldrich	≥99%
Diacetyl		Merck	≥97%
Diacetyl		Aldrich	97%
Phenol		Fluka	≥99.5%
Toluene	Tol	Sigma-Aldrich	≥99.9%
Milli-Q water			
Dimethylsulfoxide		Aldrich	≥ 99.9%
Isobutylmethyl ketone	IBMK	Merck	≥ 99.9%
Methanol		J. T. Baker	≥ 99.8%

2.3.1. Aqueous –phase reaction systems

The catalytic tests were performed under nitrogen (autogeneous pressure) in batch tubular glass micro-reactors (total capacity of ca. 5 cm³) with pear-shaped bottom and equipped with a valve for gas purging and a PTFE-coated magnetic stirring bar (Chapters 3-7). Prior to the catalytic reaction, the reaction mixture was stirred at a.t. for ca. 1 min to completely dissolve the saccharide in the aqueous phase and then it was immersed in a thermostatically controlled oil bath. The instant the reaction began (zero time) was taken as the instant that the micro-reactor was immersed in the oil bath. Each sample was taken from an individual batch run experiment.

Typically, the dehydration of the saccharides was carried out at 170 °C, using a biphasic solvent system (1 cm³ total volume) consisting of Milli-Q water and toluene (0.3:0.7 v/v, Figure 2.1). The biphasic solvent system is interesting for the simultaneous separation of Fur/Hmf from the aqueous phase as it is formed.^{34,35} The reaction of the saccharides takes place in the aqueous phase (where they dissolve completely) and the product Fur or Hmf is transferred into the organic phase, avoiding undesired reactions.³⁶ The saccharides tested in the biphasic solvent systems were (monosaccharides) D-xylose (100 g.dm⁻³, 0.67 M) in Chapters 3-8, D-fructose and D-glucose (100 g.dm⁻³, 0.56 M) in Chapter 4, (disaccharides) D-sucrose, D-maltose and D-cellobiose (100 g.dm⁻³, 0.29 M), and (polysaccharides) D-xylan, inulin and starch (33.3 g.dm⁻³) in Chapter 4. The amount of the catalyst in the reaction medium was typically 20 g.dm⁻³.

Catalytic tests using solely water as solvent were also performed. The saccharide tested was D-xylose (100 g.dm⁻³, 0.67 M) in Chapter 5 using 0.3 cm³ of solvent, and in Chapters 6 and 7 using 1 cm³ of solvent). The amount of the catalyst in the reaction medium was 20 g.dm⁻³.

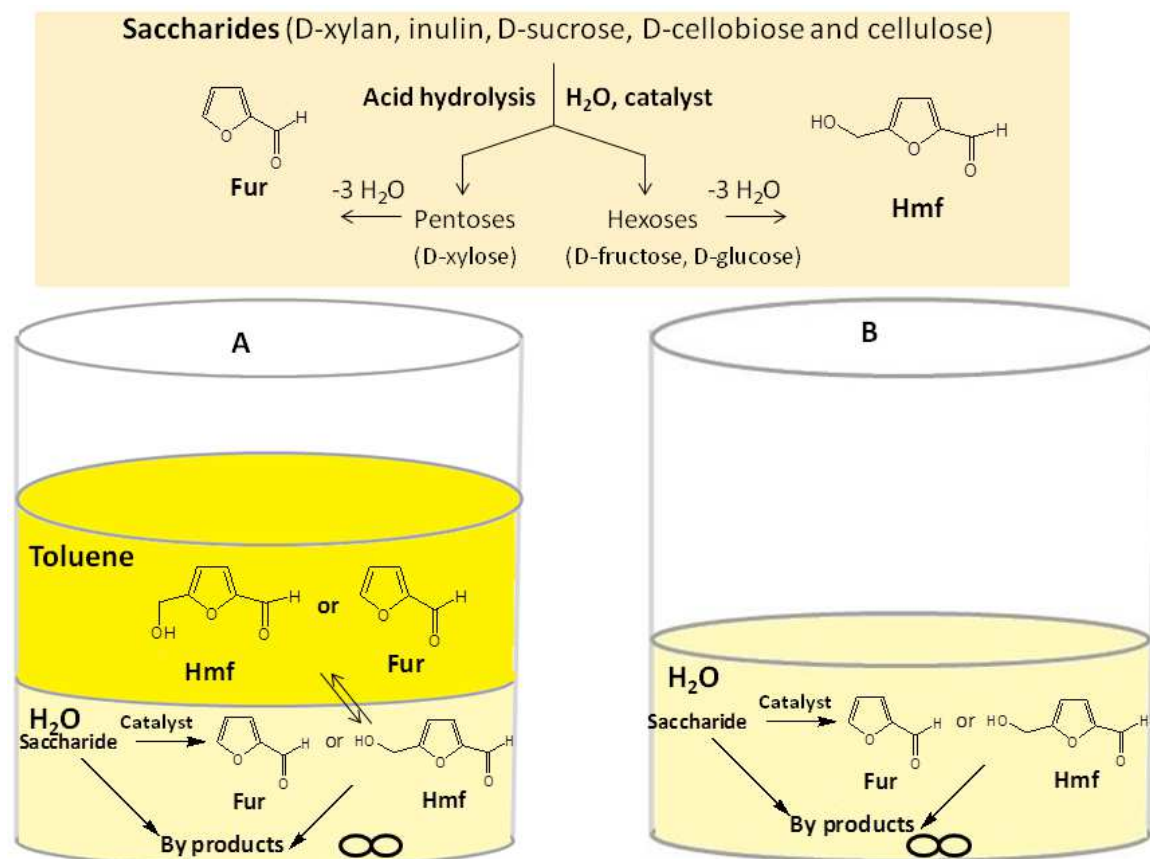


Figure 2.1- Schematic representation of the aqueous-phase acid hydrolysis and dehydration of saccharides into 2-furaldehyde (Fur) and 5-hydroxymethyl-2-furaldehyde (Hmf), using a biphasic solvent system (A) or solely water as solvent (B).

The stirring rates used were optimised to avoid internal mass transfer limitations. For H-MCM-22(24) and ITQ-2(24) (Chapter 6) the initial reaction rates (based on the conversion at 1 h reaction) were similar for stirring rates at or above 700 r.p.m: 1.6, 2.4 and 2.3 mmol.g_{cat}⁻¹.h⁻¹ for H-MCM-22(24) and 2.1, 2.0 and 2.1 mmol.g_{cat}⁻¹.h⁻¹ for ITQ-2(24) at 600, 700 and 800 r.p.m respectively (Chapter 6). In parallel with these results, for ZrW(Cl) (Chapter 7) the initial reaction rates (based on the conversion at 30 min reaction) were similar above 700 r.p.m: 9.4, 12.4 and 12.1 mmol.g_{cat}⁻¹.h⁻¹ at 600, 700 and 900 r.p.m, respectively. The same applies for the BEA and BEATUD-1 catalysts (Chapter 5) in that the Xyl conversions at 30 min were similar for stirring rates

in the range 700-800 r.p.m (ca. 9.3 and 5.7 $\text{mmol}\cdot\text{g}_{\text{cat}}^{-1}\cdot\text{h}^{-1}$ respectively) and slightly lower for 600 r.p.m in the case of BEA (a decrease in conversion of ca. 7% was observed, Chapter 5). The calculated initial reaction rates were typically based on conversions at 30 min for BEA and BEATUD-1 (Chapter 5) and at 60 min for H-MCM-22(24) and ITQ-2(24) (Chapter 6). Initially the reaction conditions are not isothermal.

2.3.2. Ionic liquid-based catalytic systems

The catalytic tests were performed under nitrogen (autogeneous pressure) in batch tubular glass micro-reactors and equipped with a valve for gas purging and a PTFE-coated magnetic stirring bar. The micro-reactors used in the studies of Chapter 8 possessed a pear-shaped bottom (total capacity of ca. 5 cm^3), and in the case of Chapter 9 round-bottomed glass reactors were used (total capacity of 7 cm^3). As carried out in the aqueous-phase reaction systems, the reaction mixture was stirred at a.t. for ca. 1 min to completely dissolve the saccharide in the IL before the catalytic reaction, and then the reactor was heated with a thermostatically controlled oil bath under magnetic stirring at 600 r.p.m in the case of [Emim]HSO₄ (Chapter 8), and at 1000 r.p.m in the case of the Cr-containing materials with [Bmim]Cl (Chapter 9). Zero time (considered as the instant the reaction began) was taken as the instant that the micro-reactor was immersed in the oil bath. Each sample was taken from an individual batch run experiment.

The catalytic tests were performed using biphasic solvent systems consisting of the IL and an extracting organic solvent (Tol or IBMK) in a 0.3:0.7 v/v ratio (Chapter 8) or using a monophasic solvent system consisting of an acid-functionalised IL (0.3 cm^3 , Chapter 8) or an IL as solvent (0.3 cm^3) coupled with a solid acid catalyst where the amount of the catalyst in the reaction medium was 50 $\text{g}\cdot\text{dm}^{-3}$ (Chapter 9, Figure 2.2). In Chapter 8, the saccharides tested were (monosaccharides) D-xylose (100 $\text{g}\cdot\text{dm}^{-3}$, 0.67 M), D-glucose and D-fructose (120 $\text{g}\cdot\text{dm}^{-3}$, 0.67 M), (disaccharides) D-sucrose, D-cellobiose, and D-maltose (120 $\text{g}\cdot\text{dm}^{-3}$, 0.35 M), (polysaccharides) D-xylan (100 $\text{g}\cdot\text{dm}^{-3}$) and inulin, starch and cellulose (120 $\text{g}\cdot\text{dm}^{-3}$). In Chapter 9, D-glucose was the substrate (50 $\text{g}\cdot\text{dm}^{-3}$, 0.28 M).

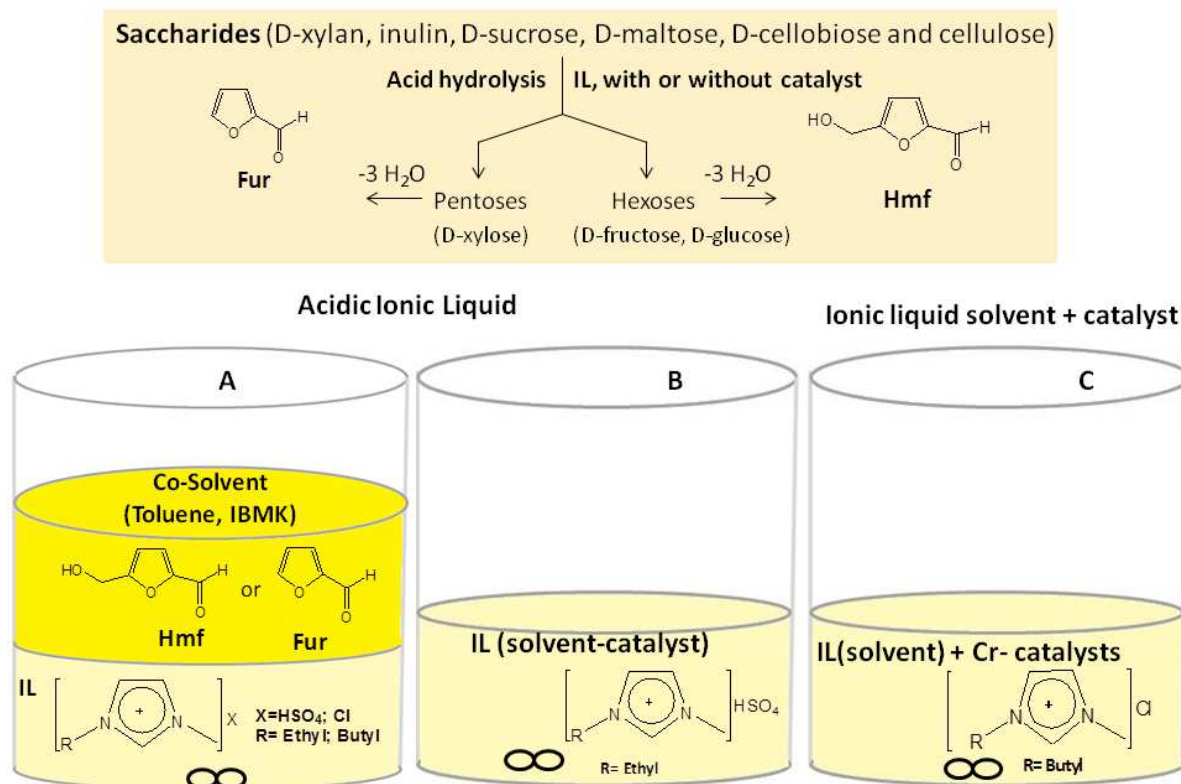


Figure 2.2- Schematic representation of the acid hydrolysis and dehydration of saccharides into 2-furaldehyde (Fur) and 5-hydroxymethyl-2-furaldehyde (Hmf) using an IL-based catalytic system under biphasic solvent conditions (A) or using an acid-functionalised IL without adding a solid acid catalyst (B) or using an IL as solvent coupled with a solid acid catalyst (C).

In Chapter 8, the catalytic reactions were carried using solely [Emim]HSO₄ as solvent and catalyst (without solid acid catalyst). Two methods were used to facilitate the separation of the target product from the IL phase. An extracting solvent (Tol or IBMK), immiscible or poorly soluble with the IL was used, or alternatively, the reaction was carried out under reduced pressure, using a water aspirator, to evaporate Fur from the IL during the catalytic reaction. In the latter case a round-bottomed glass reactor (total capacity of 25 cm³) was used and charged with D-xylose (18 wt.%) and [Emim]HSO₄ (5 g). The reactor was connected to a Liebig condenser with circulating water cooled to ca. 15 °C (Figure 2.3). The quasi-horizontally positioned condenser was connected through a vacuum adapter to a 10 cm³ round bottomed flask for collection, which was cooled with liquid nitrogen-frozen ice. The fed reactor was degassed under vacuum and placed in a water-filled ultrasound bath (50 W, 40 kHz) for ca. 15 min at a.t. prior to immersion in the oil bath and heating at 100 °C for 4 h.



Figure 2.3- Experimental setup used for the D-xylose/[Emim]HSO₄ reaction system under reduced pressure (Chapter 8).

2.3.3. Recovery of the solid acid catalysts

After each batch run at a certain reaction time, the reactor was removed from the oil bath and cooled to a.t. Then the reaction mixture was centrifuged to 3500 r.p.m to separate the catalyst (Figure 2.4 A). The separated solid catalysts were used in consecutive batch runs. Prior to reuse, the solids were washed with methanol (Chapters 3-6) or with deionised water in the case of ZrW(Cl), Zr(NO₃), ZrW-MP and ZrWAl-MP (Chapter 7) and Cr-containing materials (Cr-Al-TUD-1, Cr-TUD-1, Cr-BEA and Cr-BEATUD-1, Chapter 9) in falcon tubes, dried at 50-60 °C overnight in an oven (Figure 2.4 B) and calcined in a muffle furnace (Figure 2.4 C) at 550 °C for 5 h for H-MCM-22(24) (Chapter 6), 450 °C for 5 h for ITQ-2(24) (Chapter 6), 450 °C for 3 h (SAPOs and Cr-Al-TUD-1, Cr-TUD-1, Cr-BEA and Cr-BEATUD-1, Chapters 3 and 9, respectively), 450 °C for 5 h (BEA, BEATUD-1, Chapter 5), ZrWAl-MP and ZrW-MP (Chapter 7) or 350 °C for 3 h (Al-TUD-1, Chapter 4) with a heating rate of 1 °C.min⁻¹ in air to remove the carbonaceous matter.

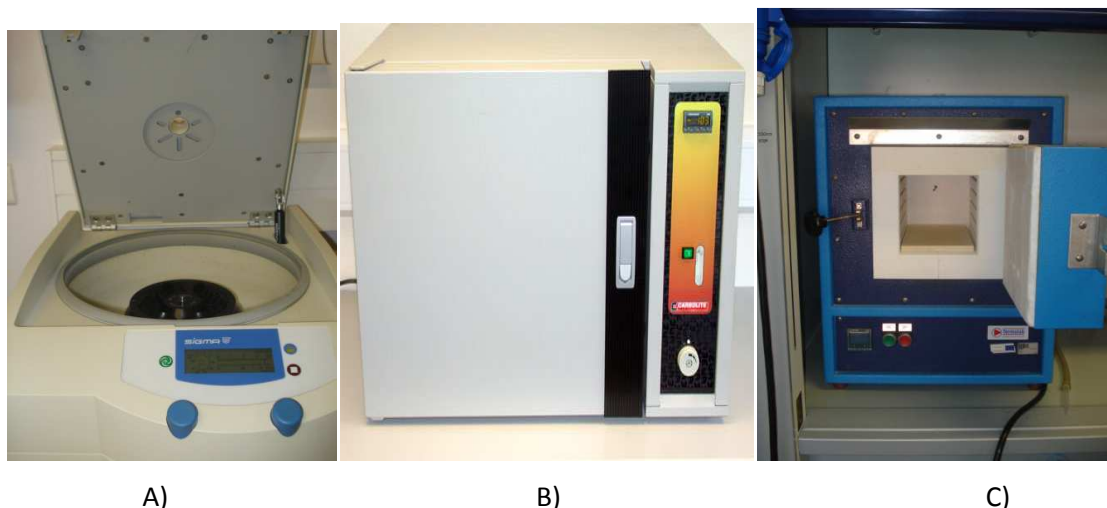


Figure 2.4- Centrifuge (A) used to separate the solid from the liquid phases; Oven used to dry the recovered powdered catalysts (B) and muffle furnace used for calcination (C).

2.4. Quantification of reaction products

The products were analysed by high performance liquid chromatography (HPLC) in isocratic mode by the internal standard method using calibration curves with authentic samples of the reagents (of D-xylose, D-(-)-fructose, D-(+)-glucose, D-(+)-cellobiose, D-(+)-sucrose, and D-(+)-maltose monohydrate) and products (Fur and Hmf) as standards used for quantification of the calibration curves. In the case of the products present in the aqueous phase (H_2O or IL) a Knauer K-1001 HPLC pump coupled to a Knauer 2300 differential refractive index detector (for sugars) and a Knauer 2600 UV detector (280 nm, for Fur and Hmf) was used. For pentose-based feedstocks a PL Hi-Plex H 300 nm x 7 nm (i.d.) ion exchange column (Polymer Laboratories Ltd, UK) was used. The mobile phase was 0.001 M H_2SO_4 with a $0.6 \text{ cm}^3 \cdot \text{min}^{-1}$ flow rate and $65 \text{ }^\circ\text{C}$ as the temperature of the column. In the case of hexose-based feedstocks, a PL Hi-Plex Ca 300 nm x 7.7 nm (i.d.) ion exchange column (Polymer Laboratories Ltd., UK) was used: the mobile phase was freshly prepared distilled and deionized water; flow rate of $0.5 \text{ cm}^3 \cdot \text{min}^{-1}$; column temperature of $80 \text{ }^\circ\text{C}$.

The products present in the organic phase were analysed using a Gilson 306 HPLC pump and a Spherisorb ODS S10 C18 column coupled to a Gilson 118 UV/Vis detector (280 nm). The mobile phase with a flow rate of $0.5 \text{ cm}^3 \cdot \text{min}^{-1}$ for SAPOs (Chapter 3), (Na,H)-MCM-22 and ITQ-

2(24) (Chapter 6), ZrW(Cl), ZrW(NO₃), ZrW-MP and ZrWAl-MP (Chapter 7) and of 0.7 cm³.min⁻¹ for [Emim]HSO₄ (Chapter 8), Al-TUD-1 (Chapter 4), BEA and BEATUD-1 (Chapter 5) consisted of a mixture of 37% (v/v) of methanol and 63% (v/v) of H₂O.

The reproducibility of the catalytic results was tested by performing two to three replicates of an individual experiment. The reported results are the average values. A good reproducibility of the results requires “real-time” sampling and HPLC analysis. The maximum average absolute deviation in these values was in the range 3-5%.

The conversion of the substrate (C_{sub}) at a reaction time t was calculated using equation (2.1) in the cases of mono/disaccharides (expressed as mol. %):

$$C_{sub} (\%) = \frac{n_o (\text{substrate}) - n_t (\text{substrate})}{n_o (\text{substrate})} \times 100 \quad (2.1)$$

where n_o (substrate) and n_t (substrate) are the initial moles of substrate and the moles of substrate at reaction time t , respectively.

For monosaccharides, the yield (Y) and selectivity (S) of the product Fur or Hmf (F) at a reaction time t were calculated using equations (2.2) and (2.3), respectively (expressed as mol. %):

$$Y (\%) = \frac{n_t (F)}{n_o (\text{saccharide})} \times 100 \quad (2.2)$$

$$S (\%) = \frac{n_t (F)}{(n_o (\text{substrate}) - n_t (\text{substrate}))} \times 100 \quad (2.3)$$

where n_F is the number of moles of F at a reaction time t .

For disaccharides and polysaccharides the F yield at a reaction time t was calculated using equation (2.4) (expressed as mol.%) and (2.5) (expressed as wt.%), respectively:

$$Y_F (\text{mol.}\%) = \frac{n_t (F)}{2x (n_o \text{ disaccharide})} \times 100 \quad (2.4)$$

$$Y_F (\text{wt.}\%) = \frac{\text{mass of } F \text{ formed}}{m_o \text{ of polysaccharide}} \times 100 \quad (2.5)$$

where n_o (disaccharides) is the initial number of moles of the disaccharide substrate and m_o (polysaccharides) is the initial mass of the polysaccharide substrate.

2.5. Identification of the reaction products

In order to identify possible by-products present in the aqueous-phase, ^1H NMR and ^{13}C NMR spectra in the liquid state were employed for the reaction solution after the reaction of D-xylose in the presence of BEA (Chapter 5) and ITQ-2(24) (Chapter 6), and for the solvent used for washing the catalyst BEA (Chapter 5). These spectra were recorded on a Bruker DRX 300 MHz spectrometer at 20 °C. The chemical shifts are quoted in parts per million from tetramethylsilane, TMS. The identification of the by-products present in the organic phase was performed by using gas chromatography-mass spectrometry (GC-MS) applied in a Trace GC 2000 Series (Thermo Quest CE Instruments)-DSQ-II (Thermo Scientific) equipped with a capillary column (DB-1MS, 30 m x 0.32 mm), using He as carrier gas (Chapter 8).

In Chapter 7, solid-phase microextraction coupled with comprehensive 2 D gas chromatography with time-of-flight mass spectrometry (SPME/GCxGC-ToFMS) analyses were carried out for the liquid phase of the reaction mixture (after separating the solid phase by centrifugation) on the same day that the respective catalytic test was performed. The vial containing the reaction solution was immersed in a thermostated bath adjusted to 40.0 ± 0.1 °C for 5 min. Then, a solid-phase microextraction (SPME) device with a fused silica fibre coating (50/30 μm divinylbenzene-carboxen-poly(dimethylsiloxane)) was immersed in the reaction solution for 20 min. After the extraction/concentration step, the SPME coating fibre was manually introduced into the GCxGC-ToFMS injection port at 250 °C and kept for 30 s for desorption. The injection port was lined with a 0.75 mm I.D. splitless glass liner and splitless injections were used (30 s). The LECO Pegasus 4 D (LECO, St. Joseph, MI, USA) GCxGC-ToFMS system consisted of an Agilent GC 7890A gas chromatograph with a dual stage jet cryogenic modulator (licensed from Zoex) and a secondary oven. The detector was a high-speed time of flight (ToF) mass spectrometer. A non-polar/polar set of columns was used: a HP-5 column (30 m x 0.32 mm I.D., 0.25 μm film thickness, J&W Scientific Inc., Folsom, CA, USA) was used as first-dimension column and a DB-FFAP (0.79 m x 0.25 μm thickness, J&W Scientific Inc., Folsom, CA, USA) was used as second-dimension column. The carrier gas was helium at a constant flow rate of $3.0 \text{ cm}^3 \cdot \text{min}^{-1}$. The primary oven temperature was programmed from 50 °C (3 min) to 230 °C (10 min) at a heating rate of $10 \text{ }^\circ\text{C} \cdot \text{min}^{-1}$. The secondary oven temperature was programmed from 70 °C (3 min) to 250 °C (10 min) at $10 \text{ }^\circ\text{C} \cdot \text{min}^{-1}$. The MS transfer line temperature and the MS source temperature was 250 °C. The modulation time was 5 s, and the modulator temperature was kept

at 20 °C offset (above primary oven). The ToFMS was operated at a spectrum storage rate of 100 spectra.s⁻¹. The mass spectrometer was operated in the EI mode at 70 eV using a range of m/z 33-500 and the voltage was -1626 V. Total ion chromatograms (TIC) were processed using the automated data processing software ChromaToF (LECO) at signal-to-noise threshold of 100. Contour plots were used to evaluate the separation general quality and for manual peak identification; a signal-to-noise threshold of 50 was used. Two commercial databases (Wiley 275 and US National Institute of Science and Technology (NIST) V 2.0-Mainlib and Replib) were used. The majority (86%) of the identified products showed mass spectral similarity matches > 850. Furthermore, a manual inspection of the mass spectra was done, combined with the use of additional data, such as the retention index (RI) value, which was determined according to the Van den Dool and Kratz RI equation.³⁷ For the determination of the RI, a C₈-C₂₀ n-alkanes series was used, and as some volatile compounds were eluted before C₈, the solvent *n*-hexane was used as C₆ standard. The experimentally calculated RI values were compared, when available, with values reported in the literature for similar chromatographic columns employed as the first dimension. The results were analysed qualitatively and thus the relative amounts of the products were not considered.

In the case of the recovered humins in Chapter 8, the solid state ¹³C NMR spectrum was recorded at 11.75 T on a Bruker DRX 500 spectrometer operating at 125.76 MHz, using a 4 mm BL CP MAS VTN probe. The sample was spun at 9.0 kHz and the contact time was 8 ms.

2.6. References

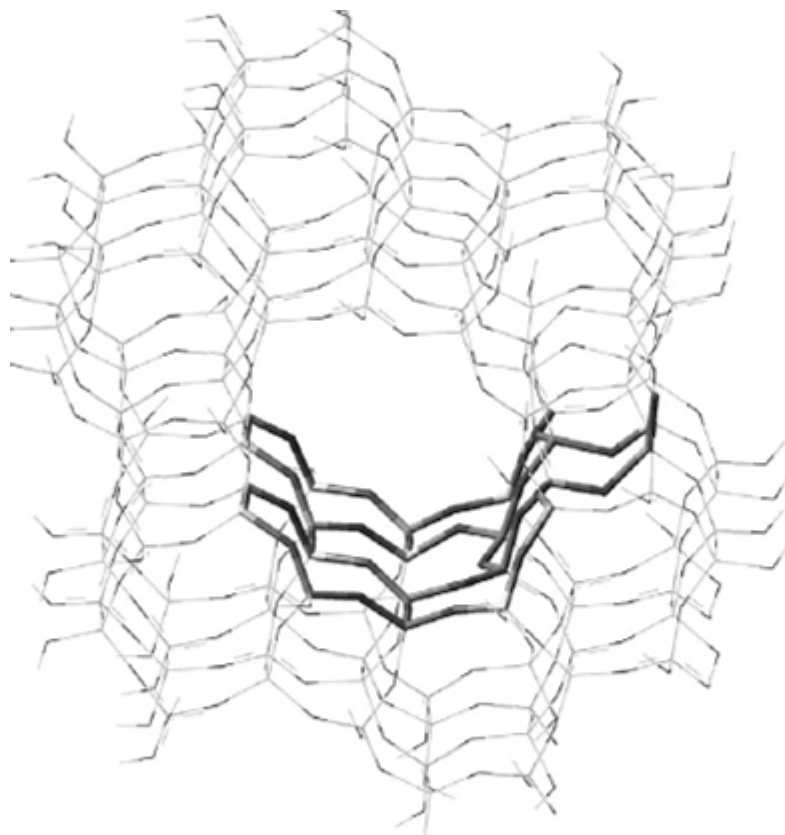
- (1) Weyda, H.; Lechert, H.: The Crystallization of Silicoaluminophosphates With the Structure-Type SAPO-5. *Zeolites* **1990**, *10*, 251-258.
- (2) Dumont, N.; Gabelica, Z.; Derouane, E. G.; Renzo, F. D.: Comparative Investigation of Different Synthesis Procedures Leading to SAPO-40. *Microporous Materials* **1994**, *3*, 71-84.
- (3) Fernandes, A.; Ribeiro, F. R.; Lourenço, J.; Gabelica, Z.: An Elegant Way to Increase Acidity in SAPOs: Use of Methylamine as Co-Template During Synthesis. In *Zeolites and Related Materials: Trends, Targets and Challenges, Proceedings of the 4th International Feza Conference*; Gedeon, A. M. P. B. F., Ed., 2008; Vol. 174; pp 281-284.
- (4) Lok, B. M.; Messina, C. A.; Patton, R. L.; Gajek, R. T.; Cannan, T. R.; Flanigen, E. M.: Crystalline Silicoaluminophosphates. In *United States Patent: US 4,440,871*; Union Carbide Corporation: USA, 1984; pp 43.
- (5) Bertolo, R.; Martins, A.; Silva, J. M.; Ribeiro, F.; Ribeiro, F. R.; Fernandes, A.: Incorporation of Niobium in SAPO-11 Materials: Synthesis and Characterization. *Microporous and Mesoporous Materials* **2011**, *143*, 284-290.

- (6) Lourenço, J. P.; Ribeiro, M. F.; Ribeiro, F. R.; Rocha, J.; Gabelica, Z.; Derouane, E. G.: Thermal and Hydrothermal Stability of the Silicoaluminophosphate SAPO-40. *Microporous Materials* **1995**, *4*, 445-453.
- (7) Lourenço, J. P.; Ribeiro, M. F.; Ribeiro, F. R.; Rocha, J.; Gabelica, Z.: Characterization of Stability and Porosity of SAPO-40 Using m-Xylene as Model Reaction. *Applied Catalysis A-General* **1996**, *148*, 167-180.
- (8) Lourenço, J. P.; Ribeiro, M. F.; Ribeiro, F. R.; Rocha, J.; Gabelica, Z.; Dumont, N.; Derouane, E. G.: *Study of Catalytic Properties of SAPO-40*; Elsevier Science Publ B V: Amsterdam, 1994; Vol. 84.
- (9) Telalović, S.; Hanefeld, U.: Noncovalent Immobilization of Chiral Cyclopropanation Catalysts on Mesoporous TUD-1: Comparison of Liquid-Phase and Gas-Phase Ion-Exchange. *Applied Catalysis A-General* **2010**, *372*, 217-223.
- (10) Shan, Z.; Jansen, J. C.; Zhou, W.; Maschmeyer, T.: Al-TUD-1, Stable Mesoporous Aluminas with High Surface Areas. *Applied Catalysis A-General* **2003**, *254*, 339-343.
- (11) Jansen, J. C.; Shan, Z.; Marchese, L.; Zhou, W.; Puil, N. V. d.; Maschmeyer, T.: A New Templating Method For Three-Dimensional Mesopore Networks. *Chemical Communications* **2001**, 713-714.
- (12) Anand, R.; Maheswari, R.; Hanefeld, U.: Catalytic Properties of the Novel Mesoporous Aluminosilicate AlTUD-1. *Journal of Catalysis* **2006**, *242*, 82-91.
- (13) Simons, C.; Hanefeld, U.; Arends, I.; Sheldon, R. A.; Maschmeyer, T.: Noncovalent Anchoring of Asymmetric Hydrogenation Catalysts on a New Mesoporous Aluminosilicate: Application and Solvent Effects. *Chemistry-A European Journal* **2004**, *10*, 5829-5835.
- (14) Waller, P.; Shan, Z. P.; Marchese, L.; Tartaglione, G.; Zhou, W. Z.; Jansen, J. C.; Maschmeyer, T.: Zeolite Nanocrystals Inside Mesoporous TUD-1: A High-Performance Catalytic Composite. *Chemistry-A European Journal* **2004**, *10*, 4970-4976.
- (15) Shan, Z.; Waller, P. W. G.; Maingary, B. G.; Anvegin, P. J.; Jansen, J. C.; Yeh, C. Y.; Maschmeyer, T.; Dautzenberg, F. M.; Marchese, L.; Pastore, H. d. O.: Zeolite Composite Method for Making and Catalytic Application Thereof. In *United States Patent: US 7,084,087 B2*; ABB Lummus Global Inc.: USA, 2006; pp 22.
- (16) Corma, A.; Fornes, V.; Triguero, J. M.; Pergher, S. B.: Delaminated Zeolites: Combining the Benefits of Zeolites and Mesoporous Materials for Catalytic Uses. *Journal of Catalysis* **1999**, *186*, 57-63.
- (17) Corma, A.; Diaz, U.; Fornes, V.; Guil, J. M.; Triguero, J. M.; Creighton, E. J.: Characterization and Catalytic Activity of MCM-22 and MCM-56 Compared With ITQ-2. *Journal of Catalysis* **2000**, *191*, 218-224.
- (18) Delitala, C.; Alba, M. D.; Becerro, A. I.; Delpiano, D.; Meloni, D.; Musu, E.; Ferino, I.: Synthesis of MCM-22 Zeolites of Different Si/Al Ratio and their Structural, Morphological and Textural Characterisation. *Microporous and Mesoporous Materials* **2009**, *118*, 1-10.
- (19) Ayala, V.; Corma, A.; Iglesias, M.; Rincon, J. A.; Sanchez, F.: Hybrid Organic - Inorganic Catalysts: A Cooperative Effect Between Support, and Palladium and Nickel Salen Complexes on Catalytic Hydrogenation of Imines. *Journal of Catalysis* **2004**, *224*, 170-177.
- (20) Schenkel, R.; Barth, J. O.; Kornatowski, J.; Lercher, J. A.: Chemical and Structural Aspects of the Transformation of the MCM-22 Precursor into ITQ-2. In *Impact of Zeolites and Other Porous Materials on the New Technologies at the Beginning of the New Millennium, Pts a and B*; Aiello, R. G. G. T. F., Ed., 2002; Vol. 142; pp 69-76.
- (21) Frontera, P.; Testa, F.; Aiello, R.; Candamano, S.; Nagy, J. B.: Transformation of MCM-22(P) into ITQ-2: The Role of Framework Aluminium. *Microporous and Mesoporous Materials* **2007**, *106*, 107-114.
- (22) Canos, A. C.; Segui, V. F.; Pergher, S. B. C.; Canos, A. C.: Oxide Catalyst for Cracking Hydrocarbonaceous Feedstock - Has Specific X-ray Diffraction Pattern and Adsorption Capacity, Increasing Active Catalytic Surface Area. In *World Intellectual Property Organization: WO 9717290-A*; Shell Int Res Mij Bv (Shel) Universidad de Valencia Politecnica (Uypv) Consejo Superior Investigaciones Cientif (Cnsj) Universidad de Valencia Politecnica Consejo Superi (Uypv): Spain, 1997.
- (23) Diaz, U.; Fornes, V.; Corma, A.: On the Mechanism of Zeolite Growing: Crystallization by Seeding with Delayed Zeolites. *Microporous and Mesoporous Materials* **2006**, *90*, 73-80.
- (24) Jácome, M. A. C.; Toledo, J. A.; Chavez, C. A.; Aguilar, M.; Wang, J. A.: Influence of Synthesis Methods on Tungsten Dispersion, Structural Deformation, and Surface Acidity in binary WO₃-ZrO₂ system. *Journal of Physical Chemistry B* **2005**, *109*, 22730-22739.

- (25) Ciesla, U.; Froba, M.; Stucky, G.; Schuth, F.: Highly Ordered Porous Zirconias From Surfactant-Controlled Syntheses: Zirconium Oxide-Sulfate and Zirconium Oxophosphate. *Chemistry of Materials* **1999**, *11*, 227-234.
- (26) Hwang, C.-C.; Chen, X.-R.; Wong, S.-T.; Chen, C.-L.; Mou, C.-Y.: Enhanced Catalytic Activity for Butane Isomerization with Alumina Promoted Tungstated Mesoporous Zirconia. *Applied Catalysis A-General* **2007**, *323*, 9-17.
- (27) Weingarten, R.; Tompsett, G. A.; Conner, W. C. J.; Huber, G. W.: Design of Solid Acid Catalysts for Aqueous-Phase Dehydration of Carbohydrates: The Role of Lewis and Brønsted Acid Sites. *Journal of Catalysis* **2011**, *279*, 174-182.
- (28) Mamman, A. S.; Lee, J. M.; Kim, Y. C.; Hwang, I. T.; Park, N. J.; Hwang, Y. K.; Chang, J. S.; Hwang, J. S.: Furfural: Hemicellulose/Xylose Derived Biochemical. *Biofuels Bioproducts & Biorefining* **2008**, *2*, 438-454.
- (29) Webster, C. E.; Drago, R. S.; Zerner, M. C.: Molecular Dimensions for Adsorptives. *Journal of the American Chemical Society* **1998**, *120*, 5509-5516.
- (30) Sjöman, E.; Mänttari, M.; Nyström, M.; Koivikko, H.; Heikkilä, H.: Separation of Xylose from Glucose by Nanofiltration from Concentrated Monosaccharide Solutions. *Journal of Membrane Science* **2007**, *292*, 106-115.
- (31) Campelo, J. M.; Lafont, F.; Marinas, J. M.: PT/SAPO-5 and PT/SAPO-11 as Catalysts for the Hydroisomerization and Hydrocracking of n-Octane. *Journal of the Chemical Society-Faraday Transactions* **1995**, *91*, 1551-1555.
- (32) Gallo, J. M. R.; Bisio, C.; Gatti, G.; Marchese, L.; Pastore, H. O.: Physicochemical Characterization and Surface Acid Properties of Mesoporous Al -SBA-15 Obtained by Direct Synthesis. *Langmuir* **2010**, *26*, 5791-5800.
- (33) Emeis, C. A.: Determination of Integrated Molar Extinction Coefficients for Infrared-Absorption Bands of Pyridine Adsorbed on Solid Acid Catalysts. *Journal of Catalysis* **1993**, *141*, 347-354.
- (34) Dam, H. E. V.; Kieboom, A. P. G.; Bekkum, H. V.: The Conversion of Fructose and Glucose in Acidic Media- Formation of Hydroxymethylfurfural. *Stärke-Starke* **1986**, *38*, 95-101.
- (35) Moreau, C.; Durand, R.; Peyron, D.; Duhamet, J.; Rivalier, P.: Selective Preparation of Furfural From Xylose Over Microporous Solid Acid Catalysts. *Industrial Crops and Products* **1998**, *7*, 95-99.
- (36) Román-Leshkov, Y.; Chheda, J. N.; Dumesic, J. A.: Phase Modifiers Promote Efficient Production of Hydroxymethylfurfural From Fructose. *Science* **2006**, *312*, 1933-1937.
- (37) Vandendool, H.; Kratz, P. D.: A Generalization of Retention Index System Including Linear Temperature Programmed Gas-Liquid Partition Chromatography. *Journal of Chromatography* **1963**, *11*, 463-471.

CHAPTER 3

Reaction of D-xylose in the presence of crystalline microporous silicoaluminophosphates (SAPOs)



Index

CHAPTER 3	163
Reaction of D-xylose in the presence of crystalline microporous silicoaluminophosphates (SAPOs).....	163
3.1. Introduction	165
3.1.1. SAPO-5.....	167
3.1.2. SAPO-11.....	168
3.1.3. SAPO-40.....	169
3.2. Results and discussion.....	170
3.2.1. Catalyst characterisation.....	170
3.2.2. Catalytic dehydration of D-xylose	175
3.2.2.1. Catalytic performance of SAPOs	175
3.2.2.2. Catalyst stability	181
3.3. Conclusions	184
3.4. References.....	184

3.1. Introduction

Two of the most commonly studied types of microporous solid acids are zeolites (aluminosilicates) and silicoaluminophosphates (SAPOs), which are important aluminosilicate-based zeolites.²⁻⁵ SAPOs can be briefly defined as molecular structures that consist of tetrahedral oxides of silicon, aluminium and phosphorous forming Si-O-Al, P-O-Al and Si-O-Si but no Si-O-P bonds.⁶ The discovery of SAPOs appeared through aluminophosphates (AIPO). The first report on aluminophosphates (AIPO) is dated from 1982 by Wilson.^{7,8} Since then, the synthesis of these materials has been widely studied and a wide range of these types of materials has been developed.⁹⁻¹¹ Microporous AIPO structures have an alternation of Al³⁺ and P⁵⁺ ions. These ions can be isomorphically replaced by heteroatoms through substitution mechanisms (Figure 3.1). A typical mechanism is the replacement of Al³⁺ by a divalent metal leading to a negatively charged framework which is compensated by the organic cationic molecules that act as structure directing agents.⁹ However, Si⁴⁺ can also be incorporated in AIPO networks, giving origin to SAPOs in 1984.^{7,12} The incorporation of silicon can be employed by two different substitution mechanisms:^{13,14} By substitution of phosphorous (SM2 substitution mechanism) or of an aluminium-phosphorous pair (SM3 substitution mechanism, Figure 3.1).^{10,15} The SM2 mechanism consists of the substitution of P⁵⁺ for Si⁴⁺ in the AIPO₄ frameworks leading to the appearance of a negative charge per each silicon ion which is balanced by the positive charge of the organic molecules inside the micropores, or protons at the Si-O-Al bridges (originating Brønsted acidity in the latter case).^{9,10} The SM2 mechanism gives an environment of a silicon atom surrounded by four aluminium atoms in the second coordination sphere (Si(OAl)₄).⁹ The amount of silicon incorporated via SM2 is limited and above certain silicon contents, both mechanisms occur.^{9,10,15} The incorporation of two Si⁴⁺ occurs via the substitution of a pair of aluminium and phosphorous ions and no charge is formed. Due to the instability of Si-O-P bonds (based on a computational study on SAPO-5),¹⁶ this mechanism is always accompanied to a certain extent by SM2 which prevents the formation of those unstable bonds.⁹ Therefore the coexistence of the SM3 and SM2 mechanisms is able to generate isolated pairs of silicon atoms with Si in Si (1Si3Al) and Si (1Si3P) configurations,¹⁷ leading to extended Si islands (silica domains) in the AIPO network, and various acid environments (Si(OAl)_n(OSi)_{4-n} (1<n<3)) located at the border of the Si island (in the interface between the islands and the Al-O-P framework). The size and concentration of the Si islands depend on the extension of SM3 to SM2;⁹ their formation is thermodynamically favoured because

high temperatures in SAPO molecular sieves promote a solid-state transformation due to the mobility of atoms (isolated silicon atoms migrate to form silicon islands in the framework).¹⁸ Although a higher number of acid sites (AS) are generated through the SM2 mechanism, the SM3 gives less amount but stronger AS that increase as the value of n in those environments decreases and as the island size increases.^{10,19} SM1 is another possible mechanism of silicon insertion which implies the substitution of aluminium for silicon, but it is not a favourable mechanism due to the formation of the unstable Si-O-P bridges.¹⁰

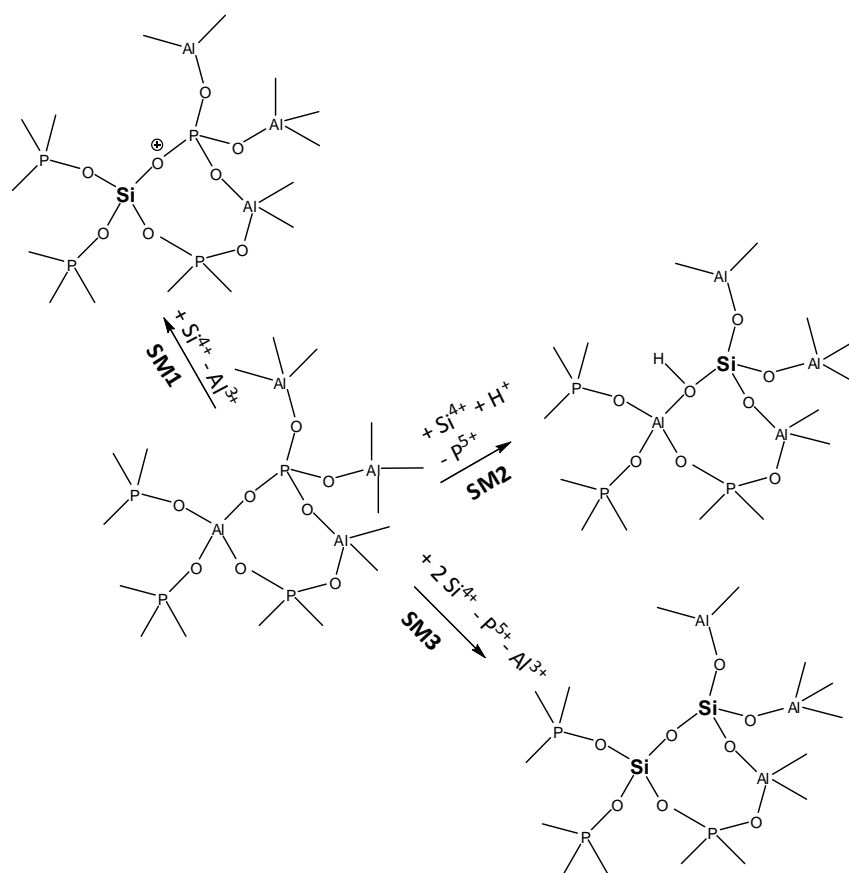


Figure 3.1- SM1, SM2 and SM3 mechanism in the transformation of AlPOs to SAPOS [adapted from ¹⁰].

In terms of catalysis, the SAPO-type materials are considered to be mildly acidic, since they are more acidic than the corresponding AlPO_4 systems but less than acid zeolites.⁷ However, since the control of the acidity of these materials can be controlled by the different mechanisms, the acidity of SAPOs is sometimes considered to be more tuneable than that of zeolites,^{10,20} which is very desirable for designing new and efficient catalysts for specific reactions.^{21,22} The

introduction of silica into the aluminophosphate structure induces ion exchange capacity and catalytic activity.²³ Therefore SAPOs are acid catalysts with very interesting properties and potential industrial applications. They have already been investigated in the isomerisation of xylene,²⁴⁻²⁶ transalkylation,²⁷ isomerisation of 1-pentene,²⁸ isopropylation of benzene,²⁹ methanol-to-hydrocarbons reaction,³⁰ and to olefins (MTO),³¹⁻³³ n-alkane cracking and hydrocracking,^{20,21} oligomerisation of propylene,³⁴ oxidative dehydrogenation of alkanes,¹⁷ transformation of alkanes,³⁵⁻³⁷ and other complex hydrocarbon transformations.³⁸

In a study of zeolites with different framework types (BEA, FAU, MFI and MOR) as catalysts for the dehydration of monosaccharides, favourable shape selective effects were reported for H-Mordenite (MOR), which possesses sufficiently large channels (6.5x7.0 Å) running in one direction.^{39,40} Besides, it is known that the size control of SAPOs is crucial to improve the catalytic activity and lifetime of the catalysts.^{11,41} These findings were relevant to screen the catalytic performance of SAPOs containing medium or large pore channels, namely SAPO-5, SAPO-11 and SAPO-40, in the dehydration of Xyl to Fur.

3.1.1. SAPO-5

The numbering of structure types of SAPO is done according to the numbering of their corresponding non-silicon substituted AlPO_4 structure. Therefore, SAPO-5 possesses the topology of AlPO_4 -5 with the same framework structure,^{26,42} which is of AFI type with a hexagonal symmetry and 1 D channels (according to the International Zeolite Association, Figure 3.2).⁴³⁻⁴⁵ The AFI framework is composed of aluminium, phosphorous and oxygen.⁴⁶ SAPO-5 is obtained by replacing at least two phosphorous atoms per unit cell in the AFI framework,^{26,47,48} being composed of alternating four and six-membered rings (4-MR and 6-MR) as secondary building units with a P6cc space group (which is a space group characteristic of hexagonal crystal systems with a C_{6v} point group that has 6 fold rotation axis and 6 minor vertical plane groups m containing the axis of rotation).²¹ The pore system consists of non-connected parallel channels of 12-MR (interconnected by 6-ring windows).^{26,42} Furthermore, in SAPO-5 each 12-MR channel is circular with pore openings of (7.3x7.3 Å).⁴² Accordingly to IUPAC, 12-MR pore apertures, SAPO-5 possesses a large pore structure.⁴⁹⁻⁵¹

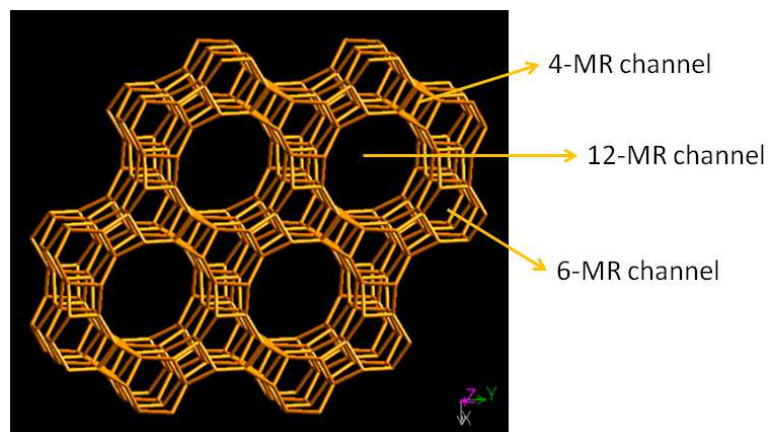


Figure 3.2- AFI framework type viewed along [001].⁴⁴

3.1.2. SAPO-11

SAPO-11 has medium pores with low density of moderate acid sites (AS),¹ belongs to 1 D pore structure and possesses the topology of AlPO_4 -11 with an AEL framework type (according to the International Zeolite Association, Figure 3.3).^{44,45,52} SAPO-11 topology consists of sheets of six-ring-six-ring-four-ring (S6R-S6R-S4R) as secondary building units, and comprises unidirectional, non-intersecting 10-MR channels (rings of ten tetrahedra),^{1,26} with elliptical pore apertures ($6.4 \times 4.4 \text{ \AA}$).²⁶ The Brønsted acid sites (B) of these structures are protons at Si-O-Al bridges located mainly inside the 10-MR channels.^{1,44,53} In SAPO-11 the silicon atoms located in the silicon islands are connected to each other by oxygen atoms; at the island borders, the O bridges connect Si to Al and Al to P.¹

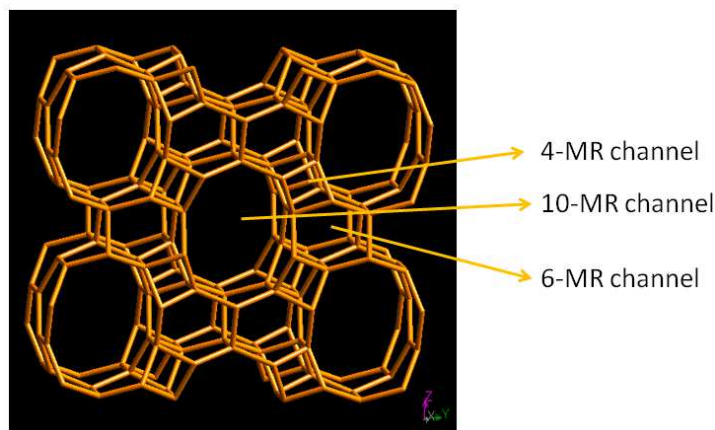


Figure 3.3- AEL framework type viewed along [001].⁴⁴

SAPO-11 can be found with different crystal sizes by controlling the aging time and temperature. The formation of crystal nuclei is favourable at lower temperatures; therefore the aging pre-treatment of the synthesis gel is employed below the normal crystallisation temperature of SAPO-11 to form a large number of nuclei with a longer time. Longer time is preferred because short aging times lead to impure SAPO-11. On the other hand, longer aging time only gives big pseudo-spherical particle aggregates, leading to small crystal size of SAPO-11 molecular sieves.^{11,54} Final products with different topology structures and morphologies are obtained during the aging process of the gels and are influenced by the changes that occur in composition and structure of the initial gel, because the nucleation of molecular sieves and the growth of crystals are affected.¹¹

3.1.3. SAPO-40

SAPO-40 was synthesised for the first time in 1984 by Lok et al.³ and presents an AFR framework topology (according to the International Zeolite Association, Figure 3.4).^{44,45} established by crystallographic methods in 1993.⁵⁵ This AFR framework consists of a large pore structure with two types of intersecting channels: 12-MR channels parallel to the z-axis and 8-MR channels parallel to the y-axis.⁵⁶ These channels intersect forming a 2 D system with pore openings of 6.7x6.9 Å and 3.7x3.7 Å respectively.⁵⁶⁻⁵⁸ A wall of 4- and 6-MR comprises a third direction (Figure 3.4).^{44,55,58} SAPO-40 has shown remarkable thermal and hydrothermal stability.⁵⁷ The acidity of SAPO-40 is related to the content and distribution of the silicon in the framework.⁵⁶

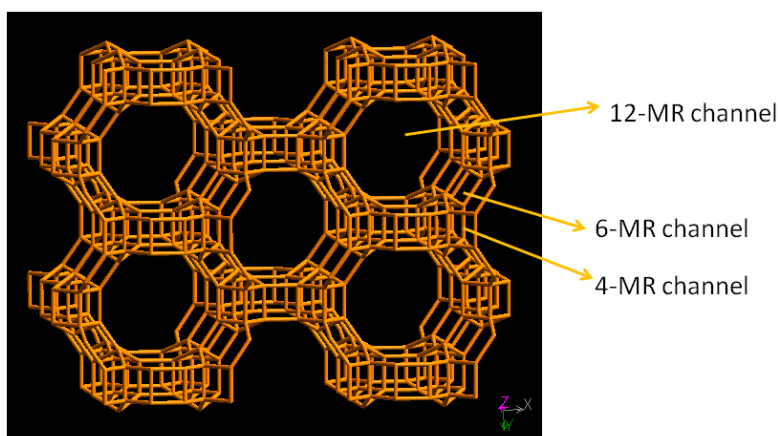


Figure 3.4- AFR framework type viewed along [001].⁴⁴

3.2. Results and discussion

3.2.1. Catalyst characterisation

In this Chapter SAPO-5, SAPO-11a, SAPO-11b and SAPO-40 materials were prepared following the procedures reported in the literature (Chapter 2). SAPO-5 was prepared as described by Weyda et al.,⁴⁸ using a mixture of an aluminophosphate gel, a gel containing the silica source and TPA as organic template. SAPO-11a and SAPO-11b were prepared by hydrothermal crystallisation according to the procedures described earlier, using pseudoboehmite aluminium, orthophosphoric acid and silica as source of aluminium, phosphorous and silicon respectively and MA and DPA as templates (for SAPO-11b) or only DPA (for SAPO 11a).^{3,59,60} SAPO-40 was prepared using pseudoboehmite alumina, orthophosphoric acid and fumed silica as aluminium, phosphorous and silicon sources as reported in the literature.^{3,61-63}

The chemical formulae of the four samples (SAPO-5, SAPO-11a, SAPO-11b and SAPO-40) are given in Table 3.1 (based on ICP-AES measurements).

Table 3.1- Structural and textural properties of the SAPOs samples.

Sample	Formula	$S_{\text{BET}}^{\text{a}}$ ($\text{m}^2 \cdot \text{g}^{-1}$)	$S_{\text{EXT}}^{\text{b}}$ ($\text{m}^2 \cdot \text{g}^{-1}$)	$V_{\text{micro}}^{\text{c}}$ ($\text{cm}^3 \cdot \text{g}^{-1}$)	Particle size (μm)
SAPO-5	$\text{Al}_{0.49}\text{P}_{0.47}\text{Si}_{0.04}\text{O}_2$	312	25	0.13	-
SAPO-11a	$\text{Al}_{0.45}\text{P}_{0.42}\text{Si}_{0.13}\text{O}_2$	274	43	0.10	1-5
SAPO-11b	$\text{Al}_{0.49}\text{P}_{0.47}\text{Si}_{0.10}\text{O}_2$	241	43	0.08	20-30
SAPO-40	$\text{Al}_{0.46}\text{P}_{0.47}\text{Si}_{0.07}\text{O}_2$	670	60	0.27	-

a) S_{BET} was estimated from the N_2 isotherms. b) S_{EXT} obtained using the t-plot method. c) V_{micro} obtained using the t-plot method.

Figure 3.5 shows the powder XRD patterns for the as-synthesised and calcined SAPO-5, SAPO-11 and SAPO-40 samples. The XRD patterns of the as-synthesised materials are identical to those reported in the literature,^{3,8} and confirmed by others for SAPO-5,^{9,21,22,26,37,38,47,64-70} SAPO-11,^{6,26,37,64,65,71-74} and SAPO-40.^{56,57,62,75,76}

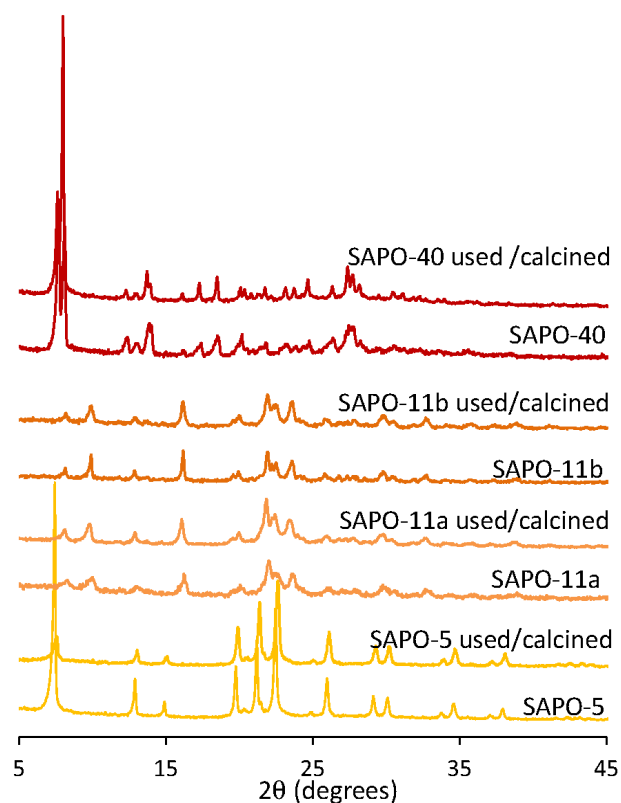


Figure 3.5- Powder XRD patterns of the fresh and used SAPO materials.

The textural properties of SAPOs were determined by nitrogen adsorption measurements at $-196\text{ }^{\circ}\text{C}$ and are collected in Table 3.1 and Figure 3.6. The adsorption isotherms of SAPO samples were of type I, which is characteristic of microporous materials.⁷⁷⁻⁸¹ An increase in adsorbed N_2 is observed at very low values of relative pressures ($p/p_0 < 0.01$) which is associated with the micropores filling mechanism.⁷⁷⁻⁸² As relative pressure approached unity a gradual increase in N_2 uptake was observed, possibly due to multi-layer adsorption in intercrystallite void spaces. The textural properties of the SAPOs are in agreement with literature data, such as V_{micro} ($0.09\text{-}0.14\text{ cm}^3\cdot\text{g}^{-1}$),^{9,64,67,68,83,84} S_{BET} ($325\text{-}359\text{ m}^2\cdot\text{g}^{-1}$),^{21,66,67} for SAPO-5, and V_{micro} ($0.09\text{ cm}^3\cdot\text{g}^{-1}$),^{64,85} S_{BET} ($235\text{-}263\text{ m}^2\cdot\text{g}^{-1}$)^{11,64,71,85} for both SAPOs 11. Although Danilina et al.⁶⁷ reported a similar S_{BET} ($325\text{ m}^2\cdot\text{g}^{-1}$) and V_{micro} ($0.10\text{ cm}^3\cdot\text{g}^{-1}$) for SAPO-5, a higher S_{EXT} was detected ($93\text{ m}^2\cdot\text{g}^{-1}$) probably due to the presence of mesoporous domains ($V_{\text{meso}}=0.12\text{ cm}^3\cdot\text{g}^{-1}$). Rather smaller specific surface areas ($S_{\text{BET}}=141\text{-}182\text{ m}^2\cdot\text{g}^{-1}$) were obtained for SAPO-5,^{22,26} and for SAPO-11 ($S_{\text{BET}}=140\text{-}208\text{ m}^2\cdot\text{g}^{-1}$),^{26,74,86} which might be correlated with the lower acid properties it revealed, which will be discussed in the next Section.⁸⁶

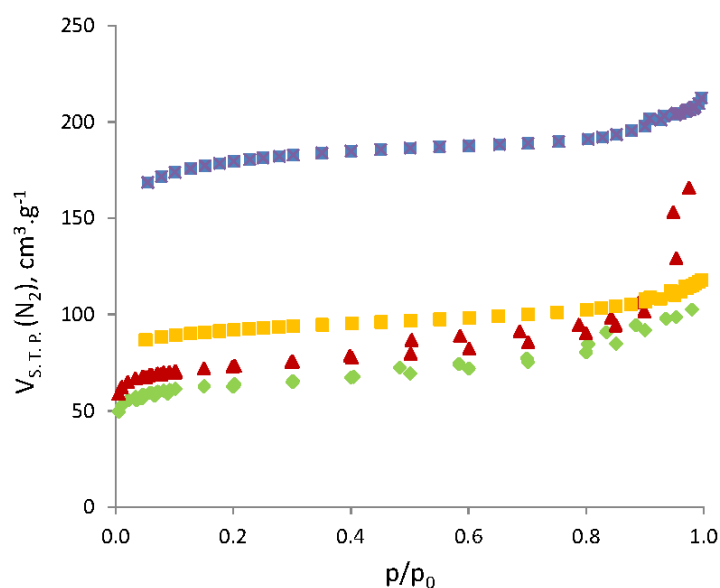


Figure 3.6- N₂ adsorption-desorption isotherms measured at -196 °C curves for SAPO-5 (orange), SAPO-11a (green), SAPO-11b (red) and SAPO-40 (blue).

SEM images of these samples are shown in Figure 3.7. Both SAPO-11 samples exhibited pseudospherical aggregates: SAPO-11b, prepared using a methylamine (MA)-based procedure, possessed aggregates with sizes between 20 and 30 μm , while SAPO-11a prepared using the MA-free procedure possessed smaller aggregates in the range 1-5 μm . These results are consistent with those reported for SAPO-11 materials prepared using the same procedure.^{64,65,71,74,85,87,88} Hexagonal prism-shaped crystals of size 3-10 μm were observed for SAPO-5, prepared with tripropylamine (TPA) as template and characteristic of AlPO₄ with an AFI topology (similar to that previously observed using as template dipropylamine (DPA),²² DPA in ethylene glycol,²⁶ or triethylamine (TEA)⁸⁴). The same morphology was obtained by other authors for SAPO-5 although with some differences in the crystal sizes (40 μm) using TPA,⁶⁴ or 15-20 μm using diethylamine (DEA).²¹ Although the organic template was not necessarily always the same, the syntheses of SAPO-5 in the mentioned works were similar and all involved hydrothermal treatment. Other morphologies have been obtained for SAPO-5 when applying different conditions, such as spherical aggregates of small crystals (with benzyl pyrrolidine and mixtures of it with TEA as structure directing agents),⁹ or rod-shaped crystals (using eutectic mixtures based on pentaerythritol and choline chloride as reaction medium by MW).⁶⁸ Spherical shapes were obtained by other authors when employing synthetic procedures similar to those used in the

present work (with TPA as template).^{65,66} Flat tabular crystals of length 2-10 μm were observed for SAPO-40, in agreement with the literature.^{55,89,90}

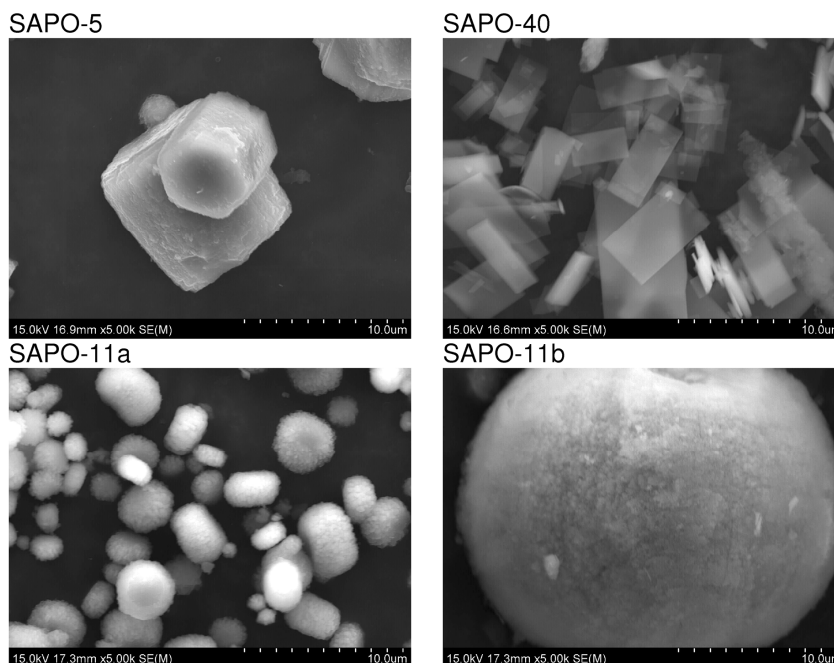


Figure 3.7- SEM images of the SAPO materials.

The introduction of silicon atoms into the framework of AlPO_4 induces Brønsted acidity.^{21,38} The acid strength is governed by the occupation of Al, Si and P atoms of the first and second shell of tetrahedral atoms around a central Si atom, their electronegativity and connectivity of tetrahedral units.^{19,91} It depends on many factors such as, bond angles, bond lengths and electrostatic potential around the AS and within the cages.¹⁰ The acid strength tends to increase with the amount of Si in the first shell and the amount of P in the second. The presence of Si islands also leads to the formation of stronger AS by forming $\text{Si}(n\text{Al})$ species ($n < 4$) at the borders of the islands.¹⁰

The acid properties of solid acids can be measured by pyridine adsorption followed by FT-IR, allowing the determination of Brønsted and Lewis acid concentrations ([B] and [L] respectively).^{92,93} The [B] is calculated by integrating the peak area of the band at 1545 cm^{-1} (C-N stretching) that results from adsorbed pyridinium ions (Hpy^+) formed by adsorption of pyridine on Brønsted acid sites (B).⁹⁴⁻¹¹¹ The area of the band at 1450 cm^{-1} is attributed to the vibration of the physical adsorbed pyridine complex formed by pyridine interactions with Lewis acid sites (L),

and is used to determine the [L].⁹⁵ The [B] and [L] were determined through equations 3.1 and 3.2, respectively.

$$[B] = \frac{A_{\text{AbsB}} \times S}{\epsilon_B \times m} \quad (3.1)$$

$$[L] = \frac{A_{\text{AbsL}} \times S}{\epsilon_L \times m} \quad (3.2)$$

in which A_{AbsB} and A_{AbsL} are the absorbances areas of Brönsted and Lewis respectively, ϵ_B and ϵ_L are the Brönsted and Lewis extinction coefficients, S is the surface area of the self-supported sample discs given by equation 3.3, and m is the mass of the sample used in the pyridine adsorption technique.

$$S = \pi r^2 \quad (3.3)$$

in which the diameter of the discs is 1.6 cm.

The molar absorption coefficients of the infrared absorption bands of pyridine adsorbed on acid sites in Si/Al-based catalysts were set equal to those determined for zeolites by Emeis.¹¹² In that study the infrared spectra of the zeolites were recorded during quantitative dosing of pyridine gas at 150 °C. The resulting values were 1.67 cm.μmol⁻¹ for the 1545 cm⁻¹ B band and 2.22 cm.μmol⁻¹ for the 1455 cm⁻¹ L band. Since there was no evidence that these integrated molar coefficients were dependent on the catalyst or the strength of the acid sites, these values could be adopted herein.

The quantitative variation of [B] and [L] in the zeotypes (SAPOs) after gas phase pyridine adsorption was analysed through the ratio shown in equation 3.4 and the amounts of AS in SAPOs are given in Table 3.2.

$$\frac{[B]}{[L]} = \frac{A_{\text{AbsB}}/\epsilon_B}{A_{\text{AbsL}}/\epsilon_L} \quad (3.4)$$

All prepared samples showed both B and L, confirmed by their interaction with pyridine after outgassing at 150 °C. The total acidity was around 120 μmol.g⁻¹ for SAPO-5 (similar to that described in previous works)²² and SAPO-11 samples, and 459 μmol.g⁻¹ for SAPO-40. However,

whereas [B] increased greatly on going from SAPO-5 and SAPO-11 to SAPO-40, [L] decreased. Although L are probably due to defective framework and/or extra-framework aluminium species, the possibility that L may arise from changes in the coordination of framework aluminium atoms upon interaction with the basic probe cannot be excluded.¹¹³ At 350 °C, pyridine desorbed more easily from the B than from the L. Thus, the ratio moderate+strong to total B (based on $[B]_{350}/[B]_{150}$) was in the range of 0.07-0.19 for all the four materials, indicating that most of the AS were of a rather weak nature. The weak Brönsted acidity is in agreement with previous studies for SAPO-11,^{65,72-74,86} SAPO-5^{21,66} and SAPO-40,⁵⁸ although stronger B have been determined for SAPO-40,^{75,56,57} SAPO-5,^{37,38,65} and SAPO-11.⁷¹ The L ratio $[L]_{350}/[L]_{150}$ was nearly 0.5 for the SAPO-5 and SAPO-11 samples, and unity for SAPO-40.

Table 3.2- Acid properties of SAPOs measured by FT-IR of adsorbed pyridine.

Sample	$[L]+[B]$ ($\mu\text{mol.g}^{-1}$) ^a	[B] ($\mu\text{mol.g}^{-1}$) ^b	[L] ($\mu\text{mol.g}^{-1}$) ^c	[L]/[B]	$[L]_{350}/[L]_{150}$ ^{d, e}	$[B]_{350}/[B]_{150}$ ^{d, e}
SAPO-5	124	78	46	0.58	0.48	0.07
SAPO-11a	119	52	67	1.30	0.45	0.12
SAPO-11b	111	75	36	0.48	0.46	0.19
SAPO-40	459	452	7	0.01	1	0.12

a) Concentration of total acid sites measured at 150 °C. b) Concentration of Brönsted acid sites. c) Concentration of Lewis acid site. d) Concentration of acid sites ratio quantified after desorption of pyridine at 150 °C ($[L]_{150}$, $[B]_{150}$). e) Concentration of acid sites ratio quantified after desorption of pyridine at 350 °C ($[L]_{350}$, $[B]_{350}$).

3.2.2. Catalytic dehydration of D-xylose

3.2.2.1. Catalytic performance of SAPOs

In the conversion of D-xylose (Xyl) to 2-Furaldehyde (Fur), three water molecules are formed per molecule of Fur formed as discussed in Chapter 1 (Figure 3.8).

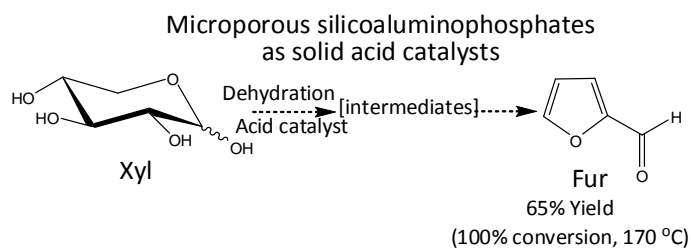


Figure 3.8- Simplified representation of the dehydration of D-xylose (Xyl) to 2-furaldehyde (Fur).

The reaction of Xyl at 170 °C in the presence of SAPO samples and under biphasic water (Wt) and toluene (Tol) conditions gave 58-65% S_{Fur} at 100% C_{Xyl} reached within 16-24 h (Figures 3.9 and 3.10, Table 3.3). In the case of the SAPO-11 samples, the higher Y_{Fur} (at 100% C_{Xyl}) was reached for the sample possessing smaller particle sizes and higher L/B ratio (Table 3.2). Usually higher catalytic activity correlated with higher total acidity. An exception is SAPO-40 which was essentially a Brønsted acid catalyst and possessed the highest total acidity, which did not correlate with its lower catalytic activity compared to the remaining SAPO samples, possibly due to differences in pore structure and surface polarity (competitive adsorption effects) and rate of catalyst deactivation by coking (catalyst surface passivation and partial pore blockage). A similar 63% Y_{Fur} was reported for the aqueous-phase reaction of Xyl (with an initial concentration of 0.05 M) in the presence of 0.03 M of H_2SO_4 at 250 °C.¹¹⁴ Under similar reaction conditions to those used in the present study, H_2SO_4 (0.03 M) gave 2% S_{Fur} at 98% C_{Xyl} within 4 h of reaction. For SAPO samples, factors which may favour Fur production are shape selectivity, acid properties (e.g. L/B ratio, discussed in the previous Section) and competitive adsorption effects. The reaction in the presence of the SAPO-11 samples gave Y_{Fur} of 34-38% at 4 h of reaction, which are comparable with that obtained for the H-Mordenite zeolite with Si/Al \approx 6 (34% Y_{Fur} at 4 h), under similar conditions.¹¹⁵ The catalytic results for SAPOs were fairly good compared with those for other solid acids tested previously as catalysts in the same reaction under similar conditions (Table 3.3).¹¹⁵⁻¹¹⁹

Table 3.3- Catalytic results for the SAPOs samples for the conversion of D-xylose (Xyl) to 2-furaldehyde (Fur) and comparison with literature data for other solid acid catalysts tested under similar conditions.

Sample	Reaction time (h)	Temperature (°C)	C_{Xyl} (%) ^d	Y_{Fur} (%) ^e	Ref
SAPO-5 ^a	6/24	170	50/99	27/62	this work
SAPO-11a ^a	4/16	170	78/100	34/65	this work
SAPO-11b ^a	4/16	170	68/100	38/61	this work
SAPO-40 ^a	6/24	170	49/100	29/58	this work
H-Mordenite	4	170	-	34	¹¹⁵
MSAZ ^b	4	160	95	39	¹¹⁶
MCM-41-SO ₃ H	24	160	72	69	¹¹⁷
del-Nu -6	6	170	87	46	¹¹⁵
H-Nu-6	6/24	170	88/98	28/52	¹¹⁵
H-AM-11	6	160	85	46	¹¹⁸
e-H-AM-11 ^c	6	160	85	39	¹¹⁸
Nb-50-MCM-41	6	160	99	39	¹¹⁸
e-Nb-50-MCM-41 ^c	6	160	92	39	¹¹⁸
Al-MCM-41	6	160	96	47	¹¹⁹

a) Reaction conditions: 0.3 Wt:0.7 Tol (v/v) biphasic solvent system, 20 g_{cat}.dm⁻³, 0.67 M Xyl. b) Alumina modified mesoporous sulfated zirconia. c) Microporous (e-H-AM-11) and mesoporous (e-Nb-50-MCM-41) niobium silicates prepared by ion-exchange method (denoted "e-"). d) Conversion of D-xylose (C_{Xyl}). e) Yield of 2-furaldehyde (Y_{Fur}).

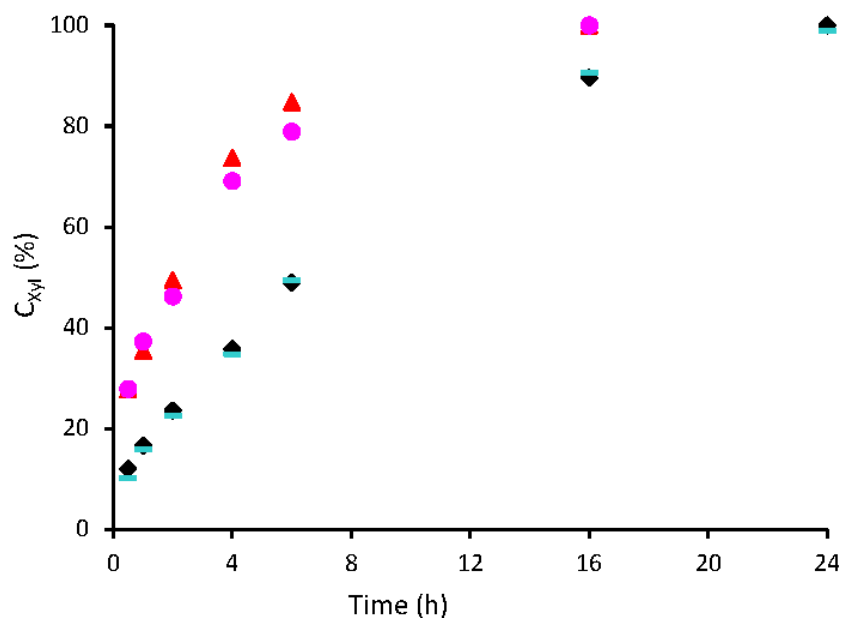


Figure 3.9- Kinetic profile of the D-xylose (Xyl) reaction in the presence of SAPO-5 (○), SAPO-11a (▲), SAPO-11b (●) and SAPO-40 (◆). Reaction conditions: 0.3 Wt:0.7 Tol (v/v) biphasic solvent system, 170 °C, 600 r.p.m, 20 g_{cat}.dm⁻³, 0.67 M Xyl.

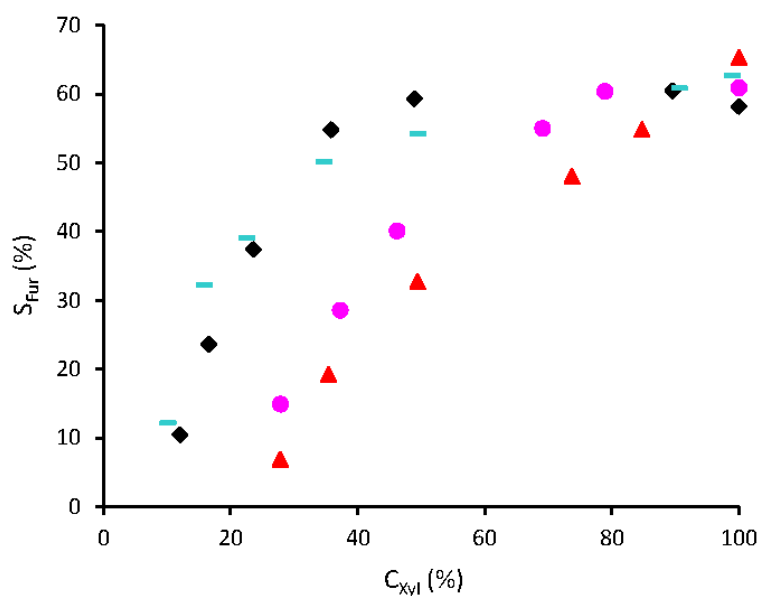


Figure 3.10- Kinetic profile of the dependence of the selectivity of 2-furaldehyde (S_{Fur}) on conversion of D-xylose (C_{Xyl}), in the presence of SAPO-5 (-), SAPO-11a (▲), SAPO-11b (●) and SAPO-40 (◆). Reaction conditions: 0.3 Wt:0.7 Tol (v/v) biphasic solvent system, 170 °C, 600 r.p.m, 20 $\text{g}_{\text{cat}}\cdot\text{dm}^{-3}$, 0.67 M Xyl.

The materials used in this work have different crystalline structures: SAPO-5 (AFI structure) and SAPO-11 (AEL structure) that consist of 1 D channel systems with pore openings of 7.3x7.3 Å and 6.4x4.4 Å, respectively, while SAPO-40 with the AFR structure consists of a 2 D channel system with pore openings of 6.7x6.9 Å and 3.7x3.7 Å. In the liquid phase the solute diffuses as a solute-solvent assemblage and catalyst-solvent interactions may reduce the effective diffusivity of Xyl within the liquid-filled pores of the SAPO materials. On the other hand, diffusivity depends on factors such as reaction temperature and viscosity of the fluid, and diffusion may be facilitated at higher temperatures. The molecular diameters (along the longest axis) of Xyl and Fur are 6.8 and 5.7 Å, respectively.¹²⁰ Considering that the “catalytic pore sizes” of zeolites are often found to exceed the crystallographic ones (by as much as 2 Å in the case of H-Mordenite, for example),¹²¹ the Xyl molecules may be able to diffuse into the channels of all three framework types, under the reaction conditions used for catalysis. Indeed, according to literature, the critical diameter (longest axis) of 8.6 Å in the D-glucose molecule is able to diffuse into the water filled 7.4 Å H-Y zeolite pore,¹²² even though in theory it is too large to enter in the H-Y zeolite. Besides the size of the solute (that affect its diffusion through the pores), other factors must be taken into

consideration, such as the structure of the substrate. The form of the D-glucose molecule in water and at 30 °C approximates that of a sphere due to its polarity and equal equatorial lengths.¹²² Deen et al.¹²³ showed that branched and spherical polysaccharides diffused faster through tracked membranes than linear polysaccharides. Netrabukkana et al.¹²² thought that the cyclic ring of D-glucose could deform and become smaller when interacting with the pore opening, allowing it to penetrate into the intracrystalline matrix. Since it is established that equilibrium between the α and β anomers of D-glucose in aqueous solutions proceeds through an acyclic intermediate,¹²² another possibility is the presence of H-Y to favour ring-opening of D-glucose into the unstable acyclic 1,2-enediol which can diffuse through the pore (possibly only at temperatures above 100 °C)¹²⁴ and thus is able to penetrate into the 7.4 Å H-Y zeolite pore.¹²²

Smaller crystallite particle sizes may enhance the overall reaction rate by increasing the number of accessible AS and decreasing the intracrystalline diffusion path lengths. To probe the existence of such effects, the catalytic activities of two SAPO-11 materials possessing different particle sizes have been compared. The conversion versus time curves for SAPO-11a (1-5 μm) and SAPO-11b (20-30 μm) were roughly coincident (Figure 3.9). SEM images for the recovered SAPO-11a and SAPO-11b solids did not show significant morphological changes (Figure 3.11, exemplified for SAPO-11a). These results suggested that the overall reaction is not strongly diffusion limited. It was noticeable that the similar reaction rate correlated with the similar total acidity,¹²⁵ and that for conversions up to about 75%, the Fur selectivities were somewhat higher for SAPO-11b than for SAPO-11a (Figure 3.10). The differences in the Fur selectivities may be partly due to the differences in the L/B ratio (Table 3.2). While there were no major differences in terms of acid strengths between the SAPO-11 samples, the number of L detected for SAPO-11a was nearly double that of SAPO-11b, and the amount of B detected for SAPO-11b was ca. 1.5 times that for SAPO-11a.

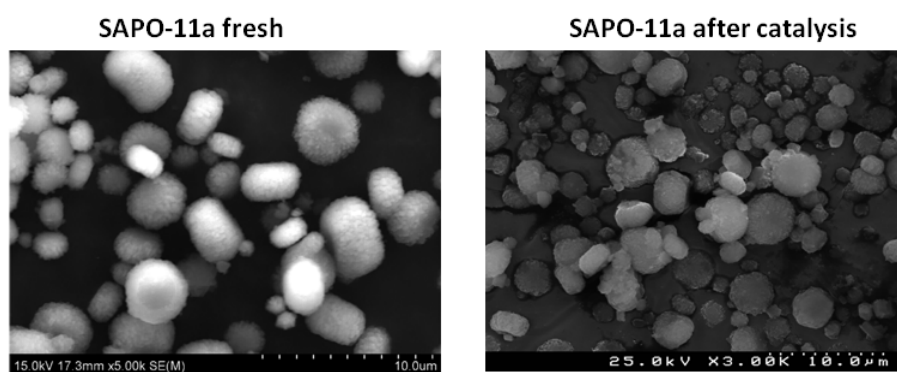


Figure 3.11- SEM images of SAPO-11a fresh and after catalysis.

In the reaction temperature range of 160-180 °C, the reaction rates (based on conversions at 2 and 4 h) increased with the temperature and the two SAPO-11 materials gave comparable conversions (Table 3.4). Similar to that observed for 170 °C, when the reaction is carried out at 160 °C or 180 °C, the Fur selectivities at similar conversions of Xyl were somewhat higher for SAPO-11b than for SAPO-11a.

Table 3.4- Reaction of D-xylose (Xyl) in the presence of SAPOs-11, at 160-180 °C.^{a)}

Samples	Temperature (°C)	C_{Xyl} (%) ^b	S_{Fur} (%) ^c
		at 2 h/4 h reaction	at 2 h/4 h reaction
SAPO-11a	160	29/46	31/50
	170	49/74	33/48
	180	76/99	26/42
SAPO-11b	160	26/49	47/58
	170	46/69	40/55
	180	73/96	36/53

a) Reaction conditions: 0.3 Wt:0.7 Tol (v/v) biphasic solvent system, 170 °C, 600 r.p.m, 20 g_{cat}.dm⁻³, 0.67 M Xyl. c) Conversion of D-xylose (C_{Xyl}). c) Selectivity of 2-furaldehyde (S_{Fur}).

The SAPO-11b and SAPO-5 samples exhibited comparable textural and acid properties, but the reaction was slower for SAPO-5 (Figure 3.9). When calculated on the basis of the surface area, the reaction rates (mmol.h⁻¹.m_{cat}⁻²) after 30 min and after 4 h of reaction followed the order (rates at 30 min; 4 h): SAPO-5 (0.13; 0.06) < SAPO-11a (0.41; 0.13) ≈ SAPO-11b (0.46; 0.14). As could be expected (since the specific surface areas were comparable), a similar trend was observed for rates calculated at the same time points on the basis of the catalyst mass (μmol.h⁻¹.g_{cat}⁻¹): SAPO-5 (41; 17) < SAPO-11a (111; 37) ≈ SAPO-11b (111; 35). Although SAPO-40 possessed the highest total acidity and the highest number of moderate+strong AS (those retaining pyridine at 350 °C), as well as the highest S_{BET} , S_{EXT} and V_{micro} , the reaction rate (on the basis of the mass of catalyst) was comparable with that observed for SAPO-5. Given the complexity of the catalytic systems it is difficult to correlate the different reaction rates with the strengths and densities of the AS for the different framework structures, and it is thus preferable to restrict the correlations to a specific structure type, as discussed above for SAPO-11.

The observed increase in the Fur selectivity with conversion for all the catalysts has been noted with other solid acid catalysts (exfoliated nanosheets,¹²⁵ layered zeolite Nu-6(1),¹¹⁵ micro and mesoporous sulfonic acids,¹¹⁷ micro and mesoporous niobium silicates,¹¹⁸ mesoporous silica supported catalysts,¹²⁶ modified sulfated zirconium¹¹⁶). The complex reaction mechanism of the conversion of Xyl to Fur involves a series of elementary steps, and the primary step of the reaction

of Xyl is possibly not rate limiting.^{114,127} On the other hand, the influence of competitive adsorption effects and changes in the surface properties of the catalysts during the reaction cannot be ruled out.

3.2.2.2. Catalyst stability

The S_{Fur} was always less than 100% (until 100% C_{Xyl}) and the originally white powders turned light brown during the reactions. No by-products were detected by gas (GC-MS of the toluene phase) or liquid (with a differential refractive index detector and an UV diode-array detection mode for the aqueous phase) chromatography, possibly because they were essentially insoluble and “non-volatile” organic compounds which were responsible for the brown colour. For the SAPO-11 materials the amount of this insoluble matter formed after 16 h reaction was estimated by removing all solids from the reaction medium by centrifugation, washing with methanol and a 50% v/v mixture of water and ethanol, drying at 65 °C and subsequently weighing and subtracting from the initial amount of catalyst. The “excess” weight corresponded to ca. 20 wt.% of the initial amount of Xyl. Using this result, the material mass balance nearly closed: (wt.% solid by-products) + (wt.% Y_{Fur}) = (20 wt.%) + (39-42 wt.%) = 59-61 wt.% Fur, compared with the 64 wt.% theoretical yield.

Differential scanning calorimetry (DSC) analyses of the fresh and used solids showed endothermic bands below 200 °C assigned to physisorbed water and volatiles. Above 200 °C, all the used catalysts exhibited exothermic bands not presented by the original catalysts (Figure 3.12 represents the curves for the two SAPO-11 samples). A small exothermic curve at ca. 330 °C appears for the unused catalysts (two SAPO-11 samples) which may be due to organic template which was not completely removed during the preparation procedures. TGA analyses of used catalysts in the temperature range of 200-550 °C indicated weight losses of 2.8-5.1%, confirming the presence of organic by-products in the washed and dried solids. The specific surface areas of the used/washed/dried SAPO-11 materials decreased significantly by a factor of ca. 12. When the washed/dried SAPO-11a was used in a second run of the Xyl reaction, the Y_{Fur} at 4 h decreased ca. 10%. Hence, the efficient regeneration of the SAPOs required removal of the organic matter, which may be accomplished by thermal treatment under air to promote the complete oxidation of the carbonaceous matter.

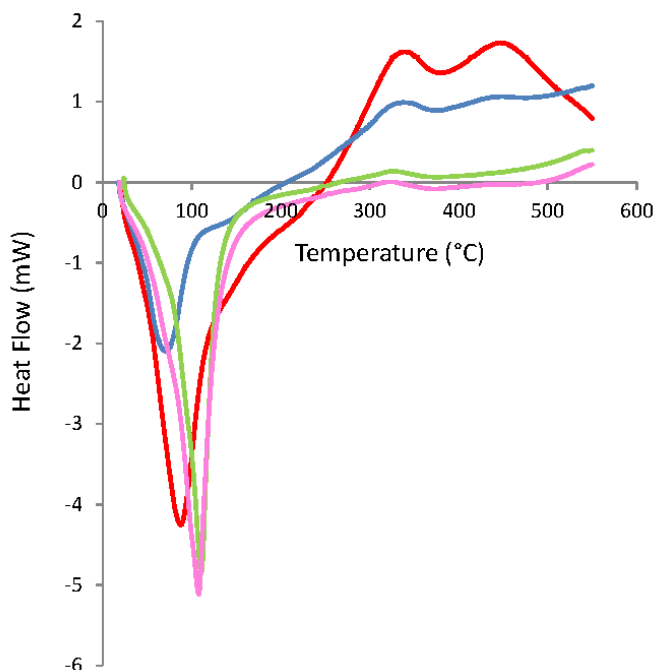


Figure 3.12- DSC curves for the two SAPO-11 samples, fresh and after 4 h of reaction: SAPO-11a fresh (pink); SAPO-11a recovered (red); SAPO-11b fresh (green); SAPO-11b recovered (blue). Reaction conditions: 0.3 Wt:0.7 Tol (v/v) biphasic solvent system, 170 °C, 20 g_{cat}.dm⁻³, 0.67 M Xyl.

The stability of the catalysts was further investigated by applying a thermal treatment (1 °C.min⁻¹ until 450 °C for 3 h, under air) after washing/drying the materials and prior to their reuse; three consecutive 4 h batch runs were performed for each sample. No significant decrease in the yield of Fur and in the conversion of Xyl was observed for any of the samples in the three consecutive runs (Figures 3.13 and 3.14 respectively). The powder XRD patterns of the fresh and recovered catalysts were quite similar indicating that the respective crystalline structures are preserved (Figure 3.5). ICP-AES analyses for the recovered SAPO-5, SAPO-11b and SAPO-40 samples showed no decrease in Si, P or Al contents (experimental error: ca. 10%). Hence the SAPO solid acids seem to be fairly stable under the reaction conditions used.

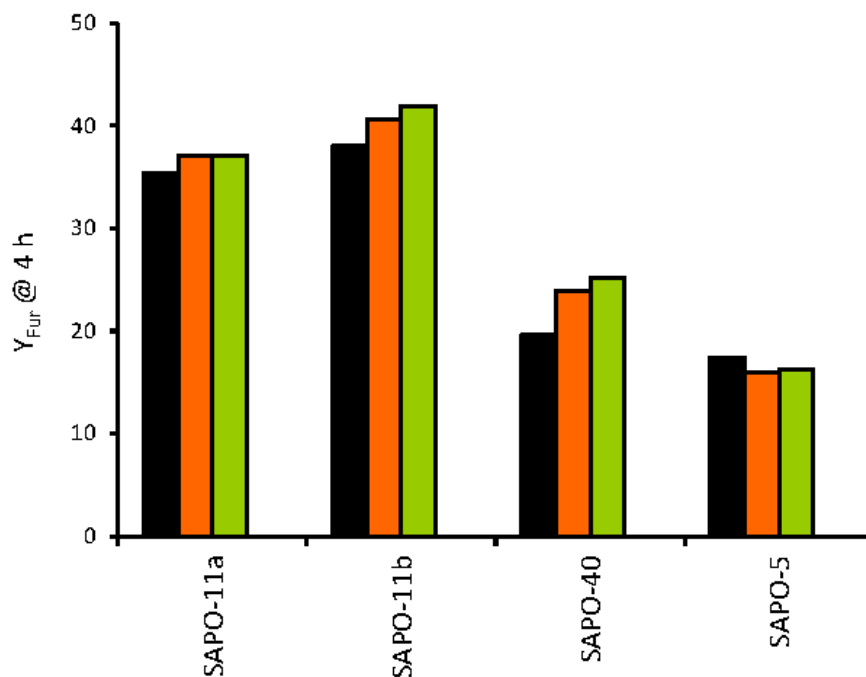


Figure 3.13- Yields of 2-furaldehyde (Y_{Fur}) in recycling runs in the presence of the SAPOs samples (4 h, 170 °C): Run 1-black bar, run 2-orange bar, run 3- green bar. Reaction conditions used: 0.3 Wt:0.7 Tol (v/v) biphasic solvent system, 170 °C, 20 $g_{cat}\cdot dm^{-3}$, 0.67 M Xyl.

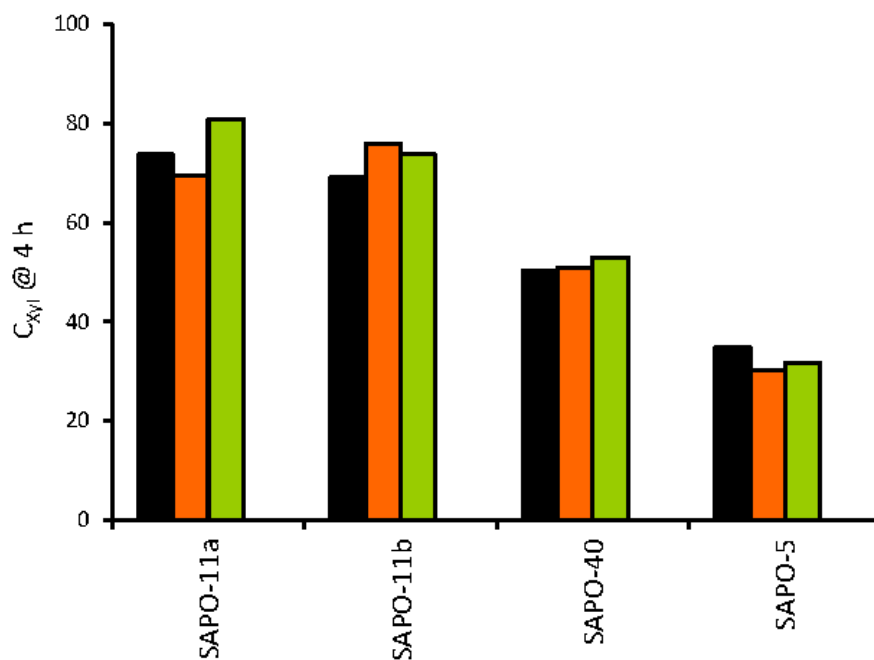


Figure 3.14- Conversions of D-xylose (C_{Xyl}) in recycling runs in the presence of the SAPOs samples (4 h, 170 °C): Run 1-black bar, run 2-orange bar, run 3- green bar. Reaction conditions: 0.3 Wt:0.7 Tol (v/v) biphasic solvent system, 170 °C, 20 $g_{cat}\cdot dm^{-3}$, 0.67 M Xyl.

3.3. Conclusions

In this work it has been demonstrated that medium pore and large pore SAPO molecular sieves can be used as recyclable solid acids for the dehydration of Xyl into Fur under aqueous-organic biphasic conditions. The similar reaction rate for the SAPO-11 materials correlated with the similar total acidity, and the differences in Fur selectivities may be partly due to the difference in the L/B ratio. Although the SAPO-11 system seems to be the most promising in this study (giving Y_{Fur} at 4 h of 34-38%, comparable with the H-Mordenite zeolite with Si/Al \approx 6), it is possible that others exhibit superior catalytic performances. On the other hand, for a specific SAPO material, the catalytic performance may be fine-tuned, based on detailed systematic investigations of the effects of the preparation method, crystallinity, morphology, silicon content and acidity on the catalytic performances: these studies may also provide insights into the factors that influence the target versus undesired reaction pathways (selectivity). When compared with other solid acids investigated previously (namely Nb-MCM-41,¹¹⁸ cesium salts of 12-tungstophosphoric acid and mesoporous silica-supported 12-tungstophosphoric acid,^{126,128} bulk and mesostructured sulfated zirconium,¹¹⁶ the investigated SAPO materials presented superior stability towards leaching (were more water-tolerant) when tested in the same reaction under comparable reaction conditions. When moving from monosaccharides to (bulkier molecules) di/polysaccharides as substrates, diffusion inside the microporous may be severely hindered. In this sense, the use of mesoporous solid acids as catalysts for the conversion of saccharides to furanic aldehydes may be preferable.

3.4. References

- (1) Sierraalta, A.; Anez, R.; Ehrmann, E.: Oniom Study of Ga/SAPO-11 Catalyst: Species Formation and Reactivity. *Journal of Molecular Catalysis A-Chemical* **2007**, *271*, 185-191.
- (2) Liu, Z. M.; Liang, J.: Methanol to Olefin Conversion Catalysts. *Current Opinion in Solid State & Materials Science* **1999**, *4*, 80-84.
- (3) Lok, B. M.; Messina, C. A.; Patton, R. L.; Gajek, R. T.; Cannan, T. R.; Flanigen, E. M.: Crystalline Silicoaluminophosphates. In *United States Patent: US 4,440,871*; Union Carbide Corporation: USA, 1984; pp 43.
- (4) Furimsky, E.: *Catalysts for Upgrading Heavy Petroleum Feeds*; Elsevier Science: Amsterdam, The Netherlands, 2007; Vol. 169.

- (5) Martenes, J. A.; Balaktishnan, I.; Grobet, P. J.; P.A., J.: On the Possibility of Generation of Brönsted Acidity by Silicon Incorporation in Very Large Pore AlPO_4 Molecular Sieves. In *Zeolite Chemistry and Catalysis, Proceeding of an International Symposium*; Jacobs, P. A., Jaeger, N. I., Kubelková, L., Wichterlov, B., Eds.; Elsevier B. V.: Prague, Czechoslovakia, 1991; Vol. 69; pp 135-143.
- (6) Prakash, A. M.; Chilukuri, S. V. V.; Bagwe, R. P.; Ashtekar, S.; Chakrabarty, D. K.: Silicoaluminophosphate Molecular Sieves SAPO-11, SAPO-31 and SAPO-41: Synthesis, Characterization and Alkylation of Toluene with Methanol. *Microporous Materials* **1996**, *6*, 89-97.
- (7) Lok, B. M.; Messina, C. A.; Patton, R. L.; Gajek, R. T.; Cannan, T. R.; Flanigen, E. M.: Silicoaluminophosphate Molecular Sieves- Another New Class of Microporous Crystalline Inorganic Solids. *Journal of the American Chemical Society* **1984**, *106*, 6092-6093.
- (8) Wilson, S. T.; Lok, B. M.; Flanigen, E. M.: Crystalline Metallophosphate Compositions. In *United States Patent: 4,310,440*; Union Carbide Corporation, New York, USA: USA, 1982; pp 27.
- (9) Hortigüela, L. G.; Alvarez, C. M.; Casas, M. G.; Garcia, R.; Pariente, J. P.: Tailoring the Acid Strength of Microporous Silicoaluminophosphates Through the Use of Mixtures of Templates: Control of the Silicon Incorporation Mechanism. *Microporous and Mesoporous Materials* **2009**, *121*, 129-137.
- (10) Pastore, H. O.; Coluccia, S.; Marchese, L.: Porous Aluminophosphates: From Molecular Sieves to Designed Acid Catalysts. In *Annual Review of Materials Research*, 2005; Vol. 35; pp 351-395.
- (11) Razavian, M.; Halladj, R.; Askari, S.: Recent Advances in Silicoaluminophosphate Nanocatalysts Synthesis Techniques and Their Effects on Particle Size Distribution. *Reviews on Advanced Materials Science* **2011**, *29*, 83-99.
- (12) Pellet, R. J.; Coughlin, P. K.; N., L. G.; Rabo, J. A.: Catalytic Cracking Process Using Silicoaluminophosphate Molecular Sieves. In *United States Patent: US 4,842,714*; UOP, Des Plaines, Illinois, USA: USA, 1989; pp 22.
- (13) Desalzarriaga, L. S.; Saldarriaga, C.; Davis, M. E.: Investigations into the Nature of a Silicoaluminophosphate with the Faujasite Structure. *Journal of the American Chemical Society* **1987**, *109*, 2686-2691.
- (14) Hasha, D.; Desalzarriaga, L. S.; Saldarriaga, C.; Hathaway, P. E.; Cox, D. F.; Davis, M. E.: Studies of Silicoaluminophosphates with The Sodalite Structure. *Journal of the American Chemical Society* **1988**, *110*, 2127-2135.
- (15) Mertens, M.; Mertens, J. A.; Grobet, P. J.; Jacobs, P. A.: *Guidelines for Mastering the Properties of Molecular Sieves: Relationships Between the Physicochemical Properties of Zeolitic Systems and Their Low Dimensionality*; Plenum Press: New York, U.S.A., 1990.
- (16) Sastre, G.; Lewis, D. W.; Catlow, C. R. A.: Structure and Stability of Silica Species in SAPO Molecular Sieves. *Journal of Physical Chemistry* **1996**, *100*, 6722-6730.
- (17) Marchese, L.; Frache, A.; Gatti, G.; Coluccia, S.; Lisi, L.; Ruoppolo, G.; Russo, G.; Pastore, H. O.: Acid SAPO-34 Catalysts for Oxidative Dehydrogenation of Ethane. *Journal of Catalysis* **2002**, *208*, 479-484.
- (18) Derewinski, M.; Peltre, M. J.; Briend, M.; Barthomeuf, D.; Man, P. P.: Solid State Transformation of SAPO-37 Molecular Sieve Above 1100 °K. *Journal of the Chemical Society-Faraday Transactions* **1993**, *89*, 1823-1828.
- (19) Barthomeuf, D.: Topological Model for the Compared Acidity of SAPOS and Sial Zeolites. *Zeolites* **1994**, *14*, 394-401.
- (20) Su, B. L.; Lamy, A.; Dzwigaj, S.; Briend, M.; Barthomeuf, D.: Oxidizing and Reducing Properties of SAPO-37 Molecular Sieve- Comparison With Acidity and Catalysis. *Applied Catalysis* **1991**, *75*, 311-320.
- (21) Wang, L. J.; Guo, C. W.; Yan, S. R.; Huang, X. D.; Li, Q. Z.: High-Silica SAPO-5 With Preferred Orientation: Synthesis, Characterization and Catalytic Applications. *Microporous and Mesoporous Materials* **2003**, *64*, 63-68.
- (22) Seelan, S.; Sinha, A. K.: Crystallization and Characterization of High Silica Silicoaluminophosphate SAPO-5. *Journal of Molecular Catalysis A-Chemical* **2004**, *215*, 149-152.
- (23) Flanigen, E. M.; Lok, B. M.; Patton, R. L.; Wilson, S. T.: Aluminophosphate Molecular Sieves and the Periodic Table. *Pure and Applied Chemistry* **1986**, *58*, 1351-1358.
- (24) Masukawa, T.; Komatsu, T.; Yashima, T.: Strong Acid Sites Generated in Aluminosilicate Region of SAPO-5. *Zeolites* **1997**, *18*, 10-17.

- (25) Urbina, M. M.; Cardoso, D.; Pariente, J. P.; Sastre, E.; Blasco, T.; Fornes, V.: Characterization and Catalytic Evaluation of SAPO-5 Synthesized in Aqueous and Two-Liquid Phase Medium in Presence of a Cationic Surfactant. *Journal of Catalysis* **1998**, *173*, 501-510.
- (26) Sinha, A. K.; Sainkar, S.; Sivasanker, S.: An Improved Method for the Synthesis of the Silicoaluminophosphate Molecular Sieves, SAPO-5, SAPO-11 and SAPO-31. *Microporous and Mesoporous Materials* **1999**, *31*, 321-331.
- (27) Hulea, V.; Bilba, N.; Lupascu, M.; Dumitriu, E.; Nibou, D.; Lebaili, S.; Kessler, H.: Study of the Transalkylation of Aromatic Hydrocarbons Over SAPO-5 Catalysts. *Microporous Materials* **1997**, *8*, 201-206.
- (28) Hocht, M.; Jentys, A.; Vinek, H.: Isomerization of 1-Pentene Over SAPO, CoAPO (AEL, AFI) Molecular Sieves and HZSM-5. *Applied Catalysis A-General* **2001**, *207*, 397-405.
- (29) Sridevi, U.; Bokade, V. V.; Satyanarayana, C. V. V.; Rao, B. S.; Pradhan, N. C.; Rao, B. K. B.: Kinetics of Propylation of Benzene over H-beta and SAPO-5 Catalysts: A Comparison. *Journal of Molecular Catalysis A-Chemical* **2002**, *181*, 257-262.
- (30) Chen, J.; Wright, P. A.; Natarajan, S.; Thomas, J. M.: Understanding the Brønsted Acidity of SAPO-5, SAPO-17, SAPO-18 and SAPO-34 and Their Catalytic Performance for Methanol Conversion to Hydrocarbons. In *Zeolites and Related Microporous Materials: State of the Art 1994*; Weitkamp, J. K. H. G. P. H. H. W., Ed., 1994; Vol. 84; pp 1731-1738.
- (31) Chen, J. S.; Wright, P. A.; Thomas, J. M.; Natarajan, S.; Marchese, L.; Bradley, S. M.; Sankar, G.; Catlow, C. R. A.; Gaiboyes, P. L.; Townsend, R. P.; Lok, C. M.: SAPO-18 Catalysts and Their Brønsted Acid Sites. *Journal of Physical Chemistry* **1994**, *98*, 10216-10224.
- (32) Stöcker, M.: Methanol to Hydrocarbons: Catalytic Materials and Their Behavior. *Microporous and Mesoporous Materials* **1999**, *29*, 3-48.
- (33) Zhu, Z. D.; Hartmann, M.; Kevan, L.: Catalytic Conversion of Methanol to Olefins on SAPO-n (n=11, 34, and 35), CrAPSO-n, and Cr-SAPO-n Molecular Sieves. *Chemistry of Materials* **2000**, *12*, 2781-2787.
- (34) Rabo, J. A.; Pellet, R. J.; Coughlin, P. K.; Samshoum, E. S.: Skeletal Rearrangement Reactions of Olefins, Paraffins and Aromatics Over Aluminophosphate Based Molecular Sieve Catalysts. In *Zeolites as Catalysts, Sorbents and Detergent Builders: Applications and Innovations, Proceedings of an International Symposium* Karge, H. G., Weitkamp, J., Eds.; Elsevier Science Ltd: Würzburg, Germany, 1989; Vol. 46; pp 1-17.
- (35) Campelo, J. M.; Lafont, F.; Marinas, J. M.: Hydroisomerization and Hydrocracking of n-Hexane on Pt/SAPO-5 and Pt/SAPO-11 Catalysts. *Zeolites* **1995**, *15*, 97-103.
- (36) Campelo, J. M.; Lafont, F.; Marinas, J. M.: Hydroisomerization and Hydrocracking of n-Heptane on Pt/SAPO-5 and Pt/SAPO-11 Catalysts. *Journal of Catalysis* **1995**, *156*, 11-18.
- (37) Meriaudeau, P.; Tuan, V. A.; Nghiem, V. T.; Lai, S. Y.; Hung, L. N.; Naccache, C.: SAPO-11, SAPO-31, and SAPO-41 Molecular Sieves: Synthesis, Characterization, and Catalytic Properties in n-Octane Hydroisomerization. *Journal of Catalysis* **1997**, *169*, 55-66.
- (38) López, C. M.; Rodríguez, K.; Méndez, B.; Montes, A.; Machado, F. J.: Influence of the Silicon Content Upon the Acidity and Catalytic Properties of AFI-Like Catalysts. *Applied Catalysis A-General* **2000**, *197*, 131-139.
- (39) Moreau, C.; Durand, R.; Pourcheron, C.; Razigade, S.: Preparation of 5-Hydroxymethylfurfural From Fructose and Precursors Over H-Form Zeolites. *Industrial Crops and Products* **1994**, *3*, 85-90.
- (40) Moreau, C.; Durand, R.; Peyron, D.; Duhamet, J.; Rivalier, P.: Selective Preparation of Furfural From Xylose Over Microporous Solid Acid Catalysts. *Industrial Crops and Products* **1998**, *7*, 95-99.
- (41) Moreau, C.; Durand, R.; Razigade, S.; Duhamet, J.; Faugeras, P.; Rivalier, P.; Ros, P.; Avignon, G.: Dehydration of Fructose to 5-Hydroxymethylfurfural Over H-Mordenites. *Applied Catalysis A-General* **1996**, *145*, 211-224.
- (42) Michalik, J.; Azuma, N.; Sadlo, J.; Kevan, L.: Silver Agglomeration in SAPO-5 and SAPO-11 Molecular Sieves. *Journal of Physical Chemistry* **1995**, *99*, 4679-4686.
- (43) Guo, Z.; Guo, C.; Jin, Q.; Li, B.; Ding, D.: Synthesis and Structure of Large AlPO₄-5 Crystals. *J Porous Mater* **2005**, *12*, 29-33.
- (44) IZA-SC-members: Zeolite Framework Types. Database of Zeolite Structures, 2012; Vol. 2012.

- (45) Meier, W.; Olson, D. H.; Baerlocher, C.; International-Zeolite-Association-Structure-Comission: *Atlas of Zeolite Structure Types*; Butterworth-Heinemann: London, 1992.
- (46) Navarro, M. V.; Puértolas, B.; García, T.; Murillo, R.; Mastral, A. M.; Gandía, F. J. V.; Castelló, D. L.; Amorós, D. C.; López, A. B.: Experimental and Simulated Propene Isotherms on Porous Solids. *Applied Surface Science* **2010**, *256*, 5292-5297.
- (47) Young, D.; Davis, M. E.: Studies on SAPO-5- Synthesis with Higher Silicon Contents. *Zeolites* **1991**, *11*, 277-281.
- (48) Weyda, H.; Lechert, H.: The Crystallization of Silicoaluminophosphates With the Structure-Type SAPO-5. *Zeolites* **1990**, *10*, 251-258.
- (49) Jacobs, P. A.; Martens, J. A.: Exploration of the Void Size and Structure of Zeolites and Molecular Sieves Using Chemical Reactions. In *Studies in Surface Science and Catalysis*; Y. Murakami, A. I., Ward, J. W., Eds.; Elsevier, 1986; Vol. Volume 28; pp 23-32.
- (50) Jacobs, P. A.; Martens, J. A.: Exploration of the Void Size and Structure of Zeolites and Molecular-Sieves Using Chemical-Reactions. *Pure and Applied Chemistry* **1986**, *58*, 1329-1338.
- (51) Nghiem, V. T.; Sapaly, G.; Meriaudeau, P.; Naccache, C.: Monodimensional Tubular Medium Pore Molecular Sieves for Selective Hydroisomerisation of Long Chain Alkanes: n-Octane Reaction on ZSM and SAPO Type Catalysts. *Topics in Catalysis* **2001**, *14*, 131-138.
- (52) Liu, Y. M.; Zhang, F. M.; Wu, H. H.; Zhang, H. J.; Yang, J. G.; Shu, X. T.; He, M. Y.: A SAPO-11 Silicoaluminophosphate Molecular Sieve With Stable Crystal Structure. *Chinese Chemical Letters* **2004**, *15*, 1258-1260.
- (53) Salehirad, F.; Anderson, M. W.: Solid-State NMR Study of Methanol Conversion Over ZSM-23, SAPO-11 and SAPO-5 Molecular Sieves. Part 2. *Journal of the Chemical Society-Faraday Transactions* **1998**, *94*, 2857-2866.
- (54) Tian, H. P.; Zhu, Z. L.; Bekheet, M. E. A.; Yuan, J. B.; Li, C. L.: Molecular Transport and SAPO-11 Crystal Growth in an $i\text{-Pr}_2\text{NH-}\text{AlPO}_4\text{-H}_3\text{PO}_4\text{-SiO}_2\text{-H}_2\text{O}$ system. *Journal of Colloid and Interface Science* **1997**, *194*, 89-94.
- (55) Dumont, N.; Gabelica, Z.; Derouane, E. G.; McCusker, L. B.: Characterization and Rietveld Refinement of the Large Pore Molecular Sieve SAPO-40. *Microporous Materials* **1993**, *1*, 149-160.
- (56) Lourenço, J. P.; Ribeiro, M. F.; Ribeiro, F. R.; Rocha, J.; Gabelica, Z.: Disproportionation of Ethylbenzene Over SAPO-40. *Reaction Kinetics and Catalysis Letters* **1996**, *59*, 219-225.
- (57) Lourenço, J. P.; Ribeiro, M. F.; Ramôa Ribeiro, F.; Rocha, J.; Gabelica, Z.: Characterization of Stability and Porosity of SAPO-40 Using m-Xylene as Model Reaction. *Applied Catalysis A: General* **1996**, *148*, 167-180.
- (58) Onida, B.; Gabelica, Z.; Lourenço, J.; Garrone, E.: Spectroscopic Characterization of Hydroxyl Groups in SAPO-40. 1. Study of the Template-Free Samples and Their Interaction with Ammonia. *The Journal of Physical Chemistry* **1996**, *100*, 11072-11079.
- (59) Fernandes, A.; Ribeiro, F. R.; Lourenço, J.; Gabelica, Z.: An Elegant Way to Increase Acidity in SAPOs: Use of Methylamine as Co-Template During Synthesis. In *Zeolites and Related Materials: Trends, Targets and Challenges, Proceedings of the 4th International Feza Conference*; Gedeon, A. M. P. B. F., Ed., 2008; Vol. 174; pp 281-284.
- (60) Bertolo, R.; Martins, A.; Silva, J. M.; Ribeiro, F.; Ribeiro, F. R.; Fernandes, A.: Incorporation of Niobium in SAPO-11 Materials: Synthesis and Characterization. *Microporous and Mesoporous Materials* **2011**, *143*, 284-290.
- (61) Dumont, N.; Gabelica, Z.; Derouane, E. G.; Renzo, F. D.: Comparative Investigation of Different Synthesis Procedures Leading to SAPO-40. *Microporous Materials* **1994**, *3*, 71-84.
- (62) Lourenço, J. P.; Ribeiro, M. F.; Ribeiro, F. R.; Rocha, J.; Gabelica, Z.; Derouane, E. G.: Thermal and Hydrothermal Stability of the Silicoaluminophosphate SAPO-40. *Microporous Materials* **1995**, *4*, 445-453.
- (63) Lourenço, J. P.; Ribeiro, M. F.; Ribeiro, F. R.; Rocha, J.; Gabelica, Z.: Characterization of Stability and Porosity of SAPO-40 Using m-Xylene as Model Reaction. *Applied Catalysis A-General* **1996**, *148*, 167-180.
- (64) Iliyas, A.; Niaki, M. H. Z.; Eić, M.; Kaliaguine, S.: Control of Hydrocarbon Cold-Start Emissions: A search for Potential Adsorbents. *Microporous and Mesoporous Materials* **2007**, *102*, 171-177.

- (65) Campelo, J. M.; Lafont, F.; Marinas, J. M.; Ojeda, M.: Studies of Catalyst Deactivation in Methanol Conversion with High, Medium and Small Pore Silicoaluminophosphates. *Applied Catalysis A: General* **2000**, *192*, 85-96.
- (66) Kumar, N.; Villegas, J. I.; Salmi, T.; Murzin, D. Y.; Heikkilä, T.: Isomerization of n-Butane to Isobutane Over Pt-SAPO-5, SAPO-5, Pt-H-Mordenite and H-Mordenite Catalysts. *Catalysis Today* **2005**, *100*, 355-361.
- (67) Danilina, N.; Krumeich, F.; Bokhoven, J. A. V.: Hierarchical SAPO-5 Catalysts Active in Acid-Catalyzed Reactions. *Journal of Catalysis* **2010**, *272*, 37-43.
- (68) Zhao, X.; Wang, H.; Kang, C.; Sun, Z.; Li, G.; Wang, X.: Ionothermal Synthesis of Mesoporous SAPO-5 Molecular Sieves by Microwave Heating and Using Eutectic Solvent as Structure-Directing Agent. *Microporous and Mesoporous Materials* **2012**, *151*, 501-505.
- (69) Roldán, R.; Sánchez, M. S.; Sankar, G.; Salguero, F. J. R.; Sanchidrián, C. J.: Influence of pH and Si Content on Si Incorporation in SAPO-5 and Their Catalytic Activity for Isomerisation of n-Heptane Over Pt Loaded Catalysts. *Microporous and Mesoporous Materials* **2007**, *99*, 288-298.
- (70) Danilina, N.; Castelanelli, S. A.; Troussard, E.; Bokhoven, J. A. v.: Influence of Synthesis Parameters on the Catalytic Activity of Hierarchical SAPO-5 in Space-Demanding Alkylation Reactions. *Catalysis Today* **2011**, *168*, 80-85.
- (71) Song, C. M.; Feng, Y.; Ma, L. L.: Characterization and Hydroisomerization Performance of SAPO-11 Molecular Sieves Synthesized by Dry Gel Conversion. *Microporous and Mesoporous Materials* **2012**, *147*, 205-211.
- (72) Zhang, D.; Barri, S. A. I.; Chadwick, D.: n-Butanol to Iso-Butene in One-Step Over Zeolite Catalysts. *Applied Catalysis A: General* **2011**, *403*, 1-11.
- (73) Lutz, W.; Kurzhals, R.; Sauerbeck, S.; Toufar, H.; Buhl, J. C.; Gesing, T.; Altenburg, W.; Jäger, C.: Hydrothermal Stability of Zeolite SAPO-11. *Microporous and Mesoporous Materials* **2010**, *132*, 31-36.
- (74) Liu, P.; Ren, J.; Sun, Y.: Influence of Template on Si Distribution of SAPO-11 and Their Performance for n-Paraffin Isomerization. *Microporous and Mesoporous Materials* **2008**, *114*, 365-372.
- (75) Lourenço, J. P.; Ribeiro, M. F.; Ribeiro, F. R.; Rocha, J.; Gabelica, Z.; Dumont, N.; Derouane, E. G.: Study of Catalytic Properties of SAPO-40. In *10th International Zeolite Conference*; Weitkamp, J. K. H. G. P. H. H. W., Ed.; Studies in Surface Science and Catalysis: Garmisch Partenkir, Germany, 1994; Vol. 84; pp 867-874.
- (76) Lourenço, J. P.; Ribeiro, M. F.; Ribeiro, F. R.; Rocha, J.; Gabelica, Z.: Solid-State NMR and Powder XRD Studies of the Structure of SAPO-40 Upon Hydration-Dehydration Cycles. *Journal of the Chemical Society, Faraday Transactions* **1995**, *91*, 2213-2215.
- (77) Sing, K. S. W.; Everett, D. H.; Haul, R. A. W.; Moscou, L.; Pierotti, R. A.; Rouquerol, F.; Siemieniewska, T.: Reporting Physisorption Data for Gas/Solid Systems With Special Reference to the Determination of Surface Area and Porosity (IUPAC Recommendations 1984). *Pure and Applied Chemistry* **1985**, *57*, 603-619.
- (78) Burgess, C. G. V.; Everett, D. H.; Nuttall, S.: Adsorption Hysteresis in Porous Materials. *Pure and Applied Chemistry* **1989**, *61*, 1845-1852.
- (79) Rouquerol, F.; Advnir, D.; Fairbridge, C. W.; Everett, D. H.; Haynes, J. H.; Pernicone, N.; Ramsay, J. D. F.; Sing, K. S. W.; Under, K. K.: Recommendations for the Characterization of Porous Solids. *Pure and Applied Chemistry* **1994**, *66*, 1739-1758.
- (80) Rouquerol, F.; Rouquerol, J.; Sing, K.: *Adsorption by Powders and Porous Solids: Principles, Methodology and Applications*; Academic Press: San Diego, USA, 1998.
- (81) Gregg, S. J.; Sing, K. S. W.: *Adsorption, Surface Area, and Porosity*; 2nd ed.; Academic Press: London, 1982.
- (82) Figueiredo, J. L.; Ribeiro, F. R.: Caracterização Físico-Química dos Catalisadores. In *Catálise Heterogénea*; Fundação Calouste Gulbenkian: Lisboa, 1987; pp 77-128.
- (83) Martens, J. A.; Grobet, P. J.; Jacobs, P. A.: Catalytic Activity and Si, Al, P Ordering in Microporous Silicoaluminophosphates of the SAPO-5, SAPO-11, and SAPO-37 Type. *Journal of Catalysis* **1990**, *126*, 299-305.
- (84) Utchariyajit, K.; Wongkasemjit, S.: Effect of Synthesis Parameters on Mesoporous SAPO-5 with AFI-Type Formation Via Microwave Radiation Using Alumatrane and Silatrane precursors. *Microporous and Mesoporous Materials* **2010**, *135*, 116-123.

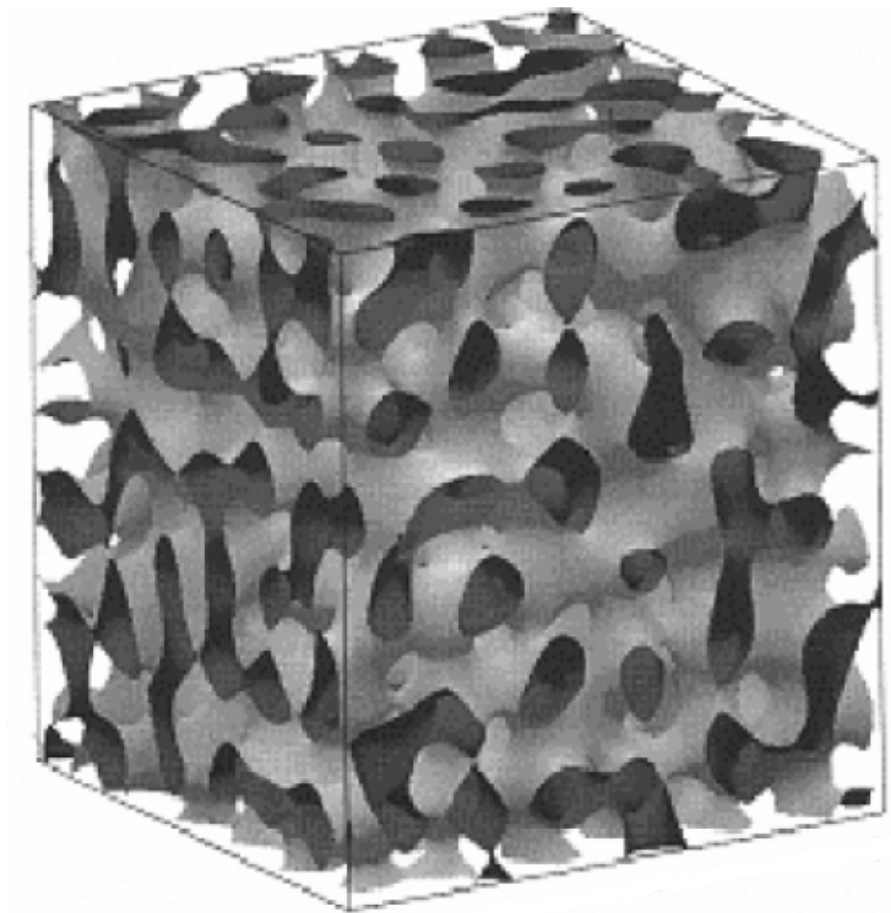
- (85) Bértolo, R.; Fernandes, A.; Ribeiro, F.; Silva, J. M.; Martins, A.; Ribeiro, F. R.: Hydroisomerization of n-Decane Over SAPO-11 Catalysts Synthesized With Methylamine as Co-Template. *Reaction Kinetics Mechanisms and Catalysis* **2010**, *99*, 183-191.
- (86) López, C. M.; Guillén, Y.; García, L.; Gómez, L.; Ramírez, A.: n-Pentane Hydroisomerization on Pt Containing H-ZSM-5, H-BEA and SAPO-11. *Catalysis Letters* **2008**, *122*, 267-273.
- (87) Fernandes, A.; Ribeiro, F.; Lourenço, J.; Gabelica, Z.: An Elegant Way to Increase Acidity in SAPOs: Use of Methylamine as Co-Template During Synthesis. In *Zeolites and Related Materials: Trends, Targets and Challenges, Proceedings of the 4th International Feza Conference*; Gedeon, A. M. P. B. F., Ed., 2008; Vol. 174; pp 281-284.
- (88) Xiaomei, Y.; Zhusheng, X.; Huaijun, M.; Yunpeng, X.; Zhijian, T.; Liwu, L.: Synthesis of SAPO-11 and MgAPO-11 Molecular Sieves in Water-Butanol Biphasic Media. *Chinese Journal of Catalysis* **2007**, *28*, 187-189.
- (89) Renzo, F. D.; Dumont, N.; Trens, P.; Gabelica, Z.: Growth Kinetics and H-Shaped Crystals of SAPO-40. *Journal of Crystal Growth* **2003**, *259*, 160-164.
- (90) Derewinski, M.; Barthomeuf, D.: High Thermal Stability of SAPO-40 in N-Octane Cracking. *Applied Catalysis A-General* **1995**, *128*, 79-88.
- (91) Barthomeuf, D.: Topology and Maximum Content of Isolated Species (Al, Ga, Fe, B, Si,...) in a Zeolitic Topology Framework- An Approach to Acid Catalysis. *Journal of Physical Chemistry* **1993**, *97*, 10092-10096.
- (92) Weglarski, J.; Datka, J.; He, H. Y.; Klinowski, J.: IR Spectroscopic Studies of the Acidic Properties of the Mesoporous Molecular Sieve MCM-41. *Journal of the Chemical Society-Faraday Transactions* **1996**, *92*, 5161-5164.
- (93) Jentys, A.; Pham, N. H.; Vinek, H.: Nature of Hydroxy Groups in MCM-41. *Journal of the Chemical Society-Faraday Transactions* **1996**, *92*, 3287-3291.
- (94) Kamarudin, N. H. N.; Jalil, A. A.; Triwahyono, S.; Mukti, R. R.; Aziz, M. A. A.; Setiabudi, H. D.; Muhid, M. N. M.; Hamdan, H.: Interaction of Zn^{2+} With Extraframework Aluminum in H-BEA Zeolite and its Role in Enhancing n-Pentane Isomerization. *Applied Catalysis A-General* **2012**, *431*, 104-112.
- (95) Luan, Z. H.; Fournier, J. A.: In Situ FTIR Spectroscopic Investigation of Active Sites and Adsorbate Interactions in Mesoporous Aluminosilicate SBA-15 Molecular Sieves. *Microporous and Mesoporous Materials* **2005**, *79*, 235-240.
- (96) Laredo, G. C.; Jesus Castillo, J.; Bolaños, J. N.; Romo, P. P.; Lagos, F. A.: Benzene Reduction in Gasoline by Alkylation With Olefins: Comparison of Beta and MCM-22 Catalysts. *Applied Catalysis A-General* **2012**, *413*, 140-148.
- (97) Hajjar, R.; Millot, Y.; Man, P. P.; Che, M.; Dzwigaj, S.: Two Kinds of Framework Al Sites Studied in BEA Zeolite by X-ray Diffraction, Fourier Transform Infrared Spectroscopy, NMR Techniques, and V Probe. *Journal of Physical Chemistry C* **2008**, *112*, 20167-20175.
- (98) Luque, R.; Budarin, V.; Clark, J. H.; Shuttleworth, P.; White, R. J.: Starbon (R) Acids in Alkylation and Acetylation Reactions: Effect of the Brønsted-Lewis Acidity. *Catalysis Communications* **2011**, *12*, 1471-1476.
- (99) Zheng, J.; Zeng, Q.; Yi, Y.; Wang, Y.; Ma, J.; Qin, B.; Zhang, X.; Sun, W.; Li, R.: The Hierarchical Effects of Zeolite Composites in Catalysis. *Catalysis Today* **2011**, *168*, 124-132.
- (100) Zhang, Q.; Xia, Q. H.; Lu, X. H.; Ma, X. T.; Su, K. X.: Gas-Phase Catalytic Synthesis of MTBE From MeOH and (Bu^tOH) Over Various Microporous H-Zeolites. *Indian Journal of Chemistry Section a-Inorganic Bio-Inorganic Physical Theoretical & Analytical Chemistry* **2009**, *48*, 788-792.
- (101) Gil, B.; Košová, G.; Čejka, J.: Acidity of MCM-58 and MCM-68 Zeolites in Comparison With Some Other 12-Ring Zeolites. *Microporous and Mesoporous Materials* **2010**, *129*, 256-266.
- (102) Zhang, Z.; Liu, S.; Zhu, X.; Wang, Q.; Xua, L.: Modification of H-Beta Zeolite by Fluorine and its Influence on Olefin Alkylation Thiophenic Sulfur in Gasoline. *Fuel Processing Technology* **2008**, *89*, 103-110.
- (103) Ordonsky, V. V.; Murzin, V. Y.; Monakhova, Y. V.; Zubavichus, Y. V.; Knyazeva, E. E.; Nesterenko, N. S.; Ivanova, I. I.: Oaturation, Strength and Accessibility of Acid Sites in Micro/Mesoporous Catalysts Obtained by Recrystallization of Zeolite BEA. *Microporous and Mesoporous Materials* **2007**, *105*, 101-110.

- (104) Bregolato, M.; Bolis, V.; Busco, C.; Ugliengo, P.; Bordiga, S.; Cavani, F.; Ballarini, N.; Maselli, L.; Passeri, S.; Rossetti, I.; Forni, L.: Methylation of Phenol Over High-Silica Beta Zeolite: Effect of Zeolite Acidity and Crystal Size on Catalyst Behaviour. *Journal of Catalysis* **2007**, *245*, 285-300.
- (105) Trasarti, A. F.; Marchi, A. J.; Apesteguia, C. R.: Design of Catalyst Systems For the One-Pot Synthesis of Menthols From Citral. *Journal of Catalysis* **2007**, *247*, 155-165.
- (106) Marques, J. P.; Gener, I.; Ayrault, P.; Bordado, J. C.; Lopes, J. M.; Ribeiro, F. R.; Guisnet, M.: Dealumination of HBEA Zeolite by Steaming and Acid Leaching: Distribution of the Various Aluminic Species and Identification of the Hydroxyl Groups. *Comptes Rendus Chimie* **2005**, *8*, 399-410.
- (107) Marques, J. P.; Gener, I.; Ayrault, P.; Lopes, J. M.; Ribeiro, F. R.; Guisnet, M.: Semi-Quantitative Estimation by IR of Framework, Extraframework and Defect Al Species of H-BEA Zeolites. *Chemical Communications* **2004**, 2290-2291.
- (108) Penzien, J.; Abraham, A.; Bokhoven, J. A. V.; Jentys, A.; Muller, T. E.; Sievers, C.; Lercher, J. A.: Generation and Characterization of Well-Defined Zn^{2+} Lewis Acid Sites in Ion Exchanged Zeolite BEA. *Journal of Physical Chemistry B* **2004**, *108*, 4116-4126.
- (109) Trombetta, M.; Busca, G.; Storaro, L.; Lenarda, M.; Casagrande, M.; Zambon, A.: Surface Acidity Modifications Induced by Thermal Treatments and Acid Leaching on Microcrystalline H-BEA Zeolite. A FTIR, XRD and MAS-NMR Study. *Physical Chemistry Chemical Physics* **2000**, *2*, 3529-3537.
- (110) Macedo, J. L. d.; Ghesti, G. F.; Dias, J. A.; Dias, S. C. L.: Liquid Phase Calorimetry and Adsorption Analyses of Zeolite Beta Acidity. *Physical Chemistry Chemical Physics : PCCP* **2008**, *10*, 1584-1592.
- (111) Guisnet, M.; Ayrault, P.; Coutanceau, C.; Alvarez, M. F.; Datka, J.: Acid Properties of Dealuminated Beta Zeolites Studied by IR Spectroscopy. *Journal of the Chemical Society-Faraday Transactions* **1997**, *93*, 1661-1665.
- (112) Emeis, C. A.: Determination of Integrated Molar Extinction Coefficients for Infrared Absorption Bands of Pyridine Adsorbed on Solid Acid Catalysts. *Journal of Catalysis* **1993**, *141*, 347-354.
- (113) Derewinski, M.; Briend, M.; Peltre, M. J.; Man, P. P.; Barthomeuf, D.: Changes in the Environment of Si and Al in SAPO-37 Zeolite During Acidity measurements. *Journal of Physical Chemistry* **1993**, *97*, 13730-13735.
- (114) Antal, M. J.; Leesomboon, T.; Mok, W. S.; Richards, G. N.: Kinetic Studies of the Reactions of Ketoses and Aldoses in Water at High Temperature 3-Mechanism of Formation of 2-Furaldehyde from D-Xylose. *Carbohydrate Research* **1991**, *217*, 71-85.
- (115) Lima, S.; Pillinger, M.; Valente, A. A.: Dehydration of D-xylose Into Furfural Catalysed by Solid Acids Derived From the Layered Zeolite Nu-6(1). *Catalysis Communications* **2008**, *9*, 2144-2148.
- (116) Dias, A. S.; Lima, S.; Pillinger, M.; Valente, A. A.: Modified Versions of Sulfated Zirconia as Catalysts for the Conversion of Xylose to Furfural. *Catalysis Letters* **2007**, *114*, 151-160.
- (117) Dias, A. S.; Pillinger, M.; Valente, A. A.: Dehydration of Xylose Into Furfural Over Micro-Mesoporous Sulfonic Acid Catalysts. *Journal of Catalysis* **2005**, *229*, 414-423.
- (118) Dias, A. S.; Lima, S.; Brandao, P.; Pillinger, M.; Rocha, J.; Valente, A. A.: Liquid-Phase Dehydration of D-xylose Over Microporous and Mesoporous Niobium Silicates. *Catalysis Letters* **2006**, *108*, 179-186.
- (119) Valente, A. A.; Dias, A. S.; Lima, S.; Brandão, P.; Pillinger, M.; Plácido, H.; Rocha, J.: Catalytic Performance of Microporous Nb and Mesoporous Nb or Al Silicates in the Dehydration of D-Xylose to Furfural. In *Perspectiva de la investigación sobre materiales en España en el siglo XXI: IX Congreso Nacional de Materiales*; Colección: Congressos n° 53 ed.; Materiales, S. E. d., Ed.; Servizo de Pulicaci3ns da Universidade de Vigo: University of Vigo, Vigo, Spain, 2006; Vol. II; pp 1203-1206.
- (120) O'Neill, R.; Ahmad, M. N. M.; Vanoye, L.; Aiouache, F.: Kinetics of Aqueous Phase Dehydration of Xylose Into Furfural Catalyzed by ZSM-5 Zeolite. *Industrial & Engineering Chemistry Research* **2009**, *48*, 4300-4306.
- (121) Webster, C. E.; Drago, R. S.; Zerner, M. C.: A Method for Characterizing Effective Pore Sizes of Catalysts. *Journal of Physical Chemistry B* **1999**, *103*, 1242-1249.
- (122) Netrabukkana, R.; Lourvanij, K.; Rorrer, G. L.: Diffusion of Glucose and Glucitol in Microporous and Mesoporous Silicate Aluminosilicate Catalysts. *Industrial & Engineering Chemistry Research* **1996**, *35*, 458-464.

- (123) Deen, W. M.; Bohrer, M. P.; Epstein, N. B.: Effects of Molecular Size and Configuration on Diffusion in Microporous Membranes. *Aiche Journal* **1981**, *27*, 952-959.
- (124) Lourvanij, K.; Rorrer, G. L.: Reactions of Aqueous Glucose Solutions Over Solid Acid Y-Zeolite Catalyst at 110-160 °C. *Industrial & Engineering Chemistry Research* **1993**, *32*, 11-19.
- (125) Dias, A. S.; Lima, S.; Carriazo, D.; Rives, V.; Pillinger, M.; Valente, A. A.: Exfoliated Titanate, Niobate and Titanoniobate Nanosheets as Solid Acid Catalysts for the Liquid-Phase Dehydration of D-Xylose Into Furfural. *Journal of Catalysis* **2006**, *244*, 230-237.
- (126) Dias, A. S.; Pillinger, M.; Valente, A. A.: Mesoporous Silica-Supported 12-Tungstophosphoric Acid Catalysts for the Liquid Phase Dehydration of D-Xylose. *Microporous and Mesoporous Materials* **2006**, *94*, 214-225.
- (127) Zeitsch, K. J.: *The Chemistry and Technology of Furfural and its Many By-Products*; 1st ed.; Elsevier Science B. V.: Amsterdam, The Netherlands, 2000; Vol. 13.
- (128) Dias, A. S.; Lima, S.; Pillinger, M.; Valente, A. A.: Acidic Cesium Salts of 12-Tungstophosphoric Acid as Catalysts for the Dehydration of Xylose into Furfural. *Carbohydrate Research* **2006**, *341*, 2946-2953.

CHAPTER 4

**Conversion of saccharides in the presence of
three-dimensional mesoporous Al-TUD-1**



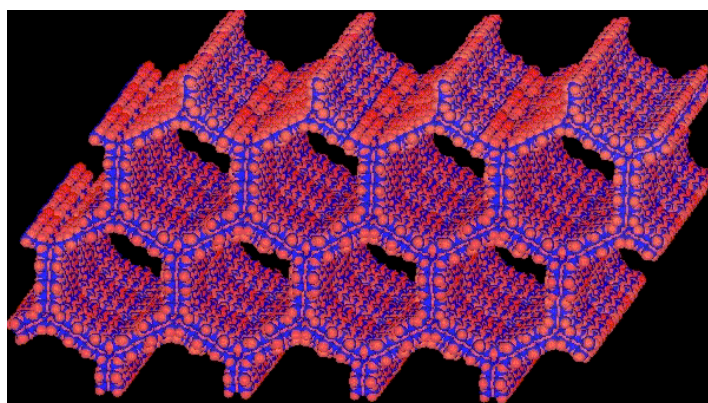
Index

CHAPTER 4	193
Conversion of saccharides in the presence of three-dimensional mesoporous Al-TUD-1	193
4.1. Introduction	195
4.2. Results and discussion.....	197
4.2.1. Catalyst characterisation.....	197
4.2.2. Hydrolysis/dehydration of carbohydrates to Fur/Hmf	203
4.2.3. Catalytic reactions of pentose-based carbohydrates to Fur	204
4.2.4. Catalytic reactions of the hexose-based carbohydrates to Hmf.....	205
4.2.5. Catalyst stability	212
4.3. Conclusions	213
4.4. References.....	214

4.1. Introduction

Of the studied catalysts, microporous zeolites or zeotype materials (such as the SAPOs samples studied in the previous Chapter) are quite promising.²⁻⁵ However, the transformation of relatively bulky saccharides may be hindered in a microporous structure because the accessibility of the pores is limited to small molecules. Hence there was an increased interest in obtaining molecular sieves with larger pore sizes and the use of mesoporous aluminosilicates may be preferable.⁶ The discovery of nanostructured mesoporous materials (M41S) came about with the introduction of supramolecular assemblies as templating agents by Mobil Oil researchers.⁷⁻⁹ The so-called M41S materials possess high specific surface areas and pore volumes with a uniform and ordered arrangement of mesopores, and controllable pore size distributions between 2 and 10 nm and the pore walls are made of amorphous silica.⁹ These features make them interesting candidates as catalysts or catalyst supports.

The first synthesis of a mesoporous silicate with a regular arrangement of pores was obtained in 1992 by the Mobil Oil Corporation.⁹ This material is known as MCM-41 (Mobil Composition of Matter number 41). It has an ordered mesostructure with 1 D hexagonal porous arrangement. It is the most widely studied of the M41S family of materials (Figure 4.1). Many other types of mesoporous materials have since then been described, such as cubic MCM-48 (Figure 4.2).



A

Figure 4.1- Representative structure of MCM-41.¹⁰

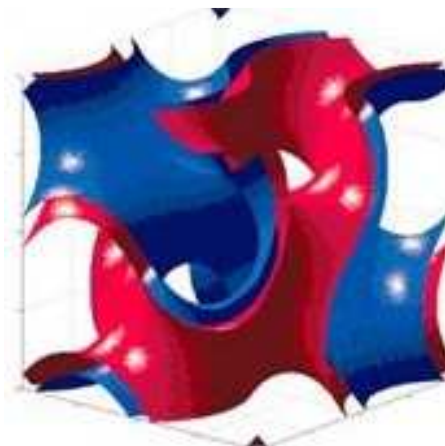
**B**

Figure 4.2- Representative structure of MCM-48.¹¹

The choice of the organic template is a key step in the synthesis of porous materials. In the case of mesoporous oxides it usually consists of supramolecular arrays such as micellar systems formed by surfactants or block copolymers as structure-directing agents.^{8,9} Economic and environmental concerns have motivated the search for low-cost and non-surfactant templating routes to mesoporous materials. An important discovery was the straightforward synthesis of the 3 D mesoporous (siliceous) oxide TUD-1 (Technische Universitat Delft), which was firstly synthesised by Shan et al.¹² in 2000.

TUD-1 can be synthesised using a silica source, water and a small and non-surfactant organic template (either triethanolamine (TENA) or tetraethyleneglycol as organic templates).¹³ The synthesis involves the polycondensation of inorganic species upon a temperature increase. Care must be taken regarding the intermolecular interaction among organic templates and inorganic species in order to have a successful formation of mesopores. For this purpose, the type of template must match with the temperature range used.¹⁴ Jansen et al.¹⁴ characterised TUD-1 as a well-defined porous material with a pore size distribution (25-250 Å in diameter), 3 D connectivities with a sponge-like or worm-like pore structure, high specific surface area (ca. 1000 m².g⁻¹) and high thermal and hydrothermal stability (at least until 1000 °C for 2 h). These features allow the access of bulky reagents to active acid sites (AS) and make TUD-1 a promising material for catalytic applications.¹³ The high specific surface area, pore volume and pore width of TUD-1 and related materials coupled with the 3 D mesoporous channel system, may facilitate a

relatively faster diffusion of molecules inside the channels, compared to 1 D pore systems in materials such as MCM-41.⁸

The purely siliceous TUD-1 may be furnished with Brönsted (B) and Lewis (L) acidity and/or redox properties by the incorporation of different metals into the framework,¹⁵ via a one-pot procedure based on the sol-gel technique.¹⁶⁻²¹ Some examples of such materials are: titanosilica (Ti-TUD-1),²²⁻²⁸ Co-TUD-1,^{23,29-34} Zr-TUD-1,^{20,35-37} Al-TUD-1,^{16-18,20,21,37-40} Cu-TUD-1,⁴¹ Fe-TUD-1,^{23,31,42-44} Cr-TUD-1,^{23,45} Mn-TUD-1,^{46,47} Mo-TUD-1,⁴⁸ V-TUD-1,^{49,50} Hf-TUD-1,⁵¹ Ga-TUD-1,^{52,53} Pd-TUD-1,⁵⁴ and Ce-TUD-1,⁵⁵ or yet bimetallic incorporation, such as Al-Zr-TUD-1.¹⁵ The high degree of framework incorporation is due to the use of a TENA in the synthesis of TUD-1, forming atrane complexes with different metals (M) which guarantees the incorporation as isolated metals instead of metal oxide clusters.^{15,48} Different metals acted similarly in the synthesis of several M-TUD-1 (M=metal).^{15-18,20-55} In this Chapter, aluminium-containing mesoporous TUD-1 (denoted as Al-TUD-1) was investigated as a solid acid catalyst in the acid-catalysed conversion of saccharides to Fur and Hmf, at 170 °C. The substrates used were D-xylose, D-fructose and D-glucose as typical monosaccharides, D-sucrose and D-cellobiose as examples of disaccharides, and D-xylan (a polymer composed mainly of D-xylose units) and inulin (a polymer of D-fructose units) as polysaccharides.

4.2. Results and discussion

4.2.1. Catalyst characterisation

In this Chapter Al-TUD-1 was synthesised as reported previously by Simons et al.¹⁸, using aluminium(III) isopropoxide and tetraethylorthosilicate (TEOS) as aluminium and silicon sources, respectively, and using TENA as organic templating agent (Chapter 2).

Elemental composition and textural properties of the prepared Al-TUD-1 are given in Table 4.1. After calcination, ICP-AES analysis indicated a Si/Al ratio of 21 for Al-TUD, which is close to the ratio of 25 used in the synthesis gel.

The powder X-ray diffraction (XRD) pattern obtained for Al-TUD-1 is characterised by the presence of a broad peak in the low angle region (around 1.4° 2θ). At higher angles the pattern

exhibited only a very broad peak centred around $24^\circ 2\theta$ (Figure 4.3), indicating that the material is amorphous,³⁷ but had characteristics of a mesostructured material.^{14,16-18,21,22,29-31,35-38,44} No evidence of crystalline Al_2O_3 phases (γ -, δ -, η -, θ -) was detected in the pattern, in accordance with the literature for the mesoporous material Al-TUD-1.^{16-18,20,21,37-40}

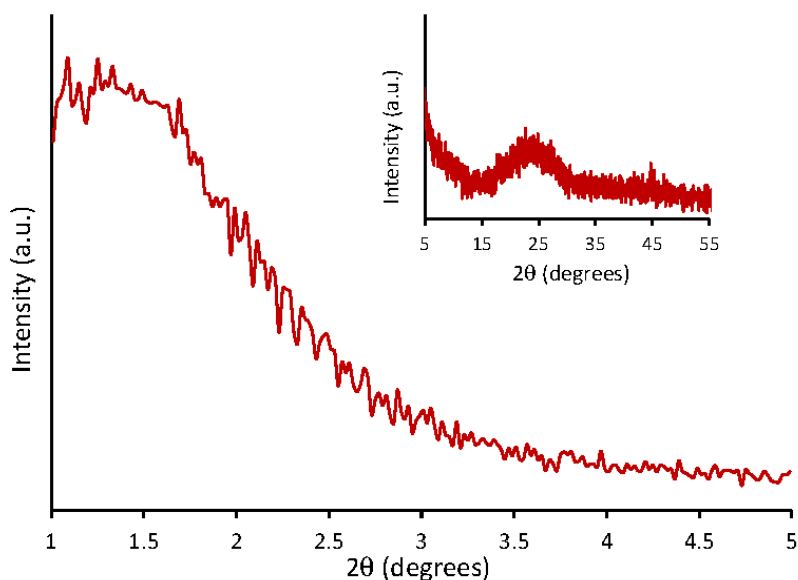


Figure 4.3- Powder XRD pattern for Al-TUD-1.

SEM analysis of Al-TUD-1 showed particles with an uneven shape and size (Figure 4.4), which is in accordance with that described in the literature for sponge or worm-like typical structures for TUD-1,¹³ in particular Al-TUD-1.¹⁷

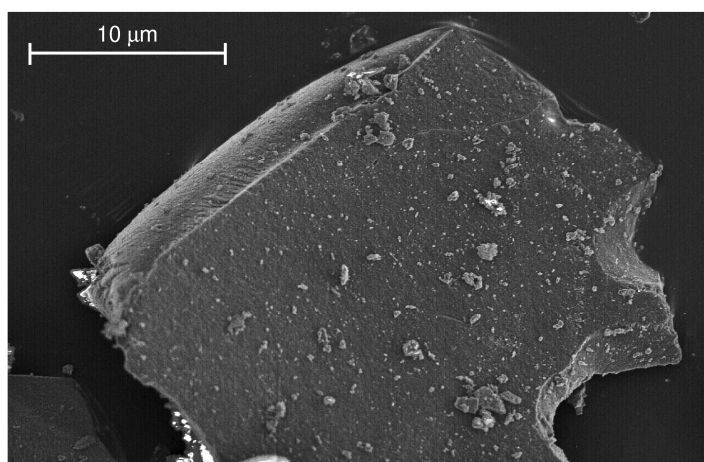


Figure 4.4- Representative SEM image of Al-TUD-1.

TEM images showed characteristics of the porous system of TUD-1 (type sponge, Figure 4.5). Probably, scaling the images, the existence of channels with approximately the width of D_p (mesoporous) measured by nitrogen adsorption at 77 K could be revealed. No crystalline nanoparticles of Al_2O_3 were detected, which indicated that the Al was incorporated into the framework, similar to previously reported studies.^{15,16}

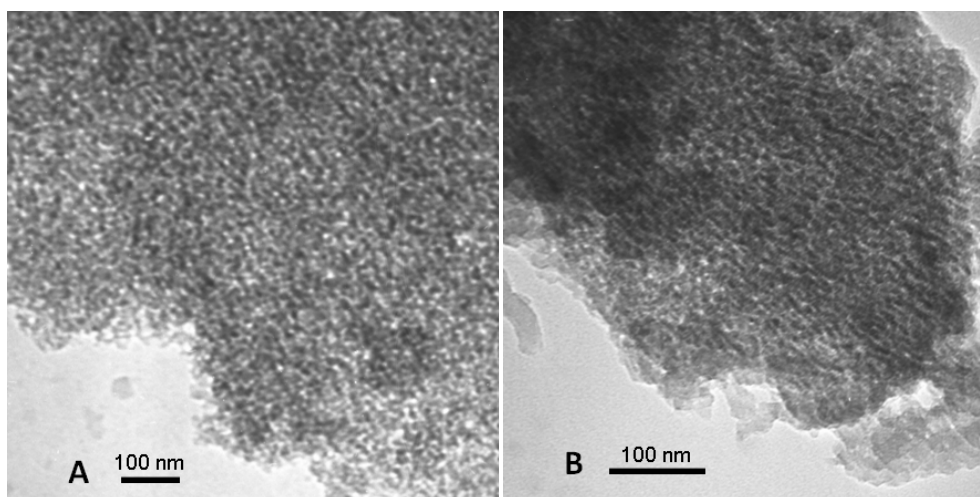


Figure 4.5- Representative TEM image of A) TUD-1 and B) Al-TUD-1.

The textural properties of Al-TUD-1 were determined by nitrogen adsorption measurements at $-196\text{ }^{\circ}\text{C}$ (Figure 4.6 and Table 4.1). Al-TUD-1 exhibited a type IV N_2 adsorption isotherm with a hysteresis loop at $p/p_0 > 0.5$ (Figure 4.6), which was consistent with the presence of a disordered mesoporous material with an interconnected (worm-like) pore network.^{19,56-58} The hysteresis loop for Al-TUD-1 seemed to be of type H-2 as it was broad, and the adsorption branch was steeper than the desorption one (almost vertical).⁵⁶⁻⁵⁸ It usually occurs in porous adsorbents with broad pore sizes and shape, when the mechanism between condensation and evaporation is different,^{56,58,59} such as porous materials with wormhole structures (TUD-1,¹⁹ and Al-TUD-1³⁸). The mesoporosity of Al-TUD-1 was also evident from the increase in nitrogen uptake at p/p_0 of ca. 0.5-0.7, as a result of the capillary condensation inside the mesopores.¹⁶ For $p/p_0 > 0.7$, the adsorption branch levels off and no more adsorption takes place in the higher relative pressure region indicating that the external surface area was negligible. Similar results were reported previously for purely siliceous and metal-incorporated TUD-1 samples.^{16-19,21,27-31,33,35-39,41,43,45-47,49-52,57,60}

Table 4.1- Si/Al molar ratio and textural properties of the prepared Al-TUD-1, and comparison with literature data for this type of material tested as catalyst in different reaction systems (liquid or gas-phase).

Si/Al (before/after catalysis)	D_p (nm)	V_p ($\text{cm}^3 \cdot \text{g}^{-1}$)	S_{meso} ($\text{m}^2 \cdot \text{g}^{-1}$)	Surface area ($\text{m}^2 \cdot \text{g}^{-1}$)	Ref
21/22 ^a	4.3 (3.9) ^c	0.77	735	757 ^h	this work
(0.5-1.5)/-	4.0-18	0.60-1.70	-	375-528 ^h	39
3.5/-	1.4 ^c	0.41 (0.08) ^d	189 ^g	357 ^h	13,38
4/-	15	1.11	-	495 ^h	21
4/-	15	1.1	-	600	18
4.9/-	2.4 ^c	0.2 ^d	204 ^g	204 ^h	13,38
10/14	3.9 ^c	-(-/0.60) ^e	-	686 ^h	16
25	3	0.75	-	760 ^h	21
25/27	3.7 ^c	0.95 ^{e,f}	-	956 ^h	15,16,20
33.3/-	3.7 ^c	0.62 ^d	-	726 ^h	44
nf ^b	4 ^c	0.63	-	528 ^h	17
50/51	3.9 ^c	-(-/0.99) ^e	-	970 ^h	16
50/-	4.3 ^c	-(-/0.7)	-	629 ^h	51
75/78	3.7 ^c	0.88 ^e	-	984 ^h	13,16
100/106	3.7 ^c	0.91 ^e	-	880 ^h	13,16

a) Determined by ICP-AES. b) nf = information not found. c) Average pore diameter calculated from the adsorption branch using BJH method and the value in parentheses calculated from the desorption branch. d) V_p is measured at $p/p_0=0.99$. Value in parenthesis refer to V_{micro} which was calculated by the t-method. e) Values in parenthesis refer to $V_{\text{micro}}/V_{\text{meso}}$ in which the V_{meso} was calculated using the t-plot method.^{16,20} f) V_p determined by BJH method.¹⁵ g) S_{meso} calculated by the t-method. h) S_{BET} determined by BET equation. The calculations for the values without an indication are not mentioned in the respective works.

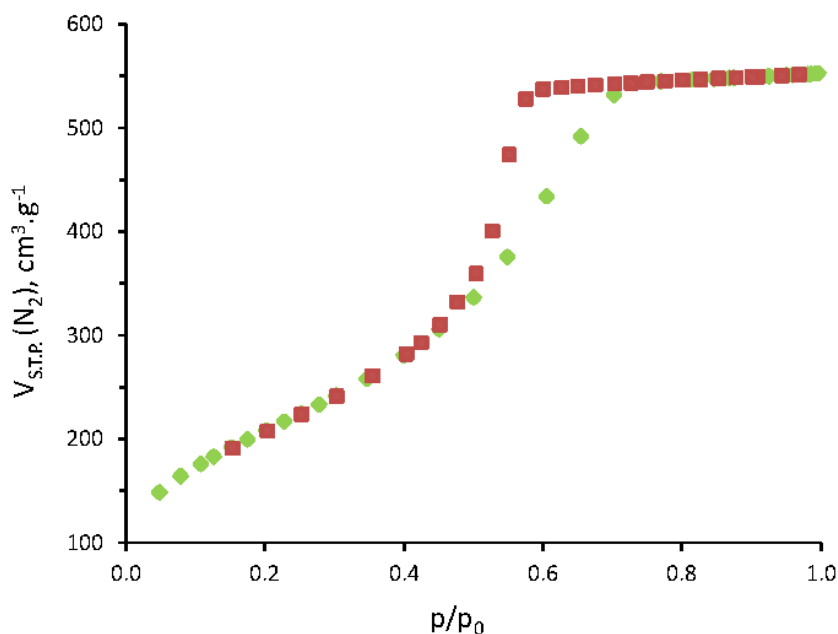


Figure 4.6- N_2 adsorption-desorption isotherm measured at $-196\text{ }^\circ\text{C}$ of Al-TUD-1. Green line is the adsorption branch; red line is the desorption branch.

The introduction of aluminium into the TUD-1 matrix generally creates hexa-, penta- and tetrahedrally coordinated aluminium.²¹ The nature of aluminium in Al-TUD-1 was investigated by using ^{27}Al -NMR spectroscopy (Figure 4.7). The spectrum obtained was very similar to that described before for Al-TUD-1 with Si/Al=4, prepared using TENA as the template,²¹ and for Al-TUD-1(30).⁶⁰ It was possible to observe the presence of aluminium species with tetrahedral coordination due to the existence of a strong resonance at $\delta=53$ ppm and hexacoordinated aluminium due to the presence of a high-field signal at $\delta=0$ ppm (Figure 4.7). An additional signal at $\delta=31$ ppm was attributed to pentacoordinated species for Al-TUD-1 with Si/Al=4.¹⁸ Anand et al.¹⁶ also obtained this third peak in an Al-TUD-1 with Si/Al=25, which they attributed to pentacoordinated aluminium or highly distorted tetrahedral sites. Other authors have reported the co-existence of the three types of aluminium species.^{16,39} These species might also be present in the Al-TUD-1 sample studied, as there is an enlargement of the peak that appears at $\delta=53$ ppm, which can overlap the signals due to pentacoordinated aluminium species.

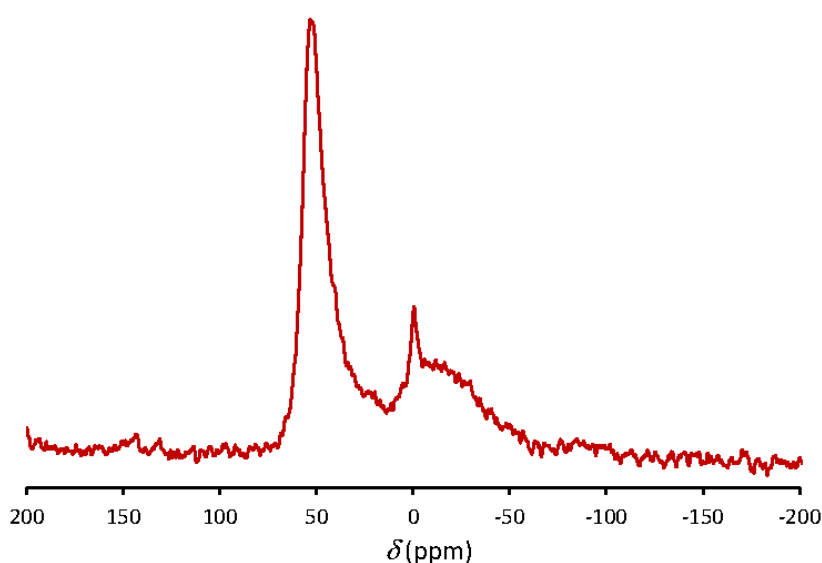


Figure 4.7- ^{27}Al MAS NMR spectrum of Al-TUD-1.

The acid properties of Al-TUD-1 were measured by adsorption of pyridine followed by FT-IR spectroscopy as explained before in Section 3.2.1.2 in Chapter 3, and [B] (band at 1545 cm^{-1}) and [L] (band at 1450 cm^{-1}) were quantified according to equations 3.1 and 3.2 described therein. The sample of Al-TUD-1 showed both L and B interacting with pyridine after outgassing at $150\text{ }^\circ\text{C}$ (Table 4.2).

Table 4.2- Acid properties of Al-TUD-1 measured by FT-IR of adsorbed pyridine and comparison with literature data.

Sample (Si/Al)	[L] ^a ($\mu\text{mol.g}^{-1}$)	[B] ^b ($\mu\text{mol.g}^{-1}$)	[L]+[B] ^c ($\mu\text{mol.g}^{-1}$)	[L]/[B]	[L] ₃₅₀ /[L] ₁₅₀	[B] ₃₅₀ /[B] ₁₅₀	Total acidity ^d ($\mu\text{mol.g}^{-1}$)	Ref
Al-TUD-1(21)	138	59	197	2.3	0.6	0.02	-	this work
Al-TUD-1(25)	24	4	28	6	-	-	370	¹⁶
Al-TUD-1(25)	-	-	-	2.4 ^c	-	-	400	¹⁵
Al-TUD-1(50)	17	2	19	2.2	-	-	220	¹⁶
Al-TUD-1(50)	133	59	192	2.2	-	-	-	⁵¹
Al-TUD-1(75)	8	2	10	4.3	-	-	210	¹⁶
Al-TUD-1(100)	8	1	9	5.4	-	-	130	¹⁶

a) Concentration of Lewis acid sites (L) based on pyridine FT-IR spectroscopic data. b) Concentration of Brønsted acid sites (B) based on pyridine FT-IR spectroscopic data. c) Total amount of acid sites based on pyridine FT-IR spectroscopic data. d) Determined by TPD-NH₃ at 200 °C.

Although the L are probably due to defective framework and/or extra-framework aluminium species, the possibility that L may also arise from tetrahedral aluminium cannot be excluded. Indeed, in a study of the adsorption of pyridine on mesoporous aluminosilicate SBA-15 molecular sieves, Luan and Fournier reported that the tetrahedral aluminium centres contributed only to L acidity.⁶¹ Normally, in crystalline zeolite materials, tetrahedral aluminium is expected to form bridging hydroxyl groups (Si-OH-Al), contributing to B acidity. However, Luan and Fourier reasoned that tetrahedral aluminium in mesoporous aluminosilicates with amorphous pore walls could contribute to L acidity due to crystallographic disorder at the atomic level.^{16,61} This can explain why the concentration of B was lower than that of L, similar to that described in the literature for Al-TUD-1 with different Si/Al ratios.^{15,51} Nevertheless, it is worth mentioning that the number of B in Al-TUD-1 may be underestimated since pyridine is a weak base (compared with, for example, ammonia) and may not be able to deprotonate the weaker AS present in the sample. However ammonia was not chosen because it may lead to an overestimate of the effective number of AS because of its smaller molecular dimensions in comparison to the saccharide molecules.⁶²

For Al-TUD-1, at 350 °C pyridine desorbed more easily from the B than from the L. Thus, the molar ratio of moderate and strong to total B ($[\text{B}]_{350}/[\text{B}]_{150}$) was 0.02, indicating that most of the AS were of a rather weak nature, which means that for Al-TUD-1 at 350 °C, the B desorbed nearly all the pyridine. The L ratio ($[\text{L}]_{350}/[\text{L}]_{150}$) was 0.6.

4.2.2. Hydrolysis/dehydration of carbohydrates to Fur/Hmf

The liquid phase conversion of different saccharides (D-xylose, D-fructose, D-glucose, D-sucrose, D-cellobiose, D-xylan and inulin) under nitrogen in the presence of AI-TUD-1 was investigated at 170 °C using a water (Wt): toluene (Tol) biphasic solvent system. The biphasic solvent system was used because as mentioned in Chapter 1, the Fur and Hmf selectivities are improved by using an organic extracting solvent since the reaction of the saccharides takes place in the aqueous phase, and the product Fur or Hmf is partially transferred into the organic phase avoiding its decomposition.^{63,64} Unless otherwise specified, product yields are reported in mol.%. The acid hydrolysis of polysaccharides gives monosaccharides, while the dehydration of pentoses and hexoses gives Fur and Hmf, respectively, via the elimination of three water molecules per molecule of monosaccharide (Figure 4.8).⁶⁵⁻⁶⁷

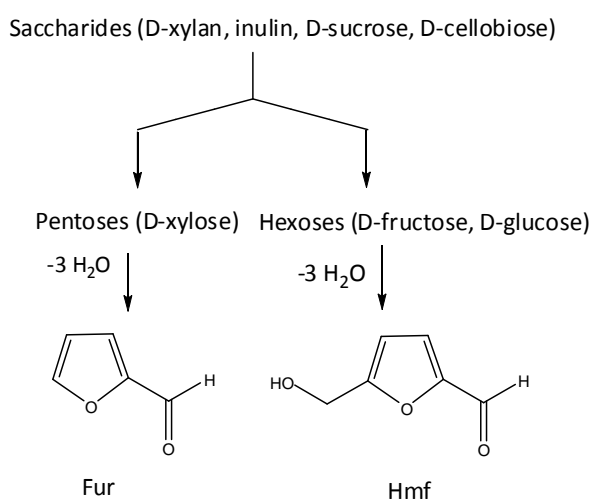


Figure 4.8- Simplified representation of the acid hydrolysis and dehydration of saccharides to 2-furaldehyde (Fur) and 5-hydroxymethyl-2-furaldehyde (Hmf).

4.2.3. Catalytic reactions of pentose-based carbohydrates to Fur

The reaction of Xyl in the presence of Al-TUD-1 gave 56/60% Y_{Fur} at 4 h/6 h (Figure 4.9). These results compared favourably with microporous silicoaluminophosphates (34-38% and 41-48% Y_{Fur} for SAPO-11 at 4 h and 6 h), used as solid acid catalysts in the same reaction, under similar conditions (Chapter 3), and with those previously reported for a delaminated zeolite del-Nu-6 (Si/Al=29), obtained by swelling and ultrasonication of a layered precursor of Nu-6(2) (46% Y_{Fur} at 6 h),⁶⁸ and zeolite H-Mordenite (Si/Al \approx 6, 34% Y_{Fur} at 4 h).⁶⁸ The reaction of Xyl with Al-TUD-1 also compared favourably with microporous H-AM-11 and ion-exchanged e-H-AM-11 (39-46% Y_{Fur} in 6 h),⁵ modified mesoporous MCM-41 materials (Al-MCM-41,⁶⁹ Nb-50-MCM-41 and ex-Nb-50-MCM-41,⁵ ca. 39-47% Y_{Fur} at 6 h),⁶⁹ and alumina modified mesoporous sulfated zirconia (MSAZ, with a Y_{Fur} of 39% in 4 h,⁷⁰ although in these cases a slightly lower temperature of 160 °C was used instead of 170 °C (Table 3.3 in Chapter 3). Comparable results were reported previously for the exfoliated material $eH_4Nb_6O_{17}$ in which a 53% Y_{Fur} (at 97% C_{Xyl}) was achieved within 6 h of reaction at 160 °C.⁷¹ Nevertheless, the synthesis of Al-TUD-1 is simpler and possibly cheaper than that of the transition metal exfoliated material.

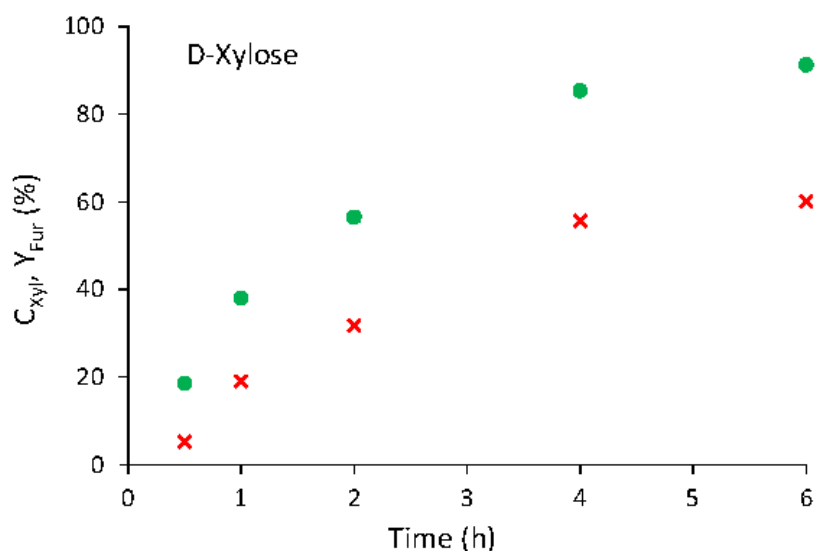


Figure 4.9- Dehydration of D-xylose in the presence of Al-TUD-1: (●) conversion of D-xylose (C_{Xyl}); (X) yield of 2-furaldehyde (Y_{Fur}). Reaction conditions: 0.3 Wt:0.7 Tol (v/v) biphasic solvent system, 170 °C, 20 $g_{cat} \cdot dm^{-3}$, 0.67 M Xyl.

The one-pot conversion (hydrolysis and dehydration) of 4-O-methyl-D-glucurono-D-xylan (D-xylan) in the presence of Al-TUD-1 gave Xyl (hydrolysis product) and Fur (dehydration product) in increasing amounts reaching 27 wt.% and 18 wt.% yield, respectively, at 6 h of reaction (Figure 4.10). The theoretical Y_{Fur} is ca. 73 wt.%.

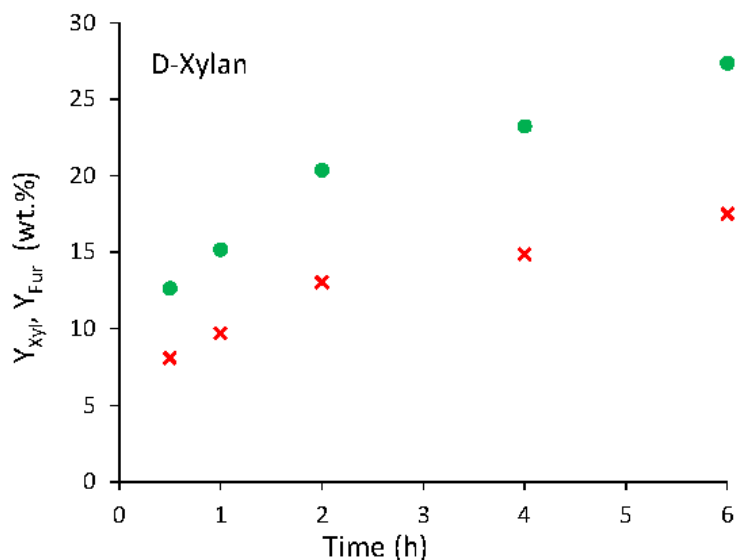


Figure 4.10- Dehydration of D-xylan in the presence of Al-TUD-1: (•) yield of D-xylose (Y_{Xyl}); (X) yield of 2-furaldehyde (Y_{Fur}). Reaction conditions: 0.3 Wt:0.7 Tol (v/v) biphasic solvent system, 170 °C, 20 $\text{g}_{\text{cat}}\cdot\text{dm}^{-3}$, 33.3 $\text{g}\cdot\text{dm}^{-3}$ D-xylan.

4.2.4. Catalytic reactions of the hexose-based carbohydrates to Hmf

Figures 4.11 and 4.12 show the catalytic results obtained for the reactions of D-fructose and D-glucose in the presence of Al-TUD-1, under similar conditions used for Xyl and D-xylan. For both hexoses, the isomers D-glucose (Glu), D-fructose (Fru) and D-mannose (Man) were simultaneously present, with the Man yield always being less than 3%. With Fru as the substrate, Glu was formed in negligible amounts (less than 3% yield). However, when the substrate was Glu, the yield of Fru reached a maximum of 16% at 61% of conversion. These results suggested that, under the applied reaction conditions, Glu has a higher tendency to isomerise to Fru than the reverse reaction, in agreement with the literature.^{63,72}

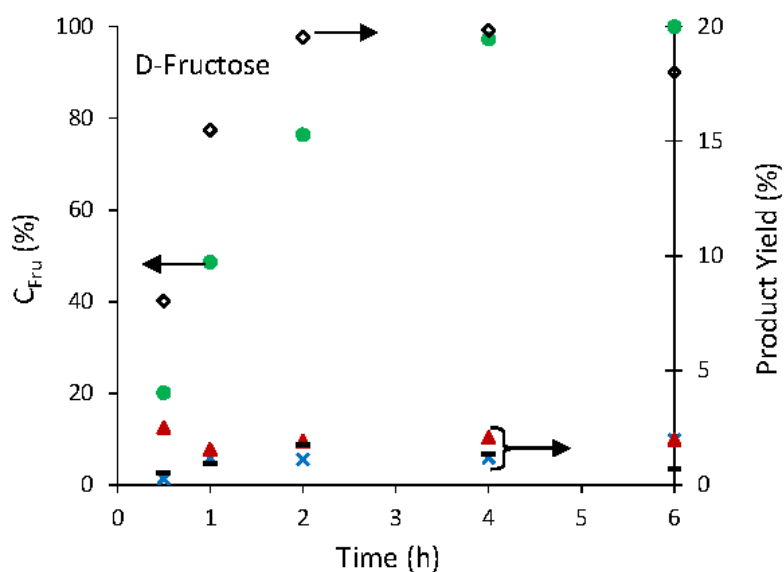


Figure 4.11- Dehydration of D-fructose in the presence of Al-TUD-1: (●) conversion of D-fructose (C_{Fru}), (▲) yield of glucose (Y_{Glu}), (◇) yield of 5-hydroxymethyl-2-furaldehyde (Y_{Hmf}), (-) yield of D-mannose (Y_{Man}) and (X) yield of 2-furaldehyde (Y_{Fur}). Reaction conditions: 0.3 Wt:0.7 Tol (v/v) biphasic solvent system, 170 °C, 20 $g_{cat}\cdot dm^{-3}$, 0.67 M Fru.

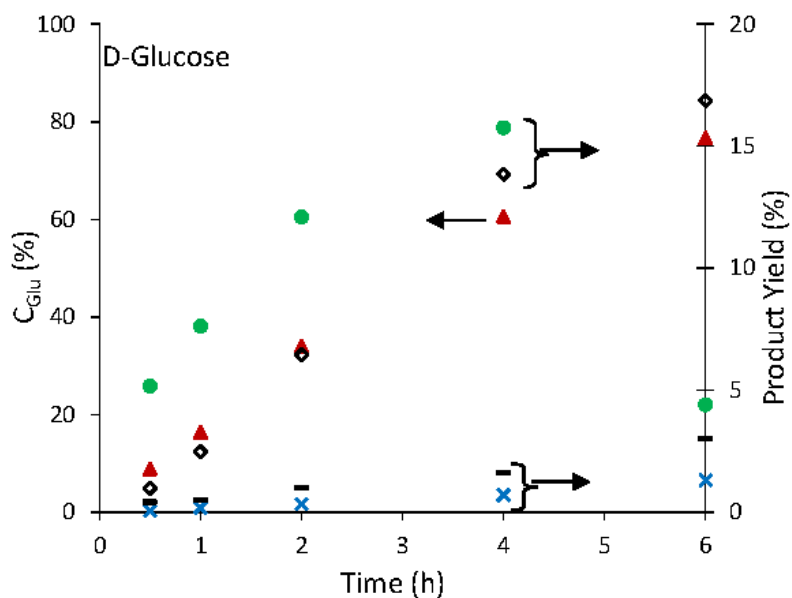


Figure 4.12- Dehydration of D-glucose in the presence of Al-TUD-1: (▲) conversion of D-glucose (C_{Glu}), (●) yield of D-fructose (Y_{Fru}), (◇) yield of 5-hydroxymethyl-2-furaldehyde (Y_{Hmf}), (-) yield of D-mannose (Y_{Man}), and (X) yield of 2-furaldehyde (Y_{Fur}). Reaction conditions used: 0.3 Wt:0.7 Tol (v/v) biphasic solvent system, 170 °C, 20 $g_{cat}\cdot dm^{-3}$, 0.67 M Glu.

Based on the kinetic profiles, it was evident that the reactivity of Fru is higher than that of Glu, giving somewhat higher Y_{Hmf} , at least until ca. 75% conversion (20% and 17% respectively). In the case of Glu, Hmf may be formed from Fru (the isomerisation product), and this pathway may be in competition with major Glu degradation pathways.⁷²⁻⁷⁴ Somewhat in parallel with those observed for AI-TUD-1, the published results for microporous zeolites used as solid acid catalysts in the conversion of hexoses to Hmf seem better for Fru than for Glu as substrate (Table 4.3). Generally, better results are then reported for the production of Hmf by the dehydration of Fru in comparison to that of Glu.^{75,76} The reaction of Glu in the presence of the zeolite H-Y (Si/Al=6.5) gave less than 10% Y_{Hmf} at ca. 75% C_{Glu} , 160 °C.⁷⁶ In contrast, the reaction of Fru in the presence of H-Beta, H-ZSM-5, H-Mordenite and H-Y Faujasite zeolites with Si/Al ratios in the range of 10-100 was quite selective towards Hmf, with one of the best results being 91% S_{Hmf} at 76% C_{Fru} for H-Mordenite(11)^{3,76}(Table 4.3). Moreau et al.^{3,76} reported that the Si/Al ratio for the zeolite catalysts influenced the rate of the reaction of Fru to Hmf, most likely due to changes in the acid properties and/or the surface polarity of the catalyst.

Table 4.3- Performance of AI-TUD-1 in the reaction of D-fructose (Fru) or D-glucose (Glu) using the biphasic solvent system (Wt:Tol)^a and comparison with literature data for zeolites as catalysts.

Catalyst	Temperature (°C)	Time (h)	$C_{\text{Fru}}/C_{\text{Glu}}$ (%) ^d	Y_{Hmf} (%) ^e	Ref
AI-TUD-1(21)	170	6	100/75	20/17	this work
H-Mordenite(11) ^b	165	1	76/-	69/-	^{76,77}
H-Mordenite(100) ^b	165	1	48/1	39/-	⁷⁷
H-Beta(15) ^b	165	1	85/-	34/-	⁷⁷
H-Y Faujasite(10) ^b	165	1	74/-	41/-	⁷⁷
H-ZSM-5(25) ^b	165	1	90/-	53/-	⁷⁷
H-Y Faujasite(6.5)	160	3	-/68	-/7	²
H-Y Faujasite ^c	150	24	-/78	-/11	⁷⁸

a) Reaction conditions: 0.3 Wt:0.7 Tol (v/v) biphasic solvent system, 170 °C, 20 $\text{g}_{\text{cat}}\cdot\text{dm}^{-3}$, 0.67 M Fru/Glu. b) Wt:IBMK= 1:5 (v/v). c) nf= information not found. d) Conversion of D-fructose (C_{Fru})/conversion of D-glucose (C_{Glu}). e) 5-Hydroxymethyl-2-furaldehyde yield (Y_{Hmf}).

The one-pot conversion of the disaccharides D-sucrose (Glu and Fru linked by an ether bond between C-1 on the Glu unit and C-2 on the Fru unit, denoted by a β -(1-2) glycosidic bond) and D-cellobiose (two Glu units linked by a β -(1-4) glycosidic bond) in the presence of AI-TUD-1 gave 100% of conversion at 1 h of reaction and 98% of conversion at 6 h of reaction, respectively, indicating that D-sucrose (Suc) is more reactive than D-cellobiose (Cel) (Figures 4.13 and 4.14). A similar relation of the substrate reactivity may be established for the zeolite H-Y Faujasite

(Si/Al=15) used as acid catalyst in the same reactions ($Y_{\text{Glu}} > 88\%$ at 90% of conversion was obtained from Cel and a quantitative yield of Fru and Glu was obtained from Suc).^{79,80}

The Si/Al ratio may have an important effect on the hydrolysis reaction rate of Suc.⁸¹ Buttersack et al.⁸¹ studied the hydrolysis over dealuminated H-Y Faujasite in which the Suc molecule adopts a conformation that allows its diffusion into the pores of the zeolite due to intensive hydrophobic interaction and adsorption over the zeolite surface. The same authors reported 90% C_{Suc} into a mixture of Fru and Glu with a selectivity close to 90% in the presence of H-Y Faujasite zeolite possessing Si/Al molar ratio of 110.⁸¹ Moreau et al.,⁷⁹ in a classical screening with different dealumination extents, demonstrated that the better compromise between catalytic activity, selectivity and by-products formation was obtained for H-Y Faujasite with a Si/Al ratio of 15 (ca.100% C_{Suc} at 152 h/100 °C, 98 wt.% Suc and ca. 100% of Fru and Glu).⁷⁹

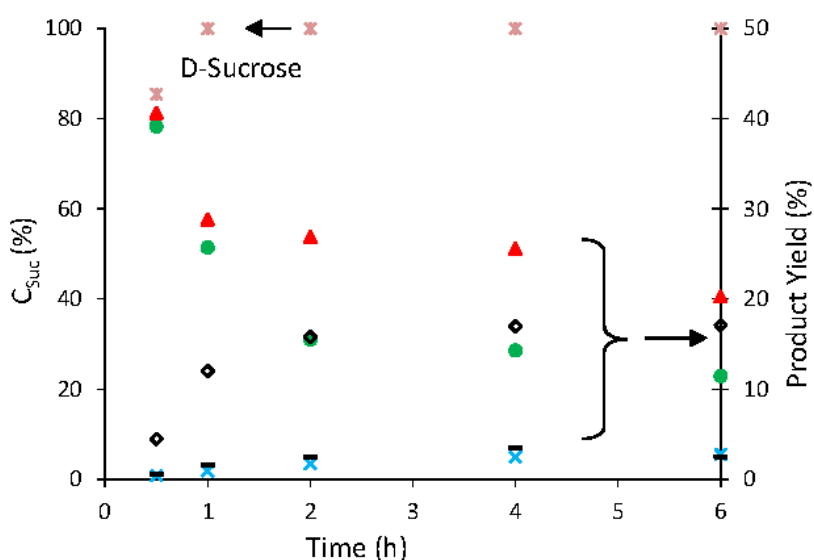


Figure 4.13- Hydrolysis and dehydration of D-sucrose in the presence of Al-TUD-1: (*) conversion of D-sucrose (C_{Suc}): (●) yield of D-fructose (Y_{Fru}), (▲) yield of D-glucose (Y_{Glu}), (◇) yield of 5-hydroxymethyl-2-furaldehyde (Y_{Hmf}), (■) yield of D-mannose (Y_{Man}), (x) yield of 2-furaldehyde (Y_{Fur}). Reaction conditions: 0.3 Wt:0.7 Tol (v/v) biphasic solvent system, 170 °C, 20 $\text{g}_{\text{cat}}\cdot\text{dm}^{-3}$, 0.29 M Suc.

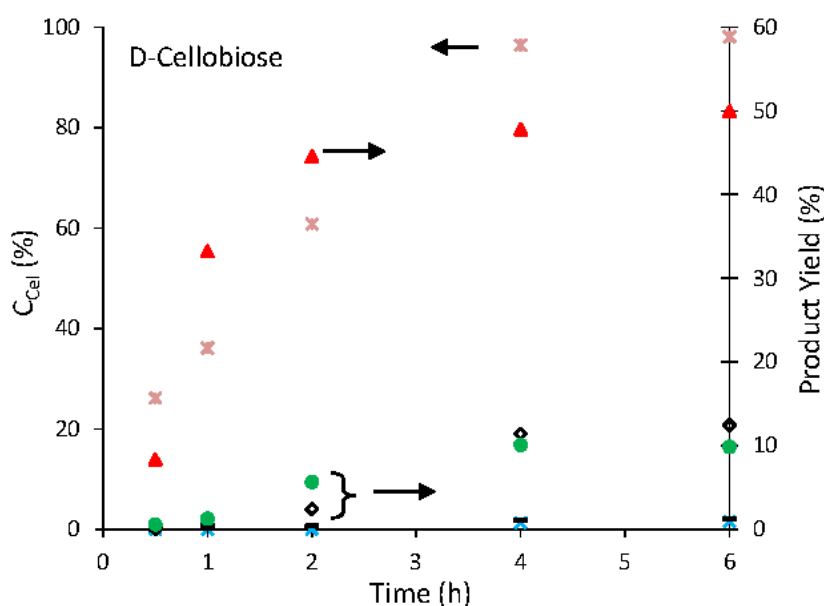


Figure 4.14- Hydrolysis and dehydration of D-cellobiose in the presence of AI-TUD-1: (*) conversion of D-cellobiose (C_{Cel}), (●) yield of 2-furaldehyde (Y_{Fru}), (▲) yield of D-glucose (Y_{Glu}), (◊) yield of 5-hydroxymethyl-2-furaldehyde (Y_{Hmf}), (-) yield of D-mannose (Y_{Man}), (x) yield of 2-furaldehyde (Y_{Fur}). Reaction conditions: 0.3 Wt:0.7 Tol (v/v) biphasic solvent system, 170 °C, 20 $\text{g}_{\text{cat}}\cdot\text{dm}^{-3}$, 0.29 M Cel.

The reaction of Suc in the presence of AI-TUD-1 gave Glu and Fru as the main products in ca. 40% yield each at 30 min of reaction, indicating that a relatively fast hydrolysis took place (Figure 4.13). After 30 min of reaction, the monosaccharide yields decreased, especially for Fru. This is consistent with the Fru reactivity being higher than that for Glu, as referred above and a maximum 17% Y_{Hmf} was reached. In the case of Cel, Glu is the main product (50% Y_{Glu}) at 6 h of reaction. The Y_{Fru} and Y_{Hmf} were 10% and 12%, respectively (Figure 4.14). For both disaccharides minor amounts of Man and Fur were formed during the 6 h of reaction (as observed with Fru and Glu as feedstocks). The undesirable reaction pathways may be similar to those occurring for Fru and Glu, as Suc and Cel are hydrolysed into these monosaccharides, giving similar results in terms of Hmf yield to those obtained with the monosaccharides (a maximum 20% and 17% Y_{Hmf} , respectively, Table 4.4).

Table 4.4- Catalytic performance of Al-TUD-1 in the conversion of D-sucrose (Suc) or D-cellobiose (Cel) to D-fructose (Fru), D-glucose (Glu) and 5-hydroxymethyl-2-furaldehyde (Hmf), and comparison with the literature data for zeolite H-Y. ^a

Catalyst	Substrate	t(h) ^c	T (°C) ^d	C (%) ^e	Y _{Fru+Glu} (%) ^f	Y _{Hmf} (%) ^g	Ref
Al-TUD-1	D-Sucrose	0.5	170	85	39+41	4	this work
Al-TUD-1	D-Sucrose	1	170	100	26+29	12	this work
Al-TUD-1	D-Sucrose	6	170	100	11+20	17	this work
H-Y (Si/Al=15) ^b	D-Sucrose	0.67	85	100	100	Traces	⁸⁰
Al-TUD-1	D-Cellobiose	0.5	170	26	0	0	this work
Al-TUD-1	D-Cellobiose	6	170	60	10+50	12	this work
H-Y (Si/Al=15) ^b	D-Cellobiose	nf ^e	150	90	88	nf ^e	⁸⁰

a) Reaction conditions: 0.3 Wt:0.7 Tol (v/v) biphasic solvent system, 170 °C, 20 g_{cat}.dm⁻³, 0.67 M Xyl. b) Using only water as solvent. c) Reaction time. d) Reaction temperature. e) Conversion at a given time. f) Total yield of D-fructose and D-glucose (Y_{Fru+Glu}). g) Yield of 5-hydroxymethyl-2-furaldehyde (Y_{Hmf}). e) nf= information not found.

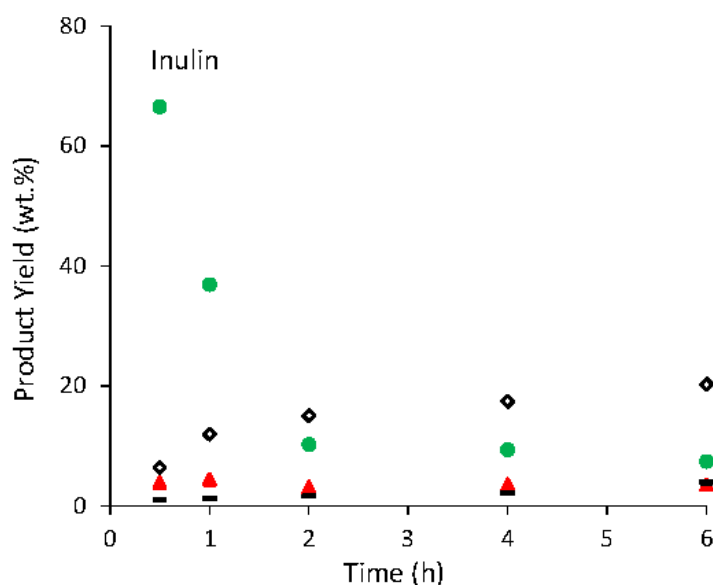


Figure 4.15- Hydrolysis and dehydration of inulin in the presence of Al-TUD-1: (●) yield of D-fructose (Y_{Fru}), (▲) yield of D-glucose (Y_{Glu}), (■) yield of D-mannose (Y_{Man}), and (◇) yield of 5-hydroxymethyl-2-furaldehyde (Y_{Hmf}). Reaction conditions: 0.3 Wt:0.7 Tol (v/v) biphasic solvent system, 170 °C, 20 g_{cat}.dm⁻³, 33.3 g. dm⁻³ inulin.

The one pot conversion of the polysaccharide inulin (a fructan, used in 33.3 wt.%) in the presence of Al-TUD-1 gave mainly Fru at 30 min of reaction (67 wt.% yield, Figure 4.15). A fast drop in the Y_{Fru} with time was accompanied by the formation of Hmf, reaching 20 wt.% yield at 6 h of reaction (the theoretical yield is ca. 78 wt.%). Glu and Man (formed by reversible isomerisation)

were also identified as minor products (< 5 wt.% yield). In face of these results it seemed that inulin could be rather selectively hydrolysed into Fru using Al-TUD-1 as catalyst, as the Y_{Hmf} at 30 min was only 9 wt.%. The selective hydrolysis of inulin (avoiding Hmf formation) was successfully carried out using H-Y zeolite (Si/Al=15) at lower reaction temperatures (ca. 92% Y_{Fru} , at 90 °C).⁸⁰

The Y_{Fur} at 91% C_{Xyl} was 60%, indicating a substantial amount of by-products (31% yield). During the reaction of Xyl the initially colourless Wt:Tol phases turned yellow-orange and the white powdered catalyst turned brown, suggesting the presence of organic by-products. However, these organic by-products were not detected in significant amounts by HPLC of the aqueous phase and GC-MS of the Tol phase. Possibly, these by-products are essentially oligo/polymeric products, formed via fragmentation and/or condensation reactions as explained in Chapter 1.^{65,82}

Similar to that observed for the Xyl dehydration, the presence of by-products in the case of the hexoses dehydration was evident by the colour build-up in the liquid phases and in the catalyst, although no significant amounts of by-products were detected. Fur was always detected in minor amounts (< 2% yield within 6 h in the reaction of each hexose), and may be formed via consecutive tautomerisation and retro aldol reactions from Glu.⁷²⁻⁷⁴ It was proposed that Glu in the cyclic form suffers consecutive tautomerisations (τ) to give 3-ketose (1,2,4,5,6-pentahydroxy 3-hexanone), which then suffers a retro aldol (RA) reaction giving arabinose, followed by dehydration to give Fur (Figure 4.16).⁸³ Another possible by-product resulting from the Hmf hydrolysis is levulinic acid. However, it was not detected by HPLC, possibly because the AS of Al-TUD-1 were not strong enough. Usually more acidic conditions are required for converting Hmf into levulinic acid than for Hmf formation.⁸⁴ According to the literature, Hmf may be involved in the formation of coke deposits on the microporous surface of aluminosilicates.⁷⁶ Taking into consideration that polymerisation reactions may be enhanced under relatively weak acidic conditions,⁸⁴ and that Al-TUD-1 possessed mainly Lewis and weak Brønsted acidity, it is possible that by-products were essentially polymers.

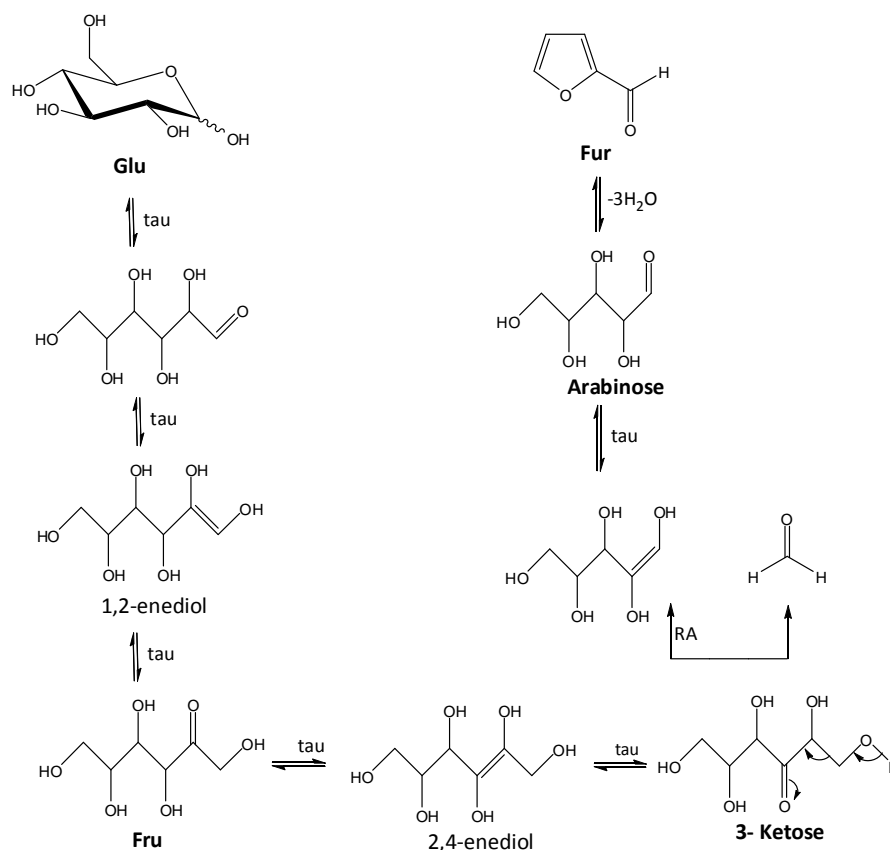


Figure 4.16- Reaction mechanism proposed by Aida et al.⁷⁴ for the conversion of D-glucose (Glu) to 2-furaldehyde (Fur); tau= tautomerisation, RA= retro aldol [adapted from ^{74,85}].

4.2.5. Catalyst stability

To test the stability and possible reusability of Al-TUD-1, the catalytic performance of the catalyst was studied for four consecutive 6 h batch runs of the Xyl reaction. The catalyst regeneration procedure is described in the experimental part (Chapter 2). The conversions of D-xylose and Fur yields in the recycling runs were quite similar (87-96% and 56-60%, respectively) (Figure 4.17). The Si/Al mole ratio of the recovered solid was 22, which is comparable to that of the fresh catalyst (Si/Al=21, Table 4.1). These results suggested that Al-TUD-1 was fairly stable under the reaction conditions used.

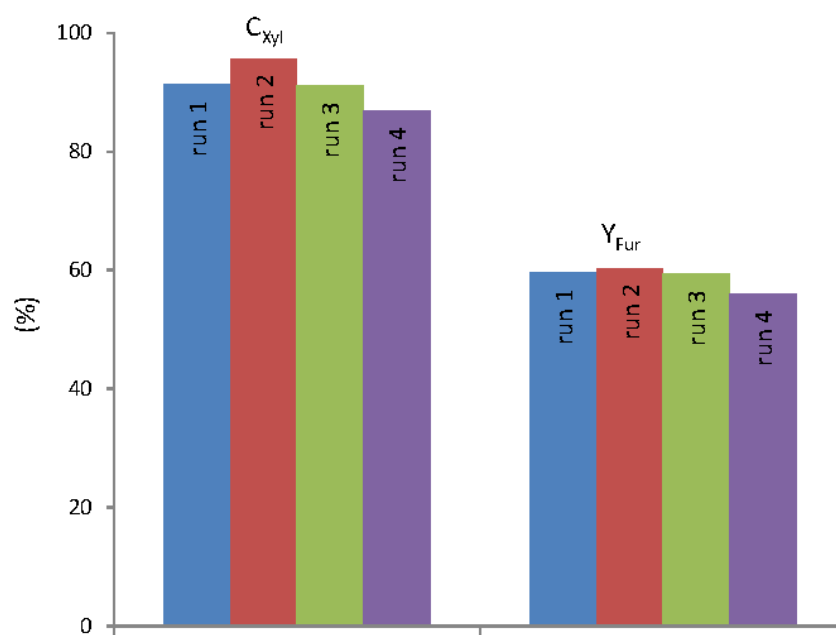


Figure 4.17- Catalytic performance of AI-TUD-1 in four consecutive 6 h batch runs at 170 °C. Reaction conditions: 0.3 Wt:0.7 Tol (v/v) biphasic solvent system, 20 g_{cat}·dm⁻³, 0.67 M Xyl.

4.3. Conclusions

The reaction of monosaccharides in the presence of AI-TUD-1, under the reaction conditions used, gave Fur (from Xyl) and Hmf (from Glu and Fru). However, the reaction of hexoses (Fru and Glu) did not seem to be selective to Hmf (17-20% Y_{Hmf} at 6 h of reaction) in comparison to the reaction of Xyl, which gave 60% Y_{Fur} at 6 h. A possible explanation might be associated to the acid properties of AI-TUD-1 (mainly L acidity and weak B acidity) being more favourable to convert Xyl into Fur than hexoses into Hmf. The one-pot hydrolysis/dehydration of the disaccharides (Suc and Cel) in the presence of AI-TUD-1 gave mainly the monosaccharides via hydrolysis, which are subsequently dehydrated into Hmf obtained in 17% and 12% Y_{Hmf} from Suc and Cel, respectively. At the maximum Y_{Hmf}, the monosaccharide yields were 31 and 59%, respectively. In the case of polysaccharides D-xylan and inulin, Fur and Hmf were formed in 18 and 20 wt.% yield within 6 h of reaction, respectively.

Based on the colour build-up of the solvents (colourless water/toluene phases turned yellow-orange) and of the catalyst (white-brown-black) during the course of the reactions, and

the fact that no significant amounts of by-products were detected, it is postulated that the formation of polymers and coke deposits may be important competitive reactions, affecting the yields of Fur and Hmf. The stability of Al-TUD-1 with Xyl as the substrate was confirmed by the approximately constant values of Xyl conversions and Fur yields (in the range of 56-60%) for at least four consecutive 6 h batch runs.

The catalytic performance of Al-TUD-1 may be improved by fine-tuning the acid properties (varying the Si/Al ratio)¹⁶ and optimising the reaction conditions. Alternatively, the mesoporous inorganic oxide matrix could be used to embed and disperse zeolite nanocrystals, which may allow enhanced acid strength (associated with the zeolite component) whilst improving the accessibility of the substrate to the AS in comparison to the bulk zeolite.

4.4. References

- (1) Hamdy, M. S.: Functionalized TUD-1: Synthesis, characterization, and (photo-)catalytic performance. Delft University of Technology, the Netherlands, 2005.
- (2) Lourvanij, K.; Rorrer, G. L.: Reactions of Aqueous Glucose Solutions Over Solid Acid Y-Zeolite Catalyst at 110-160 °C. *Industrial & Engineering Chemistry Research* **1993**, *32*, 11-19.
- (3) Moreau, C.; Durand, R.; Pourcheron, C.; Razigade, S.: Preparation of 5-Hydroxymethylfurfural From Fructose and Precursors Over H-Form Zeolites. *Industrial Crops and Products* **1994**, *3*, 85-90.
- (4) Moreau, C.: Zeolites and Related Materials for the Food and Non Food Transformation of Carbohydrates. *Agro Food Industry Hi-Tech* **2002**, *13*, 17-26.
- (5) Dias, A. S.; Lima, S.; Brandao, P.; Pillinger, M.; Rocha, J.; Valente, A. A.: Liquid-Phase Dehydration of D-xylose Over Microporous and Mesoporous Niobium Silicates. *Catalysis Letters* **2006**, *108*, 179-186.
- (6) Netrabukkana, R.; Lourvanij, K.; Rorrer, G. L.: Diffusion of Glucose and Glucitol in Microporous and Mesoporous Silicate Aluminosilicate Catalysts. *Industrial & Engineering Chemistry Research* **1996**, *35*, 458-464.
- (7) Degnanm, T. F. J.: Mesoporous Materials (M41S): From Discovery to Application. In *Dekker Encyclopedia of Nanoscience and Nanotechnology*; Schwarz, J. A., Contescu, C. I., Putvera, K., Eds.; Taylor and Francis: Oxfordshire, United Kingdom, 2004; Vol. 6 Volume Set.
- (8) Beck, J. S.; Vartuli, J. C.; Roth, W. J.; Leonowicz, M. E.; Kresge, C. T.; Schmitt, K. D.; Chu, C. T. W.; Olson, D. H.; Sheppard, E. W.; McCullen, S. B.; Higgins, J. B.; Schlenker, J. L.: A new Family of Mesoporous Molecular Sieves Prepared With Liquid Crystal Templates. *Journal of the American Chemical Society* **1992**, *114*, 10834-10843.
- (9) Kresge, C. T.; Leonowicz, M. E.; Roth, W. J.; Vartuli, J. C.; Beck, J. S.: Ordered Mesoporous Molecular Sieves Synthesized by a Liquid Crystal Template Mechanism. *Nature* **1992**, *359*, 710-712.
- (10) ZNMG-Project-4: Zeolite and Nanostructure Materials Laboratory. Universiti Teknoogi: Malaysia, 2012; Vol. 2012.
- (11) Anderson, M. W.; Ohsuna, T.; Sakamoto, Y.; Liu, Z.; Carlsson, A.; Terasaki, O.: Modern Microscopy Methods for the Structural Study of Porous Materials. *Chemical Communications* **2004**, 907-916.

- (12) Shan, Z.; Maschmeyer, T.; Jansen, J. C.: Inorganic Oxides With Mesoporosity or Combined Meso- and Microporosity and Process for the Preparation Thereof. In *World Intellectual Property Organization: WO 00/15551*; Olsteinm Elliot, M., Roseland, New Jersey, U.S.A.: U.S.A., 2000; pp 35.
- (13) Telalović, S.; Ramanathan, A.; Mul, G.; Hanefeld, U.: TUD-1: Synthesis and Application of a Versatile Catalyst, Carrier, Material. *Journal of Materials Chemistry* **2010**, *20*, 642-658.
- (14) Jansen, J. C.; Shan, Z.; Marchese, L.; Zhou, W.; Puil, N. V. d.; Maschmeyer, T.: A New Templating Method For Three-Dimensional Mesopore Networks. *Chemical Communications* **2001**, 713-714.
- (15) Telalović, S.; Ramanathan, A.; Ng, J. F.; Maheswari, R.; Kwakernaak, C.; Soulimani, F.; Brouwer, H. C.; Chuah, G. K.; Weckhuysen, B. M.; Hanefeld, U.: On the Synergistic Catalytic Properties of Bimetallic Mesoporous Materials Containing Aluminum and Zirconium: The Prins Cyclisation of Citronellal. *Chemistry-A European Journal* **2011**, *17*, 2077-2088.
- (16) Anand, R.; Maheswari, R.; Hanefeld, U.: Catalytic Properties of the Novel Mesoporous Aluminosilicate AlTUD-1. *Journal of Catalysis* **2006**, *242*, 82-91.
- (17) Shan, Z.; Jansen, J. C.; Zhou, W.; Maschmeyer, T.: Al-TUD-1, Stable Mesoporous Aluminas with High Surface Areas. *Applied Catalysis A-General* **2003**, *254*, 339-343.
- (18) Simons, C.; Hanefeld, U.; Arends, I.; Sheldon, R. A.; Maschmeyer, T.: Noncovalent Anchoring of Asymmetric Hydrogenation Catalysts on a New Mesoporous Aluminosilicate: Application and Solvent Effects. *Chemistry-A European Journal* **2004**, *10*, 5829-5835.
- (19) Zhang, Z.-X.; Bai, P.; Xu, B.; Yan, Z.-F.: Synthesis of Mesoporous Alumina TUD-1 With High Thermostability. *J Porous Mater* **2006**, *13*, 245-250.
- (20) Telalović, S.; Ng, J. F.; Maheswari, R.; Ramanathan, A.; Chuah, G. K.; Hanefeld, U.: Synergy Between Brønsted Acid Sites and Lewis Acid Sites. *Chemical Communications* **2008**, 4631-4633.
- (21) Telalović, S.; Hanefeld, U.: Noncovalent Immobilization of Chiral Cyclopropanation Catalysts on Mesoporous TUD-1: Comparison of Liquid-Phase and Gas-Phase Ion-Exchange. *Applied Catalysis A-General* **2010**, *372*, 217-223.
- (22) Shan, Z.; Gianotti, E.; Jansen, J. C.; Peters, J. A.; Marchese, L.; Maschmeyer, T.: One-Step Synthesis of a Highly Active, Mesoporous, Titanium-Containing Silica by Using Bifunctional Templating. *Chemistry-A European Journal* **2001**, *7*, 1437-1443.
- (23) Anand, R.; Hamdy, M. S.; Gkourgkoulas, P.; Maschmeyer, T.; Jansen, J. C.; Hanefeld, U.: Liquid Phase Oxidation of Cyclohexane Over Transition Metal Incorporated Amorphous 3D-Mesoporous Silicates M-TUD-1 (M = Ti, Fe, Co and Cr). *Catalysis Today* **2006**, *117*, 279-283.
- (24) Karmakar, B.; Chowdhury, B.; Banerji, J.: Mesoporous Titanosilicate Ti-TUD-1 Catalyzed Knoevenagel Reaction: An Efficient Green Synthesis of Trisubstituted Electrophilic Olefins. *Catalysis Communications* **2010**, *11*, 601-605.
- (25) Karmakar, B.; Nayak, A.; Chowdhury, B.; Banerji, J.: A Highly Efficient, Eco-Friendly, Room Temperature Synthesis of Bis(indol-3-yl)methanes Using the Mesoporous Titanosilicate Ti-TUD-1: Electrophilic Substitution Reactions of Indoles - Part XXIII. *Arkivoc* **2009**, 209-216.
- (26) Prasad, M. R.; Hamdy, M. S.; Mul, G.; Bouwman, E.; Drent, E.: Efficient Catalytic Epoxidation of Olefins With Silylated Ti-TUD-1 Catalysts. *Journal of Catalysis* **2008**, *260*, 288-294.
- (27) Shan, Z.; Jansen, J. C.; Marchese, L.; Maschmeyer, T.: Synthesis, Characterization and Catalytic Testing of a 3-D Mesoporous Titanosilica, Ti-TUD-1. *Microporous and Mesoporous Materials* **2001**, *48*, 181-187.
- (28) Tanglumlert, W.; Yang, S.-T.; Jeong, K.-E.; Jeong, S.-Y.; Ahn, W.-S.: Facile Synthesis of Ti-TUD-1 for Catalytic Oxidative Desulfurization of Model Sulfur Compounds. *Research on Chemical Intermediates* **2011**, *37*, 1267-1273.
- (29) Anand, R.; Hamdy, M. S.; Hanefeld, U.; Maschmeyer, T.: Liquid-Phase Oxidation of Cyclohexane Over Co-TUD-1. *Catalysis Letters* **2004**, *95*, 113-117.
- (30) Hamdy, M. S.; Ramanathan, A.; Maschmeyer, T.; Hanefeld, U.; Jansen, J. C.: Co-TUD-1: A Ketone-Selective Catalyst for Cyclohexane Oxidation. *Chemistry-A European Journal* **2006**, *12*, 1782-1789.
- (31) Hamdy, M. S.; Mul, G.; Wei, W.; Anand, R.; Hanefeld, U.; Jansen, J. C.; Moulijn, J. A.: Fe, Co and Cu-Incorporated TUD-1: Synthesis, Characterization and Catalytic Performance in N₂O Decomposition and Cyclohexane Oxidation. *Catalysis Today* **2005**, *110*, 264-271.

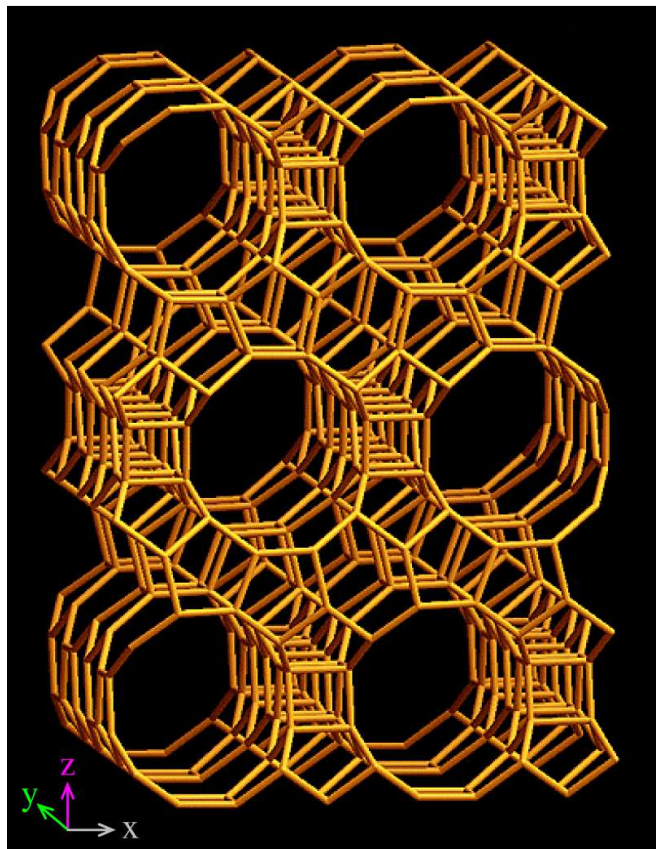
- (32) Wang, H.; Wang, B.; Quek, X.-Y.; Wei, L.; Zhao, J.; Li, L.-J.; Park, M. B. C.; Yang, Y.; Chen, Y.: Selective Synthesis of (9,8) Single Walled Carbon Nanotubes on Cobalt Incorporated TUD-1 Catalysts. *Journal of the American Chemical Society* **2010**, *132*, 16747-16749.
- (33) Quek, X.-Y.; Tang, Q.; Hu, S.; Yang, Y.: Liquid Phase Trans-Stilbene Epoxidation Over Catalytically Active Cobalt Substituted TUD-1 Mesoporous Materials (Co-TUD-1) Using Molecular Oxygen. *Applied Catalysis A: General* **2009**, *361*, 130-136.
- (34) Ramanathan, A.; Hamdy, M. S.; Parton, R.; Maschmeyer, T.; Jansen, J. C.; Hanefeld, U.: Co-TUD-1 Catalysed Aerobic Oxidation of Cyclohexane. *Applied Catalysis A: General* **2009**, *355*, 78-82.
- (35) Ramanathan, A.; Villalobos, M. C. C.; Kwakernaak, C.; Telalović, S.; Hanefeld, U.: Zr-TUD-1: A Lewis Acidic, Three-Dimensional, Mesoporous, Zirconium-Containing Catalyst. *Chemistry-A European Journal* **2008**, *14*, 961-972.
- (36) Ramanathan, A.; Klomp, D.; Peters, J. A.; Hanefeld, U.: Zr-TUD-1: A Novel Heterogeneous Catalyst for the Meerwein-Ponndorf-Verley Reaction. *Journal of Molecular Catalysis A-Chemical* **2006**, *260*, 62-69.
- (37) Telalović, S.; Hanefeld, U.: Investigation of the Cyanosilylation Catalysed by Metal-Siliceous Catalysts. *Catalysis Communications* **2011**, *12*, 493-496.
- (38) Neves, I. C.; Botelho, G.; Machado, A. V.; Rebelo, P.; Ramoa, S.; Pereira, M. F. R.; Ramanathan, A.; Pescarmona, P.: Feedstock Recycling of Polyethylene Over AlTUD-1 Mesoporous Catalyst. *Polymer Degradation and Stability* **2007**, *92*, 1513-1519.
- (39) Shan, Z.; Jansen, J. C.; Yeh, C. Y.; Angevine, P. J.; Maschmeyer, T.: Mesoporous Aluminium Oxide, Preparation and Use Thereof. In *United States Patent Application Publication: US 2007/0170096 A1*; Dilworth & Barrese, LLP, Uniondale, NY, U.S.A.: USA, 2007; pp 23.
- (40) Norek, M.; Neves, I. C.; Peters, J. A.: ^1H Relaxivity of Water in Aqueous Suspensions of Gd^{3+} -Loaded NaY Nanozeolites and AlTUD-1 Mesoporous Material: the Influence of Si/Al Ratio and Pore Size. *Inorganic Chemistry* **2007**, *46*, 6190-6196.
- (41) Maheswari, R.; Pachamuthu, M. P.; Anand, R.: Copper Containing TUD-1: Synthesis, Characterization and Catalytic Behavior in Liquid-Phase Oxidation of Ethylbenzene. *J Porous Mater* **2012**, *19*, 103-110.
- (42) Hamdy, M. S.; Mul, G.; Jansen, J. C.; Ebaid, A.; Shan, Z.; Overweg, A. R.; Maschmeyer, T.: Synthesis, Characterization, and Unique Catalytic Performance of the Mesoporous Material Fe-TUD-1 in Friedel-Crafts Benzoylation of Benzene. *Catalysis Today* **2005**, *100*, 255-260.
- (43) Tušar, N. N.; Ristić, A.; Cecowski, S.; Arčon, I.; Lázár, K.; Amenitsch, H.; Kaučič, V.: Local Environment of Isolated Iron in Mesoporous Silicate Catalyst FeTUD-1. *Microporous and Mesoporous Materials* **2007**, *104*, 289-295.
- (44) Wei, W.; Moulijn, J. A.; Mul, G.: FAPO and Fe-TUD-1: Promising Catalysts for N_2O Mediated Selective Oxidation of Propane? *Journal of Catalysis* **2009**, *262*, 1-8.
- (45) Hamdy, M. S.; Berg, O.; Jansen, J. C.; Maschmeyer, T.; Arafat, A.; Moulijn, J. A.; Mul, G.: Chromium-Incorporated TUD-1 as a New Visible Light-Sensitive Photo-Catalyst for Selective Oxidation of Propane. *Catalysis Today* **2006**, *117*, 337-342.
- (46) Maheswari, R.; Anand, R.; Imran, G.: MnTUD-1: Synthesis, Characterization and Catalytic Behavior in Liquid-Phase Oxidation of Cyclohexane. *J Porous Mater* **2012**, *19*, 283-288.
- (47) Ramanathan, A.; Archipov, T.; Maheswari, R.; Hanefeld, U.; Roduner, E.; Glaser, R.: Synthesis, Characterization and Catalytic Properties of the Novel Manganese-Containing Amorphous Mesoporous Material MnTUD-1. *The Journal of Physical Chemistry C* **2008**, *112*, 7468-7476.
- (48) Hamdy, M. S.; Mul, G.: Synthesis, Characterization and Catalytic Performance of Mo-TUD-1 Catalysts in Epoxidation of Cyclohexene. *Catalysis Science & Technology* **2012**, *in press*.
- (49) Guo, Z.; Zhou, C.; Hu, S.; Chen, Y.; Jia, X.; Lau, R.; Yang, Y.: Epoxidation of trans-Stilbene and cis-Cyclooctene Over Mesoporous Vanadium Catalysts: Support Composition and Pore Structure Effect. *Applied Catalysis A: General* **2012**, *419-420*, 194-202.
- (50) Hu, S.; Liu, D.; Li, L.; Guo, Z.; Chen, Y.; Borgna, A.; Yang, Y.: Highly Selective 1-Heptene Isomerization over Vanadium Grafted Mesoporous Molecular Sieve Catalysts. *Chemical Engineering Journal* **2010**, *165*, 916-923.
- (51) Li, L.; Koranyi, T. I.; Sels, B. F.; Pescarmona, P. P.: Highly-Efficient Conversion of Glycerol to Solketal Over Heterogeneous Lewis Acid Catalysts. *Green Chemistry* **2012**, *14*, 1611-1619.

- (52) Mandal, S.; SinhaMahapatra, A.; Rakesh, B.; Kumar, R.; Panda, A.; Chowdhury, B.: Synthesis, Characterization of Ga-TUD-1 Catalyst and its Activity Towards Styrene Epoxidation Reaction. *Catalysis Communications* **2011**, *12*, 734-738.
- (53) Karmakar, B.; Sinhamahapatra, A.; Panda, A. B.; Banerji, J.; Chowdhury, B.: Ga-TUD-1: A New Heterogeneous Mesoporous Catalyst for the Solventless Expedient Synthesis of α -Aminonitriles. *Applied Catalysis A: General* **2011**, *392*, 111-117.
- (54) Chen, Y.; Guo, Z.; Chen, T.; Yang, Y.: Surface-Functionalized TUD-1 Mesoporous Molecular Sieve Supported Palladium for Solvent-Free Aerobic Oxidation of Benzyl Alcohol. *Journal of Catalysis* **2010**, *275*, 11-24.
- (55) Water, L. G. A. d. V.; Bulcock, S.; Masters, A. F.; Maschmeyer, T.: Ce-TUD-1: Synthesis, Characterization, and Testing of a Versatile Heterogeneous Oxidation Catalyst. *Industrial & Engineering Chemistry Research* **2007**, *46*, 4221-4225.
- (56) Sangwichien, C.; Aranovich, G. L.; Donohue, M. D.: Density Functional Theory Predictions of Adsorption Isotherms With Hysteresis Loops. *Colloids and Surfaces A-Physicochemical and Engineering Aspects* **2002**, *206*, 313-320.
- (57) Blin, J. L.; Léonard, A.; Su, B. L.: Well-Ordered Spherical Mesoporous Materials CMI-1 Synthesized via an Assembly of Decaoxyethylene Cetyl Ether and TMOS. *Chemistry of Materials* **2001**, *13*, 3542-3553.
- (58) Sing, K. S. W.: Characterization of Adsorbents. In *Adsorption, Science and Technology*; Rodrigues, A. E., Levan, M. D., Tondeur, D., Eds.; Kluwer Academic Publishers: Dordrecht, the Netherlands, 1989; Vol. 158 pp 3-14.
- (59) Rouquerol, F.; Rouquerol, J.; Sing, K.: *Adsorption by Powders and Porous Solids Principles, Methodology and Applications*; Academic Press: San Diego, California, U.S.A., 1999.
- (60) Zhou, J.; Hua, Z.; Shi, J.; He, Q.; Guo, L.; Ruan, M.: Synthesis of a Hierarchical Micro/Mesoporous Structure by Steam-Assisted Post-Crystallization. *Chemistry – A European Journal* **2009**, *15*, 12949-12954.
- (61) Luan, Z. H.; Fournier, J. A.: In Situ FTIR Spectroscopic Investigation of Active Sites and Adsorbate Interactions in Mesoporous Aluminosilicate SBA-15 Molecular Sieves. *Microporous and Mesoporous Materials* **2005**, *79*, 235-240.
- (62) Gallo, J. M. R.; Bisio, C.; Gatti, G.; Marchese, L.; Pastore, H. O.: Physicochemical Characterization and Surface Acid Properties of Mesoporous Al -SBA-15 Obtained by Direct Synthesis. *Langmuir* **2010**, *26*, 5791-5800.
- (63) Dam, H. E. V.; Kieboom, A. P. G.; Bekkum, H. V.: The Conversion of Fructose and Glucose in Acidic Media- Formation of Hydroxymethylfurfural. *Stärch-Starke* **1986**, *38*, 95-101.
- (64) Moreau, C.; Durand, R.; Peyron, D.; Duhamet, J.; Rivalier, P.: Selective Preparation of Furfural From Xylose Over Microporous Solid Acid Catalysts. *Industrial Crops and Products* **1998**, *7*, 95-99.
- (65) Zeitsch, K. J.: *The Chemistry and Technology of Furfural and its Many By-Products*; 1st ed.; Elsevier Science B. V.: Amsterdam, The Netherlands, 2000; Vol. 13.
- (66) Lichtenhaler, F. W.: The Key Sugars of Biomass: Availability, Non-Food Uses and Future Developments Lines. In *Biorefineries-Industrial Processes and Products: Status Quo and Future Directions*; Kamm, B., Gruber, P. R., Kamm, M., Eds.; Wiley VCH: New York, U.S.A., 2006; Vol. 2; pp 3-59.
- (67) Moreau, C.; Belgacem, M. N.; Gandini, A.: Recent Catalytic Advances in the Chemistry of Substituted Furans from Carbohydrates and in the Ensuing Polymers. *Topics in Catalysis* **2004**, *27*, 11-30.
- (68) Lima, S.; Pillinger, M.; Valente, A. A.: Dehydration of D-xylose Into Furfural Catalysed by Solid Acids Derived From the Layered Zeolite Nu-6(1). *Catalysis Communications* **2008**, *9*, 2144-2148.
- (69) Valente, A. A.; Dias, A. S.; Lima, S.; Brandão, P.; Pillinger, M.; Plácido, H.; Rocha, J.: Catalytic Performance of Microporous Nb and Mesoporous Nb or Al Silicates in the Dehydration of D-Xylose to Furfural. In *Perspectiva de la investigación sobre materiales en España en el siglo XXI: IX Congreso Nacional de Materiales*; Colección: Congressos nº 53 ed.; Materiales, S. E. d., Ed.; Servizo de Pulicaci3ns da Universidade de Vigo: University of Vigo, Vigo, Spain, 2006; Vol. II; pp 1203-1206.
- (70) Dias, A. S.; Lima, S.; Pillinger, M.; Valente, A. A.: Modified Versions of Sulfated Zirconia as Catalysts for the Conversion of Xylose to Furfural. *Catalysis Letters* **2007**, *114*, 151-160.

- (71) Dias, A. S.; Lima, S.; Carriazo, D.; Rives, V.; Pillinger, M.; Valente, A. A.: Exfoliated Titanate, Niobate and Titanoniobate Nanosheets as Solid Acid Catalysts for the Liquid-Phase Dehydration of D-Xylose Into Furfural. *Journal of Catalysis* **2006**, *244*, 230-237.
- (72) Asghari, F. S.; Yoshida, H.: Acid-Catalyzed Production of 5-Hydroxymethylfurfural From D-fructose in Subcritical Water. *Industrial & Engineering Chemistry Research* **2006**, *45*, 2163-2173.
- (73) Antal, M. J.; Mok, W. S. L.; Richards, G. N.: Kinetic-Studies of the Reactions of Ketoses and Aldoses in Water at High Temperature .1. Mechanism of Formation of 5-(Hydroxymethyl)-2-Furaldehyde from D-Fructose and Sucrose. *Carbohydrate Research* **1990**, *199*, 91-109.
- (74) Aida, T. M.; Sato, Y.; Watanabe, M.; Tajima, K.; Nonaka, T.; Hattori, H.; Arai, K.: Dehydration of D-Glucose in High Temperature Water at Pressures up to 80 MPa. *Journal of Supercritical Fluids* **2007**, *40*, 381-388.
- (75) Corma, A.; Iborra, S.; Velty, A.: Chemical Routes for the Transformation of Biomass into Chemicals. *Chemical Reviews* **2007**, *107*, 2411-2502.
- (76) Moreau, C.; Durand, R.; Razigade, S.; Duhamet, J.; Faugeras, P.; Rivalier, P.; Ros, P.; Avignon, G.: Dehydration of Fructose to 5-Hydroxymethylfurfural Over H-Mordenites. *Applied Catalysis A-General* **1996**, *145*, 211-224.
- (77) Rivalier, P.; Duhamet, J.; Moreau, C.; Durand, R.: Development of a Continuous Catalytic Heterogeneous Column Reactor With Simultaneous Extraction of an Intermediate Product by an Organic-Solvent Circulating in Counter-Current Manner With the Aqueous Phase. *Catalysis Today* **1995**, *24*, 165-171.
- (78) Lourvanij, K.; Rorrer, G. L.: Reaction Rates for the Partial Dehydration of Glucose to Organic Acids in Solid-Acid, Molecular-Sieving Catalyst Powders. *Journal of Chemical Technology and Biotechnology* **1997**, *69*, 35-44.
- (79) Moreau, C.; Durand, R.; Alies, F. R.; Cotillon, M.; Frutz, T.; Theoleyre, M. A.: Hydrolysis of Sucrose in the Presence of H-Form Zeolites. *Industrial Crops and Products* **2000**, *11*, 237-242.
- (80) Moreau, C.; Durand, R.; Duhamet, J.; Rivalier, P.: Hydrolysis of Fructose and Glucose Precursors in the Presence of H-form Zeolites 1. *Journal of Carbohydrate Chemistry* **1997**, *16*, 709-714.
- (81) Buttersack, C.; Laketic, D.: Hydrolysis of Sucrose by Dealuminated Y-Zeolite. *Journal of Molecular Catalysis* **1994**, *94*, L283-L290.
- (82) Antal, M. J.; Leesomboon, T.; Mok, W. S.; Richards, G. N.: Kinetic Studies of the Reactions of Ketoses and Aldoses in Water at High Temperature 3-Mechanism of Formation of 2-Furaldehyde from D-Xylose. *Carbohydrate Research* **1991**, *217*, 71-85.
- (83) Kabyemela, B. M.; Adschiri, T.; Malaluan, R. M.; Arai, K.: Glucose and Fructose Decomposition in Subcritical and Supercritical Water: Detailed Reaction Pathway, Mechanisms, and Kinetics. *Industrial & Engineering Chemistry Research* **1999**, *38*, 2888-2895.
- (84) Kuster, B. F. M.; Temmink, H. M. G.: The Influence of pH and Weak-Acid anions on the Dehydration of D-fructose. *Carbohydrate Research* **1977**, *54*, 185-191.
- (85) Srokol, Z.; Bouche, A.-G.; Estrik, A. V.; Strik, R. C. J.; Maschmeyer, T.; Peters, J. A.: Hydrothermal Upgrading of Biomass to Biofuel; Studies on Some Monosaccharide Model Compounds. *Carbohydrate Research* **2004**, *339*, 1717-1726.

CHAPTER 5

Reaction of D-xylose in the presence of zeolite Beta (BEA) and a micro/mesoporous (BEATUD-1) composite material



Zeolite BEA viewed along $[100]$ ¹

Index

CHAPTER 5	219
Reaction of D-xylose in the presence of zeolite Beta (BEA) and a micro/mesoporous (BEATUD-1) composite material	219
5.1. Introduction	221
5.1.1. Zeolite Beta (BEA).....	223
5.1.2. Microporous/mesoporous BEATUD-1.....	224
5.2. Results and discussion.....	225
5.2.1. Catalysts characterisation	225
5.2.2. Catalytic dehydration of D-xylose	237
5.2.2.1. Catalytic performance of zeolite BEA and composite BEATUD-1	237
5.2.2.2. Identification of the reaction products	242
5.2.2.3. Catalyst stability	249
5.3. Conclusions	251
5.4. References.....	252

5.1. Introduction

As mentioned previously, heterogeneous porous solid catalysts present several advantages over homogeneous catalysts mainly due to the easier catalyst separation after the reaction, leading to a reduction in the costs of separation techniques, which are quite demanding for homogeneous systems.² However there are critical requirements to be considered such as thermal stability and water-tolerance. SAPOs and Al-TUD-1 demonstrated to be water-tolerant porous solid acid catalysts used in the conversion of saccharides to furanic aldehydes. Successfully investigated materials include crystalline inorganic oxides, namely the zeolites H-Y Faujasite, H-Mordenite,³ H-ZSM-5,⁴ microporous niobium silicates,^{5,6} titanoniobate nanosheets,⁷ and a delaminated zeolite obtained by the swelling and ultrasonication of a layered precursor of Nu-6(2)⁸. It is possible to fine-tune the acid properties of microporous or mesoporous materials, to improve the catalytic performance in Fur production for making them excellent catalysts for one-pot multi-step processes.⁹ The number of acid sites (AS) can be maximised per unit weight of catalyst and the acid strength of those sites can be modified by changing the composition, such as the Si/Al ratio. It is also desirable to increase their accessibility to the reactant molecules by producing a material with the appropriate surface area and porosity. In the case of multistep reactions the solid catalysts should preferably possess large surface areas and optimum adsorption characteristics.⁹ To achieve these characteristics the initial concentration of reactants in the synthesis mixture, the pH and aging time of the synthesis gel are important parameters.^{9,10}

Aluminosilicate catalysts are known to be more attractive in terms of production costs and/or availability in comparison to transition-metal containing ones. They can be amorphous or crystalline in which the presence of tetrahedrally coordinated aluminium generates a negatively charged framework, which in turn is compensated by cations, such as hydronium cations (Figure 5.1).⁹ Zeolites are crystalline aluminosilicates with well-defined structures that contain aluminium, silicon and oxygen in their regular framework. They are built up of a 3 D array of tetrahedral units TO_4 ($T=Si, Al$) with each apical oxygen atom bridging two adjacent tetrahedra. Zeolites are one of the most important families of crystalline microporous solids. Since zeolite frameworks are typically anionic (network of SiO_4 tetrahedra is neutral while AlO_4 bears a negative charge), charge compensating cations (Na^+ , K^+ or NH_4^+) populate the pores to maintain electrical neutrality.¹¹ The general formula of a zeolite is $M_{x/m}[(AlO_2)_x(SiO_2)_y]zH_2O$, where M is the cation with valence m, z is the number of water molecules in each unit cell, and x and y are integers.¹²

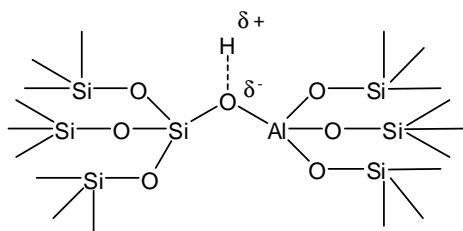


Figure 5.1- Structure of an amorphous and crystalline aluminosilicate [adapted from ⁹].

Zeolites belong to a class named tectosilicates although they have the particularity of having open channels and cavities of molecular dimensions which does not happen with other members of the tectosilicate family (e.g. SiO_2 groups, Feldspathoid group). The dimensions of the cavities and channels (ca. 0.3 to 1.5 nm) in their structures give these materials unique properties such as, the ability to adsorb molecules of various sizes and shapes.¹³ Zeolites can be classified into small pore zeolites with 8 membered rings (MR) pore apertures (3.0-4.5 Å), medium pore zeolites with 10-MR pore apertures (4.5-6.0 Å) and large pore zeolites with 12-MR apertures (6.0-8.0 Å) of which zeolite Beta is an example, represented in Figure 5.2.¹¹

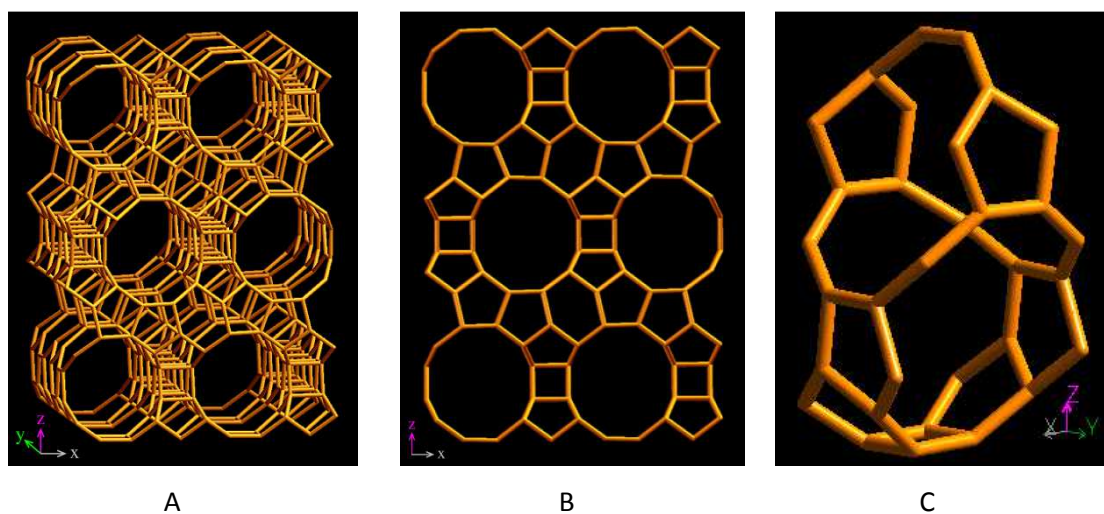


Figure 5.2- Structure of zeolite BEA viewed along [100] (A and B) and along [001] (C).¹

Despite all the advantages, an important drawback is the formation of coke, which may lead to drops in Fur selectivity. Reducing the crystallite size of the catalyst to the nanoscale would increase the surface area to micropore volume ratio and decrease the diffusion path lengths,

which may avoid severe coking. On the other hand, the reduction in crystallite size may enhance the L/B ratio, which may be beneficial since Lewis acids may stabilise intermediate species and enhance selectivity towards Fur.¹⁴ However, nanosized materials tend to pose concerns related to health, the environment, and technical issues (e.g. ease of handling, high pressure drops, up-flow clogging of equipment, and demanding separation techniques such as nanofiltration). Composite materials consisting of zeolite nanocrystals embedded in a mesoporous inorganic oxide matrix may benefit from the catalytic properties associated with the zeolite nanocrystals, while minimising the nanoscale-related drawbacks.¹⁵⁻²⁴

Taking into account these considerations, the dehydration of Xyl into Fur in the presence of zeolite H-Beta and a micro/mesoporous BEATUD-1 composite material as catalysts was investigated and the results are compared with those for bulk nanocrystalline zeolite H-Beta (denoted BEA).

5.1.1. Zeolite Beta (BEA)

Zeolite BEA is included in the group of high silica zeolites (with a $\text{Si/Al} \geq 10$). This group of zeolites was described between the late 1960s and early 1970s and is synthesised at the Mobil Research and Development Laboratories of the “high silica zeolites”.²⁵⁻²⁷ Beta has a specific strength and density of AS that allow achieving superior levels of conversion at lower reaction temperatures than catalysts based only on silica,²⁸ and it was the first zeolite to be discovered by R. L. Wadlinger, G. T. Kerr and E. J. Rosinski in 1967.^{26,27} However its complex structure was only completely determined in 1988.²⁸⁻³⁰ The most interesting property is its highly disordered framework.³¹ It consists of an intergrowth of three distinct polymorphs³²: polymorph A, B and C, built from different stacking of the same building layer.³² The structure of polymorph C was determined by several different techniques (SEM, powder XRD and TGA).³³ The structures of polymorphs A and B were proposed on the basis of high resolution electron microscopy (HREM) images and electron diffraction (ED) patterns.³⁴ At first, zeolite Beta was accepted as a highly faulted intergrowth of only two polymorphs A and B in a 60:40 ratio that grew as 2 D sheets randomly alternated between each other.³³ Both polymorphs have a 3 D network of 12-MR pore systems in which the intergrowth does not significantly affect the pores in two of the dimensions, where two mutually perpendicular straight channels with elliptical pore apertures of (6.4x7.6 Å)

run in the x and y directions (Figures 5.2 A and B).³⁵ However in the crystallographic faulting direction, the pore system might become tortuous, where a sinusoidal channel of $5.5 \times 5.5 \text{ \AA}$ runs parallel to the z direction (Figure 5.2 C).³⁶ The third polymorph C has a 3 D pore system formed by linear channels of nearly circular 12-MR (ca. 6.9 \AA).³² In the case of the other two polymorphs (A and B) one of the channels is sinusoidal.³³ Polymorph C also differs from A and B polymorphs because it contains double 4-MR (D4-MR) per unit cell as secondary building units that do not appear in polymorphs A or B.³³ The different polymorphs consist of layers formed by 5- and 6-MR that may be stacked in different sequences forming 12-MR pores (Figure 5.3).^{31,32,37,38}

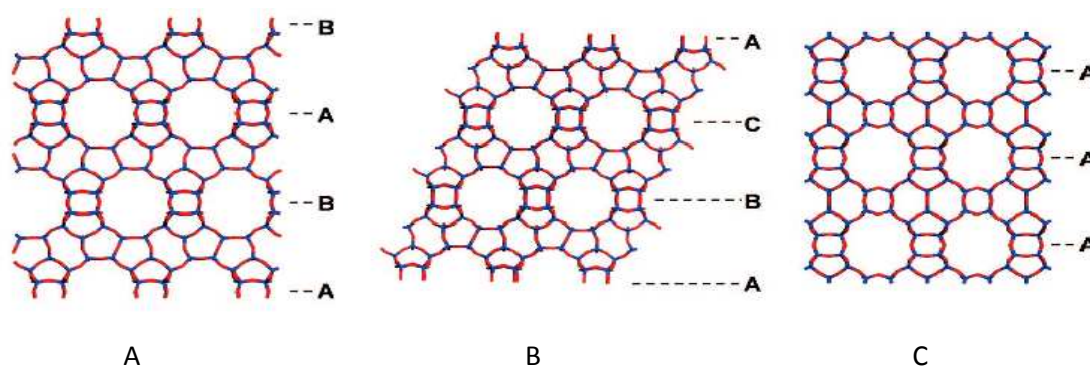


Figure 5.3- Framework structures of A) polymorph A, B) polymorph B and C) polymorph C of zeolite Beta, showing the different stackings of the 12-MR pores as A) ABAB (shears with alternating translations), B) ABCABC (shears in the same direction) and C) AA.³²

The surface of the zeolite BEA studied herein with a Si/Al=12 allows organophobic-hydrophilic selectivity, in contrast to zeolites with higher Si/Al ratios.³⁹ It favours the adsorption of polar molecules (such as the substrate studied, Xyl) and interacts weakly with organic molecules, like the product Fur. Therefore zeolite Beta is adequate for converting Xyl to Fur.

5.1.2. Microporous/mesoporous BEATUD-1

The micro/mesoporous composite material consisting of BEA zeolite nanocrystals embedded in a TUD-1 type mesoporous inorganic oxide matrix was denoted as BEATUD-1. The features of TUD-1⁴⁰ have been described in detail in Chapter 4. The composites can be prepared

by blending pre-formed zeolite nanocrystals into the synthesis mixture of a mesoporous carrier. Additional advantages of these composites may include the ability to maintain stable the catalyst component on the carrier, improving its lifetime, and its use for catalyst formulations allowing enhanced porosity of extrudates and fairly good control over composition, size and morphology of the catalyst component. The choice of a 3 D mesoporous silica matrix of the type TUD-1 is attractive since its preparation is based on a relatively low cost, non-surfactant templating route, and may be advantageous in relation to a 2 D material in terms of facilitated internal diffusion.

5.2. Results and discussion

5.2.1. Catalysts characterisation

In this Chapter zeolite BEA and composite BEATUD-1 were prepared in accordance with the procedure described by Maschmeyer et al. (Chapter 2).^{15,16} Zeolite Beta in the proton form (BEA) was obtained by calcination of the commercial ammonium-form of the Beta powder. The composite BEATUD-1 was prepared by embedding H-Beta nanocrystallites (40 wt.%) in the 3 D mesoporous silica TUD-1.^{15,16}

The powder XRD patterns are shown in Figure 5.4. From this Figure it is possible to see that the XRD patterns of the bulk nanocrystalline zeolite BEA and the composite BEATUD-1 were similar, showing the characteristic diffraction peaks of zeolite BEA at $2\theta=7.2^\circ$ and 22.3° .^{15,24,35,41-157} The low angle peak was broadened due to the presence of an intergrowth of different polymorphs (mainly A and B) in the crystals.

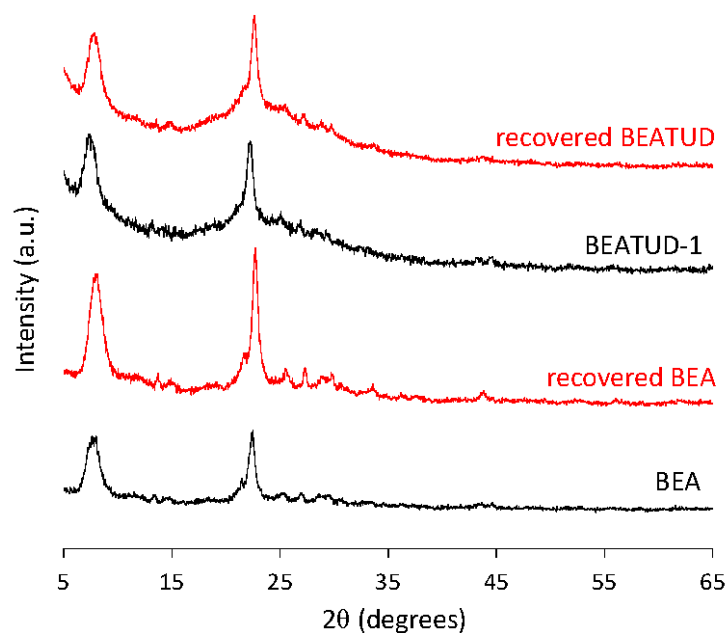


Figure 5.4- Powder XRD patterns of the fresh and recovered catalysts.

TEM images of the zeolite BEA and the composite BEATUD-1 were collected in order to determine the size and morphology of the crystals or aggregates (Figure 5.5).¹⁵⁸ These images of zeolite Beta showed that the sample consisted of small crystallites with a size of about 20-30 nm, which were clustered to give larger particles with dimensions in the range of 100-200 nm (Figure 5.5a). Comparable results for crystallite sizes from 15 to 60 nm, which further aggregated, are described in the literature.^{24,48,56,69,71,93,157,159}

The high resolution (HR) TEM image shown in Figure 5.5 b clearly showed that the aggregates of Beta crystals had lattice fringes uniformly aligned with the aggregates. Lattice fringes are characteristic of the zeolite Beta, and are in agreement with that described by Kuechl et al.,⁶² and others.^{42,91,143,158,160,161} Some authors had obtained irregular spherical H-Beta particles,^{24,55,159,162,163} or cubic-shape particles.¹⁶⁴ According to Kuechl et al.⁶² the parallel nature of the lattice fringes for adjacent crystals might have two different interpretations. One of them says that the individual crystals are nucleated in solution and then attached later in an oriented fashion which lowers the overall free energy of the synthesis medium (the crystals attach to one another in an energetically favourable manner). The multiple nucleation sites on a gel particle is the other hypothesis that may explain the adjacent crystals formed in parallel fringes.⁶² The highly faulted structure of zeolite Beta observed in the TEM images (Figure 5.5 b) is in good agreement with the XRD data (the boarder peak at $2\theta=7.2^\circ$), suggesting the presence of two polymorphs

typical for zeolite BEA.⁴¹ For BEATUD-1, TEM characterisation showed a 3 D sponge- or wormlike mesoporous matrix with some dark gray domains that may be attributed to the embedded zeolite particles (Figure 5.5 c) in accord with the literature for a BEATUD-1 composite with a zeolite loading of 16-20 wt%.^{15,157} HRTEM images (Figure 5.5 d) confirmed that BEATUD-1 is a composite of nanocrystalline BEA particles and an amorphous mesoporous matrix (TUD-1), whereby the microporosity is resulting from the crystalline zeolite particles and the mesoporous phase from the amorphous component. The TEM studies generally revealed aggregates (about 50-200 nm) of nanocrystals surrounded by the mesoporous matrix. Areas containing isolated BEA nanocrystals (about 20-30 nm) embedded in the matrix were also observed. The presence of small aggregates is in agreement with previous findings for a BEATUD-1 composite with a zeolite loading of 40 wt%,¹⁵ and can be attributed to the combined effect of the synthesis conditions and the high zeolite loading. Despite the presence of these aggregates, the TEM studies (Figure 5.5 d) indicated that the nanocrystalline BEA particles were fairly evenly distributed in the mesoporous matrix, similar to that reported by Waller et al.¹⁵ for these types of materials.

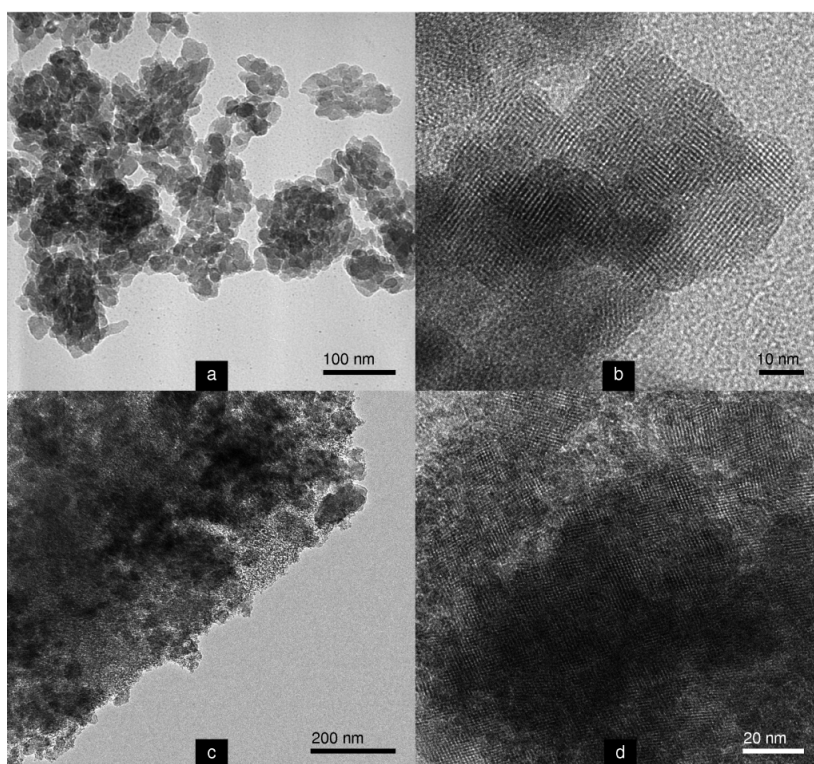


Figure 5.5- TEM images of BEA (a and b) and BEATUD-1 (c and d). The amorphous carbon support film used for BEA (b) appears as the mottled background in the upper and lower right-hand parts of the micrograph; a holey carbon film was used for BEATUD-1 to clearly distinguish the mesoporous silica matrix of the composite from the background of the support.

Elemental composition and textural properties of the zeolite BEA, BEATUD-1 and TUD-1 are given in Table 5.1. To assess the textural properties of these materials (BEA, BEATUD-1 and TUD-1), nitrogen adsorption measurements were performed at $-196\text{ }^{\circ}\text{C}$ (Figure 5.6). The adsorption isotherm of BEA clearly showed a significant increase in N_2 uptake at $p/p_0 < 0.01$, typically associated with the filling of micropores (characteristic of type I adsorption isotherms).¹⁶⁵⁻¹⁶⁹ Afterwards a gradual increase in N_2 uptake was observed as p/p_0 approached unity, most likely due to multilayer adsorption on the external surface of the nanocrystallites, accounting for a significant external surface area ($S_{\text{EXT}}=176\text{ m}^2\cdot\text{g}^{-1}$, Table 5.1). The pore size distribution (PSD) of BEA shows a very broad and weak maximum centred on a pore width of ca. 7 nm, which probably arises from the inter-nanocrystallite empty void spaces. BEATUD-1 and purely siliceous TUD-1 exhibited type IV isotherms, typical of mesoporous materials and a hysteresis loop at $p/p_0 > 0.4$ which is associated with capillary condensation/evaporation in mesopores.^{165,166,168-175} The PSDs showed maxima at pore widths of ca. 4.5 nm for BEATUD-1 and 7.0 nm for TUD-1. In contrast to TUD-1, BEATUD-1 possesses microporosity arising from the zeolite component, although the composite is essentially mesoporous. This is consistent with the literature data for zeolite nanocrystals BEA,^{15,52,111,128,140,176,177} and the composite BEATUD-1 (Table 5.1).¹⁵

Table 5.1- Elemental composition and textural properties of BEA, BEATUD-1 and TUD-1 and comparison with literature data.

Sample	Al (mmol.g ⁻¹)	Si/Al (before/after catalysis)	V _{micro} (cm ³ .g ⁻¹)	V _p (cm ³ .g ⁻¹)	Surface area (m ² .g ⁻¹)	S _{EXT} (m ² .g ⁻¹)	D _{p(meso)} (nm)	Average size (μm)	Ref
BEA	0.96	12/13 ^c	0.18 ^e	0.69	643 ^m	176	-	0.02 (crystals) [*]	this work
BEA	-	nf ^d	0.12 ^e	-	598(399/199) ⁿ	-	0.7	-	15
BEA	1.14	10.6/-	0.21 (0.63) ^f	0.84 ^k	662 ^o	-	-	0.02-0.03 (crystals)	62
H-Beta	-	12.5/-	-	-	674 ^p	-	-	0.1 (particle)	178
H-Beta	-	12.5/-	0.22	0.68 ^k	741 ^m	-	-	-	67
H-Beta	-	12.5/-	0.18 (0.04) ^f	-	517 (367/29) ⁿ	-	-	0.01 (crystals)	163
H-Beta	-	12.5/-	0.22 (0.89) ⁱ	-	582 ^m	-	-	-	179
H-Beta	-	12.5/-	0.11	0.63 ^k	667 (329/-) ^q	-	3.8	0.5 (particle)	93
H-Beta	-	12.5/-	0.11	0.86 ^k	734 (346/-) ^q	-	4.7	0.03 (crystals)	93
H-Beta	-	12.5/-	0.19 (0.45) ^f	0.64 ^k	-	245 ^u	-	0.03-0.05 (crystals) and 0.3-1 (particles)	180
H-Beta	-	12.5	-	0.23 ^k	574 ^r	-	0.65 ^w	-	74
H-Beta	-	12.5	0.21 ^g	-	538 ^m	-	-	-	126
H-Beta	-	12.5	0.16	0.59 ^k	558 (350/-) ^m	-	-	-	129
H-Beta	-	-	0.14 ^h	-	-	431 ^v	-	-	111
H-Beta	-	nf ^d	-	0.84 ^k	615 ^m	-	-	-	181
H-Beta	-	nf ^d	0.18 ^e	-	633 ^m	-	-	-	182
H-Beta	-	nf ^d	-	0.22 ^k	442 ^p	-	4.5	-	183
H-Beta	-	12.4/-	0.21 ^e	-	-	220 ^x	-	0.5-0.8 (particles)	177
H-Beta	-	12.0/-	0.16	-	627 (303/-) ^s	-	-	0.1-0.4 (crystals)	52
H-Beta	-	12.0/-	0.22 ^e	0.65 ^k	696 ^m	170 ^x	-	1-10 (crystals)	184
H-Beta	-	12.0/-	0.24(0.05)	-	563 ^m	-	-	-	185
H-Beta	-	11.6/-	0.22 (0.89) ⁱ	-	582 ^m	-	-	0.07 (crystals)	186
H-Beta	-	10.8/-	-	0.91	739 ^p	-	-	-	187
H-Beta	-	10/-	-	-	573 ^m	-	-	-	188
H-Beta	-	10/-	-	-	360 ^m	-	-	0.05 (crystals)	101
H-Beta	-	8/-	0.25 (2.42) ^j	-	651 ^m	168 ^x	>50 ^y	0.05-0.15 (crystals)	143
H-Beta	-	14.5/-	-	-	578 ^m	-	-	-	51

H-Beta	-	15/-	-	0.23	575 ^m	-	-	-	113
H-Beta	-	20/-	-	0.26 ^l	585 ^m	-	-	-	189
H-Beta	-	21/-	-	0.27 ^l	625 ^m	-	-	-	138
H-Beta	-	22/-	-	0.24	750 ^p	-	-	-	114
H-Beta	-	24.4/-	0.20 (0.58)	-	663 ^m	-	-	-	190
H-Beta	-	25.0/-	-	-	608 ^m	-	0.67	-	191
H-Beta ^a	-	27.5/	-	0.74	613 ^m	228 ^x	-	0.0002-0.0008 (particles)	192
H-Beta	-	32/-	0.29	-	319 ^m	185 ^x	-	-	90
H-Beta ^a	-	33/-	0.23	-	713 ^m	102 ^x	-	0.015 (crystals)	91
H-Beta	-	35	0.26 ^e	0.26 ^k	563 ^m	27	-	0.2 (crystal)	193-195
H-Beta	-	220/-	0.20 ^e	-	- (-/82) ^t	-	-	-	43
BEATUD-1	0.38	34/33 ^c	0.05 ^e	0.70	712 ^m	-	4.5 ^y	15 (particles) [*]	this work
BEATUD-1 (16 wt.%) ^b	-	nf ^d	-	1.1	710 ^m	-	9.1	-	157
BEATUD-1 (20 wt.%) ^b	-	nf ^d	0.07	1.1	725 (161/564) _n	-	7.4 (0.7) ^z	-	15
BEATUD-1 (40 wt.%) ^b	-	nf ^d	0.09	1.1	642 (289/353) ⁿ	-	9.1(0.7) _z	0.08-1.4 (crystals)	15
BEATUD-1 (60 wt.%) ^b	-	nf ^d	0.1	1	639 (377/262) ⁿ	-	9.0(0.7) _z	-	15
TUD-1	-	-	-	0.83	617 ^m	-	7.0 ^y	>20 (particles)	this work
TUD-1	-	nf ^d	-	1.0	757 (61/696) ⁿ	-	6.3	-	15

a) Determined by TPD (temperature programmed desorption of ammonia). b) Loading of zeolite Beta in the composite. c) Determined by ICP-AES. d) Information not found. e) V_{micro} determined by t-plot. f) V_{micro} determined by the t-plot method and the value in parentheses refers to V_{meso} which was calculated as $V_p - V_{\text{micro-g}}$. g) V_{micro} determined by t-plot. h) V_{micro} determined by α_s -plot. i) V_{meso} determined by the BJH method at $0.1 < p/p_0 < 1$ and V_{meso} (value in parenthesis) was calculated using Dubinin-Astakhov method ($n=4$) at $p/p_0 < 0.1$. j) V_{micro} and V_{meso} determined by BJH method. k) V_p calculated by the maximum adsorption amount of nitrogen at $p/p_0 \approx 0.99$. l) V_p determined by Dubinin-Radushkevich method. m) S_{BET} calculated by the BET equation and values in parentheses refers to $S_{\text{micro}}/S_{\text{meso}}$. n) S_{BET} calculated by the BET equation and the values in parenthesis refers to $S_{\text{micro}}/S_{\text{meso}}$, in which the S_{micro} was determined by the t-plot method and $S_{\text{meso}} = S_{\text{BET}} - S_{\text{micro}}$. o) Surface area determined by N_2 isotherms. p) Determination of the surface area not mentioned. q) S_{BET} calculated with the multipoint BET equation with linear region in the p/p_0 range of 0.05-0.35 and the values in parentheses refers to $S_{\text{micro}}/S_{\text{meso}}$. r) S_{BET} calculated using adsorption data in the p/p_0 range of 0.05 to 0.20. s) S_{BET} calculated by the BET equation and the value in parentheses refers to $S_{\text{micro}}/S_{\text{meso}}$ in which S_{micro} determined by t-plot method. t) S_{meso} determined by the t-plot method. u) S_{EXT} determined by t-plot curves for the relative pressures p/p_0 in the range 0.1-0.3. v) S_{EXT} determined by the α_s -plot. x) S_{EXT} determined by t-plot method. w) D_p (average pore diameter) determined by Horvath-Kawazoe method. y) D_p determined by the BJH method. z) Value in parenthesis refers to microporous average diameter. *) Estimated by electron microscopy. The calculations for the values without an indication are not mentioned in the respective works.

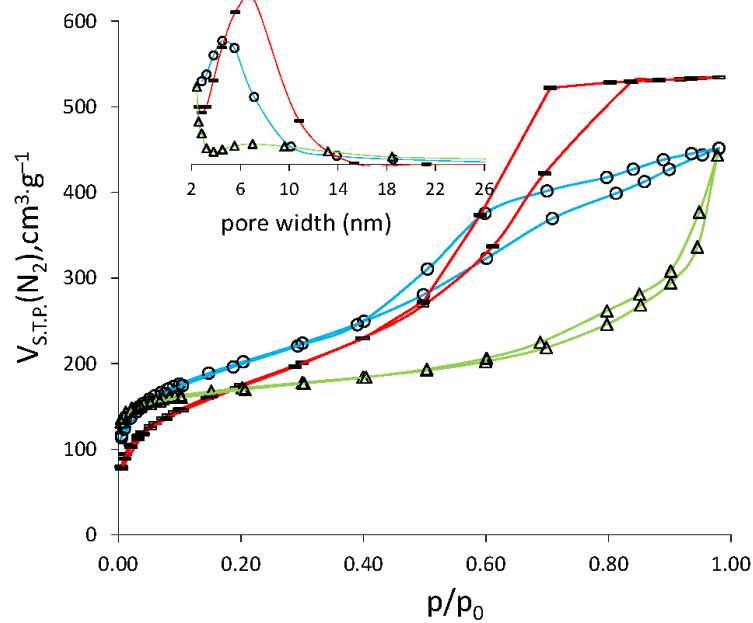


Figure 5.6- N₂ adsorption-desorption isotherms measured at -196 °C and pore size distribution curves for BEA (Δ), BEATUD-1 (O) and TUD-1 (-).

When comparing with the literature data, similar significant external surface areas were obtained for zeolite Beta ($S_{EXT}=168-185 \text{ m}^2.\text{g}^{-1}$, Table 5.1).^{90,143,184} Other authors achieved even higher external surface areas ($S_{EXT}=220-245 \text{ m}^2.\text{g}^{-1}$).^{177,180,192} Lower external surface areas were also obtained ($S_{EXT}=27-102 \text{ m}^2.\text{g}^{-1}$); however in those cases, the specific surface areas were similar to that obtained in the present work ($S_{BET}=563-713 \text{ m}^2.\text{g}^{-1}$ compared to $643 \text{ m}^2.\text{g}^{-1}$, Table 5.1).^{91,193-195} In the work of Waller et al.,¹⁵ as the amount of zeolite in the composite BEATUD-1 decreased, an increase in the mesoporous surface area was observed due to the mesoporosity of TUD-1 ($S_{meso}=262 \text{ m}^2.\text{g}^{-1}$ for BEATUD-1 with 60 wt.% of BEA compared to $564 \text{ m}^2.\text{g}^{-1}$ for BEATUD-1 with 16 wt.% of BEA, Table 5.1).^{15,157}

Based on the aluminium contents of BEA and BEATUD-1 measured by ICP-AES (Table 5.1) it was possible to estimate that the amount of zeolite BEA in BEATUD-1 was 40 wt.% (by comparing the aluminium contents of BEA and the composite BEATUD-1), which was the same as that used in the synthesis gel. This result suggested that the zeolite was completely incorporated in the final material.

^{27}Al MAS NMR is important because it is an effective tool for characterising the structure of zeolites. It allows differentiating aluminium-containing species with different structures or different chemical environments because they have different chemical shifts in the ^{27}Al MAS NMR spectra.^{112,196} It has been widely used to determine the coordination number,^{87,197,198} and local structure of specific aluminium species in zeolites.⁸⁷ According to crystallographic data, zeolite Beta contains three or nine different T-sites, depending on the type of polymorphs present.^{28,29,199-201} Nevertheless, these T-sites in the Beta framework can be resolved into only two or three due to small differences in the chemical shifts of the T-sites.¹⁹⁷ The regular coordination of aluminium in the zeolite framework is tetrahedral.¹⁹⁷ Figure 5.7 shows the ^{27}Al MAS NMR spectra of BEA and BEATUD-1. Both of them exhibited two groups of peaks at about 55 ppm and a larger peak at 0 ppm, which were attributed to aluminium species in tetrahedral framework (Al_{tet}) and octahedral coordination (Al_{oct}), respectively, in agreement with the literature data for zeolite Beta.^{84,95,112,113,125,150,154,182,196,200,202-205} Normally the peak at 0 ppm is ascribed to extra-framework octahedral aluminium species which are formed during calcination.^{206,207} However, in the case of the acid zeolite Beta octahedral framework aluminium might also be present.¹⁹⁷ Specific framework tetrahedral T-sites tend to convert to framework-associated octahedral sites during the calcination.²⁰⁰ Bourgeat-Lami et al.²⁰⁸ were the first to suggest the existence of octahedral framework aluminium species at 0 ppm in zeolite Beta. This type of framework octahedral aluminium can only be formed in the presence of water.^{202,206,209} According to Bokhoven et al.¹⁹⁷ the Brönsted acid zeolite attracts water molecules to stabilise the strong electric field induced by the proton, delocalising the cationic charge. Since the zeolite is not able to accommodate many strong electrical field centers throughout the framework, the water molecules are attracted and part of the framework tetrahedral aluminium may be converted to octahedral aluminium, reducing the electrical field in the framework.¹⁹⁷ It was proposed by the authors that this aluminium might be connected to the framework via one or two oxygen atoms.¹⁹⁷ Alternatively, an aluminium atom may be connected via four oxygen atoms to the framework and coordinated by one water molecule and one hydronium ion.^{155,202,208,210,211} The aluminium in octahedral coordination might result from the hydrolysis of the Al-O bond.²⁰⁶ Abraham et al.²⁰⁰ verified that in zeolite H-Beta, octahedrally coordinated framework-associated aluminium atoms could be quantitatively reverted into tetrahedral coordination, and that the amount of these octahedral aluminium species decreases with increasing Si/Al ratio, and are absent in samples with very high-Si/Al ratios.²⁰⁰ This theory was confirmed by Woolery et al.²¹² that reported that the peak in the region of 0 ppm corresponding to octahedral aluminium can be converted to the tetrahedral

coordination by alkali ion-exchange or by treatment with NH_3 ; and by Bockhoven et al.^{213,214} reporting that all the octahedral aluminium of an acid zeolite was converted to tetrahedral aluminium by heating above 100 °C.

The ^{27}Al MAS NMR spectrum obtained for BEA was very similar to that reported by Beers et al.²¹⁵ for a commercial zeolite Beta in the H^+ -form with a bulk Si/Al ratio of 13 (ref CP 814 E-22), and Li et al.¹¹² for Beta (Si/Al=15). Besides the sharp peak at 0 ppm that can be assigned to a framework connected octahedral aluminium (reported for acidic zeolite Beta), there is a broad centred around -18 ppm that could be due to extra-framework (octahedral) aluminium oxide amorphous species left over from the synthesis (Figure 5.7).²¹⁵ Furthermore a few authors had obtained a third signal at ca. 25 ppm, which was attributed to pentacoordinated aluminium or to an aluminium atom in highly distorted tetrahedral coordination.^{145,216-218} However this was not verified in the present work (Figure 5.7).

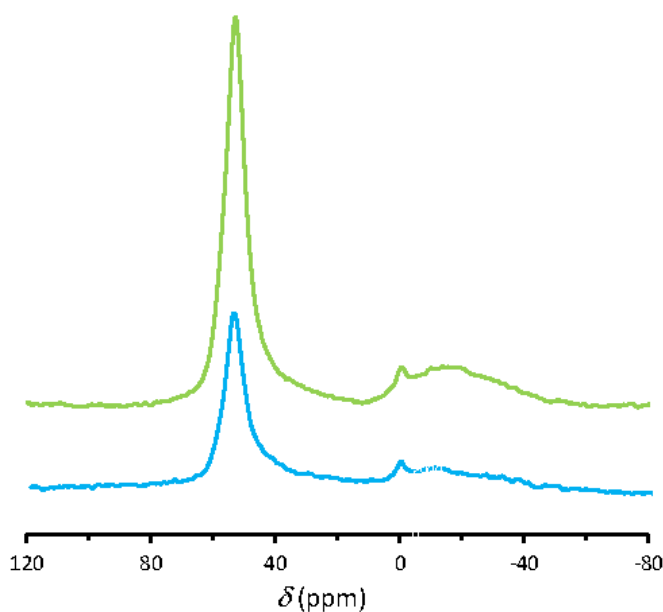


Figure 5.7- ^{27}Al MAS NMR spectra of BEA (green) and BEATUD-1 (blue).

Engelhardt et al.²¹⁹ considered that the peak at 0 ppm was due to extra-framework octahedral aluminium and proposed that relative proportions of tetrahedral framework and octahedral aluminium could be directly determined from the peak intensities (I) of the tetrahedral aluminium, Al_{tet} , and the octahedral aluminium, Al_{oct} , signals.²¹⁹ According to the authors, the Si/Al ratio of the tetrahedral framework species $(\text{Si}/\text{Al})_{\text{fr}}$ could be calculated using the equation 5.1 ($(\text{Si}/\text{Al})_{\text{tot}}$ is the total ratio of Si/Al):

$$\left(\frac{\text{Si}}{\text{Al}}\right)_{\text{fr}} = \left(\frac{\text{Si}}{\text{Al}}\right)_{\text{tot}} \times \frac{(I_{\text{Altet}} + I_{\text{Al oct}})}{I_{\text{Altet}}} \quad (5.1)$$

$A(\text{Si}/\text{Al})_{\text{fr}}$ of 15.8 was obtained which was higher than the value of 12 obtained from ICP-AES (Table 5.1). The difference between the NMR and ICP-AES results represents the contribution from octahedral aluminium in the sample (that can be framework and extra-framework as discussed above) assuming that all the aluminium were detected by ^{27}Al MAS NMR spectrum.¹²⁵ According to the literature, octahedral species in zeolite BEA might be associated with Lewis acid sites (L).^{197,212,220,221}

The acidity of aluminosilicates investigated by FT-IR may be associated with bridging hydroxyl groups (Si-OH-Al) formed by tetrahedral aluminium,²²² (ca. 3600 cm^{-1} on the FT-IR spectra),^{223,224} hydroxyl groups, such as internal or terminal silanol Si-OH groups (3740 cm^{-1}),^{223,224} and Al-OH groups (3780 and 3680 cm^{-1})^{208,224} on the surface of the aluminosilicate which are usually weakly acidic.^{155,238} The measurement of the acid properties of the prepared catalysts (BEA and BEATUD-1) was performed by FT-IR studies of adsorbed pyridine after outgassing at $150\text{ }^{\circ}\text{C}$. In the case of zeolite BEA and composite BEATUD-1 the presence of Si-OH terminal groups was evident by the presence of an intense band at ca. 3745 cm^{-1} (Figure 5.8), similar to reported in the literature.^{205,222,225-228}

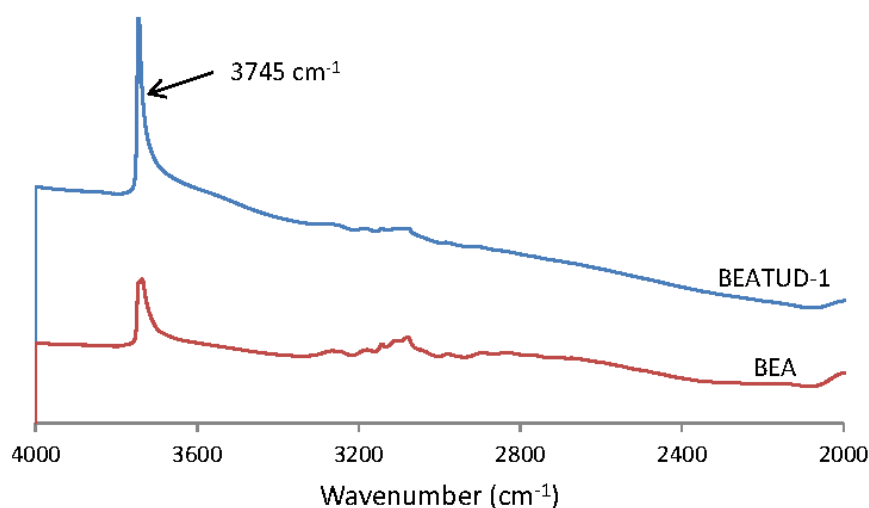


Figure 5.8- FT-IR spectra of BEA and BEATUD-1 after pyridine adsorption and outgassing at $150\text{ }^{\circ}\text{C}$.

BEA and BEATUD-1 possessed both B and L interacting with pyridine after outgassing at 150 °C. The concentrations of B and L were determined as explained previously in Section 3.2.1.2 of Chapter 3. In this sense, the [B] (band at ca. 1545 cm^{-1}) and [L] (band at ca. 1450 cm^{-1}) for the zeolite BEA and composite BEATUD-1 were determined through equations 3.1 and 3.2, as specified in Chapter 3 (Table 5.2). Figure 5.9 shows the FT-IR spectra of the catalysts with adsorbed pyridine, after outgassing at 150 °C. The band at ca. 1490 cm^{-1} is attributed to L and B, 1620 cm^{-1} to L and 1640 cm^{-1} to B, which is similar to the literature.^{70,222,229} Other authors did not made reference to the bands at 1620 and 1640 cm^{-1} .^{226,230,231}

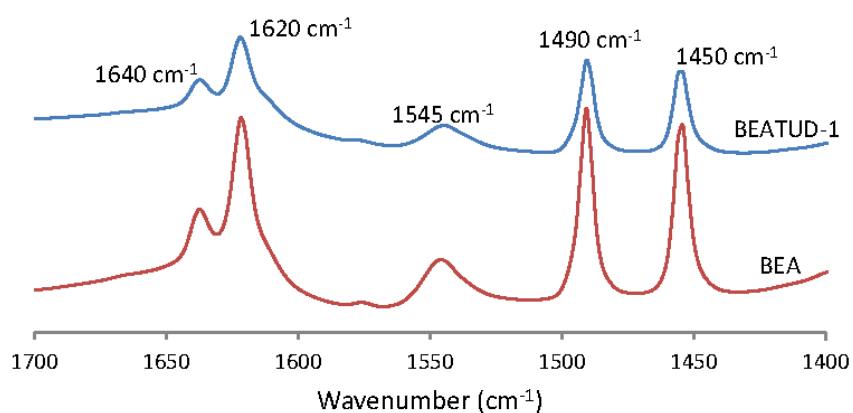


Figure 5.9- FT-IR spectra of BEA and BEATUD-1 after pyridine adsorption and outgassing at 150 °C.

The total amount of AS was greater for BEA than for BEATUD-1 (Table 5.2). The total amount of AS found in the literature for zeolite BEA was also higher than the total amount of AS found for BEATUD-1 reported herein (Table 5.2).^{70,92,163,178,191,222,225-227,229,231-236} The [B] was lower than the [L]. A similar behaviour was verified for zeolite Beta with a Si/Al of ca. 13-31,^{70,178,225-227,229,234} but the opposite was also obtained for zeolite Beta samples with a similar Si/Al ratio (11-13),^{163,222,227,233-235} or higher Si/Al ratio of 42-60.^{92,232} In BEA the positively charged extra-framework aluminium species may neutralise the negative charge of AlO_4 tetrahedra and decrease the [B].¹⁵⁵ In terms of the L/B molar ratio and acid strengths, the acid properties of BEA and BEATUD-1 were somewhat comparable.

The effect of the outgassing temperature on the [L] and [B] was also investigated, and it was observed a decrease in the amount of detected AS with an increase in the outgassing temperature (Figure 5.10). The ratios of the amounts of AS were measured at 150 °C and 350 °C. At 350 °C, pyridine desorbed more easily from the B than from the L. The molar ratio of

moderate and strong to total B at 350 °C and 150 °C ($[B]_{350}/[B]_{150}$) was in the range of 0.2-0.3 (for both samples), indicating that most of the B were of a rather weak nature. In the case of L ratio ($[L]_{350}/[L]_{150}$) this value was 0.8, which means that these were stronger due to the fact that they almost did not desorb the pyridine at a temperature of 350 °C.

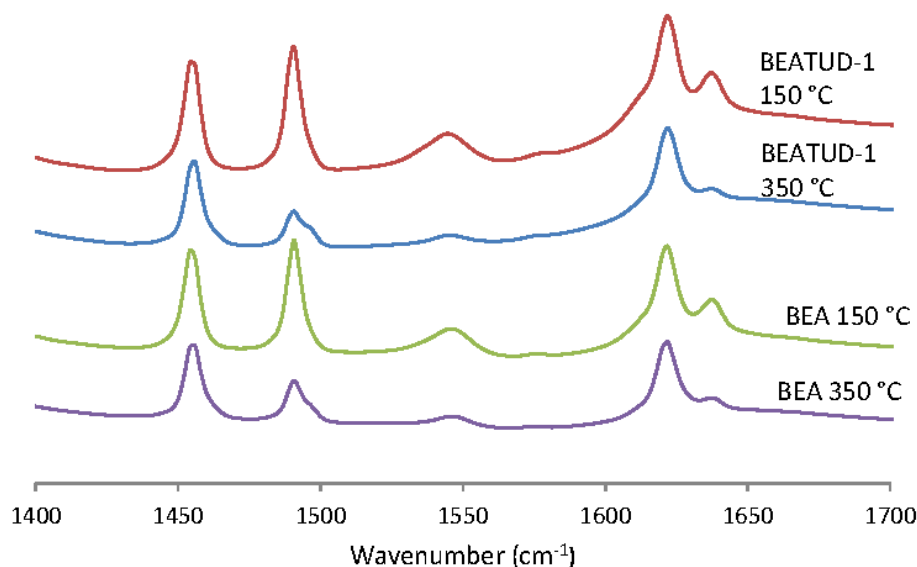


Figure 5.10- Effect of the outgassing temperature on BEA and BEATUD-1 after pyridine adsorption.

Table 5.2- Acid properties measured by FT-IR of adsorbed pyridine of BEA and BEATUD-1 and comparison with literature data.

Sample (Si/Al)	T_{ads} (°C) ^b	T_{des} (°C) ^c	$[L]$ ^d $\mu\text{mol.g}^{-1}$	$[B]$ ^e $\mu\text{mol.g}^{-1}$	$[L]+[B]$ $\mu\text{mol.g}^{-1}$	$[L]/[B]$	Ref
BEA(12)	150	150	199	152	351	1.31	this work
Beta(11.1) ^a	147	147	382	513	895	0.75	222
BEA(12.5)	150	150	240	580	820	0.41	163
BEA(12.5)	450	450	400	320	720	1.25	178
BEA(12.5) ^a	170	170	190	153	343	1.23	227
BEA(12.5)	350	350	-	-	-	0.16	233
Beta(12.5)	150	150	248	96	344	2.58	234
Beta(13.0)	250	250	128	180	308	0.71	235
Beta(15.0) ^a	200	200	469	372	841	0.83 (1.2) ^f	226
Beta(16.5) ^a	180	180	100	194	294	0.52 (0.95) ^f	231
Beta(25)	200	200	-	-	-	1.33	236
Beta(25)	152	152	151	150	301	0.50	191
Beta(26.4)	150	150	340	315	655	1.08	225
Beta(30)	200	200	269	66	335	4.08	229

Beta(30.6)	200	200	-	-	-	2.99	⁷⁰
Beta(42)	150	150	107	189	296	0.57	⁹²
Beta(60)	350	350	-	-	-	0.66	²³²
BEATUD-1(34)	150	150	114	95	209	1.19	this work

a) These values were converted to mmol.g^{-1} considering that the values reported for unit cell were given per moles and considering that the unit cell is dehydrated. b) Temperature of pyridine adsorption (T_{ads}) used to determine Brönsted and Lewis acid sites concentrations. c) Temperature of pyridine desorption (T_{des}) used to determine Brönsted and Lewis acid sites concentrations. d) Concentration of Lewis acid sites, [L]. e) Concentration of Brönsted acid sites [B]. f) Values in parenthesis were calculated according to the equation: $(1.5 \times (A_{\text{AbsB}}/A_{\text{AbsL}}))$, where $A_{\text{AbsB}}/A_{\text{AbsL}}$ is the absorbance area ratio and 1.5 is the extinction coefficient ratio (ϵ_L/ϵ_B).

The aluminium concentration in zeolite BEA ($960 \mu\text{mol.g}^{-1}$, Table 5.1) was higher than the total number of AS ($351 \mu\text{mol.g}^{-1}$, Table 5.2). This is consistent with the literature, which indicated that the number of AS is different from the total number of aluminium atoms present in the zeolite even when all their centres are accessible to pyridine.²²⁷ Gil et al.²²⁷ reported that this can be due to the fact that zeolites are not perfect structures and therefore part of the aluminium does not form the protonated Si-O-Al bridges: some form weak Al-OH groups or are present as Lewis acid sites. Lewis acid sites do not have infrared absorption bands however they can be detected after adsorption of base molecules, e.g. pyridine.²²⁷ On the other hand, pyridine is a relatively strong base that can be protonated by Si-OH-Al groups, Si-OH or Al-OH.²³⁷ These two facts (possible formation of Al-OH groups or Lewis acid sites; and protonation of pyridine) act in opposite directions and the number of Brönsted acid sites detected by pyridine adsorption depends on the domination of one factor over the other.²²⁷

5.2.2. Catalytic dehydration of D-xylose

5.2.2.1. Catalytic performance of zeolite BEA and composite BEATUD-1

The reaction of Xyl in the presence of BEATUD-1 under water-toluene biphasic solvent conditions (denoted Wt:tol), at 170°C (Figure 5.11), gave 74 % Y_{Fur} at 98% C_{Xyl} (reached at 8 h of reaction, Table 5.3). At 6 h of reaction, the C_{Xyl} was 94%, compared with only 20% of purely siliceous TUD-1, and 23% without a catalyst, indicating that the zeolite component was responsible for accelerating the reaction of Xyl. These results compared favourably with

microporous silicoaluminophosphates (Chapter 3: 34-38% and 41-48% Y_{Fur} for SAPO-11 at 4 h and 6 h), and Al-TUD-1 (Chapter 4: 60% Y_{Fur} at 6 h) used as solid acid catalysts in the same reaction, under similar conditions.

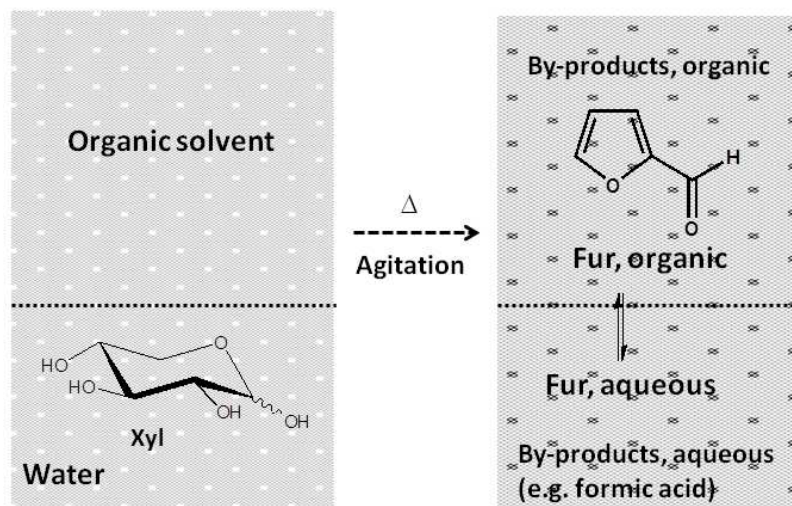


Figure 5.11- Schematic representation of the reaction of D-xylose (Xyl) to 2-furaldehyde (Fur) under aqueous-organic biphasic solvent conditions. The dots represent the powdered solid acid catalyst.

Table 5.3- Catalytic performance of BEA, BEATUD-1 or TUD-1 in the reaction of D-xylose (Xyl) using the biphasic solvent system (Wt:Tol) and comparison with literature data for other catalysts.

Catalysts	T (°C) ^c	t (h) ^d	C_{Xyl} (%) ^e	Y_{Fur} (%) ^f	Initial reaction rate ($\text{mmol} \cdot \text{g}_{\text{cat}}^{-1} \cdot \text{h}^{-1}$) ^g	Ref
BEA1.0 (Si/Al=12) ^a	170	4/6	98/100	54/49	9.3 (C_{Xyl} (30 min)=46.3%)	this work
BEA0.4 ^a	170	6	97	56	9.6 (C_{Xyl} (30 min)=19.2%)	this work
BEA0.4/TUD0.6 ^a	170	6	94	58	4.3 (C_{Xyl} (30 min)=21.5%)	this work
BEATUD-1 (Si/Al=34) ^a	170	6/8	94/98	69/74	5.7 (C_{Xyl} (30 min)=28.3%)	this work
TUD-1 ^a	170	6	20	13	5.6 (C_{Xyl} (30 min)=28%)	this work
Al-TUD-1 (Si/Al=21)	170	6	91	60	3.7 (C_{Xyl} (30 min)=18.6%)	Chapter 4
No catalyst	170	6	23	12	-	this work
H-Y Faujasite (Si/Al=5)	160	6	94	39	-	^{5,238}
H-Y Faujasite (Si/Al=15) ^b	170	0.83	51	42	24 (C_{Xyl} (30min)=48%)	³
H-Nu-6(2)	170	6	90	45	1.1 (C_{Xyl} (30 min)=5.7%)	⁸
del-Nu-6(1)	170	6	90	48	2.3 (C_{Xyl} (30 min)=11.4%)	⁸
H-Mordenite (Si/Al=6)	160	6	79	28	-	^{5,238}
H-Mordenite (Si/Al=11) ^b	170	0.83	37	33	15 (C_{Xyl} (30min)=30%)	³

a) The amount of the catalyst in the reaction medium was always $20 \text{ g}_{\text{cat}} \cdot \text{dm}^{-3}$ except for BEA0.4 ($8 \text{ g}_{\text{cat}} \cdot \text{dm}^{-3}$). In the case of BEA0.4/TUD0.6 it was used 8 g of BEA0.4 with the remaining of TUD-1 to give a total of $20 \text{ g}_{\text{cat}} \cdot \text{dm}^{-3}$. b) The concentration of D-xylose was 0.5 M Xyl and the amount of the catalyst in the reaction medium was $20 \text{ g}_{\text{cat}} \cdot \text{dm}^{-3}$. c) Temperature of reaction. d) Reaction time. e) D-xylose conversion at the specified reaction time (C_{Xyl}). f) 2-Furaldehyde yield at the specified reaction time (Y_{Fur}). g) Initial reaction rate was determined for 30 min of D-xylose conversion (C_{Xyl}). Reaction conditions: 0.3 Wt:0.7 Tol (v/v) biphasic solvent system, 170 °C, $20 \text{ g}_{\text{cat}} \cdot \text{dm}^{-3}$, 0.67 M Xyl.

Other water tolerant crystalline inorganic solid acids (containing Al and Si) have already been tested in the reaction of Xyl using water and toluene as solvents. A few examples are shown in Table 5.3. After comparing these results, it seems that the composite BEATUD-1 exhibited superior catalytic performance in the dehydration of Xyl to Fur under similar reaction conditions (0.3 Wt:0.7 Tol (v/v) biphasic solvent system, 160-170 °C). The catalytic performance of BEATUD-1 in terms of Fur yield compares quite favourably with all of the previously tested catalysts (74% Y_{Fur} compared to 28-48% Y_{Fur}), even for H-Y Faujasite(5), H-Nu-6(2) and the delaminated zeolite del-Nu-6(2) with similar C_{Xyl} (90-94%) at which 39-48% Y_{Fur} were reached (Table 5.3). Decreasing the amount of the catalyst in the reaction medium from 20 $\text{g}_{\text{BEATUD-1}} \cdot \text{dm}^{-3}$ to 5 $\text{g}_{\text{BEATUD-1}} \cdot \text{dm}^{-3}$ led to somewhat lower Y_{Fur} at 6 h (69 and 59%, respectively). More recently, Kim et al.²³⁹ reported for zeolite BEA(25) in the same reaction at 140 °C and under similar biphasic solvent conditions, 40% Y_{Fur} (90% C_{Xyl}) at 4 h, exhibiting superior activity than that for zeolites H-Ferrierite(20), and H-Mordenite(20), which gave 35% Y_{Hmf} (ca. 80% C_{Xyl}) under similar reaction conditions.

The dehydration of Xyl in the presence of BEATUD-1 was carried out using solely water as the solvent for comparison with the biphasic solvent system (Wt:Tol). A high C_{Xyl} of 81% was obtained at 6 h, but the Y_{Fur} was poor (25%) in comparison to the Wt:Tol solvent system (69%, Figures 5.12- 5.14). Hence, the biphasic solvent system is beneficial, because the reaction of Xyl (insoluble in Tol) takes place only in the aqueous phase, and the in situ extraction of Fur from the aqueous phase (containing Xyl and polar intermediates) into the organic phase may enhance Fur yields by avoiding its decomposition through consecutive reactions with intermediates in the aqueous phase. The partition ratio of Fur (PR_{Fur}) calculated as indicated in equation 5.2 varied in the range 8-10 for different reaction times (measured at a.t.). Hence, changes in the product distribution with time did not significantly affect the partition ratio of Fur. Increasing the reaction temperature in the range of 160-180 °C for the Wt:Tol system had a beneficial effect on initial reaction rate and Fur yield. Initial reaction rate ($\text{mmol} \cdot \text{g}_{\text{cat}}^{-1} \cdot \text{h}^{-1}$) followed the order: 3.4 (160 °C) < 5.7 (170 °C) < 8.2 (180 °C), and Fur yield at 30 min of reaction followed the order: 4% (160 °C) < 14% (160 °C) < 14% (170 °C) < 27% (180 °C). Hence, increasing the reaction temperature may be advantageous for process intensification.

$$\text{PR}_{\text{Fur}} = \frac{\text{moles of Fur in Tol}}{\text{moles of Fur in } W_t} \quad (5.2)$$

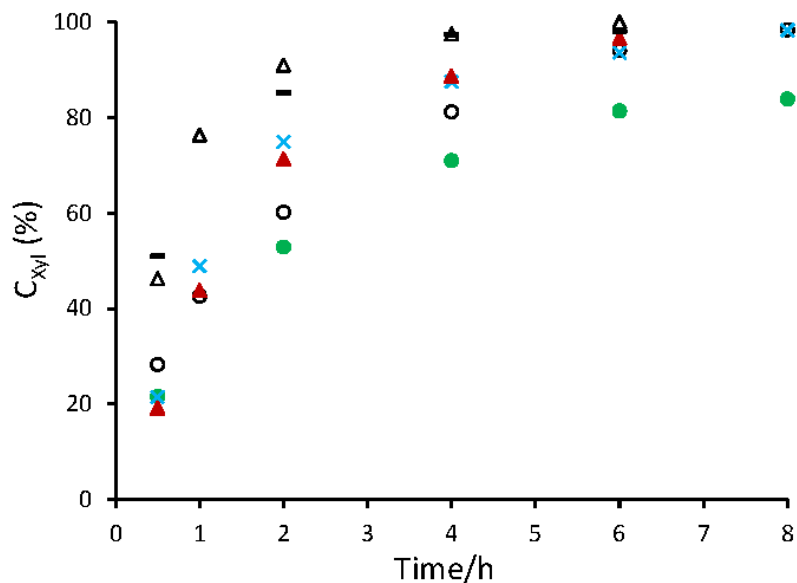


Figure 5.12- D-xylose conversion (C_{Xyl}) in the presence of BEA1.0 (Δ), BEA0.4 (\blacktriangle), physical mixture BEA0.4/TUD0.6 (\times), or BEATUD-1 (O) for 0.3 Wt:0.7 Tol (v/v) biphasic solvent system ; BEATUD-1 (\bullet) or BEA (-) for solely Wt (0.3 cm^3), $170 \text{ }^\circ\text{C}$, 0.67 M Xyl . Amount of catalyst in the reaction medium: $20 \text{ g}_{\text{cat}}\cdot\text{dm}^{-3}$ for BEA1.0 and BEATUD-1; $8 \text{ g}_{\text{BEA}}\cdot\text{dm}^{-3}$ for BEA0.4 and $8 \text{ g}_{\text{BEA}}\cdot\text{dm}^{-3} + 12 \text{ g}_{\text{TUD-1}}\cdot\text{dm}^{-3}$ for BEA0.4/TUD0.6.

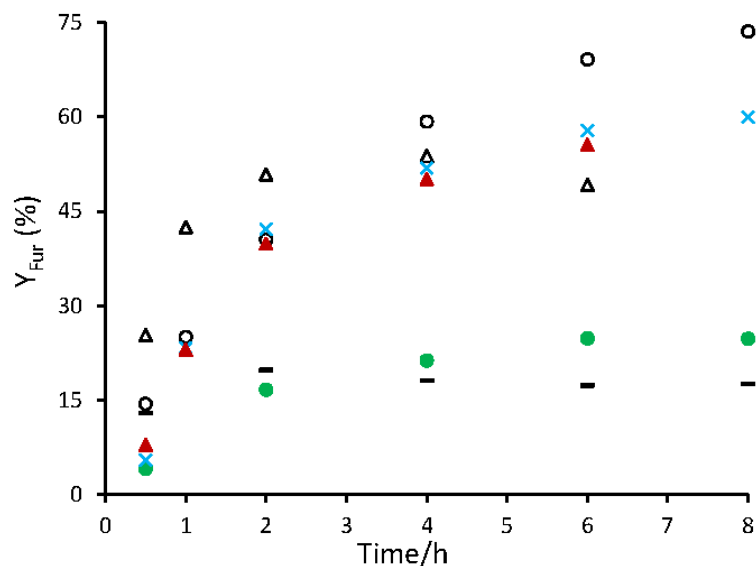


Figure 5.13- Dependence of the yield of 2-furaldehyde (Y_{Fur}) on time for the reaction of D-xylose in the presence of BEA1.0 (Δ), BEA0.4 (\blacktriangle), physical mixture BEA0.4/TUD0.6 (\times), or BEATUD-1 (O) for 0.3 Wt:0.7 Tol (v/v) biphasic solvent system; BEATUD-1 (\bullet) or BEA (-) for solely Wt (0.3 cm^3), $170 \text{ }^\circ\text{C}$, 0.67 M Xyl . Amount of catalyst in the reaction medium: $20 \text{ g}_{\text{cat}}\cdot\text{dm}^{-3}$ for BEA1.0 and BEATUD-1; $8 \text{ g}_{\text{BEA}}\cdot\text{dm}^{-3}$ for BEA0.4 and $8 \text{ g}_{\text{BEA}}\cdot\text{dm}^{-3} + 12 \text{ g}_{\text{TUD-1}}\cdot\text{dm}^{-3}$ for BEA0.4/TUD0.6.

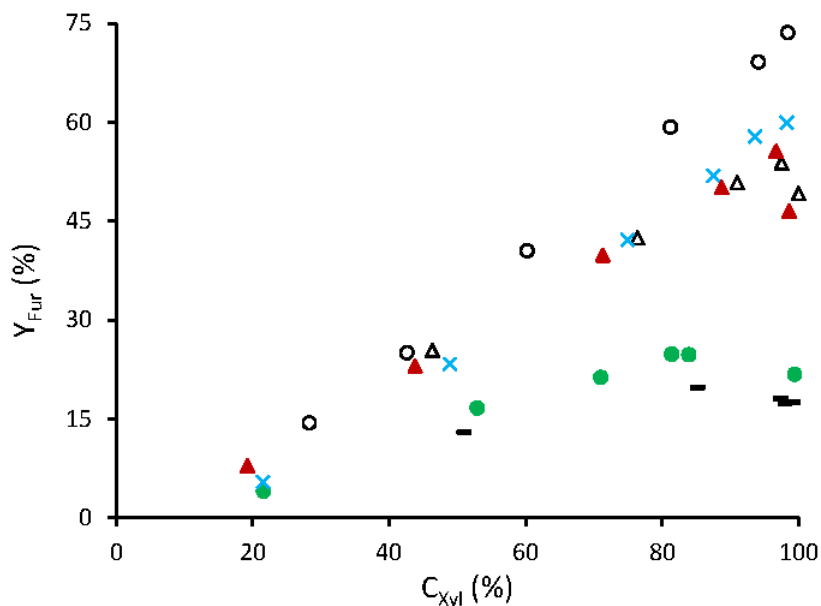


Figure 5.14- Yield of 2-furaldehyde (Y_{Fur}) versus the conversion of D-xylose (C_{Xyl}) for the reaction of D-xylose in the presence of BEA1.0 (Δ), BEA0.4 (\blacktriangle), physical mixture BEA0.4/TUD0.6 (\times), or BEATUD-1 (O) for 0.3 Wt:0.7 Tol (v/v) biphasic solvent system; BEATUD-1 (\bullet) or BEA ($-$) for solely Wt (0.3 cm^3) 170 °C, 0.67 M Xyl. Amount of catalyst in the reaction medium: $20 \text{ g}_{cat} \cdot \text{dm}^{-3}$ for BEA1.0 and BEATUD-1; $8 \text{ g}_{BEA} \cdot \text{dm}^{-3}$ for BEA0.4 and $8 \text{ g}_{BEA} \cdot \text{dm}^{-3} + 12 \text{ g}_{TUD-1} \cdot \text{dm}^{-3}$ for BEA0.4/TUD0.6.

The reaction of Xyl in the presence of BEA, used in the same quantity (20 mg) as BEATUD-1, at 170 °C (experiment denoted BEA1.0) gave 42% Y_{Fur} at 1 h (Figures 5.12 and 5.13), which was somewhat comparable to that reported by Moreau et al.³ for dealuminated H-Y Faujasite and H-Mordenite zeolites possessing similar Si/Al ratio (10-15), used as catalysts in the same reaction and under similar conditions (33-42% Y_{Fur} at 50 min, Table 5.3).

The beneficial effects of using Wt:Tol biphasic solvent system instead of solely water as solvent mentioned above for BEATUD-1 were also observed for BEA: 17 and 54% Y_{Fur} at 4 h reaction for the Wt and Wt:Tol solvent systems, respectively (Figures 5.12-5.14).

The reaction of Xyl using the biphasic system (Wt:Tol) was faster for BEA1.0 than for BEATUD-1 (Figures 5.12-5.14). It is possible that the catalytic reaction took place on the internal and external surface of the BEA nanocrystallites (micropore volume was much lower than the total pore volume, Table 5.2). The initial reaction rate calculated on the basis of the mass of catalyst (9.3 and $5.7 \text{ mmol} \cdot \text{g}^{-1} \cdot \text{h}^{-1}$ for BEA and BEATUD-1, respectively, Table 5.3) correlated with the amount of AS in the catalysts, which was higher for BEA than for BEATUD-1 (351 and $209 \text{ } \mu\text{mol} \cdot \text{g}^{-1}$, respectively, Table 5.2);⁷ possibly the silica embedding the nanocrystallites may limit the

access to some of the AS. On the other hand, the initial reaction rate calculated on the basis of the total amount of AS $[L]+[B]$ was similar for BEA1.0 and BEATUD-1 (26 and 27 $\text{mol}\cdot\text{mol}_{L+B}^{-1}\cdot\text{h}^{-1}$, respectively). A 2.5-fold decrease in the mass of BEA used (experiment BEA0.4) led to lower C_{Xyl} at 6 h than that for BEA1.0 (Figures 5.13 and 5.14), but a similar initial reaction rate ($9.6 \text{ mmol}\cdot\text{g}^{-1}\cdot\text{h}^{-1}$ for BEA0.4 compared to $9.3 \text{ mmol}\cdot\text{g}^{-1}\cdot\text{h}^{-1}$ for BEA1.0, Table 5.3). In the studied range of the amount of the catalyst in the reaction medium ($8\text{-}20 \text{ g}_{\text{BEA}}\cdot\text{dm}^{-3}$), the plots of the Fur yield against Xyl conversion were roughly coincident (Figure 5.14). The reaction in the presence of the physical mixture BEA0.4/TUD0.6 took place at a similar rate to that for BEA0.4, suggesting that the reaction rate was essentially governed by the acid properties of the zeolite fraction. Furthermore, considering the plots of Fur yield against the conversion of Xyl, BEA0.4/TUD0.6 and BEA0.4 gave similar Fur yield for C_{Xyl} up to ca. 80%, and for higher conversions of Xyl slightly higher yields of Fur are reached for the physical mixture: 60 and 56% Y_{Fur} at 97-98% C_{Xyl} for BEA0.4/TUD0.6 and BEA0.4, respectively. A significant improvement in the yield of Fur at higher conversion of Xyl, was observed for the composite BEATUD-1, which gave 74% Y_{Fur} , while BEA gave 54% for the same C_{Xyl} of 98% (Table 5.3). These improvements might be due to favourable competitive adsorption effects caused by the surrounding silica matrix in the zeolite nanocrystallites, minimising undesired reactions (the used BEATUD-1 catalyst contained a lower amount of carbonaceous matter than BEA as discussed ahead in Section 5.2.3).

5.2.2.2. Identification of the reaction products

During the reaction under study in the presence of BEATUD-1, the water and toluene phases turned yellow, suggesting the formation of by-products. As detailed in the Introduction Section 1.3, the reaction mechanism of the acid-catalysed conversion of Xyl to Fur involves a series of elementary steps with the formation of three molecules of water per molecule of Fur formed, and several undesired side reactions may take place.

The HPLC analysis of the aqueous phase showed some minor peaks, which may include formic acid (based on the comparison of peak retention times with that for an authentic sample) formed by fragmentation reactions of Xyl.²⁴⁰ Oligo/polymeric by-products are also expected to be formed by condensation reactions through Fur intermediates.²⁴¹ To test the stability of Fur under

the reaction conditions used, the reaction was carried out with Fur as the substrate (instead of Xyl) in the presence of BEA and gave 3% C_{Fur} at 6 h, suggesting that Fur is relatively stable.⁴

In order to identify other possible by-products, the aqueous-phase was extracted with dichloromethane, giving a yellow solution, and then both of the organic phases were analysed by GC-MS. However, no major by-products were detected in the Tol phase or in the dichloromethane extract, which could be due to the soluble by-products being essentially of low volatility. To get some insight into the nature of the soluble/low volatile by-products formed, the reaction of Xyl was carried out in the presence of BEA using D_2O as solvent instead of H_2O , at 170 °C for 8 h. After separating the solid catalyst, the reaction solution was analysed by 1H (Figure 5.15) and ^{13}C NMR spectroscopy (Figure 5.16).

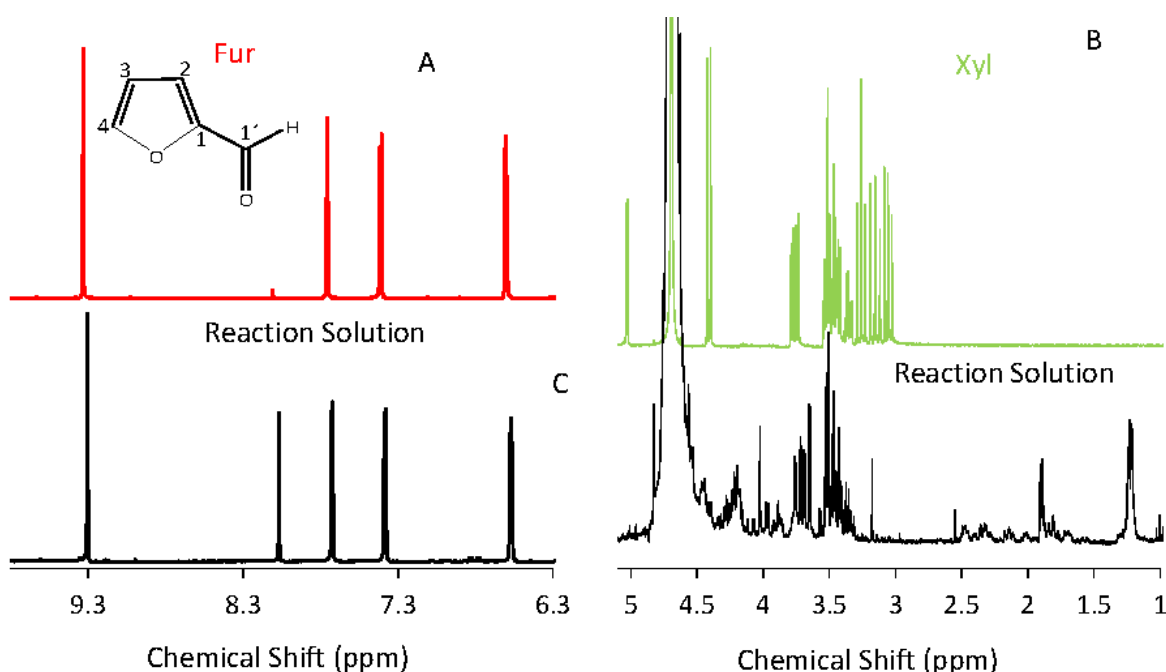


Figure 5.15- 1H NMR spectra of the solution obtained after separation of the solid phase from the reaction mixture of D-xylose (Xyl) in the presence of BEA using D_2O as solvent (C). The spectra of 2-furaldehyde, Fur (A) and D-xylose, Xyl (B) are given for comparison. Reaction conditions: D_2O (1 cm^3), 8 h, 170 °C, $20\text{ g}_{BEA}\cdot\text{dm}^{-3}$, 0.67 M Xyl.

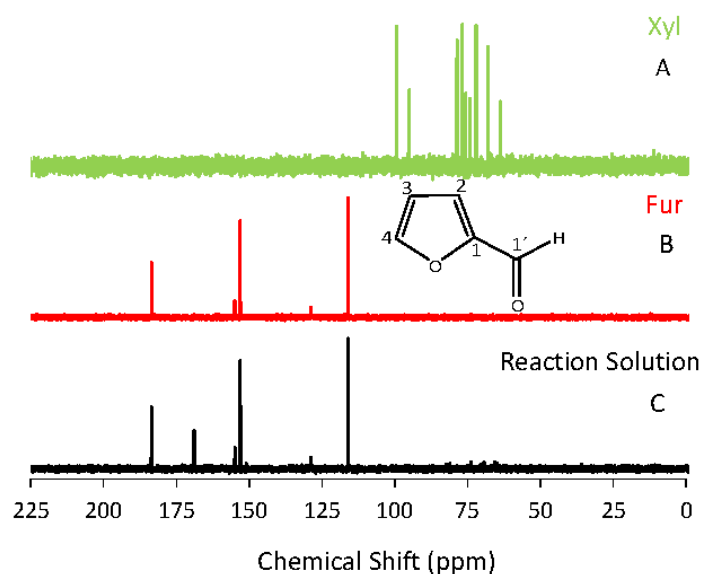


Figure 5.16- ^{13}C NMR spectrum of the reaction solution obtained after the reaction of D-xylose (Xyl) in the presence of BEA using D_2O as solvent (C). The spectra of D-xylose, Xyl (A) and 2-furaldehyde, Fur (B) are given for comparison. Reaction conditions: D_2O (1 cm^3), 8 h, $170\text{ }^\circ\text{C}$, $20\text{ g}_{\text{BEA}}\cdot\text{dm}^{-3}$, 0.67 M Xyl.

As expected, the ^1H NMR spectrum of the reaction mixture showed four characteristic peaks of Fur at 9.3 (H-1'), 7.8 (H-4), 7.4 (H-2) and 6.6 ppm (H-3) (Figure 5.15 C). In the ^{13}C NMR spectrum, the five characteristic peaks of Fur were 184 (C-1'), 157 (C-4), 155 (C-1), 128 (C-2) and 116 ppm (C-3). According to Antal et al.²⁴⁰ Fur is probably formed from the cyclic form of Xyl, and the open chain forms fragmentation products such as organic acids (e.g. lactic and formic) and glyceraldehyde. The ^1H NMR spectrum of lactic acid is characterised by the presence of a signal at 1.41 ± 0.1 ppm (as a doublet generated by the 3 protons of $-\text{CH}_3$ coupled to the proton $-\text{CH}$) and another at 4.37 ppm (as a quartet generated by the proton $-\text{CH}$ coupled to the 3 protons of $-\text{CH}_3$).²⁴²⁻²⁴⁵ In the ^1H NMR spectrum obtained herein (Figure 5.15) signals appear at 1.2 ppm and 4.2 ppm, which are more closely with those reported by Francisco et al.,²⁴⁶ who did not specify the pD ($\sim\text{pH}+0.41$) (1.25 ppm due to the doublet and 4.21 ppm due to the quartet). Although the quartet resonance of lactic acid arising from its α -proton is more sensitive to pD changes than the doublet arising from the methyl group protons,²⁴³ the possibility that the signal at 1.2 ppm (Figure 5.15) is due to lactic acid cannot be ruled out. Nevertheless, to be more certain, the pD of

the reaction solution could have been measured and compared against a spectrum of lactic acid obtained at the same pD.

The intense signals at 8.07 ppm in the ^1H NMR (Figure 5.15) and 168.9 ppm in the ^{13}C NMR (Figure 5.16) can be assigned to formic acid. This is in agreement with the literature.^{247,248} In sub/supercritical water conditions, organic acids may act as homogeneous catalysts in the reaction of Xyl.^{4,240,249} However it has been reported that even though formic acid and lactic acid are formed under sub/supercritical water conditions, they do not seem to play an important role in the decomposition of Fur because no noticeable changes in the Fur concentrations or solid deposition were observed an hour after the formic acid was detected.⁴

Xyl, which is essentially in the pyranose form in D_2O (Figure 5.15), was not detected in the catalytic reaction mixture, indicating that the C_{Xyl} was 100%, consistent with the kinetic data (Table 5.3).

Apart from the resonances due to Fur, formic acid and possibly lactic acid, the spectra of the reaction mixture still exhibit numerous weak to very weak signals in the range of 3.3-4.3 ppm (δ_{H}) and 65-85 ppm (δ_{C}), which are typical regions for carbohydrate H-C-O or $\text{H}_2\text{C-O}$ groups; weak peaks at $\delta_{\text{H}} < 2$ ppm may be assigned to methyl or methylene carbon atoms. These signals were probably due to fragmentation products of Xyl; however product identification was complicated by the overlapping of individual signals, especially in the ^1H NMR spectrum.

The presence of organic by-products was evident in the catalysts as the originally white colour of BEATUD-1 and BEA powders changed to brown during the catalytic reaction, and remained so after washing with toluene, methanol, ethanol and acetone. In a study of the reaction of Xyl in the presence of H-ZSM-5, O'Neill et al.⁴ concluded that H-ZSM-5 sample tested possessed relatively large pores of 1.2 nm. According to the authors this value does not represent the effective pore size of H-ZSM-5 but represents an estimate of the average pore size, reflecting the contribution of the external surface to the total surface (internal plus external). The high value of the pore size could possibly indicate the co-existence of two phases: one crystalline with microporous characteristics and the other with more open porosity.⁴ Consequently Fur (0.57 nm) would have a longer residence time in the pore structure, allowing Fur rearrangements to form oligomers (with possible furan-ring cleavage). These oligomers led to large molecules (coke) not able to diffuse easily in and out of the channels becoming entrapped in the porous structure, and causing pore blockage and passivation of the catalyst surface ("poisoning" of AS).⁴ Accordingly, Fur loss reactions can lead to the formation of bulky by-products. In the case of zeolite

nanocrystallites it is possible that coke was formed on the internal (strongly adsorbed and/or entrapped) and external surfaces (strongly adsorbed).

In order to get more insight into the nature of the carbonaceous matter (verified by DSC and TGA measurements discussed in detail in the Section 5.2.2.3 “Catalytic stability”), the used BEA catalyst was characterised by ^{13}C CP MAS NMR spectroscopy (Figure 5.17 C). The spectrum showed peaks characteristic of Fur at 113, 117-137, 151 and 178 ppm. Besides Fur it was noticeable the existence of other compounds by the presence of two very broad peaks centred at 33 and 208 ppm, and several relatively narrow and weak peaks in the region 60-80 ppm. The two broad peaks may correspond to saturated carbon-carbon bonds and aldehyde/ketone groups, respectively, while the narrow peaks may be due to fragments related to Xyl.

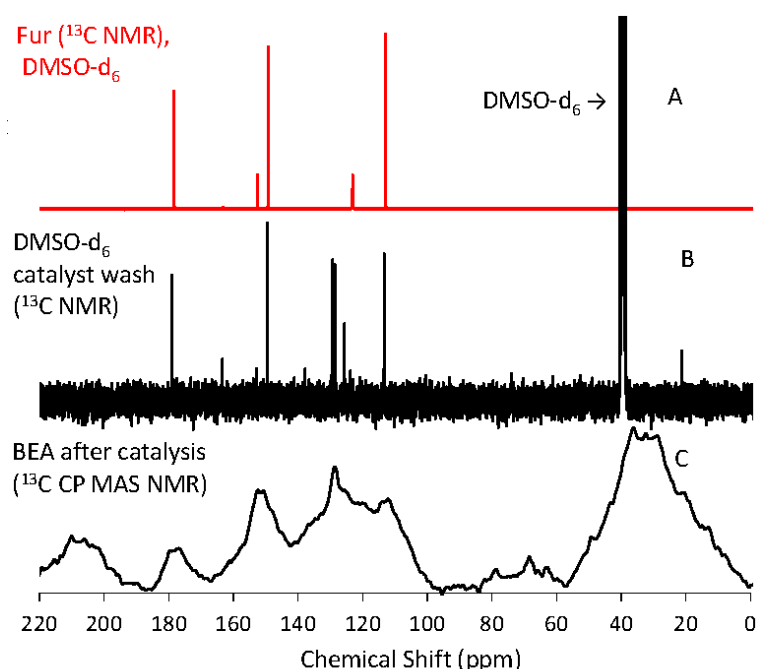


Figure 5.17- ^{13}C NMR spectrum of 2-furaldehyde (Fur) in DMSO-d_6 (A); ^{13}C NMR spectrum of the solution obtained after washing the used BEA with DMSO-d_6 (B); ^{13}C CP MAS NMR spectrum of BEA after catalysis using D_2O as solvent (C). Reaction conditions: D_2O (1 cm^3), 8 h, $170\text{ }^\circ\text{C}$, $20\text{ g}_{\text{BEA}}\cdot\text{dm}^{-3}$, 0.67 M Xyl.

Attempts were made to remove organic compounds from the used BEA by further washing the catalyst with DMSO-d_6 (giving DMSO-d_6 catalyst wash), obtaining the ^{13}C NMR spectrum of the resultant solution (Figure 5.17 B). A comparison with the liquid and solid ^{13}C NMR

spectra indicated that the compounds which gave rise to the peaks centred at 33, 60-80 and 208 ppm in the MAS NMR spectrum of used BEA were not removed by washing with DMSO- d_6 , and were therefore essentially insoluble products. The liquid-state ^{13}C NMR spectrum (DMSO- d_6 catalyst wash, Figure 5.17 B), exhibited the characteristic resonances of Fur (Figure 5.17 A) and extra lines at 21.4, 125.7, 128.6, 129.3 and 163.4 ppm. The signals between 125 and 130 ppm can be assigned to alkenyl groups (RCH=CHR), while the single line at 21.4 ppm can be assigned to a methyl or methylene carbon atom. These results were congruent with the appearance of several overlapping signals or multiplets in the region 7.1-7.3 ppm and a singlet at 2.30 ppm in the ^1H NMR spectrum of DMSO- d_6 catalyst wash (Figure 5.18).

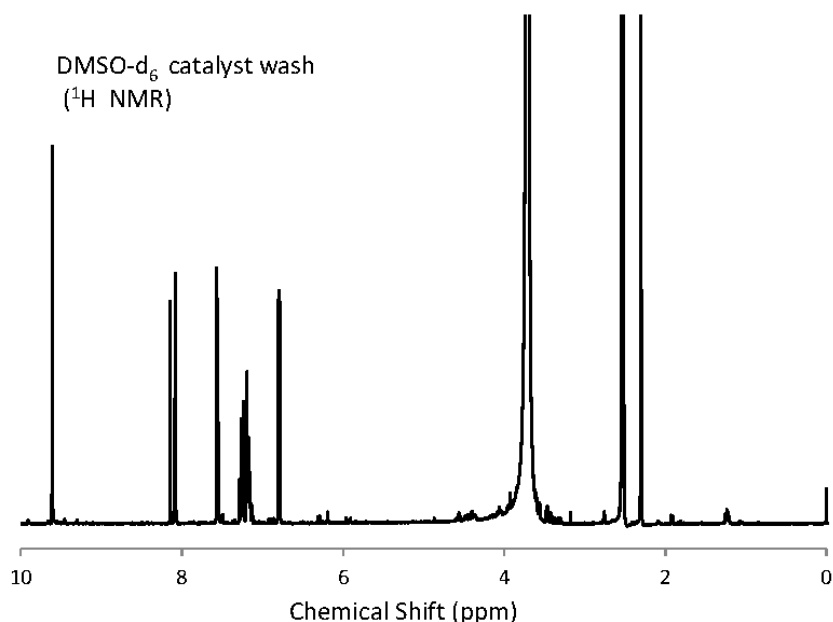


Figure 5.18- ^1H NMR spectrum of the solution obtained after washing the used BEA with DMSO- d_6 . Reaction conditions: D_2O (1 cm^3), 8 h, $170\text{ }^\circ\text{C}$, $20\text{ g}_{\text{BEA}}\cdot\text{dm}^{-3}$, 0.67 M Xyl .

More elaborate characterisation studies are needed to identify the product(s) responsible for these signals. Furthermore, the weak line that appears at 163.4 ppm in the ^{13}C NMR spectrum for the catalyst wash (Figure 5.17 B) and at 8.1 ppm in the ^1H NMR spectrum for the same sample (Figure 5.15) was assigned to a residual amount of formic acid. It was noteworthy that the resonances between 125 and 130 ppm (^{13}C NMR spectrum of DMSO- d_6 catalyst wash) matched with the fairly narrow peak at 128.5 ppm and the shoulder at 125.7 ppm in the ^{13}C CP MAS NMR spectrum of the used BEA (prior to washing with DMSO- d_6 , Figure 5.17 C).

The FT-IR spectra of the as-prepared and used BEA were quite similar (Figure 5.19) with the main difference being the appearance of a new band centred at ca. 1700 cm^{-1} which may be assigned to the aldehyde/ketone groups that gave rise to the broad signal at ca. 208 ppm in the ^{13}C CP MAS NMR spectrum of the recovered BEA (Figure 5.17 C). A very weak band at ca. 1470 cm^{-1} was also observed which may be due to Fur or related by-products. The failure to observe additional IR bands from by-products may be due to the overlap of these bands with the more intense bands of the aluminosilicate matrix, as well as to the low concentration and/or the amorphous and complex chemical nature of the by-products. The comparison of the FT-IR spectra of the as-prepared and used BEA suggested that the chemical nature of BEA was essentially preserved under the applied hydrothermal reaction conditions.

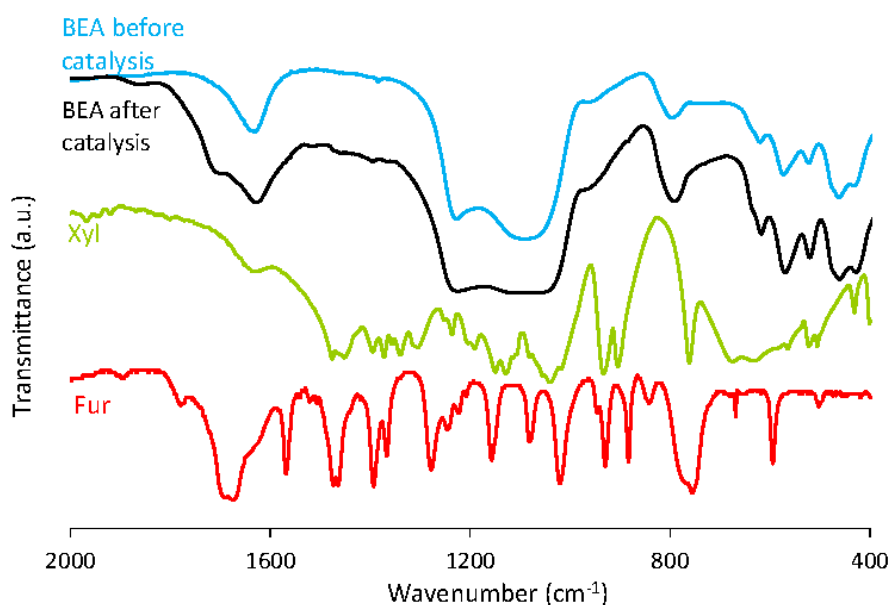


Figure 5.19- FT-IR spectra of BEA before and after reaction of D-xylose (Xyl) using D_2O as solvent. Reaction conditions: D_2O (1 cm^3), 8 h, $170\text{ }^\circ\text{C}$, $20\text{ g}_{\text{BEA}}\cdot\text{dm}^{-3}$, 0.67 M Xyl . The spectra of D-xylose (Xyl) and 2-furaldehyde (Fur) are given for comparison.

Overall, it seems that the carbonaceous matter contained aldehyde/ketone groups, fragments related to Xyl and (un)saturated carbon-carbon bonds, which were possible to extract with DMSO.

5.2.2.3. Catalyst stability

Thermal analyses (TGA, DSC) were performed under air for the solids recovered (washed and dried at 65 °C overnight) from the reaction in the presence of BEATUD-1, BEA1.0, BEA0.4 and BEA0.4/TUD0.6 after reaching ca. 98% C_{Xyl} . Figure 5.20 shows the DSC curves for BEATUD-1 and BEA. The presence of organic matter in the four samples was confirmed by DSC, which showed exothermic features above 200 °C (not observed for the as-prepared samples). An endothermic peak was detected below 200 °C, attributed to desorption of physisorbed water and volatiles.

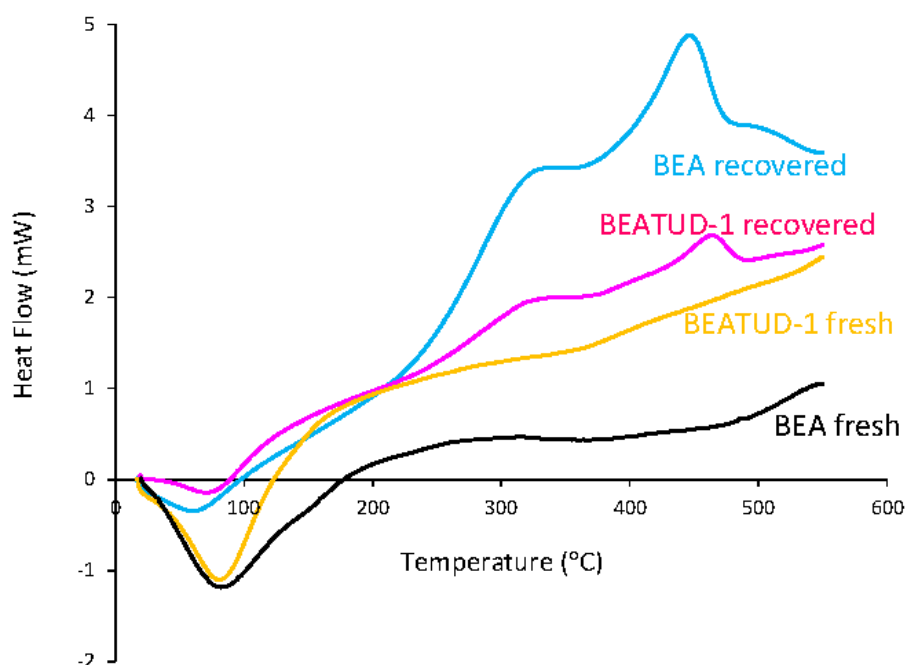


Figure 5.20- DSC curves for fresh BEA and BEATUD-1 and after 98% of D-xylose conversion (C_{Xyl}). Reaction conditions: 0.3 Wt:0.7 Tol (v/v) biphasic solvent system, 170 °C, 20 $g_{BEA} \cdot dm^{-3}$, 0.67 M Xyl.

The amount of carbonaceous matter of the samples recovered, washed and dried at 65 °C, was estimated from the TGA curves in the temperature range of 200-600 °C by calculating the weight loss in this range. No significant variation in mass was observed for the as-prepared materials, whereas for the recovered solids, these values gave 24, 31 and 15 wt.% for BEA0.4, BEA1.0 and BEATUD-1 solids, respectively. Hence, BEATUD-1 possessed the lowest amount of carbonaceous matter and gave the highest Y_{Fur} (74%) at high C_{Xyl} (98%).

To examine the reusability of BEA and BEATUD-1 catalysts, a total of four consecutive 6 h batch runs were carried out (details about the catalyst regeneration procedure applied after each batch run are described in the experimental part, Chapter 2). As shown in Figure 5.21, the conversion of Xyl and the yield of Fur at 6 h reaction remained fairly constant for the consecutive runs. The powder XRD patterns of the as-prepared and used catalysts were similar (Figure 5.4), as were the Si/Al ratios determined by ICP-AES (33 and 13 for recovered BEATUD-1 and BEA, respectively). These results suggested that BEA and BEATUD-1 were quite stable under the applied reaction conditions. The total Fur productions for the four runs were of 20 and 29 $\text{mmol}_{\text{Fur}} \cdot \text{g}_{\text{cat}}^{-1}$ for BEA and BEATUD-1, respectively (theoretical value, 100% $Y_{\text{Fur}} = 40 \text{ mmol}_{\text{Fur}} \cdot \text{g}_{\text{cat}}^{-1}$). When BEATUD-1 was recovered without applying the thermal treatment and reused in a second run, the yield of Fur_r at 6 h decreased by a factor of ca. 1.8, revealing the negative effect of coke on Fur production.

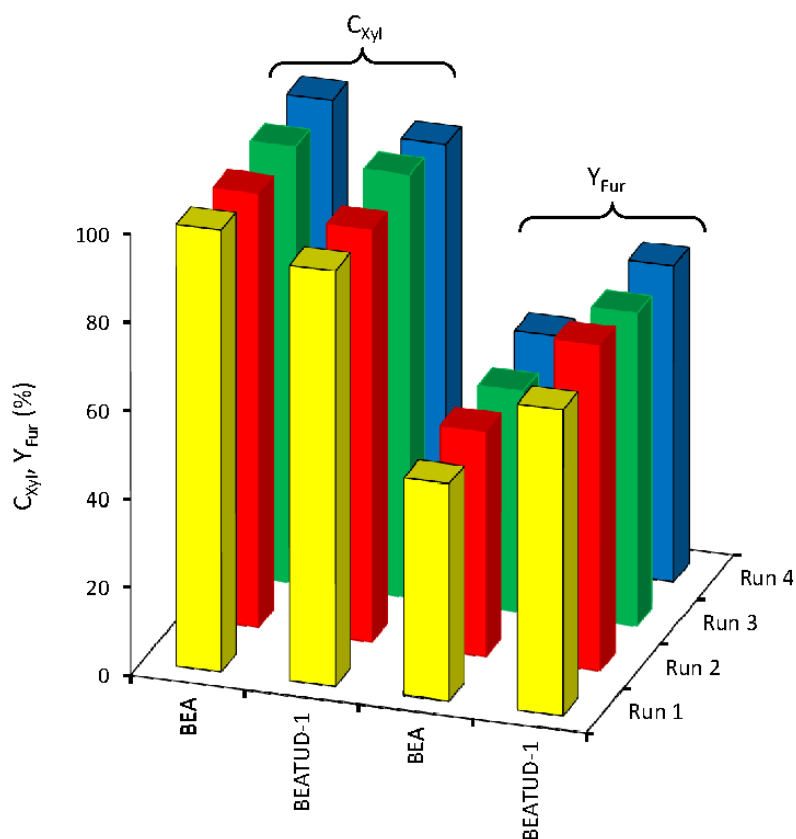


Figure 5.21- Catalytic performance of BEA and BEATUD-1 in four consecutive 6 h batch runs. Reaction conditions: 0.3 Wt:0.7 Tol (v/v) biphasic solvent system, 8 h, 170 °C, 20 $\text{g}_{\text{BEA}} \cdot \text{dm}^{-3}$, 0.67 M Xyl.

5.3. Conclusions

The composite BEATUD-1 consisting of commercial nanocrystalline zeolite BEA in the protonic form incorporated in a TUD-1 mesoporous matrix (denoted BEATUD-1) was an efficient catalyst for the acid catalysed conversion of Xyl into Fur, without the need for catalyst replacement during at least four runs (similar yields of Fur were reached). In comparison to the bulk nanocrystalline zeolite BEA, BEATUD-1 gave a lower reaction rate (on the same catalyst mass basis), which correlated with the lower total amount of AS ([L]+[B]) of BEATUD-1 in comparison to BEA. Initial reaction rate was ca. $9.3 \text{ mmol.g}_{\text{cat}}^{-1}.\text{h}^{-1}$ for BEA and $5.7 \text{ mmol.g}_{\text{cat}}^{-1}.\text{h}^{-1}$ for BEATUD-1 (on the basis of total amount of acid sites, the initial reaction rates were similar for the two catalysts, ca. $27 \text{ mol.mol}_{\text{L+B}}^{-1}.\text{h}^{-1}$).

The catalyst stability of BEA seemed as good as that for BEATUD-1. However, the yield of Fur at very high C_{Xyl} (98%) was higher for BEATUD-1 (74%) than for bulk BEA (54%) or the physical mixture consisting of BEA plus TUD-1 silica (60%). On the other hand, the amount of carbonaceous matter was lower for BEATUD-1 than for BEA. Based on solid- and liquid-state NMR studies it seemed that carbonaceous matter contained aldehyde/ketone groups, Xyl-related fragments and (un)saturated carbon-carbon bonds.

The improved performance of the composite BEATUD-1 may be due to favourable competitive adsorption effects caused by the surrounding silica matrix. Catalytic tests showed that the strong adsorption/entrapment of organic matter in the catalyst had a major negative effect on the catalytic performance, although this drawback can be successfully overcome by, for example, thermally regenerating the catalyst.

Further improvements in the catalytic performance for composites of the type BEATUD-1 may be possible by fine-tuning properties such as the Si/Al ratio, which can change the total amount of AS and catalyst surface polarity, and the zeolite loading, which may affect the dispersion and the number of accessible AS of the zeolite. Alternatively, the preparation of zeolite catalysts with significantly enhanced external specific surface area may allow improved catalytic performances. In this sense in the next Chapter it was studied the catalytic performance of the high external surface area ITQ-2, obtained by delamination of a layered precursor of zeolite MCM-22.

5.4. References

- (1) IZA-SC-members: Zeolite Framework Types. Database of Zeolite Structures, 2012; Vol. 2012.
- (2) Rinaldi, R.; Schuth, F.: Design of Solid Catalysts for the Conversion of Biomass. *Energy & Environmental Science* **2009**, *2*, 610-626.
- (3) Moreau, C.; Durand, R.; Peyron, D.; Duhamet, J.; Rivalier, P.: Selective Preparation of Furfural From Xylose Over Microporous Solid Acid Catalysts. *Industrial Crops and Products* **1998**, *7*, 95-99.
- (4) O'Neill, R.; Ahmad, M. N. M.; Vanoye, L.; Aiouache, F.: Kinetics of Aqueous Phase Dehydration of Xylose Into Furfural Catalyzed by ZSM-5 Zeolite. *Industrial & Engineering Chemistry Research* **2009**, *48*, 4300-4306.
- (5) Dias, A. S.; Lima, S.; Brandao, P.; Pillinger, M.; Rocha, J.; Valente, A. A.: Liquid-Phase Dehydration of D-xylose Over Microporous and Mesoporous Niobium Silicates. *Catalysis Letters* **2006**, *108*, 179-186.
- (6) Dias, A. S.; Lima, S.; Pillinger, M.; Valente, A. A.: Furfural and Furfural-Based Industrial Chemicals. In *Ideas in Chemistry and Molecular Sciences: Advances in Synthetic Chemistry*; Pignataro, B., Ed.; Wiley-VCH: Weinheim, Germany, 2010; pp 165-186.
- (7) Dias, A. S.; Lima, S.; Carriazo, D.; Rives, V.; Pillinger, M.; Valente, A. A.: Exfoliated Titanate, Niobate and Titanoniobate Nanosheets as Solid Acid Catalysts for the Liquid-Phase Dehydration of D-Xylose Into Furfural. *Journal of Catalysis* **2006**, *244*, 230-237.
- (8) Lima, S.; Pillinger, M.; Valente, A. A.: Dehydration of D-xylose Into Furfural Catalysed by Solid Acids Derived From the Layered Zeolite Nu-6(1). *Catalysis Communications* **2008**, *9*, 2144-2148.
- (9) Climent, M. J.; Corma, A.; Iborra, S.: Heterogeneous Catalysts for the One-Pot Synthesis of Chemicals and Fine Chemicals. *Chemical Reviews* **2011**, *111*, 1072-1133.
- (10) Corma, A.: Inorganic Solid Acids and Their Use in Acid-Catalyzed Hydrocarbons Reactions. *Chemical Reviews* **1995**, *95*, 559-614.
- (11) Price, G. L.: TU Chemical Engineering Zeolite Page. Price, G. L.: Price's Home Page, 2012; Vol. 2012.
- (12) Seader, J. D.; Henley, E. J.: *Separation Process Principles*; John Wiley & Sons Incorporation: New York, USA, 1998.
- (13) Illia, G. J. D. S.; Sanchez, C.; Lebeau, B.; Patarin, J.: Chemical Strategies to Design Textured Materials: From Microporous and Mesoporous Oxides to Nanonetworks and Hierarchical Structures. *Chemical Reviews* **2002**, *102*, 4093-4138.
- (14) Mansilla, H. D.; Baeza, J.; Urzua, S.; Maturana, G.; Villasenor, J.; Duran, N.: Acid-Catalysed Hydrolysis of Rice Hull: Evaluation of Furfural Production. *Bioresource Technology* **1998**, *66*, 189-193.
- (15) Waller, P.; Shan, Z. P.; Marchese, L.; Tartaglione, G.; Zhou, W. Z.; Jansen, J. C.; Maschmeyer, T.: Zeolite Nanocrystals Inside Mesoporous TUD-1: A High-Performance Catalytic Composite. *Chemistry-A European Journal* **2004**, *10*, 4970-4976.
- (16) Shan, Z.; Waller, P. W. G.; Maingary, B. G.; Anvegine, P. J.; Jansen, J. C.; Yeh, C. Y.; Maschmeyer, T.; Dautzenberg, F. M.; Marchese, L.; Pastore, H. d. O.: Zeolite Composite Method for Making and Catalytic Application Thereof. In *United States Patent: US 7,084,087 B2*; ABB Lummus Global Inc.: USA, 2006; pp 22.
- (17) Mavrodinova, V.; Popova, M.; Valchev, V.; Nickolov, R.; Minchev, C.: Beta Zeolite Colloidal Nanocrystals Supported on Mesoporous MCM-41. *Journal of Colloid and Interface Science* **2005**, *286*, 268-273.
- (18) Petkov, N.; Holzl, M.; Metzger, T. H.; Mintova, S.; Bein, T.: Ordered Micro/Mesoporous Composite Prepared as Thin Films. *Journal of Physical Chemistry B* **2005**, *109*, 4485-4491.
- (19) Oers, C. J. V.; Stevens, W. J. J.; Bruijn, E.; Mertens, M.; Lebedev, O. I.; Tendeloo, G. V.; Meynen, V.; Cool, P.: Formation of a Combined Micro- and Mesoporous Material Using Zeolite Beta Nanoparticles. *Microporous and Mesoporous Materials* **2009**, *120*, 29-34.

- (20) Xia, Y. D.; Mokaya, R.: On the Synthesis and Characterization of ZSM-5/MCM-48 Aluminosilicate Composite Materials. *Journal of Materials Chemistry* **2004**, *14*, 863-870.
- (21) Wang, J.; Groen, J. C.; Yue, W.; Zhou, W.; Coppens, M.-O.: Single-Template Synthesis of Zeolite ZSM-5 Composites With Tunable Mesoporosity. *Chemical Communications* **2007**, 4653-4655.
- (22) Wang, J.; Groen, J. C.; Yue, W.; Zhou, W.; Coppens, M.-O.: Facile Synthesis of ZSM-5 Composites With Hierarchical Porosity. *Journal of Materials Chemistry* **2008**, *18*, 468-474.
- (23) Wang, J.; Yue, W.; Zhou, W.; Coppens, M.-O.: TUD-C: A Tunable, Hierarchically Structured Mesoporous Zeolite Composite. *Microporous and Mesoporous Materials* **2009**, *120*, 19-28.
- (24) Xu, H.; Guan, J.; Wu, S.; Kan, Q.: Synthesis of Beta/MCM-41 Composite Molecular Sieve With High Hydrothermal Stability in Static and Stirred Condition. *Journal of Colloid and Interface Science* **2009**, *329*, 346-350.
- (25) Ribeiro, F. R.; Rodrigues, A. E.; Rollmann, L. D.; Naccache, C.: *Zeolites: Science and Technology*; Martinus Nijhoff Publishers: The Hague, The Netherlands, 1984; Vol. 80.
- (26) Wadlinger, R. L.; Kerr, G. T.; Township, L.; County, M.; Rosinski, E. K.: Catalytic Composition of a Crystalline Zeolite. In *United States Patent Office: 3,308,069*; Mobil Oil Corporation, a corporation of New York USA, 1967; pp 6.
- (27) Wadlinger, R. L.; Kerr, G. T.; Rosinski, E. K.: Catalytic Composition of a Crystalline Zeolite. In *United States Patent: Reissued 28,341*; Mobil Oil Corporation: USA, 1975; pp 7.
- (28) Newsam, J. M.; Treacy, M. M. J.; Koetsier, W. T.; Degruyter, C. B.: Structural Characterization of Zeolite Beta. *Proceedings of the Royal Society of London Series a-Mathematical Physical and Engineering Sciences* **1988**, *420*, 375-405.
- (29) Treacy, M. M. J.; Newsam, J. M.: 2 New 3 Dimensional 12-Ring Zeolite Frameworks of Which Zeolite Beta is a Disordered Intergrowth. *Nature* **1988**, *332*, 249-251.
- (30) Higgins, J. B.; Lapiere, R. B.; Schlenker, J. L.; Rohrman, A. C.; Wood, J. D.; Kerr, G. T.; Rohrbaugh, W. J.: The framework of Topology of Zeolite Beta. *Zeolites* **1988**, *8*, 446-452.
- (31) Lohse, U.; Altrichter, B.; Fricke, R.; Pilz, W.; Schreier, E.; Garkisch, C.; Jancke, K.: Synthesis of Zeolite Beta .2. Formation of Zeolite Beta and Titanium-Beta via an Intermediate Layer Structure. *Journal of the Chemical Society-Faraday Transactions* **1997**, *93*, 505-512.
- (32) Corma, A.; Moliner, M.; Cantin, A.; Diaz-Cabanas, M. J.; Lorda, J. L.; Zhang, D.; Sun, J.; Jansson, K.; Hovmoller, S.; Zou, X.: Synthesis and Structure of Polymorph B of Zeolite Beta. *Chemistry of Materials* **2008**, *20*, 3218-3223.
- (33) Corma, A.; Navarro, M. T.; Rey, F.; Rius, J.; Valencia, S.: Pure Polymorph C of Zeolite Beta Synthesized by Using Framework Isomorphous Substitution as a Structure-Directing Mechanism. *Angewandte Chemie-International Edition* **2001**, *40*, 2277-2280.
- (34) Liu, Z.; Ohsuna, T.; Terasaki, O.; Cambor, M. A.; Cabanas, M. J. D.; Hiraga, K.: The First Zeolite With Three-Dimensional Intersecting Straight-Channel System of 12-Membered Rings. *Journal of the American Chemical Society* **2001**, *123*, 5370-5371.
- (35) Wu, J.-S.; Chiang, A. S. T.; Tsai, T.-C.: Some Observations on the Synthesis of Colloidal Beta Zeolite from a Clear Precursor Sol. *Science of Advanced Materials* **2011**, *3*, 1011-1018.
- (36) Yuntong, N.: Synthesis of Fine Chemicals Over Zeolitic and Microporous/Mesoporous Materials. National University of Singapore, 2007.
- (37) Stevens, A. P.; Cox, P. A.: Postulated Mechanism for Faulting in Zeolite Beta. *Journal of the Chemical Society-Chemical Communications* **1995**, 343-345.
- (38) Marker, B.; Böhme, R.; Gies, H.: Superposition Structure of Zeolite Beta. In *Proceedings from the Ninth International Zeolite Conference*; Ballmoos, R. V. H., J. B.; Treacy, M. M. J., Ed.; Butterworth-Heinemann: Montreal, 1992; Vol. 2; pp 425.
- (39) Guisnet, M.; Gilson, J.-P.: *Zeolites for Cleaner Technologies*; Imperial College Press: London, UK, 2002; Vol. 3.
- (40) Jansen, J. C.; Shan, Z.; Marchese, L.; Zhou, W.; Puil, N. V. d.; Maschmeyer, T.: A New Templating Method For Three-Dimensional Mesopore Networks. *Chemical Communications* **2001**, 713-714.
- (41) Mintova, S.; Valtchev, V.; Onfroy, T.; Marichal, C.; Knözinger, H.; Bein, T.: Variation of the Si/Al Ratio in Nanosized Zeolite Beta Crystals. *Microporous and Mesoporous Materials* **2006**, *90*, 237-245.
- (42) Shah, A. K.; Khan, N.-u. H.; Sethia, G.; Saravanan, S.; Kureshy, R. I.; Abdi, S. H. R.; Bajaj, H. C.: Tin Exchanged Zeolite as Catalyst for Direct Synthesis of Alpha-Amino Nitriles Under Solvent-Free Conditions. *Applied Catalysis A-General* **2012**, *419*, 22-30.

- (43) Verboekend, D.; Vilé, G.; Ramírez, J. P.: Mesopore Formation in USY and Beta Zeolites by Base Leaching: Selection Criteria and Optimization of Pore-Directing Agents. *Crystal Growth & Design* **2012**, *12*, 3123-3132.
- (44) Esquivel, D.; Cruz-Cabeza, A. J.; Jimenez-Sanchidrian, C.; Romero-Salguero, F. J.: Enhanced Concentration of Medium Strength Bronsted Acid Sites in Aluminium-Modified beta Zeolite. *Catalysis Letters* **2012**, *142*, 112-117.
- (45) Shekara, B. M. C.; Prakash, B. S. J.; Bhat, Y. S.: Microwave-Induced Deactivation-Free Catalytic Activity of BEA Zeolite in Acylation Reactions. *Journal of Catalysis* **2012**, *290*, 101-107.
- (46) Rodríguez, M. T.; Arzaluz, M. G.; Alvarez, V. M.; Pliego, J. A.; Pergher, S.: Alkylation of Benzene with Propylene in a Flow-Through Membrane Reactor and Fixed-Bed Reactor: Preliminary Results. *Materials* **2012**, *5*, 872-881.
- (47) Duan, A.; Wan, G.; Zhang, Y.; Zhao, Z.; Jiang, G.; Liu, J.: Optimal Synthesis of Micro/Mesoporous Beta Zeolite from Kaolin Clay and Catalytic Performance for Hydrodesulfurization of Diesel. *Catalysis Today* **2011**, *175*, 485-493.
- (48) Cao, F.; Wu, Y.; Gu, J.; Wang, J.: Hydrothermal Synthesis of Nanocrystalline Zeolite Beta by Acid-Catalyzed Hydrolysis of Tetraethylorthosilicate. *Materials Chemistry and Physics* **2011**, *130*, 727-732.
- (49) Kamimura, Y.; Tanahashi, S.; Itabashi, K.; Sugawara, A.; Wakihara, T.; Shimojima, A.; Okubo, T.: Crystallization Behavior of Zeolite Beta in OSDA-Free, Seed-Assisted Synthesis. *Journal of Physical Chemistry C* **2011**, *115*, 744-750.
- (50) Fang, S.-Y.; Chiang, A. S. T.; Kao, H.-M.: Increasing the Productivity of Colloidal Zeolite Beta by Posthydrolysis Evaporation. *Industrial & Engineering Chemistry Research* **2010**, *49*, 12191-12196.
- (51) Liu, P.; Yao, Y.; Wang, J.: Using Beta-MCM41 Composite Molecular Sieves as Supports of Bifunctional Catalysts for the Hydroisomerization of n-Heptane. *Reaction Kinetics Mechanisms and Catalysis* **2010**, *101*, 465-475.
- (52) Kamimura, Y.; Chaikittisilp, W.; Itabashi, K.; Shimojima, A.; Okubo, T.: Critical Factors in the Seed-Assisted Synthesis of Zeolite Beta and "Green Beta" from OSDA-Free Na⁺-Aluminosilicate Gels. *Chemistry-An Asian Journal* **2010**, *5*, 2182-2191.
- (53) Qian, L.; Yue, B.; Pei, S.; Zhang, L.; Ye, L.; Cheng, J.; Tsang Shik, C.; He, H.: Reforming of CH₄ with CO₂ over Rh/H-Beta: Effect of Rhodium Dispersion on the Catalytic Activity and Coke Resistance. *Chinese Journal of Chemistry* **2010**, *28*, 1864-1870.
- (54) Wang, D.; Liu, Z.; Wang, H.; Xie, Z.; Tang, Y.: Shape-Controlled Synthesis of Monolithic ZSM-5 Zeolite With Hierarchical Structure and Mechanical Stability. *Microporous and Mesoporous Materials* **2010**, *132*, 428-434.
- (55) Selvin, R.; Roselin, L. S.; Kumar, K. P.; Arul, S.: Nanocrystalline Zeolite Beta: An Efficient Catalyst for the Regioselective Alcoholysis of Epichlorohydrin. *Science of Advanced Materials* **2010**, *2*, 190-194.
- (56) Liu, S.-P.; Chen, L.; Wang, Y. M.: The Synthesis of Mesoporous Zeolite Beta Aggregates Without the Use of Second Template and Additive. *Solid State Sciences* **2010**, *12*, 1070-1075.
- (57) Jin, C.; Zhang, Y.; Gao, W.; Cui, L.: Anionic Emulsion-Mediated Synthesis of Zeolite Beta. *International Journal of Modern Physics B* **2010**, *24*, 3236-3241.
- (58) Liu, P.; Zhang, X.; Yao, Y.; Wang, J.: Alkaline Earth Metal Ion-Exchanged Beta Zeolite Supported Pt Catalysts for Hydroisomerization of n-Heptane. *Reaction Kinetics Mechanisms and Catalysis* **2010**, *100*, 217-226.
- (59) Toktarev, A. V.; Malysheva, L. V.; Paukshtis, E. A.: Effect of Thermal Treatment Conditions on the Acid Properties of Zeolite Beta. *Kinetics and Catalysis* **2010**, *51*, 318-324.
- (60) Parker, W. O., Jr.; Angelis, A. d.; Flego, C.; Millini, R.; Perego, C.; Zanardi, S.: Unexpected Destructive Dealumination of Zeolite Beta by Silylation. *Journal of Physical Chemistry C* **2010**, *114*, 8459-8468.
- (61) Dzwigaj, S.; Millot, Y.; Methivier, C.; Che, M.: Incorporation of Nb(V) into BEA Zeolite Investigated by XRD, NMR, IR, DR UV-vis, and XPS. *Microporous and Mesoporous Materials* **2010**, *130*, 162-166.
- (62) Kuechl, D. E.; Benin, A. I.; Knight, L. M.; Abrevaya, H.; Wilson, S. T.; Sinkler, W.; Mezza, T. M.; Willis, R. R.: Multiple Paths to Nanocrystalline High Silica Beta Zeolite. *Microporous and Mesoporous Materials* **2010**, *127*, 104-118.

- (63) Wang, Y.; Jiang, Z.; Li, H.; Yang, D.: Chitosan Membranes Filled by GPTMS-Modified Zeolite Beta Particles With Low Methanol Permeability for DMFC. *Chemical Engineering and Processing* **2010**, *49*, 278-285.
- (64) Wan, G.; Duan, A.; Zhang, Y.; Zhao, Z.; Jiang, G.; Zhang, D.; Gao, Z.: Zeolite Beta Synthesized With Acid-Treated Metakaolin and its Application in Diesel Hydrodesulfurization. *Catalysis Today* **2010**, *149*, 69-75.
- (65) Merg, J. C.; Rossett, F.; Penha, F. G.; Pergher, S. B. C.; Petkowicz, D. I.; dos Santos, H. Z.: Titanium Oxide Incorporation on Zeolites For Heterogeneous Photocatalysis. *Química Nova* **2010**, *33*, 1525-1528.
- (66) Modhera, B.; Chakraborty, M.; Bajaj, H. C.; Parikh, P. A.: Simultaneous n-Hexane Isomerization and Benzene Saturation Over Pt/Nano-Crystalline Zeolite Beta. *Reaction Kinetics Mechanisms and Catalysis* **2010**, *99*, 421-429.
- (67) Dragoi, B.; Rakic, V.; Dumitriu, E.; Auroux, A.: Adsorption of Organic Pollutants Over Microporous Solids Investigated by Microcalorimetry Techniques. *Journal of Thermal Analysis and Calorimetry* **2010**, *99*, 733-740.
- (68) Liu, P.; Zhang, X.; Yao, Y.; Wang, J.: Pt catalysts Supported on Beta Zeolite Ion-Exchanged With Cr(III) for Hydroisomerization of n-Heptane. *Applied Catalysis A-General* **2009**, *371*, 142-147.
- (69) Parmentier, J.; Valtchev, V.; Gaslain, F.; Tosheva, L.; Ducrot-Boisgontier, C.; Möller, J.; Patarin, J.; Vix-Guterl, C.: Effect of the Zeolite Crystal Size on the Structure and Properties of Carbon Replicas Made by a Nanocasting Process. *Carbon* **2009**, *47*, 1066-1073.
- (70) Zhang, Q.; Xia, Q. H.; Lu, X. H.; Ma, X. T.; Su, K. X.: Gas-Phase Catalytic Synthesis of MTBE From MeOH and (Bu^tOH) Over Various Microporous H-Zeolites. *Indian Journal of Chemistry Section a-Inorganic Bio-Inorganic Physical Theoretical & Analytical Chemistry* **2009**, *48*, 788-792.
- (71) Hou, Q.; Zheng, B.; Bi, C.; Luan, J.; Zhao, Z.; Guo, H.; Wang, G.; Li, Z.: Liquid-Phase Cascade Acylation/Dehydration Over Various Zeolite Catalysts to Synthesize 2-Methylantraquinone Through an Efficient One-Pot Strategy. *Journal of Catalysis* **2009**, *268*, 376-383.
- (72) Lee, F. Y.; Lv, L.; Su, F.; Liu, T.; Liu, Y.; Sow, C. H.; Zhao, X. S.: Incorporation of Titanium into Polymorph C for Catalytic Epoxidation of Cyclohexene. *Microporous and Mesoporous Materials* **2009**, *124*, 36-41.
- (73) Hadjiivanov, K.; Penkova, A.; Kefirov, R.; Dzwigaj, S.; Che, M.: Influence of Dealumination and Treatments on the Chromium Speciation in Zeolite CrBEA. *Microporous and Mesoporous Materials* **2009**, *124*, 59-69.
- (74) Xu, X.; Zhao, X.; Sun, L.; Liu, X.: Adsorption Separation of Carbon Dioxide, Methane and Nitrogen on Monoethanol Amine Modified Beta-Zeolite. *Journal of Natural Gas Chemistry* **2009**, *18*, 167-172.
- (75) Liu, P.; Wang, J.; Zhang, X.; Wei, R.; Ren, X.: Catalytic Performances of Dealuminated H-Beta Zeolite Supported Pt Catalysts Doped With Cr in Hydroisomerization of n-Heptane. *Chemical Engineering Journal* **2009**, *148*, 184-190.
- (76) Jakob, A.; Valtchev, V.; Soulard, M.; Faye, D.: Syntheses of Zeolite Beta Films in Fluoride Media and Investigation of Their Sorption Properties. *Langmuir* **2009**, *25*, 3549-3555.
- (77) Modhera, B.; Chakraborty, M.; Parikh, P. A.; Jasra, R. V.: Synthesis of Nano-Crystalline Zeolite Beta: Effects of Crystallization Parameters. *Crystal Research and Technology* **2009**, *44*, 379-385.
- (78) Mahalakshmi, M.; Priya, S. V.; Arabindoo, B.; Palanicharnly, M.; Murugesan, V.: Photocatalytic Degradation of Aqueous Propoxur Solution Using TiO₂ and H-Beta Zeolite-Supported TiO₂. *Journal of Hazardous Materials* **2009**, *161*, 336-343.
- (79) Li, H.; Li, M.; Chu, Y.; Nie, H.: Influence of Different Modified Beta Zeolite on Skeletal Isomerization of n-Hexene in the Presence of Hydrogen. *Microporous and Mesoporous Materials* **2009**, *117*, 635-639.
- (80) Dzwigaj, S.; Janas, J.; Gurgul, J.; Socha, R. P.; Shishido, T.; Che, M.: Do Cu(II) Ions Need Al Atoms in Their Environment to Make CuSiBEA Active in the SCR of NO by Ethanol or Propane? A spectroscopy and Catalysis Study. *Applied Catalysis B-Environmental* **2009**, *85*, 131-138.
- (81) Huang, Z.; Su, J.-F.; Guo, Y.-H.; Su, X.-Q.; Teng, L.-J.: Synthesis of Well-Crystallized Zeolite Beta at Large Scale and its Synthesis of Well-Crystallized Zeolite Beta at Large Scale and its Incorporation into Polysulfone Matrix for Gas Separation. *Chemical Engineering Communications* **2009**, *196*, 969-986.

- (82) Shen, B.; Wang, P.; Yi, Z.; Zhang, W.; Tong, X.; Liu, Y.; Guo, Q.; Gao, J.; Xu, C.: Synthesis of Zeolite Beta from Kaolin and Its Catalytic Performance For FCC Naphtha Aromatization. *Energy & Fuels* **2009**, *23*, 60-64.
- (83) Maheswari, R.; Pachamuthu, M. P.; Anand, R.: Copper Containing TUD-1: Synthesis, Characterization and Catalytic Behavior in Liquid-Phase Oxidation of Ethylbenzene. *J Porous Mater* **2012**, *19*, 103-110.
- (84) Hajjar, R.; Millot, Y.; Man, P. P.; Che, M.; Dzwigaj, S.: Two Kinds of Framework Al Sites Studied in BEA Zeolite by X-ray Diffraction, Fourier Transform Infrared Spectroscopy, NMR Techniques, and V Probe. *Journal of Physical Chemistry C* **2008**, *112*, 20167-20175.
- (85) Viswanadham, N.; Kamble, R.; Saxena, S. K.; Garg, M. O.: Studies on Octane Boosting of Industrial Feedstocks on Pt/H-BEA Zeolite. *Fuel* **2008**, *87*, 2394-2400.
- (86) Li, Y.; Chung, T.-S.: Exploratory Development of Dual-Layer Carbon-Zeolite Nanocomposite Hollow Fiber Membranes With High Performance for Oxygen Enrichment and Natural Gas Separation. *Microporous and Mesoporous Materials* **2008**, *113*, 315-324.
- (87) Li, X.; Zhang, W.; Liu, S.; Xu, L.; Han, X.; Bao, X.: Olefin Metathesis over Heterogeneous Catalysts: Interfacial Interaction Between Mo Species and a H-Beta-Al₂O₃ composite support. *Journal of Physical Chemistry C* **2008**, *112*, 5955-5960.
- (88) Pacula, A.; Mokaya, R.: Synthesis and High Hydrogen Storage Capacity of Zeolite-Like Carbons Nanocast Using as-Synthesized Zeolite Templates. *Journal of Physical Chemistry C* **2008**, *112*, 2764-2769.
- (89) Zhang, Y.; Wang, Y.; Bu, Y.: Vapor Phase Beckmann Rearrangement of Cyclohexanone Oxime on H-Beta Zeolites Treated by Ammonia. *Microporous and Mesoporous Materials* **2008**, *107*, 247-251.
- (90) Zhang, X.; Zhong, J.; Wang, J.; Gao, J.; Liu, A.: Trimerization of Butene over Ni-doped Zeolite Catalyst: Effect of Textural and Acidic Properties. *Catalysis Letters* **2008**, *126*, 388-395.
- (91) Aguadoa, J.; Serrano, D. P.; Rodriguez, J. M.: Zeolite Beta With Hierarchical Porosity Prepared From Organofunctionalized Seeds. *Microporous and Mesoporous Materials* **2008**, *115*, 504-513.
- (92) Ordonsky, V. V.; Murzin, V. Y.; Monakhova, Y. V.; Zubavichus, Y. V.; Knyazeva, E. E.; Nesterenko, N. S.; Ivanova, I. I.: Oaturation, Strength and Accessibility of Acid Sites in Micro/Mesoporous Catalysts Obtained by Recrystallization of Zeolite BEA. *Microporous and Mesoporous Materials* **2007**, *105*, 101-110.
- (93) Ding, L.; Zheng, Y.; Hong, Y.; Ring, Z.: Effect of Particle Size on the Hydrothermal Stability of Zeolite Beta. *Microporous and Mesoporous Materials* **2007**, *101*, 432-439.
- (94) Tosheva, L.; Valtchev, V. P.; Mihailova, B.; Doyle, A. M.: Zeolite Beta Films Prepared Via the Langmuir-Blodgett Technique. *Journal of Physical Chemistry C* **2007**, *111*, 12052-12057.
- (95) Li, X.; Zhang, W.; Liu, S.; Xu, L.; Han, X.; Bao, X.: The Role of Alumina in the Supported Mo/HBeta-Al₂O₃ Catalyst for Olefin Metathesis: A high-Resolution Solid-State NMR and Electron Microscopy Study. *Journal of Catalysis* **2007**, *250*, 55-66.
- (96) Penkova, A.; Dzwigaj, S.; Kefirov, R.; Hadjiivanov, K.; Che, M.: Effect of the Preparation Method on the State of Nickel Ions in BEA Zeolites. A study by Fourier Transform Infrared Spectroscopy of Adsorbed CO and NO, Temperature-Programmed Reduction, and X-ray Diffraction. *Journal of Physical Chemistry C* **2007**, *111*, 8623-8631.
- (97) Zarama, M. C. P.; Rios, J. S. V.; Alba, M. D.; Castro, M. A.: Contribution to the Hydrothermal Synthesis of Zeolite Beta and its Modifications with Gallium. *J Porous Mater* **2007**, *14*, 239-242.
- (98) Sun, J.; Zhu, G.; Chen, Y.; Li, J.; Wang, L.; Peng, Y.; Li, H.; Qiu, S.: Synthesis, Surface and Crystal Structure Investigation of the Large Zeolite Beta Crystal. *Microporous and Mesoporous Materials* **2007**, *102*, 242-248.
- (99) Kadgaonkar, M. D.; Kasture, M. W.; Bhange, D. S.; Joshi, P. N.; Ramaswamy, V.; Kumar, R.: NCL-7, A Novel All Silica Analog of Polymorph B Rich Member of BEA Family: Synthesis and Characterization. *Microporous and Mesoporous Materials* **2007**, *101*, 108-114.
- (100) Yang, Z.; Xia, Y.; Mokaya, R.: Enhanced Hydrogen Storage Capacity of High Surface Area Zeolite-Like Carbon Materials. *Journal of the American Chemical Society* **2007**, *129*, 1673-1679.
- (101) Bregolato, M.; Bolis, V.; Busco, C.; Ugliengo, P.; Bordiga, S.; Cavani, F.; Ballarini, N.; Maselli, L.; Passeri, S.; Rossetti, I.; Forni, L.: Methylation of Phenol Over High-Silica Beta Zeolite: Effect of Zeolite Acidity and Crystal Size on Catalyst Behaviour. *Journal of Catalysis* **2007**, *245*, 285-300.

- (102) Mihalyi, R. M.; Pal-Borbely, G.; Beyer, H. K.; Szegedi, A.; Koranyi, T. I.: Characterization of Aluminum and Boron Containing Beta Zeolites Prepared By Solid-State Recrystallization of Magadlite. *Microporous and Mesoporous Materials* **2007**, *98*, 132-142.
- (103) Kang, S.; Gong, Y.; Dou, T.; Zhang, Y.; Zheng, Y.: Preparation and Characterization of Zeolite Beta With Low SiO₂/Al₂O₃ ratio. *Petroleum Science* **2007**, *4*, 70-74.
- (104) Malki, E.-M. E.; Massiani, P.; Che, M.: Introduction of Vanadium Species in Beta Zeolite by Solid-State Reaction: Spectroscopic Study of V Speciation and Molecular Mechanism. *Research on Chemical Intermediates* **2007**, *33*, 749-774.
- (105) Agullo, J.; Kumar, N.; Berenguer, D.; Kubicka, D.; Marcilla, A.; Gomez, A.; Salmi, T.; Murzin, D. Y.: Catalytic Pyrolysis of Low Density Polyethylene Over H-Beta, H-Y, H-Mordenite, and H-Ferrierite Zeolite Catalysts: Influence of Acidity and Structures. *Kinetics and Catalysis* **2007**, *48*, 535-540.
- (106) Kumaran, G. M.; Garg, S.; Soni, K.; Prasad, V. V. D. N.; Sharma, L. D.; Dhar, G. M.: Catalytic Functionalities of H-Beta Zeolite-Supported Molybdenum Hydrotreating Catalysts. *Energy & Fuels* **2006**, *20*, 1784-1790.
- (107) Ding, L.; Zheng, Y.; Zhang, Z.; Ring, Z.; Chen, J.: Effect of Agitation on the Synthesis of Zeolite Beta and its Synthesis Mechanism in Absence of Alkali Cations. *Microporous and Mesoporous Materials* **2006**, *94*, 1-8.
- (108) Anandan, S.; Vinu, A.; Venkatachalam, N.; Arabindoo, B.; Murugesan, V.: Photocatalytic Activity of ZnO Impregnated H-Beta and Mechanical Mix of ZnO/H-Beta in the Degradation of Monocrotophos in Aqueous Solution. *Journal of Molecular Catalysis A-Chemical* **2006**, *256*, 312-320.
- (109) Bordoloi, A.; Devassy, B. M.; Niphadkar, P. S.; Joshi, P. N.; Halligudi, S. B.: Shape Selective Synthesis of Long-Chain Linear Alkyl Benzene (LAB) With Al-MCM-41/Beta Zeolite Composite Catalyst. *Journal of Molecular Catalysis A-Chemical* **2006**, *253*, 239-244.
- (110) Dzwigaj, S.; Che, M.: Incorporation of Co(II) in Dealuminated BEA Zeolite at Lattice Tetrahedral Sites Evidenced by XRD, FTIR, Diffuse Reflectance UV-vis, EPR, and TPR. *Journal of Physical Chemistry B* **2006**, *110*, 12490-12493.
- (111) Fojtíková, P. P.; Mintova, S.; Čejka, J.; Žilková, N.; Zukal, A.: Porosity of micro/mesoporous composites. *Microporous and Mesoporous Materials* **2006**, *92*, 154-160.
- (112) Li, X. J.; Zhang, W. P.; Liu, S. L.; Han, X. W.; Xu, L. Y.; Bao, X. H.: A High-Resolution MAS NMR Study on the Potential Catalysts Mo/H-Beta for Olefin Metathesis: The Interaction of Mo Species With H-Beta Zeolite. *Journal of Molecular Catalysis A-Chemical* **2006**, *250*, 94-99.
- (113) Saravanamurugan, S.; Palanichamy, M.; Hartmann, M.; Murugesan, V.: Knoevenagel Condensation Over Beta and Y Zeolites in Liquid Phase Under Solvent Free Conditions. *Applied Catalysis A-General* **2006**, *298*, 8-15.
- (114) Narasimharao, K.; Hartmann, M.; Thiel, H. H.; Ernst, S.: Novel Solid Basic Catalysts by Nitridation of Zeolite Beta at Low Temperature. *Microporous and Mesoporous Materials* **2006**, *90*, 377-383.
- (115) Tosheva, L.; Hözl, M.; Metzger, T. H.; Valtchev, V.; Mintova, S.; Bein, T.: Zeolite Beta films Synthesized From Basic and Near-Neutral Precursor Solutions and Gels. *Materials Science & Engineering C-Biomimetic and Supramolecular Systems* **2005**, *25*, 570-576.
- (116) Panpranot, J.; Toophorm, U.; Praserttham, P.: Effect of Particle Size on the Hydrothermal Stability and Catalytic Activity of Polycrystalline Beta Zeolite. *J Porous Mater* **2005**, *12*, 293-299.
- (117) Pergher, S. B. C.; Oliveira, L. C. A.; Smaniotto, A.; Petkowicz, D. I.: Magnetic Zeolites for Removal of Metals in Water. *Química Nova* **2005**, *28*, 751-755.
- (118) Zheng, Y.; Wang, X. X.; Li, Z. H.; Fu, X. Z.; Wei, K. M.: Study of the Reaction of Tetramethyltin With H-Beta Zeolite. *Journal of Organometallic Chemistry* **2005**, *690*, 3187-3192.
- (119) Naydenov, V.; Tosheva, L.; Sterte, J.: Self-Bonded Zeolite Beta/MCM-41 Composite Spheres. *J Porous Mater* **2005**, *12*, 193-199.
- (120) Holmberg, B. A.; Hwang, S. J.; Davis, M. E.; Yan, Y. S.: Synthesis and Proton Conductivity of Sulfonic Acid Functionalized Zeolite BEA Nanocrystals. *Microporous and Mesoporous Materials* **2005**, *80*, 347-356.
- (121) Zhang, Y. J.; Wang, Y. Q.; Bu, Y. F.; Mi, Z. T.; Wu, W.; Min, E.; Han, S.; Fu, S. B.: Beckmann Rearrangement of Cyclohexanone Oxime Over H-Beta Zeolite and H-Beta Zeolite-Supported Boride. *Catalysis Communications* **2005**, *6*, 53-56.

- (122) Markus, H.; Arvela, P. M.; Kumar, N.; Heikkilä, T.; Lehto, V. P.; Sjöholm, R.; Holmbom, B.; Salmi, T.; Murzin, D. Y.: Reactions of Hydroxymatairesinol Over Supported Palladium Catalysts. *Journal of Catalysis* **2006**, *238*, 301-308.
- (123) Kasture, M. W.; Niphadkar, P. S.; Sharanappa, N.; Mirajkar, S. R.; Bokade, V. V.; Joshi, P. N.: Isopropylation of Benzene Catalyzed by H-Beta Zeolite Catalysts With Different Crystallinities. *Journal of Catalysis* **2004**, *227*, 375-383.
- (124) Gautier, B.; Smaïhi, M.: Template Extraction From Surface Functionalised Zeolite Beta Nanoparticles. *New Journal of Chemistry* **2004**, *28*, 457-461.
- (125) Adebajo, M. O.; Long, M. A.; Frost, R. L.: Spectroscopic and XRD Characterisation of Zeolite Catalysts Aactive for the Oxidative Methylation of Benzene With Methane. *Spectrochimica Acta Part a-Molecular and Biomolecular Spectroscopy* **2004**, *60*, 791-799.
- (126) Nakao, R.; Kubota, Y.; Katada, N.; Nishiyama, N.; Kunimori, K.; Tomishige, K.: Performance and Characterization of BEA Catalysts for Catalytic Cracking. *Applied Catalysis A-General* **2004**, *273*, 63-73.
- (127) Omegna, A.; Vasic, M.; Bokhoven, J. A. v.; Pirngruber, G.; Prins, R.: Dealumination and Realumination of Microcrystalline Zeolite Beta: an XRD, FTIR and Quantitative Multinuclear (MQ) MAS NMR Study. *Physical Chemistry Chemical Physics* **2004**, *6*, 447-452.
- (128) Prokešová, P.; Mintova, S.; Čejka, J.; Bein, T.: Preparation of Nanosized Micro/Mesoporous Composites. *Materials Science & Engineering C-Biomimetic and Supramolecular Systems* **2003**, *23*, 1001-1005.
- (129) Oliveira, A. M. d.; Pergher, S. B. C.; Moro, C. C.; Baibich, I. M.: Nitric Oxide Decomposition on Copper Supported on Zeolites. *Química Nova* **2004**, *27*, 226-230.
- (130) Prokešová, P.; Mintova, S.; Čejka, J.; Bein, T.: Preparation of Nanosized Micro/Mesoporous Composites via Simultaneous Synthesis of Beta/MCM-48 Phases. *Microporous and Mesoporous Materials* **2003**, *64*, 165-174.
- (131) Xia, Q. H.; Shen, S. C.; Song, J.; Kawi, S.; Hidajat, K.: Structure, Morphology, and Catalytic Activity of Beta Zeolite Synthesized in a Fluoride Medium for Asymmetric Hydrogenation. *Journal of Catalysis* **2003**, *219*, 74-84.
- (132) Oumi, Y.; Nemoto, S.; Nawata, S.; Fukushima, T.; Teranishi, T.; Sano, T.: Effect of the Framework Structure on the Dealumination-Realumination Behavior of Zeolite. *Materials Chemistry and Physics* **2002**, *78*, 551-557.
- (133) Nares, R.; Ramirez, J.; Alejandre, A. G.; Louis, C.; Klimova, T.: Ni/H-Beta Zeolite Catalysts Prepared by Deposition-Precipitation. *Journal of Physical Chemistry B* **2002**, *106*, 13287-13293.
- (134) Shi, Y. F.; Gao, Y.; Yuan, W. K.: Some Characterization of Beta Zeolite for Alkylation of Benzene in Near Critical. *Catalysis Today* **2002**, *74*, 91-100.
- (135) Assabumrungrat, S.; Kiatkittipong, W.; Seviton, N.; Praserttham, P.; Goto, S.: Kinetics of Liquid Phase Synthesis of Ethyl tert-Butyl Ether from tert-Butyl Alcohol and Ethanol Catalyzed by Beta Zeolite Supported on Monolith. *International Journal of Chemical Kinetics* **2002**, *34*, 292-299.
- (136) Roberge, D. M.; Hausmann, H.; Holderich, W. F.: Dealumination of Zeolite Beta by Acid Leaching: A New Insight With Two-Dimensional Multi-Quantum and Cross Polarization ²⁷Al MAS NMR. *Physical Chemistry Chemical Physics* **2002**, *4*, 3128-3135.
- (137) Naydenov, V.; Tosheva, L.; Sterte, J.: Palladium-Containing Zeolite Beta Macrostructures Prepared by Resin Macrottemplating. *Chemistry of Materials* **2002**, *14*, 4881-4885.
- (138) Oumi, Y.; Mizuno, R.; Azuma, K.; Nawata, S.; Fukushima, T.; Uozumi, T.; Sano, T.: Reversibility of Dealumination-Realumination Process of BEA Zeolite. *Microporous and Mesoporous Materials* **2001**, *49*, 103-109.
- (139) Schoeman, B. J.; Babouchkina, E.; Mintova, S.; Valtchev, V. P.; Sterte, J.: The Synthesis of Discrete Colloidal Crystals of Zeolite Beta and Their Application in the Preparation of Thin Microporous Films. *J Porous Mater* **2001**, *8*, 13-22.
- (140) Tosheva, L.; Mihailova, B.; Valtchev, V.; Sterte, J.: Zeolite Beta Spheres. *Microporous and Mesoporous Materials* **2001**, *48*, 31-37.
- (141) Dzwigaj, S.; Massiani, P.; Davidson, A.; Che, M.: Role of Silanol Groups in the Incorporation of V in Beta Zeolite. *Journal of Molecular Catalysis A-Chemical* **2000**, *155*, 169-182.
- (142) Yang, C.; Xu, Q. H.; Hu, C.: Boronation and Galliation of Zeolites Beta in an Alkaline Medium. *Materials Chemistry and Physics* **2000**, *63*, 55-66.

- (143) Schmidt, I.; Madsen, C.; Jacobsen, C. J. H.: Confined Space synthesis. A Novel Route to Nanosized Zeolites. *Inorganic Chemistry* **2000**, *39*, 2279-2283.
- (144) Ramirez, S.; Dominguez, J. M.; Viniegra, M.; Menorval, L. C. d.: Specific Behavior of Beta Zeolites Upon the Modification of the Surface Acidity by Cs and Li Exchange. *New Journal of Chemistry* **2000**, *24*, 99-104.
- (145) Trombetta, M.; Busca, G.; Storaro, L.; Lenarda, M.; Casagrande, M.; Zambon, A.: Surface Acidity Modifications Induced by Thermal Treatments and Acid Leaching on Microcrystalline H-BEA Zeolite. A FTIR, XRD and MAS-NMR Study. *Physical Chemistry Chemical Physics* **2000**, *2*, 3529-3537.
- (146) Rakshe, B.; Ramaswamy, V.; Ramaswamy, A. V.: Acidity and m-Xylene Isomerization Activity of Large Pore, Zirconium Containing Alumino-Silicate With BEA Structure. *Journal of Catalysis* **1999**, *188*, 252-260.
- (147) Cambor, M. A.; Corma, A.; Valencia, S.: Characterization of Nanocrystalline Zeolite Beta. *Microporous and Mesoporous Materials* **1998**, *25*, 59-74.
- (148) Jia, C. J.; Beaunier, P.; Massiani, P.: Comparison of Conventional and Solid-State Ion Exchange Procedures for the Incorporation of Lanthanum in H-Beta Zeolite. *Microporous and Mesoporous Materials* **1998**, *24*, 69-82.
- (149) Lee, Y. K.; Park, S. H.; Rhee, H. K.: Transalkylation of Toluene and 1,2,4-Trimethylbenzene Over Large Pore Zeolites. *Catalysis Today* **1998**, *44*, 223-233.
- (150) Cambor, M. A.; Corma, A.; Valencia, S.: Synthesis in Fluoride Media and Characterisation of Aluminosilicate Zeolite Beta. *Journal of Materials Chemistry* **1998**, *8*, 2137-2145.
- (151) Lohse, U.; Altrichter, B.; Donath, R.; Fricke, R.; Jancke, K.; Parlitz, B.; Schreier, E.: Synthesis of Zeolite Beta .1. Using Tetraethylammonium Hydroxide Bromide With Addition of Chelates as Templating Agents. *Journal of the Chemical Society-Faraday Transactions* **1996**, *92*, 159-165.
- (152) Yang, C.; Xu, Q. H.: Aluminated Zeolites Beta and Their Properties .1. Aluminated Zeolites Beta. *Journal of the Chemical Society-Faraday Transactions* **1997**, *93*, 1675-1680.
- (153) Chien, S. H.; Ho, J. C.; Mon, S. S.: Hydrothermal Synthesis and Characterization of the Vanadium Containing Zeolite Beta. *Zeolites* **1997**, *18*, 182-187.
- (154) Borade, R. B.; Clearfield, A.: Preparation of Aluminum Rich Beta Zeolite. *Microporous Materials* **1996**, *5*, 289-297.
- (155) Jia, C.; Massiani, P.; Barthomeuf, D.: Characterization by Infrared and Nuclear Magnetic Resonance Spectroscopies of Calcined Beta Zeolite. *Journal of the Chemical Society-Faraday Transactions* **1993**, *89*, 3659-3665.
- (156) Zhang, D.; Duan, A.; Zhao, Z.; Wang, X.; Jiang, G.; Liu, J.; Wang, C.; Jin, M.: Synthesis, Characterization and Catalytic Performance of Meso/Microporous Material Beta-SBA-15-Supported Ni-Mo Catalysts for Hydrodesulfurization of Dibenzothiophene. *Catalysis Today* **2011**, *175*, 477-484.
- (157) Shan, Z.; Zhou, W.; Jansen, J. C.; Yeh, C. Y.; Koegler, J. H.; Maschmeyer, T.: Incorporation of Nano-Sized Zeolites Into a Mesoporous Matrix, TUD-1. In *Nanoporous Materials iii*; Sayari, A., Jaroniec, M., Eds., 2002; Vol. 141; pp 635-640.
- (158) Petushkov, A.; Merilis, G.; Larsen, S. C.: From Nanoparticles to Hierarchical Structures: Controlling the Morphology of Zeolite Beta. *Microporous and Mesoporous Materials* **2011**, *143*, 97-103.
- (159) Landau, M. V.; Tavor, D.; Regev, O.; Kaliya, M. L.; Herskowitz, M.; Valtchev, V.; Mintova, S.: Colloidal Nanocrystals of Zeolite Beta Stabilized in Alumina Matrix. *Chemistry of Materials* **1999**, *11*, 2030-2037.
- (160) Moushey, D. L.; Smirniotis, P. G.: n-Heptane Hydroisomerization over Mesoporous Zeolites made by Utilizing Carbon Particles as the Template for Mesoporosity. *Catalysis Letters* **2009**, *129*, 20-25.
- (161) Bernasconi, S.; Kokhoven, J. A.; Krumeich, F.; Pirngruber, G. D.; Prins, R.: Formation of Mesopores in Zeolite Beta by Steaming: A Secondary Pore Channel System in the (001) Plane. *Microporous and Mesoporous Materials* **2003**, *66*, 21-26.
- (162) Gu, Y.; Cui, N.; Yu, Q.; Li, C.; Cui, Q.: Study on the Influence of Channel Structure Properties in the Dehydration of Glycerol to Acrolein Over H-Zeolite Catalysts. *Applied Catalysis A-General* **2012**, *429*, 9-16.
- (163) Zheng, J.; Zeng, Q.; Yi, Y.; Wang, Y.; Ma, J.; Qin, B.; Zhang, X.; Sun, W.; Li, R.: The Hierarchical Effects of Zeolite Composites in Catalysis. *Catalysis Today* **2011**, *168*, 124-132.

- (164) Egeblad, K.; Kustova, M.; Klitgaard, S. K.; Zhu, K.; Christensen, C. H.: Mesoporous Zeolite and Zeotype Single Crystals Synthesized in Fluoride Media. *Microporous and Mesoporous Materials* **2007**, *101*, 214-223.
- (165) Gregg, S. J.; Sing, K. S. W.: *Adsorption, Surface Area, and Porosity*; 2nd ed.; Academic Press: London, 1982.
- (166) Burgess, C. G. V.; Everett, D. H.; Nuttall, S.: Adsorption Hysteresis in Porous Materials. *Pure and Applied Chemistry* **1989**, *61*, 1845-1852.
- (167) Rouquerol, F.; Avnir, D.; Fairbridge, C. W.; Everett, D. H.; Haynes, J. H.; Pernicone, N.; Ramsay, J. D. F.; Sing, K. S. W.; Under, K. K.: Recommendations for the Characterization of Porous Solids. *Pure and Applied Chemistry* **1994**, *66*, 1739-1758.
- (168) Rouquerol, F.; Rouquerol, J.; Sing, K.: *Adsorption by Powders and Porous Solids: Principles, Methodology and Applications*; Academic Press: San Diego, USA, 1998.
- (169) Sing, K. S. W.; Everett, D. H.; Haul, R. A. W.; Moscou, L.; Pierotti, R. A.; Rouquerol, J.; Siemieniowska, T.: Reporting Physisorption Data for Gas Solid Systems With Special Reference to the Determination of Surface Area and Porosity (Recommendations 1984). *Pure and Applied Chemistry* **1985**, *57*, 603-619.
- (170) Figueiredo, J. L.; Ribeiro, F. R.: Caracterização Físico-Química dos Catalisadores. In *Catálise Heterogênea*; Fundação Calouste Gulbenkian: Lisboa, 1987; pp 77-128.
- (171) Rouquerol, J.; Avnir, D.; Fairbridge, C. W.; Everett, D. H.; Haynes, J. H.; Pernicone, N.; Ramsay, J. D. F.; Sing, K. S. W.; Unger, K. K.: Recommendations for the Characterization of Porous Solids. *Pure and Applied Chemistry* **1994**, *66*, 1739-1758.
- (172) Sangwichien, C.; Aranovich, G. L.; Donohue, M. D.: Density Functional Theory Predictions of Adsorption Isotherms With Hysteresis Loops. *Colloids and Surfaces A-Physicochemical and Engineering Aspects* **2002**, *206*, 313-320.
- (173) Blin, J. L.; Léonard, A.; Su, B. L.: Well-Ordered Spherical Mesoporous Materials CMI-1 Synthesized via an Assembly of Decaoxyethylene Cetyl ether and TMOS. *Chemistry of Materials* **2001**, *13*, 3542-3553.
- (174) Sing, K. S. W.: Characterization of Adsorbents. In *Adsorption, Science and Technology*; Rodrigues, A. E., Levan, M. D., Tondeur, D., Eds.; Kluwer Academic Publishers: Dordrecht, the Netherlands, 1989; Vol. 158 pp 3-14.
- (175) Rouquerol, F.; Rouquerol, J.; Sing, K.: *Adsorption by Powders and Porous Solids Principles, Methodology and Applications*; Academic Press: San Diego, California, U.S.A., 1999.
- (176) El Roz, M.; Lakiss, L.; Valtchev, V.; Mintova, S.; Thibault-Starzyk, F.: Cold Plasma as Environmentally Benign Approach for Activation of Zeolite Nanocrystals. *Microporous and Mesoporous Materials* **2012**, *158*, 148-154.
- (177) Bisio, C.; Martra, G.; Coluccia, S.; Massiani, P.: FT-IR Evidence of Two Distinct Protonic Sites in BEA Zeolite: Consequences on Cationic Exchange and on Acido-Basic Properties in the Presence of Cesium. *Journal of Physical Chemistry C* **2008**, *112*, 10520-10530.
- (178) Bejblová, M.; Zones, S. I.; Čejka, J.: Highly Selective Synthesis of Acetylferrocene by Acylation of Ferrocene Over Zeolites. *Applied Catalysis A- General* **2007**, *327*, 255-260.
- (179) Cruz-Cabeza, A. J.; Esquivel, D.; Jimenez-Sanchidrian, C.; Romero-Salguero, F. J.: Metal-Exchanged Beta Zeolites as Catalysts for the Conversion of Acetone to Hydrocarbons. *Materials* **2012**, *5*, 121-134.
- (180) Moreau, P.; Finiels, A.; Meric, P.; Fajula, F.: Acetylation of 2-Methoxynaphthalene in the Presence of Beta Zeolites: Influence of Reaction Conditions and Textural Properties of the Catalysts. *Catalysis Letters* **2003**, *85*, 199-203.
- (181) Ramos, M. J.; Casas, A.; Rodríguez, L.; Romero, R.; Pérez, A.: Transesterification of Sunflower Oil Over Zeolites Using Different Metal Loading: A Case of Leaching and Agglomeration Studies. *Applied Catalysis A-General* **2008**, *346*, 79-85.
- (182) Costa, A. E.; Cerqueira, H. S.; Ferreira, J. M. M.; Ruiz, N. M. S.; Menezes, S. M. C.: BEA and MOR as Additives for Light Olefins Production. *Applied Catalysis A-General* **2007**, *319*, 137-143.
- (183) Bian, J. J.; Liu, J.; Wang, X. S.; Liu, X. M.; Bao, X. H.: Characterization of the Deposit on Zeolite Beta Catalyzed Benzene Propylation. *Materials Chemistry and Physics* **2003**, *77*, 406-410.
- (184) Bernasconi, S.; Pirngruber, G. D.; Prins, R.: Influence of the Properties of Zeolite BEA on its Performance in the Nitration of Toluene and Nitrotoluene. *Journal of Catalysis* **2004**, *224*, 297-303.

- (185) Kubicek, N.; Vaudry, F.; Chiche, B. H.; Hudec, P.; Di Renzo, F.; Schulz, P.; Fajula, F.: Stabilization of Zeolite Beta for Fcc Application by Embedding in Amorphous Matrix. *Applied Catalysis A-General* **1998**, *175*, 159-171.
- (186) Esquivel, D.; Cabeza, A. J. C.; Sanchidrian, C. J.; Salguero, F. J. R.: Local Environment and Acidity in Alkaline and Alkaline-Earth Exchanged Beta Zeolite: Structural Analysis and Catalytic Properties. *Microporous and Mesoporous Materials* **2011**, *142*, 672-679.
- (187) Neatu, F.; Coman, S.; Parvulescu, V. I.; Poncelet, G.; Vos, D. D.; Jacobs, P.: Heterogeneous Catalytic Transformation of Citronellal to Menthol in a Single Step on Ir-Beta Zeolite Catalysts. *Topics in Catalysis* **2009**, *52*, 1292-1300.
- (188) Savidha, R.; Pandurangan, A.: Isopropylation of Toluene: A Comparative Study of Microporous Zeolites and Mesoporous MCM-41 Materials. *Applied Catalysis A-General* **2004**, *276*, 39-50.
- (189) Oumi, Y.; Jintsugawa, I.; Kikuchi, S.; Nawata, S.; Fukushima, T.; Teranishi, T.; Sano, T.: Co-Incorporation of Al and Ga Into BEA Zeolite by the pH Control Method. *Microporous and Mesoporous Materials* **2003**, *66*, 109-116.
- (190) Fernandes, L. D.; Monteiro, J. L. F.; Aguiar, E. F. S.; Martinez, A.; Corma, A.: Ethylbenzene Hydroisomerization Over Bifunctional Zeolite Based Catalysts: The Influence of Framework and Extraframework Composition and Zeolite Structure. *Journal of Catalysis* **1998**, *177*, 363-377.
- (191) Trasarti, A. F.; Marchi, A. J.; Apesteguia, C. R.: Design of Catalyst Systems For the One-Pot Synthesis of Menthols From Citral. *Journal of Catalysis* **2007**, *247*, 155-165.
- (192) Dimitrova, R.; Gunduz, G.; Spassova, M.: A Comparative Study on the Structural and Catalytic Properties of Zeolites Type ZSM-5, Mordenite, Beta and MCM-41. *Journal of Molecular Catalysis A-Chemical* **2006**, *243*, 17-23.
- (193) Aguado, J.; Serrano, D. P.; San Miguel, G.: Analysis of Products Generated from the Thermal and Catalytic Degradation of Pure and Waste Polyolefins Using Py-GC/MS. *Journal of Polymers and the Environment* **2007**, *15*, 107-118.
- (194) Miguel, G. S.; Aguado, J.; Serrano, D. P.; Escola, J. M.: Thermal and Catalytic Conversion of Used Tyre Rubber and its Polymeric Constituents Using Py-GC/MU. *Applied Catalysis B-Environmental* **2006**, *64*, 209-219.
- (195) Aguado, J.; Serrano, D. P.; Miguel, G. S.; Escola, J. M.; Rodriguez, J. M.: Catalytic Activity of Zeolitic and Mesostructured Catalysts in the Cracking of Pure and Waste Polyolefins. *Journal of Analytical and Applied Pyrolysis* **2007**, *78*, 153-161.
- (196) Kao, H. M.; Chen, Y. C.: ^{27}Al and ^{19}F Solid-State NMR Studies of Zeolite H-Beta Dealuminated With Ammonium Hexafluorosilicate. *Journal of Physical Chemistry B* **2003**, *107*, 3367-3375.
- (197) Bokhoven, J. A. v.; Koningsberger, D. C.; Kunkeler, P.; Bekkum, H. v.; Kentgens, A. P. M.: Stepwise Dealumination of Zeolite Beta at specific T-sites Observed with ^{27}Al MAS and ^{27}Al MQ MAS NMR. *Journal of the American Chemical Society* **2000**, *122*, 12842-12847.
- (198) Kentgens, A. P. M.: A Practical Guide to Solid-State NMR of Half-Integer Quadrupolar Nuclei With Some Applications to Disordered Systems. *Geoderma* **1997**, *80*, 271-306.
- (199) Fyfe, C. A.; Strobl, H.; Kokotailo, G. T.; Pasztor, C. T.; Barlow, G. E.; Bradley, S.: Correlations Between Lattice Structures of Zeolites and Their ^{29}Si MAS NMR Spectra- Zeolites KZ-2, ZSM-12 and Beta. *Zeolites* **1988**, *8*, 132-136.
- (200) Abraham, A.; Lee, S. H.; Shin, C. H.; Hong, S. B.; Prins, R.; Bokhoven, J. A. v.: Influence of Framework Silicon to Aluminium Ratio on Aluminium Coordination and Distribution in Zeolite Beta Investigated by ^{27}Al MAS and ^{27}Al MQ MAS NMR. *Physical Chemistry Chemical Physics* **2004**, *6*, 3031-3036.
- (201) Stelzer, J.; Paulus, M.; Hunger, M.; Weitkamp, J.: Hydrophobic Properties of All-Silica Zeolite Beta. *Microporous and Mesoporous Materials* **1998**, *22*, 1-8.
- (202) Ménorval, L. C. d.; Buckermann, W.; Figueras, F.; Fajula, F.: Influence of Adsorbed Molecules on the Configuration of Framework Aluminum Atoms in Acidic Zeolite-Beta. A ^{27}Al MAS NMR study. *Journal of Physical Chemistry* **1996**, *100*, 465-467.
- (203) Zhang, W. M.; Smirniotis, P. G.; Gangoda, M.; Bose, R. N.: Brønsted and Lewis Acid Sites in Dealuminated ZSM-12 and Beta Zeolites Characterized by NH_3 -STPD, FT-IR, and MAS NMR spectroscopy. *Journal of Physical Chemistry B* **2000**, *104*, 4122-4129.
- (204) Muller, M.; Harvey, G.; Prins, R.: Quantitative Multinuclear MAS NMR Studies of Zeolites. *Microporous and Mesoporous Materials* **2000**, *34*, 281-290.

- (205) Penzien, J.; Abraham, A.; Bokhoven, J. A. V.; Jentys, A.; Muller, T. E.; Sievers, C.; Lercher, J. A.: Generation and Characterization of Well-Defined Zn²⁺ Lewis Acid Sites in Ion Exchanged Zeolite BEA. *Journal of Physical Chemistry B* **2004**, *108*, 4116-4126.
- (206) Wouters, B. H.; Chen, T. H.; Grobet, P. J.: Reversible Tetrahedral-Octahedral Framework Aluminum Transformation in Zeolite Y. *Journal of the American Chemical Society* **1998**, *120*, 11419-11425.
- (207) Klinowski, J.; Thomas, J. M.; Fyfe, C. A.; Gobbi, G. C.: Monitoring of Structural Changes Accompanying Ultrastabilization of Faujasitic Zeolite Catalysts. *Nature* **1982**, *296*, 533-536.
- (208) Lami, E. B.; Massiani, P.; Direnzo, F.; Espiau, P.; Fajula, F.; Courieres, T. D.: Study of the State of Aluminium in Zeolite Beta. *Applied Catalysis* **1991**, *72*, 139-152.
- (209) Eerden, A. M. J. v. d.; Bokhoven, J. A. v.; Smith, A. D.; Koningsberger, D. C.: Apparatus for in Situ X-Ray Absorption Fine Structure Studies on Catalytic Systems in the Energy Range 1000 eV < E < 3500 eV. *Review of Scientific Instruments* **2000**, *71*, 3260-3266.
- (210) Beck, L. W.; Haw, J. F.: Multinuclear NMR-Studies Reveal a Complex Acid Function for Zeolite-Beta. *Journal of Physical Chemistry* **1995**, *99*, 1076-1079.
- (211) Kiricsi, I.; Flego, C.; Pazzuconi, G.; Parker, W. O.; Millini, R.; Perego, C.; Bellussi, G.: Progress Toward Understanding Zeolite Beta Acidity- An Air and ²⁷Al NMR Spectroscopy Study. *Journal of Physical Chemistry* **1994**, *98*, 4627-4634.
- (212) Woolery, G. L.; Kuehl, G. H.; Timken, H. C.; Chester, A. W.; Vartuli, J. C.: On the Nature of Framework Brønsted and Lewis Acid Sites in ZSM-5. *Zeolites* **1997**, *19*, 288-296.
- (213) Bokhoven, J. A. v.; Eerden, A. M. J. v. d.; Koningsberger, D. C.: Three-Coordinate Aluminum in Zeolites Observed With in Situ X-Ray Absorption Near-Edge Spectroscopy at the AlK-Edge: Flexibility of Aluminum Coordinations in Zeolites. *Journal of the American Chemical Society* **2003**, *125*, 7435-7442.
- (214) Bokhoven, J. A. v.; Eerden, A. M. J. v. d.; Koningsberger, D. C.: Flexible Aluminium Coordination of Zeolites as Function of Temperature and Water Content, an in-Situ Method to Determine Aluminium Coordinations. In *Impact of Zeolites and Other Porous Materials on the New Technologies at the Beginning of the New Millennium, Pts a and B*; Aiello, R., Giordano, G., Testa, F., Eds., 2002; Vol. 142; pp 1885-1890.
- (215) Beers, A. E. W.; Bokhoven, J. A. v.; Lathouder, K. M. d.; Kapteijn, F.; Moulijn, J. A.: Optimization of Zeolite Beta by Steaming and Acid Leaching for the Acylation of Anisole with Octanoic Acid: A Structure-Activity Relation. *Journal of Catalysis* **2003**, *218*, 239-248.
- (216) Lippmaa, E.; Samoson, A.; Magi, M.: High Resolution ²⁷Al NMR of Aluminosilicates. *Journal of the American Chemical Society* **1986**, *108*, 1730-1735.
- (217) Gilson, J. P.; Edwards, G. C.; Peters, A. W.; Rajagopalan, K.; Wormsbecher, R. F.; Roberie, T. G.; Shatlock, M. P.: Pentacoordinated Aluminium in Zeolites and Aluminosilicates. *Journal of the Chemical Society-Chemical Communications* **1987**, 91-92.
- (218) Chen, F. R.; Davis, J. G.; Fripiat, J. J.: Aluminium Coordination and Lewis Acidity in Transition Aluminas. *Journal of Catalysis* **1992**, *133*, 263-278.
- (219) Engelhardt, G.: Solid State NMR Spectroscopy Applied to Zeolites In *Introduction to Zeolite Science and Practice: Studies in Surface Science and Catalysis*; Bekkum, H. V. F., E. M.; Jansen, J. C., Ed.; Elsevier Science Publishers BV: Amsterdam, The Netherlands, 1991; Vol. 58; pp 285-316.
- (220) Bokhoven, J. A. v.; Koningsberger, D. C.; Kunkeler, P.; Bekkum, H. v.: Influence of Steam Activation on Pore Structure and Acidity of Zeolite Beta: An AlK Edge XANES Study of Aluminum Coordination. *Journal of Catalysis* **2002**, *211*, 540-547.
- (221) Haouas, M.; Bernasconi, S.; Kogelbauer, A.; Prins, R.: An NMR Study of the Nitration of Toluene Over Zeolites by HNO₃-Ac₂O. *Physical Chemistry Chemical Physics* **2001**, *3*, 5067-5075.
- (222) Guisnet, M.; Ayrault, P.; Coutanceau, C.; Alvarez, M. F.; Datka, J.: Acid Properties of Dealuminated Beta Zeolites Studied by IR Spectroscopy. *Journal of the Chemical Society-Faraday Transactions* **1997**, *93*, 1661-1665.
- (223) Corma, A.; Fornes, V.; Melo, F. V.; Monton, J. B.; Orchilles, A. V.: Catalytic Cracking of a Vacuum Gas Oil and n-Heptane on H-Beta Zeolites With Different Si/Al Ratios. *Abstr. Pap. Am. Chem. Soc.* **1987**, *194*, 14-PETR.
- (224) Corma, A.; Fornes, V.; Melo, F.; Perezpariente, J.: Zeolite Beta Structure, Activity, and Selectivity for Catalytic Cracking. *American Chemical Society Symposium Series* **1988**, *375*, 49-63.

- (225) Marques, J. P.; Gener, I.; Ayrault, P.; Bordado, J. C.; Lopes, J. M.; Ribeiro, F. R.; Guisnet, M.: Dealumination of HBEA Zeolite by Steaming and Acid Leaching: Distribution of the Various Aluminic Species and Identification of the Hydroxyl Groups. *Comptes Rendus Chimie* **2005**, *8*, 399-410.
- (226) Xie, Z. K.; Chen, Q. L.; Zhang, C. F.; Bao, J. Q.; Cao, Y. H.: Influence of Citric Acid Treatment on the Surface Acid Properties of Zeolite Beta. *Journal of Physical Chemistry B* **2000**, *104*, 2853-2859.
- (227) Gil, B.; Košová, G.; Čejka, J.: Acidity of MCM-58 and MCM-68 Zeolites in Comparison With Some Other 12-Ring Zeolites. *Microporous and Mesoporous Materials* **2010**, *129*, 256-266.
- (228) Macedo, J. L. d.; Ghesti, G. F.; Dias, J. A.; Dias, S. C. L.: Liquid Phase Calorimetry and Adsorption Analyses of Zeolite Beta Acidity. *Physical Chemistry Chemical Physics* **2008**, *10*, 1584-1592.
- (229) Laredo, G. C.; Jesus Castillo, J.; Bolaños, J. N.; Romo, P. P.; Lagos, F. A.: Benzene Reduction in Gasoline by Alkylation With Olefins: Comparison of Beta and MCM-22 Catalysts. *Applied Catalysis A-General* **2012**, *413*, 140-148.
- (230) Kamarudin, N. H. N.; Jalil, A. A.; Triwahyono, S.; Mukti, R. R.; Aziz, M. A. A.; Setiabudi, H. D.; Muhid, M. N. M.; Hamdan, H.: Interaction of Zn^{2+} With Extraframework Aluminum in H-BEA Zeolite and its Role in Enhancing n-Pentane Isomerization. *Applied Catalysis A-General* **2012**, *431*, 104-112.
- (231) Xie, Z. K.; Bao, J. Q.; Yang, Y. Q.; Chen, Q. L.; Zhang, C. F.: Effect of Treatment with $NaAlO_2$ Solution on the Surface Acid Properties of Zeolite Beta. *Journal of Catalysis* **2002**, *205*, 58-66.
- (232) Zhang, Z.; Liu, S.; Zhu, X.; Wang, Q.; Xua, L.: Modification of H-Beta Zeolite by Fluorine and its Influence on Olefin Alkylation Thiophenic Sulfur in Gasoline. *Fuel Processing Technology* **2008**, *89*, 103-110.
- (233) Macedo, J. L. d.; Ghesti, G. F.; Dias, J. A.; Dias, S. C. L.: Liquid Phase Calorimetry and Adsorption Analyses of Zeolite Beta Acidity. *Physical Chemistry Chemical Physics : PCCP* **2008**, *10*, 1584-1592.
- (234) Selli, E.; Forni, L.: Comparison Between the Surface Acidity of Solid Catalysts Determined by TPD and FT-IR Analysis of Pre-Adsorbed Pyridine. *Microporous and Mesoporous Materials* **1999**, *31*, 129-140.
- (235) O'Sullivan, P.; Forni, L.; Hodnett, B. K.: The Role of Acid Site Strength in the Beckmann Rearrangement. *Industrial & Engineering Chemistry Research* **2001**, *40*, 1471-1475.
- (236) Luque, R.; Budarin, V.; Clark, J. H.; Shuttleworth, P.; White, R. J.: Starbon (R) Acids in Alkylation and Acetylation Reactions: Effect of the Brønsted-Lewis Acidity. *Catalysis Communications* **2011**, *12*, 1471-1476.
- (237) Trombetta, M.; Busca, G.; Rossini, S.; Piccoli, V.; Cornaro, U.; Guercio, A.; Catani, R.; Willey, R. J.: FT-IR Studies on Light Plefin Skeletal Isomerization Catalysis III. Surface Acidity and Activity of Amorphous and Crystalline Catalysts Belonging to the $SiO_2-Al_2O_3$ System. *Journal of Catalysis* **1998**, *179*, 581-596.
- (238) Valente, A. A.; Dias, A. S.; Lima, S.; Brandão, P.; Pillinger, M.; Plácido, H.; Rocha, J.: Catalytic Performance of Microporous Nb and Mesoporous Nb or Al Silicates in the Dehydration of D-Xylose to Furfural. In *Perspectiva de la investigación sobre materiales en España en el siglo XXI: IX Congreso Nacional de Materiales*; Colección: Congressos n° 53 ed.; Materiales, S. E. d., Ed.; Servizo de Pulicaciós da Universidade de Vigo: University of Vigo, Vigo, Spain, 2006; Vol. II; pp 1203-1206.
- (239) Kim, S. B.; You, S. J.; Kim, Y. T.; Lee, S. M.; Lee, H.; Park, K.; Park, E. D.: Dehydration of D-xylose Into Furfural Over H-Zeolites. *Korean Journal of Chemical Engineering* **2011**, *28*, 710-716.
- (240) Antal, M. J.; Leesomboon, T.; Mok, W. S.; Richards, G. N.: Kinetic Studies of the Reactions of Ketoses and Aldoses in Water at High Temperature 3-Mechanism of Formation of 2-Furaldehyde from D-Xylose. *Carbohydrate Research* **1991**, *217*, 71-85.
- (241) Zeitsch, K. J.: *The Chemistry and Technology of Furfural and its Many By-Products*; 1st ed.; Elsevier Science B. V.: Amsterdam, The Netherlands, 2000; Vol. 13.
- (242) Wevers, R. A.; Engelke, U. F.: The Magician from Transsylvania on the Use of Proton NMR Spectroscopy in the Clinical Chemistry Laboratory. *Ned Tijdschr Klin Chem Labgeneesk* **2005**, *30*, 272-275.
- (243) Wevers, R. A.; Engelke, U.; Wendel, U.; Dejong, J. G. N.; Gabreels, F. J. M.; Heerschap, A.: Standardized Method for High-Resolution 1H NMR of Celebrospinal Fluid. *Clinical Chemistry* **1995**, *41*, 744-751.
- (244) Brown, G.: The Power of NMR: the Beginning. *Education in Chemistry* **2008**, *45*, 108-116.

(245) Ramanjooloo, A.; Bhaw-Luximon, A.; Jhurry, D.; Cadet, F.: ^1H NMR Quantitative Assessment of Lactic Acid Produced by Biofermentation of Cane Sugar Juice. *Spectroscopy Letters* **2009**, *42*, 296-304.

(246) Francisco, M.; Bruinhorst, A. v. d.; Kroon, M. C.: New Natural and Renewable Low Transition Temperature Mixtures (LTTMs): Screening as Solvents for Lignocellulosic Biomass Processing. *Green Chemistry* **2012**, *14*, 2153-2157.

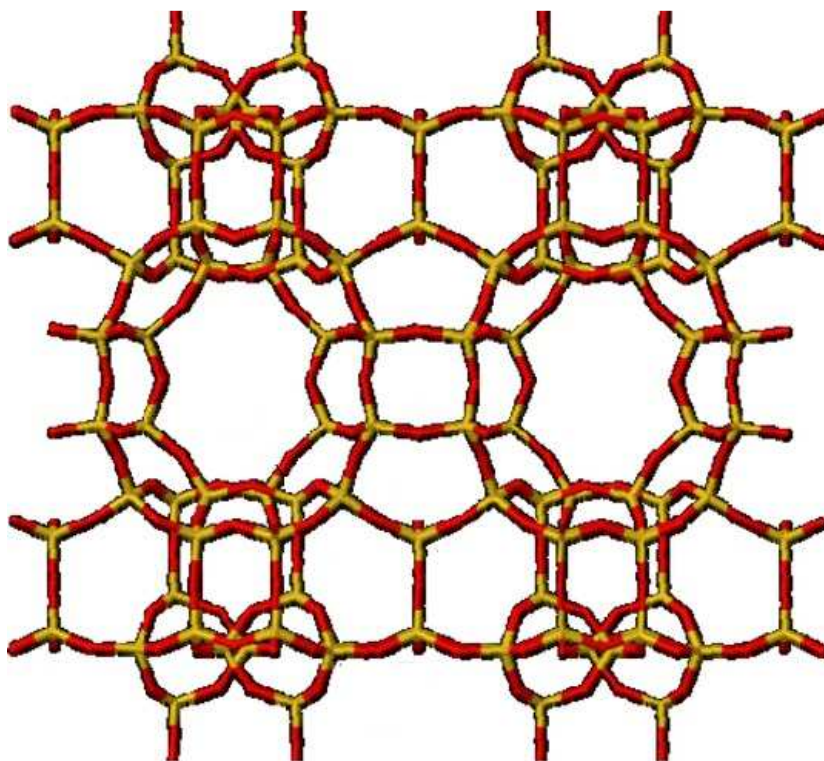
(247) Campo, G. d.; Berregi, I.; Caracena, R.; Zuriarrain, J.: Quantitative Determination of Caffeine, Formic Acid, Trigonelline and 5-(Hydroxymethyl)furfural in Soluble Coffees by ^1H NMR Spectrometry. *Talanta* **2010**, *81*, 367-371.

(248) Yoshida, K.; Wakai, C.; Matubayasi, N.; Nakahara, M.: NMR Spectroscopic Evidence for an Intermediate of Formic Acid in the Water Gas Shift Reaction. *Journal of Physical Chemistry A* **2004**, *108*, 7479-7482.

(249) Jing, Q.; Lu, X. Y.: Kinetics of Non-Catalyzed Decomposition of D-Xylose in High Temperature Liquid Water. *Chin. J. Chem. Eng.* **2007**, *15*, 666-669.

CHAPTER 6

Reaction of D-xylose in the presence of zeolite H-MCM-22 and delaminated ITQ-2



Structure of one layer of MCM-22 ¹

Index

CHAPTER 6	265
Reaction of D-xylose in the presence of zeolite H-MCM-22 and delaminated ITQ-2	265
6.1. Introduction	267
6.1.1. Zeolite H-MCM-22	268
6.1.2. Delaminated ITQ-2	270
6.2. Results and discussion.....	272
6.2.1. Catalyst characterisation.....	272
6.2.2. Catalytic dehydration of D-xylose	285
6.2.2.1. Catalytic performance of H-MCM-22 and ITQ-2(24) in water-organic biphasic solvent system	285
6.2.2.2. Catalytic performance of H-MCM-22 and ITQ-2(24) using solely water as solvent...	290
6.2.2.3. Identification of the reaction products	292
6.2.2.4. Catalyst stability	294
6.3. Conclusions	296
6.4. References.....	297

6.1. Introduction

Porous aluminosilicates are promising solid acid catalysts in the dehydration of Xyl to Fur. They exhibit catalytic activity in acid catalysed reactions and fulfill important requirements that are put on solid acid catalysts, such as being water-tolerant (minimal levelling-off of the acid strength in water), hydrothermally stable (crystalline structure integrity and stability towards metal leaching) and presenting a good thermal stability when the catalyst regeneration requires thermal decomposition of accumulated carbonaceous deposits (typically in the range 350-550 °C), or chemical stability if carbonaceous deposits are to be removed by harsh chemical treatments (e.g. liquid-phase oxidising conditions),^{2,3} as mentioned in Chapter 1. From the literature data, other families of porous inorganic solids can be pointed as fairly robust materials for this catalytic application, but aluminosilicates (bulk catalysts) in particular are relatively cheap and versatile materials with respect to the type of crystallinity and pore structures (micro/meso/macropores; 1 D, 2 D or 3 D pore systems), acid properties and surface polarity (varying the Si/Al ratio), and possibility of being prepared with particle/crystallite sizes down to the nano-scale.

Microporous 3 D structures impose size constraints on the reactants, intermediates and products. In a pioneering work by Moreau et al.,⁴ zeolites revealed to be effective solid acids for the conversion of saccharides into Fur; in the case of H-Mordenite and H-Y Faujasite with Si/Al atomic ratio in the range 2-15, 90-96% S_{Fur} was reached at 27-37% C_{Xyl} at 170 °C, although selectivity dropped considerably as conversion increased.⁴ O'Neill et al.⁵ found a similar trend in Fur selectivity with conversion of Xyl for zeolite ZSM-5 as catalyst, and explained these results on the basis of enhanced Fur loss reactions inside the pore system, which may eventually cause pore blockage and deactivation of the catalyst. Accordingly, efforts have been focused on increasing pore sizes, allowing a wider application of these materials in fine chemicals, pharmaceuticals and petrochemical industries. Various synthetic approaches have improved the catalytic performance of zeolites, such as decreasing the zeolite crystallite sizes to the nano scale to increase the specific surface/pore volume ratio (as discussed in previous Chapter 5) and delaminating lamellar precursors of zeolites into aggregates of sheets with zeolitic nature and enhanced specific surface area.⁶ In this Chapter, H-MCM-22 zeolite possessing a medium-pore framework (MWW) and its delaminated counterpart, were tested as catalysts in the dehydration of Xyl into Fur.

6.1.1. Zeolite H-MCM-22

The zeolite H-MCM-22 possesses a 3 D MWW-type framework (Figures 6.1 and 6.2) and was discovered by Mobil in 1990.⁷ Like zeolite beta (discussed in the previous Chapter) MCM-22 belongs to the group of high silica zeolites ($\text{Si/Al} \geq 10$) and crystallises in the form of thin platelets.^{1,8} It presents a complex pore system characterised by the presence of both medium and large pores,⁹ in which the internal MWW-type structure consists of two independent pore systems, both accessible only through 10-membered ring apertures (10-MR),^{1,8,10,11} and specific surface area is commonly in the range¹¹ 300-500 $\text{m}^2.\text{g}^{-1}$. The first pore system is 3 D, formed by MWW large super cages (with an inner free diameter of ca. 7.1 Å and with an unusually large inner height of 18.2 Å) and composed of 12-MR, only accessible through elliptical 10-MR apertures (4.0x5.5 Å).^{1,11-13} The [001] plane of MCM-22 crystals are terminated by open (half-cut) MWW cages (pores in the form of cups).⁸ The aluminium sites in these cups give rise to strong acid sites on the external surface, similar to the Brønsted acid sites on the internal surface.¹²⁻¹⁶ The second pore system is defined by a 2 D circular 10-MR sinusoidal channel system with a uniform diameter (4.1x5.1 Å) throughout the structure (medium-pore),¹ and does not contain cages.¹³ The two pore systems are independent.¹³

The acid sites on the external surface of MCM-22 can be accessed by relatively bulky organic molecules, making MCM-22 an interesting catalyst for a wide variety of reactions.¹³ Hence, the distribution of the framework aluminium atoms and acidic hydroxyl groups of the MWW-type framework structures are particularly interesting.¹ The properties of MCM-22 zeolite may be influenced by several factors, such as the synthesis method and conditions (variation of the silica gel composition),^{10,17} having a strong impact on crystal size and morphology.¹⁸

MCM-22 had been proposed with both hexagonal and orthorhombic forms,^{10,19} Kennedy et al.²⁰ determined by NMR studies that for highly-siliceous zeolites the orthorhombic one is favoured with 13 non-equivalent tetrahedral sites, that can be Si or Al. According to Kennedy et al.¹⁹ the Al-O bonds (1.75 Å in length) are longer than Si-O (1.61 Å in length).

MCM-22 zeolite can be formed via two different synthesis methods,²¹ either by calcination of a lamellar precursor herein denoted as Pre-MCM-22, during which, the OH groups condense in the lamellar layers to form the 3 D MWW-type framework structure;²² or alternatively by direct hydrothermal synthesis from a synthesis gel (which is typical for zeolites).²¹ The Pre-MCM-22 already contains the sinusoidal system within hexagonal individual layers

(thickness of ca. 25 Å) perpendicularly aligned to the central axis z and separated by the organic template hexamethylenimine.^{7,22-25}

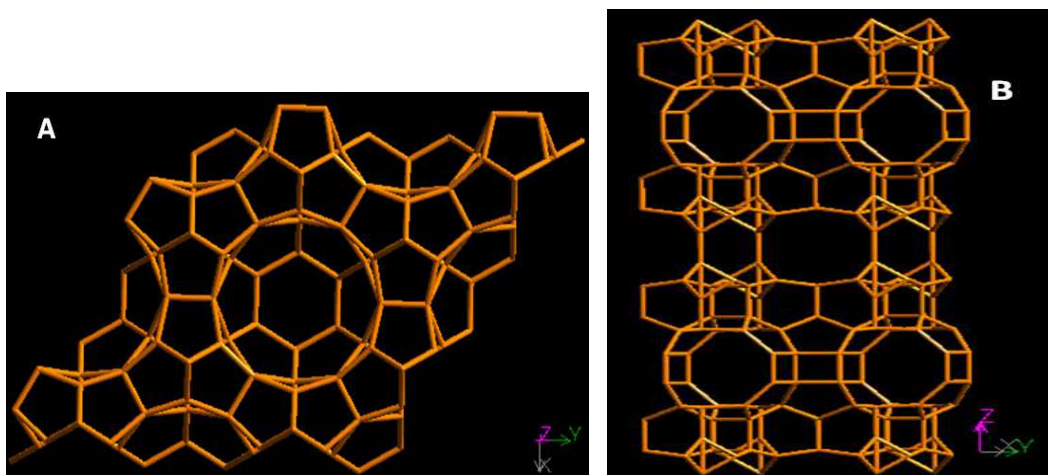


Figure 6.1- Structures of MWW-type framework projected along [001] (A), and projected along [100] (B).²⁶

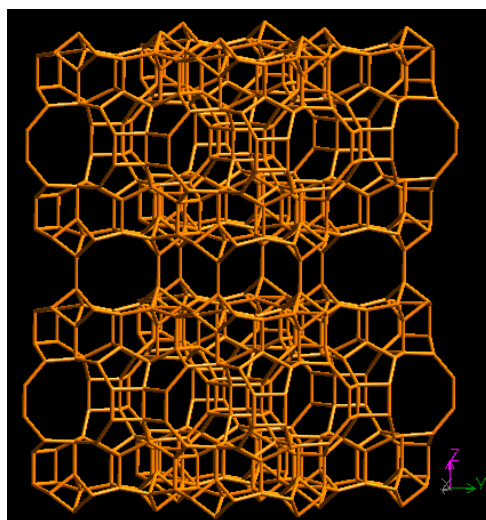


Figure 6.2- Structure of MWW-type framework viewed normal to [001].²⁶

6.1.2. Delaminated ITQ-2

The maximum diameter of the pore-rings of MCM-22 is ca. 5.5 Å or 6.2 Å based on atomic or Norman radii, respectively.^{1,11,27} Since Xyl molecules possess an approximate molecular diameter of 6.8 Å,²⁸ access to the internal catalyst surface of MCM-22 through the 10-MR apertures may be impeded. In order to enhance the external surface area available for the catalytic reactions, Corma et al.²⁹⁻³² developed a delamination procedure to transform Pre-MCM-22 into the first delaminated material obtained through zeolite precursors, known as ITQ-2 (Figure 6.3).²⁹ ITQ-2 is obtained when Pre-MCM-22 layers are exfoliated and oriented randomly but predominantly edge-to-face,⁵ allowing easier access of the reactants to the zeolite AS.²³ When Pre-MCM-22 is calcined, then MCM-22 is obtained (Figure 6.3).^{33,34}

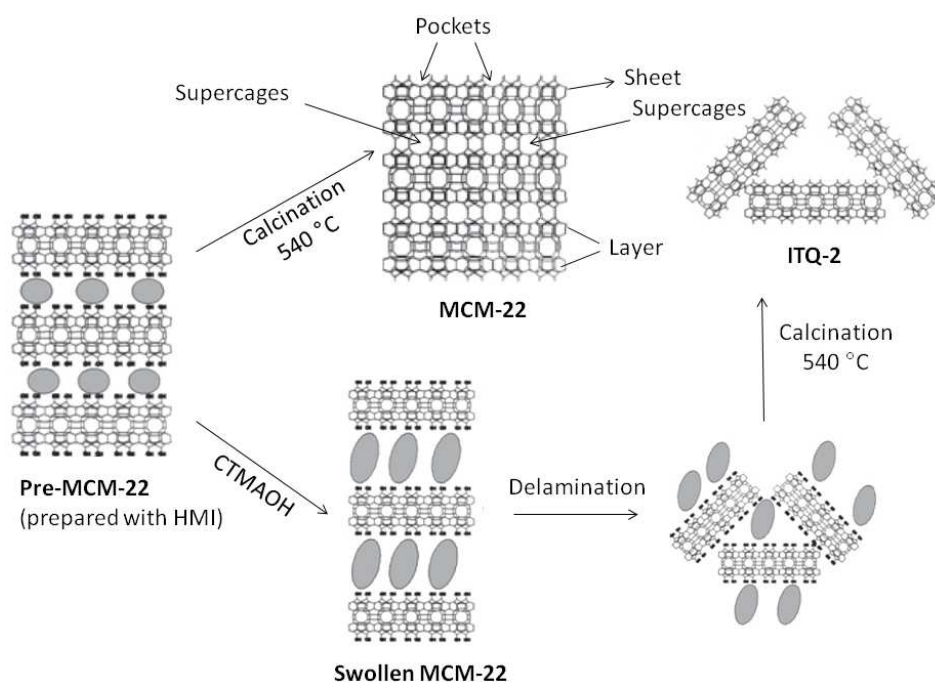


Figure 6.3- Schematic representation of MCM-22 and ITQ-2 obtained from Pre-MCM-22; HMI- hexamethylenamine, CTMAOH- cetyltrimethylammonium hydroxide [adapted from^{35,36}].

ITQ-2 is a material with a very high external specific surface area (ca. 600-800 m².g⁻¹) and consists of 2.5 nm thick sheets possessing a hexagonal array of half-open supercages (cup-shaped open pores) facing out each side of the sheets (with a diameter of ca. 7.1 Å, formed by a 12-MR).

The cups have a height of 7.0 Å with bottoms connected by a double 6-MR unit, and a circular 10-MR sinusoidal channel system running between the cups, inside the sheet (Figure 6.4).^{29-32,35,37} ITQ-2 is a promising catalyst with possible advantages compared to amorphous oxides and microporous zeolites; it retains its shape selectivity; reduced diffusion or pore-size limitations in accessing the active sites; possesses short range order and is disordered in long range,^{38,39} narrow distribution of the pores and well defined microporosity.³⁹ It has a corrugated surface structure allowing the chemical reactions to occur at active sites located in the half cage.⁴⁰ ITQ-2 can be more active and more selective than MCM-22, as shown by Corma et al.²⁹ The lack of long-range periodic order makes conventional analysis of XRD data not suitable for determining the structure of ITQ-2.³⁹ The proposed structure of ITQ-2 was determined on the basis of high-resolution electron microscopy, gas adsorption isotherms and infrared spectroscopy.^{29,35,40}

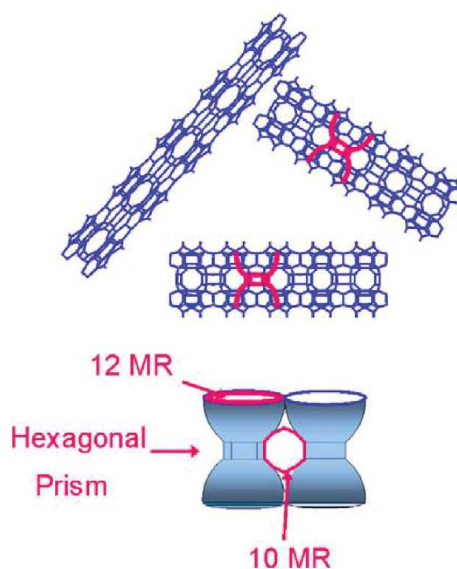


Figure 6.4- Schematic representation of the structure of ITQ-2.⁴¹

In this work, the dehydration of Xyl to Fur was investigated in the presence of MCM-22 and ITQ-2 catalysts, using a biphasic Wt:Tol solvent system or solely water as solvent, at 170 °C.

6.2. Results and discussion

6.2.1. Catalyst characterisation

In this Chapter (Na,H)-MCM-22(X) and ITQ-2(24) materials were prepared as described in the literature (Chapter 2).^{31,32} Na-MCM-22(X) materials were obtained through calcination of the previously prepared Pre-MCM-22(X), which were prepared as described in the literature,^{30,31} using sodium aluminate and silica (as aluminium and silicon sources) and hexamethylenimine as the organic template; X (the atomic ratio of Si/Al) was determined to be of 24 and 38 by ICP-AES measurements. ITQ-2(24) was prepared by delamination of Pre-MCM-22(30), by the addition of aqueous cetyltrimethyl-ammonium hydroxide/bromide (prepared by ion-exchange of CTMABr using Amberlite IRA-400 (OH)) and aqueous tetrapropylammonium hydroxide/bromide.

The ion-exchange and calcination treatments applied to Na-MCM-22(24) and Na-MCM-22(38) to give H-MCM-22(24) and H-MCM-22(38), respectively, did not affect the Si/Al atomic ratio.

The delamination procedure applied to Pre-MCM-22(30) gave the material ITQ-2(24) with a slightly lower Si/Al atomic ratio, possibly due to slight dissolution of silica during the delamination process.^{42,43}

The powder XRD patterns of the (Na,H)-MCM-22 samples obtained are in good agreement with the literature data for a MWW-type framework topology (Figure 6.5).^{10,12,13,17,23,29,31,36,39,44-98} The XRD pattern of ITQ-2(24) revealed a significant reduction in the long-range order as a result of the delamination procedure, in agreement with the literature data.^{29,31,36,41-43,46,51,53,56,73,83,93,99-101}

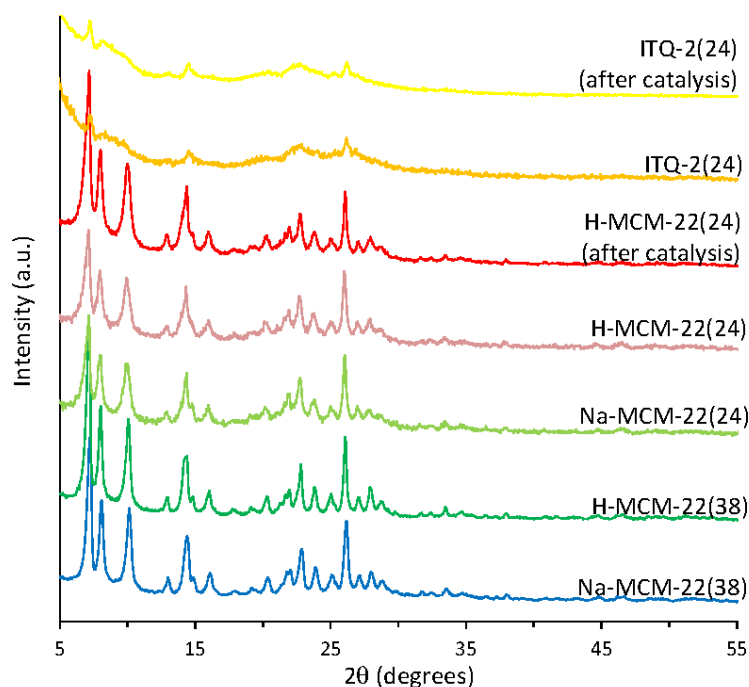


Figure 6.5- Powder XRD patterns of as-prepared H-MCM-22(24) and ITQ-2(24) and the corresponding used/calined (after catalysis) solids.

The SEM analyses showed that the (Na,H)-MCM-22 samples consisted of thin plate-like crystallites of a few hundreds of nanometers to ca. 1 μm wide, and ITQ-2(24) consisted of particles of irregular shapes (exemplified for Na-MCM-22(24) and ITQ-2(24), Figure 6.6 and for H-MCM-22(24) and H-MCM-22(38), Figure 6.7). A platelet-like morphology for MCM-22 was also observed by other authors. Some of them reported sizes $\leq 1 \mu\text{m}$ in length,^{46,74,85,87,88,102,103} in agreement to the findings in this work. Others found the same platelet-like morphology for MCM-22 but for sizes $>1 \mu\text{m}$.^{17,47,55,61-63,72,75,90,95,96,104-111} Smiešková et al.¹¹² reported that MCM-22 consisted of clusters composed of platelet type particles of about $\leq 1 \mu\text{m}$ in length. Other morphologies were observed by other authors for MCM-22 such as circular crystals, with diameters of 0.8-1 μm for MCM-22(50) and much smaller (0.03-0.05 μm) for MCM-22(15), in accordance with the higher crystallinity of MCM-22(50) and higher external surface area of MCM-22(15) (141 $\text{m}^2\cdot\text{g}^{-1}$ compared to 97 $\text{m}^2\cdot\text{g}^{-1}$ for MCM-22(50)),⁸⁸ hollow spheres with 6-7 μm in diameter,⁵¹ spheres with a hole inside with diameters from 1-2 μm ,^{60,77} 3-10 μm ,^{100,113} and 13-16 μm ,^{67,68} hexagonal lamellar crystals with lengths of ca. 0.5-0.6 μm ,⁷⁴ and crystal chips with diameters of 5-10 μm .⁵⁹ A not well defined sheet for MCM-22 with 5 μm in length was reported.¹³ The irregular particle shapes typical of ITQ-2 were confirmed before (with loss of the platelet

morphology of MCM-22(P)).^{43,54} In contrast, ITQ-2 consisted of thin platelets similar to MCM-22, but with the formation of more agglomerates or more fragments.^{46,114} Similar to what some authors observed for MCM-22, hollow spheres were also observed for ITQ-2 but with more fragments,⁵¹ or spheres with smaller diameters of 1 μm when compared to MCM-22 (3-10 μm).¹⁰⁰

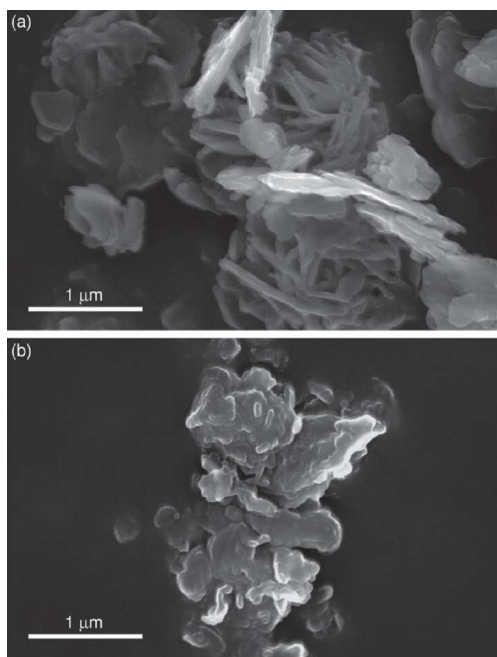


Figure 6.6- SEM images of a) Na-MCM-22(24) and b) ITQ-2(24).

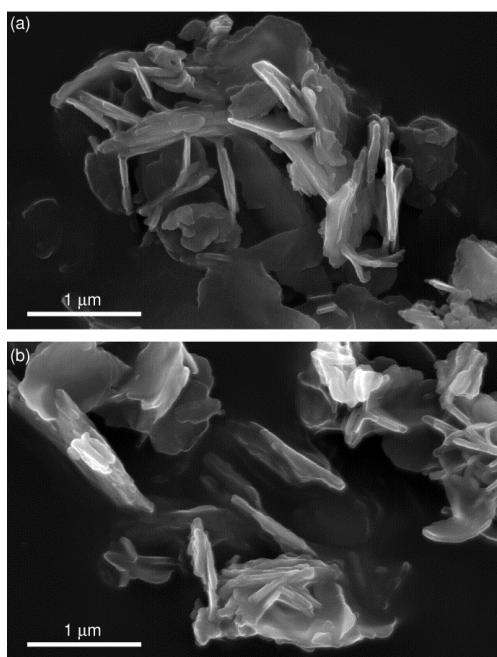


Figure 6.7- SEM images of a) H-MCM-22(24) and b) H-MCM-22(38).

Figure 6.8 shows a representative HRTEM image of Na-MCM-22(24) crystallite viewed along the 10-MR channels (bright spots), perpendicular to the z-direction. The images generally showed the stacking of MWW sheets with a thickness ranging from 150 to 300 nm, corresponding to the thickness of the platelet crystals. As expected, the 10-MR channels were separated by 1.2 nm, and the thickness of the layers was ca. 2.5 nm. MWW sheets with different ranges of thickness were reported. A few authors reported sheets with thickness of 100-500 nm (similar to the obtained in this work),^{55,75,96,108} others in the range of 1000-2500 nm,^{63,105} others reported sheets with less than 100 nm of thickness,^{74,87,88,102} or even smaller (≥ 50 nm).^{74,85,103} HRTEM images of ITQ-2(24) showed much more fragmented crystals consisting of fewer sheets than Na-MCM-22(24), and even single layers of 2.5 nm thickness (Figure 6.8 b). Similar results for ITQ-2 were reported earlier by Corma et al.³⁵

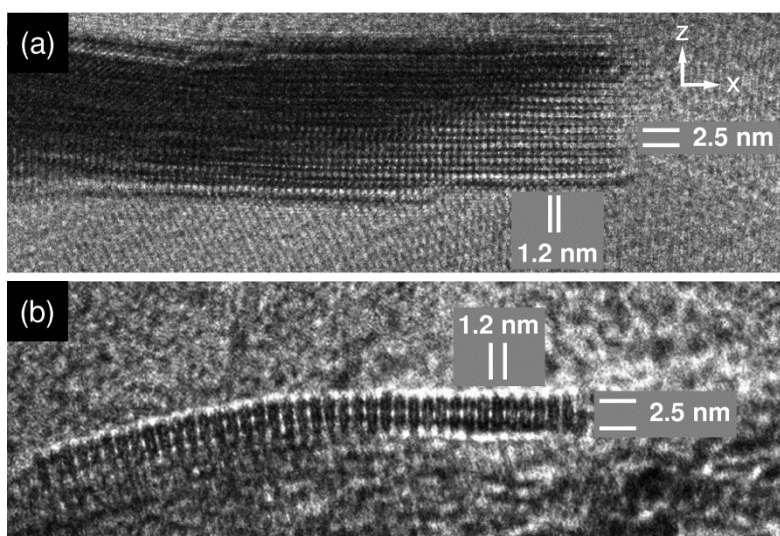


Figure 6.8- HRTEM images of a) Na-MCM-22(24) and an b) ITQ-2(24) layer, viewed along the 10-MR channels, perpendicular to the z-direction.

The (Na,H)-MCM-22 materials exhibited type I adsorption isotherms, typical of microporous materials,¹¹⁵⁻¹¹⁹ with an enhanced increase in the amount of adsorbed N_2 at high relative pressures (p/p_0) which is most likely due to multilayer adsorption on the external surface of the crystallites (exemplified for Na-MCM-22(24) and ITQ-2(24) in Figure 6.9); H-MCM-22(24), Na-MCM-22(38) and H-MCM-22(38) (Figure 6.10). These results are in agreement with the literature data.^{17,31,54,56,60,73,75,101,111,120,121}

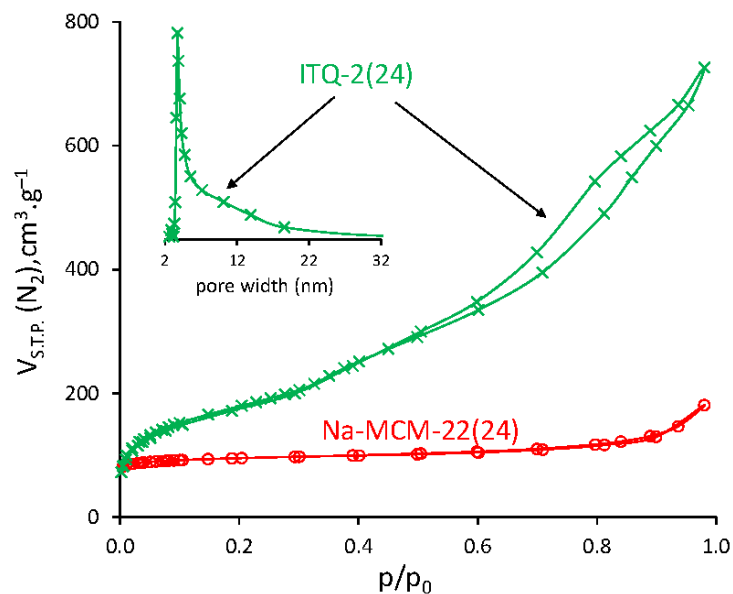


Figure 6.9- N_2 adsorption-desorption isotherms measured for Na-MCM-22(24) and ITQ-2(24), at $-196\text{ }^\circ\text{C}$.

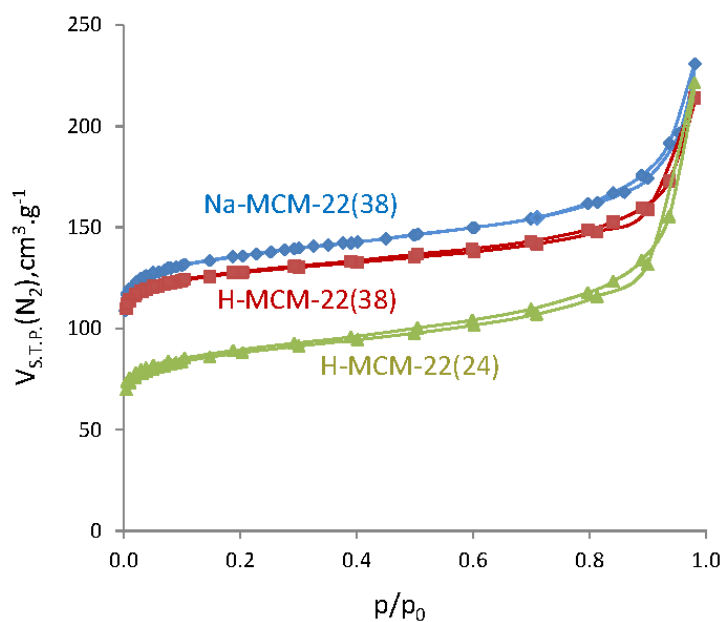


Figure 6.10- N_2 adsorption-desorption isotherms measured for H-MCM-22(24), Na-MCM-22(38) and H-MCM-22(38), at $-196\text{ }^\circ\text{C}$.

The external surface areas (S_{EXT}) of these samples were significant ($48\text{--}74\text{ m}^2\text{.g}^{-1}$, Table 6.1), which was consistent with the rather small crystallite sizes observed by electron microscopy (Figure 6.6). The ion-exchange/calcination treatments did not affect significantly the textural

properties of the Na-MCM-22 samples. The adsorption-desorption isotherms for ITQ-2(24) exhibited a hysteresis loop at $p/p_0 > 0.5$, indicating the presence of mesoporosity and the pore size distribution curve (PSD) exhibited a maximum pore diameter (D_p) at ca. 3.7 nm (Figure 6.9), in agreement with the literature data.^{31,41,54,56,73,101,121} The much higher S_{EXT} ($611 \text{ m}^2 \cdot \text{g}^{-1}$) obtained for ITQ-2(24) compared to the (Na,H)-MCM-22 materials ($48\text{-}74 \text{ m}^2 \cdot \text{g}^{-1}$), was consistent with a successful delamination procedure.

Table 6.1- Elemental composition and textural properties of (Na,H)-MCM-22 and ITQ-2(24) catalysts and comparison with literature data for other delaminated zeolites.

Sample (Si/Al) ^a	V_p ($\text{cm}^3 \cdot \text{g}^{-1}$)	V_{micro}/V_{meso} ($\text{cm}^3 \cdot \text{g}^{-1}$)	Surface area ($\text{m}^2 \cdot \text{g}^{-1}$)	S_{EXT} ($\text{m}^2 \cdot \text{g}^{-1}$)	D_p (nm)	Ref
Na-MCM-22(24)	0.28	0.12 ^e /-	361 ^j	52 ^r	-	this work
H-MCM-22(24)	0.34	0.10 ^e /-	333 ^j	74 ^r	-	this work
Na-MCM-22(38)	0.22	0.19 ^e /-	564 ^j	62 ^r	-	this work
H-MCM-22(38)	0.33	0.18 ^e /-	497 ^j	48 ^r	-	this work
MCM-22(7)	-	0.14 ^f /-	518 ^k	-	-	75
MCM-22(12)	-	0.16 ^e /0.24	481 ^l	106 ^r	-	46
MCM-22(12)	-	-	432 ^l	-	-	122
MCM-22(14)	0.19	-	689	-	-	91
MCM-22(15)	-	-	453 ^m	-	-	123,124
MCM-22(15)	0.31	0.16 ^e /-	451(310/-) ⁿ	141 ^s	-	93,125
MCM-22(15)	-	0.16/0.61	503 ^l	-	-	126
MCM-22(15)	0.47	-	654 ^l	-	-	44
H-MCM-22(15)	0.65 ^c	0.15 ^e /0.48 ^h	501 ^l	-	-	52,61
H-MCM-22(15)	-	-	458 ^l	-	-	127
MCM-22(15)	-	-	487 ^l	-	-	59
MCM-22(16)	-	-	432 ^o	-	-	84
H-MCM-22(16)	0.31	0.21 ^e or 0.20 ^h /0.10 ^g	566 ^l	132 ^r	-	128
H-MCM-22(16)	-	0.16 ^f /-	553 ^l	-	-	55
H-MCM-22(17)	-	-	460 (350/-) ^l	110 ^r	-	129
MCM-22(18)	-	0.16 ^e /-	-	110 ^r	-	73
MCM-22(18)	0.17 ^d	0.14 ^e /-	435 (303/-) ⁿ	132 ^s	-	130
H-MCM-22(19)	0.28 ^d	0.23 ^e /-	524 ^l	127 ^r	-	56
MCM-22(21)	0.27	0.21 ^e /0.06 ^g	586 ^l	-	-	83
MCM-22(21)	-	0.18 ^f or 0.21 ^h /-	597 ^p	-	-	17
H-MCM-22(22)	0.43	0.18/-	493 ^l	-	-	131
H-MCM-22(23)	0.22 ^d	0.14 ^e /0.08 ^g	401 (318/-) ⁿ	83 ^s	-	51
H-MCM-22(28)	0.16	-	530	-	-	91
MCM-22(29)	-	-	481 ^l	-	-	1
H-MCM-22(30)	-	-	451 ^l	-	-	132
H-MCM-22(31)	0.41	-	452	-	-	133
MCM-22(40)	0.52	0.16 ^e /0.36 ^g	418 (337/-)	93	-	107
MCM-22(40)	-	-	329 ^l	-	-	1
MCM-22(46)	-	0.11 ^e or 0.13 ^h /-	356 ^p	-	-	17
H-MCM-22(46)	0.18 ^d	0.11 ^e /0.07 ^g	396 (311/-) ⁿ	85 ^s	-	51

MCM-22(50)	0.52 ^d	0.18 ^e /-	451 (355/-) ⁿ	96 ^s	-	36
MCM-22(50)	-	0.12/-	400 ^l	150	-	134
MCM-22(50)	-	0.12/-	400 ^l	82	-	135
MCM-22(50)	-	-	453 (244/-) ^l	111 ^r	-	31
MCM-22(50)	-	0.18/-	456 ^l (342/-)	114	-	25
MCM-22(50)	0.22	0.14/-	358 ^l (290/-)	68	2.4	62,64
ITQ-2						
ITQ-2(24)	1.12	0.01 ^e /-	623 ^j	611 ^r	3.7 ^t	this work
ITQ-2(14)	-	0.12 ^e /-	560 (239/-) ⁿ	331 ^s	-	93
ITQ-2(15)	-	-	573 ^m	-	-	123
ITQ-2(17)	-	0.16 ^e /0.57	679 ^l	268 ^r	-	46
ITQ-2(17)	-	-	730 (60/-) ^l	670 ^r	-	129
ITQ-2(18)	-	0.05 ^e /-	-	529 ^r	-	73
ITQ-2(18)	-	0.25 ^e /0.03 ^g	772 ^l	-	-	83
ITQ-2(19)	0.69 ^d	0.03 ^e /-	676 ^l	625 ^r	-	56
ITQ-2(24)	0.66 ^d	0.08 ^e /0.58 ^g	859 ⁿ	657 ^s	-	51
ITQ-2(24)	0.47	0.04 ^e /-	562 ⁿ	430 ^s	-	125
ITQ-2(25)	-	-	632 ^m	-	-	124
ITQ-2(30)	0.38	-/0.24 ^l	468 ^m (-/175) ^q	-	3.3	100
ITQ-2(50)	0.95 ^d	0.02 ^e /-	854 (45/-) ⁿ	756 ^s	-	36
ITQ-2(50)	-	-	840 (50/-) ^l	790 ^r	-	31
ITQ-2(50)	0.99	0.04/-	895(60/-) ⁿ	-	-	136
ITQ-2(58)	-	0.01/-	806 ^l	750	-	134
ITQ-2(58)	-	0.01/-	806 ^l	706	-	135
ITQ-2(nf) ^b	0.77	-	835 ^l	-	-	137
ITQ-2(nf) ^b	0.60	-	884 ^m	-	-	138
ITQ-2(pure silica)	0.76 ^d	-	822 ^l	-	3.7 ^t	41
ITQ-2(pure silica)	-	0.01/-	700 ^m	-	-	139
H-Nu-6(2)(32)	0.01	-	20 ^l	-	-	6
del-Nu-6(1)(29)	0.07	-	151 ^l	6 ^r	-	6

a) The bulk Si/Al atomic ratio of the catalysts is given in parenthesis. b) nf= information not found. c) Total pore volume for $p/p_0 < 0.9$. d) V_p determined by BJH adsorption method. e) V_{micro} calculated by t-plot. f) V_{micro} calculated by αs plot. g) $V_{meso} = V_p - V_{micro}$. h) V_{micro} calculated by Dubinin-Raduskevitch method. i) V_{meso} calculated by BJH method. j) S_{BET} calculated for p/p_0 in the range 0.01-0.10. k) Specific surface area calculated from the B point of the isotherm. l) S_{BET} values in parenthesis refers to S_{micro}/S_{meso} in which $S_{micro} = S_{BET} - S_{EXT}$. m) Not mentioned how the surface area was calculated. n) S_{BET} values in parenthesis refers to S_{micro}/S_{meso} in which S_{micro} is calculated by t-plot. o) S_{BET} determined from N_2 adsorption data for the proton form of each zeolite. p) Surface area determined by Dubinin-Raduskevitch method. q) S_{micro} determined by BJH method. r) S_{EXT} calculated from the t-plot method. s) S_{EXT} calculated by the difference between S_{BET} and S_{micro} . t) Average pore diameter (D_p) determined by BJH method. The calculations for the values without an indication are not mentioned in the respective works.

The delamination process is better succeeded for lower Si/Al ratios as can be seen for the values reported in the literature data (Table 6.1). The higher specific surface area was always observed for the delaminated ITQ-2 ($623-895 \text{ m}^2 \cdot \text{g}^{-1}$) compared to (Na,H)-MCM-22 materials ($401-597 \text{ m}^2 \cdot \text{g}^{-1}$ and Si/Al ratio between 7-29; $329-456 \text{ m}^2 \cdot \text{g}^{-1}$ and Si/Al ratio between 40-50). Even the lower ITQ-2 surface areas reported ($468-560 \text{ m}^2 \cdot \text{g}^{-1}$) were higher than the MCM-22 counterparts (e.g. $560 \text{ m}^2 \cdot \text{g}^{-1}$ obtained for ITQ-2 and $451 \text{ m}^2 \cdot \text{g}^{-1}$ for MCM-22)⁹³ (Table 6.1). Exceptionally, a

higher surface area was observed for MCM-22 ($654 \text{ m}^2 \cdot \text{g}^{-1}$) by Laredo et al.⁴⁴ In general, the S_{EXT} for ITQ-2 ($268\text{-}790 \text{ m}^2 \cdot \text{g}^{-1}$) was high compared to (Na,H)-MCM-22 materials ($68\text{-}150 \text{ m}^2 \cdot \text{g}^{-1}$), and the V_{micro} values were normally higher for MCM-22 materials (0.11 to $0.24 \text{ cm}^3 \cdot \text{g}^{-1}$) than in ITQ-2 ($0.01\text{-}0.08 \text{ cm}^3 \cdot \text{g}^{-1}$). Liu et al.¹⁰⁰ reported a low S_{meso} of $175 \text{ m}^2 \cdot \text{g}^{-1}$ for ITQ-2, which probably is an indication of an unsuccessful delamination. Yang et al.⁴⁶ reported the same value of V_{micro} for ITQ-2 and MCM-22 ($0.16 \text{ cm}^3 \cdot \text{g}^{-1}$), however the V_{meso} of the former was ca. 2.3 times greater ($0.57 \text{ cm}^3 \cdot \text{g}^{-1}$) than the latter ($0.24 \text{ cm}^3 \cdot \text{g}^{-1}$), which is consistent with the mesoporosity associated with ITQ-2 and observed through the nitrogen adsorption isotherms (Figure 6.9).

The ^{27}Al MAS NMR spectra of the Na-MCM-22 samples exhibited an asymmetric peak with maximum at ca. 56 ppm and a shoulder at ca. 50 ppm (Figure 6.11), assigned to tetrahedrally coordinated framework aluminium (denoted Al_{fr}), which may have non-equivalent chemical environments with different T-O-T angles.^{19,37,41,99,140} The tetrahedral aluminium at ca. 50 ppm was assigned to aluminium atoms in sites T6 and T7,^{1,17,37,51} while the peak at 56 ppm was assigned to T1-T5 and T8, since T6 and T7 have larger T-O-T angles,⁵¹ or only T1, T3, T4, T5 and T8 (Figure 6.12).^{1,17,19,37} The average Al-O-Si angles in the zeolite framework of 152° and 164° were assigned for the chemical shifts at ca. 55 ppm and ca. 48 ppm respectively.¹⁴¹ This spectrum is in agreement with the literature for MCM-22 before calcination.^{1,10,19,23,37,43,49,51,59,76,98,140,142} Other authors observed a single peak at 54 ppm, associated with Al_{fr} in tetrahedral environment and indicating that aluminium was effectively incorporated in the silica framework.^{143,144} In the present work, the spectra of the H-MCM-22 samples exhibited an additional (narrow, weaker) peak at ca. 0 ppm, assigned to extra-framework aluminium species (denoted $\text{Al}_{\text{ext-fr}}$) formed during the ion-exchange/calcination treatments,^{91,99,133} which is similar to that reported in the literature.^{17,19,23,47,51,61,78,79,91,94,132,133,142,145-147} An additional peak at 61 ppm was reported sometimes as a shoulder of the ca. 50 and 55 ppm peaks assigned to tetrahedrally coordinated Al_{fr} ,^{19,23,142,147,148} and to T2 sites.⁷ Delitala et al.¹⁷ identified a peak at ca. 30 ppm that was attributed to distorted tetrahedral or pentacoordinated $\text{Al}_{\text{ext-fr}}$. Similar peak at ca. 30 ppm was also observed by other authors.^{78,94,148}

The relative amounts of the Al_{fr} and $\text{Al}_{\text{ext-fr}}$ species were determined from the areas of the respective peaks ($A(\text{Al}_{\text{fr}})$ = area of the peak in the range of 35-70 ppm; $A(\text{Al}_{\text{ext-fr}})$ = area of the peak centred at 0 ppm). The ratio $A(\text{Al}_{\text{fr}})/A(\text{Al}_{\text{ext-fr}})$ equals 8.4 for H-MCM-22(24) and 9.4 for H-MCM-22(38). These results are in agreement with the literature data in that higher Si/Al ratios of H-MCM-22 can lead to higher relative amounts of tetrahedral aluminium.^{1,43,133} The ^{27}Al NMR

spectrum of ITQ-2(24) revealed the presence of Al_{fr} (ca. 55 ppm) and $\text{Al}_{\text{ext-fr}}$ species (0 ppm), in agreement with the literature data.^{43,51,99}

The $A(\text{Al}_{\text{fr}})/A(\text{Al}_{\text{ext-fr}})$ ratio for ITQ-2(24) was equal to 8.5 which was similar to that observed for its counterpart H-MCM-22(24).

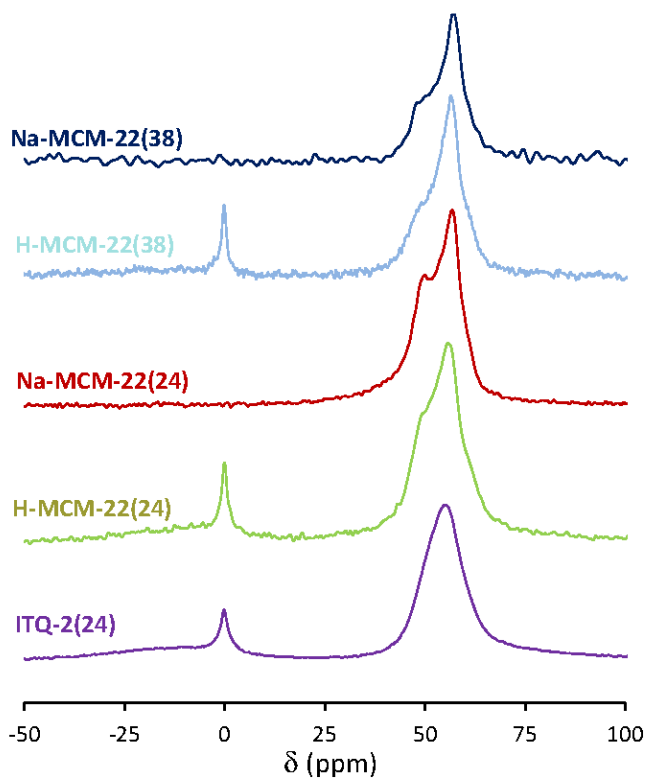


Figure 6.11- ^{27}Al MAS NMR spectra of the prepared catalysts (Na,H)-MCM-22 and ITQ-2(24).

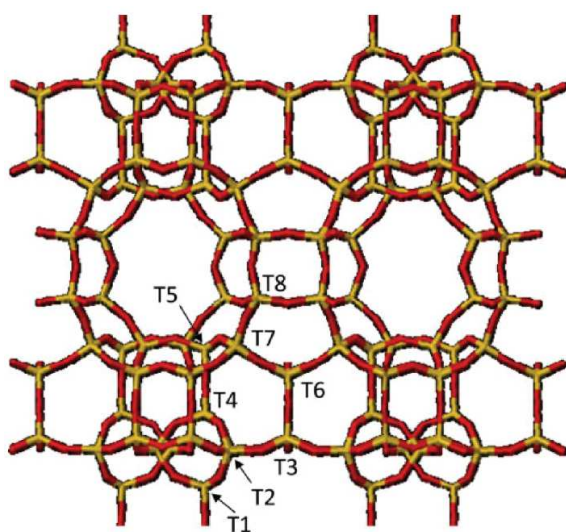


Figure 6.12- Schematic representation of non-equivalent tetrahedral positions in one layer of MCM-22. The T1 and T3-T8 sites may be occupied by Al and Si, while T2 sites contain only Si.¹

The FT-IR spectrum of ITQ-2(24) showed a band at ca. 956 cm^{-1} assigned to terminal Si-OH groups, which was poorly resolved in the case of H-MCM-22(24), further suggesting that delamination occurred to a significant extent in the preparation of ITQ-2(24) (Figure 6.13).^{29,31,99}

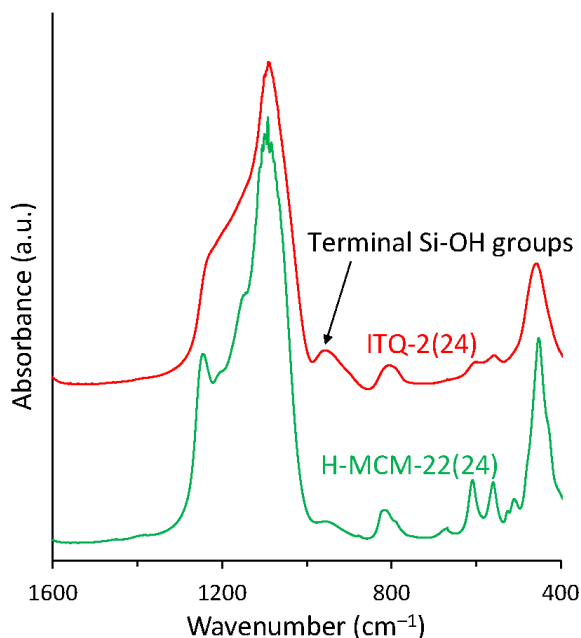


Figure 6.13- FT-IR spectra, in the framework region of H-MCM-22(24) and ITQ-2(24).

As mentioned in Section 5.2.1.2. from Chapter 5, the acidity of aluminosilicates investigated by FT-IR may be associated with bridging hydroxyl groups (Si-OH-Al) formed by tetrahedral aluminium.¹⁴⁹ (ca. 3600 cm^{-1} in the FT-IR spectra),^{150,151} hydroxyl groups, such as internal or terminal silanol Si-OH groups (3740 cm^{-1}),^{150,151} and Al-OH groups (3780 and 3680 cm^{-1})^{151,152} on the surface of the aluminosilicate which are usually weakly acidic.^{155,238} The measurement of the acid properties of the prepared catalysts was performed by FT-IR studies of adsorbed pyridine after outgassing at $150\text{ }^{\circ}\text{C}$. In the case of ITQ-2(24) the presence of Si-OH terminal groups was evident by the presence of an intense band at 3743 cm^{-1} (Figure 6.13). The presence of Si-OH groups was also observed in the case of the zeolite H-MCM-22(24) and H-MCM-22(38), although with much lower relative intensities (Figure 6.14). The ratio between the intensities of FT-IR bands due to acidic groups depends on the zeolite composition, preparation procedure, and subsequent thermal treatment conditions.^{153,154}

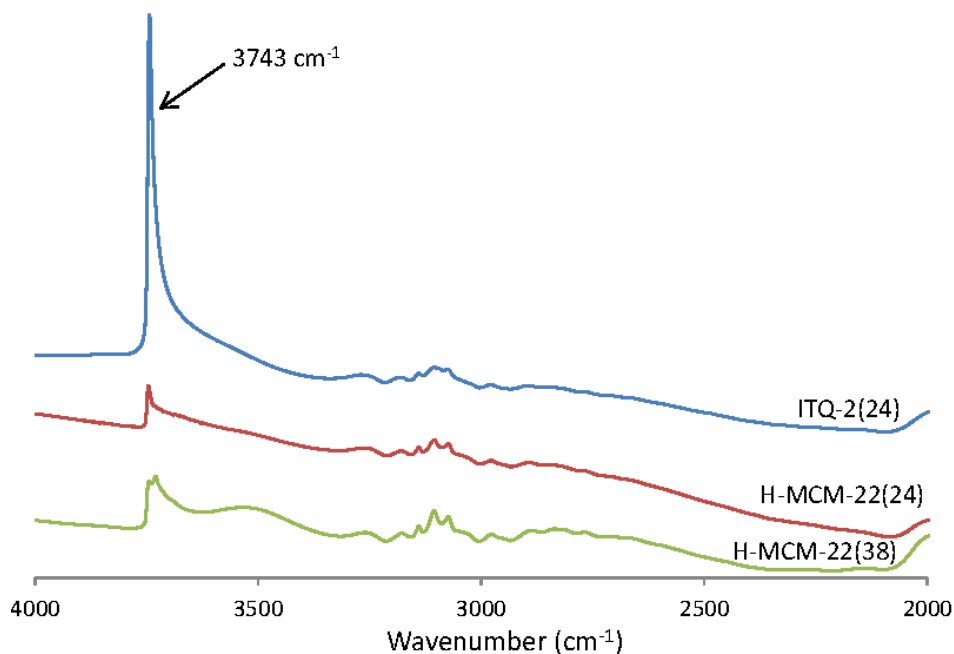


Figure 6.14- FT-IR spectra of ITQ-2(24), H-MCM-22(24) and H-MCM-22(38) after pyridine adsorption and outgassing at 150 °C.

All the prepared materials possessed both B and L interacting with pyridine after outgassing at 150 °C. The concentration of B and L were determined as explained previously in Section 3.2.1.2 of Chapter 3. In this sense, the [B] (band at ca. 1545 cm⁻¹) and [L] (band at ca. 1450 cm⁻¹) for ITQ-2(24) and H-MCM-22 were determined through equations 3.1 and 3.2, specified in Chapter 3 (Table 6.2). Figure 6.15 shows the FT-IR spectra of the catalysts with adsorbed pyridine, after outgassing at 150 °C. The band at ca. 1490 cm⁻¹ is attributed to L and B, 1620 cm⁻¹ to L and 1640 cm⁻¹ to B, which is in accordance with the literature.^{44,56,61,62,132,155}

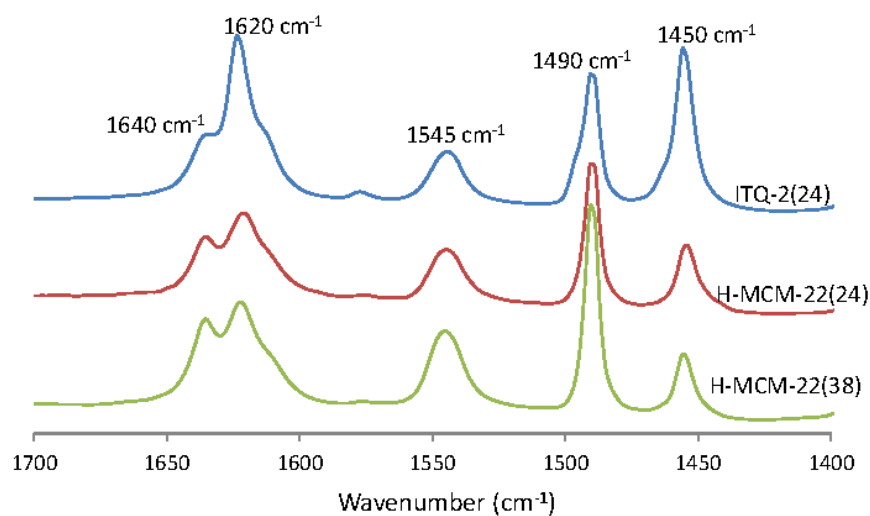


Figure 6.15- FT-IR spectra of ITQ-2(24), H-MCM-22(24) and H-MCM-22(38) after pyridine adsorption and outgassing at 150 °C.

The H-MCM-22 materials possessed mainly Brønsted acid sites (B), and comparable ratio of [L]/[B] (0.4-0.6, Figure 6.15). The H-MCM-22(24) sample possessed higher total amount of ([L]+[B]) in comparison to H-MCM-22(38), which was consistent with the lower Si/Al ratio for the former (Table 6.2), and with the literature for two MCM-22 samples with different Si/Al ratios (total acidity of 78.2 mmol.g⁻¹ for MCM-22(15) and of 41 mmol.g⁻¹ for MCM-22(50) after pyridine outgassing at 250 °C).⁸⁸ The ITQ-2(24) sample possessed a similar total amount of acid sites (AS) to H-MCM-22(24), while the [L]/[B] ratio was higher for ITQ-2(24) (a similar trend has been reported in the literature³⁰).

The effect of the outgassing temperature on the [L] and [B] was also investigated, and a decrease in the amount of detected AS was observed with an increase in outgassing temperature. The ratios of the amounts of AS measured at 150 °C and 250 °C ($[L]_{150}/[L]_{250}$ and $[B]_{150}/[B]_{250}$) were both equal to 1.1 for H-MCM-22(24), whereas for ITQ-2(24) $[L]_{150}/[L]_{250}=1.4$ and $[B]_{150}/[B]_{250}=2.6$. Hence, the surface acidity (particularly the Brønsted acidity) for ITQ-2(24) was weaker.

The [L]/[B] ratio for these types of materials reported in the literature (pyridine adsorption in a temperature range of 100 to 200 °C) is given in Table 6.2; in general for H-MCM-22, [B] was greater than [L]; exceptions were reported by Ling et al.,¹³² and Wang et al.⁵⁶ The higher [L]+[B] seemed to be correlated to the higher aluminium content, as observed for H-MCM-22(24) (204 μmol.g⁻¹) in comparison to H-MCM-22(38) (168 μmol.g⁻¹), and literature data for

H-MCM-22 with lower Si/Al ratios of 15-19 ($411-457 \mu\text{mol.g}^{-1}$).^{44,56,61} The same trend was reported for ITQ-2(24) and ITQ-2(19),⁵⁶ in which the total amount of AS were 198 and $276 \mu\text{mol.g}^{-1}$, respectively (Table 6.2). Meloni et al.¹⁵⁵ reported a considerably higher acidity for H-MCM-22(30) ($371 \mu\text{mol.g}^{-1}$) when compared to the results reported in this Chapter ($204 \mu\text{mol.g}^{-1}$ for H-MCM-22(24)).

Table 6.2- Acid properties measured by FT-IR of adsorbed pyridine of (Na,H)-MCM-22 and ITQ-2(24) catalysts and comparison with literature data.

Catalyst (Si/Al) ^a	T _{ads} (°C) ^b	T _{des} (°C) ^c	[L]+[B] ^d ($\mu\text{mol.g}^{-1}$)	[L] ^e ($\mu\text{mol.g}^{-1}$)	[B] ^f ($\mu\text{mol.g}^{-1}$)	[L]/[B] ^g	Ref
H-MCM-22(24)	150	150	204	58	145	0.4	this work
H-MCM-22(38)	150	150	168	63	105	0.6	this work
H-MCM-22(15)	200	200	457	106	351	0.3	⁴⁴
H-MCM-22(15)	110	110	411	159	252	0.6	⁶¹
H-MCM-22(19)	100	100	424	160	264	0.6	⁵⁶
H-MCM-22(30)	200	200	383	217	166	1.3	¹³²
H-MCM-22(30)	150	150	371	43	328	0.13	¹⁵⁵
H-MCM-22(49)	200	200	-	-	-	0.4	⁶²
ITQ-2(24)	150	150	198	99	99	1.0	this work
ITQ-2(19)	100	100	276	158	118	1.3	⁵⁶

a) The Si/Al atomic ratio of the catalyst is given in parenthesis. b) Temperature of pyridine adsorption (T_{ads}) used to determine Brønsted and Lewis acid sites concentrations. c) Temperature of pyridine desorption (T_{des}) used to determine Brønsted and Lewis acid sites concentrations. d) Sum of the total de Brønsted acid sites [B] plus Lewis acid sites [L]. e) Concentration of Lewis acid sites. f) Concentration of Brønsted acid sites. g) Ratio of the amounts of Lewis to Brønsted acid sites.

For comparison, the acid properties of ITQ-2(24) and H-MCM-22(24) were measured using collidine as the base probe molecule. Due to its steric bulk (ca. 7.4 \AA), the collidine molecule is not expected to enter the pores of the MWW-type framework structure,^{156,157} meaning it should only interact with B (giving [B]_{col}) located on the external surface or at the pore entrances. On the other hand, collidine is a stronger base (pKa ca. 7.4) than pyridine (pKa ca. 5.3).¹⁵⁸ The [B]_{col} for H-MCM-22(24) and ITQ-2(24) was 45 and $153 \mu\text{mol.g}^{-1}$, respectively (the reproducibility was checked in duplicate experiments). The lower [B]_{col} for H-MCM-22(24) than for ITQ-2(24) is most likely due to steric constraints (inaccessibility of the AS on the internal surface to the bulky collidine molecules). For ITQ-2(24), [B]_{col} was greater than [B] determined using pyridine, most likely due to the fact that collidine is a stronger base than pyridine and thus it interacts with AS which were too weak for interaction with pyridine. Based on the above results, it seems that while the delamination procedure led to enhanced surface area of ITQ-2(24), the surface acidity became relatively weak.

6.2.2. Catalytic dehydration of D-xylose

6.2.2.1. Catalytic performance of H-MCM-22 and ITQ-2(24) in water-organic biphasic solvent system

The catalysts were tested in the aqueous-phase reaction of Xyl to give Fur, using a biphasic solvent system (0.3 water:0.7 toluene (v/v), denoted Wt:Tol), at 170 °C. As mentioned before, Xyl dissolves completely in water and is insoluble in toluene, whereas Fur is distributed in the two liquid phases with a partition ratio in the range of 8-10, at a.t. calculated through equation 5.2 described in Chapter 5. Hence, the use of Tol as co-solvent allows the simultaneous extraction of Fur as it is formed, into the upper organic phase, which may avoid consecutive Fur loss reactions. The reaction of Xyl in the presence of H-MCM-22(24) gave 70% of Y_{Fur} at 92% C_{Xyl} , reached at 16 h (Figures 6.16 and 6.17). The kinetic curves for H-MCM-22(24) and its parent basic form, Na-MCM-22(24), were roughly coincident (Figure 6.16); the initial reaction rate for H-MCM-22(24) and Na-MCM-22(24) was 2.4 and 2.9 $\text{mmol}\cdot\text{g}_{\text{cat}}^{-1}\cdot\text{h}^{-1}$, respectively (based on the conversion of Xyl after 1 h of reaction). However, higher yields of Fur were reached for H-MCM-22(24) than for Na-MCM-22(24) (Figure 6.17). In the case of Na-MCM-22(38) the initial reaction rate was very poor (only 0.84 $\text{mmol}\cdot\text{g}_{\text{cat}}^{-1}\cdot\text{h}^{-1}$; slower than Na-MCM-22(24)). At 24 h of reaction the $C_{\text{Xyl}}/Y_{\text{Fur}}$ was 98%/47% for Na-MCM-22(24), 87%/51% for Na-MCM-22(38) and 82%/60% for H-MCM-22(38).

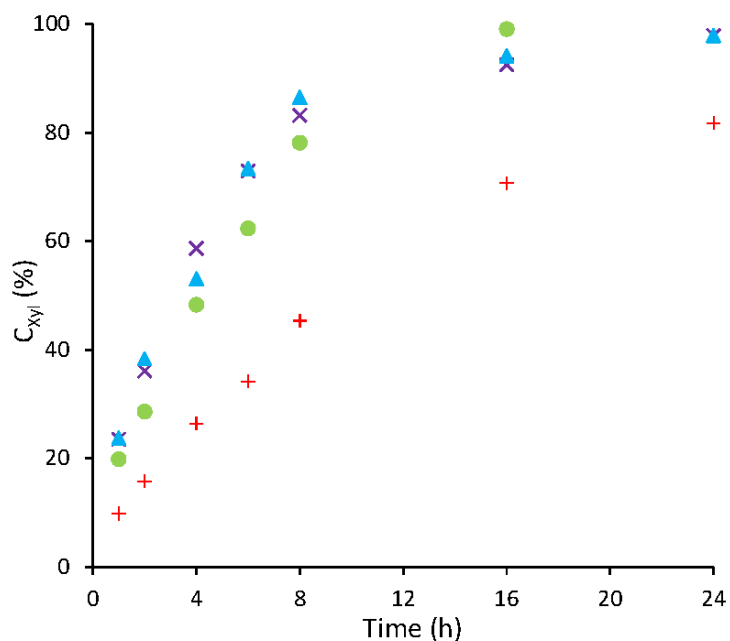


Figure 6.16- Kinetic profiles of the reaction of D-xylose (Xyl) in the presence of Na-MCM-22(24) (▲), H-MCM-22(24) (x), H-MCM-22(38) (+) or ITQ-2(24) (●). Reaction conditions: 0.3 Wt:0.7 Tol (v/v) biphasic solvent system, 170 °C, 20 $\text{g}_{\text{cat}}\cdot\text{dm}^{-3}$, 0.67 M Xyl.

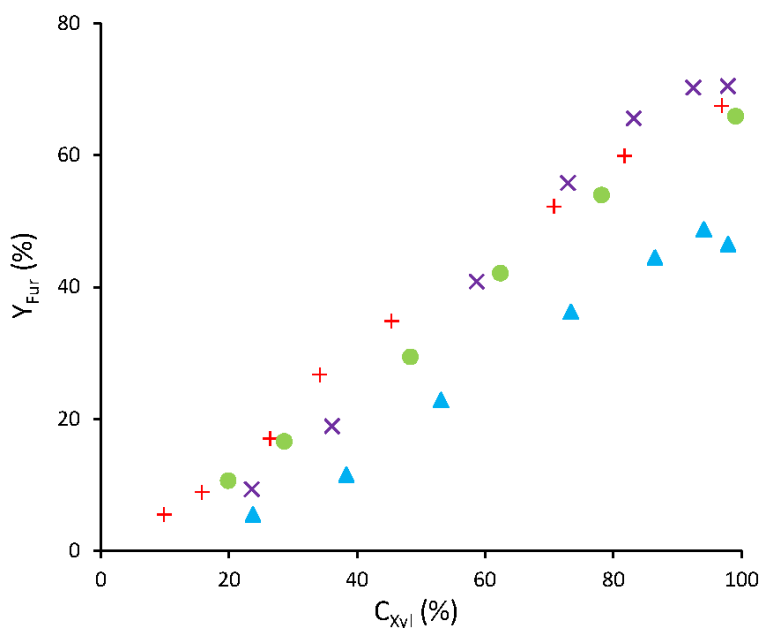


Figure 6.17- Dependence of the yield of 2-furaldehyd (Y_{Fur}) on the conversion of D-xylose (C_{Xyl}) curves for Na-MCM-22(24) (▲), H-MCM-22(24) (x), H-MCM-22(38) (+) or ITQ-2(24) (●). Reaction conditions: 0.3 Wt:0.7 Tol (v/v) biphasic solvent system, 170 °C, 20 $\text{g}_{\text{cat}}\cdot\text{dm}^{-3}$, 0.67 M Xyl.

The influence of the Si/Al ratio of the catalyst on the reaction of Xyl was investigated by comparing the catalytic performances of H-MCM-22(24) and H-MCM-22(38). For H-MCM-22(38), the initial reaction rate was $1.0 \text{ mmol.g}_{\text{cat}}^{-1}.\text{h}^{-1}$ (compared to $2.4 \text{ mmol.g}_{\text{cat}}^{-1}.\text{h}^{-1}$ for H-MCM-22(24)), and a 71% C_{Xyl} was reached at 16 h of reaction (Figure 6.16). The higher catalytic activity observed for H-MCM-22(24) (92% C_{Xyl} at 16 h compared to 82% C_{Xyl} at 24 h for H-MCM-22(38)) correlated with the higher total amount of acid sites determined by FT-IR studies of adsorbed pyridine (Tables 6.2 and 6.3). The yield of Fur reached at ca. 98% C_{Xyl} was 68% for H-MCM-22(38) and 71% for H-MCM-22(24) (Figure 6.17). Hence, the decrease in the Si/Al ratio of the H-MCM-22 zeolite led to an increase in the total amount of AS which, in turn, improved the catalytic activity in the reaction of Xyl, without affecting significantly the Fur selectivity.

The catalytic activity of (medium-pore) H-MCM-22(24) was intermediate (92% C_{Xyl} , 16 h) between that previously reported for the small-pore zeolite H-Nu-6 (2) (Si/Al=32), (59% C_{Xyl} , 6 h),⁶ and large-pore zeolite BEA (Si/Al=12) (98% C_{Xyl} at 4 h, in Chapter 5), used as catalysts in the same reaction under similar conditions (Table 6.3). Nevertheless, the maximum yield of Fur reached was highest for H-MCM-22(24). For comparison, the reaction of Xyl was carried out, under similar reaction conditions, in the presence of the protonic form of a commercial sample of ZSM-5 (Alfa Aesar; ammonium form; Si/Al=11.5, $425 \text{ m}^2.\text{g}^{-1}$), which is a medium-pore zeolite with the MFI framework type. The acquired zeolite was heated under static air at a rate of $1 \text{ }^\circ\text{C}.\text{min}^{-1}$ to $550 \text{ }^\circ\text{C}$, and maintained at this temperature for 10 h, giving the tested H-ZSM-5(11.5). The C_{Xyl} and Y_{Fur} at 6 h/16 h were 88%/98% and 60%/61%, respectively. Compared with the prepared H-MCM-22 samples, the H-ZSM-5(11.5) catalyst was more active (for the more active H-MCM-22(24), 73%/92% C_{Xyl} at 6 h/16 h), but led to lower yields of Fur at high conversions (at ca. 98% C_{Xyl} : 71%, 69% and 61% Y_{Fur} for H-MCM-22(24), H-MCM-22(38), and H-ZSM-5(11.5), respectively). O' Neill et al.⁵ investigated the reaction of Xyl in the presence of H-ZSM-5 with Si/Al=28. In that study, a maximum of ca. 33% Y_{Fur} was reached within 60 min, at $180 \text{ }^\circ\text{C}$, and afterwards the yield of Fur tended to drop with time (reaction conditions: 0.67 M Xyl and $30 \text{ g}_{\text{cat}}.\text{dm}^{-3}$) under pressurised He atmosphere. The yield of Fur reported for the reaction temperature of $160 \text{ }^\circ\text{C}$ was lower (ca. 12% Y_{Fur} at 1 h).

The presence of basic sites in the catalysts can promote undesirable reactions such as the aldolisation decomposition of the saccharide into oligomeric acid products.^{159,160} Particularly in the investigated catalyst H-ZSM-5, the average pore size was ca. 1.2 nm which is far greater than the molecular diameters of both Xyl and Fur, and this was considered as a possible cause of the formation of considerable amounts of by-products (oligomers).⁵

The results obtained for (Na-H)-MCM-22 samples compared favourably in terms of yield of Fur to the zeolites H-Mordenite or H-Y Faujasite tested under similar conditions in previously reported works (Table 6.3).

Table 6.3- Catalytic performance of prepared catalysts in the reaction of D-xylose (Xyl), using a biphasic solvent system (Wt:Tol) at 170 °C, and comparison with literature data for other aluminosilicate catalysts.

Catalyst (Si/Al) ^a	time (h)	C _{Xyl} (%) ^b	Y _{Fur} (%) ^c	Ref
Na-MCM-22(24)	24	98	47	this work
H-MCM-22(24)	16	92	70	this work
Na-MCM-22(38)	24	87	58	this work
H-MCM-22(38)	24/32	82/97	60/68	this work
ITQ-2(24)	6/16	60/99	66	this work
H-ZSM-5(11.5)	6/16	88/98	60/61	this work
Al-TUD-1(21)	6	91	60	Chapter 4
BEA(12)	4/6	98/100	54/49	Chapter 5
BEATUD-1(34)	6/8	94/98	69/74	Chapter 5
H-Nu-6(2) (32)	6	59	28	⁶
del-Nu-6(1) (29)	6	87	46	⁶
H-Y Faujasite(15)	0.83	51	42	⁴
H-Mordenite(11)	0.83	37	33	⁴

a) The Si/Al atomic ratio of the catalyst is given in parenthesis. b) Conversion of D-xylose (C_{Xyl}) at a specified reaction times. c) 2-Furaldehyde yield (Y_{Fur}) at specified reaction times. Reaction conditions: 0.3 Wt:0.7 Tol (v/v) biphasic solvent system, 170 °C, 20 g_{cat}·dm⁻³, 0.67 M Xyl.

The reaction of Xyl was further investigated in the presence of ITQ-2(24), using the biphasic Wt:Tol solvent system at 170 °C, which gave a Y_{Fur} of 66% at 99% C_{Xyl} reached at 16 h (Figures 6.16 and 6.17). In terms of the maximum yield of Fur reached, these results were superior to those reported previously for a delaminated solid acid (denoted del-Nu-6(1)) prepared by exfoliation of the lamellar precursor Nu-6(1) (46% Y_{Fur}),⁶ comparable to a mesoporous Al-TUD-1 material (60% Y_{Fur}, Chapter 4), and lower than that for a BEATUD-1 composite (74% Y_{Fur}, Chapter 5), used as catalysts in the same reaction under similar conditions (ITQ-2(24) possessed comparatively lower catalytic activity, Table 6.3). It is difficult to establish clear structure-activity relationships between different types of aluminosilicate catalysts. The catalytic performances may be due to an interplay of different factors such as morphology, crystalline structure, porosity, surface polarity and acid properties. A common feature, however, was the apparent fairly high stability of the aluminosilicate catalysts investigated, under the applied reaction conditions (discussed in Section 6.2.2.4 for H-MCM-22 materials and ITQ-2(24)). It is worth mentioning that

these comparisons merely summarise literature data obtained under similar reaction conditions, and do not serve to “rate” the different families of catalysts (the physical-chemical properties of different types of catalysts may be optimised).

A comparison of the catalytic results for ITQ-2(24) and H-MCM-22(24) showed no major differences in terms of reaction rate (Figure 6.16): ITQ-2(24) gave an initial reaction rate of $2.0 \text{ mmol.g}_{\text{cat}}^{-1}.\text{h}^{-1}$ and a C_{Xyl} at 8 h of 78%, while H-MCM-22(24) gave $2.4 \text{ mmol.g}_{\text{cat}}^{-1}.\text{h}^{-1}$ and a C_{Xyl} of 83%. The catalytic performances of ITQ-2(24) and H-MCM-22(24) were similar despite their considerably different S_{EXT} ($611 \text{ m}^2.\text{g}^{-1}$ for ITQ-2(24) and $52 \text{ m}^2.\text{g}^{-1}$ for H-MCM-22(24) (Figure 6.17 and Table 6.1). The catalytic results correlated fairly well with the similar total concentration of AS ($[\text{L}]+[\text{B}]$) measured for the two catalysts using pyridine as probe molecule (Tables 6.2 and 6.3). The catalytic activity did not correlate with the $[\text{B}]_{\text{col}}$ which was higher for ITQ-2(24) ($153 \mu\text{mol.g}^{-1}$) than for H-MCM-22(24) ($45 \mu\text{mol.g}^{-1}$); possibly the stronger base collidine interacts with some AS which were too weak for catalysing the reaction of Xyl. The Fur yield versus Xyl conversion curves were also comparable for the two catalysts, and the Y_{Fur} reached at ca. 99% of C_{Xyl} was 71% for H-MCM-22(24) and 66% for ITQ-2(24) (Figure 6.17). Hence ITQ-2(24) stood on a similar footing to H-MCM-22(24) (the Si/Al ratio was the same for the two materials) in terms of catalytic performance in the reaction of Xyl.

A clear assessment of the location (external/internal surfaces) of the effective AS was not trivial. As mentioned in Section 6.1.1., the intrazeolite void space of the MWW pore structure is accessible through the 10-MR apertures,²⁹ and the maximum pore diameter is 5.5 \AA or 6.2 \AA based on atomic or Norman radii, respectively.²⁷ It is reported that the Xyl molecules (in which the hemiacetal isomers are predominant in solution) possess an approximate molecular diameter of 6.8 \AA ,²⁸ and the critical, maximum and kinetic diameters of Fur are reported to be 4.56 \AA , 5.99 \AA and 5.5 \AA , respectively.²⁷ Based on these data, and taking into consideration that in the liquid phase the solute molecules are solvated by the solvent, the access of Xyl (and possibly Fur) molecules to the internal surface of the MWW-type framework may be severely hindered. It has been reported for benzene as substrate and zeolite MCM-22 as catalyst that the reaction takes place essentially on the external surface.^{156,161} Molecular dynamics simulations indicated that benzene (kinetic diameter of 5.85 \AA)¹⁶² presents low diffusivity in either of the two pore systems of the MWW-type structure.¹⁶³ Assuming that the reaction of Xyl takes places essentially on the external surface of the catalysts, the similar catalytic performances of ITQ-2(24) and H-MCM-22(24) despite their considerably different S_{EXT} , may be due to weaker overall acidity in the former case (some AS may be inactive or possess relatively low intrinsic catalytic activity).

The reaction of Xyl in the presence of ITQ-2(24) at 155 °C was slower (an initial reaction rate of $0.8 \text{ mmol.g}_{\text{cat}}^{-1}.\text{h}^{-1}$) and led to a lower 55% Y_{Fur} (at 98% C_{Xyl} , reached at 24 h of reaction) than that observed at 170 °C (initial reaction rate of $2.0 \text{ mmol.g}_{\text{cat}}^{-1}.\text{h}^{-1}$; 66% Y_{Fur} at 99% C_{Xyl} , reached at 16 h reaction). For the reaction temperature of 170 °C, and at constant amount of the catalyst (ITQ-2(24)) in the reaction medium, total volume of liquid phases and catalyst/Xyl mass ratio, changing the 0.3 Wt:0.7 Tol (v/v) solvents ratio affects the yield of Fur: for a Wt:Tol of 1:1 v/v, 51% Y_{Fur} was reached at 98% C_{Xyl} and 16 h of reaction, which is lower than that observed for a Wt:Tol of 0.3:0.7 v/v, 66% Y_{Fur} .

6.2.2.2. Catalytic performance of H-MCM-22 and ITQ-2(24) using solely water as solvent

The reaction of Xyl was further investigated in the presence of ITQ-2(24) and H-MCM-22(24), using solely water as solvent (Wt), at 170 °C. The amount of the catalyst in the reaction medium, catalyst/ Xyl ratio, and the initial concentration of Xyl in water were the same for the Wt:Tol biphasic system and solely water. The kinetic profiles for ITQ-2(24) and H-MCM-22(24) were very similar until 8 h of reaction (Figure 6.18), which correlated with the similar total concentration of AS ($[L]+[B]$) for the two catalysts (Table 6.2). The yield of Fur versus Xyl conversion curves were comparable, giving 52-54% Y_{Fur} at 97% C_{Xyl} (Figure 6.19). The comparable performances for these two catalysts using the Wt system paralleled that observed for the biphasic Wt:Tol system. For the two solvent systems, at reaction times longer than 8 h, ITQ-2(24) gave slightly higher conversions than H-MCM-22(24), possibly due to slower catalyst deactivation (coking) in the former case. The maximum yields for Fur reached at high conversions of Xyl were somewhat lower when the simultaneous extraction of Fur was not performed, due to the enhanced formation of by-products (discussed in Section 6.2.2.3).

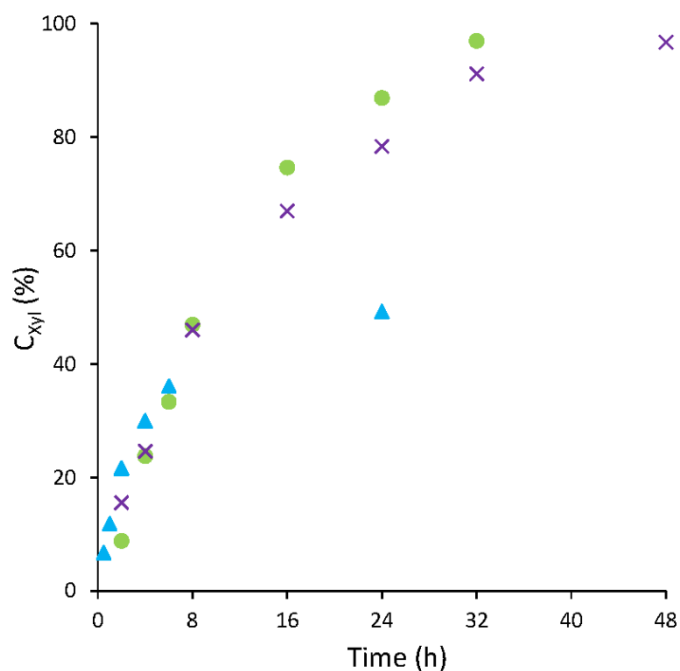


Figure 6.18- Kinetic profiles of the reaction of the conversion of D-xylose (C_{Xyl}) for H-MCM-22(24)(x), ITQ-2(24) (●) and H_2SO_4 (▲), used as catalysts. Reaction conditions: 1 cm^3 Wt or 4 mM H_2SO_4 , $170\text{ }^\circ\text{C}$, $20\text{ g}_{\text{cat}}\cdot\text{dm}^{-3}$, 0.67 M Xyl.

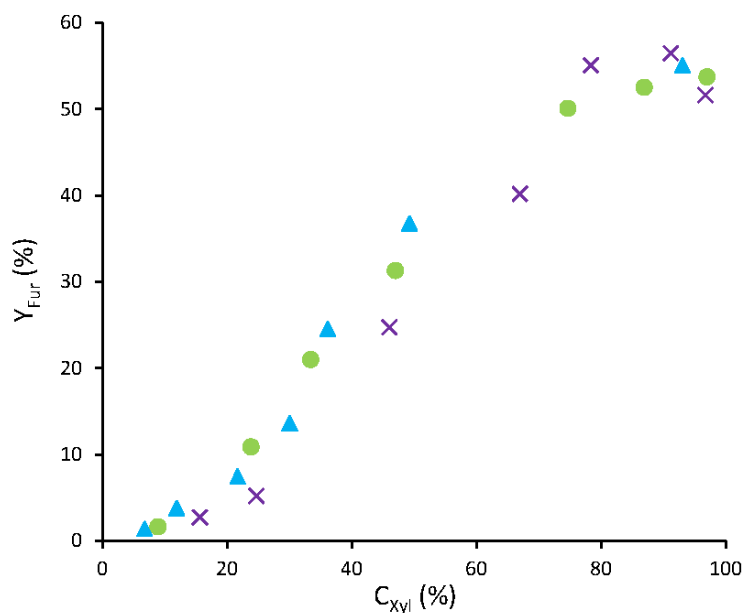


Figure 6.19- Dependence of the yield of 2-furaldehyde (Y_{Fur}) on the conversion of D-xylose (C_{Xyl}) for H-MCM-22(24) (x), ITQ-2(24) (●) and H_2SO_4 (▲), used as catalysts. Reaction conditions: 1 cm^3 Wt or 4 mM H_2SO_4 , $170\text{ }^\circ\text{C}$, $20\text{ g}_{\text{cat}}\cdot\text{dm}^{-3}$, 0.67 M Xyl. The kinetic profile for H_2SO_4 was measured until 72 h of reaction.

For comparison, the reaction of Xyl was carried out in the presence of 4 mM of H₂SO₄ as catalyst instead of the solid acids. The initial amount of liquid acid was comparable to the total amount of AS in the loaded solid acid catalysts. Although the kinetic profile until 8 h reaction was similar for H₂SO₄ and the solid acid catalysts, H₂SO₄ gave much lower conversions at longer reaction times (Figure 6.18). The pronounced retardation of the reaction of Xyl in the presence of H₂SO₄ may be due to the partial decomposition of the catalyst through its possible participation in the formation of sulfur-containing by-products,¹⁶⁴⁻¹⁶⁶ and/or to the decrease in the concentration of active Brønsted acid species due to the protonation of Fur.^{165,166} The yield of Fur versus the Xyl conversion profile for H₂SO₄ (55% Y_{Fur} at 93% C_{Xyl} at 72 h) was comparable to those for the solid acid catalysts (Figure 6.19).

6.2.2.3. Identification of the reaction products

To get insight into the type of by-products formed, the reaction of Xyl was carried out in the presence of ITQ-2(24) using D₂O as solvent at 170 °C for 24 h, and the reaction mixture was analysed by ¹H and ¹³C NMR spectroscopy, similar to that described in Chapter 5. The presence of Xyl in the reaction solution was hardly detected in the spectra (Figure 6.20), which was consistent with the catalytic results (97% C_{Xyl} at 24 h). The main peaks were relative to Fur: 9.4 (H-1'), 7.8 (H-4), 7.5 (H-2) and 6.6 ppm (H-3) in ¹H NMR; 183.6 (C-1'), 155 (C-4), 153.1 (C-1), 128.7 (C-2) and 116.2 ppm (C-3) in ¹³C NMR (Figure 6.21). Formic acid was detected (169 ppm and 8.1 ppm in the ¹³C and ¹H NMR spectra, respectively), which may be formed via the decomposition of Fur.^{5,167-169} The ¹H NMR spectrum exhibited weak to very weak signals in the range of 3-4.5 ppm which may be due to carbohydrate H-C-O or H₂C-O groups. The absence of ¹H NMR signals near 1.4 ppm and 4.3 ppm rules out the presence of significant amounts of lactic acid in the reaction solution of the reaction of Xyl with ITQ-2(24) as the catalyst, similar to that discussed in Chapter 5 for BEA tested as catalyst in the same reaction, under similar conditions. Weak peaks below 2 ppm may be assigned to methyl/methylene carbon atoms. Fragmentation reactions of Xyl can take place to form oxygenated aliphatic compounds.^{169,170}

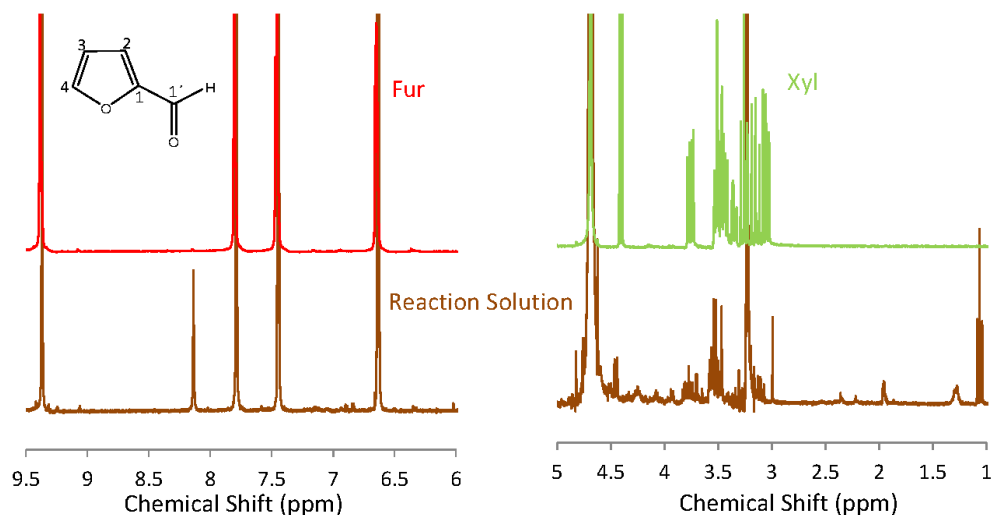


Figure 6.20- ^1H NMR spectrum of the solution obtained after separation of the solid phase from the reaction mixture of D-xylose (Xyl) in the presence of ITQ-2(24) using D_2O as solvent. The spectra of 2-furaldehyde (Fur) and D-xylose (Xyl) are given for comparison. Reaction conditions: D_2O (1 cm^3), 24 h, $170\text{ }^\circ\text{C}$, $20\text{ g}_{\text{ITQ-2}}\cdot\text{dm}^{-3}$, 0.67 M Xyl.

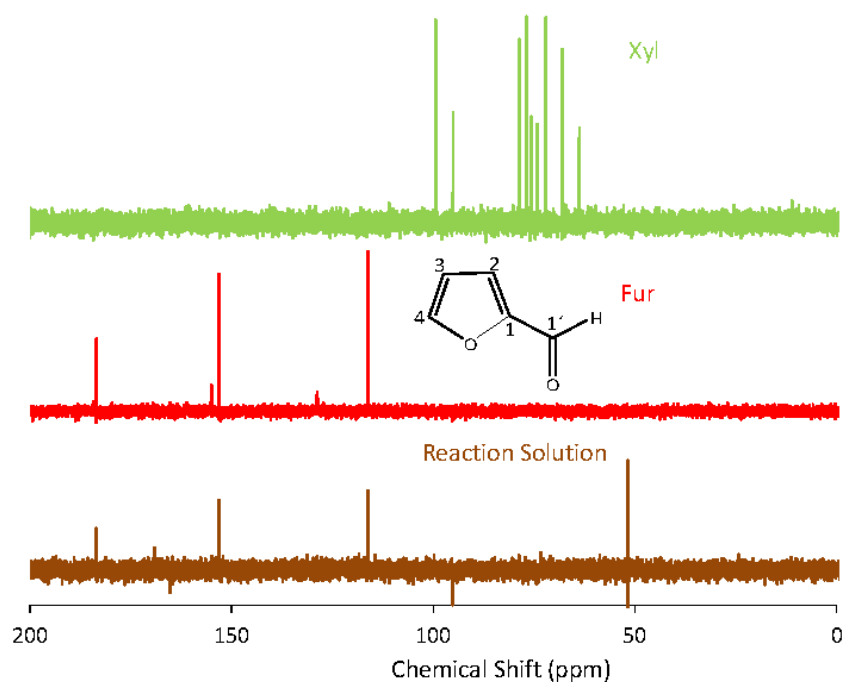


Figure 6.21- ^{13}C NMR spectrum of the reaction solution obtained after the reaction of D-xylose (Xyl) in the presence of ITQ-2(24) using D_2O as solvent. The spectra of 2-furaldehyde (Fur) and D-xylose (Xyl) are given for comparison. Reaction conditions: D_2O (1 cm^3), 8 h, $170\text{ }^\circ\text{C}$, $20\text{ g}_{\text{ITQ-2}}\cdot\text{dm}^{-3}$, 0.67 M Xyl.

Figure 6.22 summarises possible pathways involved in the formation of by-products in the conversion of Xyl to Fur.

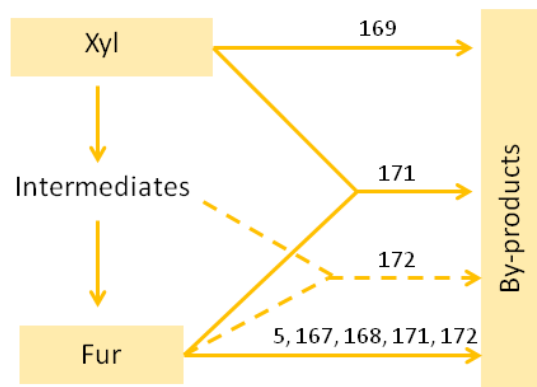


Figure 6.22- Possible pathways for the formation of by-products in the D-xylose to 2-furaldehyde reaction systems.^{5,167-169,171,172}

6.2.2.4. Catalyst stability

After at least 98% C_{xyl} was reached, the H-MCM-22(24) and ITQ-2(24) catalysts were separated from the reaction mixture by centrifugation, washed with methanol and dried at 50 °C overnight, giving pale brown powders. For each solid, the DSC analysis showed an endothermic band below 200 °C assigned to desorption of physisorbed water and strong exothermic bands above 200 °C (which were not observed for the fresh catalysts) assigned to the combustion of organic matter (Figure 6.23). The amount of organic matter in the used catalysts (measured by TGA by the weight loss in the temperature range of 220-700 °C) was similar for H-MCM-22(24) and ITQ-2(24) (ca. 12 wt.%). However, the DSC profiles were different, suggesting that the chemical nature of the carbonaceous matter was different for the two catalysts. The spectrum of by-products formed may be influenced by the [L]/[B] acid site ratio,¹⁷³ and/or textural properties (by-products may become strongly adsorbed/entrapped inside the MWW-type microporous structure). TGA analyses of H-MCM-22(24) and ITQ-2(24) catalysts revealed higher amounts of organic deposits using the solely Wt reaction system (18-21 wt.% for the solids recovered after 24 h of reaction) in comparison to the Wt:Tol one (12 wt.%). The catalytic contribution to the decomposition of Fur was minor: less than 5%, obtained in separate catalytic tests using Fur as

the substrate instead of Xyl. Hence, Fur loss reactions may be essentially due to its reaction with Xyl or intermediates of the reaction of Xyl.

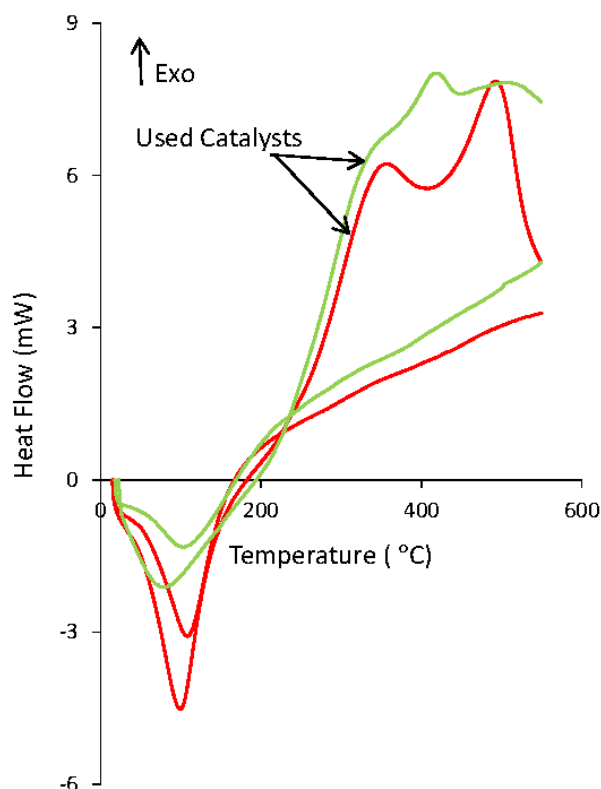


Figure 6.23- DSC curves for the as-prepared H-MCM-22(24) (green line) and ITQ-2(24) (red line) catalysts, and the respective solids recovered from the reaction of D-xylose (Xyl) after ca. 98% of conversion was reached (used catalysts). Reaction conditions: 0.3 Wt:0.7 Tol (v/v) biphasic solvent system, 170 °C, 20 $\text{g}_{\text{cat}}\cdot\text{dm}^{-3}$, 0.67 M Xyl.

The stability of the H-MCM-22(24) and ITQ-2(24) catalysts was investigated by recycling the solid acids, under biphasic solvent conditions, at 170 °C. The washing of the used catalysts with different solvents (methanol, acetone, toluene, water) failed to efficiently remove the organic matter from the catalysts. Therefore, prior to reuse, the solids were calcined at either 450 °C (ITQ-2(24)) or 550 °C (H-MCM-22(24)) for 5 h with a heating rate of 1 °C.min⁻¹ to leave a residual amount of organic matter of less than 1 wt.%. The higher temperature required (550 °C) for the complete combustion of the organic matter in the case of H-MCM-22(24) was consistent with the thermal analyses data. The yields of Fur in four consecutive 6 h batch runs were similar for H-MCM-22(24) and ITQ-2(24) (Figure 6.24). When the used H-MCM-22(24) catalyst was

treated at 450 °C instead of 550 °C, the yield of Fur decreased in recycling runs (Figure 6.24), most likely due to the incomplete removal of organic matter (the calcined solid was very light brown in colour and contained ca. 4 wt.% organic matter).

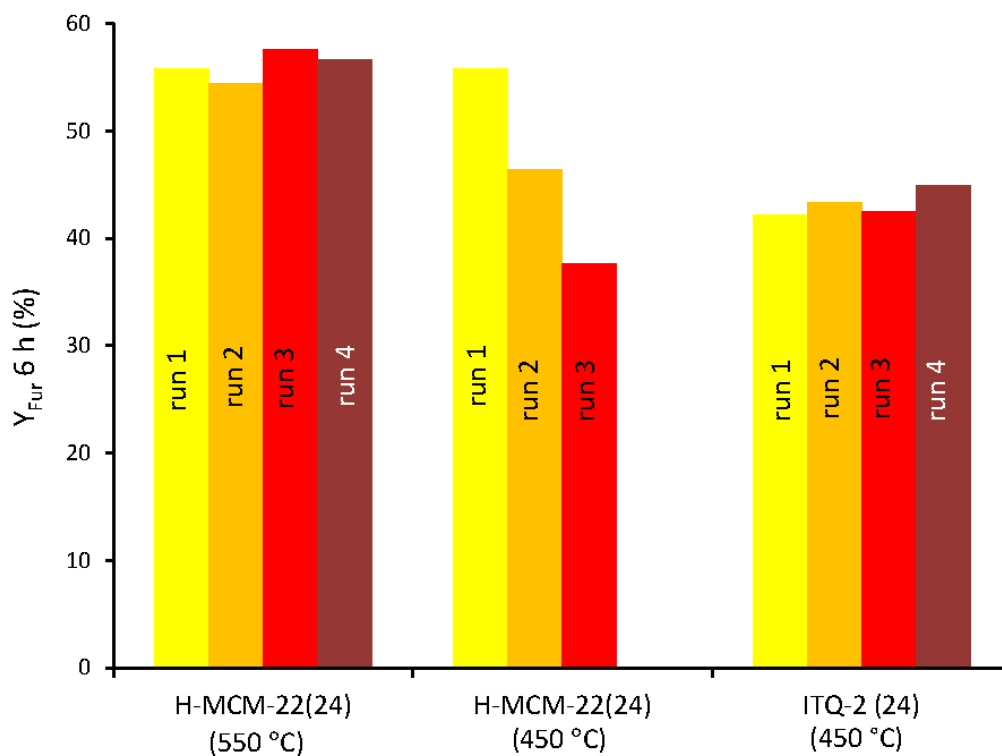


Figure 6.24- Yield of 2-furaldehyde (Y_{Fur}) in four consecutive 6 h batch runs of the reaction of D-xylose (Xyl) in the presence of regenerated catalysts H-MCM-22(24) or ITQ-2(24). Reaction conditions: 0.3 Wt:0.7 Tol (v/v) biphasic solvent system, 170 °C, 20 $\text{g}_{\text{cat}}.\text{dm}^{-3}$, 0.67 M Xyl.

The powder XRD patterns (Figure 6.5) and the Si/Al ratios (measured by ICP-AES) of the used/calcined H-MCM-22(24) and ITQ-2(24) catalysts were similar to those of the respective fresh catalysts (Si/Al=25 and 24, respectively).

6.3. Conclusions

The aqueous phase dehydration of Xyl into Fur was investigated under batch mode in the presence of H-MCM-22 zeolite or its delaminated counterpart (ITQ-2) possessing enhanced

external surface area, using a biphasic water:toluene solvent mixture or solely water as the solvent (Wt:Tol and Wt reaction system, respectively), at 170 °C. Y_{Fur} of up to 71% and 56% were reached at more than 96% of C_{Xyl} for the Wt:Tol and Wt systems, respectively for H-MCM-22(24). Sulfuric acid as catalyst (4 mM; Wt reaction system) gave comparable Y_{Fur} (55% at 93% C_{Xyl}) to H-MCM-22(24) in the Wt system (56% Y_{Fur} at 91% C_{Xyl}). Decreasing the Si/Al ratio (in the range of 38-24) of H-MCM-22, increased the total amount of ([L]+[B]), which led to an improvement in the catalytic activity, without affecting significantly the Fur selectivity. For the two Wt and Wt/Tol solvent systems, the ITQ-2(24) catalyst exhibited comparable catalytic performance to its H-MCM-22 counterpart (with the same Si/Al of 24), which correlated with the similar total amounts of [L]+[B] AS of these materials. No structural modifications or leaching phenomena were detected for the used catalysts (thermally regenerated to remove organic deposits), and the yields of Fur in consecutive batch runs are similar. A difference between H-MCM-22(24) and ITQ-2(24) was the less energy intensive conditions required for the thermal regeneration of ITQ-2(24) (450 °C compared to 550 °C for H-MCM-22(24)), which might be related with some differences in the chemical nature of the carbonaceous matter, based on DSC analyses, and an apparently slower catalyst deactivation by coking in the case of ITQ-2(24). Although the enhanced $S_{\text{EXT}}/S_{\text{BET}}$ ratio was effectively accomplished for ITQ-2(24) through the delamination procedure, a concomitant weakening of the surface acidity seemed to have occurred, which should be avoided in order to optimise the catalytic performance and take the highest value/profit possible out of the application of a more refined catalyst preparation procedure.

6.4. References

- (1) Gil, B.; Marszalek, B.; Ilnicka, A. M.; Olejniczak, Z.: The Influence of Si/Al Ratio on the Distribution of OH Groups in Zeolites with MWW Topology. *Topics in Catalysis* **2010**, *53*, 1340-1348.
- (2) Corma, A.: Inorganic Solid Acids and Their Use in Acid-Catalyzed Hydrocarbon Reactions. *Chemical Reviews* **1995**, *95*, 559-614.
- (3) Maxwell, I. E.; Stork, W. H. J.: Hydrocarbon Processing with Zeolites. In *Introduction to Zeolite Science and Practice*; H. van Bekkum, E. M. F., Jansen, J. C., Eds.; Elsevier: Studies in Surface Science and Catalysis, 1991; Vol. Volume 58; pp 571-630.
- (4) Moreau, C.; Durand, R.; Peyron, D.; Duhamet, J.; Rivalier, P.: Selective Preparation of Furfural From Xylose Over Microporous Solid Acid Catalysts. *Industrial Crops and Products* **1998**, *7*, 95-99.
- (5) O'Neill, R.; Ahmad, M. N. M.; Vanoye, L.; Aiouache, F.: Kinetics of Aqueous Phase Dehydration of Xylose Into Furfural Catalyzed by ZSM-5 Zeolite. *Industrial & Engineering Chemistry Research* **2009**, *48*, 4300-4306.

- (6) Lima, S.; Pillinger, M.; Valente, A. A.: Dehydration of D-xylose Into Furfural Catalysed by Solid Acids Derived From the Layered Zeolite Nu-6(1). *Catalysis Communications* **2008**, *9*, 2144-2148.
- (7) Rubin, M. K.; Chu, P.: Composition of Synthetic Porous Crystalline Material, its Synthesis and Use. In *United States Patent: 4,954,325*; Mobil Oil Corporation, New York, N.Y.: USA, 1990; pp 16.
- (8) Lawton, S.; Leonowicz, M. E.; Partridge, R.; Chu, P.; Rubin, M. K.: Twelve-Ring Pockets on the External Surface of MCM-22 Crystals. *Microporous and Mesoporous Materials* **1998**, *23*, 109-117.
- (9) Berlier, G.; Pourny, M.; Bordiga, S.; Spoto, G.; Zecchina, A.; Lamberti, C.: Coordination and Oxidation Changes Undergone by Iron Species in Fe-MCM-22 Upon Template Removal, Activation and Redox Treatments: an in Situ IR, and XANES Study. *Journal of Catalysis* **2005**, *229*, 45-54.
- (10) Aiello, R.; Crea, F.; Testa, F.; Demortier, G.; Lentz, P.; Wiame, M.; Nagy, J. B.: Synthesis and Characterization of Aluminosilicate MCM-22 in Basic Media in the Presence of Fluoride Salts. *Microporous and Mesoporous Materials* **2000**, *35-6*, 585-595.
- (11) Leonowicz, M. E.; Lawton, J. A.; Lawton, S. L.; Rubin, M. K.: MCM-22 - A Molecular Sieve with 2 Independent Multidimensional Channel Systems. *Science* **1994**, *264*, 1910-1913.
- (12) Čejka, J.; Krejčí, A.; Žilková, N.; Kotrla, J.; Ernst, S.; Weber, A.: Activity and Selectivity of Zeolites MCM-22 and MCM-58 in the Alkylation of Toluene with Propylene. *Microporous and Mesoporous Materials* **2002**, *53*, 121-133.
- (13) Juttu, G. G.; Lobo, R. F.: Characterization and Catalytic Properties of MCM-56 and MCM-22 Zeolites. *Microporous and Mesoporous Materials* **2000**, *40*, 9-23.
- (14) Du, H. W.; Kalyanaraman, M.; Cambor, M. A.; Olson, D. H.: Hydrocarbon Sorption Properties of Pure Silica MCM-22 Type Zeolite. *Microporous and Mesoporous Materials* **2000**, *40*, 305-312.
- (15) Degnan, T. F.; Smith, C. M.; Venkat, C. R.: Alkylation of Aromatics With Ethylene and Propylene: Recent Developments in Commercial Processes. *Applied Catalysis A-General* **2001**, *221*, 283-294.
- (16) Park, S. H.; Rhee, H. K.: Shape Selective Conversion of 1,2,4-Trimethylbenzene Over Zeolite Nu-87. *Catalysis Today* **2000**, *63*, 267-273.
- (17) Delitala, C.; Alba, M. D.; Becerro, A. I.; Delpiano, D.; Meloni, D.; Musu, E.; Ferino, I.: Synthesis of MCM-22 Zeolites of Different Si/Al Ratio and their Structural, Morphological and Textural Characterisation. *Microporous and Mesoporous Materials* **2009**, *118*, 1-10.
- (18) Pinho, P. d. S. D. d.; Silva, M. I. P. d.: Síntese e Caracterização da Zeólita MCM-22. In *VIII Congresso Brasileiro de Engenharia Química em Iniciação Científica*: Uberlândia, Minas Gerais, Brasil, 2009.
- (19) Kennedy, G. J.; Lawton, S. L.; Fung, A. S.; Rubin, M. K.; Steuernagel, S.: Multinuclear MAS NMR Studies of Zeolites MCM-22 and MCM-49. *Catalysis Today* **1999**, *49*, 385-399.
- (20) Kennedy, G. J.; Lawton, S. L.; Rubin, M. K.: ²⁹Si MAS NMR-Studies of a High-Silica Form of The Novel Molecular Sieve- MCM-22. *Journal of the American Chemical Society* **1994**, *116*, 11000-11003.
- (21) Roth, W. J.: Synthesis of Delaminated and Pillared Zeolitic Materials. In *Studies in Surface Science and Catalysis*; Čejka, J., Bekkum, v. B., Corma, C., Ferdi, S., Eds.; Elsevier, 2007; Vol. 168; pp 221-239.
- (22) Leite, R. C. N.; Sousa, B. V.; Rodrigues, M. G. F.: Caracterização e Síntese Estática da Zeólita MCM-22. In *4º Congresso Brasileiro de Pesquisa e Desenvolvimento em Petróleo e Gás*; Brazilian Association for Research and Development in Petroleum and Natural Gas: Campinas, São Paulo, Brazil, 2007.
- (23) Lawton, S. L.; Fung, A. S.; Kennedy, G. J.; Alemany, L. B.; Chang, C. D.; Hatzikos, G. H.; Lissy, D. N.; Rubin, M. K.; Timken, H. K. C.; Steuernagel, S.; Woessner, D. E.: Zeolite MCM-49: A Three-Dimensional MCM-22 Analogue Synthesized by in Situ Crystallization. *Journal of Physical Chemistry* **1996**, *100*, 3788-3798.
- (24) He, Y. J.; Nivarthi, G. S.; Eder, F.; Seshan, K.; Lercher, J. A.: Synthesis, Characterization and Cactivity of the Pillared Molecular Sieve MCM-36. *Microporous and Mesoporous Materials* **1998**, *25*, 207-224.
- (25) Diaz, U.; Fornes, V.; Corma, A.: On the Mechanism of Zeolite Growing: Crystallization by Seeding with Delayed Zeolites. *Microporous and Mesoporous Materials* **2006**, *90*, 73-80.
- (26) IZA-SC-members: Zeolite Framework Types. Database of Zeolite Structures, 2012; Vol. 2012.
- (27) Jae, J.; Tompsett, G. A.; Foster, A. J.; Hammond, K. D.; Auerbach, S. M.; Lobo, R. F.; Huber, G. W.: Investigation Into the Shape Selectivity of Zeolite Catalysts for Biomass Conversion. *Journal of Catalysis* **2011**, *279*, 257-268.

- (28) Sjöman, E.; Mänttari, M.; Nyström, M.; Koivikko, H.; Heikkilä, H.: Separation of Xylose from Glucose by Nanofiltration From Concentrated Monosaccharide Solutions. *Journal of Membrane Science* **2007**, *292*, 106-115.
- (29) Corma, A.; Fornes, V.; Pergher, S. B.; Maesen, T. L. M.; Buglass, J. G.: Delaminated Zeolite Precursors as Selective Acidic Catalysts. *Nature* **1998**, *396*, 353-356.
- (30) Corma, A.; Fornes, V.; Triguero, J. M.; Pergher, S. B.: Delaminated Zeolites: Combining the Benefits of Zeolites and Mesoporous Materials for Catalytic Uses. *Journal of Catalysis* **1999**, *186*, 57-63.
- (31) Corma, A.; Diaz, U.; Fornes, V.; Guil, J. M.; Triguero, J. M.; Creighton, E. J.: Characterization and Catalytic Activity of MCM-22 and MCM-56 Compared With ITQ-2. *Journal of Catalysis* **2000**, *191*, 218-224.
- (32) Canos, A. C.; Segui, V. F.; Pergher, S.: Oxide Materials and Catalyst Compositions Containing Them. In *World Intellectual Property Organization: WO 97/17290*; Shell Internationale Research Maatschappij B. V., The Netherlands: Spain, 1997; pp 32.
- (33) Roth, W. J.; Kresge, C. T.; Vartuli, J. C.; Leonowicz, M. E.; Fung, A. S.; McCullen, S. B.: MCM-36: The First Pillared Molecular Sieve with Zeolite Properties. In *Studies in Surface Science and Catalysis*; Beyer, H. K., Kiricsi, H. G. K. I., Nagy, J. B., Eds.; Elsevier, 1995; Vol. 94; pp 301-308.
- (34) Mochida, I.; Eguchi, S.; Hironaka, M.; Nagao, S.; Sakanishi, K.; Whitehurst, D. D.: The Effects of Seeding in the Synthesis of Zeolite MCM-22 in The Presence of Hexamethylenimine. *Zeolites* **1997**, *18*, 142-151.
- (35) Corma, A.; Fornés, V.; Guil, J. M.; Pergher, S.; Maesen, T. L. M.; Buglass, J. G.: Preparation, Characterisation and Catalytic Activity of ITQ-2, a Delaminated Zeolite. *Microporous and Mesoporous Materials* **2000**, *38*, 301-309.
- (36) Aguilar, J.; Pergher, S. B. C.; Detoni, C.; Corma, A.; Melo, F. V.; Sastre, E.: Alkylation of Biphenyl with Propylene Using MCM-22 and ITQ-2 Zeolites. *Catalysis Today* **2008**, *133*, 667-672.
- (37) Maheshwari, S.; Jordan, E.; Kumar, S.; Bates, F. S.; Penn, R. L.; Shantz, D. F.; Tsapatsis, M.: Layer Structure Preservation During Swelling, Pillaring, and Exfoliation of a Zeolite Precursor. *Journal of the American Chemical Society* **2008**, *130*, 1507-1516.
- (38) Canos, A. C.; Segui, V. F.; Pergher, S. B. C.: Oxide Materials and Catalyst Compositions Containing Them. In *United States Patent: US 6,231,751 B1*; Universidad Politecnica de Valencia, Spain: USA, 2001; pp 8.
- (39) Narkhede, V. V.; Gies, H.: Crystal Structure of MCM-22 (MWW) and Its Delaminated Zeolite ITQ-2 from High-Resolution Powder X-Ray Diffraction Data: An Analysis Using Rietveld Technique and Atomic Pair Distribution Function. *Chemistry of Materials* **2009**, *21*, 4339-4346.
- (40) Corma, A.; Fornes, V.; Rey, F.: Delaminated Zeolites: An Efficient Support for Enzymes. *Advanced Materials* **2002**, *14*, 71-74.
- (41) Concepcion, P.; Lopez, C.; Martinez, A.; Puentes, V. E.: Characterization and Catalytic Properties of Cobalt Supported on Delaminated ITQ-6 and ITQ-2 Zeolites for the Fischer-Tropsch Synthesis Reaction. *Journal of Catalysis* **2004**, *228*, 321-332.
- (42) Schenkel, R.; Barth, J. O.; Kornatowski, J.; Lercher, J. A.: Chemical and Structural Aspects of the Transformation of the MCM-22 Precursor Into ITQ-2. In *Impact of Zeolites and Other Porous Materials on the New Technologies at the Beginning of the New Millennium, Pts a and B*; Aiello, R., Giordano, G., Testa, F., Eds., 2002; Vol. 142; pp 69-76.
- (43) Frontera, P.; Testa, F.; Aiello, R.; Candamano, S.; Nagy, J. B.: Transformation of MCM-22(P) into ITQ-2: The Role of Framework Aluminium. *Microporous and Mesoporous Materials* **2007**, *106*, 107-114.
- (44) Laredo, G. C.; Jesus Castillo, J.; Bolaños, J. N.; Romo, P. P.; Lagos, F. A.: Benzene Reduction in Gasoline by Alkylation With Olefins: Comparison of Beta and MCM-22 Catalysts. *Applied Catalysis A-General* **2012**, *413*, 140-148.
- (45) Jiang, T.; Zhang, Q.; Wang, T.-J.; Zhang, Q.; Ma, L.-L.: High Yield of Pentane Production by Aqueous-Phase Reforming of Xylitol Over Ni/HZSM-5 and Ni/MCM22 Catalysts. *Energy Conversion and Management* **2012**, *59*, 58-65.
- (46) Yang, S.-T.; Kim, J.-Y.; Kim, J.; Ahn, W.-S.: CO₂ Capture Over Amine-Functionalized MCM-22, MCM-36 and ITQ-2. *Fuel* **2012**, *97*, 435-442.
- (47) Wang, X.; Dai, W.; Wu, G.; Li, L.; Guan, N.; Hunger, M.: Phosphorus Modified HMCM-22: Characterization and Catalytic Application in Methanol-to-Hydrocarbons Conversion. *Microporous and Mesoporous Materials* **2012**, *151*, 99-106.

- (48) Oliveira, A. M. d.; Pergher, S. B. C.; Moro, C. C.; Baibich, I. M.: Nitric Oxide Decomposition on Copper Supported on Zeolites. *Química Nova* **2004**, *27*, 226-230.
- (49) Mihalyi, R. M.; Kollar, M.; Kiraly, P.; Karoly, Z.; Mavrodinova, V.: Effect of Extra-Framework Al Formed by Successive Steaming and Acid Leaching of Zeolite MCM-22 on its Structure and Catalytic Performance. *Applied Catalysis A-General* **2012**, *417*, 76-86.
- (50) Goergen, S.; Fayad, E.; Laforge, S.; Magnoux, P.; Rouleau, L.; Patarin, J.: Synthesis of Layered MCM-22(P) in the Presence of Hexamethonium Cations and its Transformation into EUO- and MWW-Type Zeolites. *J Porous Mater* **2011**, *18*, 639-650.
- (51) Wang, J.; Tu, X.; Hua, W.; Yue, Y.; Gao, Z.: Role of the Acidity and Porosity of MWW-Type Zeolites in Liquid-Phase Reaction. *Microporous and Mesoporous Materials* **2011**, *142*, 82-90.
- (52) Miltenburg, A. v.; Menorval, L. C. d.; Stocker, M.: Characterization of the Pore Architecture Created by Alkaline Treatment of HMC22 Using ¹²⁹Xe NMR Spectroscopy. *Catalysis Today* **2011**, *168*, 57-62.
- (53) Makita, K.; Hirota, Y.; Egashira, Y.; Yoshida, K.; Sasaki, Y.; Nishiyama, N.: Synthesis of MCM-22 Zeolite Membranes and Vapor Permeation of Water/Acetic Acid Mixtures. *Journal of Membrane Science* **2011**, *372*, 269-276.
- (54) Xu, L.; Xing, H.; Wu, S.; Guan, J.; Jia, M. J.; Kan, Q.: Synthesis, Characterization and Catalytic Performance of a Novel Zeolite ITQ-2-Like by Treating MCM-22 Precursor with H₂O₂. *Bulletin of Materials Science* **2011**, *34*, 1605-1610.
- (55) Kollár, M.; Kolev, I.; Mihályi, M. R.; Mavrodinova, V.: Transformations of Alkyl Aromatics Over Delaminated MCM-22 Zeolites and Their Composites With Mesoporous MCM-41 Silicate. *Applied Catalysis A-General* **2011**, *393*, 59-70.
- (56) Wang, J.; Jaenicke, S.; Chuah, G. K.; Hua, W.; Yue, Y.; Gao, Z.: Acidity and Porosity Modulation of MWW Type Zeolites for Nopol Production by Prins Condensation. *Catalysis Communications* **2011**, *12*, 1131-1135.
- (57) Yang, J.; Yang, J. Y.; Zhou, Y.; Wei, F.; Lin, W. G.; Zhu, J. H.: Hierarchical Functionalized MCM-22 Zeolite for Trapping Tobacco Specific Nitrosamines (TSNAs) in Solution. *Journal of Hazardous Materials* **2010**, *179*, 1031-1036.
- (58) Fernández, M. B.; Sánchez M, J. F.; Tonetto, G. M.; Damiani, D. E.: Hydrogenation of sunflower oil over different palladium supported catalysts: Activity and selectivity. *Chemical Engineering Journal* **2009**, *155*, 941-949.
- (59) Liu, X.; Li, Y.; Chen, B.; Liu, Y.: Preparation Self-Bonded Zeolite MCM-22 Bodies by Vapor-Phase Transport Method. *J Porous Mater* **2009**, *16*, 745-748.
- (60) Freire, R. M.; Batista, A. H. M. d.; Filho, A. G. S. d.; Filho, J. M.; Saraiva, G. D.; Oliveira, A. C.: High Catalytic Activity of Nitrogen-Containing Carbon from Molecular Sieves in Fine Chemistry. *Catalysis Letters* **2009**, *131*, 135-145.
- (61) Miltenburg, A. v.; Pawlesa, J.; Bouzga, A. M.; Žilková, N.; Čejka, J.; Stöcker, M.: Alkaline Modification of MCM-22 to a 3D Interconnected Pore System and its Application in Toluene Disproportionation and Alkylation. *Topics in Catalysis* **2009**, *52*, 1190-1202.
- (62) Li, Y.; Xue, B.; He, X.: Synthesis of Ethylbenzene by Alkylation of Benzene with Diethyl Carbonate Over Parent MCM-22 and Hydrothermally Teated MCM-22. *Journal of Molecular Catalysis A-Chemical* **2009**, *301*, 106-113.
- (63) Wu, Y.; Ren, X.; Wang, J.: Facile Synthesis and Morphology Control of Zeolite MCM-22 Via a Two-Step Sol-Gel Route With Tetraethyl Orthosilicate as Silica Source. *Materials Chemistry and Physics* **2009**, *113*, 773-779.
- (64) Xue, B.; Li, Y.; Deng, L.: Selective Synthesis of p-Xylene by Alkylation of Toluene With Dimethyl Carbonate Over MgO-Modified MCM-22. *Catalysis Communications* **2009**, *10*, 1609-1614.
- (65) Liu, X.; Li, Y.; Chen, B.; Niu, T.: In Situ Preparation of Self-Bonded Zeolite MCM-22 Bodies By Vapor-Phase Transport Method. *Journal of Materials Science* **2009**, *44*, 3211-3217.
- (66) Xu, G.; Zhu, X.; Niu, X.; Liu, S.; Xie, S.; Li, X.; Xu, L.: One-Pot Synthesis of High Silica MCM-22 Zeolites and Their Performances in Catalytic Cracking of 1-Butene to Propene. *Microporous and Mesoporous Materials* **2009**, *118*, 44-51.
- (67) Wu, Y.; Ren, X.; Wang, J.: Effect of Microwave-Assisted Aging on the Static Hydrothermal Synthesis of Zeolite MCM-22. *Microporous and Mesoporous Materials* **2008**, *116*, 386-393.

- (68) Wu, Y.; Ren, X.; Lu, Y.; Wang, J.: Crystallization and Morphology of Zeolite MCM-22 Influenced by Various Conditions in the Static Hydrothermal Synthesis. *Microporous and Mesoporous Materials* **2008**, *112*, 138-146.
- (69) Mihályi, R. M.; Lázár, K.; Kollár, M.; Lónyi, F.; Pál-Borbély, G.; Szegedi, A.: Structure, Acidity and Redox Properties of MCM-22 Ferrisilicate. *Microporous and Mesoporous Materials* **2008**, *110*, 51-63.
- (70) Shang, Y.; Yang, P.; Jia, M.; Zhang, W.; Wu, T.: Modification of MCM-22 Zeolites With Silylation Agents: Acid Properties and Catalytic Performance for the Skeletal Isomerization of n-Butene. *Catalysis Communications* **2008**, *9*, 907-912.
- (71) Srinivasu, P.; Vinu, A.; Hishita, S.; Sasaki, T.; Ariga, K.; Mori, T.: Preparation and Characterization of Novel Microporous Carbon Nitride With Very High Surface Area Via Nanocasting Technique. *Microporous and Mesoporous Materials* **2008**, *108*, 340-344.
- (72) Kumar, G. S.; Saravanamurugan, S.; Hartmann, M.; Palanichamy, M.; Murugesan, V.: Synthesis, Characterisation and Catalytic Performance of H-MCM-22 of Different Silica to Alumina Ratios. *Journal of Molecular Catalysis A-Chemical* **2007**, *272*, 38-44.
- (73) Inagaki, S.; Kamino, K.; Kikuchi, E.; Matsukata, M.: Shape Selectivity of MWW-Type Aluminosilicate Zeolites in the Alkylation of Toluene with Methanol. *Applied Catalysis A-General* **2007**, *318*, 22-27.
- (74) Yang, P.; Shang, Y.; Yu, J.; Wang, J.; Zhang, M.; Wu, T.: One-Step Synthesis of Methyl Isobutyl Ketone From Acetone Over Pd/MCM-22 Zeolites. *Journal of Molecular Catalysis A-Chemical* **2007**, *272*, 75-83.
- (75) Kollár, M.; Mihályi, R. M.; Borbely, G. P.; Valyon, J.: Micro/Mesoporous Aluminosilicate Composites From Zeolite MCM-22 Precursor. *Microporous and Mesoporous Materials* **2007**, *99*, 37-46.
- (76) Vuono, D.; Pasqua, L.; Testa, F.; Aiello, R.; Fonseca, A.; Koranyi, T. I.; Nagy, J. B.: Influence of NaOH and KOH on the Synthesis of MCM-22 and MCM-49 Zeolites. *Microporous and Mesoporous Materials* **2006**, *97*, 78-87.
- (77) Albuquerque, A.; Marchese, L.; Lisi, L.; Pastore, H. O.: V,Al -MCM-22: A Novel Acid/Redox Bifunctional Molecular Sieve. *Journal of Catalysis* **2006**, *241*, 367-377.
- (78) Liu, L.; Ma, D.; Chen, H. Y.; Zheng, H.; Cheng, M. J.; Xu, Y. D.; Bao, X. H.: Methane Dehydroaromatization on Mo/HMCM-22 Catalysts: Effect of SiO₂/Al₂O₃ ratio of HMCM-22 zeolite supports. *Catalysis Letters* **2006**, *108*, 25-30.
- (79) Xia, J. C.; Mao, D. S.; Tao, W. C.; Chen, Q. L.; Zhang, Y. H.; Tang, Y.: Dealumination of H-MCM-22 by Various Methods and its Application in One-Step Synthesis of Dimethyl Ether From Syngas. *Microporous and Mesoporous Materials* **2006**, *91*, 33-39.
- (80) Zhu, X. X.; Liu, S. L.; Song, Y. Q.; Xu, L. Y.: Post-Treatment With Ammonium Hexafluoro Silicate: An Effective Way to Synthesize High Silica MCM-22 Zeolite. *Catalysis Communications* **2005**, *6*, 742-746.
- (81) Ravishankar, R.; Li, M. M.; Borgna, A.: Novel Utilization of MCM-22 Molecular Sieves as Supports of Cobalt Catalysts in the Fischer-Tropsch Synthesis. *Catalysis Today* **2005**, *106*, 149-153.
- (82) Laforge, S.; Ayrault, P.; Manin, D.; Guisnet, M.: Acidic and Catalytic Properties of MCM-22 and MCM-36 Zeolites Synthesized From the Same Precursors. *Applied Catalysis A-General* **2005**, *279*, 79-88.
- (83) Dumitriu, E.; Meloni, D.; Monaci, R.; Solinas, V.: Liquid-Phase Alkylation of Phenol With t-Butanol Over Various Catalysts Derived From MWW-Type Precursors. *Comptes Rendus Chimie* **2005**, *8*, 441-456.
- (84) Han, B.; Lee, S. H.; Shin, C. H.; Cox, P. A.; Hong, S. B.: Zeolite Synthesis Using Flexible Diquaternary Alkylammonium Ions (C_nH_{2n+1})₂HN+(CH₂)₅N+H(C_nH_{2n+1})₂ with n=1-5 as structure-directing agents. *Chemistry of Materials* **2005**, *17*, 477-486.
- (85) Yang, P. P.; Yu, J. F.; Wang, Z. L.; Xu, M. P.; Liu, Q. S.; Wu, T. H.: Synthesis, Characterization of MCM-22 and Catalytic Activity in One-Step Synthesis of Methyl Isobutyl Ketone. *Reaction Kinetics and Catalysis Letters* **2005**, *84*, 129-135.
- (86) Miao, S. J.; Liu, L.; Lian, Y. X.; Zhu, X. X.; Zhou, S. T.; Wang, Y.; Bao, X. H.: On the Reactivity of Mo Species for Methane Partial Oxidation on Mo/H-MCM-22 Catalysts. *Catalysis Letters* **2004**, *97*, 209-215.
- (87) Tsai, C. C.; Zhong, C. Y.; Wang, I.; Liu, S. B.; Chen, W. H.; Tsai, T. C.: Vapor Phase Beckmann Rearrangement of Cyclohexanone Oxime Over MCM-22. *Applied Catalysis A-General* **2004**, *267*, 87-94.

- (88) Pergher, S. B. C.; Corma, A.; Fornes, V.: Preparation and Characterization of MCM-22 Zeolite and its Layered Precursor. *Quimica Nova* **2003**, *26*, 795-802.
- (89) Dumitriu, E.; Secundo, F.; Patarin, J.; Fehete, L.: Preparation and Properties of Lipase Immobilized on MCM-36 Support. *Journal of Molecular Catalysis B-Enzymatic* **2003**, *22*, 119-133.
- (90) Balkus, K. J.; Gbery, G.; Deng, Z. S.: Preparation of Partially Oriented Zeolite MCM-22 Membranes Via Pulsed Laser Deposition. *Microporous and Mesoporous Materials* **2002**, *52*, 141-150.
- (91) Okumura, K.; Hashimoto, M.; Mimura, T.; Niwa, M.: Acid Properties and Catalysis of MCM-22 With Different Al Concentrations. *Journal of Catalysis* **2002**, *206*, 23-28.
- (92) Shu, Y. Y.; Ma, D.; Xu, L. Y.; Xu, Y. D.; Bao, X. H.: Methane Dehydro-Aromatization Over Mo/MCM-22 Catalysts: A Highly Selective Catalyst For the Formation of Benzene. *Catalysis Letters* **2000**, *70*, 67-73.
- (93) Martínez, A.; Valencia, S.; Murciano, R.; Cerqueira, H. S.; Costa, A. F.; Aguiar, E. S. F.: Catalytic Behavior of Hybrid CO/SiO₂-(Medium Pore) Zeolite Catalysts During the One-Stage Conversion of Syngas to Gasoline. *Applied Catalysis A-General* **2008**, *346*, 117-125.
- (94) Ma, D.; Deng, F.; Fu, R. Q.; Dan, X. W.; Bao, X. H.: MAS MMR Studies on the Dealumination of Zeolite MCM-22. *Journal of Physical Chemistry B* **2001**, *105*, 1770-1779.
- (95) Kumar, N.; Lindfors, L. E.: Synthesis, Characterization and Application of H-MCM-22, Ga-MCM-22 and Zn-MCM-22 Zeolite Catalysts in the Aromatization of n-Butane. *Applied Catalysis A-General* **1996**, *147*, 175-187.
- (96) Ravishankar, R.; Bhattacharya, D.; Jacob, N. E.; Sivasanker, S.: Characterization and Catalytic Properties of Zeolite MCM-22. *Microporous Materials* **1995**, *4*, 83-93.
- (97) Corma, A.; Corell, C.; Fornes, V.; Kolodziejski, W.; Perezpariente, J.: Infrared Spectroscopy, Thermoprogrammed Desorption, and Nuclear Magnetic Resonance Study of the Acidity, Structure, and Stability of Zeolite MCM-22. *Zeolites* **1995**, *15*, 576-582.
- (98) Ravishankar, R.; Sen, T.; Sivasanker, S.; Ganapathy, S.: Multinuclear MAS NMR Spectroscopic Study of the Zeolite MCM-22. *Journal of the Chemical Society-Faraday Transactions* **1995**, *91*, 3549-3552.
- (99) Jung, H. J.; Park, S. S.; Shin, C.-H.; Park, Y.-K.; Hong, S. B.: Comparative Catalytic Studies on the Conversion of 1-Butene and n-Butane to Isobutene Over MCM-22 and ITQ-2 Zeolites. *Journal of Catalysis* **2007**, *245*, 65-74.
- (100) Liu, B. J.; Huo, H. J.; Meng, Q. M.; Gao, S. S.: Synthesis of ITQ-2 Zeolite Under Static Conditions and Its Properties. *Science in China Series B-Chemistry* **2006**, *49*, 148-154.
- (101) Ogino, I.; Nigra, M. M.; Hwang, S.-J.; Ha, J.-M.; Rea, T.; Zones, S. I.; Katz, A.: Delamination of Layered Zeolite Precursors under Mild Conditions: Synthesis of UCB-1 via Fluoride/Chloride Anion-Promoted Exfoliation. *Journal of the American Chemical Society* **2011**, *133*, 3288-3291.
- (102) Dahlhoff, G.; Barsnick, U.; Holderich, W. F.: The Use of MCM-22 as Catalyst for the Beckmann Rearrangement of Cyclohexanone Oxime to Epsilon-Caprolactam. *Applied Catalysis A-General* **2001**, *210*, 83-95.
- (103) Wu, P.; Kan, Q. B.; Wang, D. Y.; Xing, H. J.; Jia, M. J.; Wu, T. H.: The Synthesis of Mo/H-MCM-36 Catalyst and its Catalytic Behavior in Methane Non-Oxidative Aromatization. *Catalysis Communications* **2005**, *6*, 449-454.
- (104) Unverricht, S.; Hunger, M.; Ernst, S.; Karge, H. G.; Weitkamp, J.: *Zeolite MCM-22-Synthesis, Dealumination and Structural Characterization*, 1994; Vol. 84.
- (105) Wu, Y.; Ren, X.; Lu, Y.; Wang, J.: Rapid Synthesis of Zeolite MCM-22 by Acid-Catalyzed Hydrolysis of Tetraethylorthosilicate. *Materials Letters* **2008**, *62*, 317-319.
- (106) Niu, X. L.; Song, Y. Q.; Xie, S. J.; Liu, S. L.; Wang, Q. X.; Xu, L. Y.: Synthesis and Catalytic Reactivity of MCM-22/Z-SM-35 Composites for Olefin Aromatization. *Catalysis Letters* **2005**, *103*, 211-218.
- (107) Mokrzycki, L.; Sulikowski, B.; Olejniczak, Z.: Properties of Desilicated ZSM-5, ZSM-12, MCM-22 and ZSM-12/MCM-41 Derivatives in Isomerization of Alpha-Pinene. *Catalysis Letters* **2009**, *127*, 296-303.
- (108) Matias, P.; Lopes, J. M.; Laforge, S.; Magnoux, P.; Guisnet, M.; Ramôa Ribeiro, F.: n-Heptane Transformation Over a H-MCM-22 Zeolite: Catalytic Role of the Pore Systems. *Applied Catalysis A: General* **2008**, *351*, 174-183.

- (109) Yang, J.; Zhou, Y.; Yang, J. Y.; Lin, W. G.; Wu, Y. J.; Lin, N.; Wang, J.; Zhu, J. H.: Capturing Nitrosamines by Zeolite MCM-22: Effect of Zeolite Structure and Morphology on Adsorption. *Journal of Physical Chemistry C* **2010**, *114*, 9588-9595.
- (110) Corma, A.; Corell, C.; Perezpariente, J.: Synthesis and Characterization of the MCM-22 Zeolite. *Zeolites* **1995**, *15*, 2-8.
- (111) Delitala, C.; Cadoni, E.; Delpiano, D.; Meloni, D.; Melis, S.; Ferino, I.: Liquid-Phase Thiophene Adsorption on MCM-22 Zeolite and Activated Carbon. *Microporous and Mesoporous Materials* **2008**, *110*, 197-215.
- (112) Smiešková, A.; Hudec, P.; Kumar, N.; Salmi, T.; Murzin, D. Y.; Jorík, V.: Aromatization of Methane on Mo Modified Zeolites: Influence of the Surface and Structural Properties of the Carriers. *Applied Catalysis A-General* **2010**, *377*, 83-91.
- (113) Kim, S. J.; Jung, K. D.; Joo, O. S.: Synthesis and Characterization of Gallosilicate Molecular Sieve With the MCM-22 Framework Topology. *J Porous Mater* **2004**, *11*, 211-218.
- (114) Prieto, G.; Martínez, A.; Concepción, P.; Tost, R. M.: Cobalt Particle Size Effects in Fischer-Tropsch Synthesis: Structural and in Situ Spectroscopic Characterisation on Reverse Micelle-Synthesised Co/ITQ-2 Model Catalysts. *Journal of Catalysis* **2009**, *266*, 129-144.
- (115) Burgess, C. G. V.; Everett, D. H.; Nuttall, S.: Adsorption Hysteresis in Porous Materials. *Pure and Applied Chemistry* **1989**, *61*, 1845-1852.
- (116) Gregg, S. J.; Sing, K. S. W.: *Adsorption, Surface Area, and Porosity*; 2nd ed.; Academic Press: London, 1982.
- (117) Sing, K. S. W.; Everett, D. H.; Haul, R. A. W.; Moscou, L.; Pierotti, R. A.; Rouquerol, F.; Siemieniowska, T.: Reporting Physisorption Data for Gas/Solid Systems With Special Reference to the Determination of Surface Area and Porosity (IUPAC Recommendations 1984). *Pure and Applied Chemistry* **1985**, *57*, 603-619.
- (118) Rouquerol, J.; Avnir, D.; Fairbridge, C. W.; Everett, D. H.; Haynes, J. H.; Pernicone, N.; Ramsay, J. D. F.; Sing, K. S. W.; Unger, K. K.: Recommendations for the Characterization of Porous Solids. *Pure and Applied Chemistry* **1994**, *66*, 1739-1758.
- (119) Rouquerol, F.; Rouquerol, J.; Sing, K.: *Adsorption by Powders and Porous Solids: Principles, Methodology and Applications*; Academic Press: San Diego, USA, 1998.
- (120) Russo, P. A.; Carrott, M. M. L. R.; Carrott, P. J. M.; Matias, P.; Lopes, J. M.; Guisnet, M.; Ribeiro, F. R.: Characterisation by Adsorption of Various Organic Vapours of the Porosity of Fresh and Coked H-MCM-22 Zeolites. *Microporous and Mesoporous Materials* **2009**, *118*, 473-479.
- (121) Huet, M. A. S.; Guenneau, F.; Gedeon, A.; Corma, A.: Probing Xe Exchange in Delaminated Zeolites by Hyperpolarized ¹²⁹Xe NMR. *Journal of Physical Chemistry C* **2007**, *111*, 5694-5700.
- (122) Barth, J. O.; Jentys, A.; Kornatowski, J.; Lercher, J. A.: Control of Acid-Base Properties of New Nanocomposite Derivatives of MCM-36 by Mixed Oxide Pillaring. *Chemistry of Materials* **2004**, *16*, 724-730.
- (123) Climent, M. J.; Corma, A.; Iborra, S.: Synthesis of Nonsteroidal Drugs With Anti-Inflammatory and Analgesic Activities With Zeolites and Mesoporous Molecular Sieve Catalysts. *Journal of Catalysis* **2005**, *233*, 308-316.
- (124) Climent, M. J.; Corma, A.; Velty, A.: Synthesis of Hyacinth, Vanilla, and Blossom Orange Fragrances: the Benefit of Using Zeolites and Delaminated Zeolites as Catalysts. *Applied Catalysis A-General* **2004**, *263*, 155-161.
- (125) Martinez, A.; Peris, E.; Sastre, G.: Dehydroaromatization of Methane Under Non-Oxidative Conditions Over Bifunctional Mo/ITQ-2 Catalysts. *Catalysis Today* **2005**, *107-08*, 676-684.
- (126) Fernandes, L. D.; Monteiro, J. L. F.; Aguiar, E. F. S.; Martinez, A.; Corma, A.: Ethylbenzene Hydroisomerization Over Bifunctional Zeolite Based Catalysts: The Influence of Framework and Extraframework Composition and Zeolite Structure. *Journal of Catalysis* **1998**, *177*, 363-377.
- (127) Ma, D.; Zhu, Q. J.; Wu, Z. L.; Zhou, D. H.; Shu, Y. Y.; Xin, Q.; Xu, Y. D.; Bao, X. H.: The Synergic Effect Between Mo Species and Acid Sites in Mo/H-MCM-22 Catalysts for Methane Aromatization. *Physical Chemistry Chemical Physics* **2005**, *7*, 3102-3109.
- (128) Bevilacqua, M.; Meloni, D.; Sini, F.; Monaci, R.; Montanari, T.; Busca, G.: A Study of the Nature, Strength, and Accessibility of Acid Sites of H-MCM-22 Zeolite. *Journal of Physical Chemistry C* **2008**, *112*, 9023-9033.

- (129) Nguyen, C. T.; Kim, D. P.; Hong, S. B.: Delaminated Zeolite Catalysed Synthesis of High-Molecular Weight Polycarbosilane as a Low Shrinkage SiC Precursor. *Journal of Polymer Science Part A-Polymer Chemistry* **2008**, *46*, 725-732.
- (130) Lacarriere, A.; Luck, F.; Świerczyński, D.; Fajula, F.; Hulea, V.: Methanol to Hydrocarbons Over Zeolites With MWW Topology: Effect of Zeolite Texture and Acidity. *Applied Catalysis A-General* **2011**, *402*, 208-217.
- (131) Dragoi, B.; Rakic, V.; Dumitriu, E.; Auroux, A.: Adsorption of Organic Pollutants Over Microporous Solids Investigated by Microcalorimetry Techniques. *Journal of Thermal Analysis and Calorimetry* **2010**, *99*, 733-740.
- (132) Tian, L.; Li, J.; Li, Y.; Chen, B.: Synthesis of Dodecylbenzene With Benzene and 1-Dodecene Over MCM-22 Zeolite Modified With Phosphorus. *Chinese Journal of Catalysis* **2008**, *29*, 889-894.
- (133) Mao, D.; Xia, J.; Chen, Q.; Lu, G.: Highly Effective Conversion of Syngas to Dimethyl Ether Over the Hybrid Catalysts Containing High-Silica HMCM-22 Zeolites. *Catalysis Communications* **2009**, *10*, 620-624.
- (134) Galletero, M. S.; Corma, A.; Ferrer, B.; Fornés, V.; García, H.: Confinement Effects at the External Surface of Delaminated Zeolites (ITQ-2): An Inorganic Mimic of Cyclodextrins. *Journal of Physical Chemistry B* **2003**, *107*, 1135-1141.
- (135) Corma, A.; Fornés, V.; Galletero, M. S.; García, H.; García, C. J. G.: Prevalence of the External Surface Over the Internal Pores in the Spontaneous Generation of Tetrathiafulvalene Radical Cation Incorporated in the Novel Delaminated ITQ-2 Zeolite. *Physical Chemistry Chemical Physics* **2001**, *3*, 1218-1222.
- (136) Corma, A.; Martínez, A.; Soria, V. M.: Catalytic Performance of the New Delaminated ITQ-2 Zeolite for Mild Hydrocracking and Aromatic Hydrogenation Processes. *Journal of Catalysis* **2001**, *200*, 259-269.
- (137) Chica, A.; Sayas, S.: Effective and Stable Bioethanol Steam Reforming Catalyst Based on Ni and Co Supported on All-Silica Delaminated ITQ-2 Zeolite. *Catalysis Today* **2009**, *146*, 37-43.
- (138) Gómez, M. V.; Cantín, A.; Corma, A.; Hoz, A. d. I.: Use of Different Microporous and Mesoporous Materials as Catalyst in the Diels-Alder and Retro-Diels-Alder Reaction Between Cyclopentadiene and p-Benzoquinone Activity of Al-, Ti- and Sn-Doped Silica. *Journal of Molecular Catalysis A-Chemical* **2005**, *240*, 16-21.
- (139) Baleizão, C.; Gigante, B.; Sabater, M. J.; García, H.; Corma, A.: On the Activity of Chiral Chromium Salen Complexes Covalently Bound to Solid Silicates for the Enantioselective Epoxide Ring Opening. *Applied Catalysis A-General* **2002**, *228*, 279-288.
- (140) Hunger, M.; Ernst, S.; Weitkamp, J.: Multinuclear Solid State NMR Investigation of Zeolite MCM-22. *Zeolites* **1995**, *15*, 188-192.
- (141) Lippmaa, E.; Samoson, A.; Magi, M.: High Resolution Aluminum ²⁷ NMR of Aluminosilicates. *Journal of the American Chemical Society* **1986**, *108*, 1730-1735.
- (142) Meriaudeau, P.; Tuel, A.; Vu, T. T. H.: On the Localization of Tetrahedral Aluminum in MCM-22 Zeolite. *Catalysis Letters* **1999**, *61*, 89-92.
- (143) Song, K.; Guan, J.; Wu, S.; Kan, Q.: Synthesis and Characterization of Strong Acidic Mesoporous Aluminosilicates Constructed of Zeolite MCM-22 Precursors. *Catalysis Communications* **2009**, *10*, 631-634.
- (144) Song, K.; Guan, J.; Wu, S.; Yang, Y.; Liu, B.; Kan, Q.: Alkylation of Phenol with tert-Butanol Catalyzed by Mesoporous Material with Enhanced Acidity Synthesized from Zeolite MCM-22. *Catalysis Letters* **2008**, *126*, 333-340.
- (145) Ma, D.; Han, X. W.; Zhou, D. H.; Yan, Z. M.; Fu, R. Q.; Xu, Y.; Bao, X. H.; Hu, H. B.; Au-Yeung, S. C. F.: Towards Guest-Zeolite Interactions: An NMR Spectroscopic Approach. *Chemistry-A European Journal* **2002**, *8*, 4557-4561.
- (146) Ma, D.; Han, X. W.; Xie, S. J.; Bao, X. H.; Hu, H. B.; Au-Yeung, S. C. F.: An Investigation of the Roles of Surface Aluminum and Acid Sites in the Zeolite MCM-22. *Chemistry-A European Journal* **2002**, *8*, 162-170.
- (147) Ma, D.; Shu, Y. Y.; Han, X. W.; Liu, X. M.; Xu, Y. D.; Bao, X. H.: Mo/HMCM-22 Catalysts for Methane Dehydroaromatization: A multinuclear MAS NMR Study. *Journal of Physical Chemistry B* **2001**, *105*, 1786-1793.

- (148) Yu, Z.; Wang, Q.; Chen, L.; Deng, F.: Brønsted/Lewis Acid Sites Synergy in H-MCM-22 Zeolite Studied by ^1H and ^{27}Al DQ-MAS NMR Spectroscopy. *Chinese Journal of Catalysis* **2012**, *33*, 129-139.
- (149) Guisnet, M.; Ayrault, P.; Coutanceau, C.; Alvarez, M. F.; Datka, J.: Acid Properties of Dealuminated Beta Zeolites Studied by IR Spectroscopy. *Journal of the Chemical Society-Faraday Transactions* **1997**, *93*, 1661-1665.
- (150) Corma, A.; Fornes, V.; Melo, F. V.; Monton, J. B.; Orchilles, A. V.: Catalytic Cracking of a Vacuum Gas Oil and n-Heptane on H-Beta Zeolites With Different Si/Al Ratios. *Abstr. Pap. Am. Chem. Soc.* **1987**, *194*, 14-PETR.
- (151) Corma, A.; Fornes, V.; Melo, F.; Perezpariente, J.: Zeolite Beta Structure, Activity, and Selectivity for Catalytic Cracking. *American Chemical Society Symposium Series* **1988**, *375*, 49-63.
- (152) Lami, E. B.; Massiani, P.; Drenzo, F.; Espiau, P.; Fajula, F.; Courieres, T. D.: Study of the State of Aluminium in Zeolite Beta. *Applied Catalysis* **1991**, *72*, 139-152.
- (153) Maache, M.; Janin, A.; Lavalley, J. C.; Joly, J. F.; Benazzi, E.: Acidity of Zeolites Beta Dealuminated by Acid Leaching- An FT-IR Study Using Different Probe Molecules (Pyridine, Carbon Monoxide). *Zeolites* **1993**, *13*, 419-426.
- (154) Dimitrova, R.; Gunduz, G.; Dimitrov, L.; Tsoncheva, T.; Yalmaz, S.; Gonzalez, E. A.: Acidic Sites in Beta Zeolites in Dependence of the Preparation Methods. *Journal of Molecular Catalysis A-Chemical* **2004**, *214*, 265-268.
- (155) Meloni, D.; Martin, D.; Ayrault, P.; Guisnet, M.: Influence of Carbonaceous Deposits on the Acidity of a Zeolite With Two Non-Interconnected Pore Systems: MCM-22. *Catalysis Letters* **2001**, *71*, 213-217.
- (156) Du, H. W.; Olson, D. H.: Surface Acidic Properties of a H-MCM-22 Zeolite: Collidine Poisoning and Hydrocarbon Adsorption Studies. *Journal of Physical Chemistry B* **2002**, *106*, 395-400.
- (157) Nesterenko, N. S.; Thibault-Starzyk, F.; Montouillout, V.; Yushchenko, V. V.; Fernandez, C.; Gilson, J. P.; Fajula, F.; Ivanova, I.: The Use of the Consecutive Adsorption of Pyridine Bases and Carbon Monoxide in the IR Spectroscopic Study of the Accessibility of Acid Sites in Microporous/Mesoporous Materials. *Kinetics and Catalysis* **2006**, *47*, 40-48.
- (158) Grandberg, I. I.; Faizova, G. K.; Kost, A. N.: Comparative Basicities of Substituted Pyridines and Electronegativity Series for Substituents in the Pyridine Series. *Khimiya Geterotsiklicheskikh Soedinenii* **1966**, *2*, 561-566.
- (159) Moreau, C.: Zeolites and Related Materials for the Food and Non Food Transformation of Carbohydrates. *Agro Food Industry Hi-Tech* **2002**, *13*, 17-26.
- (160) Brujin, J. M. d.: Monosaccharides in Alkaline Medium: Isomerization, Degradation, Oligomerization. University of Technology, Delft, The Netherlands, 1986.
- (161) Corma, A.; Soria, V. M.; Schnoefeld, E.: Alkylation of Benzene With Short-Chain Olefins Over MCM-22 Zeolite: Catalytic Behaviour and Kinetic Mechanism. *Journal of Catalysis* **2000**, *192*, 163-173.
- (162) Talu, O.; Guo, C. J.; Hayhurst, D. T.: Heterogeneous Adsorption Equilibria With Comparable Molecule and Pore Sizes. *Journal of Physical Chemistry* **1989**, *93*, 7294-7298.
- (163) Sastre, G.; Catlow, C. R. A.; Corma, A.: Diffusion of Benzene and Propylene in MCM-22 Zeolite. A Molecular Dynamics Study. *Journal of Physical Chemistry B* **1999**, *103*, 5187-5196.
- (164) Gilbert, E. E.; Jones, E. P.: Sulfonation and Sulfation. *Industrial and Engineering Chemistry* **1961**, *53*, 501-507.
- (165) Frost, J. W.; Bui, V.: Sulfonation of Polyhydroxyaromatics. In *International Application Published Under the Patent Cooperation Treaty (PCT): WO 2011/022588 A1*; Draths Corporation, Science Parkway, Okemos, MI, USA: USA, 2011; pp 13.
- (166) Frost, J.; Bul, V.: Sulfonation of Polyhydroxyaromatics. In *United States Patent Application Publication: US 2011/0046412 A1*; Draths Corporation, Okemos, MI, USA: USA, 2011; pp 5.
- (167) Williams, D. L.; Dunlop, A. P.: Kinetics of Furfural Destruction in Acidic Aqueous Media. *Industrial and Engineering Chemistry* **1948**, *40*, 239-241.
- (168) Dunlop, A. P.: Furfural Formation and Behavior. *Industrial and Engineering Chemistry* **1948**, *40*, 204-209.
- (169) Antal, M. J.; Leesomboon, T.; Mok, W. S.; Richards, G. N.: Kinetic Studies of the Reactions of Ketoses and Aldoses in Water at High Temperature 3-Mechanism of Formation of 2-Furaldehyde from D-Xylose. *Carbohydrate Research* **1991**, *217*, 71-85.

(170) Bonn, G.; Rinderer, M.; Bobleter, O.: Hydrothermal Degradation and Kinetic Studies of 1,3-Dihydroxy-2-Propane and 2,3-Dihydroxypropanal. *Journal of Carbohydrate Chemistry* **1985**, *4*, 67-77.

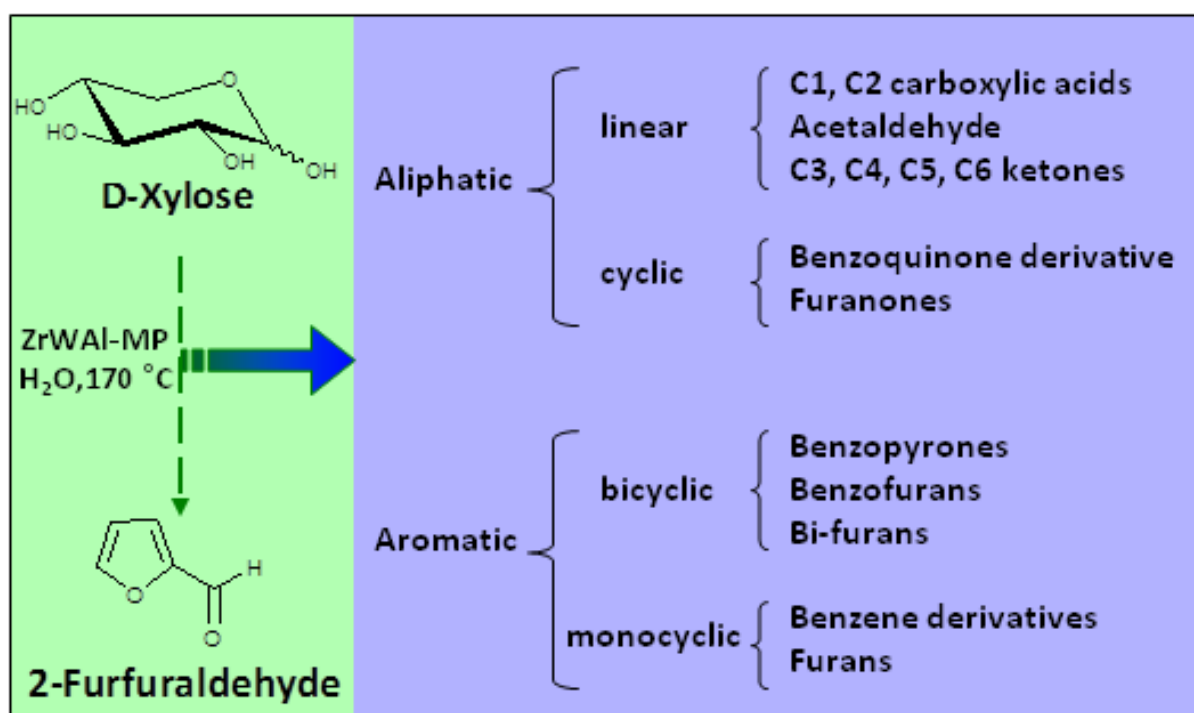
(171) Weingarten, R.; Cho, J.; Conner, W. C., Jr.; Huber, G. W.: Kinetics of Furfural Production by Dehydration of Xylose in a Biphasic Reactor With Microwave Heating. *Green Chemistry* **2010**, *12*, 1423-1429.

(172) Zeitsch, K. J.: *The Chemistry and Technology of Furfural and its Many By-Products*; 1st ed.; Elsevier Science B. V.: Amsterdam, The Netherlands, 2000; Vol. 13.

(173) Weingarten, R.; Tompsett, G. A.; Conner, W. C. J.; Huber, G. W.: Design of Solid Acid Catalysts for Aqueous-Phase Dehydration of Carbohydrates: The Role of Lewis and Brønsted Acid Sites. *Journal of Catalysis* **2011**, *279*, 174-182.

CHAPTER 7

Reaction of D-xylose in the presence of mixed zirconium tungsten oxides



Index

CHAPTER 7	307
Reaction of D-xylose in the presence of mixed zirconium tungsten oxides	307
7.1. Introduction	309
7.1.1. Mixed zirconium-tungsten materials, ZrW(X) (X=Cl, NO ₃) and ZrWAl	310
7.2. Results and discussion.....	312
7.2.1. Catalyst characterisation.....	312
7.2.2. Catalytic dehydration of D-xylose	322
7.2.2.1. Catalytic performance of ZrW(X), ZrW-MP and ZrWAl-MP materials	322
7.2.2.2. Identification of the reaction products	324
7.2.2.3. Catalyst stability	331
7.3. Conclusions	334
7.4. References.....	335

7.1. Introduction

The complex mechanism for the dehydration of D-xylose involves a series of elementary steps, and it may be accompanied by several types of undesirable side reactions (e.g. fragmentation of Xyl and reactions of Fur with other products or with itself).¹⁻¹¹ The understanding of the influence of the acid and textural properties of porous solids on the catalytic reaction is not straightforward. Due to the complex reaction systems (many types of side reactions may occur, leading to complex mixtures of by-products), each elementary step may depend differently on the catalytic properties of porous solids. The development of new solid acid catalysts has been essential to replace homogeneous catalysts (disadvantages described in Chapter 1), and other solid acids that present certain limitations. For example, the small pores (< 2 nm) of zeolites make them difficult to use in reactions that involve the use of high molecular weight components.¹² Sulfated zirconia catalysts, known as super acids, become deactivated during reactions (release of volatile sulfur containing pollutants).^{13,14} Solid acids based on supported metal oxides such as tungstated zirconia (ZrW) are potential candidates to replace mineral acids, or sulfated zirconia, which are harmful to the environment.¹⁵⁻¹⁷ Although ZrW is much less active than sulfated zirconia, it offers a very important advantage as the WO_x units in ZrW are much more stable than sulfate groups in sulfated zirconia at high temperatures and in reductive atmospheres.¹⁸ ZrW materials are almost 100% selective for branched alkanes and undergo only slow deactivation,¹⁹ which is not irreversible when the catalyst is properly prepared.²⁰ ZrW was very active for isomerisation of C4 and C8 alkanes.²¹⁻²³ Recently, Weingarten et al.,⁶ in a comparative study using different types of solid acids as catalysts in the aqueous-phase dehydration of Xyl, reported that a commercial zirconium-tungsten mixed oxide catalyst (XZO 1251, MEL Chemicals, WO_3 content of 15 wt.%), with relatively high concentration of Lewis acid sites, was more active (and less selective to Fur) than an amorphous (mainly Brønsted type) zirconium phosphate catalyst, and less active than Brønsted microporous H-Y zeolite (Si/Al=30) in Fur loss reactions (strong adsorption and subsequent decomposition of Fur on the catalyst's microporous surface).⁶ A specific family of catalysts may be focused on to help establish structure-activity relationships by modifying the physicochemical properties. ZrW catalysts have attracted interest, presenting an advantage over heteropolytungstates in that they retain structural integrity during high temperature oxidative treatments (> 600 °C), in contrast with heteropolytungstates that decompose to bulk WO_3 at much lower temperatures (400 °C).²⁴ In this

sense, in this Chapter mixed zirconium tungsten oxides pre-prepared by co-condensation (ZrW(X), X=NO₃, Cl; X is related to the type of zirconium precursor), or impregnation (with or without aluminium) on mesophases of mesoporous zirconia (ZrW-MP, ZrWAl-MP), were investigated as solid acid catalysts in the aqueous phase dehydration of Xyl into Fur, at 170 °C.

7.1.1. Mixed zirconium-tungsten materials, ZrW(X) (X=Cl, NO₃) and ZrWAl

Zirconium-tungsten mixed oxides (ZrW) are fairly stable (thermally and chemically),^{21,22} versatile solid acid catalysts and several types are commercially available. The tungsten atoms in the surface of zirconium-tungsten oxides may be octahedrally coordinated,²⁵ interconnected via W-O-W bridges,^{25,26} or anchored to the support by W-O-Zr bonds.²⁵ Tungstated zirconias were first discovered in 1988 by Hino and Arata,^{21,27} as strong solid acids, and demonstrated to be active catalysts at low-temperature (30-50 °C). Since then, these types of materials have received much attention, due to the good combination of activity and selectivity in acid catalysed reactions,^{16,18,21,28-30} and particular interest arose in the catalysis literature due to their industrial application for converting C4-C8 paraffins to highly branched species that upgrade the gasoline octane number.^{21,22,29,31-39} The good correlation between activity and selectivity can be explained as a consequence of balanced surface acid properties, density of acid sites (AS),⁴⁰⁻⁴⁴ and high thermal stability.^{16,18,20,22,24,25,30,39,42,43,45-49} 12-Tungstophosphoric acid (H₃PW₁₂O₄₀) and ZrW present the strongest acid sites among tungsten oxide-based materials.²⁴ For ZrW materials, it is accepted that the strong acidity is due to the strong interaction between zirconia and tungstate (WO₃ species on ZrO₂ support surfaces create strongly acidic sites^{18,21-23,25}) or by the presence of ZrW clusters.^{17,18} XRD patterns indicated that distorted octahedral W⁶⁺ species dominate on the ZrO₂ surface,^{23,50} and UV-vis spectra demonstrated that WO₃ domain sizes increase with loading.²³ WO₃ clusters formed on ZrW materials have the ability to delocalise negative charges (caused by the slight reduction of W⁶⁺ centers) among several surface oxygen atoms, which allows hydrogen atoms in OH surface groups and hydrocarbons to interact, retaining the cationic character.^{16,24,25,30,42,43,45,46} The temporary negative charge imbalance might lead to the formation of Brönsted acid centers on the support (WO₃)_m, [W⁶⁻ⁿO₃] [n-H⁺] (Figure 7.1).²⁴ The formation of B acid sites by H₂ requires L acid sites in the form of W⁶⁺ centers within neutral WOx domains. These L acid sites can be titrated by H atoms to produce active Brönsted acid sites.⁴³ Several authors

had confirmed the presence of Lewis acid sites on these materials by infrared studies of adsorbed ammonia and pyridine.^{18,51,52} A balance between Brønsted and Lewis acidity may be required for a high activity.^{22,47,48}

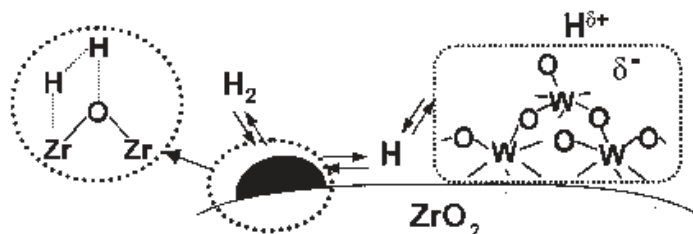


Figure 7.1- Mechanism for the formation of Brønsted acid site.⁴³

ZrW(X) materials are used in different types of catalytic reactions, including dehydrations, such as those of 2-butanol,^{42,53} tert-butanol,⁵⁴ methanol,^{30,53,55} 1-propanol and 2-propanol,⁵⁴ 2-propenol,⁵⁶ and of glycerol to acrolein.⁵⁷⁻⁶⁵ The acid-base behaviour of solids is a crucial parameter in a catalytic reaction.²⁸ Structure-activity relationships of ZrW-type materials have also been applied in the study of different types of acid-catalysed reactions (the textural and acid properties of ZrW(X) materials may be finely tuned through different synthetic approaches/conditions). The acidity of these types of oxides depends on various parameters after the preparation procedures such as the nature of the precursors, precipitation procedures, concentration of dopant, and calcination temperature.^{48,66,67} Galano et al.²⁸ found that the Lewis acidity of the ZrW system decreases with the W loading which was consistent with their theoretical calculations.²⁸ Not all the Brønsted acid sites in the WO_3 domain are equally acidic. The sites at the edge of the domain are the most acidic ones. In that study of Galano et al.²⁸, the Brønsted (B) acidity also decreased with the increase in the number of units in the polymeric domains, as the B acid sites disappear due to the condensation phenomenon of superficial tungstate monomeric species.²⁸ Despite the extensive research on the active AS, the methods to improve the activity of ZrW catalysts still need to be developed. One disadvantage is the low surface area of ZrO_2 ($< 100 \text{ m}^2 \cdot \text{g}^{-1}$) in catalytic reactions, especially liquid phase reactions.

In the case of the dehydration of Xyl into Fur, it may be advantageous to prepare mesoporous versions (denoted MP) of ZrW catalysts with enhanced amounts of effective AS and higher surface area, similar to other procedures.¹⁷ Catalyst preparation approaches in this

direction can involve using a templating agent (for generating mesoporosity) and/or doping the catalyst with aluminium (attempting to enhance acidity).^{68,69}

7.2. Results and discussion

7.2.1. Catalyst characterisation

In this Chapter ZrW(X) (X=Cl, NO₃) materials were prepared by the co-precipitation method as reported in the literature (Chapter 2).⁷⁰ The mesoporous ZrW-MP and ZrWAl-MP materials were prepared via incipient wetness impregnation on a pre-prepared templated zirconium hydroxide support which was prepared by following the procedure described by Ciesla et al.⁷¹ (a surfactant-based synthesis).

The elemental composition and specific surface area (S_{BET}) of the prepared catalysts are given in Table 7.1.

The semi-quantitative analyses of the crystalline phases were performed using the Reference Intensity Ratio (RIR) method applied to the XRD data of the prepared materials (Figure 7.2). The RIR method is based upon scaling all diffraction data to the diffraction of standard reference materials. The intensity of a diffraction peak is a combination of many factors, which by using the RIR method are scaled to a common reference and reduced to a constant, with the exception of concentration of the analyte. The scale factor is determined by equation 7.1.

$$\frac{\text{Intensity (Analyte)}}{\text{Intensity (Reference)}} = \frac{I}{I_r} = \frac{(\mu \times \gamma \times \rho_r)}{(\mu_r \times \gamma_r \times \rho)} \quad (7.1)$$

in which μ is the linear attenuation coefficient, γ is the absolute scale factor and ρ is the density of crystalline phase. The subscript r corresponds to the reference. The variables in the equation 7.1 are calculated by single crystal determinations from atomic and unit cell parameters with the use of atomic scattering factors and published constants.⁷² Experimentally, I/I_r can be determined by taking the ratio of the strongest line of the pattern to the intensity of the strongest line of the reference in a 50/50 weight mixture. The fraction of phase a, X_a , can be calculated by applying the equation 7.2.

$$I_{ia} = \frac{K_{ia} \times X_a}{\rho_a \times \mu_a} \quad (7.2)$$

in which I_{ia} is the intensity of reflection i of phase a , K_{ia} contains structure factor, multiplicity, Lorentz-polarisation factor, temperature factor and scale factor for reflection i of phase a , ρ_a is the density of phase a , and μ_a is the linear attenuation coefficient of phase a . The variables K_{ia} , ρ_a and μ_a are calculated by single crystal determinations from atomic and unit cell parameters. In an alternatively way, Reddy et al.⁷³ reported that the percent composition of each phase could be calculated from the Gaussian areas $h \times w$ in which h is height and w is the width at half-height as described in equations 7.3 and 7.4:

$$\% \text{Monoclinic} = \frac{\sum (h \times w)_{\text{monoclinic}}}{\sum (h \times w)_{\text{monoclinic and tetragonal}}} \quad (7.3)$$

$$\% \text{Tetragonal} = \frac{\sum (h \times w)_{\text{tetragonal}}}{\sum (h \times w)_{\text{monoclinic and tetragonal}}} \quad (7.4)$$

The ZrW(X) materials were composed predominantly of tetragonal zirconia (t-ZrO₂) and contained ca. 20 wt.% of (thermodynamically stable) monoclinic zirconia (m-ZrO₂). The ZrO₂ material prepared for comparison was predominantly monoclinic (contains 8 wt.% of t-ZrO₂). These results are in agreement with the literature data for the bulk ZrO₂ (monoclinic),⁷³⁻⁷⁷ and ZrW(X) type materials (tetragonal).^{22,31,73,74,76-78}

When tungsten is incorporated, the monoclinic phase tends to disappear due to stabilisation of the tetragonal phase.^{16,30,54,69,76,79-81} Only t-ZrO₂ was detected for the ZrW-MP and ZrWAl-MP materials, similar to that reported previously for ZrWAl materials.^{31,69,82} For all prepared materials no crystalline phases of WO_x were detected.¹⁶

Table 7.1- Elemental composition and specific surface area of the prepared materials ZrW(Cl), ZrW(NO₃), ZrW-MP, ZrWAl-MP and bulk ZrO₂.

Sample	Calcination Temperature (°C)	Crystalline (wt.%)		W/Zr	S _{BET} (m ² .g ⁻¹)	D _p (nm)	Ref.
		m-ZrO ₂	t-ZrO ₂				
ZrW(Cl) ^a	800	19 ^f	81 ^f	0.11 (0.10) ^h	48	17 ^h	this work
ZrW(NO ₃) ^a	800	23 ^f	77 ^f	0.09 ^h	51	-	this work
ZrW _{3.6}	650	-	-	-	54	-	¹⁸
ZrW _{8.6}	825	-	-	-	46	-	¹⁸
ZrW _{10.5}	825	-	-	-	46	-	¹⁸
ZrW _{13.6}	825	-	-	-	42	-	¹⁸

ZrW _{5.1} (OH) ^b	600	-	-	-	52	-	30
ZrW _{10.1} (OH) ^b	800	-	-	-	42	-	30
ZrW ₁₅ (OH) ^b	800	-	-	-	46	-	30
ZrW _{19.5} (OH) ^b	800	-	-	-	48	-	30
ZrW _{23.3} (OH) ^b	800	-	-	-	43	-	30
ZrW _{26.6} (OH) ^b	700	-	-	-	57	-	30
ZrW _{11.3} (OH) ^b	800	26 ^g	74 ^g	-	66	23 ⁱ	83
ZrW ₁₀ (NO ₃) ^a	900	-	-	-	56	15 ^h	31
ZrW ₁₀ (NO ₃) ^a	950	-	-	-	49	15 ^h	31
ZrW ₁₈ (NO ₃) ^a	850	-	-	-	57	15 ^h	31
ZrW ₁₈ (NO ₃) ^a	900	-	-	-	47	15 ^h	31
ZrW ^b	500	-	-	-	53	-	80
ZrW ^b	800	-	-	-	36	2 ^h	84
ZrW _{10.6} ^b	800	-	-	-	51	-	85
ZrW _{18.2} ^b	800	-	-	-	48	-	85
ZrWSi ^b	800	-	-	-	44	-	86
Zr-W ^b	800	-	-	-	44	4-18 ^j	78
ZrW ₁₀ ^b	825	-	-	-	54	3 ^h	87
ZrW ₁₂ ^b	825	-	-	-	51	3 ^h	87
ZrW ^b	850	-	-	-	54	-	88
ZrW ^b	650	32	68	-	35	-	77
Zr ₆₃ W _{15.5} ^a	500	-	-	0.25 ⁱ	62	5	22
ZrW ₆ ^b	650	-	-	-	63	-	89
ZrW ^b	650	-	-	-	64	-	73
ZrW-MP ^b	800	0 ^f	100 ^f	0.10 (0.13) ^h	102	4.5 ^h	this work
ZrW ₁₅ ^b	470	-	-	-	70	-	74
ZrW _{10.5}	650	-	-	-	82	-	18
ZrW _{13.6}	650	-	-	-	88	-	18
ZrW _{19.0}	650	-	-	-	96	-	18
ZrW _{10.1} (OH) ^b	500	-	-	-	89	-	30
ZrW ₁₅ (OH) ^b	500	-	-	-	96	-	30
ZrW _{19.5} (OH) ^b	600	-	-	-	91	-	30
ZrW _{26.6} (OH) ^b	500	-	-	-	98	-	30
ZrW _{23.3} (OH) ^b	500	-	-	-	113	-	30
ZrW ₁₀ ^b	700	-	-	-	89	8 ^h	31
ZrW _{19.8} ^c	700	-	-	-	91	-	76
ZrW ₁₀ ^b	700	-	-	-	100	8 ^h	31
ZrW ₁₂ ^b	700	-	-	-	105	-	90
ZrW ₁₈ ^b	700	-	-	-	101	-	90
Zr _{1.0} W _{7.5} Si	800	-	-	-	107	>2 ^h	84
ZrW _{19.6} ^c	600	-	-	-	121	-	76
ZrW ₁₀ ^d	500	-	-	-	130	3 ^h	87
ZrW ₁₀ Si ₂₀ ^b	800	-	-	-	94	9-10 ^j	91
ZrW ₁₄ Si ₂₀ ^b	800	-	-	-	89	9-10 ^j	91
ZrW ₅ -MP ^e	550	-	-	-	477	5.5 ^j	17
ZrW-MP	nf	-	-	1.03	275	3.7 ^h	92
ZrWAl-MP ^b	800	0 ^f	100 ^f	0.09 (0.07) ^j	133	3.8 ^h	this work
ZrW _{7.91} Al _{1.34} ^b	630	-	-	-	134	3.1	69
ZrWAl ^{a, b}	650	-	-	-	114	-	82

ZrW _{27.4} AlSi ^b	nf	-	-	-	126	5.8 ^k	93
ZrO ₂	800	92 ^f	8 ^f	-	12	-	this work
ZrO ₂	800	-	-	-	8	-	94
ZrO ₂	800	-	-	-	12	-	84
ZrO ₂	700	-	-	-	12	-	90
ZrO ₂	470	-	-	-	16	-	74
ZrO ₂	1025	-	-	-	18	-	18
ZrO ₂	800	-	-	-	18	-	85
ZrO ₂	nf	-	-	-	57-60	-	80

a) Synthesised by co-precipitation. b) Synthesised by impregnation. c) Synthesised by ion-exchange. d) Activated by temperature. e) Synthesised by condensation. f) Semi-quantitative analyses of the constituent crystalline phases (monoclinic zirconia, m-ZrO₂; tetragonal zirconia, t-ZrO₂) determined by Reference Intensity Ratio (RIR) method applied to the XRD data. g) Semi-quantitative analyses of the constituent crystalline phases (monoclinic zirconia, m-ZrO₂; tetragonal zirconia, t-ZrO₂) determined by Rietveld method. h) Surface atomic ratio of W/Zr determined by EDX. Values in brackets are for the bulk elemental analyses using ICP-AES. i) W/Zr determined by elemental analysis. j) (W+Al)/Zr=0.15 (EDX) or 0.14 (ICP-AES). h) Maximum pore diameter (D_p) by BJH equation from the adsorption branch of the isotherm. i) Medium pore diameter. j) Average pore size distribution. k) Calculated by XRD lines at ca. 50° 2θ.

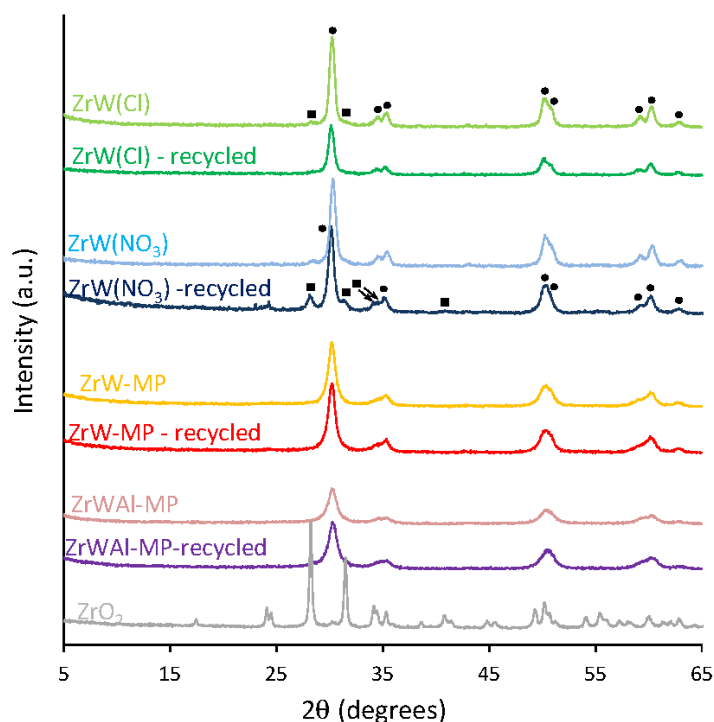


Figure 7.2- XRD patterns of the unused and recycled catalysts. For ZrW(Cl) and ZrW(NO₃) the main peaks of the ZrO₂ crystalline phases are marked as (■) m-ZrO₂ and (●) t-ZrO₂.

The SEM images showed that the ZrW(X) materials were composed of particles (ca. 1-50 μm size) with irregular morphologies, and the mesoporous materials (ZrW-MP and ZrWAl-MP) consisted of spherical particles with ca. 3 μm diameters (Figure 7.3). SEM-EDX and chemical mapping showed fairly homogeneous dispersions of Zr, W and Al (in the case of ZrWAl-MP), and

the atomic ratio W/Zr was ca. 0.1 for all the prepared materials (Figure 7.3 and Table 7.1). In the case of ZrWAl-MP the atomic ratio (W+Al)/Zr was 0.15 (Al/W=0.07). The bulk atomic ratios measured by ICP-AES were comparable to those obtained by EDX (Table 7.1), further supporting fairly homogeneous dispersions of the constituent elements (W, Zr, Al), and consistent with the absence of crystalline WO_x phases in the XRD patterns of all the prepared materials.

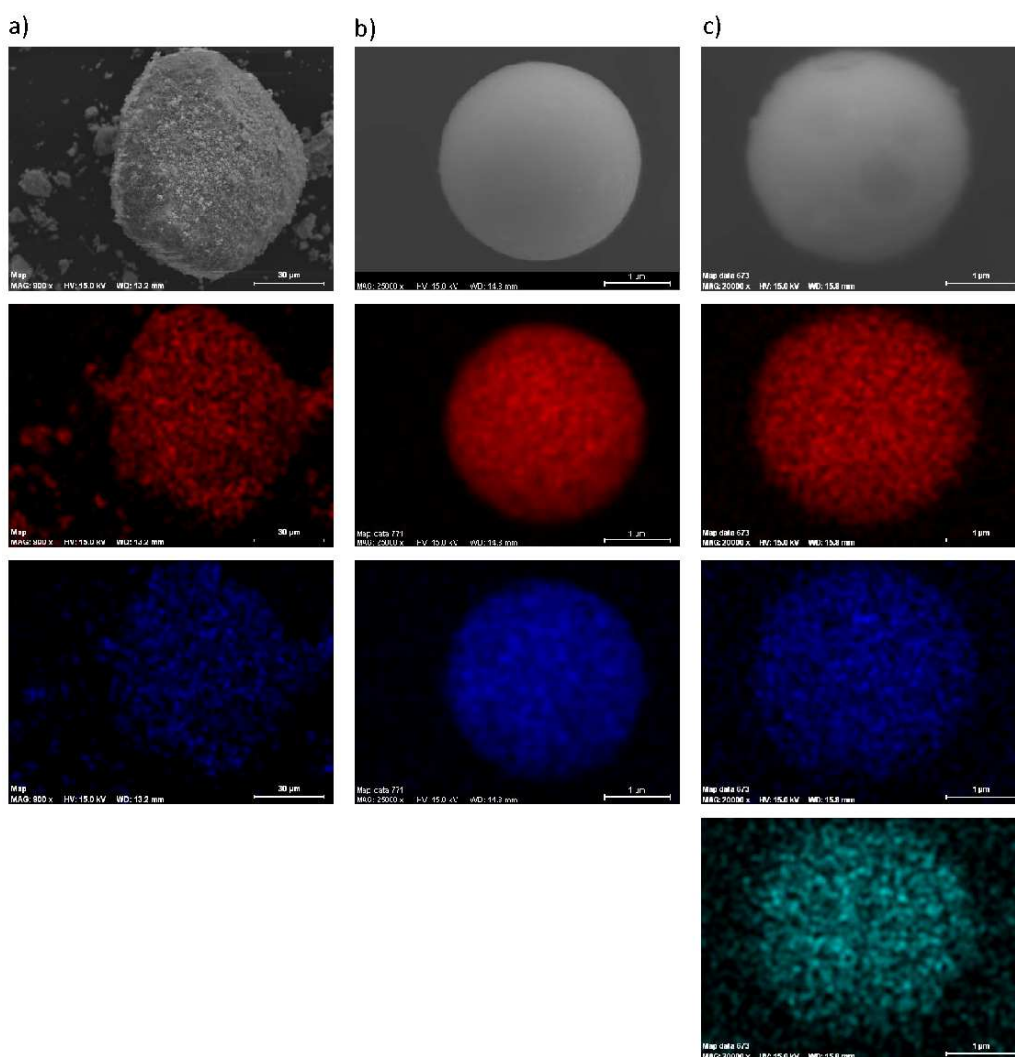


Figure 7.3- SEM images (top) and chemical mapping (Zr-red; W-dark blue; Al-light blue) for: a) ZrW(Cl), b) ZrW-MP, c) ZrWAl-MP.

The N_2 sorption isotherms measured at $-196\text{ }^\circ\text{C}$ for the ZrW(X) materials exhibited a hysteresis loop at high relative pressures (above 0.6) and very broad pore size distributions (ca. 2-52 nm, Figure 7.4 for ZrW(Cl)). The values of S_{BET} for these materials ($48\text{-}51\text{ m}^2\cdot\text{g}^{-1}$) were similar

and are in agreement with those reported in the literature for related ZrW materials ($S_{\text{BET}}=35\text{-}66\text{ m}^2\cdot\text{g}^{-1}$, Table 7.1).^{18,22,30,31,73,77,78,80,83-89} The ZrW-MP and ZrWAI-MP materials exhibited type IV isotherms (in accordance with the literature data for these types of materials),^{17,87,92,93} higher $S_{\text{BET}}=100\text{-}133\text{ m}^2\cdot\text{g}^{-1}$ (Table 7.1) and narrower pore size distributions (between ca. 2 and 7 nm width), inset of Figure 7.4, when compared to the ZrW(X) materials. Similar pore sizes were reported previously for a commercial zirconia-tungstate material,⁸⁷ and other types of ZrW (3.7-5.5 nm),^{17,92} ZrWAI (3.1 nm),⁶⁹ and ZrWAlSi⁹³ (5.8 nm) catalysts. Similar specific surface areas were reported for materials of the type ZrW ($S_{\text{BET}}=82\text{-}130\text{ m}^2\cdot\text{g}^{-1}$),^{18,30,31,76,87,90} ZrWAI ($S_{\text{BET}}=114\text{-}134\text{ m}^2\cdot\text{g}^{-1}$),^{69,82,93} ZrWSi ($S_{\text{BET}}=89\text{-}107\text{ m}^2\cdot\text{g}^{-1}$),^{84,91} and ZrWAlSi ($S_{\text{BET}}=126\text{ m}^2\cdot\text{g}^{-1}$)⁹³ (Table 7.1). Other authors reported different specific surface area values for ZrW type materials, which were higher than the values obtained in this work ($S_{\text{BET}}=365\text{-}477\text{ m}^2\cdot\text{g}^{-1}$),^{17,92} or lower ($S_{\text{BET}}=70\text{ m}^2\cdot\text{g}^{-1}$)⁷⁴ than ZrW-MP materials obtained herein ($S_{\text{BET}}=102\text{-}133\text{ m}^2\cdot\text{g}^{-1}$).

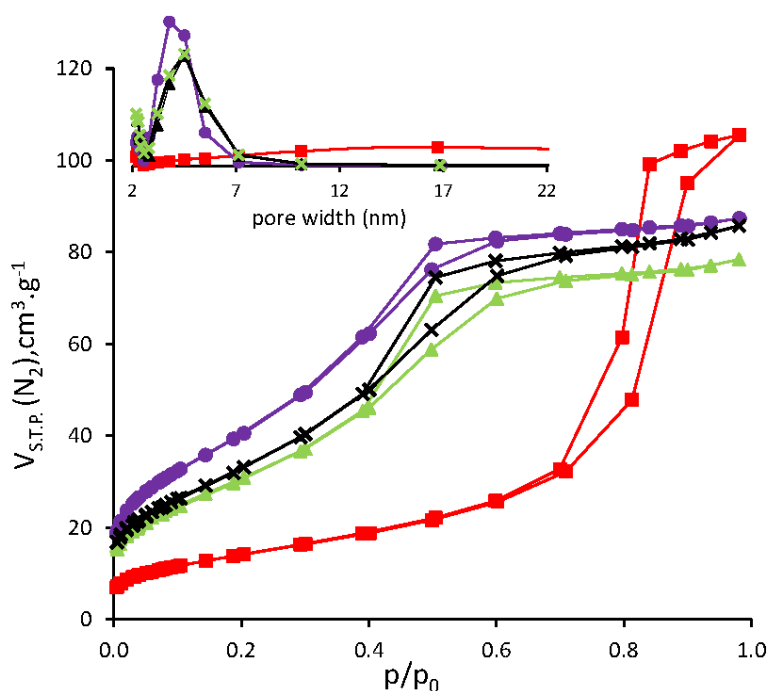


Figure 7.4- Nitrogen adsorption-desorption isotherms measured at $-196\text{ }^{\circ}\text{C}$ for ZrWCl (■), ZrW-MP (unused (▲); recycled (X)) and ZrWAI-MP (●). The inset shows the respective pore size distribution curves using the same symbols.

According to the literature,^{69,76,87,95} the calcination temperature of the prepared materials may influence the surface area which tends to decrease with the increase in the temperature of

calcination, and consequently, the tungsten surface density increases.⁷⁶ Melezhyk et al.⁹⁵ reported that the decrease in the specific surface area may be related to the growth of the crystals of zirconia, which was consistent with the narrowing of the intense peak attributed to t-ZrO₂ at ca. $2\theta=35^\circ$.⁹⁵ The type of the calcination atmosphere also seems to influence the surface area of the materials, in which static air (in comparison with nitrogen or oxygen) gave the highest specific surface area.⁸⁷ The low S_{BET} verified in some cases may be related to the penetration of the doped W-oxide into the pores of the zirconia.⁷⁷ The S_{BET} value for the bulk ZrO₂ was inferior to the modified zirconia,^{84,90} and similar to literature data ($S_{\text{BET}}=8-18 \text{ m}^2 \cdot \text{g}^{-1}$).^{18,74,84,85,90,94}

The Raman spectra of the prepared materials are shown in Figure 7.5. The results for the essentially monoclinic ZrO₂ were given for comparison. The spectra of the tungsten-containing materials showed similarities between each other and were very different from that of monoclinic ZrO₂, partly due to the predominant t-ZrO₂ phase in the former materials.³⁰ The characteristic band of t-ZrO₂ at ca. $625-640 \text{ cm}^{-1}$ was present, which is in accord with the literature.^{18,76,77,92}

Bands characteristic of crystalline WO₃ (typically at ca. $800-810 \text{ cm}^{-1}$, $710-720 \text{ cm}^{-1}$ and ca. 270 cm^{-1}) were hardly detected (consistent with the XRD data),^{25,31} suggesting that crystalline WO₃ was not formed on the surface of W-ZrO₂.⁷³ This is in accord with the literature for ZrW type materials.^{73,74,76,77,88,89,96} However, in exceptional cases these typical WO₃ bands were observed for ZrW type materials.^{31,80} Broad bands in the region $930-1020 \text{ cm}^{-1}$ may be assigned to the terminal W=O bonds which may be isolated or polymeric mono oxo tungsten species.^{30,49,73,77,89,92,96,97} Geometrically different WO_x species on the surface may be present when the bands in the region $930-1020 \text{ cm}^{-1}$ present shoulder peaks.²⁵ These may be octahedrally and tetrahedrally coordinated WO_x species. According to a few authors, the band at ca. 930 cm^{-1} was attributed to a symmetric vibration mode of (WO₄)²⁻ anions in tetrahedral symmetry.^{76,78,80,98,99} These anions are thought to form an amorphous phase after exchange with the hydroxyl groups of the zirconium precursor, in which Zr⁴⁺ cations become surrounded by WO₄²⁻,⁷⁶ allowing the crystallisation of zirconia in the tetragonal phase during calcination.^{25,76} Another possibility to obtain WO₄²⁻ in tetrahedral symmetry occurs when the interaction of W surface species with the support is weak and these species are surrounded by protons.⁷⁶

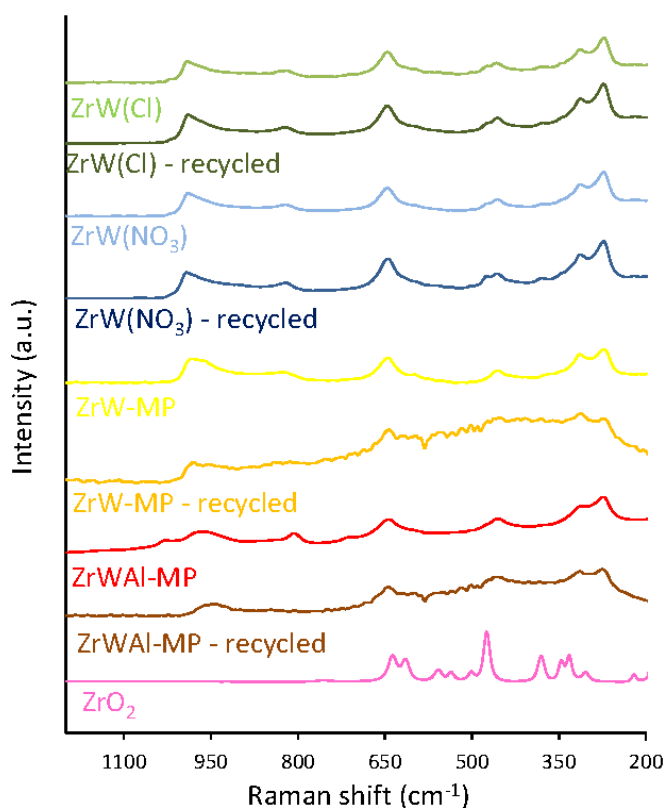


Figure 7.5- Raman spectra of unused and recycled catalysts.

Raman bands assigned to $\nu(\text{W}=\text{O})$ depend on the base strength of the ligands to which the W atom is coordinated and therefore might suffer slight shifts. The stronger the basicity of the oxide ligands is, the weaker is the W=O bond and the lower is the frequency of $\nu(\text{W}=\text{O})$.¹⁰⁰ The presence of water can also lead to a shift of the band of the W=O groups to lower frequencies, due to the strong interaction with water by hydrogen bonding; the band of W-O-Zr stretching cannot be unequivocally assigned due to the overlap with other broad signals.⁸⁹ The W-O-W characteristic band remains unchanged in the presence of water.⁸⁹ Additionally, the bands at 840 cm^{-1} , $900\text{--}910\text{ cm}^{-1}$ and $820\text{--}830\text{ cm}^{-1}$ can also be present and they were attributed to the antisymmetric stretching vibration of tetrahedral W^{6+} ,⁷⁸ W-O-Zr stretching vibration of WO_x species anchored to the support,^{78,89,97,101} and W-O-W, respectively.^{76,78,88,89,97,101} A low intensity band at ca. $800\text{--}820\text{ cm}^{-1}$ was observed in the case of $\text{ZrW}(\text{X})$ and ZrW-MP materials which may be attributed to W-O-W vibrations. The presence of W-O-W stretching modes is indicative that the WO_x surface structure consists of poorly defined oligomeric or polymeric species that are influenced by their interaction with the ZrO_2 surface, and most likely cover the support

surface.^{89,101} Sunita et al.⁷⁴ had also observed a band at ca. 825 cm^{-1} but the authors here had attributed this absorption to W-O-Zr vibrations instead of W-O-W.⁷⁴

All the prepared materials possessed both B and L interacting with pyridine after outgassing at $150\text{ }^{\circ}\text{C}$. The concentrations of B and L were determined as explained previously in Section 3.2.1.2 of Chapter 3. In this sense, the [B] (band at ca. 1545 cm^{-1}) and [L] (band at ca. 1450 cm^{-1}) for ZrW(X) materials were determined through equations 3.1 and 3.2 as specified in Chapter 3 (Figure 7.6). Besides the characteristic bands at 1545 cm^{-1} and at 1450 cm^{-1} , bands at 1490 cm^{-1} (sum of L and B), 1620 cm^{-1} (due to L) and 1640 cm^{-1} (due to B) were also observed, similar to that observed for H-MCM-22(24) and ITQ-2(24) in Chapter 6. FT-IR spectra of all prepared catalysts exhibited similar bands (Figure 7.6), and the ratio [L]/[B] varied in the range 1.2-1.4 (Table 7.2). Similar FT-IR spectra of adsorbed pyridine were obtained for ZrW type materials.^{28,31} Sunita et al.⁷⁴ only obtained bands at 1490 cm^{-1} and 1545 cm^{-1} .

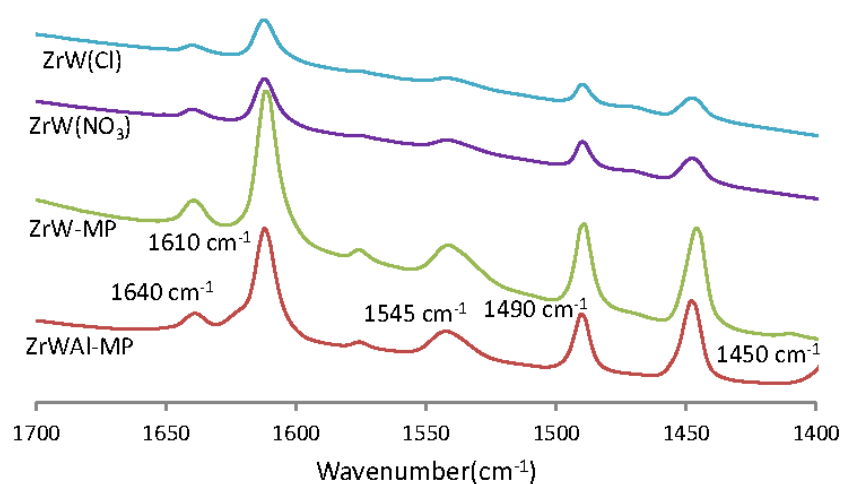


Figure 7.6- FT-IR spectra of ZrWAl-MP, ZrW-MP, ZrW(NO₃) and ZrW(Cl) after pyridine adsorption and outgassing at $150\text{ }^{\circ}\text{C}$.

The effect of the temperature in the [L] and [B] was also analysed (Figure 7.7).

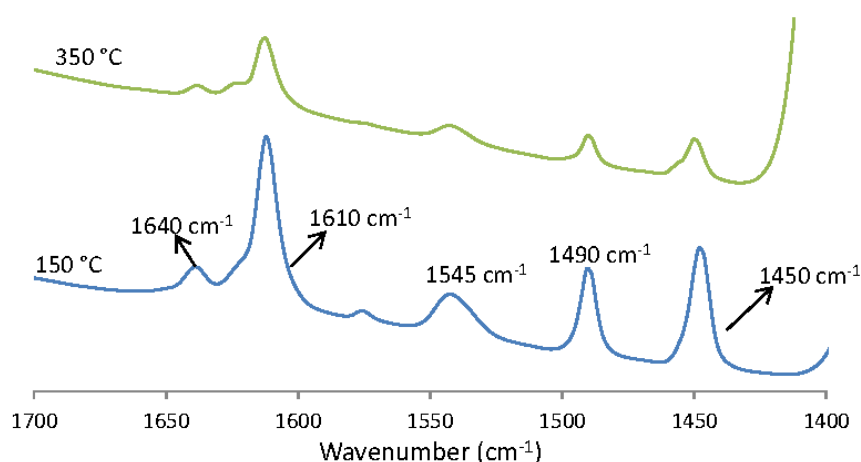


Figure 7.7- Effect of the outgassing temperature on ZrWAl-MP after pyridine adsorption.

The acid properties of the ZrW(X) materials were similar in terms of the total amount of AS ($[L]+[B]$) and acid strengths (based on the molar ratios of $[L]$ and $[B]$ measured at 350 °C and 150 °C, denoted as $[L]_{350}/[L]_{150}$ and $[B]_{350}/[B]_{150}$, respectively). The total amount of $[B]+[L]$ was considerably greater for ZrW-MP than for the ZrW(X) materials which may be partly related to the higher S_{BET} in the former case, enhancing the accessibility of the AS to the base probe (the W/Zr molar ratios were similar for the three materials). The ZrW-MP possessed similar acid strengths to the ZrW(X) materials. In comparison to ZrW-MP, the ZrWAl-MP material possessed somewhat higher $[B]+[L]$ (and S_{BET}), and slightly stronger Brönsted acidity. These results compared favourably with those for ZrW type material (W/Zr of ca. 0.10, Table 7.2).

Table 7.2- Acid properties measured by FT-IR of adsorbed pyridine of the prepared materials (ZrW(Cl), ZrW(NO₃), ZrW-MP and ZrWAl-MP) after outgassing at 150 °C.

Sample	$[B]+[L]^a$ ($\mu\text{mol.g}^{-1}$)	$[L]$ ($\mu\text{mol.g}^{-1}$)	$[B]$ ($\mu\text{mol.g}^{-1}$)	$[L]/[B]$	$[L]_{350}/[L]_{150}^b$	$[B]_{350}/[B]_{150}^c$	Ref
ZrW(Cl)	38	22	16	1.4	0.2	<0.1	this work
ZrW(NO ₃)	39	21	18	1.2	0.2	<0.1	this work
ZrW-MP	111	61	50	1.2	0.2	<0.1	this work
ZrWAl-MP	127	74	53	1.4	0.2	0.2	this work
PdZrW	55	-	-	0.8	-	-	¹⁰²

a) Sum of the total Brönsted acid sites $[B]$ plus Lewis acid sites $[L]$. b) Ratio between the concentration of Lewis acid sites $[L]$ at 350 °C and at 150 °C. c) Ratio between the concentration of Brönsted acid sites $[B]$ at 350 °C and at 150 °C.

7.2.2. Catalytic dehydration of D-xylose

7.2.2.1. Catalytic performance of ZrW(X), ZrW-MP and ZrWAl-MP materials

The mesoporous ZrW-MP and ZrWAl-MP catalysts led to higher yields of Fur at comparable reaction times, in comparison to the ZrW(X) catalysts (Figure 7.8), which correlated with the higher total amounts of AS of the former two catalysts (Table 7.2). In comparison to ZrW-MP, the ZrWAl-MP catalyst led to higher yields of Fur at high conversions of Xyl (52% Y_{Fur} at 98% C_{Xyl} for ZrWAl-MP compared to 41% Y_{Fur} at 100% C_{Xyl} for ZrW-MP, Figure 7.9), suggesting that the combined effects of enhanced S_{BET} and surface acidity favoured the dehydration of Xyl into Fur.

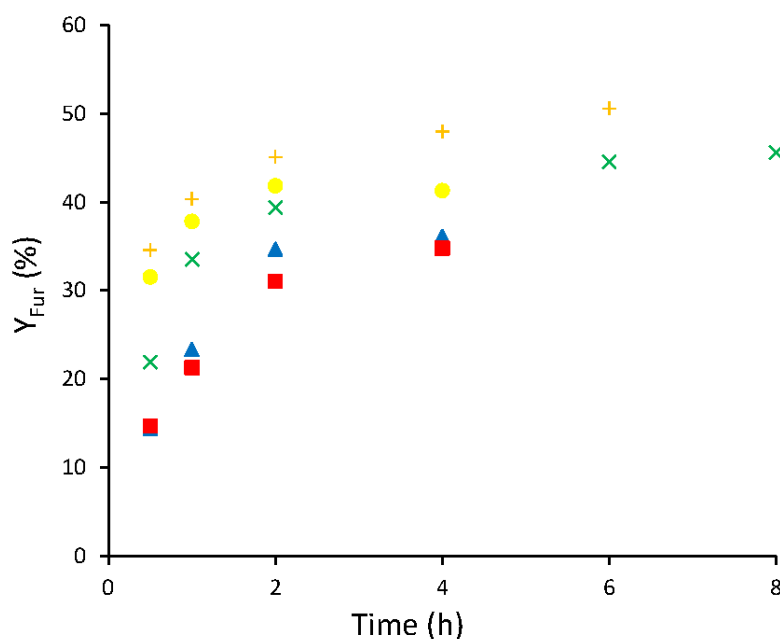


Figure 7.8- Yield of 2-furaldehyde (Y_{Fur}) versus reaction time for the catalysts ZrW(Cl) (■), ZrW(NO₃) (▲), ZrW-MP (●), and ZrWAl-MP (+) for 0.3 Wt:0.7 Tol (v/v) biphasic solvent system and (X) for solely Wt (1 cm³). Reaction conditions: 170 °C, 20 g_{cat}·dm⁻³, 0.67 M Xyl.

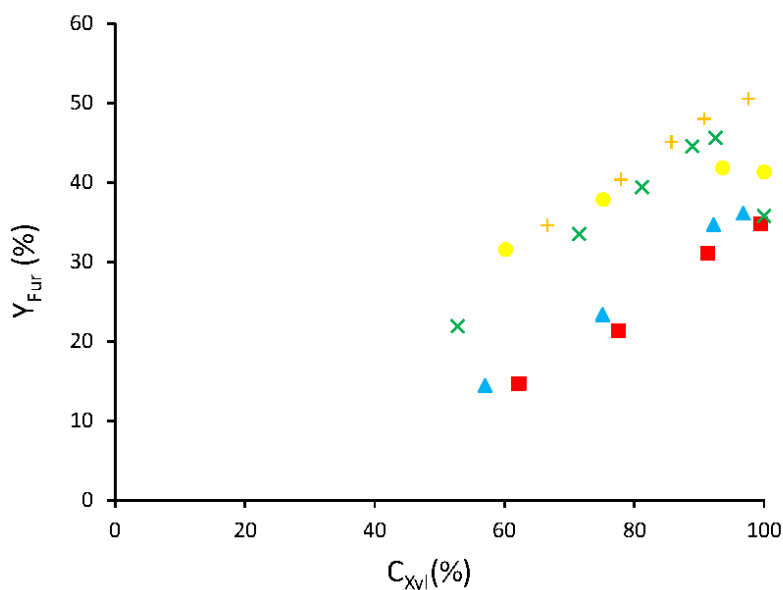


Figure 7.9- Yield of 2-furaldehyde (Y_{Fur}) versus conversion of D-xylose (C_{Xyl}) for the catalysts ZrW(Cl) (■), ZrW(NO₃) (▲), ZrW-MP (●), and ZrWAl-MP (+) for 0.3 Wt:0.7 Tol (v/v) biphasic solvent system and (X) for solely Wt (1 cm³). Reaction conditions: 170 °C, 20 g_{cat}.dm⁻³, 0.67 M Xyl.

For comparison with the biphasic solvent system, the reaction of Xyl in the presence of ZrWAl-MP was carried out using solely water as solvent, at 170 °C (the amount of catalyst in the reaction medium and the total volume of reaction mixture were the same for the two sets of reaction conditions). The yield of Fur at similar Xyl conversions was lower for the water system than for the biphasic solvent system (Figure 7.9). The water and biphasic solvent systems led to comparable yields of Fur until ca. 90% C_{Xyl} (46-48% Y_{Fur}). Afterwards the Y_{Fur} dropped to 36% when C_{Xyl} reached 100% in the case of the water system, whereas in the case of the biphasic solvent system, the Y_{Fur} increased to 52% at 98% C_{Xyl} (Figure 7.9). In a previous study for the dehydration of Xyl in the presence of tungstated zirconia (ZrW, XZO 1251 with WO₃ content 15 wt.%, supplied by MEL Chemicals) using solely water it was reported that 16% Y_{Fur} was reached at 96% C_{Xyl} , 160 °C (0.33 M Xyl; 7.5 g_{cat}.dm⁻³).⁶

7.2.2.2. Identification of the reaction products

The identification of by-products may help to identify factors influencing the side reactions, important for tailoring the properties of solid acid catalysts for the target reaction.

The InsolOrg products identification (also known as humins) is not trivial, as discussed in Chapter 5 for the reaction of Xyl in the presence of micro/mesoporous composite BEATUD-1 and in Chapter 6 for ITQ-2(24) under similar conditions to those used in the present work. The FT-IR and ^{13}C MAS NMR spectra were quite complex and it was only possible to identify clearly Xyl, Fur and formic acid (the organic matter possessed aldehyde/ketose groups, fragments related to Xyl and (un)saturated carbon-carbon bonds) as shown in Chapters 5 and 6.

With respect to the water soluble by-products, only formic acid was detected by HPLC (using a UV diode array detector), which according to the literature, may be formed via fragmentation of sugars under acidic hydrothermal conditions,^{103,104} or hydrolytic fission of the aldehyde group of Fur.^{7-9,105} However, the yellow colour of the liquid phases of the reaction mixtures indicated the presence of other types of by-products besides formic acid. Therefore, a more detailed study to identify water soluble by-products of the reaction of Xyl in the presence of ZrWAl-MP, using water as solvent, at 170 °C, was carried out by employing solid-phase microextraction (SPME) coupled with comprehensive two-dimensional gas chromatography (GCxGC) with time-of-flight mass spectrometry (ToFMS). The SPME/GCxGC-ToFMS technique allowed the separation and identification of water soluble reaction products which were sufficiently volatile under the applied analytical conditions (details given in the experimental part, Section 2.4 of Chapter 2). For comparison, the analysis was performed for the reaction of Fur in the presence of ZrWAl-MP, at 170 °C.

The identified reaction by-products are listed in Table 7.3 (many more products were detected, which were not clearly identified). Figures 7.10 and 7.11 show the 1 D and 3 D TIC GCxGC-ToFMS obtained. A complex mixture of reaction products was obtained for the reaction of Xyl in the presence of ZrWAl-MP, at 170 °C and 4 h. When using Fur as the substrate instead of Xyl a much narrower spectrum of reaction products was detected (Figure 7.12).

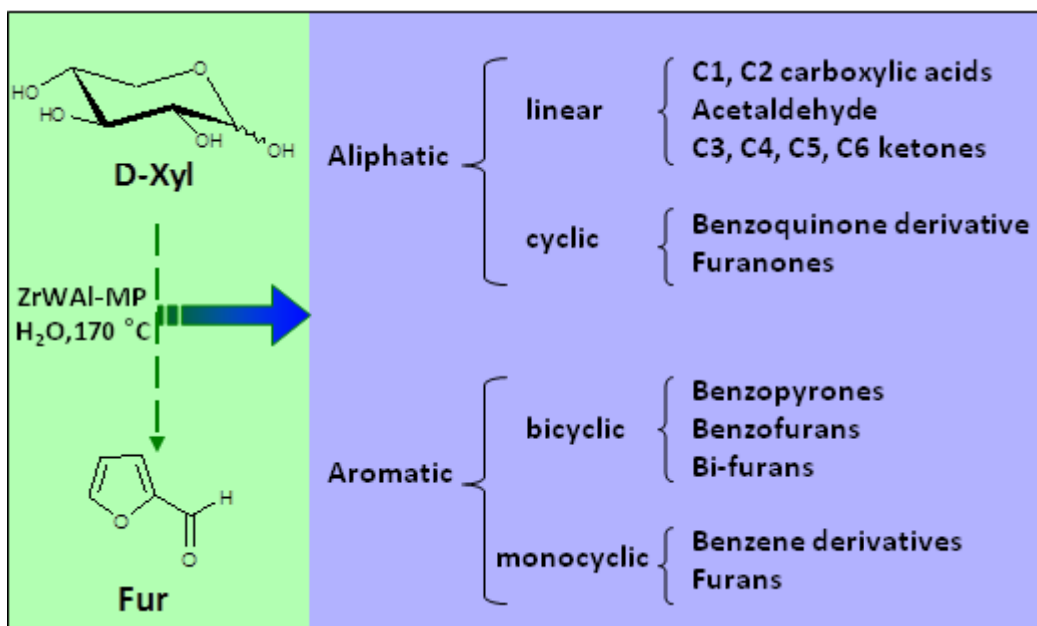


Figure 7.10- Products formed in the reaction of D-xylose (Xyl) in the presence of ZrWAl-MP, using solely water (1 cm³) as solvent, at 170 °C, identified by GCxGC-ToFMS.

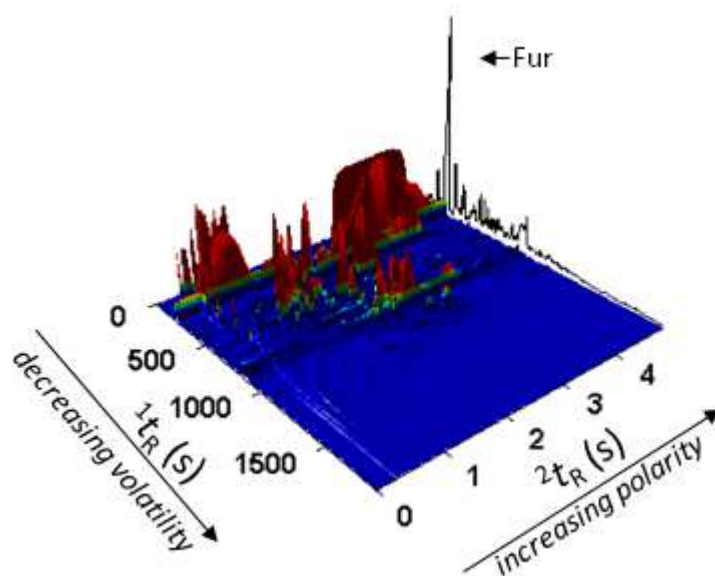
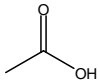
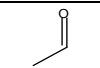
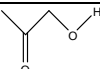
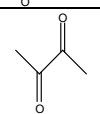
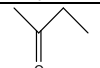
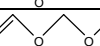
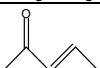
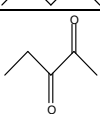
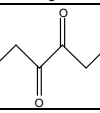
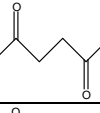
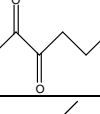
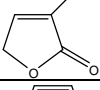
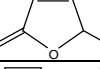
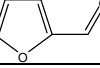
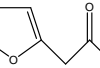
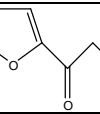
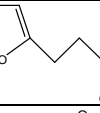
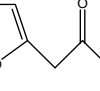
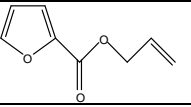
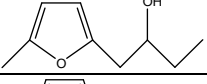
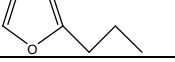
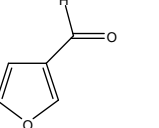
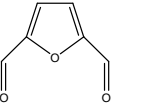
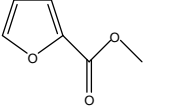
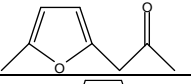
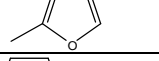
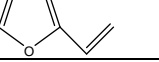
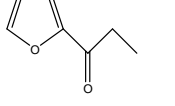
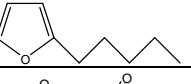
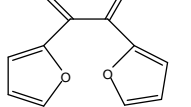
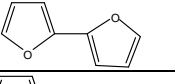
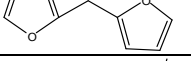
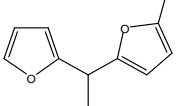
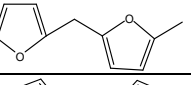
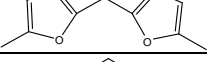
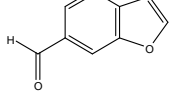
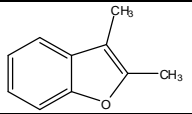
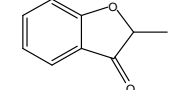
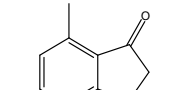
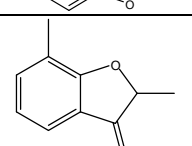
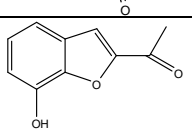
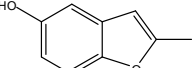
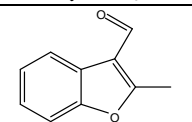
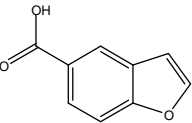
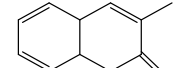
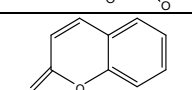
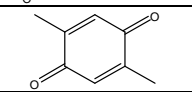
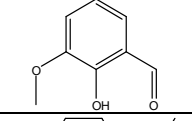
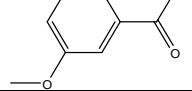
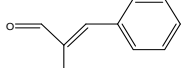
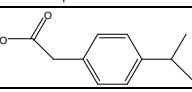
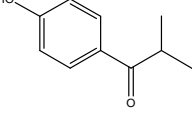


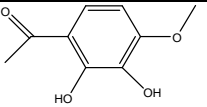
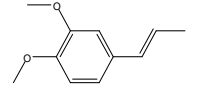
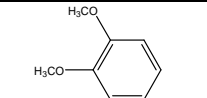
Figure 7.11- TIC GCxGC-ToFMS representation (1 D and 3 D) of the reaction mixture with D-xylose (Xyl) as substrate. Reaction conditions: solely Wt (1 cm³), 170 °C, 20 g_{cat}·dm⁻³, 0.67 M Xyl, 4 h.

Table 7.3- Reaction products detected by GCxGC-ToFMS for the reaction of D-xylose (Xyl) in the presence of ZrWAl-MP, at 170 °C.^a

Reaction Product		Similarity	RI ^b	RI [ref] ^c
Molecular structure	Name of compound			
	acetic acid	997	-	-
	Acetaldehyde	979	564	≅500 ¹⁰⁶
	1-hydroxy-2-propanone	999	824	-
	2,3-butanedione	994	585	592 ¹⁰⁷
	2-butanone	892	589	602 ¹⁰⁸
	methoxy methyl vinyl ether	963	863	-
	3-penten-2-one	959	702	735 ¹⁰⁹
	2,3-pentanedione	886	652	696 ¹¹⁰
	3,4-hexanedione	993	801	800 ^{111,112}
	2,5-hexanedione	971	980	93 ¹⁰⁹
	2,3-hexanedione	961	777	786 ¹¹³
	3-methyl-2(5H)-furanone	942	1022	983 ¹¹⁴
	5-methyl-2(5H)-furanone	950	990	954 ¹¹⁵
	2-Furaldehyde	975	863	852 ¹¹⁶
	(1-(furan-2-yl)-propan-2-one	948	963	952 ¹¹⁷
	1-(5-methylfuran-2-yl)butan-1-one	844	1255	-
	1-(2-furyl)-butan-3-one	943	1083	-
	1-(2-furanyl)-2-butanone	967	1063	-

	2-propenyl ester 2-furancarboxylic acid	875	1087	-
	1-(5-methylfuran-2-yl)butan-2-ol	829	1226	-
	2-propyl-furan	880	874	861 ¹¹⁸
	3-furaldehyde * ^d	967	849	849 ¹¹⁹
	2,5-furandicarboxaldehyde * ^d	802	1040	1079 ¹²⁰
	methyl furan-2-carboxylate * ^d	947	984	983 ¹¹⁹
	1-(5-methyl-2-furyl)-2-propanone * ^d	956	1063	1056 ¹²¹
	2-methyl-furan * ^d	970	601.	603 ¹²²
	vinylfuran * ^d	959	677	723 ¹²³
	1-(2-furanyl)-2-propanone * ^d	948	963	952 ¹¹⁷
	2-pentylfuran * ^d	816	1039	1001 ¹²⁴
	di-2-furanyl-ethanedione	930	1599	-
	2,2'-bifuran	953	1044	1047 ¹²³
	2,2'-methylenebis-furan	948	1092	1090 ¹²⁵
	2,2'-ethylidenebis(5-methylfuran)	920	1320	-
	2-(2-furanylmethyl)-5-methyl-furan	933	1191	1195 ¹²⁶
	2,2'-methylenebis-(5-methyl-furan)	785	1272	1290 ¹²⁶
	benzo[b]furan-6-carboxaldehyde	994	1291	-

	2,3-dimethylbenzofuran	838	1237	1199 ¹²⁷
	2-methyl-3(2H)-benzofuranone	890	1243	-
	4-methyl-3(2H)-benzofuranone	949	1302	-
	2,7-dimethyl-3(2H)-benzofuranone	858	1321	-
	2-acetyl-7-hydroxybenzofuran	895	1443	-
	2-methyl-5-hydroxybenzofuran	908	1384	-
	2-methyl-benzofurane-3-carboxaldehyde	919	1409	-
	benzo[b]furan-5-carboxylic acid	867	1668	-
	3-methyl-2H-chromen-2-one	932	1443	1493 ¹²⁸
	2H-chromen-2-one	880	1390	1376 ¹²⁸
	2,5-dimethyl-1,4-benzoquinone	945	1128	1129 ¹²⁹
	2-hydroxy-3-methoxybenzaldehyde	897	1299	1298 ¹²⁸
	(1-(3-methoxyphenyl)-ethanone)	937	1261	1297 ¹²⁸
	2-methyl-3-phenyl-2-propenal	899	1219	1207 ¹⁰⁹
	4-(1-methylethyl)-phenyl acetate	764	1450	1454 ¹³⁰
	1-(4-hydroxyphenyl)-2-methyl-1-propanone	886	1321	-

	2,3-dihydroxy-4-methylacetophenone	907	1397	-
	(E)-3,4-dimethoxy-1-propenylbenzene	814	1547	1500 ^{109,131}
	1,2-dimethoxybenzene	863	1123	1147 ¹²⁸

a) Reaction conditions: solely Wt (1 cm^3), $170 \text{ }^\circ\text{C}$, $20 \text{ g}_{\text{cat}} \cdot \text{dm}^{-3}$, 0.67 M Xyl , 4 h reaction. b) The symbol * indicates that the same product was detected for 2-furaldehyde as substrate. c) Retention index (RI) obtained through the modulated chromatogram. d) Retention index reported in the literature for one dimensional GC with 5% phenylmethylpolysiloxane GC column or equivalent.

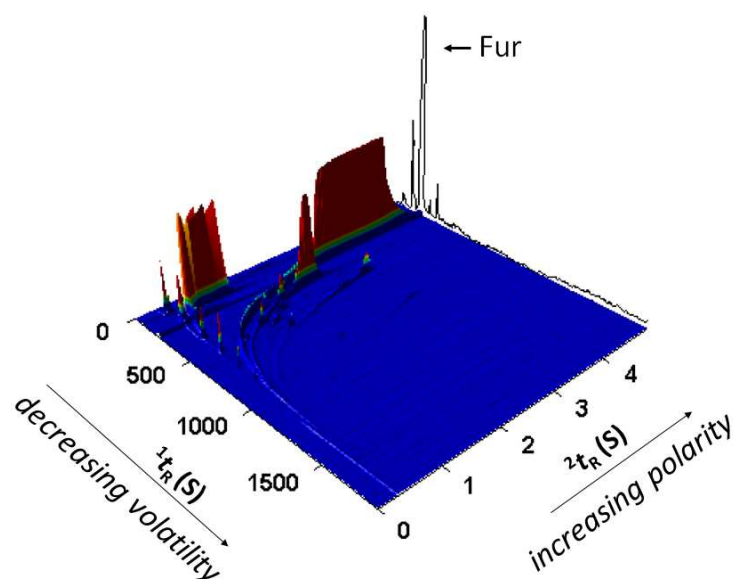


Figure 7.12- TIC GCxGC-ToFMS representation (1 and 3 D) of the reaction mixture for 2-furaldehyde (Fur) as substrate, in the presence of ZrWAI-MP using solely water as solvent. Reaction conditions: Solely Wt (1 cm^3), $170 \text{ }^\circ\text{C}$, 0.67 M Fur , 6 h.

The products formed in the reaction of Xyl may be grouped into aliphatic and aromatic compounds (Figure 7.10). A major chromatographic peak was identified as Fur. The aliphatic by-products consisted of linear carbon chains of up to six carbon atoms, possessing hydroxyl, carbonyl and/or carboxylic acid functional groups. According to the literature, monosaccharides may undergo fragmentations through complex reaction mechanisms involving retro aldolisation, hydrolysis and/or oxidative fission pathways, which may be accompanied by enolisation and dehydration reactions leading to a variety of compounds.¹³²⁻¹³⁹ The aliphatic by-products

possessing less than five carbon atoms identified in the reaction of Xyl include acetic acid, acetaldehyde, 1-hydroxy-2-propanone, 2,3-butanedione and 2-butanone (Table 7.3). The first four of these are possible sugar fragmentation products,¹⁰³ and were not detected with Fur as the substrate.

2,3-Pentadione and hexadione products were formed in the reaction of Xyl and not of Fur. According to the literature 2,3-pentadione may be formed through a series of reactions involving aldol reactions of butanedione (detected in this work) with formaldehyde or of acetaldehyde (detected in this work) with 1-hydroxy-2-propanone.¹⁴⁰ The mechanism of formation of the hexadiones is not clear. It has been reported that 2,5-hexadione is a possible product of the reaction of 2,5-dimethylfuran (not detected in this work) with water.¹⁴¹ It is worth mentioning that the by-products may react with Xyl (e.g. Xyl bound to a non-carbohydrate moiety) and/or Fur, and fragmentation and recombination of carbohydrate fragments may take place, further enhancing the complexity of the overall reaction mechanism.

Furanone products were detected, namely 3-methyl-2(5H)-furanone and 5-methyl-2(5H)-furanone, for Xyl and not for Fur as substrate. A similar compound identified as 5-methyl-3(2H)-furanone was previously reported as the product of the reaction of 2-deoxy- D-erythro-pentose in aqueous acidic medium.¹⁴²

Several compounds possessing one furan ring were detected and some (noted with the symbol * in Table 7.3, e.g. methyl-furan-2-carboxylate) were common to the reactions of Xyl and Fur. Furan derivatives possessing two furan rings were formed (e.g. di-2-furanyl-ethanedione), and related by-products have been reported previously for the reactions of pentoses^{143,144} and hexoses.¹³² 2,5-Dimethyl-1,4-benzoquinone was detected for the reaction of Xyl and not of Fur, as well as a variety of aromatic by-products possessing a benzene ring, suggesting that the formation of these by-products involved intermediates of the reaction of Xyl. Monocyclic compounds included hydroxyacetophenones and hydroxybenzaldehydes, and bicyclic compounds were benzopyrone and benzofuran derivatives. It is worth mentioning that phenolic compounds can be readily transformed into coloured products (as mentioned above the reaction solutions were yellow). Aromatic compounds of the type benzopyrone and acetophenone possessing hydroxyl functional groups have been identified as by-products of the reaction of Xyl under acidic conditions.^{145,146}

The reaction of Fur (as the substrate) in the absence or presence of ZrWAI-MP, at 170 °C (water system), gave 16% and 24% C_{Xyl} at 4 h reaction, respectively. In the case of the biphasic

solvent system no measurable conversion of Fur was observed, which was consistent with the favourable effects of the biphasic solvent system in avoiding Fur loss reactions.

7.2.2.3. Catalyst stability

DSC analyses (exemplified for ZrWAl-MP in Figure 7.13) of the used catalysts exhibited two exothermic bands in the temperature range 200-550 °C which did not appear for the respective unused catalysts and were therefore attributed to the decomposition of InsolOrg.

The amount of water-insoluble organic matter (designated as InsolOrg) was determined by TGA of the washed/dried solids (after reaching a C_{Xyl} of 98-100%), based on the mass loss in the temperature range 200-600 °C, and expressed as $\frac{\text{mass of InsolOrg}}{\text{initial mass of Xyl}}$ ($\text{mg}\cdot\text{g}_{\text{Xyl}}^{-1}$) (Figure 7.13).

The amount of InsolOrg was similar for ZrWAl-MP ($154 \text{ mg}\cdot\text{g}_{\text{Xyl}}^{-1}$) and ZrW-MP ($133 \text{ mg}\cdot\text{g}_{\text{Xyl}}^{-1}$). A greater amount of InsolOrg was formed for the water system ($197 \text{ mg}\cdot\text{g}_{\text{Xyl}}^{-1}$) in comparison to the biphasic solvent system ($154 \text{ mg}\cdot\text{g}_{\text{Xyl}}^{-1}$, Figure 7.13). These results are in agreement with the partition ratio of Fur (PR_{Fur}) that was calculated as specified in equation 5.2 in Chapter 5 and measured at a.t., and gave a variation in the range 7 ± 0.7 throughout the reaction. Hence, as Fur is formed it is dissolved favourably in the organic phase, which does not dissolve Xyl (or similarly polar intermediates). Therefore the higher yield of Fur and lower amount of InsolOrg formed at high conversions in the case of the biphasic solvent system may be partly due to:

- i) reduction in the concentration of Fur in the aqueous phase and consequently the lower extension of Fur loss reactions involving Xyl and/or polar intermediates,^{1,7-9,11}
- ii) competitive adsorption effects minimising consecutive reactions of Fur (mainly Tol solvated) on the catalyst surface (polar, hydrophilic).

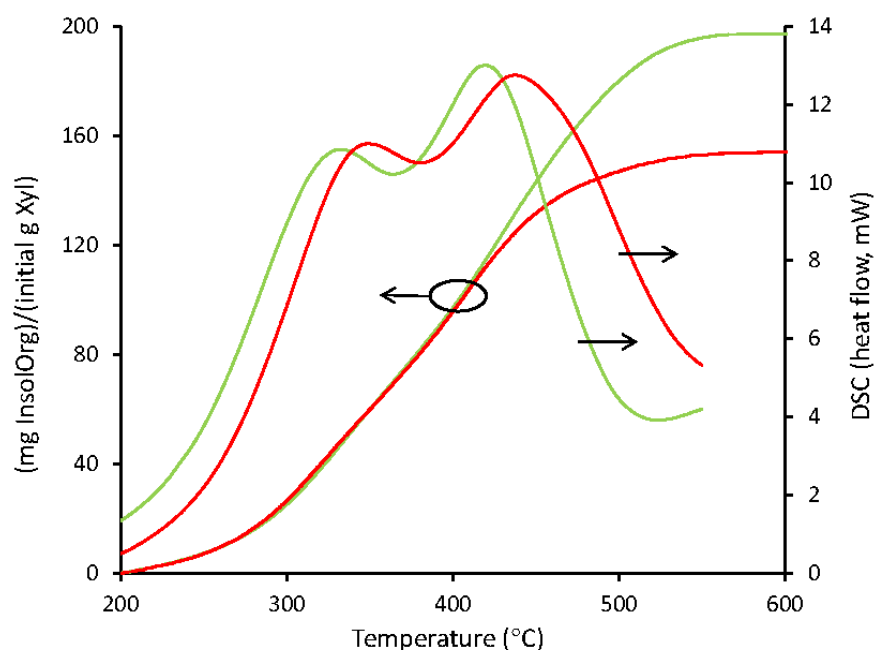


Figure 7.13- TGA (represented as (mass of InsolOrg)/(initial mass of D-Xylose) and DSC curves for the ZrWAl-MP catalyst separated (washed/dried) from the reaction mixture after reaching at least 98% of D-xylose conversion (C_{Xyl}), using the 0.3 Wt:0.7 Tol (v/v) biphasic solvent system (red lines) or solely Wt (1 cm^3) (green lines). Reaction conditions: $170 \text{ }^\circ\text{C}$, $20 \text{ g}_{\text{cat}}\cdot\text{dm}^{-3}$, 0.67 M Xyl .

The thermally regenerated ZrW-MP and ZrWAl-MP catalysts (details given in the experimental part, Section 2.3 in Chapter 2) were reused in three consecutive 4 h batch runs (similar conditions have been reported previously for efficiently regenerating a zirconia catalyst used in the conversion of cellulose at $180 \text{ }^\circ\text{C}$).¹⁴⁷ The used catalysts were brownish in colour and the solvent washing procedures failed to restore the original white colour of the as-prepared catalysts (in contrast to that observed for the thermal treatment). For each catalyst, the yields of Fur in recycling runs were comparable (Figure 7.14). It is worth mentioning that for the washed/dried ZrW-MP catalyst which was not subjected to the thermal treatment, the yield of Fur dropped considerably from 41% for the first batch run to 13% for the second one, possibly due to the catalyst surface passivation by adsorbed organic compounds.

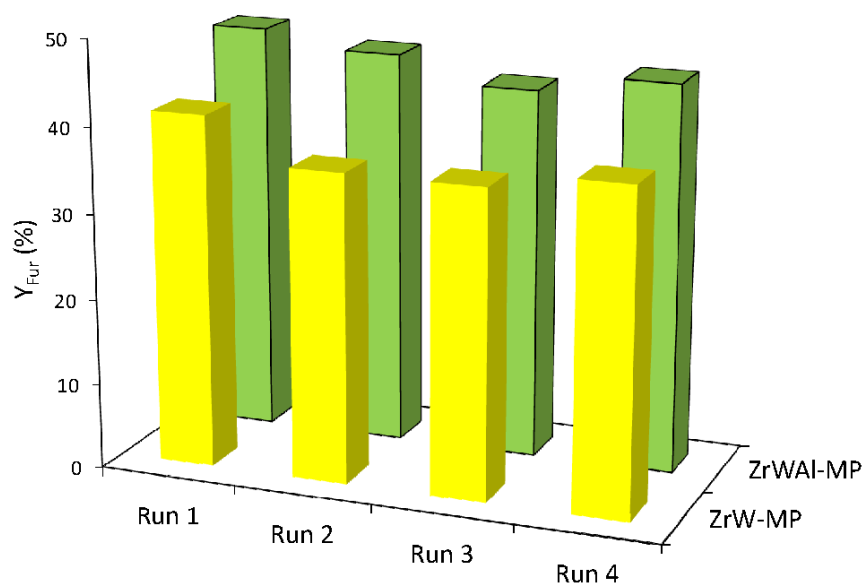


Figure 7.14- Yield of 2-furaldehyde (Y_{Fur}) in recycling runs of the reaction of D-xylose (Xyl) in the presence of ZrWAI-MP or ZrW-MP. Reaction conditions: 0.3 Wt:0.7 Tol (v/v) biphasic solvent system, 170 °C, 20 $g_{cat} \cdot dm^{-3}$, 0.67 M Xyl, 4 h.

The XRD patterns and Raman spectra for the used/regenerated ZrW-MP catalysts were similar to those for the respective unused catalysts (Figures 7.3 and 7.6). The Raman spectra for the used/regenerated catalysts exhibited higher background noise.

The stability of the mesoporous structure was confirmed by the similar textural properties (type IV isotherms, S_{BET} and pore size distribution) of the used/regenerated ZrW-MP (109-133 $m^2 \cdot g^{-1}$; pore size distribution between ca. 2 and 7 nm width) and ZrWAI-MP (133-143 $m^2 \cdot g^{-1}$; pore size distribution between ca. 2.5 and 6 nm width) catalysts (Figure 7.4).

ICP-AES analyses of the aqueous phase of the reaction mixtures indicated no measurable leaching of Zr, W or Al. Based on these results it seems that ZrW-MP and ZrWAI-MP were fairly stable catalysts.

7.3. Conclusions

Zirconium-tungsten mixed oxides were relatively active catalysts in the aqueous phase reaction of Xyl, at 170 °C. The catalysts prepared by co-condensation (ZrW(X)) led to more than 90% C_{Xyl} within 2 h of reaction, but Y_{Fur} were less than 35%. The yield of Fur at a similar conversion of Xyl could be improved by using a templating agent to give ZrW-MP with enhanced specific surface area and amount of accessible AS (41% Y_{Fur} at 100% C_{Xyl}), and furthermore by doping the inorganic material with aluminium to give ZrWAl-MP (51% Y_{Fur} at 98% C_{Xyl}).

SPME/GCxGC-ToFMS analyses were carried out for the reaction of Xyl, showing that a complex mixture of water soluble by-products was obtained. Detailed systematic studies using this technique may give valuable insights into the overall reaction mechanisms of the conversion of carbohydrate biomass, important for identifying factors (catalyst properties, reaction conditions) affecting product selectivities.

Catalyst recycling tests and characterisation of the recovered solids revealed that ZrW-MP and ZrWAl-MP were fairly stable catalysts under the applied reaction conditions. For the ZrWAl-MP catalyst, the yields of Fur were higher when using the biphasic Wt:Tol solvent system instead of solely water as the solvent (40% at 93% C_{Xyl}). On the other hand, the yields of Fur reached for ZrWAl-MP using solely water as the solvent (cheaper, cleaner), were higher than those for the ZrW(X) catalysts coupled with the biphasic solvent system.

By fine-tuning the catalytic properties of these types of solid acid catalysts it may be possible to further improve their catalytic performances. Furthermore, tungsten/aluminium modified zirconias may be promising (versatile) catalysts for converting cellulose/glucose (most abundant terrestrial poly/monosaccharides) to added value products such as Hmf. The product distribution obtained in the aqueous reaction of Glu in the presence of aluminium-zirconium mixed oxides at 180 °C was found to be dependent on the acid-base properties of the catalysts.⁶⁸

ZrO₂ is effective in the isomerisation of Glu using water as solvent, at 200 °C.¹⁴⁸ McNeff et al.¹⁴⁷ demonstrated the feasibility of using a continuous process coupled with stable porous heterogeneous metal oxide catalysts (zirconia, titania) for the conversion of cellulose to Hmf in fairly good yields.¹⁴⁷ More recently, Chambon et al.⁵⁹ reported that tungstated zirconia and tungstated alumina exhibited remarkable catalytic activity and stability in the depolymerisation of cellulose. A major limitation of the aqueous phase conversion of cellulose is the reduced solubility

of the polysaccharide in water. In this sense, high expectations have been put on the use of ionic liquids as solvents (investigated in the next two Chapters using different approaches).

7.4. References

- (1) Zeitsch, K. J.: *The Chemistry and Technology of Furfural and its Many By-Products*; 1st ed.; Elsevier Science B. V.: Amsterdam, The Netherlands, 2000; Vol. 13.
- (2) Antal, M. J.; Leesomboon, T.; Mok, W. S.; Richards, G. N.: Kinetic Studies of the Reactions of Ketoses and Aldoses in Water at High Temperature 3-Mechanism of Formation of 2-Furaldehyde from D-Xylose. *Carbohydrate Research* **1991**, *217*, 71-85.
- (3) Antal, M. J.; Mok, W. S. L.; Richards, G. N.: Kinetic Studies of the Reactions of Ketoses and Aldoses in Water at High Temperature. 2. 4-Carbon Model Compounds for the Reactions of Sugars in Water at High Temperature. *Carbohydrate Research* **1990**, *199*, 111-115.
- (4) Mansilla, H. D.; Baeza, J.; Urzua, S.; Maturana, G.; Villasenor, J.; Duran, N.: Acid-Catalysed Hydrolysis of Rice Hull: Evaluation of Furfural Production. *Bioresource Technology* **1998**, *66*, 189-193.
- (5) Binder, J. B.; Blank, J. J.; Cefali, A. V.; Raines, R. T.: Synthesis of Furfural from Xylose and Xylan. *ChemSusChem* **2010**, *3*, 1268-1272.
- (6) Weingarten, R.; Tompsett, G. A.; Conner, W. C. J.; Huber, G. W.: Design of Solid Acid Catalysts for Aqueous-Phase Dehydration of Carbohydrates: The Role of Lewis and Brønsted Acid Sites. *Journal of Catalysis* **2011**, *279*, 174-182.
- (7) O'Neill, R.; Ahmad, M. N. M.; Vanoye, L.; Aiouache, F.: Kinetics of Aqueous Phase Dehydration of Xylose Into Furfural Catalyzed by ZSM-5 Zeolite. *Industrial & Engineering Chemistry Research* **2009**, *48*, 4300-4306.
- (8) Williams, D. L.; Dunlop, A. P.: Kinetics of Furfural Destruction in Acidic Aqueous Media. *Industrial and Engineering Chemistry* **1948**, *40*, 239-241.
- (9) Dunlop, A. P.: Furfural Formation and Behavior. *Industrial and Engineering Chemistry* **1948**, *40*, 204-209.
- (10) Bonn, G.; Rinderer, M.; Bobleter, O.: Hydrothermal Degradation and Kinetic Studies of 1,3-Dihydroxy-2-Propane and 2,3-Dihydroxypropanal. *Journal of Carbohydrate Chemistry* **1985**, *4*, 67-77.
- (11) Weingarten, R.; Cho, J.; Conner, W. C., Jr.; Huber, G. W.: Kinetics of Furfural Production by Dehydration of Xylose in a Biphasic Reactor With Microwave Heating. *Green Chemistry* **2010**, *12*, 1423-1429.
- (12) Peters, T. A.; Benes, N. E.; Holmen, A.; Keurentjes, J. T. F.: Comparison of Commercial Solid Acid Catalysts for the Esterification of Acetic Acid with Butanol. *Applied Catalysis A-General* **2006**, *297*, 182-188.
- (13) Chen, F. R.; Coudurier, G.; Joly, J. F.; Vedrine, J. C.: Superacid and Catalytic Properties of Sulfated Zirconia. *Journal of Catalysis* **1993**, *143*, 616-626.
- (14) Srinivasan, R.; Keogh, R. A.; Milburn, D. R.; Davis, B. H.: Sulfated Zirconia Catalysts-Characterization by TGA/DTA Mass-Spectrometry. *Journal of Catalysis* **1995**, *153*, 123-130.
- (15) Thomas, J. M.: Solid Acid Catalysts. *Scientific American* **1992**, *266*, 112-118.
- (16) Soultanidis, N.; Zhou, W.; Psarras, A. C.; Gonzalez, A. J.; Iliopoulou, E. F.; Kiely, C. J.; Wachs, I. E.; Wong, M. S.: Relating n-Pentane Isomerization Activity to the Tungsten Surface Density of WO_x/ZgO₂. *Journal of the American Chemical Society* **2010**, *132*, 13462-13471.
- (17) Kim, T. Y.; Park, D. S.; Choi, Y.; Baek, J.; Park, J. R.; Yi, J.: Preparation and Characterization of Mesoporous Zr-WO_x/SiO₂ Catalysts for the Esterification of 1-Butanol with Acetic Acid. *Journal of Materials Chemistry* **2012**, *22*, 10021-10028.

- (18) Scheithauer, M.; Cheung, T. K.; Jentoft, R. E.; Grasselli, R. K.; Gates, B. C.; Knozinger, H.: Characterization of WO_x/ZrO_2 by Vibrational Spectroscopy and n-Pentane Isomerization Catalysis. *Journal of Catalysis* **1998**, *180*, 1-13.
- (19) Kuba, S.; Gates, B. C.; Vijayanand, P.; Grasselli, R. K.; Knozinger, H.: An Active and Selective Alkane Isomerisation Catalyst: Iron- and Platinum-Promoted Tungstated Zirconia (pg 321, 2001). *Chemical Communications* **2001**, 508-508.
- (20) Kuba, S.; Lukinskas, P.; Ahmad, R.; Jentoft, F. C.; Grasselli, R. K.; Gates, B. C.; Knozinger, H.: Reaction Pathways in n-Pentane Conversion Catalyzed by Tungstated Zirconia: Effects of Platinum in the Catalyst and Hydrogen in the Fed. *Journal of Catalysis* **2003**, *219*, 376-388.
- (21) Hino, M.; Arata, K.: Synthesis of Solid Superacid of Tungsten-Oxide Supported on Zirconia and its Catalytic Action for Reactions of Butane and Pentane. *Journal of the Chemical Society-Chemical Communications* **1988**, 1259-1260.
- (22) Santiesteban, J. G.; Vartuli, J. C.; Han, S.; Bastian, R. D.; Chang, C. D.: Influence of the Preparative Method on the Activity of Highly Acidic WO_x/ZrO_2 and the Relative Acid Activity Compared With Zeolites. *Journal of Catalysis* **1997**, *168*, 431-441.
- (23) Iglesia, E.; Barton, D. G.; Soled, S. L.; Miseo, S.; Baumgartner, J. E.; Gates, W. E.; Fuentes, G. A.; Meitzner, G. D.: Selective Isomerization of Alkanes on Supported Tungsten Oxide Acids. In *Studies in Surface Science and Catalysis*; Joe W. Hightower, W. N. D. E. I., Alexis, T. B., Eds.; Elsevier, 1996; Vol. Volume 101; pp 533-542.
- (24) Barton, D. G.; Soled, S. L.; Iglesia, E.: Solid Acid Catalysts Based on Supported Tungsten Oxides. *Topics in Catalysis* **1998**, *6*, 87-99.
- (25) Scheithauer, M.; Grasselli, R. K.; Knozinger, H.: Genesis and Structure of WO_x/ZrO_2 Solid Acid Catalysts. *Langmuir* **1998**, *14*, 3019-3029.
- (26) Boyse, R. A.; Ko, E. I.: Crystallization Behavior of Tungstate on Zirconia and Its Relationship to Acidic Properties. *Journal of Catalysis* **1997**, *171*, 191-207.
- (27) Arata, K.: Solid Superacids. In *Advances in Catalysis*; D.D. Eley, H. P., Paul, B. W., Eds.; Academic Press, 1990; Vol. Volume 37; pp 165-211.
- (28) Galano, A.; Gattorno, G. R.; García, E. T.: A Combined Theoretical-Experimental Study on the Acidity of WO_x-ZrO_2 systems. *Physical Chemistry Chemical Physics* **2008**, *10*, 4181-4188.
- (29) Hino, M.; Arata, K.: Synthesis of Solid Superacid of Molybdenum Oxide Supported on Zirconia and its Catalytic Action. *Chemistry Letters* **1989**, 971-972.
- (30) Medgaarden, E. I. R.; Knowles, W. V.; Kim, T.; Wong, M. S.; Zhou, W.; Kiely, C. J.; Wachs, I. E.: New Insights into the Nature of the Acidic Catalytic Active Sites Present in ZrO_2 -Supported Tungsten Oxide Catalysts. *Journal of Catalysis* **2008**, *256*, 108-125.
- (31) Boyse, R. A.; Ko, E. I.: Crystallization Behavior of Tungstate on Zirconia and its Relationship to Acidic Properties .1. Effect of Preparation Parameters. *Journal of Catalysis* **1997**, *171*, 191-207.
- (32) Chang, C. D.; Kresge, C. T.; Santiesteban, J. G.; Vartuli, J. C.: Method for Preparing a Modified Solid Oxide. In *United States Patent: 5,510,309*; Mobil Oil Corporation, Fairfax, Virginia, USA: USA, 1996; pp 8.
- (33) Chan, J. Y. G.; Santiesteban, J. G.; Stern, D. L.: Catalyst Comprising a Modified Solid Oxide. In *United States Patent: 5,719,097*: USA, 1998; pp 11.
- (34) Chang, C. D.; Guiseppi, T. D.; Santiesteban, J. G.: Method for Preparing a Modified Solid Oxide. In *United States Patent: 5,780,382*; Mobil Oil Corporation, Virginia, USA: USA, 1998; pp 10.
- (35) Chan, J. Y. G.; Guiseppi, T. D.; Han, S.; Santiesteban, J. G.; Stern, D. L.: Method for Preparing a Modified Solid Oxide. In *United States Patent:5,854,170*; Mobil Oil Corporation, Virginia, USA: USA, 1998; pp 13.
- (36) Chan, J. Y. G.; Santiesteban, J. G.; Stern, D. L.: Isomerization Process. In *United States Patent:6,080,904*; Mobil Oil Corporation, Virginia, USA: USA, 2000; pp 11.
- (37) Gillespie, R. P.: Isomerization Catalyst and Processes. In *United States Patent: US 6,818,589 B1*; UOP LLC, Illinois, USA: USA, 2004; pp 15.
- (38) Gillespie, R. P.: Isomerization Catalyst and Processes. In *United States Patent: US 6,977,322 B2*; UOP LLC, Illinois, USA: USA, 2005; pp 15.
- (39) Zhou, W.; Medgaarden, E. I. R.; Knowles, W. V.; Wong, M. S.; Wachs, I. E.; Kiely, C. J.: Identification of Active Zr- WO_x Clusters on a ZrO_2 Support for Solid Acid Catalysts. *Nature Chemistry* **2009**, *1*, 722-728.

- (40) De Rossi, S.; Ferraris, G.; Valigi, M.; Gazzoli, D.: WO_x/ZrO₂ catalysts Part 2. Isomerization of n-Butane. *Applied Catalysis A-General* **2002**, *231*, 173-184.
- (41) Triwahyono, S.; Yamada, T.; Hattori, H.: IR Study of Acid Sites on WO₃-ZrO₂ and Pt/WO₃-ZrO₂. *Applied Catalysis A-General* **2003**, *242*, 101-109.
- (42) Baertsch, C. D.; Komala, K. T.; Chua, Y. H.; Iglesia, E.: Genesis of Brønsted Acid sites During Dehydration of 2-Butanol on Tungsten Oxide Catalysts. *Journal of Catalysis* **2002**, *205*, 44-57.
- (43) Wilson, R. D.; Barton, D. G.; Baertsch, C. D.; Iglesia, E.: Reaction and Deactivation Pathways in Xylene Isomerization on Zirconia Modified by Tungsten Oxide. *Journal of Catalysis* **2000**, *194*, 175-187.
- (44) Lecarpentier, S.; Gestel, J. v.; Thomas, K.; Houalla, M.: Study of Ir/WO₃/ZrO₂-SiO₂ Ring Opening Catalysts Part I: Characterization. *Journal of Catalysis* **2007**, *245*, 45-54.
- (45) Barton, D. G.; Soled, S. L.; Meitzner, G. D.; Fuentes, G. A.; Iglesia, E.: Structural and Catalytic Characterization of Solid Acids Based on Zirconia Modified by Tungsten Oxide. *Journal of Catalysis* **1999**, *181*, 57-72.
- (46) Baertsch, C. D.; Soled, S. L.; Iglesia, E.: Isotopic and Chemical Titration of Acid Sites in Tungsten Oxide Domains Supported on Zirconia. *Journal of Physical Chemistry B* **2001**, *105*, 1320-1330.
- (47) Vartuli, J. C.; Santiesteban, J. G.; Traverso, P.; Martinez, N. C.; Chang, C. D.; Stevenson, S. A.: Characterization of the Acid Properties of Tungsten/Zirconia Catalysts Using Adsorption Microcalorimetry and n-Pentane Isomerization Activity. *Journal of Catalysis* **1999**, *187*, 131-138.
- (48) Calabro, D. C.; Vartuli, J. C.; Santiesteban, J. G.: The Characterization of Tungsten-Oxide-Modified Zirconia Supports for Dual Functional Catalysis. *Topics in Catalysis* **2002**, *18*, 231-242.
- (49) Barton, D. G.; Shtein, M.; Wilson, R. D.; Soled, S. L.; Iglesia, E.: Structure and Electronic Properties of Solid Acids Based on Tungsten Oxide Nanostructures. *Journal of Physical Chemistry B* **1999**, *103*, 630-640.
- (50) Larsen, G.; Lotero, E.; Parra, R. D.: Tungsta and Platinum-Tungsta Supported on Zirconia Catalysts for Alkane Isomerization. In *Studies in Surface Science and Catalysis*; Joe W. Hightower, W. N. D. E. I., Alexis, T. B., Eds.; Elsevier, 1996; Vol. Volume 101; pp 543-551.
- (51) Larsen, G.; Raghavan, S.; Marquez, M.; Lotero, E.: Tungsta Supported on Zirconia and Alumina catalysts: Temperature-Programmed Desorption/Reaction of Methanol and Pyridine DRIFTS Studies. *Catalysis Letters* **1996**, *37*, 57-62.
- (52) Baertsch, C. D.; Wilson, R. D.; Barton, D. G.; Soled, S. L.; Iglesia, E.: Structure and Surface Properties of ZrO₂-supported WO₃ nanostructures. In *Studies in Surface Science and Catalysis*; Avelino Corma, F. V. M. S. M., José Luis, G. F., Eds.; Elsevier, 2000; Vol. Volume 130; pp 3225-3230.
- (53) Herrera, J. E.; Kwak, J. H.; Hu, J. Z.; Wang, Y.; Peden, C. H. F.: Effects of Novel Supports on the Physical and Catalytic Properties of Tungstophosphoric Acid for Alcohol Dehydration Reactions. *Topics in Catalysis* **2008**, *49*, 259-267.
- (54) Larsen, G.; Lotero, E.; Petkovic, L. M.; Shobe, D. S.: Alcohol Dehydration Reactions Over Tungstated Zirconia Catalysts. *Journal of Catalysis* **1997**, *169*, 67-75.
- (55) Ramos, F. S.; Farias, A. M. D. d.; Borges, L. E. P.; Monteiro, J. L.; Fraga, M. A.; Aguiar, E. F. S.; Appel, L. G.: Role of Dehydration Catalyst Acid Properties on One-Step DME Synthesis Over Physical Mixtures. *Catalysis Today* **2005**, *101*, 39-44.
- (56) Trens, P.; Peckett, J. W.; Stathopoulos, V. N.; Hudson, M. J.; Pomonis, P. J.: Phosphotungstate Anions Supported on Spherical Beads of Carbon as Highly Efficient Catalysts for the Dehydration of Propan-2-ol to Propene. *Applied Catalysis A-General* **2003**, *241*, 217-226.
- (57) Garbay, P. L.; Millet, J. M. M.; Loridant, S.; Baca, V. B.; Rey, P.: New Efficient and Long-Life Catalyst for Gas-Phase Glycerol Dehydration to Acrolein. *Journal of Catalysis* **2011**, *280*, 68-76.
- (58) Sereshki, B. R.; Balan, S. J.; Patience, G. S.; Dubois, J. L.: Reactive Vaporization of Crude Glycerol in a Fluidized Bed Reactor. *Industrial & Engineering Chemistry Research* **2010**, *49*, 1050-1056.
- (59) Chambon, F.; Rataboul, F.; Pinel, C.; Cabiac, A.; Guillon, E.; Essayem, N.: Cellulose Hydrothermal Conversion Promoted by Heterogeneous Brønsted and Lewis Acids: Remarkable Efficiency of Solid Lewis Acids to Produce Lactic Acid. *Applied Catalysis B-Environmental* **2011**, *105*, 171-181.
- (60) Chai, S.-H.; Wang, H.-P.; Liang, Y.; Xu, B.-Q.: Sustainable Production of Acrolein: Preparation and Characterization of Zirconia-Supported 12-Tungstophosphoric Acid Catalyst for Gas-Phase Dehydration of Glycerol. *Applied Catalysis A-General* **2009**, *353*, 213-222.
- (61) Paul, S.; Katryniok, B.; Dumeignil, F.: Method for Preparing Acrolein from Glycerol or Glycerine. In *Demande Internationale Publiée en Vertu du Traité de Coopération en Matière de Brevets*

(PCT): WO 2011/083254 A1; Adisseo France S. A. S., Centre National de la Recherche Scientifique, Université Lille 1- Sciences et Technologies: France, 2011; pp 23.

(62) Chai, S.-H.; Wang, H.-P.; Liang, Y.; Xu, B.-Q.: Sustainable Production of Acrolein: Gas-Phase Dehydration of Glycerol over 12-Tungstophosphoric Acid Supported on ZrO₂ and SiO₂. *Green Chemistry* **2008**, *10*, 1087-1093.

(63) Alsahme, A. M.; Wiper, P. V.; Khimyak, Y. Z.; Kozhevnikova, E. F.; Kozhevnikov, I. V.: Solid Acid Catalysts Based on H₃PW₁₂O₄₀ Heteropolyacid and Catalytic Properties at a Gas-Solid Interface. *Journal of Catalysis* **2010**, *276*, 181-189.

(64) Paul, S.; Katryniok, B.; Dumeignil, F.; Capron, M.: Procédé de Préparation D' Acroleine Par Deshydratation Catalytique de Glycerol ou Glycerine. In *France Patent: FR 2954312-A1*; Adisseo France S.A.S.; Centre National de la Recherche Scientifique; Université de Lille 1 Sciences et Technologies: France, 2011.

(65) Hölderich, W.; Ülgen, A.: Heterogenkatalysatoren für die Dehydratisierung von Glycerin. In *German Patent: DE 102008027350 A1*; Frankenthal, Germany: Germany, 2009.

(66) Arata, K.: Preparation of Superacids by Metal Oxides for Reactions of Butanes and Pentanes. *Applied Catalysis A-General* **1996**, *146*, 3-32.

(67) Macht, J.; Baertsch, C. D.; Lozano, M. M.; Soled, S. L.; Wang, Y.; Iglesia, E.: Support Effects on Brönsted Acid Site Densities and Alcohol Dehydration Turnover Rates on Tungsten Oxide Domains. *Journal of Catalysis* **2004**, *227*, 479-491.

(68) Zeng, W.; Cheng, D.-g.; Chen, F.; Zhan, X.: Catalytic Conversion of Glucose on Al-Zr Mixed Oxides in Hot Compressed Water. *Catalysis Letters* **2009**, *133*, 221-226.

(69) Hwang, C.-C.; Chen, X.-R.; Wong, S.-T.; Chen, C.-L.; Mou, C.-Y.: Enhanced Catalytic Activity for Butane Isomerization with Alumina-Promoted Tungstated Mesoporous Zirconia. *Applied Catalysis A-General* **2007**, *323*, 9-17.

(70) Jácome, M. A. C.; Toledo, J. A.; Chavez, C. A.; Aguilar, M.; Wang, J. A.: Influence of Synthesis Methods on Tungsten Dispersion, Structural Deformation, and Surface Acidity in binary WO₃-ZrO₂ system. *Journal of Physical Chemistry B* **2005**, *109*, 22730-22739.

(71) Ciesla, U.; Froba, M.; Stucky, G.; Schuth, F.: Highly Ordered Porous Zirconias From Surfactant-Controlled Syntheses: Zirconium Oxide-Sulfate and Zirconium Oxophosphate. *Chemistry of Materials* **1999**, *11*, 227-234.

(72) ICDD-International-Centre-for-Diffracton-Data: <http://www.icdd.com/>. 2012.

(73) Reddy, B. M.; Patil, M. K.; Reddy, G. K.; Reddy, B. T.; Rao, K. N.: Selective Tert-Butylation of Phenol Over Molybdate- and Tungstate-Promoted Zirconia Catalysts. *Applied Catalysis A-General* **2007**, *332*, 183-191.

(74) Sunita, G.; Devassy, B. M.; Vinu, A.; Sawant, D. P.; Balasubramanian, V. V.; Halligudi, S. B.: Synthesis of Biodiesel over Zirconia-Supported Isopoly and Heteropoly Tungstate Catalysts. *Catalysis Communications* **2008**, *9*, 696-702.

(75) Chakravarty, R.; Shukla, R.; Tyagi, A. K.; Dash, A.; Venkatesh, M.: Nanocrystalline Zirconia: A Novel Sorbent for the Preparation of ¹⁸W/¹⁸Re generator. *Applied Radiation and Isotopes* **2010**, *68*, 229-238.

(76) Loridant, S.; Feche, C.; Essayem, N.; Figueras, F.: WO_x/ZrO₂ Catalysts Prepared by Anionic Exchange: In Situ Raman Investigation From the Precursor Solutions to the Calcined Catalysts. *Journal of Physical Chemistry B* **2005**, *109*, 5631-5637.

(77) Reddy, B. M.; Sreekanth, P. M.; Reddy, V. R.: Modified Zirconia Solid Acid Catalysts for Organic Synthesis and Transformations. *Journal of Molecular Catalysis A-Chemical* **2005**, *225*, 71-78.

(78) Figueras, F.; Palomeque, J.; Loridant, S.; Fèche, C.; Essayem, N.; Gelbard, G.: Influence of the Coordination on the Catalytic Properties of Supported W Catalysts. *Journal of Catalysis* **2004**, *226*, 25-31.

(79) Jácome, M. A. C.; Chavez, C. A.; Bokhimi, X.; Antonio, J. A. T.: Generation of WO₃-ZrO₂ Catalysts from Solid Solutions of Tungsten in Zirconia. *Journal of Solid State Chemistry* **2006**, *179*, 2663-2673.

(80) Ji, W. J.; Hu, J. Q.; Chen, Y.: The Structure and Surface Acidity of Zirconia-Supported Tungsten Oxides. *Catalysis Letters* **1998**, *53*, 15-21.

(81) Vaudagna, S. R.; Canavese, S. A.; Comelli, R. A.; Figoli, N. S.: Platinum Supported WO_x-ZrO₂: Effect of Calcination Temperature and Tungsten Loading. *Applied Catalysis A-General* **1998**, *168*, 93-111.

- (82) Reddy, B. M.; Sreekanth, P. M.; Yamada, Y.; Kobayashi, T.: Surface Characterization and Catalytic Activity of Sulfate-, Molybdate- and Tungstate-Promoted Al₂O₃-ZrO₂ solid acid catalysts. *Journal of Molecular Catalysis A-Chemical* **2005**, *227*, 81-89.
- (83) Jácome, M. A.; Toledo, J. A.; Chavez, C.; Aguilar, M.; Wang, J. A.: Influence of Synthesis Methods on Tungsten Dispersion, Structural Deformation, and Surface Acidity in Binary WO₃-ZrO₂ system. *Journal of Physical Chemistry B* **2005**, *109*, 22730-22739.
- (84) Busto, M.; Lovato, M. E.; Vera, C. R.; Shimizu, K.; Grau, J. M.: Silica Supported Tungsta-Zirconia Catalysts for Hydroisomerization-Cracking of Long Alkanes. *Applied Catalysis A-General* **2009**, *355*, 123-131.
- (85) Valigi, M.; Gazzoli, D.; Pettiti, I.; Mattei, G.; Colonna, S.; Rossi, S. D.; Ferraris, G.: WO_x/ZrO₂ Catalysts Part 1. Preparation, Bulk and Surface Characterization. *Applied Catalysis A-General* **2002**, *231*, 159-172.
- (86) Maksimov, G. M.; Litvak, G. S.; Budneva, A. A.; Paukshtis, E. A.; Salanov, A. N.; Likholobov, V. A.: WO₃/MO₂ (M = Zr, Sn, Ti) Heterogeneous Acid Catalysts: Synthesis, Study, and Use in Cumene Hydroperoxide Decomposition. *Kinetics and Catalysis* **2006**, *47*, 564-571.
- (87) Boyse, R. A.; Ko, E. I.: Commercially Available Zirconia-Tungstate as a Benchmark Catalytic Material. *Applied Catalysis A-General* **1999**, *177*, L131-L137.
- (88) Boyse, R. A.; Ko, E. I.: Study of Tungsten Oxide and Sulfate Interactions on Doubly-Doped Zirconia Aerogels. *Catalysis Letters* **1997**, *49*, 17-23.
- (89) Kuba, S.; Heydorn, P. C.; Grasselli, R. K.; Gates, B. C.; Che, M.; Knozinger, H.: Redox Properties of Tungstated Zirconia Catalysts: Relevance to the Activation of n-Alkanes. *Physical Chemistry Chemical Physics* **2001**, *3*, 146-154.
- (90) Kaucký, D.; Wichterlová, B.; Dedecek, J.; Sobalik, Z.; Jakubec, I.: Effect of the Particle Size and Surface Area of Tungstated Zirconia on the WO_x Nuclearity and n-Heptane Isomerization Over Pt/WO₃-ZrO₂. *Applied Catalysis A-General* **2011**, *397*, 82-93.
- (91) Boyse, R. A.; Ko, E. I.: Crystallization Behavior of Tungstate on Zirconia and its Relationship to Acidic Properties - II. Effect of Silica. *Journal of Catalysis* **1998**, *179*, 100-110.
- (92) Sarkar, A.; Pramanik, S.; Achariya, A.; Pramanik, P.: A Novel Sol-Gel Synthesis of Mesoporous ZrO₂-MoO₃/WO₃ mixed oxides. *Microporous and Mesoporous Materials* **2008**, *115*, 426-431.
- (93) Vu, T. M.; Gestel, J. v.; Gilson, J. P.; Collet, C.; Dath, J. P.; Duchet, J. C.: Platinum Tungstated Zirconia Isomerization Catalysts - Part I. Characterization of Acid and Metal Properties. *Journal of Catalysis* **2005**, *231*, 453-467.
- (94) Yori, J. C.; Pieck, C. L.; Parera, J. M.: Phosphate as Promoter of Zirconia for Alkane Isomerization Reactions. *Catalysis Letters* **1998**, *52*, 227-229.
- (95) Melezhyk, O. V.; Prudius, S. V.; Brei, V. V.: Sol-Gel Polymer-Template Synthesis of Mesoporous WO₃/ZrO₂. *Microporous and Mesoporous Materials* **2001**, *49*, 39-44.
- (96) Scheithauer, M.; Jentoft, R. E.; Gates, B. C.; Knozinger, H.: n-Pentane Isomerization Catalyzed by Fe- and Mn-Containing Tungstated Zirconia Characterized by Raman Spectroscopy. *Journal of Catalysis* **2000**, *191*, 271-274.
- (97) Kuba, S.; Lukinskas, P.; Grasselli, R. K.; Gates, B. C.; Knozinger, H.: Structure and Properties of Tungstated Zirconia Catalysts for Alkane Conversion. *Journal of Catalysis* **2003**, *216*, 353-361.
- (98) Busca, G.: Differentiation of Mono-Oxo and Polyoxo and of Monomeric and Polymeric Vanadate, Molybdate and Tungstate Species in Metal Oxide Catalysts by IR and Raman Spectroscopy. *Journal of Raman Spectroscopy* **2002**, *33*, 348-358.
- (99) Nyquist, R.; Kagel, R.; Putzig, C.; Leugers, M.: *Handbook of Infrared and Raman Spectra of Inorganic Compounds and Organic Salts*; Academic Press: San Diego, USA, 1997; Vol. 1.
- (100) Alejandre, A. G.; Castillo, P.; Ramirez, J.; Ramis, G.; Busca, G.: Redox and Acid Reactivity of Wolframyl Centers on Oxide Carriers: Brønsted, Lewis and Redox Sites. *Applied Catalysis A-General* **2001**, *216*, 181-194.
- (101) Hsu, C. Y.; Heimbuch, C. R.; Armes, C. T.; Gates, B. C.: A Highly-Active Solid Superacid Catalyst for n-Butane Isomerization- A Sulfated Oxide Containing Iron, Manganese and Zirconium. *Journal of the Chemical Society-Chemical Communications* **1992**, 1645-1646.
- (102) Wang, L.; Xu, S.; Chu, W.; Yang, W.: Effect of Structure of Pd/WO₃-ZrO₂ Catalyst on Its Activity for Direct Oxidation of Ethylene to Acetic Acid. *Chinese Journal of Catalysis* **2009**, *30*, 864-872.

- (103) Antal, M. J.; Mok, W. S. L.; Richards, G. N.: Kinetic-Studies of the Reactions of Ketoses and Aldoses in Water at High Temperature .1. Mechanism of Formation of 5-(Hydroxymethyl)-2-Furaldehyde from D-Fructose and Sucrose. *Carbohydrate Research* **1990**, *199*, 91-109.
- (104) Ahmad, T.; Kenne, L.; Olsson, K.; Theander, O.: The Formation of 2-Furaldehyde and Formic Acid From Pentoses in Slightly Acidic Deuterium Oxide Studied by ¹H NMR Spectroscopy. *Carbohydrate Research* **1995**, *276*, 309-320.
- (105) Rose, I. C.; Epstein, N.; Watkinson, A. P.: Acid-Catalyzed 2-Furaldehyde (Furfural) Decomposition Kinetics. *Industrial & Engineering Chemistry Research* **2000**, *39*, 843-845.
- (106) Qian, M.; Reineccius, G.: Potent Aroma Compounds in Parmigiano Reggiano Cheese Studied Using a Dynamic Headspace (Purge-Trap) Method. *Flavour and Fragrance Journal* **2003**, *18*, 252-259.
- (107) Schnermann, P.; Schieberle, P.: Evaluation of Key Odorants in Milk Chocolate and Cocoa Mass by Aroma Extract Dilution Analyses. *Journal of Agricultural and Food Chemistry* **1997**, *45*, 867-872.
- (108) Halarewicz, K. C.; Kowalska, T.: A Study of the Dependence of the Kovats Retention Index on the Temperature of Analysis on Stationary Phases of Different Polarity. *Acta Chromatographica* **2003**, *13*, 69-80.
- (109) Pino, J. A.; Mesa, J.; Munoz, Y.; Marti, M. P.; Marbot, R.: Volatile Components from Mango (*Mangifera indica* L.) Cultivars. *Journal of Agricultural and Food Chemistry* **2005**, *53*, 2213-2223.
- (110) Rychlik, M.; Schieberle, P.; Grosch, W.: *Compilation of Odor Thresholds, Odor Quantities and Retention Indices of Key Food Odorants*; Institut für Lebensmittelchemie der Technischen Universität München and Deutsche Forschungsanstalt für Lebensmittelchemie: München, 1998.
- (111) Whitfield, F. B.; Mottram, D. S.: Heterocyclic Volatiles Formed by Heating Cysteine or Hydrogen Sulfide with 4-Hydroxy-5-methyl-3 (2H)-furanone at pH 6.5. *Journal of Agricultural and Food Chemistry* **2001**, *49*, 816-822.
- (112) Whitfield, F. B.; Mottram, D. S.: Investigation of the Reaction Between 4-Hydroxy-5-methyl-3(2H)-furanone and Cysteine or Hydrogen Sulfide at pH 4.5. *Journal of Agricultural and Food Chemistry* **1999**, *47*, 1626-1634.
- (113) Pino, J.; Marbot, R.; Rosado, A.: Volatile Constituents of Star Apple (*Chrysophyllum Cainito* L.) from Cuba. *Flavour and Fragrance Journal* **2002**, *17*, 401-403.
- (114) Mateo, J.; Zumalacarregui, J. M.: Volatile Compounds in Chorizo and Their Changes During Ripening. *Meat Science* **1996**, *44*, 255-273.
- (115) Jürgens, A.; Dötterl, S.: Chemical Composition of Another Volatiles in Ranunculaceae: Genera-Specific Profiles in Anemone, Aquilegia, Caltha, Pulsatilla, Ranunculus, and Trollius species. *American Journal of Botany* **2004**, *91*, 1969-1980.
- (116) Goodner, K. L.: Practical Retention Index Models of OV-101, DB-1, DB-5, and DB-Wax for Flavor and Fragrance Compounds. *Lwt-Food Science and Technology* **2008**, *41*, 951-958.
- (117) Parker, J. E.; Hassell, G. M. E.; Mottram, D. S.; Guy, R. C. E.: Sensory and Instrumental Analyses of Volatiles Generated During the Extrusion Cooking of Oat Flours. *Journal of Agricultural and Food Chemistry* **2000**, *48*, 3497-3506.
- (118) Gomez, E.; Ledbetter, C. A.; Hartsell, P. L.: Volatile Compounds in Apricot, Plum, and Their Interspecific Hybrids. *Journal of Agricultural and Food Chemistry* **1993**, *41*, 1669-1676.
- (119) Kaškonienė, V.; Venskutonis, P. R.; Čeksterytė, V.: Composition of Volatile Compounds of Honey of Various Floral Origin and Beebread Collected in Lithuania. *Food Chemistry* **2008**, *111*, 988-997.
- (120) Vichi, S.; Santini, C.; Natali, N.; Riponi, C.; Tamames, E. L.; Buxaderas, S.: Volatile and Semi-Volatile Components of Oak Wood Chips Analysed by Accelerated Solvent Extraction (ASE) Coupled to Gas Chromatography-Mass Spectrometry (GC-MS). *Food Chemistry* **2007**, *102*, 1260-1269.
- (121) Elmore, J. S.; Mottram, D. S.; Enser, M.; Wood, J. D.: Effect of the Polyunsaturated Fatty Acid Composition of Beef Muscle on the Profile of Aroma Volatiles. *Journal of Agricultural and Food Chemistry* **1999**, *47*, 1619-1625.
- (122) Engel, E.; Baty, C.; Corre, D. I.; Souchon, I.; Martin, N.: Flavor-Active Compounds Potentially Implicated in Cooked Cauliflower Acceptance. *Journal of Agricultural and Food Chemistry* **2002**, *50*, 6459-6467.
- (123) Risticvic, S.: HS-SPME-GC-TOFMS Methodology for Verification of Geographical Origin and Authenticity Attributes of Coffee Samples. University of Waterloo, 2008.

- (124) Jordan, M. J.; Margaria, C. A.; Shaw, P. E.; Goodner, K. L.: Aroma Active Components in Aqueous Kiwi Fruit Essence and Kiwi Fruit Puree by GC-MS and Multidimensional GC/GC-O. *Journal of Agricultural and Food Chemistry* **2002**, *50*, 5386-5390.
- (125) Risticvic, S.; Carasek, E.; Pawliszyn, J.: Headspace Solid-Phase Microextraction-Gas Chromatographic-Time-of-Flight Mass Spectrometric Methodology for Geographical Origin Verification of Coffee. *Analytica Chimica Acta* **2008**, *617*, 72-84.
- (126) Ames, J. M.; Guy, R. C. E.; Kipping, G. J.: Effect of pH, Temperature, and Moisture on the Formation of Volatile Compounds in Glycine/Glucose Model Systems. *Journal of Agricultural and Food Chemistry* **2001**, *49*, 4315-4323.
- (127) Tosun, G.; Kahriman, N.; Albay, C. G.; Karaoğlu, S. A.; Yayli, N.: Antimicrobial Activity and Volatile Constituents of the Flower, Leaf, and Stem of *Paeonia Daurica* Grown in Turkey. *Turkish Journal of Chemistry* **2011**, *35*, 145-153.
- (128) Adams, R. P.: *Identification of Essential Oil Components by Gas Chromatography/Mass Spectroscopy*; Allured Publishing Corporation: Illinois, USA, 1995.
- (129) Hill, V. M.; Isaacs, N. S.; Ledward, D. A.; Ames, J. M.: Effect of High Hydrostatic Pressure on the Volatile Components of a Glucose-Lysine Model System. *Journal of Agricultural and Food Chemistry* **1999**, *47*, 3675-3681.
- (130) Ghorab, A. H. E.; Mansour, A. F.; Massry, K. F. E.: Effect of Extraction Methods on the Chemical Composition and Antioxidant Activity of Egyptian Marjoram (*Majorana hortensis* Moench). *Flavour and Fragrance Journal* **2004**, *19*, 54-61.
- (131) Macleod, G.; Ames, J. M.: Gas Chromatography Mass-Spectrometry of the Volatile Components of Cooked Scorzonera. *Phytochemistry* **1991**, *30*, 883-888.
- (132) Chheda, J. N.; Dumesic, J. A.: An Overview of Dehydration, Aldol-Condensation and Hydrogenation Processes for Production of Liquid Alkanes from Biomass Derived Carbohydrates. *Catalysis Today* **2007**, *123*, 59-70.
- (133) Brujin, J. M. d.: *Monosaccharides in Alkaline Medium: Isomerization, Degradation, Oligomerization*. University of Technology, Delft, The Netherlands, 1986.
- (134) Kabyemela, B. M.; Adschiri, T.; Malaluan, R. M.; Arai, K.: Glucose and Fructose Decomposition in Subcritical and Supercritical Water: Detailed Reaction Pathway, Mechanisms, and Kinetics. *Industrial & Engineering Chemistry Research* **1999**, *38*, 2888-2895.
- (135) Yu, Y.; Lou, X.; Wu, H.: Some Recent Advances in Hydrolysis of Biomass in Hot-Compressed, Water and its Comparisons With Other Hydrolysis Methods. *Energy & Fuels* **2008**, *22*, 46-60.
- (136) Asghari, F. S.; Yoshida, H.: Acid-Catalyzed Production of 5-Hydroxymethylfurfural From D-fructose in Subcritical Water. *Industrial & Engineering Chemistry Research* **2006**, *45*, 2163-2173.
- (137) Sasaki, M.; Hayakawa, T.; Arai, K.; Adschiri, T.: Hydrothermal Reactions and Techniques. In *Proceedings of the Seventh International Symposium on Hydrothermal Reactions*; Feng, J. L., Chen, J. S., Shi, Z., Eds.; World Scientific Publishing Co. Pte., Ltd.: Changchun, China, 2003; pp 169-176.
- (138) Aida, T. M.; Sato, Y.; Watanabe, M.; Tajima, K.; Nonaka, T.; Hattori, H.; Arai, K.: Dehydration of D-Glucose in High Temperature Water at Pressures up to 80 MPa. *Journal of Supercritical Fluids* **2007**, *40*, 381-388.
- (139) Rasrendra, C. B.; Makertihartha, I. G. B. N.; Adisasmito, S.; Heeres, H. J.: Green Chemicals From D-glucose: Systematic Studies on Catalytic Effects of Inorganic Salts on the Chemo-Selectivity and Yield in Aqueous Solutions. *Topics in Catalysis* **2010**, *53*, 1241-1247.
- (140) Nursen, H. E.: *The Maillard Reaction: Chemistry, Biochemistry and Implications*; Royal Society of Chemistry: Great Britain, 2005.
- (141) Chidambaram, M.; Bell, A. T.: A Two-Step Approach for the Catalytic Conversion of Glucose to 2,5-Dimethylfuran in Ionic Liquids. *Green Chemistry* **2010**, *12*, 1253-1262.
- (142) Seydel, J. K.; Garrett, E. R.; Diller, W.; Schaper, K. J.: 5-Methyl-3(2H)-Furanone From Acid Catalyzed Solvolysis of 2-Deoxy-D-Ribose. *Journal of Pharmaceutical Sciences* **1967**, *56*, 858-862.
- (143) Karinen, R.; Vilonen, K.; Niemela, M.: Biorefining: Heterogeneously Catalyzed Reactions of Carbohydrates for the Production of Furfural and Hydroxymethylfurfural. *ChemSusChem* **2011**, *4*, 1002-1016.
- (144) Malherbe, R. R.; Martinez, J. O.; Navarro, E.: Furfural Oligomerization Within H-Fe-FAU Zeolite. *Journal of Materials Science Letters* **1993**, *12*, 1037-1038.

(145) Popoff, T.; Theander, O.: Formation of Aromatic Compounds from D-Glucuronic Acid and D-Xylose Under Slightly Acidic Conditions. *Journal of the Chemical Society D-Chemical Communications* **1970**, 1576a.

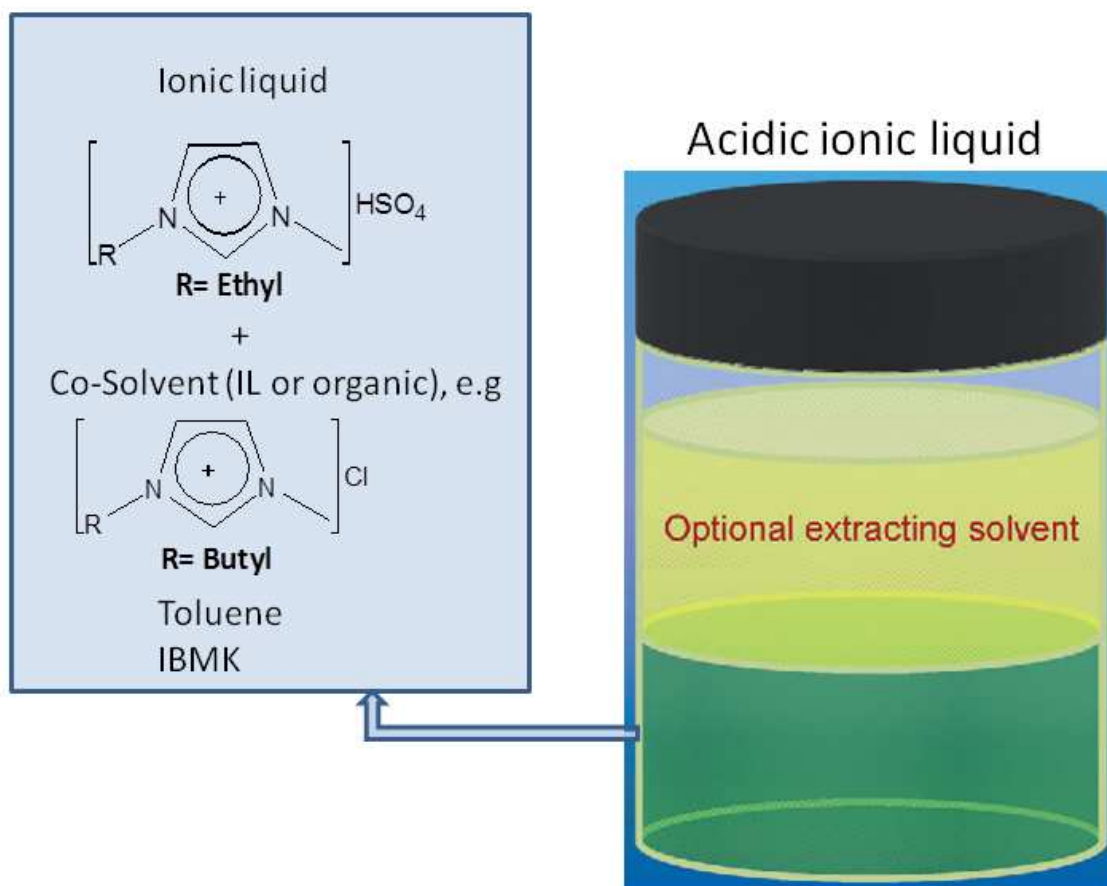
(146) Popoff, T.; Theander, O.: Formation of Aromatic Compounds From Carbohydrates. 1. Reaction of D-Glucuronic Acid, D-Galacturonic Acid, D-Xylose, and L-Arabinose in Slightly Acidic, Aqueous Solution. *Carbohydrate Research* **1972**, *22*, 135-149.

(147) McNeff, C. V.; Nowlan, D. T.; McNeff, L. C.; Yan, B.; Fedie, R. L.: Continuous Production of 5-Hydroxymethylfurfural From Simple and Complex Carbohydrates. *Applied Catalysis A-General* **2010**, *384*, 65-69.

(148) Watanabe, M.; Aizawa, Y.; Iida, T.; Nishimura, R.; Inomata, H.: Catalytic Glucose and Fructose Conversions With TiO₂ and ZrO₂ in Water at 473 K: Relationship Between Reactivity and Acid-Base Property Determined by TPD Measurement. *Applied Catalysis A-General* **2005**, *295*, 150-156.

CHAPTER 8

Conversion of saccharides into furanic aldehydes using homogeneous ionic liquid-based catalytic systems



Schematic representation of ILs systems

Index

CHAPTER 8	343
Conversion of saccharides into furanic aldehydes using homogeneous ionic liquid-based catalytic systems.....	343
8.1. Introduction	345
8.2. Results and discussion.....	346
8.2.1. [Emim]HSO ₄ characterisation	346
8.2.2. Dehydration of monosaccharides in ionic liquids.....	348
8.2.2.1. Reaction using [Emim]HSO ₄ -based catalytic systems under N ₂ atmosphere.....	348
8.2.2.2. Reaction using [Emim]HSO ₄ -based catalytic systems under reduced pressure.....	351
8.2.2.3. Reaction of hexoses using [Emim]HSO ₄ /co-solvent systems under N ₂ atmosphere	352
8.2.2.4. One-pot hydrolysis/dehydration of di/polysaccharides in ionic liquids.....	354
8.2.2.5. Identification of the reaction products	356
8.2.2.6. IL stability and reuse under N ₂ atmosphere.....	359
8.2.2.7. IL stability and reuse under reduced pressure	361
8.3. Conclusions	361
8.4. References.....	362

8.1. Introduction

Ionic liquids (ILs) have been tested as solvents and/or catalysts, due to the interesting properties they display when compared to common organic solvents used in carbohydrate chemistry.¹ ILs have several advantages as mentioned in Chapter 1, fulfilling some of the green chemistry requirements, like having almost no vapour pressure (avoiding atmospheric pollution problems typically associated with volatile organic solvents and product contamination with solvents in distillation processes), and some can be quite stable at high temperatures. Furthermore, IL solvents open up a window of opportunities for the dissolution of carbohydrates.¹ For example, cellulose, which is one of the most abundant natural polymers and attractive renewable feedstock, is practically insoluble in water and most organic solvents. In an early study, Swatloski et al.² reported that cellulose could be dissolved in ILs. Cellulose dissolves in [Bmim]Cl under conventional (100 °C) or microwave-assisted heating.² When cellulose is dissolved in an IL the β -glycosidic bonds are more susceptible to acid-catalysed hydrolysis at relatively low temperatures (100 °C) and low catalyst loading.^{1,3-5} Different studies have demonstrated the potential of hydrophilic ionic liquids (ILs) for the conversion of saccharides to Fur and Hmf. The state of the art of IL based catalytic systems used in the conversion of carbohydrates to furanic aldehydes under mild reaction conditions, is described in detail in Chapter 1. Most of the published work on the use of ILs for the conversion of saccharides has focused on the hexose monosaccharides D-fructose (Fru) and D-glucose (Glu). The published work with ILs using D-xylose to obtain Fur has been less studied.

Lansalot-Matras et al.⁶ firstly reported on the dehydration of D-fructose in the presence of Amberlyst-15 or p-TsOH as catalysts, using solvent mixtures of DMSO (the latter enhanced dissolution of D-fructose in the IL medium) and [Bmim]BF₄ or [Bmim]PF₆, which gave 75-80% Y_{Hmf} within 24 h, at 80 °C. In another study, the dehydration of fructose in 1-H-3-methyl imidazolium chloride, [Hmim]Cl gave 92% Y_{Hmf} within 15-45 min at 90 °C.⁷ The acidic IL 3-allyl-1-(4-sulfonylchloride butyl) imidazolium trifluoromethanesulfonate was also effective in converting Fru to Hmf, using DMSO as solvent, at 100 °C, under microwave radiation: ca. 85% Y_{Hmf} was reached within 4 min.⁸ Immobilisation of this IL in silica gel gave an effective and reusable solid catalyst, with no decay in Hmf yields after seven runs.⁸ Zhang et al.,⁹ reported on the use of several metal chlorides in 1-alkyl-3-methylimidazolium chloride ([Amim]Cl, A=alkyl) ILs for dehydration of Glu, a more demanding saccharide than Fru for Hmf production at 100 °C. These authors found that

CrCl_2 in $[\text{Emim}]\text{Cl}$ (E=ethyl) was a singularly effective catalytic system, affording up to 70% Y_{Hmf} at ca. 95% C_{Glu} (3 h reaction), and negligible amounts of levulinic acid were formed. Several explanations of the high Hmf yield achieved in imidazolium chloride ILs have been put forward, such as the low concentration of water present in the reaction medium (avoiding the subsequent hydration of Hmf to levulinic acid), the formation of complexes between the IL and the sugar (decreasing the activation barrier for Hmf formation),⁷ and the formation of complexes between the sugar and the metal chlorides in the ILs.⁹

This Chapter focuses on the dehydration of pentose (D-xylose) and hexose (D-fructose and D-glucose) monosaccharides, and the one-pot hydrolysis of di/polysaccharides and subsequent dehydration of the corresponding monosaccharides into Fur or Hmf, using the acidic IL 1-ethyl-3-methyl imidazolium hydrogen sulfate supplied by Merck KGaA ($[\text{Emim}]\text{HSO}_4$) (Figure 8.1), at 100 °C. A comparative study with 1-butyl-3-methyl imidazolium chloride ($[\text{Bmim}]\text{Cl}$) (Figure 8.1) or $[\text{Emim}]\text{HSO}_4/[\text{Bmim}]\text{Cl}$ mixtures was also carried out and the effect of adding chromium chloride was investigated, with the aim of enhancing the selectivity of the dehydration of Glu to Hmf.



Figure 8.1- Molecular structures of $[\text{Emim}]\text{HSO}_4$ and $[\text{Bmim}]\text{Cl}$.

More recent studies have been reported for the conversion of Xyl and related polysaccharides to Fur using IL-based catalytic systems. Sievers et al.¹⁰ reported 14% Y_{Hmf} using $[\text{Bmim}]\text{Cl}$ and H_2SO_4 as catalyst at 120 °C/94 min. Binder et al.¹¹ improved the Y_{Fur} to 45% using DMA/CrCl_2 coupled to $[\text{Emim}]\text{Cl}$ at 100 °C/2 h.

8.2. Results and discussion

8.2.1. $[\text{Emim}]\text{HSO}_4$ characterisation

The ^1H NMR and ^{13}C NMR spectra of $[\text{Emim}]\text{HSO}_4$ are given in Figures 8.2 and 8.3.

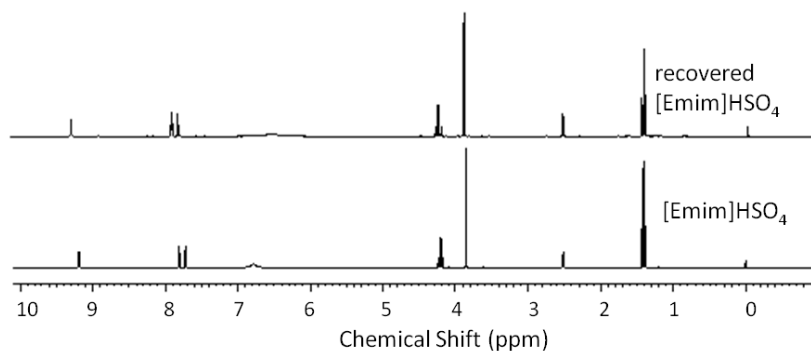


Figure 8.2- ¹H NMR spectra of fresh and recovered (from a catalytic test) [Emim]HSO₄.

The ¹H NMR data for [Emim]HSO₄ (300.13 MHz, 20 °C, DMSO-d₆, TMS) can be summarised as follows : δ = 1.41 (t, 3 H, CH₃CH₂), 3.86 (s, 3H, N-CH₃), 4.20 (q, 2H, N-CH₂CH₃), 7.72 (s, 1H, CH), 7.81 (s, 1H, CH) and 9.19 (s, 1H, CH).

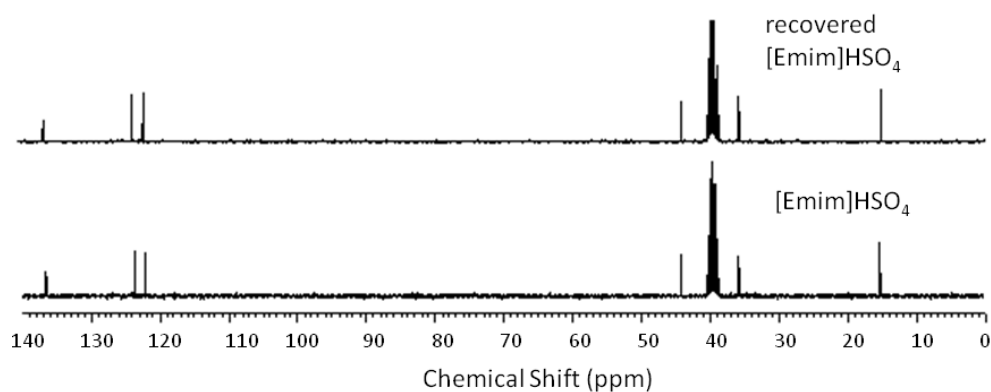


Figure 8.3- ¹³C NMR spectra of fresh and recovered (from a catalyst test) [Emim]HSO₄.

The ¹³C NMR data for [Emim]HSO₄ (75.47 MHz, 20 °C, DMSO-d₆, TMS) can be summarised as follows: δ =15.2 (CH₃CH₂), 35.7 (N-CH₃), 44.1 (N-CH₂), 122 (CH), 123.6 (CH) and 136.4 (CH).

8.2.2. Dehydration of monosaccharides in ionic liquids

8.2.2.1. Reaction using [Emim]HSO₄-based catalytic systems under N₂ atmosphere

The reaction of Xyl in [Emim]HSO₄ (0.67 M Xyl) at 100 °C gave 86% C_{Xyl} and 72% S_{Fur} at 30 min (Table 8.1). These results were fairly good, for example, in comparison to that reported for the reaction of Xyl carried out in the presence of Keggin-type heteropolytungstate (ca. 0.07 M) or sulfuric acid (0.01 M), using DMSO as solvent (a commonly used solvent to promote selectivity to the furan derivative).¹² After 4 h at 140 °C, these reaction systems gave 58-63% Y_{Fur}.¹³

When toluene (Tol) was used as a co-solvent with [Emim]HSO₄, a liquid-liquid biphasic solvent system was obtained, which gave approximately half of the Y_{Fur} (33%) achieved without a co-solvent (62% Y_{Fur}), at 30 min. However, the Y_{Fur} for the biphasic solvent system reached 84% at 6 h (Figure 8.4, Table 8.1), which was higher than the maximum observed without a co-solvent (62% Y_{Fur} at 30 min).

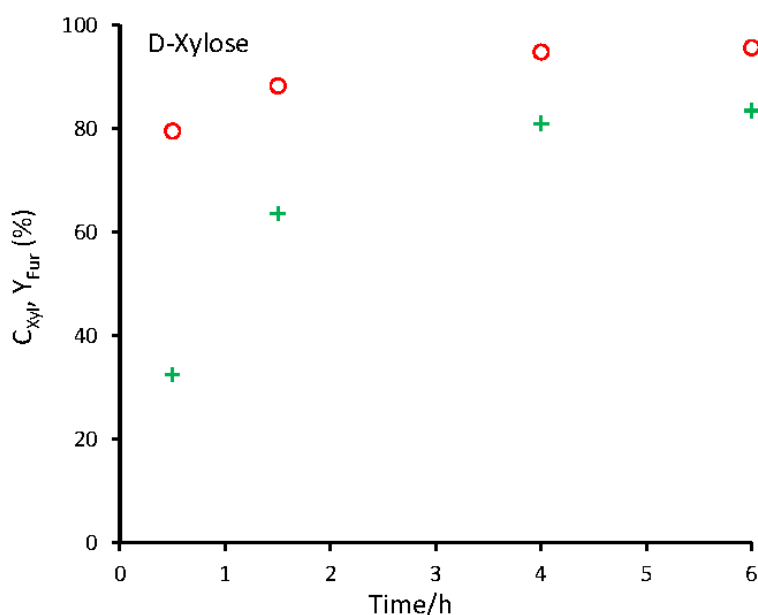


Figure 8.4- Conversion of D-Xylose (C_{Xyl}) (○) and yield of 2-furaldehyde (Y_{Fur}) (+) versus time for the reaction carried out in [Emim]HSO₄/Tol. Reaction conditions: 0.3 Wt:0.7 Tol (v/v) biphasic solvent system, 100 °C, 0.67 M Xyl.

Table 8.1- Conversion of mono/disaccharides to 2-furaldehyde (Fur) and/or 5-hydroxymethyl-2-furaldehyde (Hmf) in the ionic liquids [Emim]HSO₄ or [Bmim]Cl under nitrogen atmosphere.

Substrate	IL/co-solvent/temperature	Concentration ^a (g.dm ⁻³)	Reaction time (h)	C _{sub} ^b (%)	Y _{Fur} ^c (%)	Y _{Hmf} ^c (%)
D-Xylose	[Emim]HSO ₄ /none/100 °C	100	0.5	86	62	-
D-Xylose	[Emim]HSO ₄ /Tol/100 °C	100	0.5	80	33	-
D-Xylose	[Emim]HSO ₄ /Tol/100 °C	100	4	95	82	-
D-Xylose	[Emim]HSO ₄ /Tol/100 °C	100	6	96	84	-
D-Xylose	[Emim]HSO ₄ /Tol/100 °C	33	4	71	71	-
D-Xylose	[Emim]HSO ₄ /Tol/100 °C	167	4	93	60	-
D-Xylose	[Emim]HSO ₄ /Tol/120 °C	100	0.5	100	58	-
D-Xylose	[Bmim]Cl/Tol/100 °C	100	4	0	-	-
D-Xylose	[Bmim]Cl/Tol/100 °C+H ₂ SO ₄	100	4	83	44	-
D-Fructose	[Emim]HSO ₄ /Tol/100 °C	120	0.5	100	-	79
D-Fructose	[Emim]HSO ₄ /IBMK/100 °C	120	0.5	100	-	88
D-Fructose	[Bmim]Cl/Tol/100 °C	120	0.5	23	-	16
D-Glucose	[Emim]HSO ₄ /Tol/80 °C	120	0.5	86	-	1
D-Glucose	[Emim]HSO ₄ /Tol/80 °C	120	4	95	-	3
D-Glucose	[Emim]HSO ₄ /Tol/80 °C	120	24	97	-	8
D-Glucose	[Emim]HSO ₄ /Tol/100 °C	120	0.5	95	-	3
D-Glucose	[Emim]HSO ₄ /Tol/100 °C	120	4	95	-	9
D-Glucose	[Bmim]Cl/Tol/100 °C	120	4	0	-	-
D-Glucose	[Bmim]Cl/Tol/100 °C+CrCl ₃ ^d	120	4	91	-	91
D-Glucose	[Bmim]Cl/IBMK/100 °C+CrCl ₃ ^d	120	4	79	-	79
D-Glucose	[Bmim]Cl/none/100 °C+CrCl ₃ ^d	120	4	83	-	81
D-Sucrose	[Bmim]Cl/IBMK/100 °C+CrCl ₃ ^d	120	4	-	-	100
D-Cellobiose	[Bmim]Cl/IBMK/100 °C+CrCl ₃ ^d	120	4	-	-	50

a) Initial concentration expressed as g feedstock/dm³ ionic liquid. b) Conversion of the substrate at time t (C_{sub}). c) 2-Furaldehyde or 5-hydroxymethyl-2-furaldehyde yield (Y_{Fur} or Y_{Hmf}) at the specified reaction time t. d) 0.04 M CrCl₃.

In contrast to that observed for the biphasic system, without a co-solvent the yield of Fur decreased with time, reaching 40%/28% after 4 h/6 h. These results paralleled those reported in the literature,^{14,15} for reactions of saccharides in aqueous phase, concerning the beneficial effect of using a co-solvent for improving Fur and Hmf yields.

Increasing the Xyl concentration from 0.22 to 0.67 M (or 33 to 100 g.dm⁻³ of IL) led to an increase in C_{Xyl} at 4 h reaction from 71 to 95% and in Y_{Fur} from 71 to 82%, under biphasic conditions (Table 8.1). A further increase in the amount of Xyl to 1.11 M (167 g.dm⁻³ IL) resulted in a decrease in the Fur yield at high conversions (60% at 93% C_{Xyl} , compared with 82% at 95% C_{Xyl} for 0.67 M Xyl). Increasing the reaction temperature from 100 °C to 120 °C (for 0.67 M Xyl) in [Emim]HSO₄/Tol accelerated the reaction, giving 100% C_{Xyl} within 30 min, and a Y_{Fur} of 58% (Table 8.1). At higher reaction temperatures, the reaction was probably so fast that the effect of the co-solvent on product selectivity became less pronounced. As the reaction proceeded the mixture became darker and increasingly viscous, and thus mass transfer limitations were expected to be important and may affect the overall reaction. Several side reactions may contribute to the loss of Fur, such as condensation reactions between Fur and intermediates of the conversion of Xyl to Fur.¹⁶ The identification of reaction products is addressed in Section 8.2.2.5. More recently, Tao et al.¹⁷ reported for the acidic IL [Sbmim]HSO₄ (50 wt.% based on the amount of the solvent mixture) in a solvent mixture of H₂O/IBMK used in the reaction of Xyl (0.70 M) that 91 wt.% Y_{Fur} was reached at 95% C_{Xyl} at 150 °C/25 min using conventional heating.¹⁷ The IL [Bmim]HPO₄ was also tested but was less effective than [Sbmim]HSO₄ under similar conditions (68 wt.% Y_{Fur} at 80% C_{Xyl}).¹⁷

For comparative purposes the reaction of Xyl was carried out in [Bmim]Cl, using Tol as co-solvent at 100 °C, with or without H₂SO₄. No reaction took place in [Bmim]Cl/Tol without H₂SO₄, at least until 4 h (Table 8.1). These results showed that the Brønsted acidity associated with the anion in [Emim]HSO₄ was responsible for Xyl dehydration to Fur. The reaction of Xyl in aqueous H₂SO₄ (0.4 M, approximately equivalent to half of the number of moles of charged [Emim]HSO₄) gave less than 5% Y_{Fur} at 38% C_{Xyl} , after 4 h at 100 °C. When H₂SO₄ (0.04 M) was added to the [Bmim]Cl/Tol mixture, 83% C_{Xyl} and 44% Y_{Fur} were reached at 4 h. For the same residence time, [Emim]HSO₄/Tol gave 82% Y_{Fur} (Figure 8.4). Fur selectivity increased with time possibly due to the fact that the reaction mechanism involves a series of elementary steps.¹³

8.2.2.2. Reaction using [Emim]HSO₄-based catalytic systems under reduced pressure

The use of volatile solvents for extraction of the target furan compounds seems less “clean” than extraction using supercritical CO₂ or reduced pressure for evaporation.¹⁸⁻²⁰ The use of supercritical CO₂ requires special expensive equipment for containment and pressure. In this work, a simple reaction-vacuum evaporation setup was used for performing the reaction of Xyl in [Emim]HSO₄ without a co-solvent at 100 °C. A control experiment carried out at 100 °C using the IL without Xyl showed that only residual water was distilled out of the IL as demonstrated in the FT-IR spectra (Figure 8.5). Since the FT-IR spectra of the IL before and after the control experiment were similar, and no colour changes were observed, the IL was stable under the applied reaction conditions.

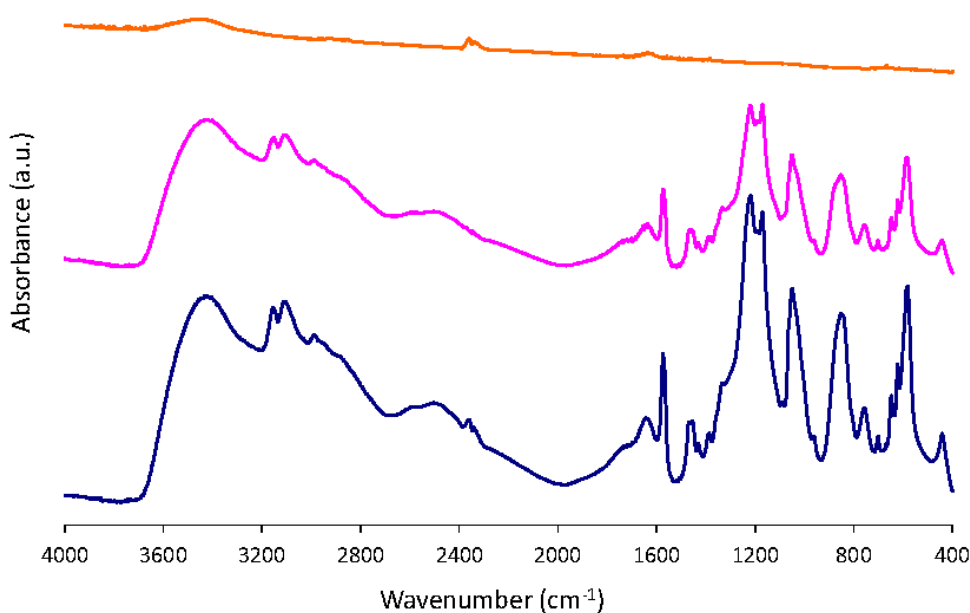


Figure 8.5- FT-IR spectra of [Emim]HSO₄ as acquired (blue line), [Emim]HSO₄ after the control experiment (vacuum drying, pink line) and the distillate obtained in that experiment (red line).

After 4 h of reaction of Xyl in [Emim]HSO₄ under reduced pressure, 84% C_{Xyl} and 15% S_{Fur} were obtained, which compared unfavourably to the results obtained under nitrogen

atmosphere, in which the S_{Fur} was 72% at a similar conversion of Xyl (86% C_{Xyl}) in only 30 min. Similar to that observed with the reaction mixture in the presence of Tol, the initially transparent mixture of the IL and Xyl became gradually darker and more viscous with increasing residence time, suggesting the formation of heavy products.

8.2.2.3. Reaction of hexoses using [Emim]HSO₄/co-solvent systems under N₂ atmosphere

The efficiency of the [Emim]HSO₄/Tol system was further investigated for the reaction of the hexoses, Glu and Fru, using an initial concentration similar to that used for Xyl (0.67 M, or 120 g.dm⁻³ IL). The reactivity of the monosaccharides (based on conversion at 30 min, Table 8.1) followed the order: Fru (100%) > Glu (95%) > Xyl (80%). As mentioned above, the yield of Fur from the reaction of Xyl increased up to 84% reached at 6 h (Figure 8.2). The reaction of Fru gave 79% Y_{Hmf} within 30 min. When [Bmim]Cl/Tol was used instead of [Emim]HSO₄/Tol, the reaction of Fru gave 16% Y_{Hmf} at 30 min, under similar conditions. Hence, the Brønsted acidity associated with [Emim]HSO₄ played a major role in the dehydration of Fru, similar to that observed for Xyl as substrate. For [Bmim]HSO₄, Hu et al.²¹ reported 56% Y_{Hmf} without a co-solvent, at 80 °C and 1 h, and very recently, Shi et al.²² reported 70% Y_{Hmf} , at 120 °C and 1 h. Another types of acidic ILs with hydrogen sulfate (HSO₄⁻) have been tested and gave lower Hmf yield, such as [Hmim]HSO₄ (24% Y_{Hmf} with DMSO as co-solvent at 90 °C/2 h, 0.46 M Fru),²³ or [NMM]HSO₄ (23% Y_{Hmf} with DMF-LiBr as co-solvent at 90 °C/2 h, 0.56 M Fru).²⁴

While Hmf may be formed in significant amounts from the reaction of Fru in [Emim]Cl at 100-120 °C, previous studies have shown that the same does not apply for the reaction of Glu in this IL, under similar reaction conditions.⁹ These results were reproduced in this work for [Emim]HSO₄ at 100 °C (Table 8.1).

For the Glu/[Emim]HSO₄/Tol system, the Hmf selectivity was very low (<9% up to 100% C_{Glu} , reached within 6 h). In a later study, Tong et al.²³ reported a similar behaviour for Glu (0.46 M) dehydration (2% Y_{Hmf} at 90 °C and 2 h using DMSO as co-solvent and [NMP]HSO₄ as solvent). The decrease in the reaction temperature from 100 to 80 °C led to lower C_{Glu} at 30 min (86% compared with 85% at 100 °C, Table 8.1), and the Hmf yield was less than 8% up to 97% C_{Glu} (reached within 24 h). More recently, Qi et al.²⁵ reported a moderate Y_{Hmf} of 37% in the absence

of a co-solvent but at a higher temperature of 200 °C and 10 min using [Bmim]HSO₄ under conventional heating.

Moreau et al.⁷ reported that the hydrolysis of Suc in 1-H-3-methyl imidazolium chloride ([Hmim]Cl) at 90 °C resulted in the very rapid cleavage of the disaccharide into Fru and Glu. However, while Fru was selectively dehydrated into Hmf in a consecutive pathway, Glu practically did not react. It has been postulated that the efficient in situ isomerisation of Glu to Fru is important to obtain high Hmf yield.^{9,26-29} In the case of the Glu/[Emim]HSO₄/Tol system, no Fru was detected by HPLC, suggesting that Glu to Fru isomerisation hardly took place, which may explain the much lower Hmf selectivities from Glu than from Fru (notwithstanding the similar reactivity of both hexoses).

Zhang et al.⁹ obtained outstanding results for the conversion of Glu into Hmf (nearly 70% Y_{Hmf} after 3 h at 100 °C) by adding CrCl₂ (0.04 M) to [Emim]Cl without a co-solvent. A series of other metal halides was tested, but the results were much poorer. As mentioned in Chapter 1, the authors proposed that a chromium chloride anion facilitates mutarotation of Glu (from α -glucopyranose to β -glucopyranose anomer) in the IL, followed by isomerisation into a fructofuranose intermediate via a chromium enolate intermediate.⁸ For comparative purposes, the reaction of Glu was carried out in [Bmim]Cl/Tol/CrCl₃ at 100 °C. CrCl₃ was chosen instead of CrCl₂ since it is more stable and easily handled under air (less toxic), much cheaper, and, on the other hand, it is very likely that Cr²⁺ is oxidised to Cr³⁺ in the IL system containing dissolved air and water (at least from the dehydration reaction). After 4 h at 100 °C, the Glu/[Bmim]Cl/CrCl₃ reaction system (without co-solvent) led to 81% Y_{Hmf} , which was much higher than that reported by Zhao et al.⁹ for the system Glu/[Emim]Cl/CrCl₃ (45% Y_{Hmf} at 100 °C/3 h). In that work when CrCl₂ was used instead of CrCl₃, an improvement to 67% of Y_{Hmf} was reached.⁹ A few other authors obtained lower 55-70% Y_{Hmf} at the same temperature and 6 h of reaction.^{9,30-34} The use of Tol as a co-solvent further improved Y_{Hmf} at 4 h to 91% (Table 8.1).

The influence of using IBMK instead of Tol as the extracting co-solvent was investigated for the Fru/[Emim]HSO₄ and Glu/[Bmim]Cl/CrCl₃ systems. The mixtures of these ILs with Tol or IBMK are biphasic. Control experiments performed without monosaccharides and analysed by GC-MS did not reveal the decomposition of the co-solvents. Whereas the use of IBMK instead of Tol led to a higher Hmf yield in the Fru/[Emim]HSO₄ reaction system, the opposite occurred for the Glu/[Bmim]Cl/CrCl₃ system (Table 8.1). These results may be due to differences in the solubility of the co-solvent in each IL (which may not be totally immiscible) and the distribution ratio of the target product in the two liquid phases. Nevertheless Li et al.³⁵ reported that the mixture of

[Bmim]HSO₄ (in catalytic amounts of 1 mol.%) and [Bmim]Cl as solvent, without the addition of a co-solvent used in the reaction of Fru (10 wt.%; 0.62 M), led to 80% Y_{Hmf} at 80 °C in 30 min.

8.2.2.4. One-pot hydrolysis/dehydration of di/polysaccharides in ionic liquids

The efficiencies of the [Emim]HSO₄/co-solvent and [Bmim]Cl/IBMK/CrCl₃ systems were further investigated in the one-pot conversion of different carbohydrate feedstocks, namely the disaccharides Suc and Cel, and the polysaccharides D-xylan, inulin, starch, and cellulose, into Hmf or Fur under nitrogen, using conditions which were chosen on the basis of preliminary catalytic tests and to facilitate comparative studies (for Xyl and di/polysaccharide, 100 g_{feedstock}·dm⁻³ in the IL; for hexoses, 120 g_{feedstocks}·dm⁻³ in the IL). The molecular structures of the different types of substrates tested are represented in Table 1.1 of the Introduction (Chapter 1). The results are shown in Figure 8.6 and were calculated on the basis of wt.% Y_{Fur} or Y_{Hmf}, and for comparative purposes the yields were also calculated for the monosaccharides. The theoretical yields (TY) are approximately 64 wt.% Y_{Fur} for Xyl, 70 wt.% Y_{Hmf} for Fru and Glu, 74 wt.% Y_{Hmf} for Suc, Mal or Cel, ca. 73 wt.% Y_{Fur} for D-xylan, and ca. 78 wt.% Y_{Hmf} for inulin. The D-xylan/[Emim]HSO₄/Tol reaction system gave nearly half the Fur TY at 4 h, and inulin/[Emim]HSO₄/IBMK gave nearly the full Hmf TY at 30 min (Figure 8.6). These results were somewhat congruent with the observed higher reactivity of Fru in comparison to Xyl in [Emim]HSO₄ (Table 8.1, Figure 8.4).

For the [Bmim]Cl/IBMK/CrCl₃ system, the reaction of Suc (a disaccharide with a β-(1-2) glycosidic bond between Glu and Fru units) gave approximately Hmf TY (73%) at 4 h. The reactions of Mal (a disaccharide with two Glu units linked by a α-(1-4) glycosidic bond) and Cel (a disaccharide with two Glu units linked by a β-(1-4) glycosidic bond) in [Bmim]Cl/IBMK/CrCl₃ gave approximately half of the Hmf TY and negligible amounts of Glu were detected (Figure 8.6). The reactions of starch (a polymer of Glu units containing α-(1-4) glycosidic bonds in a linear fashion (amylose) and α-(1-6) in a branched fashion (amylopectin)) and cellulose (a polymer of Glu units linked by β-(1-4) glycosidic bonds) in [Bmim]Cl/IBMK/CrCl₃ gave negligible Hmf yield, for residence times up to 4 h. No hydrolysis products were detected and the appearance of the reaction

mixture remained unchanged, suggesting that practically no reaction of these polysaccharides took place.

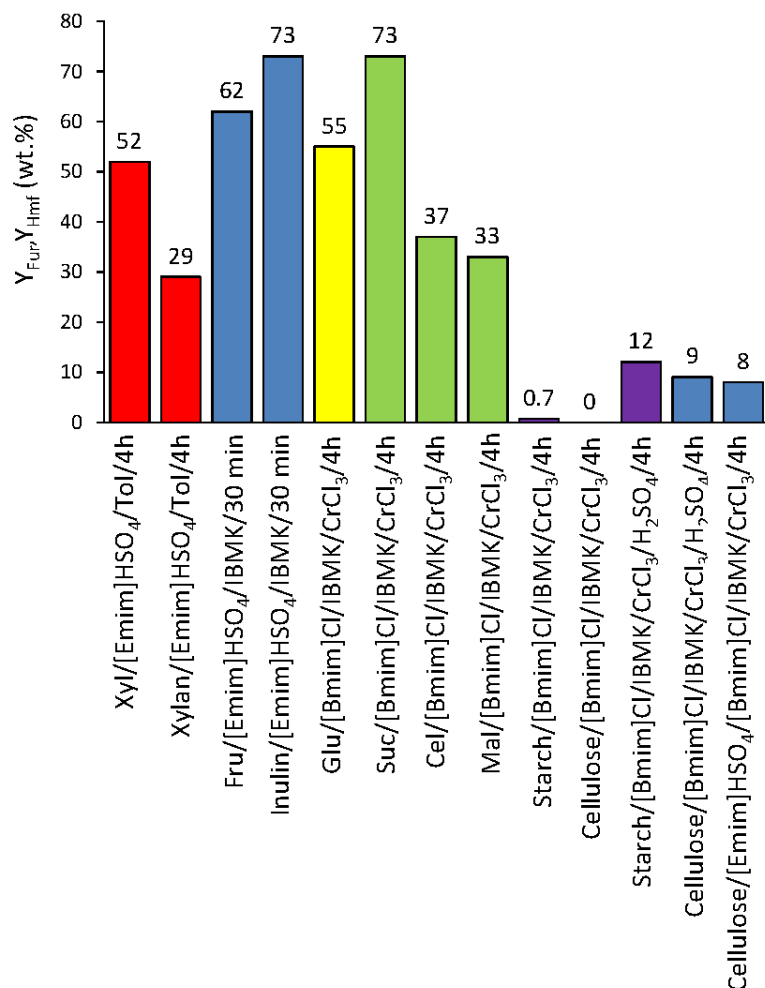


Figure 8.6- Yields of 2-furaldehyde, Y_{Fur} (from Xyl/D-xylan) or 5-hydroxymethyl-2-furaldehyde, Y_{Hmf} (from the remaining substrates) obtained in IL co-solvent biphasic system at 100 °C (initial concentration of feedstock of 100 g.dm⁻³ or 120 g.dm⁻³ for pentose or hexose-based carbohydrates, respectively, in the IL). In general, theoretical yields vary between 70 and 80 wt.%.

The dissolution of cellulose in [Amim]Cl ILs was greatly assisted by the high chloride ion concentration, which led to disruption of the extensive hydrogen bonding network present in its macrostructure.^{2,36-38} Accordingly, the sluggish reaction for cellulose/[Bmim]Cl/IBMK/CrCl₃ was probably not due entirely to solubility limitations. A possible explanation is that the hydrolysis step is rate limiting and demands a stronger acidity (Brønsted rather than Lewis type). Li and

Zhao³⁹ reported that cellulose hydrolysis takes place in [Bmim]Cl in the presence of HCl or H₂SO₄ as catalysts at 100 °C, under atmospheric pressure and without pretreatment.

After stirring the IL/cellulose mixtures for 5 min at 100 °C, a solution was obtained in the case of [Emim]HSO₄ (and the mixture was light brown), whereas a heterogeneous mixture was obtained for [Bmim]Cl (apparently cellulose did not completely dissolve, and no colour change in the reaction mixture was observed), suggesting that cellulose dissolved better in [Emim]HSO₄. Prior to the reaction at 100 °C, the mixtures were treated in an ultrasound bath (50 W, 40 KHz) for 15 min, at a.t. Based on these findings and those by Zhang et al.,⁹ an attempt was made to simultaneously enhance the hydrolysis reaction rate of cellulose (using [Emim]HSO₄ for enhancing polysaccharide solubility and giving Brönsted acidity) and enhance selectivity of the reaction of Glu to Hmf using ([Bmim]Cl/IBMK/CrCl₃) in a single reactor, at 100 °C. Hence, a mixed IL system consisting of [Bmim]Cl/[Emim]HSO₄ (2:1 v/v)/IBMK/CrCl₃ was used and led to 8 wt.% Y_{Hmf} after 4 h at 100 °C (Figure 8.6). Similar results were obtained when H₂SO₄ (0.04 M) was added to the [Bmim]Cl/IBMK/CrCl₃ system: 9 and 12% Y_{Hmf} for the reactions of cellulose and starch, respectively. The acidic IL [Sbmim]HSO₄ was tested by Tao et al.⁴⁰ in the one pot hydrolysis/dehydration of cellulose to Hmf in which the Y_{Hmf} was 15-24 wt.% using IBMK as co-solvent at 150 °C and 5 h.

The reaction of Glu using [Emim]HSO₄/Tol/CrCl₃ led to 96% C_{Glu} and 7 wt.% Y_{Hmf} at 4 h, which was similar to that observed for [Emim]HSO₄/Tol (6 wt.% Y_{Hmf}). Hence, the rather low Hmf yield for the cellulose reaction in the [Bmim]Cl/[Emim]HSO₄ (2:1, v/v)/IBMK/CrCl₃ system may be due to the lack of selectivity in the dehydration of Glu. The CrCl₂/[Bmim]Cl system reported by Zhang et al.,⁹ was successful in converting Glu into Hmf due to the formation of a higher halogenated anion complex. The mixed sulfate/chromium chloride IL acid systems may form different types of species, which may change (in nature and amount) during the course of the reaction as the concentration of water varies.

8.2.2.5. Identification of the reaction products

No by-products of the Xyl reaction in [Emim]HSO₄/Tol at 100 °C or 120 °C were detected by HPLC of the IL phase (using a diode array detector) and GC-MS analysis of the Tol phase

showed a few very weak peaks, which were not clearly identified. Thus, it was postulated that the by-products are mainly heavier products resulting from condensation reactions.

The exact nature of the black residue formed in the reaction of Xyl/[Emim]HSO₄ at 100 °C under reduced pressure was unknown. Elemental analysis revealed C, H, N and S contents of 45.7, 4.9, 4.8 and 8.0 wt.%, respectively (C:N:S mole ratio of 15:1.4:1), suggesting that the residue contains the IL or an insoluble derivative thereof. The calculated values for the pure IL were: C, 34.6; H, 5.8; N, 13.45; S, 15.4% (C:N:S mole ratio of 6:2:1). The solid state ¹³C CP MAS NMR spectrum of the recovered solid showed a complex series of overlapping resonances between 0 and 200 ppm (Figure 8.7): δ = 23.1, 44.3, 53, 89.5, 120, 131.5, 144.2 and 159.0 ppm. The signals up to 53 ppm were presumably due to the methyl and/or methylene carbon atoms, while those in the range 90-160 ppm were likely to arise from the carbon atoms of furan and/or imidazole/imidazolium rings. An alternative assignment for the peak at 90 ppm was a CH or CH₂ carbon bonded to two oxygen atoms (e.g. hemi-acetal), while the peak at 159 ppm may be due to the carbonyl group of an ester (since the FT-IR spectrum showed a new adsorption band at ca. 1700 cm⁻¹, that is attributed to a carbonyl stretching vibration, Figure 8.8).

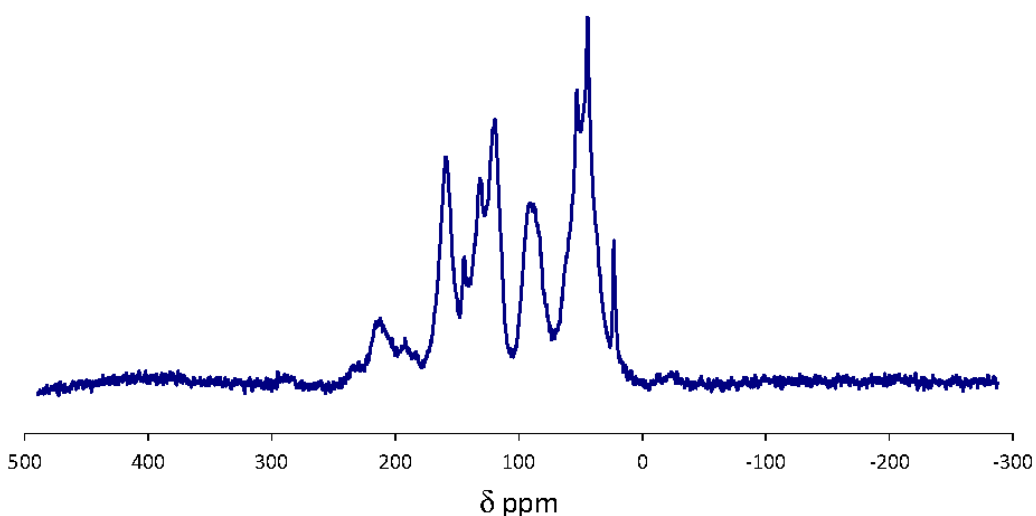


Figure 8.7-¹³C CP MAS NMR spectrum of the recovered solid after a catalytic batch run using D-xylose (Xyl)/[Emim]HSO₄ at 100 °C/4 h.

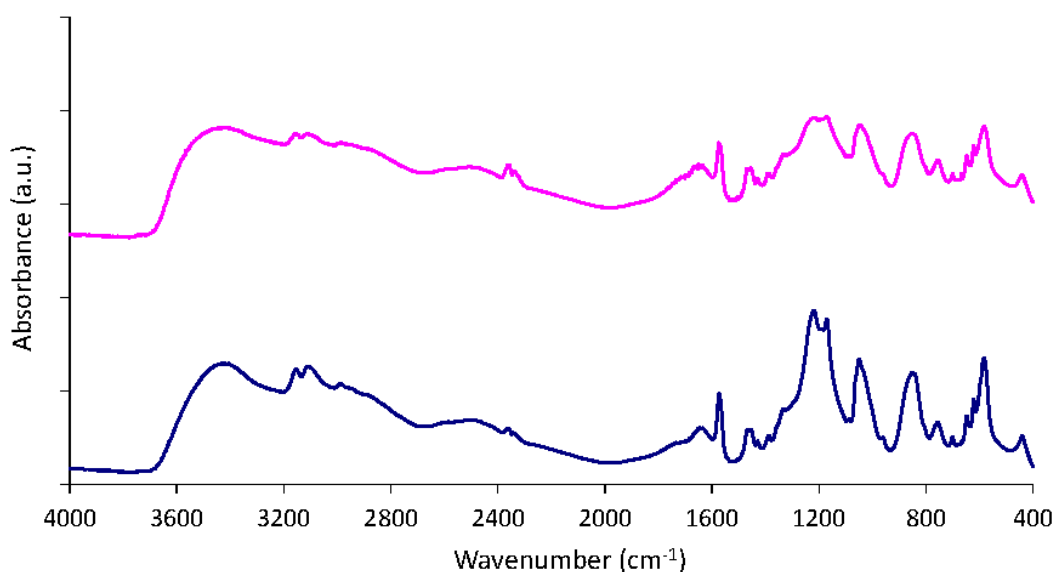


Figure 8.8- FT-IR spectra of [Emim]HSO₄ as acquired (blue line), and dark solid phase obtained from the reaction of D-xylose (Xyl) using [Emim]HSO₄ at 100 °C/4 h.

Levulinic and formic acids, which are common by-products formed in the aqueous phase reactions of hexoses under acidic conditions (via decomposition of Hmf), were not detected by HPLC (using diode array detector) in the reactions of hexoses using [Emim]HSO₄/Tol at 100 °C/6 h or 80 °C/24 h.

The decomposition of Glu may give several by-products, such as other sugars (e.g. mannose) via isomerisation, C-C bond scission via a retro aldol condensation and subsequent retro aldolisation, and non-furan cyclic ethers via dehydration.^{9,41} GC-MS analysis of the Glu/[Emim]HSO₄/Tol system after 6 h at 100 °C was performed to identify any volatile by-products. The chromatograms presented a few very weak peaks, which could not be fully and clearly identified. In the reaction of Fru, 5,5'-oxy-dimethylene-bis(2-furaldehyde), a symmetric ether of Hmf, was detected, which may be formed via condensation of Hmf.⁴² This product has also been detected in the thermal decomposition of Hmf.⁴³ Possibly, the by-products were mainly heavy/non-volatile compounds.

8.2.2.6. IL stability and reuse under N₂ atmosphere

The stability of the [Emim]HSO₄/Tol system (under N₂ atmosphere) was investigated by recovering and reusing the IL phase in four consecutive runs at 100 °C (0.67 M in the IL). Prior to each reuse of the IL, the two liquid phases were separated by decantation. Acetonitrile (miscible with [Emim]HSO₄) was added to the IL phase with stirring, which facilitated the subsequent separation of dark residues by centrifugation. Acetonitrile and water were removed from the solution by evaporation under reduced pressure, giving the recovered IL free of Fur (ascertained by HPLC and FT-IR spectroscopy, Figure 8.10). The C_{Xyl} and Y_{Fur} at 4 h remained nearly constant at ca. 93 and 85% in the four consecutive runs (Figure 8.9).

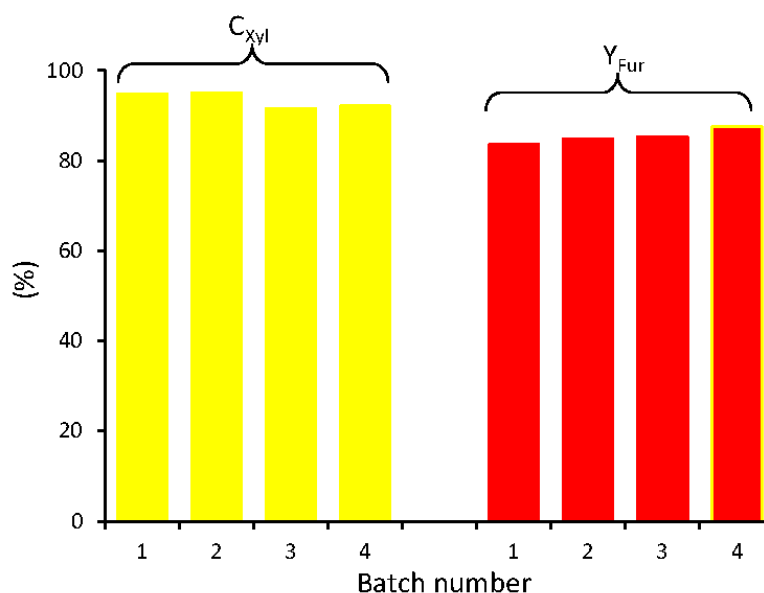


Figure 8.9- Conversion of D-xylose (C_{Xyl}) to 2-furaldehyde (Fur) in [Emim]HSO₄/Tol for four consecutive 4 h runs at 100 °C, using the same IL charged initially to the reaction vessel. Reaction conditions: 0.3 Wt:0.7 Tol (v/v) biphasic solvent system, 100 °C, 0.67 M Xyl.

The recycling of the [Emim]HSO₄/Tol system using 167 g_{Xyl}.dm⁻³ in the IL (1.11 M Xyl) gave a turn over number of 1.25 after seven runs at 100 °C. The CNS microanalyses, FT-IR (Figure 8.10), ¹H and ¹³C NMR spectra of the fresh and recovered IL were very similar (Figures 8.2 and 8.3).

These results demonstrated that [Emim]HSO₄ was fairly stable and can be efficiently recycled under the reaction conditions used (catalytic reaction under N₂ atmosphere).

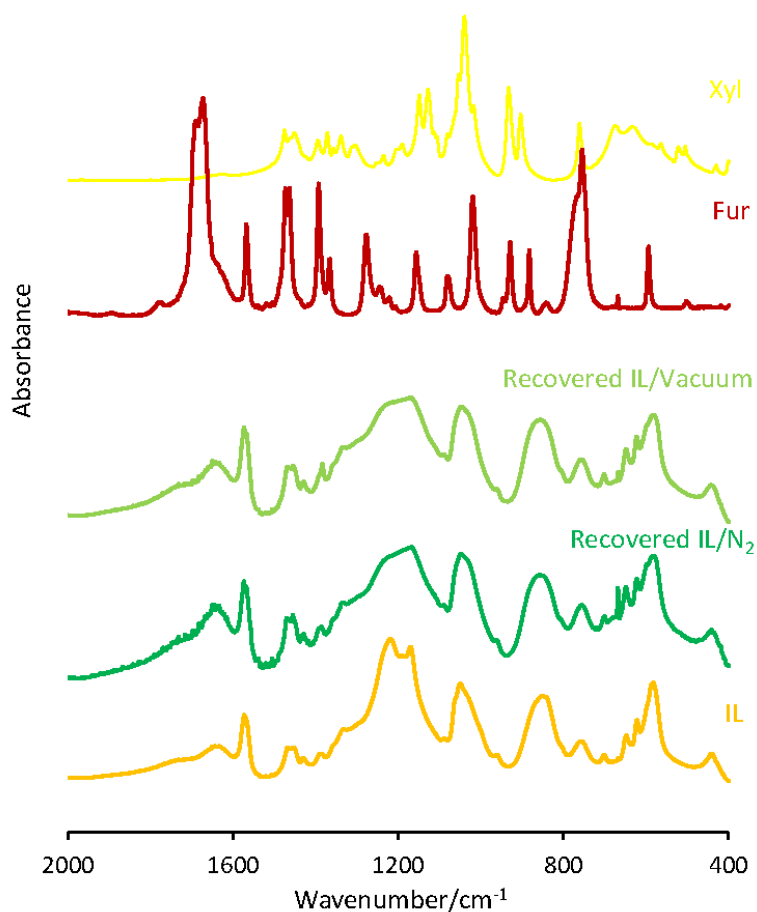


Figure 8.10- FT-IR spectra of pure [Emim]HSO₄ (IL) and IL recovered from the reaction of D-xylose (Xyl) carried out in [Emim]HSO₄/Tol under nitrogen, or in [Emim]HSO₄ under reduced pressure. The spectra of D-xylose (Xyl) and 2-furaldehyde (Fur) are given for comparison.

The weak and sharp band at ca. 650 cm⁻¹ in the spectrum of the recovered IL under N₂ atmosphere was attributed to a residual amount of acetonitrile that was not completely separated from the IL during work-up procedures.

8.2.2.7. IL stability and reuse under reduced pressure

In the absence of Tol and under reduced pressure, the black residues formed during the reaction were separated by centrifugation and membrane filtration, leaving a transparent, pale yellow liquid. Excess water (and possibly other volatile products) in the IL was distilled off under reduced pressure. The amount of Xyl in the recovered IL was ca. 1 wt.% (measured by HPLC) of the initial amount of Xyl charged to the reactor. The FT-IR spectra (Figure 8.10) and the elemental analysis data of pure and recovered IL were similar. For the two runs applied, the distillate consisted of two separate colourless liquids, which were identified by FT-IR spectroscopy as being Fur and water. For the second run, 81% C_{Xyl} and 22% S_{Fur} were reached in 4 h. The similar results for both runs suggested that the IL was recyclable, as observed for the reactions carried out under nitrogen. In summary, the Y_{Fur} at 4 h are 12-18% for the reduced pressure system compared to 40% for the IL without Tol, and 81% for the IL/Tol biphasic system

8.3. Conclusions

It has been shown that the dehydration of Xyl and Fru, and on the other hand, the one-pot hydrolysis and dehydration of di/polysaccharides containing Fru units, in [Emim]HSO₄/co-solvent gave fairly high yields of Fur or Hmf (80-90%) at 100 °C. The reaction of Xyl in [Emim]HSO₄/Tol at 100 °C gave better results (82% Y_{Fur} at 4 h) than previously reported DMSO/(Keggin-type heteropolytungstates or sulfuric acid) system at 140 °C.¹³ Furthermore, better results were achieved with [Emim]HSO₄ than with aqueous H₂SO₄, under similar conditions. Removal of Fur by evaporation under reduced pressure (instead of solvent extraction) gave poorer results, although it should be possible to improve on the 18% Y_{Fur} obtained at 4 h by optimising the pressure in the system, the design and dimensions of the setup, the mixing efficiency of the reaction mixture, and the reaction temperature and residence time. For both methods of Fur removal, the IL can be recovered and reused without a significant drop in the yields of Fur in recycling runs. In considering the potential of acidic ILs such as [Emim]HSO₄ to replace sulfuric acid in processes for the transformation of saccharides into Fur and Hmf, it must be recalled that H₂SO₄ is very hygroscopic and difficult to dry in vacuum, and when heated it emits

highly toxic fumes, which include sulfur trioxide, leading to the accumulation of acidic waste. The use of [Emim]HSO₄ instead of H₂SO₄ may allow process intensification with reuse of the acid IL.

Although [Emim]HSO₄ was effective in converting Fru (88% Y_{Hmf} at 30 min) and polymers containing these units into Hmf, it was poorly selective in Glu dehydration. The [Bmim]Cl/Tol/CrCl₃ system of Zhao et al.⁹ was quite effective in converting Glu and related disaccharides into Hmf, but not polysaccharides such as cellulose and starch. For the latter feedstocks, the addition of [Emim]HSO₄ to cellulose/[Bmim]Cl/CrCl₃ enhanced Hmf yield, presumably by accelerating the hydrolysis step. However, the dehydration of Glu monomers to Hmf was poorly selective (8-9% Y_{Hmf}) compared to Xyl for the same system without [Emim]HSO₄, most likely due to the formation of different active species from those formed in the absence of the sulfated anions.

A drawback of the IL/CrCl₃ systems is that chromium (especially chromium (VI), which can be formed from chromium (III) in aqueous environments) poses risks to human health and the environment, which would mean that any process based on these systems would be subject to very stringent environmental controls. Nevertheless, the results showed that hydrophilic ILs may be promising for Fur and Hmf production from sugar feedstocks, allowing relatively easy work-up procedures for isolating the target product(s), reuse of the acidic medium and operation under relatively mild conditions. Attempts to find IL systems for selectively processing feeds composed of mixed Fru and Glu-based saccharides remains a challenge.

In the next Chapter 9, the use of the IL [Bmim]Cl coupled to chromium-containing silicates in the conversion of Glu (more demanding substrate than Fru) to Hmf will be discussed.

8.4. References

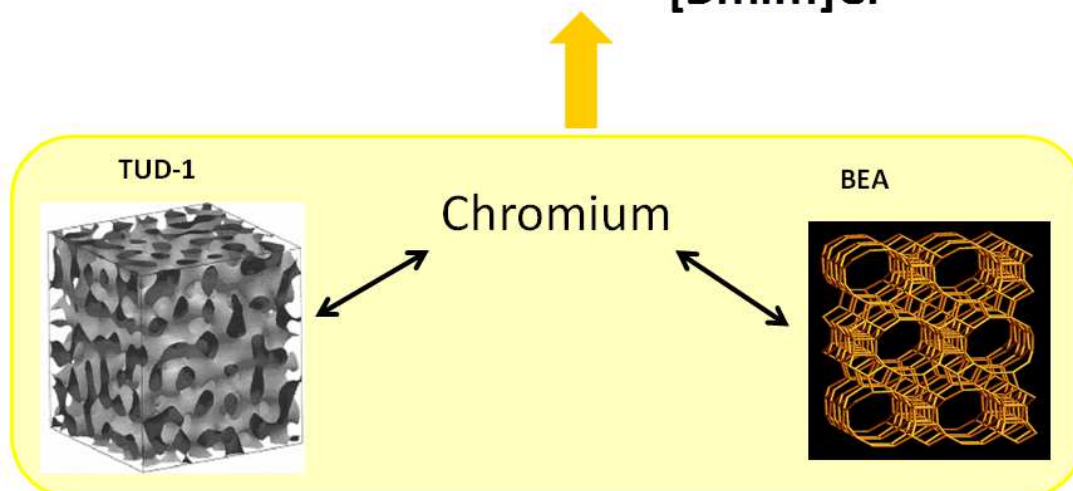
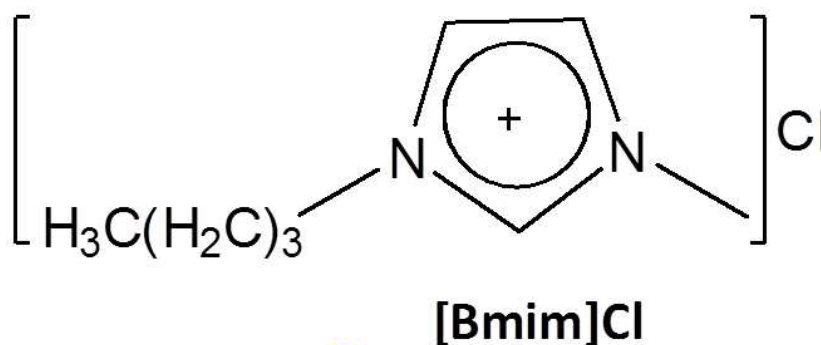
- (1) Bourbigou, H. O.; Magna, L.; Morvan, D.: Ionic liquids and Catalysis: Recent Progress from Knowledge to Applications. *Applied Catalysis A-General* **2010**, *373*, 1-56.
- (2) Swatloski, R. P.; Spear, S. K.; Holbrey, J. D.; Rogers, R. D.: Dissolution of Cellose With Ionic Liquids. *Journal of the American Chemical Society* **2002**, *124*, 4974-4975.
- (3) Feng, L.; Chen, Z.-I.: Research Progress on Dissolution and Functional Modification of Cellulose in Ionic Liquids. *Journal of Molecular Liquids* **2008**, *142*, 1-5.
- (4) Zakrzewska, M. E.; Lukasik, E. B.; Lukasik, R. B.: Solubility of Carbohydrates in Ionic Liquids. *Energy & Fuels* **2010**, *24*, 737-745.
- (5) Pinkert, A.; Marsh, K. N.; Pang, S.; Staiger, M. P.: Ionic Liquids and Their Interaction with Cellulose. *Chemical Reviews* **2009**, *109*, 6712-6728.

- (6) Lansalot-Matras, C.; Moreau, C.: Dehydration of Fructose into 5-Hydroxymethylfurfural in the Presence of Ionic Liquids. *Catalysis Communications* **2003**, *4*, 517-520.
- (7) Moreau, C.; Finiels, A.; Vanoye, L.: Dehydration of Fructose and Sucrose into 5-Hydroxymethylfurfural in the Presence of 1-H-3-Methyl Imidazolium Chloride Acting Both as Solvent and Catalyst. *Journal of Molecular Catalysis A-Chemical* **2006**, *253*, 165-169.
- (8) Bao, Q.; Qiao, K.; Tomida, D.; Yokoyama, C.: Preparation of 5-Hydroxymethylfurfural by Dehydration of Fructose in the Presence of Acidic Ionic Liquid. *Catalysis Communications* **2008**, *9*, 1383-1388.
- (9) Zhao, H.; Holladay, J. E.; Brown, H.; Zhang, Z. C.: Metal chlorides in ionic liquid solvents convert sugars to 5-hydroxymethylfurfural. *Science* **2007**, *316*, 1597-1600.
- (10) Sievers, C.; Musin, I.; Marzialetti, T.; Olarte, M. B. V.; Agrawal, P. K.; Jones, C. W.: Acid-Catalyzed Conversion of Sugars and Furfurals in an Ionic-Liquid Phase. *ChemSusChem* **2009**, *2*, 665-671.
- (11) Binder, J. B.; Blank, J. J.; Cefali, A. V.; Raines, R. T.: Synthesis of Furfural from Xylose and Xylan. *ChemSusChem* **2010**, *3*, 1268-1272.
- (12) Chheda, J. N.; Roman-Leshkov, Y.; Dumesic, J. A.: Production of 5-Hydroxymethylfurfural and Furfural by Dehydration of Biomass Derived Mono- and Polysaccharides. *Green Chemistry* **2007**, *9*, 342-350.
- (13) Dias, A. S.; Pillinger, M.; Valente, A. A.: Liquid Phase Dehydration of D-xylose in the Presence of Keggin-Type Heteropolyacids. *Applied Catalysis A-General* **2005**, *285*, 126-131.
- (14) Moreau, C.: Zeolites and Related Materials for the Food and Non Food Transformation of Carbohydrates. *Agro Food Industry Hi-Tech* **2002**, *13*, 17-26.
- (15) Román-Leshkov, Y.; Chheda, J. N.; Dumesic, J. A.: Phase Modifiers Promote Efficient Production of Hydroxymethylfurfural From Fructose. *Science* **2006**, *312*, 1933-1937.
- (16) Zeitsch, K. J.: *The Chemistry and Technology of Furfural and its Many By-Products*; 1st ed.; Elsevier Science B. V.: Amsterdam, The Netherlands, 2000; Vol. 13.
- (17) Tao, F.; Song, H.; Chou, L.: Efficient Process for the Conversion of Xylose to Furfural With Acidic Ionic Liquid. *Canadian Journal of Chemistry-Revue Canadienne De Chimie* **2011**, *89*, 83-87.
- (18) Kim, Y. C.; Lee, H. S.: Selective Synthesis of Furfural From Xylose with Supercritical Carbon Dioxide and Solid Acid Catalyst. *Journal of Industrial and Engineering Chemistry* **2001**, *7*, 424-429.
- (19) Bicker, M.; Kaiser, D.; Ott, L.; Vogel, H.: Dehydration of D-Fructose to Hydroxymethylfurfural in Sub- and Supercritical Fluids. *Journal of Supercritical Fluids* **2005**, *36*, 118-126.
- (20) Asghari, F. S.; Yoshida, H.: Acid-Catalyzed Production of 5-Hydroxymethylfurfural From D-fructose in Subcritical Water. *Industrial & Engineering Chemistry Research* **2006**, *45*, 2163-2173.
- (21) Hu, S.; Zhang, Z.; Zhou, Y.; Han, B.; Fan, H.; Li, W.; Song, J.; Xie, Y.: Conversion of Fructose to 5-Hydroxymethylfurfural Using Ionic Liquids Prepared From Renewable Materials. *Green Chemistry* **2008**, *10*, 1280-1283.
- (22) Shi, C.; Zhao, Y.; Xin, J.; Wang, J.; Lu, X.; Zhang, X.; Zhang, S.: Effects of Cations and Anions of Ionic Liquids on the Production of 5-Hydroxymethylfurfural From Fructose. *Chemical Communications* **2012**, *48*, 4103-4105.
- (23) Tong, X.; Li, Y.: Efficient and Selective Dehydration of Fructose to 5-Hydroxymethylfurfural Catalyzed by Brønsted-Acidic Ionic Liquids. *ChemSusChem* **2010**, *3*, 350-355.
- (24) Tong, X.; Ma, Y.; Li, Y.: An Efficient Catalytic Dehydration of Fructose and Sucrose to 5-Hydroxymethylfurfural With Protic Ionic Liquids. *Carbohydrate Research* **2010**, *345*, 1698-1701.
- (25) Qi, X.; Watanabe, M.; Aida, T. M.; Smith, R. L.: Synergistic Conversion of Glucose into 5-Hydroxymethylfurfural in Ionic Liquid-Water Mixtures. *Bioresource Technology* **2012**, *109*, 224-228.
- (26) Tong, X.; Ma, Y.; Li, Y.: Biomass Into Chemicals: Conversion of Sugars to Furan Derivatives by Catalytic Processes. *Applied Catalysis A-General* **2010**, *385*, 1-13.
- (27) Karinen, R.; Vilonen, K.; Niemela, M.: Biorefining: Heterogeneously Catalyzed Reactions of Carbohydrates for the Production of Furfural and Hydroxymethylfurfural. *ChemSusChem* **2011**, *4*, 1002-1016.
- (28) Torres, A. I.; Daoutidis, P.; Tsapatsis, M.: Continuous Production of 5-Hydroxymethylfurfural From Fructose: A Design Case Study. *Energy & Environmental Science* **2010**, *3*, 1560-1572.
- (29) Corma, A.; Iborra, S.; Velty, A.: Chemical Routes for the Transformation of Biomass into Chemicals. *Chemical Reviews* **2007**, *107*, 2411-2502.

- (30) Binder, J. B.; Raines, R. T.: Simple Chemical Transformation of Lignocellulosic Biomass into Furans for Fuels and Chemicals. *Journal of the American Chemical Society* **2009**, *131*, 1979-1985.
- (31) Pidko, E. A.; Degirmenci, V.; Santen, R. A. V.; Hensen, E. J. M.: Glucose Activation by Transient Cr²⁺ dimers. *Angewandte Chemie* **2010**, *122*, 2584-2588.
- (32) Pidko, E. A.; Degirmenci, V.; Santen, R. A. V.; Hensen, E. J. M.: Glucose Activation by Transient Cr²⁺ Dimers. *Angewandte Chemie-International Edition* **2010**, *49*, 2530-2534.
- (33) Hu, S.; Zhang, Z.; Song, J.; Zhou, Y.; Han, B.: Efficient Conversion of Glucose into 5-Hydroxymethylfurfural Catalyzed by a Common Lewis Acid SnCl₄ in an Ionic Liquid. *Green Chemistry* **2009**, *11*, 1746-1749.
- (34) Zhang, Y.; Pidko, E. A.; Hensen, E. J. M.: Molecular Aspects of Glucose Dehydration by Chromium Chlorides in Ionic Liquids. *Chemistry-A European Journal* **2011**, *17*, 5281-5288.
- (35) Li, C.; Zhao, Z. K.; Wang, A.; Zheng, M.; Zhang, T.: Production of 5-Hydroxymethylfurfural in Ionic Liquids Under High Fructose Concentration Conditions. *Carbohydrate Research* **2010**, *345*, 1846-1850.
- (36) Zhu, S. D.; Wu, Y. X.; Chen, Q. M.; Yu, Z. N.; Wang, C. W.; Jin, S. W.; Ding, Y. G.; Wu, G.: Dissolution of Cellulose with Ionic Liquids and its Application: A Mini-Review. *Green Chemistry* **2006**, *8*, 325-327.
- (37) Gutowski, K. E.; Broker, G. A.; Willauer, H. D.; Huddleston, J. G.; Swatloski, R. P.; Holbrey, J. D.; Rogers, R. D.: Controlling the Aqueous Miscibility of Ionic Liquids: Aqueous Biphasic Systems of Water-Miscible Ionic Liquids and Water-Structuring Salts for Recycle, Metathesis, and Separations. *Journal of the American Chemical Society* **2003**, *125*, 6632-6633.
- (38) Remsing, R. C.; Hernandez, G.; Swatloski, R. P.; Masefski, W. W.; Rogers, R. D.; Moyna, G.: Solvation of Carbohydrates in N,N'-Dialkylimidazolium Ionic Liquids: A Multinuclear NMR Spectroscopy Study. *Journal of Physical Chemistry B* **2008**, *112*, 11071-11078.
- (39) Li, C.; Zhao, Z. K.: Efficient Acid-Catalyzed Hydrolysis of Cellulose in Ionic Liquid. *Advanced Synthesis & Catalysis* **2007**, *349*, 1847-1850.
- (40) Tao, F.; Song, H.; Chou, L.: Catalytic Conversion of Cellulose to Chemicals in Ionic Liquid. *Carbohydrate Research* **2011**, *346*, 58-63.
- (41) Kabyemela, B. M.; Adschiri, T.; Malaluan, R. M.; Arai, K.: Kinetics of Glucose Epimerization and Decomposition in Subcritical and Supercritical Water. *Industrial & Engineering Chemistry Research* **1997**, *36*, 1552-1558.
- (42) Moreau, C.; Belgacem, M. N.; Gandini, A.: Recent Catalytic Advances in the Chemistry of Substituted Furans from Carbohydrates and in the Ensuing Polymers. *Topics in Catalysis* **2004**, *27*, 11-30.
- (43) Chambel, P.; Oliveira, M. B.; Andrade, P. B.; Fernandes, J. O.; Seabra, R. M.; Ferreira, M. A.: Identification of 5,5'-Oxy-dimethylene-bis(2-furaldehyde) by Thermal Decomposition of 5-Hydroxymethyl-2-furfuraldehyde. *Food Chemistry* **1998**, *63*, 473-477.

CHAPTER 9

Conversion of D-glucose in the presence of micro/mesoporous (chromium, aluminium)-containing silicates using an ionic liquid solvent



Index

CHAPTER 9	365
Conversion of D-glucose in the presence of micro/mesoporous (chromium, aluminium)-containing silicates using an ionic liquid solvent	365
9.1. Introduction	367
9.1.1. Cr-TUD-1 and Cr-Al-TUD-1	368
9.1.2. Cr-BEA and Cr-BEATUD-1	369
9.2. Results and discussion.....	370
9.2.1. Catalyst characterisation.....	370
9.2.2. Catalytic dehydration of D-glucose	377
9.2.2.1. Catalytic performance of Cr-TUD-1, Cr-Al-TUD-1, Cr-BEA and Cr-BEATUD-1 in the presence of [Bmim]Cl, DMSO or water.....	378
9.2.2.2. Catalyst stability.....	380
9.3. Conclusions	387
9.4. References.....	388

9.1. Introduction

D-Glucose (Glu) is the major monosaccharide building block obtained from carbohydrate biomass that can be converted into the promising platform chemical 5-(hydroxymethyl)-2-furaldehyde (Hmf).³ However, the reaction of Glu to Hmf is rather demanding in comparison to that for fructose (Fru) as substrate, partly due to the fact that the reaction mechanism is complex, involving several elementary steps with different acid-base requirements. Zhao et al.⁴⁻⁶ reported one of the most effective catalytic systems known to date for the conversion of Glu to Hmf, consisting of chromium salts as homogeneous Lewis acid catalysts dissolved in an ionic liquid (IL) solvent under mild reaction conditions.⁴⁻⁶ CrCl₂ coupled with 1-ethyl-3-methyl imidazolium chloride ([Emim]Cl) led to ca. 70% Y_{Hmf} at 95% C_{Glu} (10 wt.% Glu, 100 °C, 3 h reaction).⁴ Since then, several chromium/IL based catalytic systems have been successfully investigated in the conversion of Glu (and related di/polysaccharides) to Hmf, generally exhibiting superior catalytic performances in comparison to IL-based catalytic systems containing other transition metals as summarised in reviews of the topic.⁷⁻¹⁰ A few other papers have been published afterwards.¹¹⁻¹⁶ The use of an IL as solvent instead of water is desirable because it avoids Hmf loss reactions, typically occurring in the aqueous media.¹⁷ Relatively low yields of Hmf have been reported for chromium salts (CrCl₂, CrSO₄) used as catalysts in the aqueous phase reaction of Glu, at 140 °C,¹⁸ or of cellulose at 180 °C.¹⁹ On the other hand, and as mentioned in Chapter 1, some ILs are favourable (non-volatile) solvents for dissolving carbohydrates such as crystalline cellulose, in comparison to water and most common organic solvents (important for process intensification),²⁰⁻²⁶ and these types of solvents can be obtained from renewable resources.²⁷

Homogeneous catalytic systems require careful work-up procedures in order to avoid losses of catalyst and contamination of effluents (requiring demanding/costly separation and purification processes and treatment/disposal of waste streams). The coupling of solid acid catalysts with ILs as solvents is a possible approach to minimise these drawbacks. Only a couple of studies can be found in the literature reporting on the reaction of Glu (or related di/polysaccharides) to Hmf using (chromium-containing solid acid)/IL catalytic systems. Physical mixtures of chromium salts and solid acids (zeolites H-Y, H-BEA, H-Mordenite, H-ZSM-5, or acidic Amberlyst ion-exchange resins) coupled with 1-butyl-3-methylimidazolium chloride ([Bmim]Cl) as IL solvent have been investigated in the conversion of cellulose to Hmf, at 120 °C, and the best result was ca. 36% Y_{Hmf} at 6 h reaction using H-Y zeolite as solid acid.²⁸ In a recent study it was

reported that the addition of ILs to aqueous solutions of Glu enhanced adsorption of the latter on zeolites.²⁹ Interesting results were reported for hydroxyapatite-supported chromium chloride (Cr-HAP) coupled with [Bmim]Cl as solvent in that this catalytic system was reused four times without significant decrease in the yield of Hmf (ca. 40% Y_{Hmf} in 2.5 min, using the microwave heating method, 400 W).³⁰

A critical issue is the stability of the solid acids in the ILs medium. According to the literature, Brønsted solid acids may undergo ion-exchange reactions in the IL medium, and the catalytic reactions may be effectively homogeneous in nature.³¹⁻³³ In the case of the Cr-HAP/IL system the homo/heterogeneous nature of the catalytic reaction was not assessed.³⁰

In this work, nanoporous chromium, aluminium-containing silicates were tested as solid acids in the reaction of Glu, using the IL [Bmim]Cl as solvent, at 120 °C. The investigated solid acids include: mesoporous TUD-1 type materials possessing chromium and/or aluminium (Al-TUD-1, Cr-Al-TUD-1, Cr-TUD-1); zeolite BEA (in the H^+ -form) and Cr-BEA, and the related micro/mesoporous composites BEATUD-1 and Cr-BEATUD-1 (Figure 9.1 A and B). Particular attention was drawn to the stabilities of the nanoporous materials in the IL medium and the influence of the type of solvent ([Bmim]Cl versus water or DMSO) on the reaction of Glu.

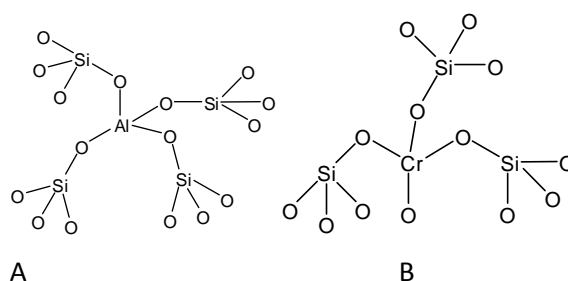


Figure 9.1- Simplified representation of aluminium (A) and chromium (B)- containing silicates in which Al^{4+} and Cr^{6+} are in tetrahedral coordination (charges are not represented for the sake of simplicity).

9.1.1. Cr-TUD-1 and Cr-Al-TUD-1

The 3 D sponge-like mesoporous material TUD-1 (studied in Chapter 4 , as catalyst in the hydrolysis/dehydration of saccharides to Fur/Hmf) has several advantages, such as being

straightforward to prepare via (relatively low-cost) non-surfactant templating routes (environmentally friendly),³¹⁻³⁶ having high specific surface areas, pore widths and volumes, and a 3 D channel system, which are favourable features for the internal diffusion of relatively bulky reactant molecules and accessibility to the active sites.

The purely siliceous TUD-1 may be furnished with Brønsted and Lewis acidity by tetrahedral incorporation of metals such as aluminium (Chapter 4), or chromium (in this work) into the framework via a one-pot procedure based on the sol-gel technique.³⁷⁻⁴⁰ In Chapter 4, Al-TUD-1 was reported to be an active and stable catalyst for the aqueous-phase dehydration of saccharides to furanic aldehydes, although the hexose-based mono/disaccharides gave less than 20% Y_{Hmf} . Since chromium-based catalytic systems are rather efficient in the conversion of hexoses, the incorporation of chromium in purely siliceous TUD-1 (Cr-TUD-1) and in Al-TUD-1 (Cr-Al-TUD-1) was carried out (Figure 9.1 A and B).

9.1.2. Cr-BEA and Cr-BEATUD-1

Following on from the good catalytic stability of BEA and BEATUD-1 (discussed in Chapter 5 in the dehydration of Xyl to Fur), in this chapter the corresponding chromium-containing versions namely Cr-BEA and Cr-BEATUD-1, were tested in the reaction of Glu as substrate to Hmf. Cr-BEA was prepared from BEA in the H^+ -form (Chapter 5) via an ion-exchange reaction, while Cr-BEATUD-1 was prepared in a similar fashion to the micro/mesoporous composite BEATUD-1 described in Chapter 5, albeit using Cr-BEA instead of BEA.

9.2. Results and discussion

9.2.1. Catalyst characterisation

In this Chapter the following materials were prepared: Al-TUD-1, Cr-Al-TUD-1 and Cr-TUD-1, BEA, BEATUD-1, Cr-BEA and Cr-BEATUD-1. As mentioned in the experimental part (Chapter 2), the aluminium and/or chromium-containing mesoporous silicas of the type TUD-1 were prepared by hydrothermal synthesis. BEA was prepared by calcination of $\text{NH}_4\text{-BEA}$, while Cr-BEA was prepared by ion-exchange of a suspension of $\text{NH}_4\text{-BEA}$ in an aqueous solution of $\text{Cr}(\text{NO}_3)_3$, further filtration and calcination. The composite Cr-BEATUD-1 was prepared by ion-exchange of BEA with chromium, similar to the procedure for Cr-BEA, excluding the calcination step.

The powder XRD patterns for Al-TUD-1, Cr-TUD-1 and Cr-Al-TUD-1 showed one broad peak at low angles (ca. $1.5^\circ 2\theta$ for Cr-TUD-1 and Cr-Al-TUD-1 and ca. $1.8^\circ 2\theta$ for Al-TUD-1, inset of Figure 9.2) and a very broad peak centred around $25^\circ 2\theta$ (Figure 9.2), indicating that these materials were amorphous, but had mesostructured features similar to that described in Chapter 4, and in agreement with the literature.^{35,37-39,41-51} No evidence of crystalline phases (e.g. alumina or chromium oxides) was detected in the patterns, similar to that described in Chapter 4 and in agreement with the literature data.^{37,38,41,42,50-54}

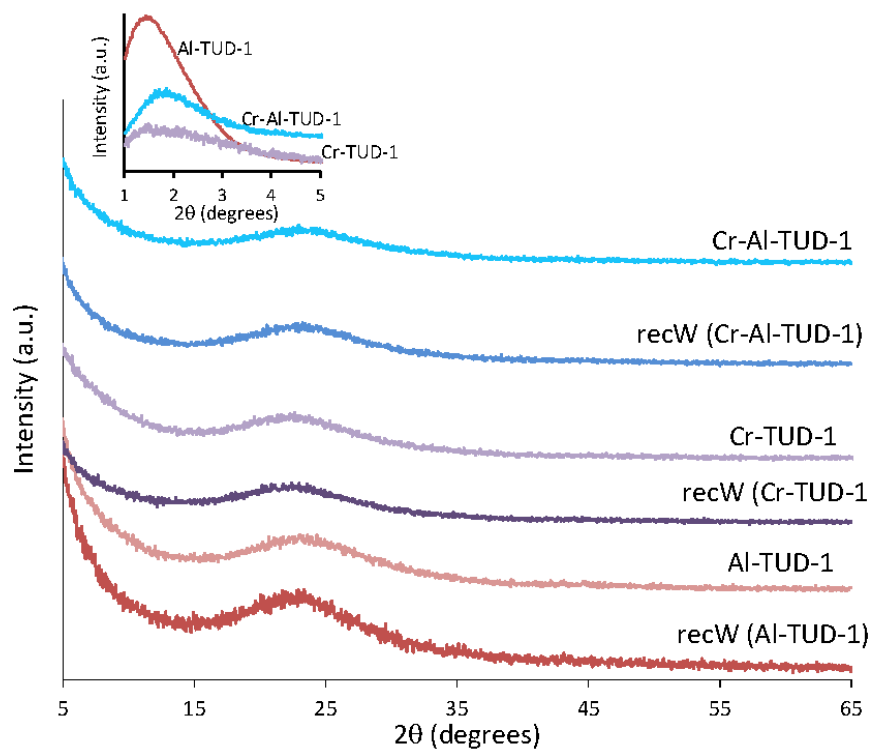


Figure 9.2- Powder XRD patterns of the fresh TUD-1 related materials (Al-TUD-1, Cr-TUD-1, and Cr-Al-TUD-1) and of the respective recW solids. The inset shows the low angle powder XRD patterns.

In the case of BEA and Cr-BEA, the XRD diffraction patterns were similar suggesting that the crystalline structure was preserved during the ion-exchange procedure (Figure 9.3). BEA and the related composite BEATUD-1 presented similar XRD patterns showing the characteristic diffraction peaks of zeolite BEA at $2\theta=7-8^\circ$ and 22.5° similar to that described in Chapter 5 and in agreement with the literature data.⁵⁵⁻¹⁸² The same applies when comparing the data for Cr-BEA and Cr-BEATUD-1.

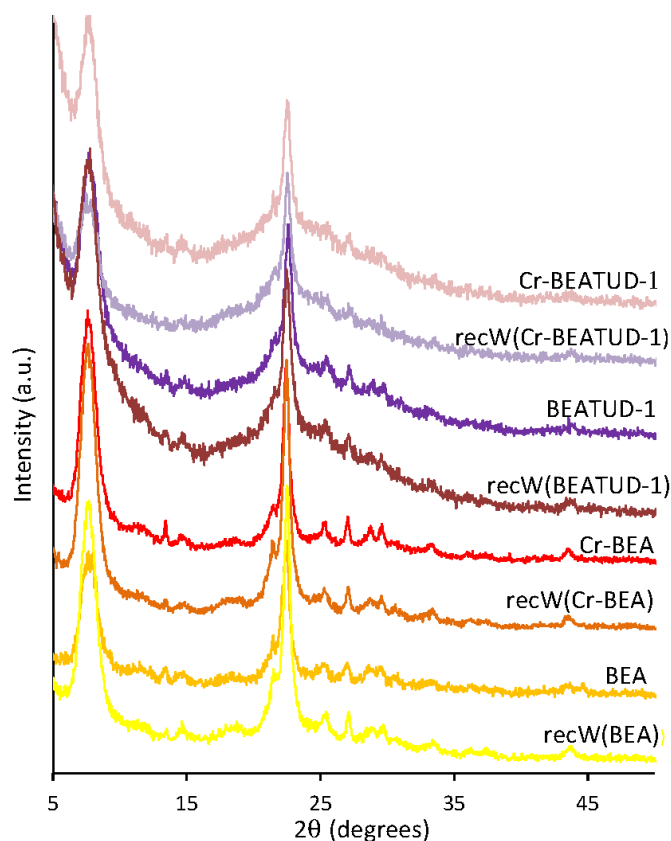


Figure 9.3- Powder XRD patterns of the fresh zeolite BEA-related materials and of the respective recW solids.

The high-resolution (HR) TEM images of Cr-BEA (exemplified in Figure 9.4a) showed small crystallites with a size of ca. 20-30 nm and the lattice fringes characteristic of zeolite Beta. In the case of Cr-BEATUD-1, HRTEM characterisation showed a 3 D sponge- or worm-like mesoporous matrix with some dark gray domains that may be attributed to the embedded zeolite particles (Figure 9.4 b), suggesting that Cr-BEATUD-1 was a composite of an amorphous mesoporous matrix and nanocrystallite Beta particles (isolated nanocrystals of ca. 20-30 nm, or aggregates of ca. 50-200 nm), which were fairly evenly distributed nanocrystals in the surrounding mesoporous matrix. The presence of small aggregates is in agreement with previous findings for a BEATUD-1 composite material with a zeolite loading of 16-20 wt.%,^{56,180} or 40 wt.%,⁵⁶ and can be attributed to the combined effect of the synthesis conditions and the high zeolite loading. These results were comparable to those previously reported in Chapter 5 for a composite material consisting of zeolite Beta and TUD-1 prepared in a similar fashion (and using the same commercial zeolite ammonia Beta powder) to that used in the present Chapter.

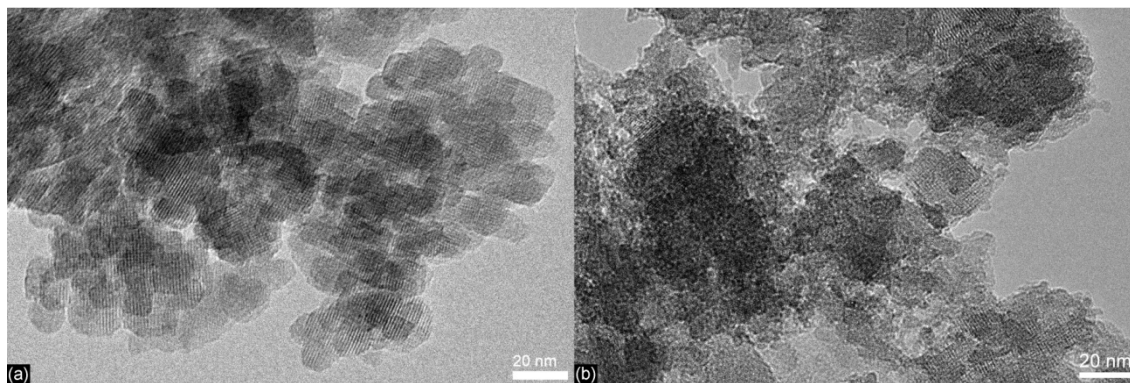


Figure 9.4- High resolution TEM images of a) Cr-BEA and b) Cr-BEATUD-1.

Table 9.1 shows the chemical composition and textural properties of the prepared materials. For Al-TUD-1 and Cr-Al-TUD-1 the atomic ratios agreed roughly with those used in the respective synthesis mixtures. For Cr-TUD-1 the Si/Cr ratio of 150 was higher than the value of 100 used in the synthesis, suggesting that a fraction of the initial amount of chromium was not incorporated in the mesoporous silicate.

The zeolite BEA and the related ion-exchanged Cr-BEA possessed similar Si/Al ratios: in the latter case, the Si/Cr ratio was 47. Based on the aluminium contents it was possible to estimate that the BEATUD-1 and Cr-BEATUD-1 composites possessed ca. 26 wt.% BEA and 33 wt.% Cr-BEA, respectively. In the case of the chromium-containing materials, the Al/Cr ratio was slightly higher for Cr-BEATUD-1 than for Cr-BEA (ca. 6 and 4, respectively), possibly due to partial leaching of chromium from BEA during the preparation of Cr-BEATUD-1.

The textural properties of Al-TUD-1 and Cr-Al-TUD-1 were similar; in comparison, the S_{BET} for Cr-TUD-1 was lower, and the PSD was wider and for greater values of pore widths (Table 9.1 and inset of Figure 9.5). In the case of the composite materials, BEATUD-1 and Cr-BEATUD-1, the PSD curves lied in the range of pore widths 2.5-10 nm (Table 9.1).

Table 9.1- Physicochemical properties of the prepared materials and comparison with the literature data.

Sample	Si/Al	Si/Cr	Al/Cr	Surface area ($\text{m}^2 \cdot \text{g}^{-1}$)	V_p ($\text{cm}^3 \cdot \text{g}^{-1}$)	PSD (pore width, nm)	Ref
Al-TUD-1	20 ^a	-	-	726 (789) ^{b,d}	0.64 (0.69) ^{b,g}	2.5-7 (2.5-7) ^{b,k}	this work
Cr-Al-TUD-1	27 (30) ^{a,b}	108	4	763 (995) ^{b,d}	0.78 (0.95) ^{b,g}	2.5-7 (2.5-7) ^{b,k}	this work
Cr-TUD-1	-	150 (261) ^{a,b}	-	484 (515) ^{b,d}	1.02 (1.14) ^{b,g}	3-17 (3-17) ^{b,k}	this work
Cr-TUD-1	-	130 ^a	-	565 ^e	1.54 ^h	8.2 ^k	³⁹
Cr-TUD-1	-	130 ^a	-	565 ^e	1.54 ⁱ	8.4 ^k	³⁴
BEA	12 ^a	-	-	634 ^d	0.74 ^g	-	this work
BEA	25 ^a	-	-	500 (365/135) ^f	nf ^j	nf ^j	¹⁸³
BEA	50 ^a	-	-	557 (430/127) ^f	nf ^j	nf ^j	¹⁸³
Cr-BEA	13 (13) ^{a,b}	47	3.6	702 (793) ^{b,d}	0.87(0.75) ^g	-	this work
Cr-BEA	25 ^a	0.99 ^c	-	488 (341/147) ^f	nf ^j	nf ^j	¹⁸³
Cr-BEA	50 ^a	0.74 ^c	-	415 (334/111) ^f	nf ^j	nf ^j	¹⁸³
BEATUD-1	31 (33) ^{a,b}	-	-	685 (722) ^{b,d}	0.78 (0.82) ^{b,g}	2.5-10 (2.5-10) ^{b,k}	this work
Cr-BEATUD-1	41 (45) ^{a,b}	236	5.8	802 (717) ^{b,d}	0.92 (0.80) ^{b,g}	2.5-10 (2.5-10) ^{b,k}	this work

a) Determined by ICP-AES. b) Values in brackets in the entries of this work refer to recovered and calcined solids (recC). c) Chromium percentage (wt.%). d) S_{BET} determined by BET equation for relative pressures p/p_0 in the range of 0.02-0.1. e) Surface area calculated from the adsorption branch of the N_2 isotherm, using the BJH method. f) S_{BET} determined by the BET equation; values in parenthesis refer to $S_{\text{micro}}/S_{\text{meso}}$. g) V_p determined using the Gurvitch equation for p/p_0 ca. 0.98. h) V_p using the BJH method. i) V_{meso} using the BJH method. j) nf= information not found. k) PDS calculated by BJH method from the adsorption branch of the isotherm. The calculations for the values without an indication are not mentioned in the respective works.

The S_{BET} tended to increase with the incorporation of chromium (Al-TUD-1 to Cr-Al-TUD-1, 726 to 763 $\text{m}^2 \cdot \text{g}^{-1}$; BEA to Cr-BEA, 634 to 702 $\text{m}^2 \cdot \text{g}^{-1}$; BEATUD-1 to Cr-BEATUD-1, 685 to 802 $\text{m}^2 \cdot \text{g}^{-1}$). According to the literature, the S_{BET} may be influenced by the chromium content; a higher amount of chromium led to higher S_{BET} in the case of Cr-TUD-1 (484 $\text{m}^2 \cdot \text{g}^{-1}$ for Cr-TUD-1(150) and 565 $\text{m}^2 \cdot \text{g}^{-1}$ for Cr-TUD-1 (130)).³⁹ Zuhairi et al.¹⁸³ observed the opposite in the case of the zeolite BEA and Cr-BEA (500-557 $\text{m}^2 \cdot \text{g}^{-1}$ for BEA(25-50) and ¹⁸³183 415-488 $\text{m}^2 \cdot \text{g}^{-1}$ for Cr-BEA(25-50)).

The TUD-1 type materials exhibited type IV N_2 adsorption-desorption isotherms at -196 °C, with a H-2 hysteresis loop (Figure 9.5), which was consistent with an interconnected (worm-like) mesoporous network characteristic of TUD-1 type materials, similar to that described in Chapter 4 and in the agreement with the literature data.^{34,37-42,44-48,50,51,53,106,184-197} The capillary condensation in the mesopores occurred in the relative pressure range of about 0.4-0.7 for Al-TUD-1 and Cr-Al-TUD-1, and 0.6-0.9 for Cr-TUD-1, above which the adsorption branch leveled off

(suggesting that the external surface area was minor). Similar results were reported previously for metal-incorporated TUD-1 samples.³⁷⁻⁴⁰

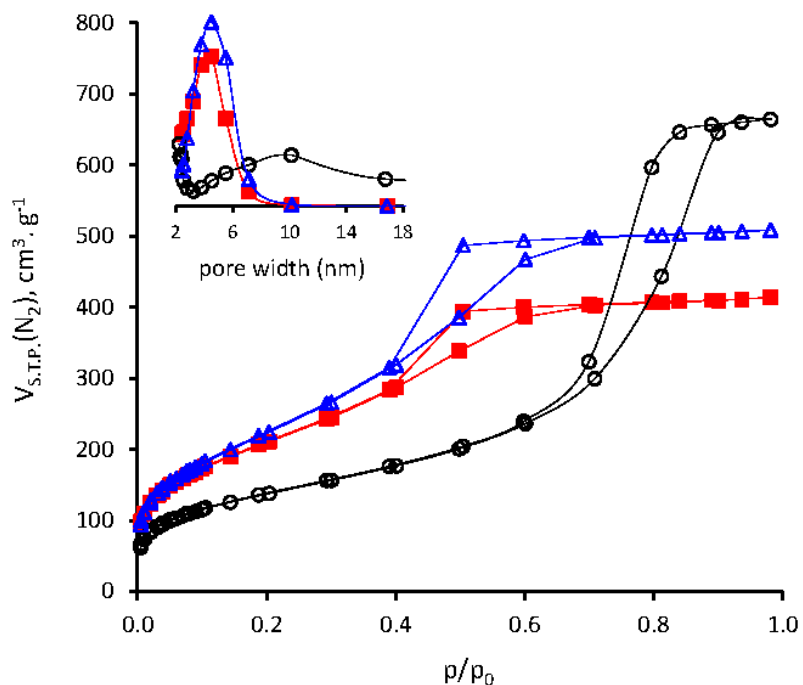


Figure 9.5- N_2 adsorption-desorption isotherms at -196 °C of Al-TUD-1 (■), Cr-Al-TUD-1 (Δ) and Cr-TUD-1 (○). The insets show the respective PSD curves (with matching symbols).

The sorption isotherms for BEA and Cr-BEA showed a significant increase in N_2 uptake at $p/p_0 < 0.01$, typically associated with the filling of micropores, followed by a gradual increase in the N_2 uptake as relative pressures approached unity (Figure 9.6),¹⁹⁸⁻²⁰² most likely due to multilayer adsorption on the external surface of the nanocrystallites. The related composite materials BEATUD-1 and Cr-BEATUD-1 exhibited type IV isotherms (Figure 9.6), typical of mesoporous materials with a hysteresis loop at $p/p_0 > 0.4$, which was associated with capillary condensation/evaporation in mesopores.^{165,166,168-175}

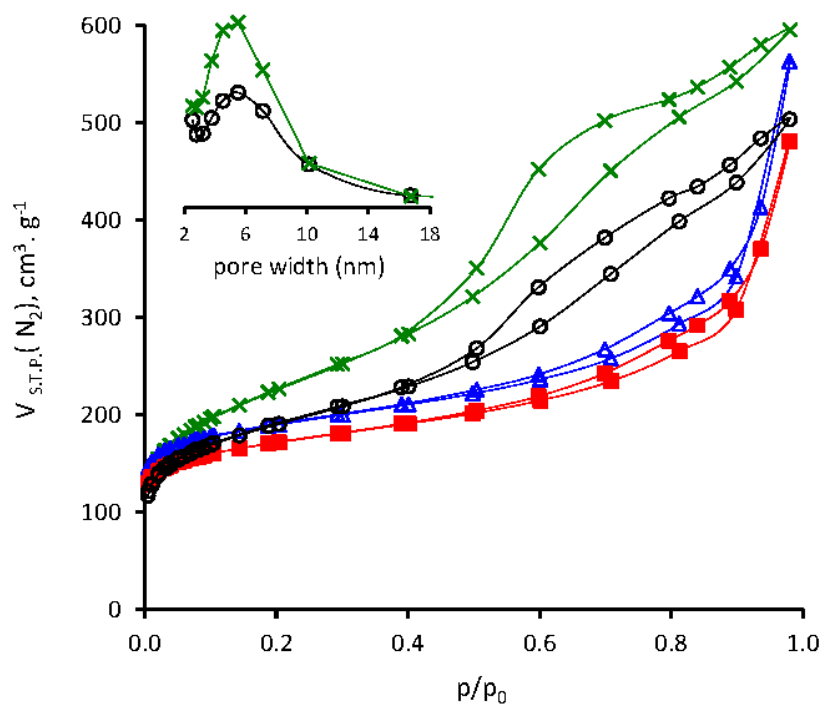


Figure 9.6- N_2 adsorption-desorption isotherms at $-196\text{ }^\circ\text{C}$ of BEA (\blacksquare), Cr-BEA (\blacktriangle), BEATUD-1 (\bigcirc) and Cr-BEATUD-1 (\times). The insets show the respective PSD curves (with matching symbols).

The yellow colour of all the chromium-containing samples suggested that the major species present was monochromate.²⁰³ Accordingly, two very broad bands at ca. 275 (220-320 nm) and 365 (320-420 nm) in the diffuse reflectance (DR) UV-vis spectra (Figure 9.7) were assigned to $O^{2-} \rightarrow Cr^{6+}$ charge transfer transitions⁶⁺ of tetrahedrally coordinated isolated Cr^{6+} .^{39,181,203-205} Similar results were reported previously for Cr-TUD-1,³⁹ and chromium-substituted BEA.^{181,205} The shoulder at 450 nm (420-520 nm) may be due to dichromate or polychromate species,^{203,204} or as proposed previously for Cr-TUD-1, distorted isolated chromate species.³⁹ The assignment of this band to octahedral Cr^{3+} species (including Cr_2O_3 -like clusters) could be excluded since no bands were detected at wavelengths greater than 600 nm, where octahedral Cr^{3+} would be expected.^{39,181,204,205}

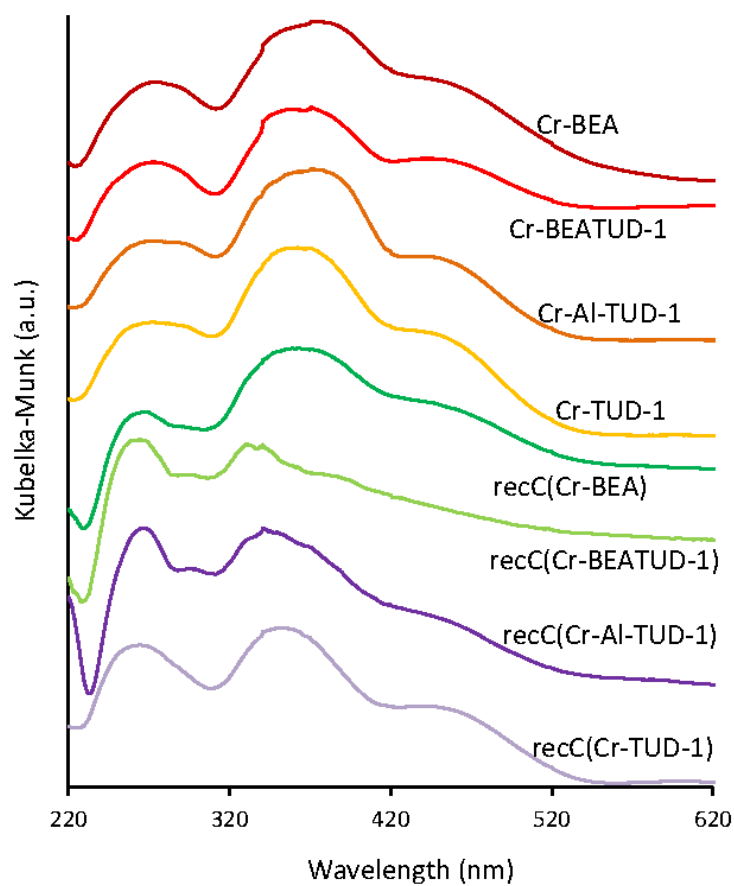


Figure 9.7- Diffuse reflectance UV-vis spectra of the chromium-containing materials and the respective recC solids.

9.2.2. Catalytic dehydration of D-glucose

The batch-wise dehydration of Glu to Hmf was investigated in the presence of the prepared micro/mesoporous materials as catalysts, using [Bmim]Cl as IL solvent, at 120 °C (experiment denoted catalytic BR, where BR stands for Batch Run, Figure 9.8). This IL was chosen since it solubilises saccharides quite well, possesses a relatively low melting point (ca. 73 °C), is readily available and relatively cheap. Furthermore it has been used successfully as solvent in the homogeneous catalytic reaction of Glu and related di/polysaccharides to Hmf.⁸⁻¹⁰ The reaction of Glu using [Bmim]Cl as solvent, without adding a catalyst, gave 1% Y_{Hmf} at 120 °C/3 h. These poor results are comparable with those reported in the literature for the same reaction using [Emim]Cl as solvent, without adding a catalyst, at 100 °C (< 5% Y_{Hmf}).^{4,206}

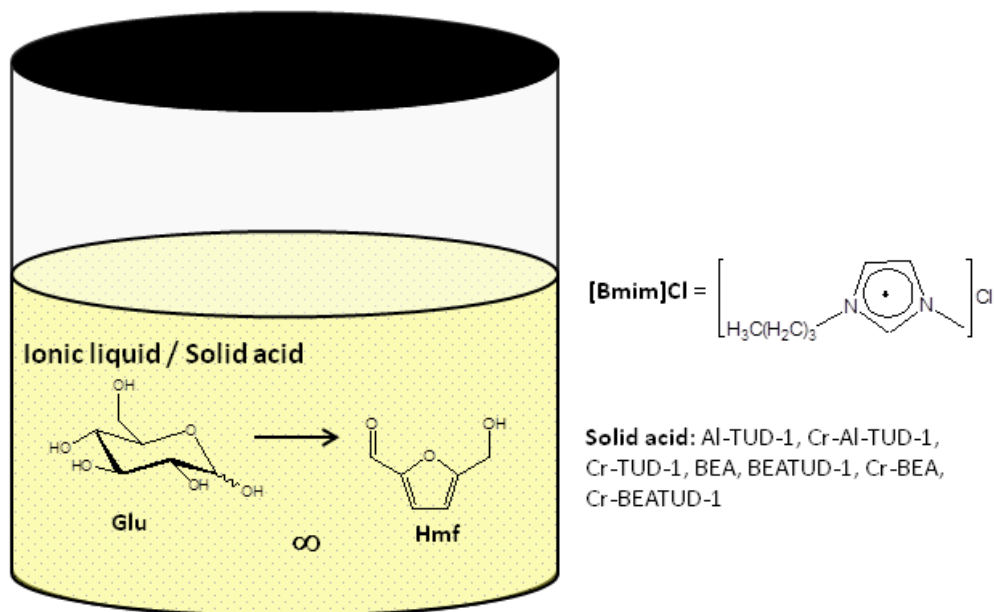


Figure 9.8- Conversion of D-glucose (Glu) into 5-(hydroxymethyl)-2-furaldehyde (Hmf) using a solid acid/[Bmim]Cl catalytic system. Reaction conditions: monophasic solvent system, [Bmim]Cl (0.3 cm^3), $120 \text{ }^\circ\text{C}$, $15 \text{ g}_{\text{cat}} \cdot \text{dm}^{-3}$, 0.28 M Glu , 3 h.

9.2.2.1. Catalytic performance of Cr-TUD-1, Cr-Al-TUD-1, Cr-BEA and Cr-BEATUD-1 in the presence of [Bmim]Cl, DMSO or water

For the reaction of Glu using the prepared solid acid/IL systems, conversions in the range 42-96% were reached at $120 \text{ }^\circ\text{C}/3 \text{ h}$ (Table 9.2-Catalytic BR).

The formation of Hmf was observed for all catalytic systems (9-58% Y_{Hmf}). By-products included Fru and/or Man (less than 12% total yield). Levulinic acid was not detected, which may be partly due to the moderately anhydrous conditions of the IL medium (the reaction of Hmf with water can give levulinic acid).

Table 9.2- Catalytic results for the reaction of D-glucose (Glu) in the presence of the prepared materials, using [Bmim]Cl as solvent, at 120 °C (Catalytic BR), and related catalytic tests for investigating catalyst stability (experiments (i), (ii), and (iii))^a

Sample	Catalytic BR		Experiment (i)		Experiment (ii)		Experiment (iii)	
	C _{Glu} ^b	Y _{Hmf} ^c	C _{Glu} ^b	Y _{Hmf} ^c	C _{Glu} ^b	Y _{Hmf} ^c	C _{Glu} ^b	Y _{Hmf} ^c
Al-TUD-1	65	9	23	1	64	9	61	9
Cr-Al-TUD-1	82	54	37	9	70	12	79	59
Cr-TUD-1	42	39	18	5	42	24	46	42
BEA	85	13	11	4	80	17	75	15
Cr-BEA	96	58	39	10	84	28	96	60
BEATUD-1	75	11	34	4	69	15	70	7
Cr-BEATUD-1	65	36	19	2	62	13	66	58

a) Experiments (i) and (ii) are relative to the recW and recC solids, respectively; experiment (iii) is relative to the recovered IL (recIL) (details in Section 9.2.2.3). b) Glucose conversion (C_{Glu}) at 3 h reaction. c) 5-Hydroxymethyl-2-furaldehyde yield (Y_{Hmf}) at 3 h reaction. Reaction conditions: [Bmim]Cl (0.3 cm³), 120 °C, 15 g_{cat}.dm⁻³, 0.28 M Glu, 3 h.

The influence of the type of solvent (water, DMSO) on the reaction was investigated for Cr-Al-TUD-1, under similar reaction conditions to those applied for [Bmim]Cl as solvent (120 °C, 3 h). For the three tested solvents, Glu was always completely dissolved in the reaction medium. For water and DMSO, the reaction of Glu was very sluggish: 3% Y_{Hmf} at 28% C_{Glu} for DMSO; 2% C_{Glu} at 3 h and no Hmf was detected for water as the solvent. These results were much poorer than those observed for the Cr-Al-TUD-1/IL system (54% Y_{Hmf}), suggesting that [Bmim]Cl was a favourable solvent for the target reaction studied.

For Al-TUD-1, the use of IL as solvent under moderate conditions did not improve the Hmf yield in comparison to that described in Chapter 4 for a similar material Al-TUD-1 (Si/Al=21) tested as catalyst in the same reaction using a biphasic Wt:Tol solvent system (< 20% Y_{Hmf} at 170 °C).

A comparative study for the different solid acid/IL systems showed that the catalytic systems without chromium led to fairly high C_{Glu} (65-85%), but low Y_{Hmf} (9-13%) compared to those observed for the related chromium-containing systems (36-58% Y_{Hmf}, Table 9.2). In the case of Al-TUD-1 and Cr-Al-TUD-1, which possessed similar Si/Al ratios and textural properties, Cr-Al-TUD-1 led to a much higher yield of Hmf. In parallel with these results, the Cr-BEA/IL and Cr-BEATUD-1/IL systems led to higher yield of Hmf than the related BEA/IL and BEATUD-1/IL systems, respectively. Similar results were reported in the literature for the reaction of Glu in the presence of a hydroxyapatite-supported chromium chloride, using [Bmim]Cl as solvent (denoted Cr-HAP/IL system), in that higher yields of Hmf were reached than the related system without chromium

(denoted HAP/IL), under similar reaction conditions: 40% and 8% Y_{Hmf} for Cr-HAP/IL and HAP/IL, respectively, at 78-81% C_{Glu} (microwave heating, 400 W, 2-3 min).³⁰

The Hmf selectivity for the Cr-TUD-1/IL system was very high (> 90% at 42% C_{Glu} , Table 9.2). Hence, while Brönsted acid sites (B) seemed to account for enhanced reaction rate of Glu, they were poorly selective in the conversion of Glu to Hmf (favouring side-reactions). Poor catalytic results have been reported in the literature for the reaction of Glu in the presence of a mixture of Brönsted acid and transition metal-containing catalysts, namely a phosphotungstic acid and chromium-containing metal-organic framework MIL-101, using [Emim]Cl as solvent (2% Y_{Hmf} , 21% C_{Glu} , at 100 °C/3 h). It was postulated that the reaction was Brönsted acid-catalysed.³²

Previously investigated IL-based homogeneous catalytic systems possessing Brönsted acidity, such as H_2SO_4 /[Emim]Cl,⁴ Brönsted acid-functionalised ILs ([Emim]HSO₄, Chapter 8), and Brönsted acid ILs ([Bmim]HSO₄ or [Hmim]HSO₄) coupled with Lewis acid CrCl_3 ,²⁰⁷ were poorly effective in the conversion of Glu to Hmf. According to the literature, and as explained in Chapter 1, the mechanism of the reaction of Glu to Hmf using chromium chloride salt/[Emim]Cl, at 100 °C, involved coordination chemistry between Lewis acid chromium species and Glu, accounting for a hydride transfer reaction and led to the isomerisation of Glu into Fru, which is an important primary step in the conversion of Glu to Hmf.^{4,208}

9.2.2.2. Catalyst stability

In order to investigate the stability of the prepared materials in the IL medium, and to assess the homo/heterogeneous nature of the catalytic reaction, each of the materials was firstly put into contact with fresh IL under similar reaction conditions to those used for the Catalytic BR experiments, but without adding Glu. After stirring for 3 h at 120 °C, the solid was separated from the IL by centrifugation, washed with milli-Q water and dried at 55 °C overnight. Afterwards, separate experiments were carried out with this solid and the recovered IL:

- i) The washed and dried solid, referred to as recW (solid acid), was tested in the reaction of Glu, using fresh IL as solvent, at 120 °C for 3 h;
- ii) The recW solid was calcined (450 °C, 3 h, heating rate of 1 °C·min⁻¹) to give recC (solid acid), which was tested in the reaction of Glu, using fresh IL as solvent, at 120 °C for 3 h;

iii) The recovered IL, referred to as recIL (“name of solid”), was used as solvent in a 3 h batch run of the reaction of Glu, at 120 °C, without adding a solid catalyst.

No drastic changes in the textural parameters (S_{BET} , V_p and PSD) were observed for the fresh and recC solids, the most significant differences were observed for Cr-Al-TUD-1 (763-995 $\text{m}^2\cdot\text{g}^{-1}$ S_{BET} , Table 9.1). The powder XRD patterns of the recovered TUD-1 and BEA-related solids were similar to those of the respective fresh materials (Figures 9.2 and 9.3, respectively). Hence, the prepared materials seemed to possess fairly good microstructural stability in the IL medium.

The FT-IR ATR spectra of the recW solids were fairly similar to those observed for the respective fresh solid acids, and did not show bands characteristic of the IL (Figures 9.9 and 9.10).

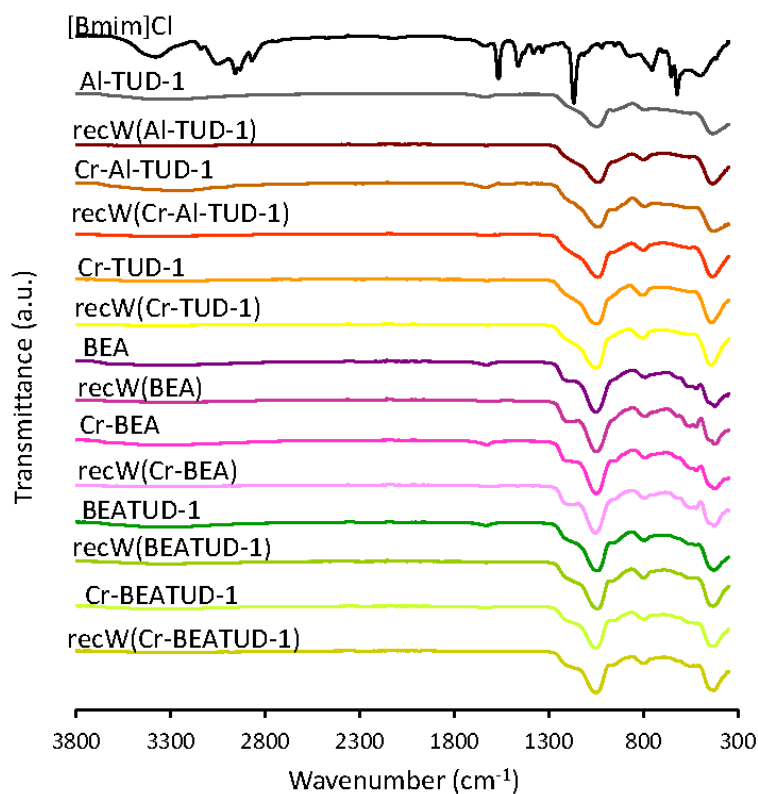


Figure 9.9- FT-IR ATR spectra of prepared materials and the respective recW solids.

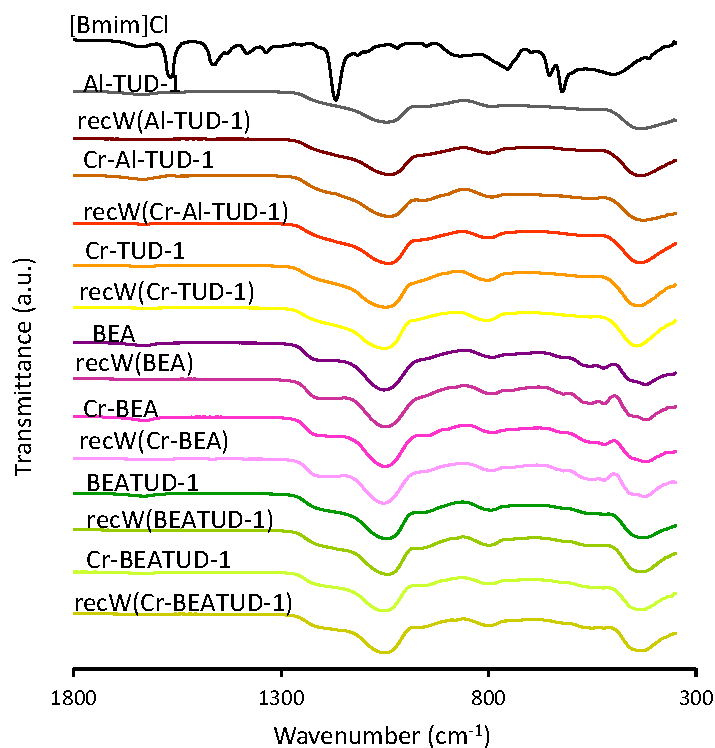


Figure 9.10- FT-IR ATR spectra of prepared materials and the respective recW solids in the range 300-1800 cm^{-1} .

The FT-IR spectra of all the recovered (recL) phases were also quite similar to that of fresh [Bmim]Cl, suggesting that this IL was relatively stable under the applied reaction conditions (Figure 9.11).

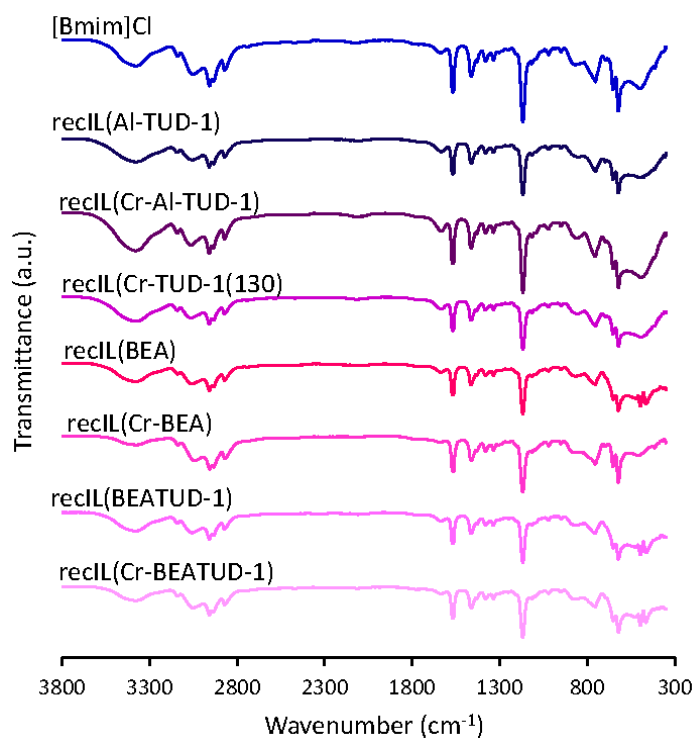


Figure 9.11- FT-IR ATR spectra of fresh [Bmim]Cl and the recovered ionic liquid (recIL) phases for the different solid acid/IL systems [denoted recIL(name of solid acid)].

The DR UV-vis spectrum of recC(Cr-BEA) was comparable with that for Cr-BEA (Figure 9.7), suggesting that the chemical nature of the surface chromium species were similar. Major differences were observed for recC(Cr-BEATUD-1) compared with Cr-BEATUD-1, suggesting that in this case modifications of the surface chromium species occurred (Figure 9.7). For recC(Cr-Al-TUD-1) and recC(Cr-TUD-1) the spectra showed three bands in similar ranges of wavelengths to those observed for the respective fresh solids, although some changes in the relative intensities were observed, which may be partly due to differences in the relative amounts of the surface chromium species.

The catalytic results for experiment (i) were poorer than those observed for the corresponding Catalytic BR experiment: the reaction of Glu was slower (for experiment (i) the values for the conversion of Glu were 0.13-0.45 times the conversion of Glu in the Catalytic BR) and the yields of Hmf were lower. For the chromium-containing systems (Cr-Al-TUD-1, Cr-TUD-1, Cr-BEA and Cr-BEATUD-1), the yields of Hmf values were a factor of 0.06-0.20 of the values for the catalytic BR, against 0.11-0.36 in the case of BEA, BEATUD-1 and Al-TUD-1 (Table 9.2). The

observed catalyst deactivation may be partly due to a) poisoning of the active sites and/or b) metal leaching.

In order to get insights into hypothesis a), the catalytic results for experiments i) and ii) were compared (Table 9.2). For the recC solids related to the prepared materials without chromium, the catalytic results were similar to those observed for the Catalytic BR experiments (64-65% C_{Glu} and 9% Y_{Hmf} for Al-TUD-1; 80-85% C_{Glu} and 13-17% Y_{Hmf} for BEA; 69-75% C_{Glu} and 11-15% Y_{Hmf} for BEATUD-1; Table 9.2), suggesting that the applied thermal treatment fully activated the recW solids. For the recC solids related to the prepared materials containing chromium, the thermal treatment led to enhanced Glu conversion, in a similar fashion to that observed for the remaining solid acids without chromium (Table 9.2). However, the yield of Hmf continued lower than those observed for the corresponding Catalytic BR experiments (Table 9.2). Nevertheless slight improvements were observed in the case of the recC solid acids containing chromium compared to the corresponding recW solid acids (9 to 12% for Cr-Al-TUD-1, 5 to 24% for Cr-TUD-1, 10 to 28% for Cr-BEA and 2 to 13% for Cr-BEATUD-1). These results suggested that chromium species (selective) are partially leached from the solids into the IL medium (hypothesis b). In fact, ICP-AES analyses for chromium in the recC solids gave residual amounts of chromium in all cases, excluding recC (Cr-TUD-1), with a Si/Cr ratio of 261 compared to 150 for the respective fresh material (Table 9.1). In contrast, the Si/Al ratios were comparable for the fresh and recovered chromium containing catalysts (Cr-Al-TUD-1, Cr-BEA and Cr-BEATUD-1, Table 9.1), suggesting that the prepared materials were fairly stable towards aluminium leaching in the IL medium: the Si/Al ratios for the recovered and calcined (recC) solid acids (recC(Cr-Al-TUD-1), recC (Cr-BEA) and recC (Cr-BEATUD-1) were 30, 13, and 45, respectively, compared to 27, 13 and 41 for the respective fresh materials (Table 9.1). According to the above discussion (in Section 9.2.2.1.) related to the roles of Brønsted and chromium Lewis acid species in the reaction of Glu, the thermally activated sites may be essentially of Brønsted acid type (active, albeit poorly selective).

Thermal analyses (TGA and DSC, under similar conditions) were carried out for recW solid acids (recW(Cr-BEA), recW(Cr-TUD-1) and recW(Cr-Al-TUD-1). The DSC curves for the fresh and recovered solids exhibited endothermic bands at temperatures lower than 175 °C and assignable to desorption of physisorbed water (Figure 9.12).

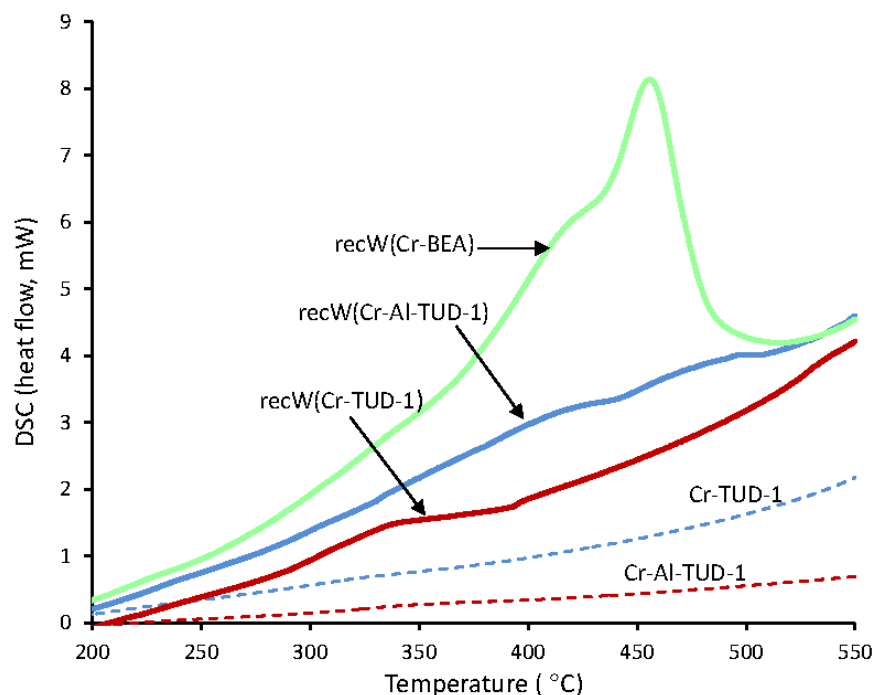


Figure 9.12- DSC curves for the recW solids related to the chromium containing solid acids and, for comparison, for fresh Cr-TUD-1 and Cr-Al-TUD-1.

Exothermic bands were observed at temperatures higher than 300 °C, only for recW solids, which may be due to the decomposition of organic matter; the latter may contribute to the observed catalyst deactivation for recW/IL systems (hypothesis a) discussed above). Based on the TGA data, the contents of organic matter were 1.2, 2.9 and 8.1 wt.% for the recW(Cr-TUD-1), recW(Cr-Al-TUD-1) and recW(Cr-BEA), respectively. The type of organic matter in the recW solids was most likely related to the cation $[Bmim]^+$ since the analysed recW solids were recovered from the solid acid/IL mixtures without Glu. It was possible that organic cations in the recW solids were converted to Brønsted acid sites upon the thermal activation treatment, accounting for the improved conversions of Glu observed for the recC solids (without enhancing the yield of Hmf, Table 9.2).

In order to get insights into the homo/heterogeneous nature of the catalytic reactions using the solid acid/IL systems, a comparative study of Catalytic BR and experiment (iii) was performed. In general, the catalytic results for these two experiments were comparable, suggesting that the catalytic reactions were essentially homogeneous in nature (Table 9.2). The active soluble species may be Brønsted acids and/or chromium Lewis acids. In terms of getting insights into the type of soluble active species, the reaction of Glu was carried out in the presence

of potassium chromate (K_2CrO_4) or dichromate ($K_2Cr_2O_7$) in which chromium is in the oxidation state +6. These salts were used in amounts equivalent to that of chromium added in the Cr-Al-TUD-1 solid acid and dissolved in the IL (7.2 mM chromium salt). For the two salt/IL systems the reaction of Glu was very sluggish: 1% Y_{Hmf} at 30-36% C_{Glu} , 120 °C/3 h. These results suggest that the active soluble species in the catalysts tested herein were not oxochromium(VI) species. Possibly, fully dissociated chromium ions were leached into the IL to give chromium chloro-complexes. Using $Cr(NO_3)_3 \cdot 9H_2O$ (in which the chromium is in the oxidation state +3) instead of the chromate salts gave an outstanding 79% Y_{Hmf} at 97% C_{Glu} , under similar catalytic reaction conditions. Figure 9.13 showed the UV-vis spectra of the recIL phases related to the solid acids, and for comparison those of freshly prepared salt/IL solutions and the respective solutions obtained after treatment under similar reaction conditions to those used for the Catalytic BR experiments, but without adding Glu (denoted heat(salt/IL)). The spectra of $Cr(NO_3)_3/IL$ and heat($Cr(NO_3)_3/IL$) were similar, suggesting that the dissolved chromium species were fairly stable under the applied reaction conditions. The same did not apply for K_2CrO_4 and $K_2Cr_2O_7$, suggesting that in the latter two cases, the dissolved species were not stable under the catalytic reaction conditions. The spectral features of recIL(Cr-Al-TUD-1), recIL(Cr-BEA) and recIL(Cr-BEATUD-1) resembled somewhat more closely those for the $Cr(NO_3)_3$ related systems than those for the K_2CrO_4 and $K_2Cr_2O_7$ systems. In the case of recIL(Cr-TUD-1), relatively intense bands appeared in the region 600-720 nm. These results suggested that the recIL phases contained active soluble Cr^{3+} species. Based on the characterisation results in Section 9.2.2.1. it was not possible to confirm the presence of Cr^{3+} in the solid acids prepared, although this possibility cannot be fully ruled out. The active soluble species may result from direct leaching of Cr^{3+} and/or from the transformation of leached metal species. Despite the presence of Cr^{3+} species in the case of $Cr(NO_3)_3/IL$ system, no bands above 600 nm characteristic of Cr^{3+} (e.g. Cr_2O_3 clusters) were observed, possibly due to the fact that in this system the Cr^{3+} species are ions and ions do not present bands in the UV-vis spectra in this region.

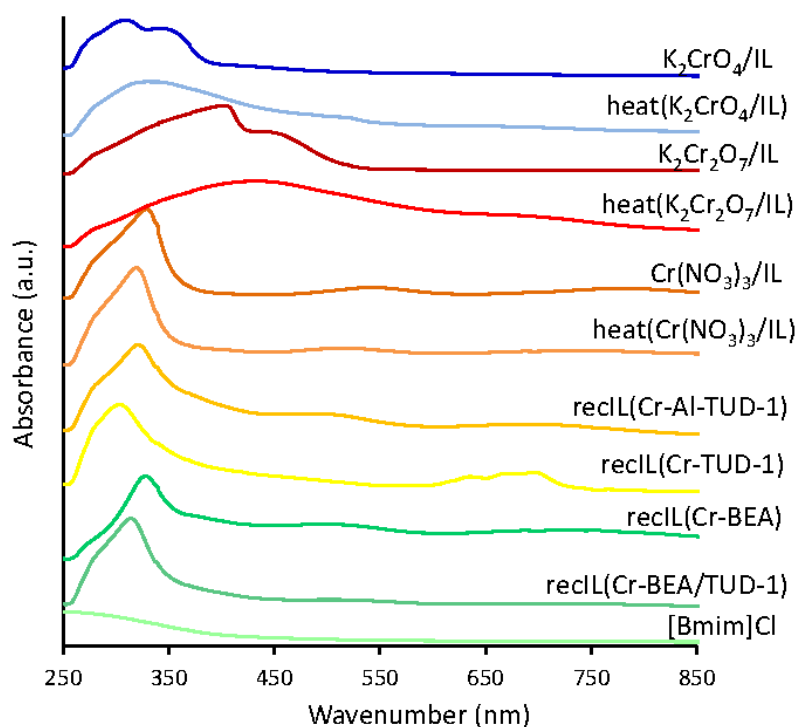


Figure 9.13- UV-vis spectra of the recIL phases related to the chromium-containing solids, and of chromium salts dissolved in the IL ([Bmim]Cl) before and after heating at 120 °C for 3 h.

9.3. Conclusions

The reaction of Glu was investigated using aluminium and/or chromium containing micro/mesoporous solid acids coupled with [Bmim]Cl as solvent, at 120 °C. The prepared materials were Al-TUD-1, Cr-Al-TUD-1, Cr-TUD-1, BEA, Cr-BEA and the related micro/mesoporous composites BEATUD-1 and Cr-BEATUD-1. The prepared materials seemed microstructurally stable in the IL medium, and the Si/Al atomic ratios were similar for the fresh and recovered solids.

The solid acids without chromium could be regenerated by thermal treatment, giving similar catalytic results to the respective fresh solids. Nevertheless, for these materials, the Y_{Hmf} were rather low (< 17%). In contrast, the (chromium-containing solid acid)/IL systems led to relatively high Y_{Hmf} (36-58%), although these materials could not be fully regenerated due to chromium leaching which led to a drop in Y_{Hmf} (12-28%). The catalytic reactions were essentially homogeneous in nature. It was postulated that Brønsted acid species seemed relatively active in

the reaction of Glu, albeit poorly selective in the conversion of Glu to Hmf. In contrast, chromium species played an effective role in the conversion of Glu to Hmf. The IL was a favourable solvent for this target reaction (in terms of yields of Hmf reached) in comparison to water or DMSO. The development of truly heterogeneous catalytic systems based on ILs for the selective reaction of Glu and related di/polysaccharides to Hmf remains a challenge.

9.4. References

- (1) Hamdy, M. S.: Functionalized TUD-1: Synthesis, characterization, and (photo-)catalytic performance. Delft University of Technology, the Netherlands, 2005.
- (2) IZA-SC-members: Zeolite Framework Types. Database of Zeolite Structures, 2012; Vol. 2012.
- (3) Karinen, R.; Vilonen, K.; Niemela, M.: Biorefining: Heterogeneously Catalyzed Reactions of Carbohydrates for the Production of Furfural and Hydroxymethylfurfural. *ChemSusChem* **2011**, *4*, 1002-1016.
- (4) Zhao, H.; Holladay, J. E.; Brown, H.; Zhang, Z. C.: Metal Chlorides in Ionic Liquid Solvents Convert Sugars to 5-Hydroxymethylfurfural. *Science* **2007**, *316*, 1597-1600.
- (5) Zhao, H.; Holladay, J. E.; Zhang, Z. C.: Method for Conversion of Carbohydrates in Ionic Liquids to Hydroxymethylfurfural. In *International Application Published under the Patent Cooperation Treaty (PCT): WO/2008/019219 A1*; Battelle Memorial Institute, Pacific Northwest Division, Intellectual Property Legal Services, Richland, USA: USA, 2008; pp 53.
- (6) Zhao, H.; Holladay, J. E.; Zhang, Z. C.: Method for Conversion of Carbohydrates in Ionic Liquids to Value-Added Chemicals. In *United States Patent: US 7,939,681 B2*; Battelle Memorial Institute, Richland, Washington, USA: USA, 2011; pp 15.
- (7) Rosatella, A. A.; Simeonov, S. P.; Frade, R. F. M.; Afonso, C. A. M.: 5-Hydroxymethylfurfural (HMF) as a Building Block Platform: Biological Properties, Synthesis and Synthetic Applications. *Green Chemistry* **2011**, *13*, 754-793.
- (8) Lima, S.; Antunes, M. M.; Pillinger, M.; Valente, A. A.: Ionic Liquids as Tools for the Acid-Catalyzed Hydrolysis/Dehydration of Saccharides to Furanic Aldehydes. *ChemCatChem* **2011**, *3*, 1686-1706.
- (9) Zakrzewska, M. E.; Lukasik, E. B.; Lukasik, R. B.: Ionic Liquid-Mediated Formation of 5-Hydroxymethylfurfural-A Promising Biomass-Derived Building Block. *Chemical Reviews* **2011**, *111*, 397-417.
- (10) Ståhlberg, T.; Fu, W.; Woodley, J. M.; Riisager, A.: Synthesis of 5-(Hydroxymethyl)furfural in Ionic Liquids: Paving the Way to Renewable Chemicals. *ChemSusChem* **2011**, *4*, 451-458.
- (11) Cao, Q.; Guo, X.; Yao, S.; Guan, J.; Wang, X.; Mu, X.; Zhang, D.: Conversion of Hexose into 5-Hydroxymethylfurfural in Imidazolium Ionic Liquids With and Without a Catalyst. *Carbohydrate Research* **2011**, *346*, 956-959.
- (12) Yuan, Z.; Xu, C.; Cheng, S.; Leitch, M.: Catalytic Conversion of Glucose to 5-Hydroxymethylfurfural Using Inexpensive Co-Catalysts and Solvents. *Carbohydrate Research* **2011**, *346*, 2019-2023.
- (13) Zhang, Y.; Pidko, E. A.; Hensen, E. J. M.: Molecular Aspects of Glucose Dehydration by Chromium Chlorides in Ionic Liquids. *Chemistry-A European Journal* **2011**, *17*, 5281-5288.
- (14) Wei, Z.; Liu, Y.; Thushara, D.; Ren, Q.: Entrainer-Intensified Vacuum Reactive Distillation Process for the Separation of 5-Hydroxymethylfurfural From the Dehydration of Carbohydrates Catalyzed by a Metal Salt-Ionic Liquid. *Green Chemistry* **2012**, *14*, 1220-1226.

- (15) Jadhav, H.; Taarning, E.; Pedersen, C. M.; Bols, M.: Conversion of D-glucose Into 5-Hydroxymethylfurfural (Hmf) Using Zeolite in BmimCl or Tetrabutylammonium Chloride (TBAC)/CrCl₂. *Tetrahedron Letters* **2012**, *53*, 983-985.
- (16) Hu, L.; Sun, Y.; Lin, L.: Efficient Conversion of Glucose into 5-Hydroxymethylfurfural by Chromium(III) Chloride in Inexpensive Ionic Liquid. *Industrial & Engineering Chemistry Research* **2012**, *51*, 1099-1104.
- (17) Patil, S. K. R.; Lund, C. R. F.: Formation and Growth of Humins via Aldol Addition and Condensation during Acid-Catalyzed Conversion of 5-Hydroxymethylfurfural. *Energy & Fuels* **2011**, *25*, 4745-4755.
- (18) Rasrendra, C. B.; Makertihartha, I. G. B. N.; Adisasmito, S.; Heeres, H. J.: Green Chemicals From D-glucose: Systematic Studies on Catalytic Effects of Inorganic Salts on the Chemo-Selectivity and Yield in Aqueous Solutions. *Topics in Catalysis* **2010**, *53*, 1241-1247.
- (19) Peng, L.; Lin, L.; Zhang, J.; Zhuang, J.; Zhang, B.; Gong, Y.: Catalytic Conversion of Cellulose to Levulinic Acid by Metal Chlorides. *Molecules* **2010**, *15*, 5258-5272.
- (20) Swatloski, R. P.; Spear, S. K.; Holbrey, J. D.; Rogers, R. D.: Dissolution of Cellose With Ionic Liquids. *Journal of the American Chemical Society* **2002**, *124*, 4974-4975.
- (21) Remsing, R. C.; Swatloski, R. P.; Rogers, R. D.; Moyna, G.: Mechanism of Cellulose Dissolution in the Ionic Liquid 1-n-Butyl-3-Methylimidazolium Chloride: a ¹³C- and ^{35/37}Cl- NMR Relaxation Study on Model Systems. *Chemical Communications* **2006**, 1271-1273.
- (22) Liebert, T.; Heinze, T.: Interaction of Ionic Liquids With Polysaccharides 5. Solvents and Reaction Media for the Modification of Cellulose. *Bioresources* **2008**, *3*, 576-601.
- (23) Pinkert, A.; Marsh, K. N.; Pang, S.; Staiger, M. P.: Ionic Liquids and Their Interaction with Cellulose. *Chemical Reviews* **2009**, *109*, 6712-6728.
- (24) Zakrzewska, M. E.; Lukasik, E. B.; Lukasik, R. B.: Solubility of Carbohydrates in Ionic Liquids. *Energy & Fuels* **2010**, *24*, 737-745.
- (25) Guo, J.; Zhang, D.; Liu, C.: A Theoretical Investigation of the Interactions Between Cellulose and 1-Butyl-3-methylimidazolium Chloride. *Journal of Theoretical and Computational Chemistry* **2010**, *09*, 611-624.
- (26) Gupta, K. M.; Hu, Z.; Jiang, J.: Mechanistic Understanding of Interactions Between Cellulose and Ionic Liquids: A Molecular Simulation Study. *Polymer* **2011**, *52*, 5904-5911.
- (27) Imperato, G.; König, B.; Chiappe, C.: Ionic Green Solvents from Renewable Resources. *European Journal of Organic Chemistry* **2007**, *2007*, 1049-1058.
- (28) Tan, M.; Zhao, L.; Zhang, Y.: Production of 5-Hydroxymethylfurfural From Cellulose in CrCl₂/Zeolite/BmimCl System. *Biomass & Bioenergy* **2011**, *35*, 1367-1370.
- (29) Francisco, M.; Mlinar, A. N.; Yoo, B.; Bell, A. T.; Prausnitz, J. M.: Recovery of Glucose from an Aqueous Ionic Liquid by Adsorption onto a Zeolite Based Solid. *Chemical Engineering Journal* **2011**, *172*, 184-190.
- (30) Zhang, Z.; Zhao, Z.: Production of 5-Hydroxymethylfurfural From Glucose Catalyzed by Hydroxyapatite Supported Chromium Chloride. *Bioresource Technology* **2011**, *102*, 3970-3972.
- (31) Glaeser, R.: Novel Process Options for the Application of Zeolites in Supercritical Fluids and Ionic Liquids. *Chemical Engineering & Technology* **2007**, *30*, 557-568.
- (32) Zhang, Y.; Degirmenci, V.; Li, C.; Hensen, E. J. M.: Phosphotungstic Acid Encapsulated in Metal-Organic Framework as Catalysts for Carbohydrate Dehydration to 5-Hydroxymethylfurfural. *ChemSusChem* **2011**, *4*, 59-64.
- (33) Rinaldi, R.; Meine, N.; Stein, J. V.; Palkovits, R.; Schueth, F.: Which Controls the Depolymerization of Cellulose in Ionic Liquids: The Solid Acid Catalyst or Cellulose? *ChemSusChem* **2010**, *3*, 266-276.
- (34) Anand, R.; Hamdy, M. S.; Gkourgkoulas, P.; Maschmeyer, T.; Jansen, J. C.; Hanefeld, U.: Liquid Phase Oxidation of Cyclohexane Over Transition Metal Incorporated Amorphous 3D-Mesoporous Silicates M-TUD-1 (M = Ti, Fe, Co and Cr). *Catalysis Today* **2006**, *117*, 279-283.
- (35) Jansen, J. C.; Shan, Z.; Marchese, L.; Zhou, W.; Puil, N. V. d.; Maschmeyer, T.: A New Templating Method For Three-Dimensional Mesopore Networks. *Chemical Communications* **2001**, 713-714.
- (36) Telalović, S.; Ramanathan, A.; Mul, G.; Hanefeld, U.: TUD-1: Synthesis and Application of a Versatile Catalyst, Carrier, Material. *Journal of Materials Chemistry* **2010**, *20*, 642-658.

- (37) Shan, Z.; Jansen, J. C.; Zhou, W.; Maschmeyer, T.: Al-TUD-1, Stable Mesoporous Aluminas with High Surface Areas. *Applied Catalysis A-General* **2003**, *254*, 339-343.
- (38) Anand, R.; Maheswari, R.; Hanefeld, U.: Catalytic Properties of the Novel Mesoporous Aluminosilicate AlTUD-1. *Journal of Catalysis* **2006**, *242*, 82-91.
- (39) Hamdy, M. S.; Berg, O.; Jansen, J. C.; Maschmeyer, T.; Arafat, A.; Moulijn, J. A.; Mul, G.: Chromium-Incorporated TUD-1 as a New Visible Light-Sensitive Photo-Catalyst for Selective Oxidation of Propane. *Catalysis Today* **2006**, *117*, 337-342.
- (40) Zhang, Z.-X.; Bai, P.; Xu, B.; Yan, Z.-F.: Synthesis of Mesoporous Alumina TUD-1 With High Thermostability. *J Porous Mater* **2006**, *13*, 245-250.
- (41) Telalović, S.; Hanefeld, U.: Noncovalent Immobilization of Chiral Cyclopropanation Catalysts on Mesoporous TUD-1: Comparison of Liquid-Phase and Gas-Phase Ion-Exchange. *Applied Catalysis A-General* **2010**, *372*, 217-223.
- (42) Simons, C.; Hanefeld, U.; Arends, I.; Sheldon, R. A.; Maschmeyer, T.: Noncovalent Anchoring of Asymmetric Hydrogenation Catalysts on a New Mesoporous Aluminosilicate: Application and Solvent Effects. *Chemistry-A European Journal* **2004**, *10*, 5829-5835.
- (43) Shan, Z.; Gianotti, E.; Jansen, J. C.; Peters, J. A.; Marchese, L.; Maschmeyer, T.: One-Step Synthesis of a Highly Active, Mesoporous, Titanium-Containing Silica by Using Bifunctional Templating. *Chemistry-A European Journal* **2001**, *7*, 1437-1443.
- (44) Anand, R.; Hamdy, M. S.; Hanefeld, U.; Maschmeyer, T.: Liquid-Phase Oxidation of Cyclohexane Over Co-TUD-1. *Catalysis Letters* **2004**, *95*, 113-117.
- (45) Hamdy, M. S.; Ramanathan, A.; Maschmeyer, T.; Hanefeld, U.; Jansen, J. C.: Co-TUD-1: A Ketone-Selective Catalyst for Cyclohexane Oxidation. *Chemistry-A European Journal* **2006**, *12*, 1782-1789.
- (46) Hamdy, M. S.; Mul, G.; Wei, W.; Anand, R.; Hanefeld, U.; Jansen, J. C.; Moulijn, J. A.: Fe, Co and Cu-Incorporated TUD-1: Synthesis, Characterization and Catalytic Performance in N₂O Decomposition and Cyclohexane Oxidation. *Catalysis Today* **2005**, *110*, 264-271.
- (47) Ramanathan, A.; Villalobos, M. C. C.; Kwakernaak, C.; Telalović, S.; Hanefeld, U.: Zr-TUD-1: A Lewis Acidic, Three-Dimensional, Mesoporous, Zirconium-Containing Catalyst. *Chemistry-A European Journal* **2008**, *14*, 961-972.
- (48) Ramanathan, A.; Klomp, D.; Peters, J. A.; Hanefeld, U.: Zr-TUD-1: A Novel Heterogeneous Catalyst for the Meerwein-Ponndorf-Verley Reaction. *Journal of Molecular Catalysis A-Chemical* **2006**, *260*, 62-69.
- (49) Wei, W.; Moulijn, J. A.; Mul, G.: FAPO and Fe-TUD-1: Promising Catalysts for N₂O Mediated Selective Oxidation of Propane? *Journal of Catalysis* **2009**, *262*, 1-8.
- (50) Telalović, S.; Hanefeld, U.: Investigation of the Cyanosilylation Catalysed by Metal-Siliceous Catalysts. *Catalysis Communications* **2011**, *12*, 493-496.
- (51) Neves, I. C.; Botelho, G.; Machado, A. V.; Rebelo, P.; Ramoa, S.; Pereira, M. F. R.; Ramanathan, A.; Pescarmona, P.: Feedstock Recycling of Polyethylene Over AlTUD-1 Mesoporous Catalyst. *Polymer Degradation and Stability* **2007**, *92*, 1513-1519.
- (52) Telalović, S.; Ng, J. F.; Maheswari, R.; Ramanathan, A.; Chuah, G. K.; Hanefeld, U.: Synergy Between Brønsted Acid Sites and Lewis Acid Sites. *Chemical Communications* **2008**, 4631-4633.
- (53) Shan, Z.; Jansen, J. C.; Yeh, C. Y.; Angevine, P. J.; Maschmeyer, T.: Mesoporous Aluminium Oxide, Preparation and Use Thereof. In *United States Patent Application Publication: US 2007/0170096 A1*; Dilworth & Barrese, LLP, Uniondale, NY, U.S.A.: USA, 2007; pp 23.
- (54) Norek, M.; Neves, I. C.; Peters, J. A.: ¹H Relaxivity of Water in Aqueous Suspensions of Gd³⁺-Loaded NaY Nanozeolites and AlTUD-1 Mesoporous Material: the Influence of Si/Al Ratio and Pore Size. *Inorganic Chemistry* **2007**, *46*, 6190-6196.
- (55) Petkov, N.; Holzl, M.; Metzger, T. H.; Mintova, S.; Bein, T.: Ordered Micro/Mesoporous Composite Prepared as Thin Films. *Journal of Physical Chemistry B* **2005**, *109*, 4485-4491.
- (56) Waller, P.; Shan, Z. P.; Marchese, L.; Tartaglione, G.; Zhou, W. Z.; Jansen, J. C.; Maschmeyer, T.: Zeolite Nanocrystals Inside Mesoporous TUD-1: A High-Performance Catalytic Composite. *Chemistry-A European Journal* **2004**, *10*, 4970-4976.
- (57) Shan, Z.; Waller, P. W. G.; Maingary, B. G.; Angevine, P. J.; Jansen, J. C.; Yeh, C. Y.; Maschmeyer, T.; Dautzenberg, F. M.; Marchese, L.; Pastore, H. d. O.: Zeolite Composite Method for Making and Catalytic Application Thereof. In *United States Patent: US 7,084,087 B2*; ABB Lummus Global Inc.: USA, 2006; pp 22.

- (58) Mavrodinova, V.; Popova, M.; Valchev, V.; Nickolov, R.; Minchev, C.: Beta Zeolite Colloidal Nanocrystals Supported on Mesoporous MCM-41. *Journal of Colloid and Interface Science* **2005**, *286*, 268-273.
- (59) Oers, C. J. V.; Stevens, W. J. J.; Bruijn, E.; Mertens, M.; Lebedev, O. I.; Tendeloo, G. V.; Meynen, V.; Cool, P.: Formation of a Combined Micro- and Mesoporous Material Using Zeolite Beta Nanoparticles. *Microporous and Mesoporous Materials* **2009**, *120*, 29-34.
- (60) Xia, Y. D.; Mokaya, R.: On the Synthesis and Characterization of ZSM-5/MCM-48 Aluminosilicate Composite Materials. *Journal of Materials Chemistry* **2004**, *14*, 863-870.
- (61) Wang, J.; Groen, J. C.; Yue, W.; Zhou, W.; Coppens, M.-O.: Single-Template Synthesis of Zeolite ZSM-5 Composites With Tunable Mesoporosity. *Chemical Communications* **2007**, 4653-4655.
- (62) Wang, J.; Groen, J. C.; Yue, W.; Zhou, W.; Coppens, M.-O.: Facile Synthesis of ZSM-5 Composites With Hierarchical Porosity. *Journal of Materials Chemistry* **2008**, *18*, 468-474.
- (63) Wang, J.; Yue, W.; Zhou, W.; Coppens, M.-O.: TUD-C: A Tunable, Hierarchically Structured Mesoporous Zeolite Composite. *Microporous and Mesoporous Materials* **2009**, *120*, 19-28.
- (64) Xu, H.; Guan, J.; Wu, S.; Kan, Q.: Synthesis of Beta/MCM-41 Composite Molecular Sieve With High Hydrothermal Stability in Static and Stirred Condition. *Journal of Colloid and Interface Science* **2009**, *329*, 346-350.
- (65) Wu, J.-S.; Chiang, A. S. T.; Tsai, T.-C.: Some Observations on the Synthesis of Colloidal Beta Zeolite from a Clear Precursor Sol. *Science of Advanced Materials* **2011**, *3*, 1011-1018.
- (66) Mintova, S.; Valtchev, V.; Onfroy, T.; Marichal, C.; Knözinger, H.; Bein, T.: Variation of the Si/Al Ratio in Nanosized Zeolite Beta Crystals. *Microporous and Mesoporous Materials* **2006**, *90*, 237-245.
- (67) Verboekend, D.; Vilé, G.; Ramírez, J. P.: Mesopore Formation in USY and Beta Zeolites by Base Leaching: Selection Criteria and Optimization of Pore-Directing Agents. *Crystal Growth & Design* **2012**, *12*, 3123-3132.
- (68) Esquivel, D.; Cruz-Cabeza, A. J.; Jimenez-Sanchidrian, C.; Romero-Salguero, F. J.: Enhanced Concentration of Medium Strength Bronsted Acid Sites in Aluminium-Modified beta Zeolite. *Catalysis Letters* **2012**, *142*, 112-117.
- (69) Shekara, B. M. C.; Prakash, B. S. J.; Bhat, Y. S.: Microwave-Induced Deactivation-Free Catalytic Activity of BEA Zeolite in Acylation Reactions. *Journal of Catalysis* **2012**, *290*, 101-107.
- (70) Rodríguez, M. T.; Arzaluz, M. G.; Alvarez, V. M.; Pliego, J. A.; Pergher, S.: Alkylation of Benzene with Propylene in a Flow-Through Membrane Reactor and Fixed-Bed Reactor: Preliminary Results. *Materials* **2012**, *5*, 872-881.
- (71) Duan, A.; Wan, G.; Zhang, Y.; Zhao, Z.; Jiang, G.; Liu, J.: Optimal Synthesis of Micro/Mesoporous Beta Zeolite from Kaolin Clay and Catalytic Performance for Hydrodesulfurization of Diesel. *Catalysis Today* **2011**, *175*, 485-493.
- (72) Cao, F.; Wu, Y.; Gu, J.; Wang, J.: Hydrothermal Synthesis of Nanocrystalline Zeolite Beta by Acid-Catalyzed Hydrolysis of Tetraethylorthosilicate. *Materials Chemistry and Physics* **2011**, *130*, 727-732.
- (73) Kamimura, Y.; Tanahashi, S.; Itabashi, K.; Sugawara, A.; Wakihara, T.; Shimojima, A.; Okubo, T.: Crystallization Behavior of Zeolite Beta in OSDA-Free, Seed-Assisted Synthesis. *Journal of Physical Chemistry C* **2011**, *115*, 744-750.
- (74) Fang, S.-Y.; Chiang, A. S. T.; Kao, H.-M.: Increasing the Productivity of Colloidal Zeolite Beta by Posthydrolysis Evaporation. *Industrial & Engineering Chemistry Research* **2010**, *49*, 12191-12196.
- (75) Liu, P.; Yao, Y.; Wang, J.: Using Beta-MCM41 Composite Molecular Sieves as Supports of Bifunctional Catalysts for the Hydroisomerization of n-Heptane. *Reaction Kinetics Mechanisms and Catalysis* **2010**, *101*, 465-475.
- (76) Kamimura, Y.; Chaikittisilp, W.; Itabashi, K.; Shimojima, A.; Okubo, T.: Critical Factors in the Seed-Assisted Synthesis of Zeolite Beta and "Green Beta" from OSDA-Free Na⁺-Aluminosilicate Gels. *Chemistry-An Asian Journal* **2010**, *5*, 2182-2191.
- (77) Qian, L.; Yue, B.; Pei, S.; Zhang, L.; Ye, L.; Cheng, J.; Tsang Shik, C.; He, H.: Reforming of CH₄ with CO₂ over Rh/H-Beta: Effect of Rhodium Dispersion on the Catalytic Activity and Coke Resistance. *Chinese Journal of Chemistry* **2010**, *28*, 1864-1870.
- (78) Wang, D.; Liu, Z.; Wang, H.; Xie, Z.; Tang, Y.: Shape-Controlled Synthesis of Monolithic ZSM-5 Zeolite With Hierarchical Structure and Mechanical Stability. *Microporous and Mesoporous Materials* **2010**, *132*, 428-434.

- (79) Selvin, R.; Roselin, L. S.; Kumar, K. P.; Arul, S.: Nanocrystalline Zeolite Beta: An Efficient Catalyst for the Regioselective Alcoholysis of Epichlorohydrin. *Science of Advanced Materials* **2010**, *2*, 190-194.
- (80) Liu, S.-P.; Chen, L.; Wang, Y. M.: The Synthesis of Mesoporous Zeolite Beta Aggregates Without the Use of Second Template and Additive. *Solid State Sciences* **2010**, *12*, 1070-1075.
- (81) Jin, C.; Zhang, Y.; Gao, W.; Cui, L.: Anionic Emulsion-Mediated Synthesis of Zeolite Beta. *International Journal of Modern Physics B* **2010**, *24*, 3236-3241.
- (82) Liu, P.; Zhang, X.; Yao, Y.; Wang, J.: Alkaline Earth Metal Ion-Exchanged Beta Zeolite Supported Pt Catalysts for Hydroisomerization of n-Heptane. *Reaction Kinetics Mechanisms and Catalysis* **2010**, *100*, 217-226.
- (83) Toktarev, A. V.; Malysheva, L. V.; Paukshtis, E. A.: Effect of Thermal Treatment Conditions on the Acid Properties of Zeolite Beta. *Kinetics and Catalysis* **2010**, *51*, 318-324.
- (84) Parker, W. O., Jr.; Angelis, A. d.; Flego, C.; Millini, R.; Perego, C.; Zanardi, S.: Unexpected Destructive Dealumination of Zeolite Beta by Silylation. *Journal of Physical Chemistry C* **2010**, *114*, 8459-8468.
- (85) Dzwigaj, S.; Millot, Y.; Methivier, C.; Che, M.: Incorporation of Nb(V) into BEA Zeolite Investigated by XRD, NMR, IR, DR UV-vis, and XPS. *Microporous and Mesoporous Materials* **2010**, *130*, 162-166.
- (86) Kuechl, D. E.; Benin, A. I.; Knight, L. M.; Abrevaya, H.; Wilson, S. T.; Sinkler, W.; Mezza, T. M.; Willis, R. R.: Multiple Paths to Nanocrystalline High Silica Beta Zeolite. *Microporous and Mesoporous Materials* **2010**, *127*, 104-118.
- (87) Wang, Y.; Jiang, Z.; Li, H.; Yang, D.: Chitosan Membranes Filled by GPTMS-Modified Zeolite Beta Particles With Low Methanol Permeability for DMFC. *Chemical Engineering and Processing* **2010**, *49*, 278-285.
- (88) Wan, G.; Duan, A.; Zhang, Y.; Zhao, Z.; Jiang, G.; Zhang, D.; Gao, Z.: Zeolite Beta Synthesized With Acid-Treated Metakaolin and its Application in Diesel Hydrodesulfurization. *Catalysis Today* **2010**, *149*, 69-75.
- (89) Merg, J. C.; Rossett, F.; Penha, F. G.; Pergher, S. B. C.; Petkowicz, D. I.; dos Santos, H. Z.: Titanium Oxide Incorporation on Zeolites For Heterogeneous Photocatalysis. *Química Nova* **2010**, *33*, 1525-1528.
- (90) Modhera, B.; Chakraborty, M.; Bajaj, H. C.; Parikh, P. A.: Simultaneous n-Hexane Isomerization and Benzene Saturation Over Pt/Nano-Crystalline Zeolite Beta. *Reaction Kinetics Mechanisms and Catalysis* **2010**, *99*, 421-429.
- (91) Dragoi, B.; Rakic, V.; Dumitriu, E.; Auroux, A.: Adsorption of Organic Pollutants Over Microporous Solids Investigated by Microcalorimetry Techniques. *Journal of Thermal Analysis and Calorimetry* **2010**, *99*, 733-740.
- (92) Liu, P.; Zhang, X.; Yao, Y.; Wang, J.: Pt catalysts Supported on Beta Zeolite Ion-Exchanged With Cr(III) for Hydroisomerization of n-Heptane. *Applied Catalysis A-General* **2009**, *371*, 142-147.
- (93) Parmentier, J.; Valtchev, V.; Gaslain, F.; Tosheva, L.; Ducrot-Boisgontier, C.; Möller, J.; Patarin, J.; Vix-Guterl, C.: Effect of the Zeolite Crystal Size on the Structure and Properties of Carbon Replicas Made by a Nanocasting Process. *Carbon* **2009**, *47*, 1066-1073.
- (94) Zhang, Q.; Xia, Q. H.; Lu, X. H.; Ma, X. T.; Su, K. X.: Gas-Phase Catalytic Synthesis of MTBE From MeOH and (Bu^tOH) Over Various Microporous H-Zeolites. *Indian Journal of Chemistry Section a-Inorganic Bio-Inorganic Physical Theoretical & Analytical Chemistry* **2009**, *48*, 788-792.
- (95) Hou, Q.; Zheng, B.; Bi, C.; Luan, J.; Zhao, Z.; Guo, H.; Wang, G.; Li, Z.: Liquid-Phase Cascade Acylation/Dehydration Over Various Zeolite Catalysts to Synthesize 2-Methylantraquinone Through an Efficient One-Pot Strategy. *Journal of Catalysis* **2009**, *268*, 376-383.
- (96) Lee, F. Y.; Lv, L.; Su, F.; Liu, T.; Liu, Y.; Sow, C. H.; Zhao, X. S.: Incorporation of Titanium into Polymorph C for Catalytic Epoxidation of Cyclohexene. *Microporous and Mesoporous Materials* **2009**, *124*, 36-41.
- (97) Xu, X.; Zhao, X.; Sun, L.; Liu, X.: Adsorption Separation of Carbon Dioxide, Methane and Nitrogen on Monoethanol Amine Modified Beta-Zeolite. *Journal of Natural Gas Chemistry* **2009**, *18*, 167-172.

- (98) Liu, P.; Wang, J.; Zhang, X.; Wei, R.; Ren, X.: Catalytic Performances of Dealuminated H-Beta Zeolite Supported Pt Catalysts Doped With Cr in Hydroisomerization of n-Heptane. *Chemical Engineering Journal* **2009**, *148*, 184-190.
- (99) Jakob, A.; Valtchev, V.; Soulard, M.; Faye, D.: Syntheses of Zeolite Beta Films in Fluoride Media and Investigation of Their Sorption Properties. *Langmuir* **2009**, *25*, 3549-3555.
- (100) Modhera, B.; Chakraborty, M.; Parikh, P. A.; Jasra, R. V.: Synthesis of Nano-Crystalline Zeolite Beta: Effects of Crystallization Parameters. *Crystal Research and Technology* **2009**, *44*, 379-385.
- (101) Mahalakshmi, M.; Priya, S. V.; Arabindoo, B.; Palanicharnly, M.; Murugesan, V.: Photocatalytic Degradation of Aqueous Propoxur Solution Using TiO₂ and H-Beta Zeolite-Supported TiO₂. *Journal of Hazardous Materials* **2009**, *161*, 336-343.
- (102) Li, H.; Li, M.; Chu, Y.; Nie, H.: Influence of Different Modified Beta Zeolite on Skeletal Isomerization of n-Hexene in the Presence of Hydrogen. *Microporous and Mesoporous Materials* **2009**, *117*, 635-639.
- (103) Dzwigaj, S.; Janas, J.; Gurgul, J.; Socha, R. P.; Shishido, T.; Che, M.: Do Cu(II) Ions Need Al Atoms in Their Environment to Make CuSiBEA Active in the SCR of NO by Ethanol or Propane? A spectroscopy and Catalysis Study. *Applied Catalysis B-Environmental* **2009**, *85*, 131-138.
- (104) Huang, Z.; Su, J.-F.; Guo, Y.-H.; Su, X.-Q.; Teng, L.-J.: Synthesis of Well-Crystallized Zeolite Beta at Large Scale and its Synthesis of Well-Crystallized Zeolite Beta at Large Scale and its Incorporation into Polysulfone Matrix for Gas Separation. *Chemical Engineering Communications* **2009**, *196*, 969-986.
- (105) Shen, B.; Wang, P.; Yi, Z.; Zhang, W.; Tong, X.; Liu, Y.; Guo, Q.; Gao, J.; Xu, C.: Synthesis of Zeolite Beta from Kaolin and Its Catalytic Performance For FCC Naphtha Aromatization. *Energy & Fuels* **2009**, *23*, 60-64.
- (106) Maheswari, R.; Pachamuthu, M. P.; Anand, R.: Copper Containing TUD-1: Synthesis, Characterization and Catalytic Behavior in Liquid-Phase Oxidation of Ethylbenzene. *J Porous Mater* **2012**, *19*, 103-110.
- (107) Hajjar, R.; Millot, Y.; Man, P. P.; Che, M.; Dzwigaj, S.: Two Kinds of Framework Al Sites Studied in BEA Zeolite by X-ray Diffraction, Fourier Transform Infrared Spectroscopy, NMR Techniques, and V Probe. *Journal of Physical Chemistry C* **2008**, *112*, 20167-20175.
- (108) Viswanadham, N.; Kamble, R.; Saxena, S. K.; Garg, M. O.: Studies on Octane Boosting of Industrial Feedstocks on Pt/H-BEA Zeolite. *Fuel* **2008**, *87*, 2394-2400.
- (109) Li, Y.; Chung, T.-S.: Exploratory Development of Dual-Layer Carbon-Zeolite Nanocomposite Hollow Fiber Membranes With High Performance for Oxygen Enrichment and Natural Gas Separation. *Microporous and Mesoporous Materials* **2008**, *113*, 315-324.
- (110) Li, X.; Zhang, W.; Liu, S.; Xu, L.; Han, X.; Bao, X.: Olefin Metathesis over Heterogeneous Catalysts: Interfacial Interaction Between Mo Species and a H-Beta-Al₂O₃ composite support. *Journal of Physical Chemistry C* **2008**, *112*, 5955-5960.
- (111) Pacula, A.; Mokaya, R.: Synthesis and High Hydrogen Storage Capacity of Zeolite-Like Carbons Nanocast Using as-Synthesized Zeolite Templates. *Journal of Physical Chemistry C* **2008**, *112*, 2764-2769.
- (112) Zhang, Y.; Wang, Y.; Bu, Y.: Vapor Phase Beckmann Rearrangement of Cyclohexanone Oxime on H-Beta Zeolites Treated by Ammonia. *Microporous and Mesoporous Materials* **2008**, *107*, 247-251.
- (113) Zhang, X.; Zhong, J.; Wang, J.; Gao, J.; Liu, A.: Trimerization of Butene over Ni-doped Zeolite Catalyst: Effect of Textural and Acidic Properties. *Catalysis Letters* **2008**, *126*, 388-395.
- (114) Aguadoa, J.; Serrano, D. P.; Rodriguez, J. M.: Zeolite Beta With Hierarchical Porosity Prepared From Organofunctionalized Seeds. *Microporous and Mesoporous Materials* **2008**, *115*, 504-513.
- (115) Ordonsky, V. V.; Murzin, V. Y.; Monakhova, Y. V.; Zubavichus, Y. V.; Knyazeva, E. E.; Nesterenko, N. S.; Ivanova, I. I.: Oature, Strength and Accessibility of Acid Sites in Micro/Mesoporous Catalysts Obtained by Recrystallization of Zeolite BEA. *Microporous and Mesoporous Materials* **2007**, *105*, 101-110.
- (116) Ding, L.; Zheng, Y.; Hong, Y.; Ring, Z.: Effect of Particle Size on the Hydrothermal Stability of Zeolite Beta. *Microporous and Mesoporous Materials* **2007**, *101*, 432-439.
- (117) Tosheva, L.; Valtchev, V. P.; Mihailova, B.; Doyle, A. M.: Zeolite Beta Films Prepared Via the Langmuir-Blodgett Technique. *Journal of Physical Chemistry C* **2007**, *111*, 12052-12057.

- (118) Li, X.; Zhang, W.; Liu, S.; Xu, L.; Han, X.; Bao, X.: The Role of Alumina in the Supported Mo/HBeta-Al₂O₃ Catalyst for Olefin Metathesis: A high-Resolution Solid-State NMR and Electron Microscopy Study. *Journal of Catalysis* **2007**, *250*, 55-66.
- (119) Penkova, A.; Dzwigaj, S.; Kefirov, R.; Hadjiivanov, K.; Che, M.: Effect of the Preparation Method on the State of Nickel Ions in BEA Zeolites. A study by Fourier Transform Infrared Spectroscopy of Adsorbed CO and NO, Temperature-Programmed Reduction, and X-ray Diffraction. *Journal of Physical Chemistry C* **2007**, *111*, 8623-8631.
- (120) Zarama, M. C. P.; Rios, J. S. V.; Alba, M. D.; Castro, M. A.: Contribution to the Hydrothermal Synthesis of Zeolite Beta and its Modifications with Gallium. *J Porous Mater* **2007**, *14*, 239-242.
- (121) Sun, J.; Zhu, G.; Chen, Y.; Li, J.; Wang, L.; Peng, Y.; Li, H.; Qiu, S.: Synthesis, Surface and Crystal Structure Investigation of the Large Zeolite Beta Crystal. *Microporous and Mesoporous Materials* **2007**, *102*, 242-248.
- (122) Kadgaonkar, M. D.; Kasture, M. W.; Bhange, D. S.; Joshi, P. N.; Ramaswamy, V.; Kumar, R.: NCL-7, A Novel All Silica Analog of Polymorph B Rich Member of BEA Family: Synthesis and Characterization. *Microporous and Mesoporous Materials* **2007**, *101*, 108-114.
- (123) Yang, Z.; Xia, Y.; Mokaya, R.: Enhanced Hydrogen Storage Capacity of High Surface Area Zeolite-Like Carbon Materials. *Journal of the American Chemical Society* **2007**, *129*, 1673-1679.
- (124) Bregolato, M.; Bolis, V.; Busco, C.; Ugliengo, P.; Bordiga, S.; Cavani, F.; Ballarini, N.; Maselli, L.; Passeri, S.; Rossetti, I.; Forni, L.: Methylation of Phenol Over High-Silica Beta Zeolite: Effect of Zeolite Acidity and Crystal Size on Catalyst Behaviour. *Journal of Catalysis* **2007**, *245*, 285-300.
- (125) Mihalyi, R. M.; Pal-Borbely, G.; Beyer, H. K.; Szegedi, A.; Koranyi, T. I.: Characterization of Aluminum and Boron Containing Beta Zeolites Prepared By Solid-State Recrystallization of Magadlite. *Microporous and Mesoporous Materials* **2007**, *98*, 132-142.
- (126) Kang, S.; Gong, Y.; Dou, T.; Zhang, Y.; Zheng, Y.: Preparation and Characterization of Zeolite Beta With Low SiO₂/Al₂O₃ ratio. *Petroleum Science* **2007**, *4*, 70-74.
- (127) Malki, E.-M. E.; Massiani, P.; Che, M.: Introduction of Vanadium Species in Beta Zeolite by Solid-State Reaction: Spectroscopic Study of V Speciation and Molecular Mechanism. *Research on Chemical Intermediates* **2007**, *33*, 749-774.
- (128) Agullo, J.; Kumar, N.; Berenguer, D.; Kubicka, D.; Marcilla, A.; Gomez, A.; Salmi, T.; Murzin, D. Y.: Catalytic Pyrolysis of Low Density Polyethylene Over H-Beta, H-Y, H-Mordenite, and H-Ferrierite Zeolite Catalysts: Influence of Acidity and Structures. *Kinetics and Catalysis* **2007**, *48*, 535-540.
- (129) Kumaran, G. M.; Garg, S.; Soni, K.; Prasad, V. V. D. N.; Sharma, L. D.; Dhar, G. M.: Catalytic Functionalities of H-Beta Zeolite-Supported Molybdenum Hydrotreating Catalysts. *Energy & Fuels* **2006**, *20*, 1784-1790.
- (130) Ding, L.; Zheng, Y.; Zhang, Z.; Ring, Z.; Chen, J.: Effect of Agitation on the Synthesis of Zeolite Beta and its Synthesis Mechanism in Absence of Alkali Cations. *Microporous and Mesoporous Materials* **2006**, *94*, 1-8.
- (131) Anandan, S.; Vinu, A.; Venkatchalam, N.; Arabindoo, B.; Murugesan, V.: Photocatalytic Activity of ZnO Impregnated H-Beta and Mechanical Mix of ZnO/H-Beta in the Degradation of Monocrotophos in Aqueous Solution. *Journal of Molecular Catalysis A-Chemical* **2006**, *256*, 312-320.
- (132) Bordoloi, A.; Devassy, B. M.; Niphadkar, P. S.; Joshi, P. N.; Halligudi, S. B.: Shape Selective Synthesis of Long-Chain Linear Alkyl Benzene (LAB) With Al-MCM-41/Beta Zeolite Composite Catalyst. *Journal of Molecular Catalysis A-Chemical* **2006**, *253*, 239-244.
- (133) Dzwigaj, S.; Che, M.: Incorporation of Co(II) in Dealuminated BEA Zeolite at Lattice Tetrahedral Sites Evidenced by XRD, FTIR, Diffuse Reflectance UV-vis, EPR, and TPR. *Journal of Physical Chemistry B* **2006**, *110*, 12490-12493.
- (134) Fojtíková, P. P.; Mintova, S.; Čejka, J.; Žilková, N.; Zúkal, A.: Porosity of micro/mesoporous composites. *Microporous and Mesoporous Materials* **2006**, *92*, 154-160.
- (135) Li, X. J.; Zhang, W. P.; Liu, S. L.; Han, X. W.; Xu, L. Y.; Bao, X. H.: A High-Resolution MAS NMR Study on the Potential Catalysts Mo/H-Beta for Olefin Metathesis: The Interaction of Mo Species With H-Beta Zeolite. *Journal of Molecular Catalysis A-Chemical* **2006**, *250*, 94-99.
- (136) Saravanamurugan, S.; Palanichamy, M.; Hartmann, M.; Murugesan, V.: Knoevenagel Condensation Over Beta and Y Zeolites in Liquid Phase Under Solvent Free Conditions. *Applied Catalysis A-General* **2006**, *298*, 8-15.

- (137) Narasimharao, K.; Hartmann, M.; Thiel, H. H.; Ernst, S.: Novel Solid Basic Catalysts by Nitridation of Zeolite Beta at Low Temperature. *Microporous and Mesoporous Materials* **2006**, *90*, 377-383.
- (138) Tosheva, L.; Hölzl, M.; Metzger, T. H.; Valtchev, V.; Mintova, S.; Bein, T.: Zeolite Beta films Synthesized From Basic and Near-Neutral Precursor Solutions and Gels. *Materials Science & Engineering C-Biomimetic and Supramolecular Systems* **2005**, *25*, 570-576.
- (139) Panpranot, J.; Toophorm, U.; Prasertthdam, P.: Effect of Particle Size on the Hydrothermal Stability and Catalytic Activity of Polycrystalline Beta Zeolite. *J Porous Mater* **2005**, *12*, 293-299.
- (140) Pergher, S. B. C.; Oliveira, L. C. A.; Smaniotto, A.; Petkowicz, D. I.: Magnetic Zeolites for Removal of Metals in Water. *Química Nova* **2005**, *28*, 751-755.
- (141) Zheng, Y.; Wang, X. X.; Li, Z. H.; Fu, X. Z.; Wei, K. M.: Study of the Reaction of Tetramethyltin With H-Beta Zeolite. *Journal of Organometallic Chemistry* **2005**, *690*, 3187-3192.
- (142) Naydenov, V.; Tosheva, L.; Sterte, J.: Self-Bonded Zeolite Beta/MCM-41 Composite Spheres. *J Porous Mater* **2005**, *12*, 193-199.
- (143) Holmberg, B. A.; Hwang, S. J.; Davis, M. E.; Yan, Y. S.: Synthesis and Proton Conductivity of Sulfonic Acid Functionalized Zeolite BEA Nanocrystals. *Microporous and Mesoporous Materials* **2005**, *80*, 347-356.
- (144) Zhang, Y. J.; Wang, Y. Q.; Bu, Y. F.; Mi, Z. T.; Wu, W.; Min, E.; Han, S.; Fu, S. B.: Beckmann Rearrangement of Cyclohexanone Oxime Over H-Beta Zeolite and H-Beta Zeolite-Supported Boride. *Catalysis Communications* **2005**, *6*, 53-56.
- (145) Markus, H.; Arvela, P. M.; Kumar, N.; Heikkilä, T.; Lehto, V. P.; Sjöholm, R.; Holmbom, B.; Salmi, T.; Murzin, D. Y.: Reactions of Hydroxymatairesinol Over Supported Palladium Catalysts. *Journal of Catalysis* **2006**, *238*, 301-308.
- (146) Kasture, M. W.; Niphadkar, P. S.; Sharanappa, N.; Mirajkar, S. R.; Bokade, V. V.; Joshi, P. N.: Isopropylation of Benzene Catalyzed by H-Beta Zeolite Catalysts With Different Crystallinities. *Journal of Catalysis* **2004**, *227*, 375-383.
- (147) Gautier, B.; Smaïhi, M.: Template Extraction From Surface Functionalised Zeolite Beta Nanoparticles. *New Journal of Chemistry* **2004**, *28*, 457-461.
- (148) Adebajo, M. O.; Long, M. A.; Frost, R. L.: Spectroscopic and XRD Characterisation of Zeolite Catalysts Active for the Oxidative Methylation of Benzene With Methane. *Spectrochimica Acta Part a-Molecular and Biomolecular Spectroscopy* **2004**, *60*, 791-799.
- (149) Nakao, R.; Kubota, Y.; Katada, N.; Nishiyama, N.; Kunimori, K.; Tomishige, K.: Performance and Characterization of BEA Catalysts for Catalytic Cracking. *Applied Catalysis A-General* **2004**, *273*, 63-73.
- (150) Omegna, A.; Vasic, M.; Bokhoven, J. A. v.; Pirngruber, G.; Prins, R.: Dealumination and Realumination of Microcrystalline Zeolite Beta: an XRD, FTIR and Quantitative Multinuclear (MQ) MAS NMR Study. *Physical Chemistry Chemical Physics* **2004**, *6*, 447-452.
- (151) Prokešová, P.; Mintova, S.; Čejka, J.; Bein, T.: Preparation of Nanosized Micro/Mesoporous Composites. *Materials Science & Engineering C-Biomimetic and Supramolecular Systems* **2003**, *23*, 1001-1005.
- (152) Oliveira, A. M. d.; Pergher, S. B. C.; Moro, C. C.; Baibich, I. M.: Nitric Oxide Decomposition on Copper Supported on Zeolites. *Química Nova* **2004**, *27*, 226-230.
- (153) Prokešová, P.; Mintova, S.; Čejka, J.; Bein, T.: Preparation of Nanosized Micro/Mesoporous Composites via Simultaneous Synthesis of Beta/MCM-48 Phases. *Microporous and Mesoporous Materials* **2003**, *64*, 165-174.
- (154) Xia, Q. H.; Shen, S. C.; Song, J.; Kawi, S.; Hidajat, K.: Structure, Morphology, and Catalytic Activity of Beta Zeolite Synthesized in a Fluoride Medium for Asymmetric Hydrogenation. *Journal of Catalysis* **2003**, *219*, 74-84.
- (155) Oumi, Y.; Nemoto, S.; Nawata, S.; Fukushima, T.; Teranishi, T.; Sano, T.: Effect of the Framework Structure on the Dealumination-Realumination Behavior of Zeolite. *Materials Chemistry and Physics* **2002**, *78*, 551-557.
- (156) Nares, R.; Ramirez, J.; Alexandre, A. G.; Louis, C.; Klimova, T.: Ni/H-Beta Zeolite Catalysts Prepared by Deposition-Precipitation. *Journal of Physical Chemistry B* **2002**, *106*, 13287-13293.
- (157) Shi, Y. F.; Gao, Y.; Yuan, W. K.: Some Characterization of Beta Zeolite for Alkylation of Benzene in Near Critical. *Catalysis Today* **2002**, *74*, 91-100.

- (158) Assabumrungrat, S.; Kiatkittipong, W.; Seviton, N.; Praserttham, P.; Goto, S.: Kinetics of Liquid Phase Synthesis of Ethyl tert-Butyl Ether from tert-Butyl Alcohol and Ethanol Catalyzed by Beta Zeolite Supported on Monolith. *International Journal of Chemical Kinetics* **2002**, *34*, 292-299.
- (159) Roberge, D. M.; Hausmann, H.; Holderich, W. F.: Dealumination of Zeolite Beta by Acid Leaching: A New Insight With Two-Dimensional Multi-Quantum and Cross Polarization ^{27}Al MAS NMR. *Physical Chemistry Chemical Physics* **2002**, *4*, 3128-3135.
- (160) Naydenov, V.; Tosheva, L.; Sterte, J.: Palladium-Containing Zeolite Beta Macrostructures Prepared by Resin Macrotemplating. *Chemistry of Materials* **2002**, *14*, 4881-4885.
- (161) Oumi, Y.; Mizuno, R.; Azuma, K.; Nawata, S.; Fukushima, T.; Uozumi, T.; Sano, T.: Reversibility of Dealumination-Realumination Process of BEA Zeolite. *Microporous and Mesoporous Materials* **2001**, *49*, 103-109.
- (162) Schoeman, B. J.; Babouchkina, E.; Mintova, S.; Valtchev, V. P.; Sterte, J.: The Synthesis of Discrete Colloidal Crystals of Zeolite Beta and Their Application in the Preparation of Thin Microporous Films. *J Porous Mater* **2001**, *8*, 13-22.
- (163) Tosheva, L.; Mihailova, B.; Valtchev, V.; Sterte, J.: Zeolite Beta Spheres. *Microporous and Mesoporous Materials* **2001**, *48*, 31-37.
- (164) Dzwigaj, S.; Massiani, P.; Davidson, A.; Che, M.: Role of Silanol Groups in the Incorporation of V in Beta Zeolite. *Journal of Molecular Catalysis A-Chemical* **2000**, *155*, 169-182.
- (165) Yang, C.; Xu, Q. H.; Hu, C.: Boronation and Galliation of Zeolites Beta in an Alkaline Medium. *Materials Chemistry and Physics* **2000**, *63*, 55-66.
- (166) Schmidt, I.; Madsen, C.; Jacobsen, C. J. H.: Confined Space synthesis. A Novel Route to Nanosized Zeolites. *Inorganic Chemistry* **2000**, *39*, 2279-2283.
- (167) Ramirez, S.; Dominguez, J. M.; Viniegra, M.; Menorval, L. C. d.: Specific Behavior of Beta Zeolites Upon the Modification of the Surface Acidity by Cs and Li Exchange. *New Journal of Chemistry* **2000**, *24*, 99-104.
- (168) Trombetta, M.; Busca, G.; Storaro, L.; Lenarda, M.; Casagrande, M.; Zambon, A.: Surface Acidity Modifications Induced by Thermal Treatments and Acid Leaching on Microcrystalline H-BEA Zeolite. A FTIR, XRD and MAS-NMR Study. *Physical Chemistry Chemical Physics* **2000**, *2*, 3529-3537.
- (169) Raksh, B.; Ramaswamy, V.; Ramaswamy, A. V.: Acidity and m-Xylene Isomerization Activity of Large Pore, Zirconium Containing Alumino-Silicate With BEA Structure. *Journal of Catalysis* **1999**, *188*, 252-260.
- (170) Cambor, M. A.; Corma, A.; Valencia, S.: Characterization of Nanocrystalline Zeolite Beta. *Microporous and Mesoporous Materials* **1998**, *25*, 59-74.
- (171) Jia, C. J.; Beaunier, P.; Massiani, P.: Comparison of Conventional and Solid-State Ion Exchange Procedures for the Incorporation of Lanthanum in H-Beta Zeolite. *Microporous and Mesoporous Materials* **1998**, *24*, 69-82.
- (172) Lee, Y. K.; Park, S. H.; Rhee, H. K.: Transalkylation of Toluene and 1,2,4-Trimethylbenzene Over Large Pore Zeolites. *Catalysis Today* **1998**, *44*, 223-233.
- (173) Cambor, M. A.; Corma, A.; Valencia, S.: Synthesis in Fluoride Media and Characterisation of Aluminosilicate Zeolite Beta. *Journal of Materials Chemistry* **1998**, *8*, 2137-2145.
- (174) Lohse, U.; Altrichter, B.; Donath, R.; Fricke, R.; Jancke, K.; Parlit, B.; Schreier, E.: Synthesis of Zeolite Beta .1. Using Tetraethylammonium Hydroxide Bromide With Addition of Chelates as Templating Agents. *Journal of the Chemical Society-Faraday Transactions* **1996**, *92*, 159-165.
- (175) Yang, C.; Xu, Q. H.: Aluminated Zeolites Beta and Their Properties .1. Almination of Zeolites Beta. *Journal of the Chemical Society-Faraday Transactions* **1997**, *93*, 1675-1680.
- (176) Chien, S. H.; Ho, J. C.; Mon, S. S.: Hydrothermal Synthesis and Characterization of the Vanadium Containing Zeolite Beta. *Zeolites* **1997**, *18*, 182-187.
- (177) Borade, R. B.; Clearfield, A.: Preparation of Aluminum Rich Beta Zeolite. *Microporous Materials* **1996**, *5*, 289-297.
- (178) Jia, C.; Massiani, P.; Barthomeuf, D.: Characterization by Infrared and Nuclear Magnetic Resonance Spectroscopies of Calcined Beta Zeolite. *Journal of the Chemical Society-Faraday Transactions* **1993**, *89*, 3659-3665.
- (179) Zhang, D.; Duan, A.; Zhao, Z.; Wang, X.; Jiang, G.; Liu, J.; Wang, C.; Jin, M.: Synthesis, Characterization and Catalytic Performance of Meso/Microporous Material Beta-SBA-15-Supported Ni-Mo Catalysts for Hydrodesulfurization of Dibenzothiophene. *Catalysis Today* **2011**, *175*, 477-484.

- (180) Shan, Z.; Zhou, W.; Jansen, J. C.; Yeh, C. Y.; Koegler, J. H.; Maschmeyer, T.: Incorporation of Nano-Sized Zeolites Into a Mesoporous Matrix, TUD-1. In *Nanoporous Materials iii*; Sayari, A., Jaroniec, M., Eds., 2002; Vol. 141; pp 635-640.
- (181) Dzwigaj, S.; Shishido, T.: State of Chromium in CrSiBEA Zeolite Prepared by the Two-Step Postsynthesis Method: XRD, FTIR, UV-Vis, EPR, TPR, and XAS Studies. *The Journal of Physical Chemistry C* **2008**, *112*, 5803-5809.
- (182) Hadjiivanov, K.; Penkova, A.; Kefirov, R.; Dzwigaj, S.; Che, M.: Influence of Dealumination and Treatments on the Chromium Speciation in Zeolite CrBEA. *Microporous and Mesoporous Materials* **2009**, *124*, 59-69.
- (183) Zuhairi, A. A.; Zailani, M. A. B.; Bhatia, S.: Comparative Study of the Deactivation of Cr-BEA, Cr-MOR and Cr-ZSM-5 in Catalytic Decomposition of VOC. *Reaction Kinetics and Catalysis Letters* **2003**, *79*, 143-148.
- (184) Shan, Z.; Jansen, J. C.; Marchese, L.; Maschmeyer, T.: Synthesis, Characterization and Catalytic Testing of a 3-D Mesoporous Titanosilica, Ti-TUD-1. *Microporous and Mesoporous Materials* **2001**, *48*, 181-187.
- (185) Quek, X.-Y.; Tang, Q.; Hu, S.; Yang, Y.: Liquid Phase Trans-Stilbene Epoxidation Over Catalytically Active Cobalt Substituted TUD-1 Mesoporous Materials (Co-TUD-1) Using Molecular Oxygen. *Applied Catalysis A: General* **2009**, *361*, 130-136.
- (186) Guo, Z.; Zhou, C.; Hu, S.; Chen, Y.; Jia, X.; Lau, R.; Yang, Y.: Epoxidation of trans-Stilbene and cis-Cyclooctene Over Mesoporous Vanadium Catalysts: Support Composition and Pore Structure Effect. *Applied Catalysis A: General* **2012**, *419-420*, 194-202.
- (187) Mandal, S.; SinhaMahapatra, A.; Rakesh, B.; Kumar, R.; Panda, A.; Chowdhury, B.: Synthesis, Characterization of Ga-TUD-1 Catalyst and its Activity Towards Styrene Epoxidation Reaction. *Catalysis Communications* **2011**, *12*, 734-738.
- (188) Zhou, J.; Hua, Z.; Shi, J.; He, Q.; Guo, L.; Ruan, M.: Synthesis of a Hierarchical Micro/Mesoporous Structure by Steam-Assisted Post-Crystallization. *Chemistry – A European Journal* **2009**, *15*, 12949-12954.
- (189) Blin, J. L.; Léonard, A.; Su, B. L.: Well-Ordered Spherical Mesoporous Materials CMI-1 Synthesized via an Assembly of Decaoxyethylene Cetyl ether and TMOS. *Chemistry of Materials* **2001**, *13*, 3542-3553.
- (190) Hu, S.; Liu, D.; Li, L.; Guo, Z.; Chen, Y.; Borgna, A.; Yang, Y.: Highly Selective 1-Heptene Isomerization over Vanadium Grafted Mesoporous Molecular Sieve Catalysts. *Chemical Engineering Journal* **2010**, *165*, 916-923.
- (191) Li, L.; Koranyi, T. I.; Sels, B. F.; Pescarmona, P. P.: Highly-Efficient Conversion of Glycerol to Solketal Over Heterogeneous Lewis Acid Catalysts. *Green Chemistry* **2012**, *14*, 1611-1619.
- (192) Ramanathan, A.; Archipov, T.; Maheswari, R.; Hanefeld, U.; Roduner, E.; Glaser, R.: Synthesis, Characterization and Catalytic Properties of the Novel Manganese-Containing Amorphous Mesoporous Material MnTUD-1. *The Journal of Physical Chemistry C* **2008**, *112*, 7468-7476.
- (193) Maheswari, R.; Anand, R.; Imran, G.: MnTUD-1: Synthesis, Characterization and Catalytic Behavior in Liquid-Phase Oxidation of Cyclohexane. *J Porous Mater* **2012**, *19*, 283-288.
- (194) Tušar, N. N.; Ristić, A.; Cecowski, S.; Arčon, I.; Lázár, K.; Amenitsch, H.; Kaučič, V.: Local Environment of Isolated Iron in Mesoporous Silicate Catalyst FeTUD-1. *Microporous and Mesoporous Materials* **2007**, *104*, 289-295.
- (195) Tanglumlert, W.; Yang, S.-T.; Jeong, K.-E.; Jeong, S.-Y.; Ahn, W.-S.: Facile Synthesis of Ti-TUD-1 for Catalytic Oxidative Desulfurization of Model Sulfur Compounds. *Research on Chemical Intermediates* **2011**, *37*, 1267-1273.
- (196) Sangwichien, C.; Aranovich, G. L.; Donohue, M. D.: Density Functional Theory Predictions of Adsorption Isotherms With Hysteresis Loops. *Colloids and Surfaces A-Physicochemical and Engineering Aspects* **2002**, *206*, 313-320.
- (197) Sing, K. S. W.: Characterization of Adsorbents. In *Adsorption, Science and Technology*; Rodrigues, A. E., Levan, M. D., Tondeur, D., Eds.; Kluwer Academic Publishers: Dordrecht, the Netherlands, 1989; Vol. 158 pp 3-14.
- (198) Gregg, S. J.; Sing, K. S. W.: *Adsorption, Surface Area, and Porosity*; 2nd ed.; Academic Press: London, 1982.

- (199) Burgess, C. G. V.; Everett, D. H.; Nuttall, S.: Adsorption Hysteresis in Porous Materials. *Pure and Applied Chemistry* **1989**, *61*, 1845-1852.
- (200) Rouquerol, F.; Avnir, D.; Fairbridge, C. W.; Everett, D. H.; Haynes, J. H.; Pernicone, N.; Ramsay, J. D. F.; Sing, K. S. W.; Under, K. K.: Recommendations for the Characterization of Porous Solids. *Pure and Applied Chemistry* **1994**, *66*, 1739-1758.
- (201) Rouquerol, F.; Rouquerol, J.; Sing, K.: *Adsorption by Powders and Porous Solids: Principles, Methodology and Applications*; Academic Press: San Diego, USA, 1998.
- (202) Sing, K. S. W.; Everett, D. H.; Haul, R. A. W.; Moscou, L.; Pierotti, R. A.; Rouquerol, J.; Siemieniewska, T.: Reporting Physisorption Data for Gas Solid Systems With Special Reference to the Determination of Surface Area and Porosity (Recommendations 1984). *Pure and Applied Chemistry* **1985**, *57*, 603-619.
- (203) Weckhuysen, B. M.; Schoonheydt, R. A.; Jehng, J. M.; Wachs, I. E.; Cho, S. J.; Ryoo, R.; Kijlstra, S.; Poels, E.: Combined DRS-RS-EXAFS-XANES-TRP Study of Supported Chromium Catalysts. *Journal of the Chemical Society-Faraday Transactions* **1995**, *91*, 3245-3253.
- (204) Weckhuysen, B. M.; Wachs, I. E.; Schoonheydt, R. A.: Surface Chemistry and Spectroscopy of Chromium in Inorganic Oxides. *Chemical Reviews* **1996**, *96*, 3327-3349.
- (205) Yuvaraj, S.; Palanichamy, M.; Krishnasamy, V.: Chromium Substitution in a Large-Pore High-Silica Zeolite BEA: Synthesis, Characterisation and Catalytic Activity. *Chemical Communications* **1996**, 2707-2708.
- (206) Binder, J. B.; Raines, R. T.: Simple Chemical Transformation of Lignocellulosic Biomass into Furans for Fuels and Chemicals. *Journal of the American Chemical Society* **2009**, *131*, 1979-1985.
- (207) Qi, X.; Watanabe, M.; Aida, T. M.; Smith, R. L., Jr.: Fast Transformation of Glucose and Di-/Polysaccharides into 5-Hydroxymethylfurfural by Microwave Heating in an Ionic Liquid/Catalyst System. *ChemSusChem* **2010**, *3*, 1071-1077.
- (208) Pidko, E. A.; Degirmenci, V.; Santen, R. A. V.; Hensen, E. J. M.: Glucose Activation by Transient Cr²⁺ Dimers. *Angewandte Chemie-International Edition* **2010**, *49*, 2530-2534.

CHAPTER 10

Conclusions and outlook

Index

CHAPTER 10	399
Conclusions and outlook	399
10.1. Conclusions	401
10.2. References.....	409

10.1. Conclusions

In the face of the declining petroleum resources and rising oil prices it is necessary to develop alternative ways to fulfill the energy needs of our industrialised society. Much research is being done exploring non-fossil carbon energy sources, such as renewable biomass. Especially the processing of plant biomass-derived carbohydrates (preferably non-edible) into added-value products seems to be at the core of the biorefinery concept. Saccharides constitute the bulk of carbohydrates and can be converted to platform chemicals such as 2-furaldehyde (Fur) or 5-hydroxymethyl-2-furaldehyde (Hmf) with wide application profiles, useful in different sectors of the chemical industry.

Fur has been produced on an industrial scale for decades (world production of ca. 250 000-300 000 ton.year⁻¹ in 2005¹⁻³ and continued until 2011)^{4,5} from biomass rich in pentosans (e.g., forest/agriculture wastes/surpluses). The hydrolysis of pentosans gives pentoses (mainly xylose, Xyl), and the latter is dehydrated into Fur. Hmf is obtained in a similar fashion from hexose-based carbohydrates, although it has not reached industrial scale production. Most industrial processes of Fur production use water as solvent, a reaction temperature in the range of 150-200 °C, and employ mineral acids as catalysts, commonly sulfuric acid. Liquid acids lead to equipment corrosion hazards and safety problems, difficult catalyst separation from the reaction products, and considerable waste disposal. For these reasons, the production of Fur is one of the industrial processes where the demand of green chemistry and technology for sustainability is stimulating the replacement of these “toxic liquid” acid catalysts by stable, recyclable, non-toxic solid acids.

In this work, solid acid catalysts as alternatives to liquid acids were investigated in the hydrolysis/dehydration of saccharides to Fur or Hmf in aqueous or ionic liquid medium, under batch mode. Porous solid acid catalysts such as zeolites have served well the petroleum-based industry, and hold promise as catalysts for these biomass conversion processes as they are relatively cheap and easily recyclable. The thermal stability of the catalyst is important due to the fact that the reaction temperatures are typically higher than 150 °C and, on the other hand, the catalyst coking phenomena are characteristically inherent to these reactions systems. Particular attention was drawn to porous inorganic oxides as solid acid catalysts due to the generally higher thermal stabilities in comparison to organic or hybrid solid acids.

The present work was divided into two major parts depending on the type of solvent used being water or an ionic liquid (IL). The choice of the solvent adds specific requirements to be put on the catalysts.

Water is the most attractive (“clean”, relatively cheap) solvent for the conversion of carbohydrate-containing biomass to furanic aldehydes. In this case, the hydrothermal stability of the catalyst is important to avoid structure collapse, leaching of the active phase into the liquid phase during the catalytic reaction and detrimental leveling-off of the acid strength by the water molecules. The tested porous inorganic oxides were crystalline or amorphous at the atomic level. Figure 10.1 summarises the type of micro/mesoporous solid acids investigated as catalysts in the aqueous phase conversion of saccharides to Fur/Hmf, and some of the catalytic best results are indicated: crystalline microporous silicoaluminophosphates (Chapter 3), Al-TUD-1 (Chapter 4), BEA and BEATUD-1 (Chapter 5), ITQ-2 (Chapter 6), and ZrW-MP and ZrWAl-MP (Chapter 7). The tested saccharides are indicated in Figure 10.2.

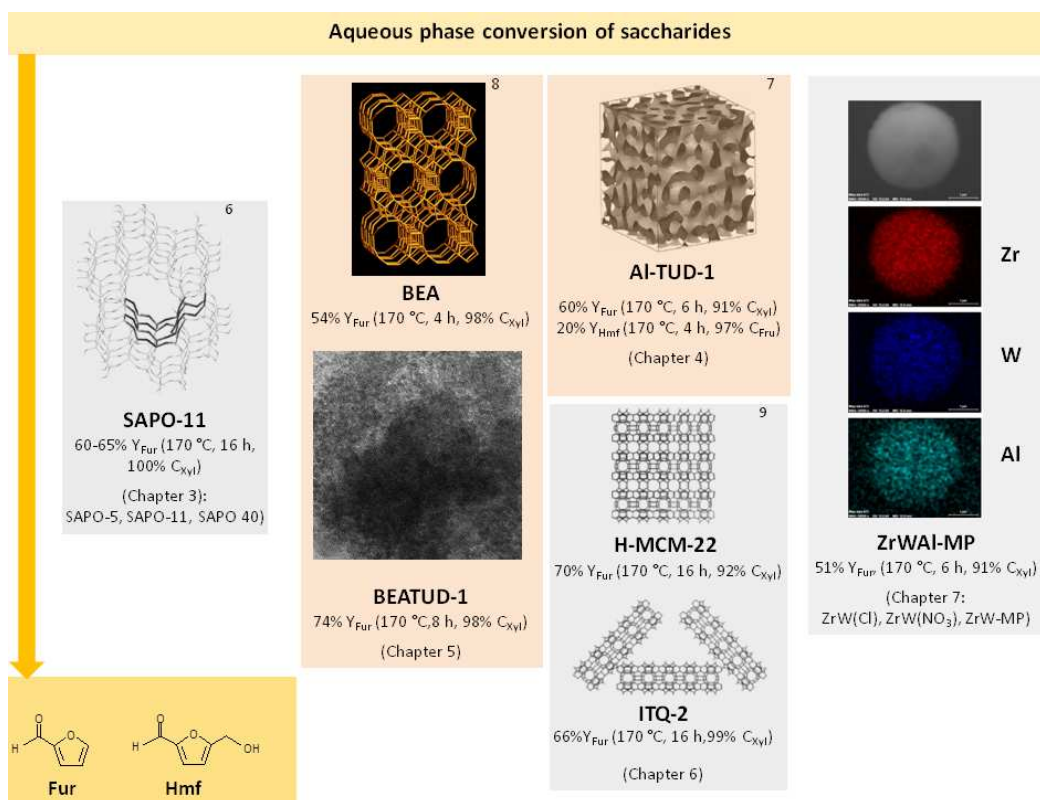


Figure 10.1- Solid acid catalysts tested in the hydrolysis/dehydration of saccharides into 2-furaldehyde (Fur) and 5-hydroxymethyl-2-furaldehyde (Hmf) in the aqueous phase. The structure images of SAPO-11, Al-TUD-1, BEA and H-MCM-22, and ITQ-2 were taken from refs ^{6,7,8} and ⁹ respectively.

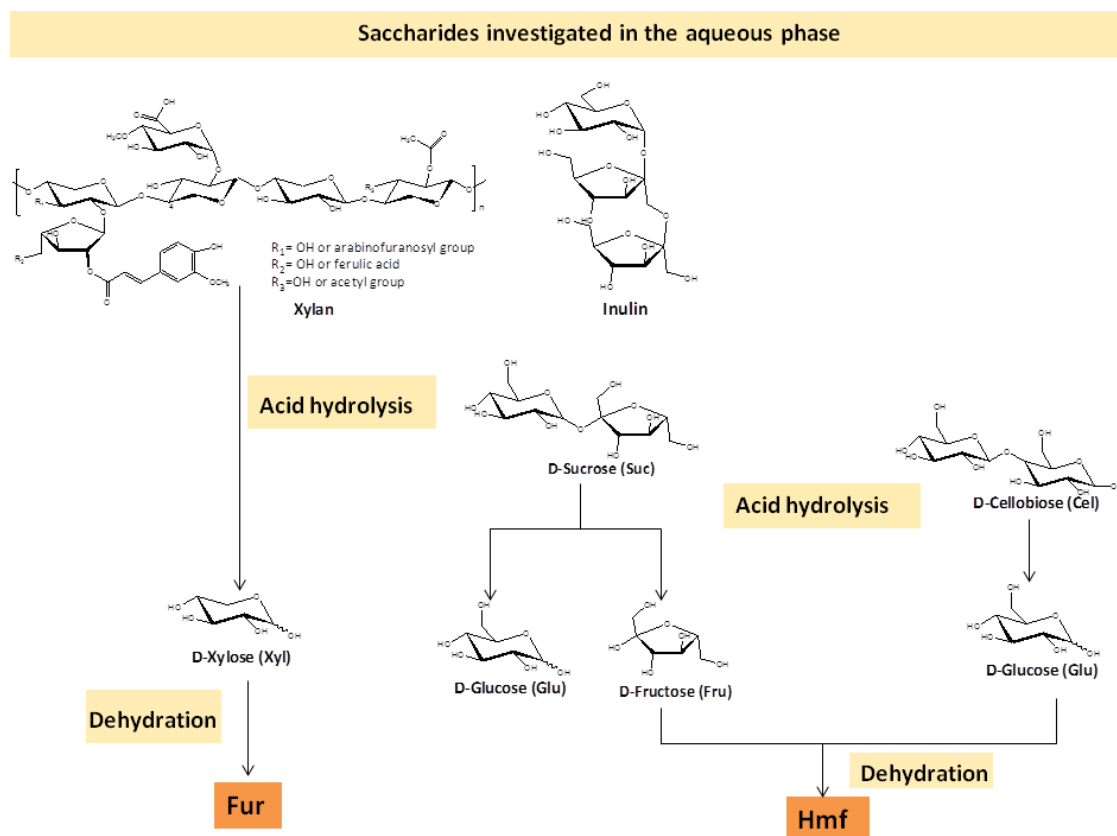


Figure 10.2- Saccharides investigated in the hydrolysis/dehydration of saccharides into 2-furaldehyde (Fur) and 5-hydroxymethyl-2-furaldehyde (Hmf) in the aqueous phase.

The tested solid acids exhibited high stability towards leaching, structure stability, and could be regenerated by thermal treatments in order to remove organic deposits, and reused giving similar Fur yields in consecutive batch runs. In general, the catalytic activity of the inorganic solid acids correlated well with the total amount (Brönsted plus Lewis) of acid sites measured using pyridine as base probe: e.g. for SAPO-11 (Chapter 3), BEA and BEATUD-1 (Chapter 5), H-MCM-22 and ITQ-2 (Chapter 6) and the modified zirconias (Chapter 7). It is preferable to restrict the correlations to a specific structure type, as discussed in Chapter 3. The type and strength of the acid sites can influence the product selectivity. Nevertheless, the textural properties of the porous inorganic oxides are important. The reactions of saccharides may be hindered in a microporous environment and catalyst deactivation by pore blockage may be relatively fast. The crystalline microporous silicoaluminophosphates possessing medium (SAPO-11) and large (SAPO-5 and SAPO-40) pores led to modest Fur yields and these were similar to that for zeolite H-Mordenite and superior to H_2SO_4 . Increasing the specific surface area and introducing

mesoporosity can enhance the amount of effective acid sites (e.g. Zr(W,Al) mixed oxides, Chapter 7) and/or reduce the amount of coke formed (e.g. BEA and BEATUD-1, Chapter 5). The catalyst synthetic approaches involved the use of an organic template for introducing mesoporosity and obtaining relatively narrow pore size distributions (Chapters 4, 5, 7), use of nanocrystalline zeolite and its embedment in a mesoporous silica matrix (Chapter 5), and delamination of the lamellar precursor Pre-MCM-22(P) (Chapter 6). It is worth noting that the investigated catalysts were mainly aluminosilicates. Aluminosilicates can be quite versatile with respect to the type of crystalline and porous structures (micro/mesopores; 1, 2 or 3 D pore systems), the acid properties and surface polarity (varying Si/Al ratio), and they may be prepared with particle/crystallite sizes down to the nano-scale.

Composite materials consisting of zeolite nanocrystals embedded in a mesoporous inorganic oxide matrix can minimise nanoscale-related drawbacks (high pressure drops or demanding separation techniques such as nanofiltration) and benefit from the advantageous catalytic properties associated with the zeolite nanocrystals. The catalytic performance of a composite catalyst consisting of H-Beta zeolite nanocrystals embedded in a TUD-1 type mesoporous inorganic oxide matrix tested in the dehydration of Xyl compared favourably with those of the (bulk) zeolite BEA and the physical mixture of BEA and silica TUD-1 (74% Y_{Fur} compared to 54% Y_{Fur} and 60% Y_{Fur} , respectively, Chapter 5).

Through delamination processes it was possible to prepare single crystalline sheets of zeolitic nature from lamellar precursors, allowing active sites to become accessible to the reagent molecules and avoid diffusion limitations and decrease the rates of the catalyst deactivation by coking. The delaminated solid ITQ-2 (Si/Al=24) possessed enhanced specific surface area and porosity compared with the lamellar precursor Pre-MCM-22(P). ITQ-2 and the zeolite counterpart H-MCM-22 were tested as catalysts in the reaction of Xyl, at 170 °C (Chapter 6); a Y_{Fur} of 71% was reached for H-MCM-22(24) and 66% for ITQ-2(24). While the delamination process considerably enhanced the external surface area of ITQ-2 in comparison to H-MCM-22, it caused modifications in the acid properties, leaving the two prepared materials (with the same Si/Al atomic ratio) on a comparable footing in terms of catalytic performance in the studied catalytic reaction. Despite their similar catalytic performances, ITQ-2(24) possessed lower amounts of insoluble organic matter, and may be advantageous in terms of energy requirements for thermal regeneration (550 °C for H-MCM-22(24) and 450 °C for ITQ-2(24)).

Mesoporous solid acid Al-TUD-1 (Si/Al=21) was tested in the reactions of mono/di/polysaccharides containing pentose or hexose units (Chapter 4). A maximum

monosaccharide yield of 31% and 59% was reached for sucrose (Suc) and cellobiose (Cel) as substrates, respectively. Al-TUD-1 was more effective in converting Xyl to Fur (60% Y_{Fur} in 6 h) than hexoses to Hmf (17-29% Y_{Hmf} in 6 h), which may be partly due to the acid properties (mainly Lewis acidity).

Further improvements in the catalytic performances of the investigated micro/mesoporous aluminosilicates may be possible by fine-tuning the textural and acid properties: the acid properties by changing the Si/Al ratio (which will also affect the catalyst surface polarity) or the amount of zeolite seeds in the cases of the composite catalysts, and the textural properties by varying the particle size ranges, the template of the mesoporous solid acids, or increasing the efficiency of the delamination procedures of the lamellar precursors (increasing extension of the delamination without destroying the acid sites). On the other hand, water as solvent can have a more detrimental effect on the catalytic reaction in the case of hexoses (Hmf is converted to organic acids).

Besides aluminosilicates and silicoaluminophosphates, zirconium-tungsten mixed oxides (Chapter 7) were investigated since they are fairly stable, versatile solid acid catalysts and some are commercially available. These types of materials were prepared by co-condensation without a templating agent (ZrW(X), in which X is related to the type of zirconium precursor) or by incipient wetness impregnation (ZrW-MP) with further doping of aluminium on ZrWAl-MP mesophases of zirconia (MP stands for mesoporous). The best results were obtained for ZrWAl-MP which led to 51% Y_{Fur} at 98% C_{Xyl} , attributed to the enhanced specific surface area and amount of accessible acid sites.

Attempts to characterise the soluble and insoluble organic by-products formed were made using TGA/DSC, FT-IR, liquid and solid state NMR techniques and GC×GC-ToFMS analyses. These studies aimed to provide mechanistic insights and identify undesired reaction pathways. Complex mixtures of soluble reaction products were obtained and the different types of side reactions may occur, such as fragmentation reactions of Xyl and condensation reactions.

The recognised high potential of Hmf as a bio-based platform chemical and the desire for its commercialisation led to an extensive study using IL-based catalytic systems with notable beneficial effects; the production of Fur and Hmf in high yields from saccharides has been made possible under relatively mild reaction conditions, using IL-based catalytic systems. With an IL-based system it is possible to suppress undesired reactions, such as the acid-hydrolysis of Hmf into formic and levulinic acids (the latter being quite difficult to separate from Hmf, increasing production costs), typically occurring in acidic aqueous solutions. Furthermore, ILs may enhance

the solubility of polysaccharides in the liquid medium. A summary of the saccharides investigated in the ionic liquid-based catalytic systems is given in Figure 10.3 and the IL systems tested in this work with some of the best catalytic results are given in Figure 10.4.

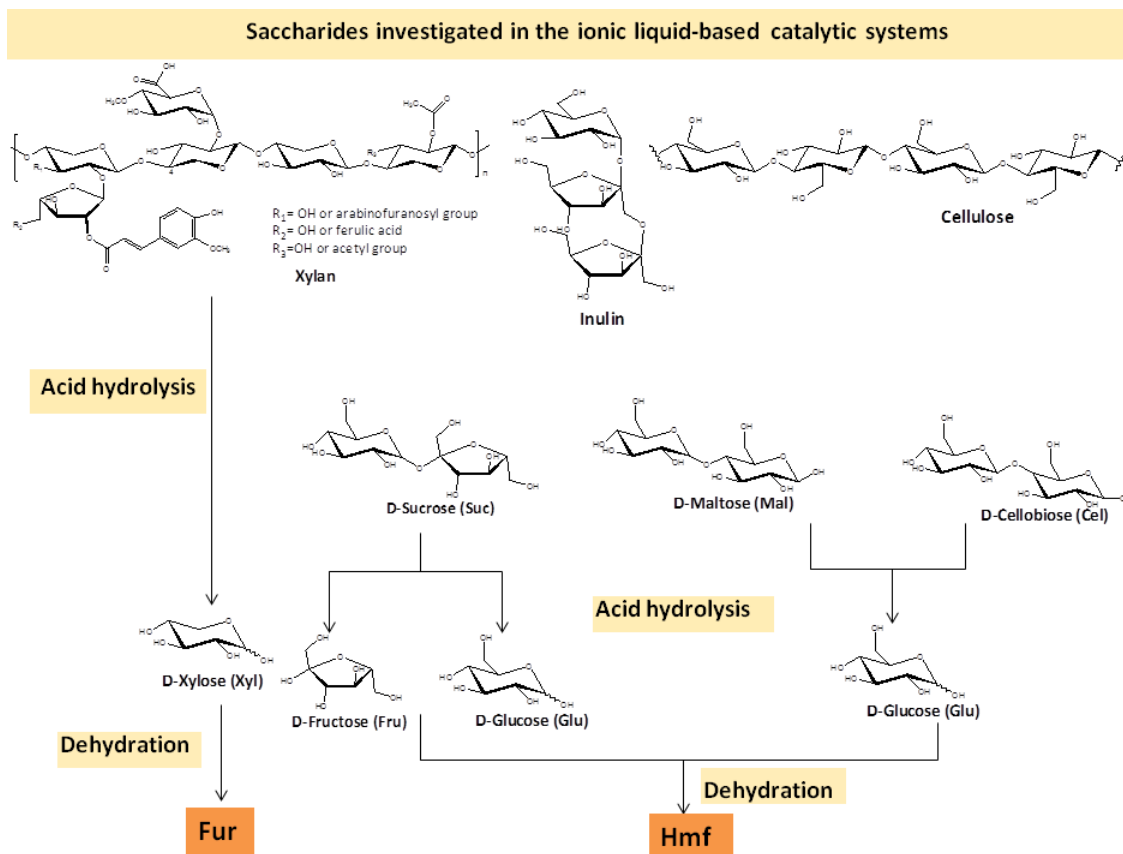


Figure 10.3- Saccharides investigated in the hydrolysis/dehydration of saccharides into 2-furaldehyde (Fur) and 5-hydroxymethyl-2-furaldehyde (Hmf) in the ionic liquid-based catalytic systems.

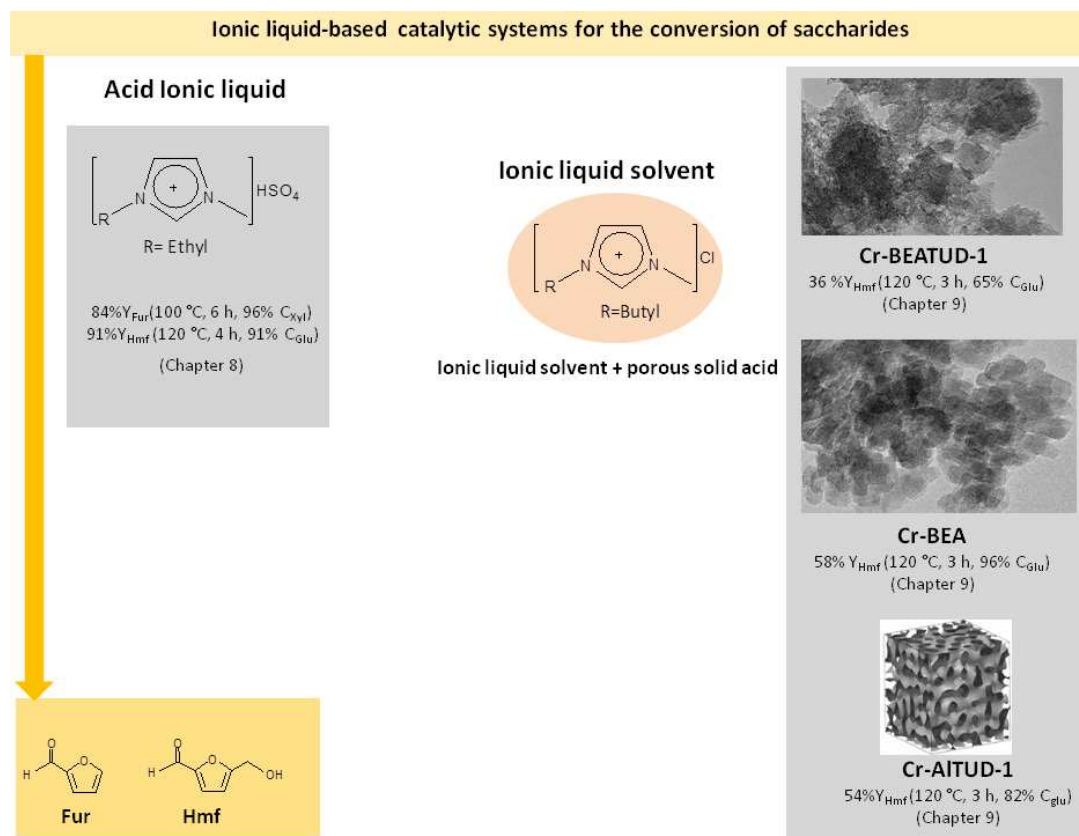


Figure 10.4- Ionic liquids tested in the hydrolysis/dehydration of saccharides into 2-furaldehyde (Fur) and 5-hydroxymethyl-2-furaldehyde (Hmf) in the ionic liquid-based catalytic systems for the conversion of saccharides: [Emim]HSO₄ as solvent and catalyst or added in catalytic amounts, and chromium containing micro/mesoporous materials coupled to [Bmim]Cl (Cr-AI-TUD-1, Cr-TUD-1, Cr-BEA, Cr-BEATUD-1).

In this work [Emim]HSO₄ was employed with dual catalyst-solvent function in the hydrolysis/dehydration of saccharides, and led to high Y_{Fur} and Y_{Hmf} (80-90%) from Xyl and Fru, respectively, under relatively mild conditions (100 °C, Chapter 8). [Emim]HSO₄ was recovered (using a relatively easy work-up procedure) and reused in subsequent cycles, and can substitute aqueous H₂SO₄ allowing process intensification with reuse of the catalytic IL phase. In contrast to that observed for the biphasic system, without an extracting solvent the Fur yield decreased with time (40%/28% after 4/6h). Removal of Fur by evaporation under reduced pressure (instead of solvent extraction) gave poorer results, although it should be possible to improve the Fur yields by optimising the control of the pressure in the system, the design of the setup, the mixing efficiency of the reaction mixture, the reaction temperature and residence time. In contrast to

aluminosilicates with water as solvent, [Emim]HSO₄ is effective in converting Fru (88% Y_{Hmf} at 30 min) and polymers containing these units into Hmf. However, [Emim]HSO₄ was poorly selective in Glu dehydration.

Attempts to find IL systems to improve the conversion of Glu (which is the major monosaccharide building block on Earth) to Hmf remains a challenge due to the more demanding reaction of Glu which has a complex reaction mechanism, involving a series of elementary steps with different acid-base properties requirements. ILs have been used as solvents coupled with many different types of catalysts, mainly homogeneous (Brønsted-type liquid mineral acids and Lewis-type metal salts), and to a much smaller extent, insoluble solid acids. One of the most effective catalytic systems to convert Glu into Hmf consists of chromium chloride salts dissolved in an imidazolium chloride IL as solvent. In this work, the dehydration of Glu using [Bmim]Cl as solvent and (Al,Cr)-silicates under mild reaction conditions was investigated (Chapter 9). The micro/mesoporous solid acids were all microstructurally stable with no detectable Al leaching. The chromium-containing solid acid/IL systems led to relatively high Y_{Hmf} (36-58%) compared to the catalysts without chromium (< 17% Y_{Hmf}). However, the chromium micro/mesoporous solid acids were unstable catalysts because the chromium species leached into solution, and the catalytic reactions were essentially homogeneous in nature. Brønsted acidity is important for the hydrolysis step (Chapter 8) but these types of active sites are deactivated in the IL medium. The development of truly heterogeneous catalytic systems for the selective conversion of Glu and related di/polysaccharides to Hmf remains a difficult challenge.

In summary, different types of heterogeneous solid acid catalysts have been identified as promising for the conversion of saccharides to Fur. The solid acids have been investigated at the lab-scale, in batch mode and are essentially powders (primary particles or aggregates of relatively small size (micrometer range). Aiming at continuous operation mode, the catalysts need to be shaped into larger physically separate entities, the shape and size of which depends on the design of the reactor and the reaction conditions. Very recently Xing et al.¹⁰ proposed a two-zone continuous biphasic reactor to produce Fur in high yields (ca.90%) from an aqueous solution of hemicellulose, with an estimate of ca. 67-80% lower energy requirements than the current industrial process. Currently, Fur is produced from a hydrolysis/dehydration process from the ground up biomass which is firstly sprayed with H₂SO₄ and then fed into a semi-batch reactor with significant quantities of steam (heat obtained from the burn of the leftover lignin and cellulose derived products).¹¹ The main countries producing Fur today are China, South Africa and

Dominican Republic.¹ The theoretical yield for this process is 0.73 kg of Fur per kg of pentosan, but in practice, this process operates at only around 33% of the theoretical yield.¹²

The implementation of heterogeneous catalytic processes for producing Fur/Hmf may partly depend on whether the processing of biomass into a liquid stream of poly, oligo or monosaccharides becomes economically feasible since otherwise severe mass transfer limitations may exist associated with solid-solid interface catalytic reactions.

The catalytic performances of the porous inorganic oxide catalysts could be explored in other catalytic routes of the chemical valorisation of carbohydrate biomass, and it may be interesting to transform them into bifunctional catalysts (important for process intensification).

10.2. References

- (1) Win, D. T.: Furfural- Gold From Garbage. *Au Journal of Technology* **2005**, *8*, 185-190.
- (2) Mamman, A. S.; Lee, J. M.; Kim, Y. C.; Hwang, I. T.; Park, N. J.; Hwang, Y. K.; Chang, J. S.; Hwang, J. S.: Furfural: Hemicellulose/Xylose Derived Biochemical. *Biofuels Bioproducts & Biorefining* **2008**, *2*, 438-454.
- (3) Huber, G. W.; Iborra, S.; Corma, A.: Synthesis of Transportation Fuels from Biomass: Chemistry, Catalysts, and Engineering. *Chemical Reviews* **2006**, *106*, 4044-4098.
- (4) Karinen, R.; Vilonen, K.; Niemela, M.: Biorefining: Heterogeneously Catalyzed Reactions of Carbohydrates for the Production of Furfural and Hydroxymethylfurfural. *ChemSusChem* **2011**, *4*, 1002-1016.
- (5) Lima, S.; Antunes, M. M.; Pillinger, M.; Valente, A. A.: Ionic Liquids as Tools for the Acid-Catalyzed Hydrolysis/Dehydration of Saccharides to Furanic Aldehydes. *ChemCatChem* **2011**, *3*, 1686-1706.
- (6) Sierraalta, A.; Anez, R.; Ehrmann, E.: Oniom Study of Ga/SAPO-11 Catalyst: Species Formation and Reactivity. *Journal of Molecular Catalysis A-Chemical* **2007**, *271*, 185-191.
- (7) Hamdy, M. S.: Functionalized TUD-1: Synthesis, characterization, and (photo-)catalytic performance. Delft University of Technology, the Netherlands, 2005.
- (8) IZA-SC-members: Zeolite Framework Types. Database of Zeolite Structures, 2012; Vol. 2012.
- (9) Corma, A.; Fornés, V.; Guil, J. M.; Pergher, S.; Maesen, T. L. M.; Buglass, J. G.: Preparation, Characterisation and Catalytic Activity of ITQ-2, a Delaminated Zeolite. *Microporous and Mesoporous Materials* **2000**, *38*, 301-309.
- (10) Xing, R.; Qi, W.; Huber, G. W.: Production of Furfural and Carboxylic Acids From Waste Aqueous Hemicellulose Solutions From the Pulp and Paper and Cellulosic Ethanol Industries. *Energy & Environmental Science* **2011**, *4*, 2193-2205.
- (11) Zeitsch, K. J.: *The Chemistry and Technology of Furfural and its Many By-Products*; 1st ed.; Elsevier Science B. V.: Amsterdam, The Netherlands, 2000; Vol. 13.
- (12) Mansilla, H. D.; Baeza, J.; Urzua, S.; Maturana, G.; Villasenor, J.; Duran, N.: Acid-Catalysed Hydrolysis of Rice Hull: Evaluation of Furfural Production. *Bioresource Technology* **1998**, *66*, 189-193.